MONITORING AND MODELING OF PAVEMENT RESPONSE AND PERFORMANCE
TASK B: NEW YORK
Pooled Fund Project TPF-5 (121)
Volume 2: I86 PCC

by
Shad M. Sargand, Issam S. Khoury,
And David Padilla-Llano

for the
Ohio Department of Transportation
Research Section
the
New York State Department of Transportation
and the
United States Department of Transportation
Federal Highway Administration

State Job Number 134287

May 2012

Ohio Research Institute for
Transportation and the Environment

1. Report No. FHWA/OH-2012/08B	2. Government Accession No.	3. Recipient's Catalog No.
4. Title and Subtitle MONITORING AND MODELING OF PAVEMENT RESPONSE AND PERFORMANCE TASK B: NEW YORK Volume 2: I86 PCC		**5. Report Date** May 2012 **6. Performing Organization Code**
7. Author(s) Shad Sargand, Issam Khoury, and David Padilla-Llano		**8. Performing Organization Report No.**
9. Performing Organization Name and Address Ohio Research Institute for Transportation and the Environment (ORITE) 141 Stocker Center Ohio University Athens OH 45701-2979		**10. Work Unit No. (TRAIS)** **11. Contract or Grant No**. Pooled Fund Project TPF-5(121) State Job No. 134287 Agreement No. 21182
12. Sponsoring Agency Name and Address Ohio Department of Transportation Innovation, Research, and Implementation Section 1980 West Broad St. Columbus OH 43223		**13. Type of Report and Period Covered** Technical Report 14. Sponsoring Agency Code

15. Supplementary Notes
Prepared in cooperation with the Ohio Department of Transportation (ODOT), the New York State Department of Transportation (NYSDOT) and the U.S. Department of Transportation, Federal Highway Administration

16. Abstract

In Cattaraugus County, New York State, Interstate 86 exhibited major distresses, and the jointed reinforced portland cement concrete pavement (JRCP) and was in need of rehabilitation by 2004. Three experimental sections were constructed in June 2006 using an unbonded overlay of jointed plain concrete pavement (JPCP). In one section the existing JRCP was *untreated*, in another it was *rubblized*, and in the third section it was *broken and seated* (B&S). Embedded sensors monitored strain, temperature, and displacement responses. The research effort included periodic monitoring of stress and strains due to environmental loads and measurement of responses induced by a falling weight deflectometer (FWD) to account for dynamic loads.

Results of this study suggest that thermal gradients in the concrete slabs induce highest vertical displacements (curling), strains, and stresses in the *untreated* section. From dynamic loads, the largest deflections and strains are induced in the *rubblized* and B&S sections, while the untreated section exhibits the least severe dynamic response. Environmental strain responses were typically more critical near the top surface of the concrete, often in tension, suggesting probable top-down cracking mechanisms. This research improves the understanding of the physical effects of these fracturing techniques on unbonded overlays through a fully monitored investigation using in-situ instrumentation.

17. Key Words	18. Distribution Statement
JPCP overlay, rubblization, break and seat, dynamic load testing, FWD, instrumented pavement	No Restrictions. This document is available to the public through the National Technical Information Service, Springfield, Virginia 22161

19. Security Classif. (of this report)	20. Security Classif. (of this page)	21. No. of Pages	22. Price
Unclassified	Unclassified	316	

SI* (MODERN METRIC) CONVERSION FACTORS

APPROXIMATE CONVERSIONS TO SI UNITS

Symbol	When You Know	Multiply By	To Find	Symbol
LENGTH				
in	inches	25.4	millimeters	mm
ft	feet	0.305	meters	m
yd	yards	0.914	meters	m
mi	miles	1.61	kilometers	km
AREA				
in^2	square inches	645.2	square millimeters	mm^2
ft^2	square feet	0.093	square meters	m^2
yd^2	square yards	0.836	square meters	m^2
ac	acres	0.405	hectares	ha
mi^2	square miles	2.59	square kilometers	km^2
VOLUME				
fl oz	fluid ounces	29.57	milliliters	mL
gal	gallons	3.785	liters	L
ft^3	cubic feet	0.028	cubic meters	m^3
yd^3	cubic yards	0.765	cubic meters	m^3
NOTE: Volumes greater than 1000 L shall be shown in m^3.				
MASS				
oz	ounces	28.35	grams	g
lb	pounds	0.454	kilograms	kg
T	short tons (2000 lb)	0.907	megagrams (or "metric ton")	Mg (or "t")
TEMPERATURE (exact)				
°F	Fahrenheit temperature	5(°F-32)/9 or (°F-32)/1.8	Celsius temperature	°C
ILLUMINATION				
fc	foot-candles	10.76	lux	lx
fl	foot-Lamberts	3.426	candela/m^2	cd/m^2
FORCE and PRESSURE or STRESS				
lbf	poundforce	4.45	newtons	N
lbf/in^2 or psi	poundforce per square inch	6.89	kilopascals	kPa

APPROXIMATE CONVERSIONS FROM SI UNITS

Symbol	When You Know	Multiply By	To Find	Symbol
LENGTH				
mm	millimeters	0.039	inches	in
m	meters	3.28	feet	ft
m	meters	1.09	yards	yd
km	kilometers	0.621	miles	mi
AREA				
mm^2	square millimeters	0.0016	square inches	in^2
m^2	square meters	10.764	square feet	ft^2
m^2	square meters	1.195	square yards	yd^2
ha	hectares	2.47	acres	ac
km^2	square kilometers	0.386	square miles	mi^2
VOLUME				
mL	milliliters	0.034	fluid ounces	fl oz
L	liters	0.264	gallons	gal
m^3	cubic meters	35.314	cubic feet	ft^3
m^3	cubic meters	1.307	cubic yards	yd^3
MASS				
g	grams	0.035	ounces	oz
kg	kilograms	2.202	pounds	lb
Mg (or "t")	megagrams (or "metric ton")	1.103	short tons (2000 lb)	T
TEMPERATURE (exact)				
°C	Celsius temperature	1.8°C + 32	Fahrenheit temperature	°F
ILLUMINATION				
lx	lux	0.0929	foot-candles	fc
cd/m^2	candela/m^2	0.2919	foot-Lamberts	fl
FORCE and PRESSURE or STRESS				
N	newtons	0.225	poundforce	lbf
kPa	kilopascals	0.145	poundforce per square inch	lbf/in^2 or psi

* SI is the symbol for the International Symbol of Units. Appropriate rounding should be made to comply with Section 4 of ASTM E380.

(Revised March 2003)

MONITORING AND MODELING OF PAVEMENT RESPONSE AND PERFORMANCE TASK B: NEW YORK Volume 2: I86 PCC

Draft Final Report

Prepared in Cooperation with the
Ohio Department of Transportation,
the
The New York State Department of Transportation,
and the
U.S. Department of Transportation,
Federal Highway Administration

Prepared by

Shad M. Sargand
Issam Khoury
David Padilla-Llano

Ohio Research Institute for Transportation and the Environment
Russ College of Engineering and Technology
Ohio University
Athens, Ohio 45701-2979

May 2012

TABLE OF CONTENTS

LIST OF TABLES

LIST OF FIGURES

ACKNOWLEDGEMENTS

On large field-oriented projects such as this, many tasks are involved and many people contribute to the successful completion of those tasks. On this project, NYSDOT personnel were needed to collect certain types of data and to secure the field sites for testing. Julián Bendaña and Wes Yang from the central office, who coordinated all activities, and the various FWD operators, who performed the FWD testing. From the Region Offices were several people who supported the research by allowing the researchers access to the road, by providing, loading, and driving dump trucks for controlled vehicle testing, and by providing traffic control.

Several people at ORITE were also necessary to complete this work, including Sam Khoury who coordinated all of the instrumentation, scheduled and trained students for the field activities and maintained contact with NYSDOT to keep everything going smoothly. Mike Krumlauf assisted with the instrumentation, and with designing and fabricating various devices used in the lab and field. Many students worked on the project team, and some wrote theses on topics associated with the project.

1 Introduction and Objectives

This report documents work by the Ohio Research Institute for Transportation and the Environment (ORITE) at Ohio University on specific tasks to be performed in New York under pooled fund study, TPF-5(121), "Monitoring and Modeling of Pavement Response and Performance," funded by the New York Department of Transportation (NYSDOT) and the Federal Highway Administration (FHWA). There are three volumes in this report, of which this is Volume 2, which presents results from the project on a jointed plain concrete pavement (JPCP) overlay on I86 at Hinsdale, near Olean, New York. The overall objectives of this project and the scope of each volume of the report are provided in Chapter 1 of Volume 1.

Brief project description: Interstate 86, Hinsdale, near Olean, in Cattaraugus County, New York. This was a jointed reinforced concrete pavement (JRCP) made of Portland Cement Concrete (PCC) that was rehabilitated in 2007 by constructing an unbonded jointed plain concrete pavement (JPCP) overlay. In the test section, three treatments were selected to apply to the existing JRCP before applying the overlay: rubblization, break and seat, or no treatment. The objective of the test was to compare the response and performance of the completed pavement with overlay as a function of the treatment applied to the original JRCP.

Because of the extensive amount of effort in this project, this report is divided into three volumes as follows: Volume 1: I490, State Route 9, and I86 Perpetual Pavement, Volume 2: I86 PCC, Volume 3: I90.

2 I86 Hinsdale, NY

2.1Project Overview and Description

Interstate 86 in Cattaraugus County, New York comprises four lanes of jointed reinforced concrete pavement (JRCP) running in the east-west direction near the town of Hinsdale. When first built in 1972, the pavement structure consisted of 229mm (9 in) JRCP with slabs 18.3m (60ft) long and 3.65m (12ft) wide; the pavement also included dowels at the joints and longitudinal tie-bars [Swart, 2006]. After 34 years of service, NYSDOT decided to rehabilitate the road, which at the time presented severe distresses and a high percentage of cracked slabs. A complete forensic study was carried on in 2006 before rehabilitation started, which found the pavement was in poor serviceability condition, which justified its rehabilitation. The rehabilitation consisted of rubblization of the existing pavement and a 225mm (8.86 in) thick hot mix asphalt (HMA) overlay. Rubblization of the existing pavement was chosen in order to diminish the distresses history in the existing concrete slabs and avoid its propagation to the new structure [Ambrosino, 2007].

The rehabilitation project also included the construction of a 2.54 km (1.58 mi) stretch of unbonded concrete overlay divided in three experimental sections, one 820 m (2690 ft) long and the other two 860 m (2822 ft) long. The main purpose of these is to evaluate two fracturing techniques widely used in New York State for the rehabilitation of concrete pavements using unbonded JPCP overlays and compare to not using any fracturing method [Bendaña, Ambrosino & Sargand, 2008]. The sections are located along the southbound lanes of the southern tier expressway between Exit 27 close to Hinsdale and exit 28 close to Cuba in Western New York, shown in the map in Figure 1. In the first section, the existing pavement was broken and seated before overlaying and it is referred herein as the *B&S Section*. In the second section, the existing pavement was rubblized before placing the JPCP overlay and it is referred herein as the *Rubblized Section*. Finally, in the third section or *Untreated Section*, the existing pavement was not treated prior to overlaying.

The cross sectional build-up consists of a 225 mm (8.86 in) JPCP overlay resting on either untreated, rubblized, or broken and seated JRCP with a 75 mm (3 in) asphalt-treated permeable base (ATPB) acting as bond-breaker interlayer between the existing and the new concrete pavement layers. Joints every 4.75 m (15.58 ft) with dowel bars spaced every 305 mm (1 ft) and tie bars along the longitudinal joint were provided. Each experimental section included four instrumented slabs with sensors and gauges to allow measuring of mechanical responses and temperatures of the pavement as described below.

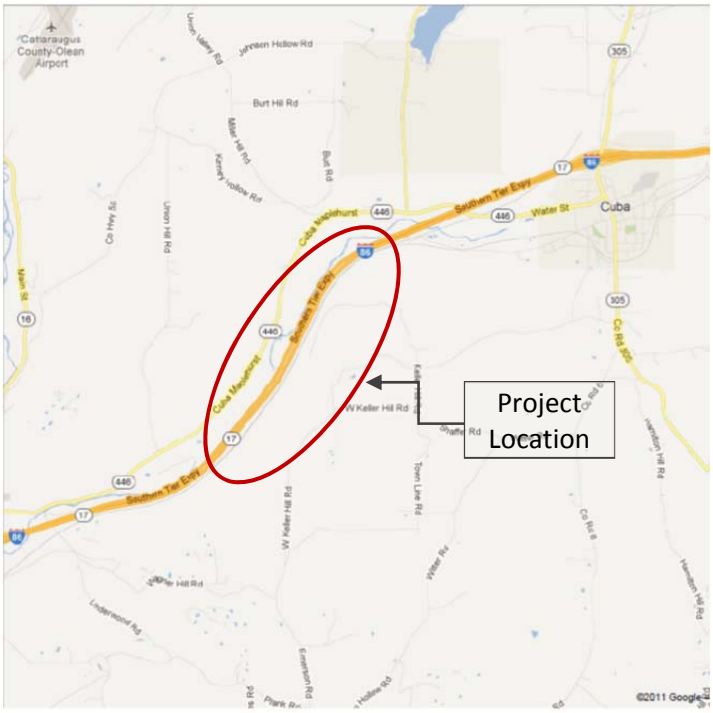

Figure 1. I-86 Project Location near Hinsdale and Cuba. [Google Maps, 2011].

2.2 Project Objectives and Report Structure

The main purpose of this project is to understand the behavior of unbonded jointed plain concrete pavement (JPCP) overlays and the differences on the responses when they are placed over rubblized, broken and seated, and untreated existing JRCP. Environmental and dynamic responses were collected from the instrumented slabs for analysis and comparisons between sections with the purpose of identifying the best option between a rubblized, broken and seated or untreated concrete bases. Comprehending the behavior of the experimental sections would help with the calibration of the Mechanistic-Empirical Pavement Design Guide (MEPDG) based catalogue of rigid pavements for the state of New York.

The study presented here is divided into four main parts. The first presents a summary of concrete overlay systems, pre-overlay treatments and pavement fracturing techniques. Additionally, it also presents a brief review of some research on the performance of existing unbonded concrete overlays under similar conditions to those of the project on Interstate 86. Methodology, description of the instrumentation used, testing procedures, and types of data collected and reduction are then described in the next section. The subsequent section presents a discussion and analysis of the response of the experimental sections due to the environmental effects. In this, the environmental strain and stresses at different places of the instrumented slabs are compared and critical locations are identified for each section. Additionally, the behaviors of the sections are compared and discussed, giving insights on the performance differences of the JPCP overlays and the different fracturing techniques. In addition, the response to the FWD testing is discussed and the responses of each section are compared on basis of the dynamic strains and FWD deflections obtained. Finally, this report ends with a summary of the findings and conclusions about the analysis presented herein. Supplemental data are provided in the appendices.

3 Literature Review

Rehabilitation of pavements is defined as the improvement of the structural and functional conditions of a pavement in order to extend its service life, and ride quality [Hall, Correa, Carpenter & Elliot, 2001]. Several rehabilitation techniques exist aimed for flexible and rigid pavement; such techniques are different depending mainly on the level of distresses observed, the traffic volume and serviceability condition of the existing structure. In the case of rigid pavements, the rehabilitation methods applicable include full or partial depth reparation, slab replacement, under-sealing, load transfer restoration, joint resealing, diamond grinding, sub-drainage improvement, asphalt or concrete overlays, and reconstruction. Among these, in this chapter the focus is on the concrete overlay technique over existing non-fractured or fractured concrete pavement.

3.1 Concrete Overlay Systems and Pre-Overlay Treatments

Concrete overlays are versatile, sustainable and the most effective rehabilitation technique; they provide increased structural capacity and serviceability with fewer or less expensive pre-overlay treatments needed and smaller traffic disruptions [Harrington, 2008]. It is required that the existing pavement integrate with the new rehabilitated structure to help on carrying the traffic load and reducing the construction time. With the increase of structural capacity and serviceability, the concrete overlay method can extend the service life of an existing pavement about 30 years [Harrington, 2008]. Concrete overlay methods are classified according to the system employed: 1. the bonded concrete overlay (BCO); and 2. unbonded concrete overlay (UBCO).

The BCO system is used to increase the structural capacity of pavements, increase serviceability, repair surface distresses, and increase ride quality [Hall et al., 2001; Harrington, 2008]. A bonded concrete overlay consists of a relatively thin (5 cm to 13 cm or 2 in to 5 in) concrete layer fully bonded to the existing pavement to work as a monolithic structure. Since BCOs are required to work as a unit with the existing structure, a detailed and careful surface preparation is essential to ensure bonding between the two layers. Hence, this makes the use of bonded overlays not economical depending on the condition and level of deterioration of the existing pavement. A distressed structure with severe cracking and damaged joints needs extensive reparations to ensure the monolitical behavior of the resulting structure, contrasting with the case of a pavement in good condition [Hall et al., 2001]. Therefore, the use of bonded concrete overlays is limited to preventive maintenance and minor rehabilitation for pavements in good to fair conditions [Harrington, 2008].

UBCO is used when severe level of distresses and condition of the existing pavement will require otherwise extensive/expensive reparations [Hall et al., 2001; Harrington, 2008]. UBCOs consist of a thicker (10 cm to 28 cm or 4 in to 11 in) concrete layer placed over the existing pavement usually separated by a bond breaker interlayer. The bond breaker interlayer, often a hot mix asphalt layer (HMA), is required to separate the overlay from the existing pavement structure when the latter is concrete. Thus, preventing excessive stresses that can develop due to relative movement between the pavement layers and which could result in reflective cracking, poor performance, and short service life of the overlay [AASHTO, 2008; Tenison & Hanson, 2009]. The thickness of the interlayer should be of at least 1in or more depending on the size of the agregate used in the HMA. The overlay is expected to behave as a new pavement structure where the existing pavement “provides a stable base” [Harrington, 2008, p. 2]. The unbonded

concrete overlay requires less or no pre-overlay treatments depending on the condition of the existing pavement. These treatments altogether with the HMA bond breaker layer are meant to help prevent reflective cracking and excesive stresses in the overlaid concrete [Hall et al., 2001; Tenison & Hanson, 2009]. When the condition of the existing pavement requires extensive repair, fracturing concrete techniques can be used. These comprise the broken or broken and seated of slabs and full depth rubblization of existing slabs. Next, a description of each of these fracturing techniques is presented.

3.2 Pavement Fracturing Techniques

Three different pavement fracturing techniques are commonly use within the United States. These three methods are: *crack and seat*, *break and seat*, and and *rubblization*. The fracturing of concrete pavements as a pre-overlay treatment is justified for two reasons: prevention of reflective cracking and avoidance of extensive and expensive repairs when the condition of the existing pavement is poor [Hall et al., 2001]. Each fracturing method is briefly described below.

Crack and Seat: Applicable only to JPCP, this method consists of the reduction of the slab effective length by breaking the existing concrete pavement into smaller pieces of no more than 3 ft (1 m) long. This is intended to reduce the vertical movements [possibly due to loss of support] without eliminating the load transfer between pieces provided by aggregate interlock. After broken, the slab pieces are seated using a heavy roller in order to re-establish the support conditions preventing related vertical movements [AASHTO, 2008; Morian, Sadasivam, Mack & Stoffels, 2006].

Break and Seat: This method is applicable to jointed reinforced concrete pavement (JRCP) and continously reinforced concrete pavement (CRCP). Similar to the crack and seat method, this method involves breaking the existing pavement structure into small pieces of no more than 2 ft (0.6 m) long. The difference is that in this method the reinforcing steel, or its bond with the concrete is broken in order to achieve reduction of the effective length of the slab [AASHTO, 2008; Morian et al., 2006].

Rubblizing: This method consists of fracturing of the concrete pavement in small pieces ranging from sand size up to 3 to 15 in (7.6 to 38 cm) at the bottom of the layer. In the rubblization process the the slabs are broken using a multi-head pavement breaker or a resonant pavement breaker. Rubblizing destroys the concrete-reinforcement bond and slab action of the existing pavement, and eliminates the reflective cracking of the overlay [Tenison & Hanson, 2009]. The rubblizing technique is applicable to any type of concrete pavement.

In this project, a comparison is made of performances between overlays on JRCP sections with no treatment, rubblization, and breaking and seating. The distinction between "break and seat" and "crack and seat" came into acceptance after most of the results on this project had been generated. As a consequence, in presenting the results in this report, the break and seat section is sometimes referred to in figures and tables as "crack and seat", "cracked and seated", "C&S" or "C/S", all of which should be understood as referring to the break and seat section, to differentiate from the rubblized and untreated sections.

3.3 Performance of existing Unbonded Concrete Overlays

Unbonded concrete overlays have shown good long-term performance indicators with little maintenance and repairs compared to projects in which other rehabilitation techniques were implemented. In 1999, ERES Consultants, Inc. published a report on the performance of unbonded concrete overlay aimed to develop guidelines for its design and construction. Different

factors were identified in this study as those of most concern for design and construction purposes. Among these factors and additionally to traffic, the climate, condition of the subgrade and existing pavement and pre-overlay treatments have important effects on the design of UBCOs [ERES Consultants Inc., 1999]. The study involved the assessment and analysis of 62 different sections that included some of the LTPP database sections. The evaluation summary of these sections showed as a general trend that thin concrete overlay performed poorly and developed more severe distresses than thicker overlays. The overlays reported generally to have performed poorly corresponded to CRCP overlays of 3 to 8 in (7.6 to 20 cm) thick, jointed concrete pavement overlays of 6 to 8 in (15 to 20 cm) thick, undoweled and with deficient or non-existent interlayer. Those overlays that performed well tended to be seven inches thick or more, with adequate non-erodible interlayer and with doweled joints in the case of JRCP and JPCP [ERES Consultants Inc., 1999].

Since climate significantly influences on the design of UBCOs, the evaluation of concrete overlays under the similar conditions to those of the project on Interstate 86 is of valuable consideration. In 1989, the Ministry of Transportation of Ontario, Canada engaged in the rehabilitation after 26 years of service of the four-lane divided Highbury Avenue (Highway 126) in the city of London, Ontario. The Highbury Avenue supported a 22,000 annual average daily traffic (AADT) during year 2000, with an 11.3% of commercial vehicles on the southbound lanes [Kazmierowski & Chan, 2005; Kazmierowski & Sturm, 1994]. The old structure consisted of a 225mm (8.86 in) thick jointed reinforced pavement supported on a 300mm (11.8 in) thick granular base. The existing JRCP in the northbound lanes (NBL) was considered to be in better condition than average and underwent diamond grinding, partial and full depth repairs. The south bound lanes (SBL) presented a more critical situation with transverse cracks, spalling of all joints and D-cracking; they were broken and seated and then overlaid using an unbonded plain concrete pavement overlay 180 mm (7.1 in) thick with no dowels and asphaltic sand hot mix interlayer of 20mm (0.8 in) thickness.

After the evaluation of the performance of the pavement done in 1992 and 1993, Kazmierowski & Sturm [1994] concluded that the strength of the pavement increased compared to the old structure. This, because of the low center-to-corner deflection ratios obtained from the falling weight deflectometer (FWD) test as well as the observed load transfer efficiency across the joints, which values were between 95% and 97% [Kazmierowski & Sturm, 1994]. After ten years of service, and with minor "full and partial depth" repairs (covering areas of 535m^2 (5760 ft^2) and 10m^2 (107 ft^2) respectively), the major distresses observed in the SBL was reported as slightly longitudinal cracking in 11 slabs in the driving lane [Kazmierowski & Chan, 2005, p. 5]. After 15 years of service, the overlay presented slightly localized faulting, moderate joint and crack spalling, severe edges drop-off as well as occasional severe reflective cracks, moderate transverse cracks, and the longitudinal cracks observed in 1999 were in a more severe condition. However, the pavement was considered to have performed well with practically constant roughness in the last five years having "acceptable ride quality and skid resistant" [Kazmierowski & Chan, 2005, p. 14].

On November 2005, Quality Engineering Solutions, Inc. [2008] started the building of a full-scale experimental concrete overlay over existing concrete pavement. A 300 ft (91 m) instrumented unbonded concrete pavement overlay underwent testing at the National Airfield Pavement Test Facility (NAPTF) located at the William J. Hughes Technical Center near Atlantic City, NJ. This test was an attempt to study the critical factors affecting the behavior of

unbonded concrete overlays for airfields. Although the purpose of this project was to evaluate the factors that affect the performance of airfield unbonded concrete overlays and provide guidance for its design, the insights, data collected and findings can be qualitatively compared to those expected from the performance of the experimental sections on Interstate 86.

The structure of the overlaid pavement consisted of two concrete slabs with an asphalt concrete interlayer resting on a subgrade of medium strength [average CBR of 7.9]. The sections were loaded up to failure and data was recorded and analyzed. This study considered different cross section for the structure of the pavement. The different variables considered included different overlay-underlying slab thickness ratios; underlying discontinuities [i.e. mismatched joints]; bonding condition of the interlayer and overlying slabs; and different gear loads and configuration: single tire, dual tire, dual tandem, and triple dual tandem [Quality Engineering Solutions Inc., 2008]. However, the study did not consider the seasonal effects on the performance despite absence of control of temperature and environmental conditions within the NAPTF facilities. Moreover, the construction period comprised at least 4 months [i.e. from Nov. 28 through March 30 when the overlay was built], and the testing took place during the next months until December 2006 in a region where seasonal changes may be an important variable on the performance of the pavement structure.

Based on the of the analysis performed, the authors concluded that the principal cracking mode was top-down longitudinal cracking due to the contra flexure bending stresses in the slabs [Quality Engineering Solutions Inc., 2008]. Additionally, the author also reported that the section with a higher overlay-underlying slab thickness ratio was the first section showing this kind of distress and that the interlayer between slabs helped preventing the propagation of top-down cracks through the depth. The authors concluded also that the influence of mismatched joints between the overlay and underlying slab was not noteworthy.

Recently, Darter, M.I., Mallela, J. & Titus-Glover, L. [2009] addressed the performance assessment of two cases of jointed plain concrete pavement (JPCP) overlay using the *Mechanistic-Empirical Pavement Design Guide, Interim Ed.: A Manual of Practice* [AASHTO, 2008]. The two cases considered include a doweled JPCP overlay over existing hot-mix asphalt (HMA) pavement located in the state of Kansas, and an overlay where the existing pavement was an existing JPCP pavement located in the state of Illinois. In this study, the authors considered different conditions of the existing pavement and their effects on the predicted performance and design of the JPCP overlay.

From the cases studied, the second case of a JPCP overlay over existing JPCP is of interest. Darter et al., 2009 state that the structural capacity of the existing pavement is a determining factor for an adequate long-term performance of the concrete overlay. The authors show that the thickness of the JPCP overlay decreases as the amount of damage in the existing structure decreases suggesting then that an assessment of the condition of the existing pavement is necessary for a good design of the JPCP overlay. This implies that the effects from the condition of the existing structure lessen as the thickness of the overlay increases. Additionally, the authors state that the overlay should be at least 2 inches thicker compared to a pavement with a "good" condition if the existing pavement is rubblized. This is attributed to the fact that rubblizing reduces the elastic modulus of the existing pavement structure [Darter et al., 2009].

3.4 Interstate 86 Related Research

The Ohio Research Institute for Transportation and the Environment (ORITE) together with the New York State Department of Transportation (NYSDOT) have been conducting research on

the behavior of three experimental sections along the interstate I86 in Cattaraugus County in New York State. This study is part of the project Monitoring and Modeling of Pavement Response and Performance of the Federal Pooled Fund and its main purpose is to compare three different rehabilitation methods for concrete pavements and provide recommendations for the design of unbonded concrete overlays [Bendaña et al., 2008]. Before construction of the experimental sections, a forensic study carried out by Swart [2006] showed that the existing JRCP presented severe distresses. Swart found the condition of the pavement to be poor based on the PCI values obtained using the procedure described by ASTM in the "*Standard Practice for Roads and Parking Lots Pavement Condition Index Surveys*" document [ASTM, 2003]. The PCI values obtained for the existing pavement at the location of each experimental section were 26 for the untreated section and 36 for both rubblized and B&S sections. Additionally, a distress survey performed before fracturing the existing JRCP showed that 80% of the slabs exhibit high severity transverse cracking at the location of the untreated and B&S sections while at the location of the rubblized section the percentage was 64%.

The experimental sections consist of an unbonded concrete overlay over jointed reinforced concrete pavement (JRCP) which received treatment before rehabilitation. In the first section, the existing pavement was left without any treatment, and over it, a 225mm (8.86 in) of jointed plain concrete pavement (JPCP) overlay with a 75mm (3.0 in) asphalt-treated permeable base (ATPB) interlayer placed in between the new and existing concrete. For the second and third sections, the existing JRCP was rubblized, and broken and seated (B&S) respectively, previous the application of the overlay [Bendaña et al., 2008]. The JPCP overlay included dowel bars for transversal joint as well as tie bars in the longitudinal joints. The sections are instrumented and data has been collected since the construction day. The analysis of the collected data and study of the performance during the first year was conducted by Bendaña et al. [2008]. From this study, the authors concluded that rubblizing is a more effective treatment method compared to the conventional overlay, and provided better support for the slabs as well as reduced the strains and stresses due to environmental effects. However, it is also mentioned that the stiffness of the rubblized section was lower compared to the other two sections as well as its effectiveness on preventing lift and high strains due to dynamic loading [Bendaña et al., 2008].

Regarding the B&S section, this provided support conditions compared to the rubblized section and reduced the induced strains and stresses due to changes in temperature [Bendaña et al., 2008]. The effectiveness of the treatment on the load transfer capability, as well as on reducing stresses and strains due to dynamic loading was dependent on the degree of support of the slabs. The authors suggested that breaking and seating the existing pavement is probably a more economical rehabilitation technique since, it provides benefits comparable to the rubblization and is less time consuming [Bendaña et al., 2008]. However, the authors also pointed out that concluding this requires the assessment of the performance over a longer period.

4 Methodology and Testing Procedures

In order to fulfill the main objective of the I86 Project described in Section 2.2, the experimental sections were instrumented with strain gauges, linear variable differential transducers (LVDT) and thermocouples. The sensors allow monitoring the behavior due to climatic changes as well as the response from the dynamic load testing using the Falling Weight Deflectometer, (FWD). The data obtained from the instrumented sections include pavement temperatures, strains and displacements due to daily climatic changes, and strain as well as deflection responses from the FWD tests. Additionally, a weather station was installed on the site to collect air temperatures, solar radiation, precipitation, wind speed, and relative humidity. From these data, the induced stresses are calculated and relationships between the different measured variables are checked such that a better understanding of the behavior of the pavement structure in each section is obtained. Moreover, this analysis will allow comparisons between the three different rehabilitation techniques and their particular influence on the behavior of the experimental sections.

The analysis and discussions presented comprises about five years of data collected since the construction day in June 2006 until August 2011. The following sections briefly describe the instrumentation plan, description of the sensors utilized, type of the data collected and the procedure of the falling weight deflectometer (FWD) test.

4.1 Instrumentation: Plan, Installation and Description

Each of the experimental section on I86 included three instrumented slabs. Instrumentation installed included: eight Honeywell linear variable differential transducers (LVDT) to measure displacements, twelve Geokon vibrating wire strain gauges to measure strains due to climatic changes, eight Vishay micro measurement strain gauges to measure strains due to dynamic loading and four thermo-set sticks each with four thermocouples equally spaced to measure the pavement temperature through the thickness of the slab. A brief description and relevant information to the work presented herein of each of the sensors is presented in the subsequent section. A more complete description of the equipment utilized, theory of operation and installation of the sensors, the wiring diagrams and labeling scheme relevant to this project has been presented before by Ambrosino [2007]. Figure 2 shows a plan view of the sensor's location and dimensions of the slabs and Table 1 shows the slab dimensions as built with the actual locations of each sensor. A description of the sensors utilized follows.

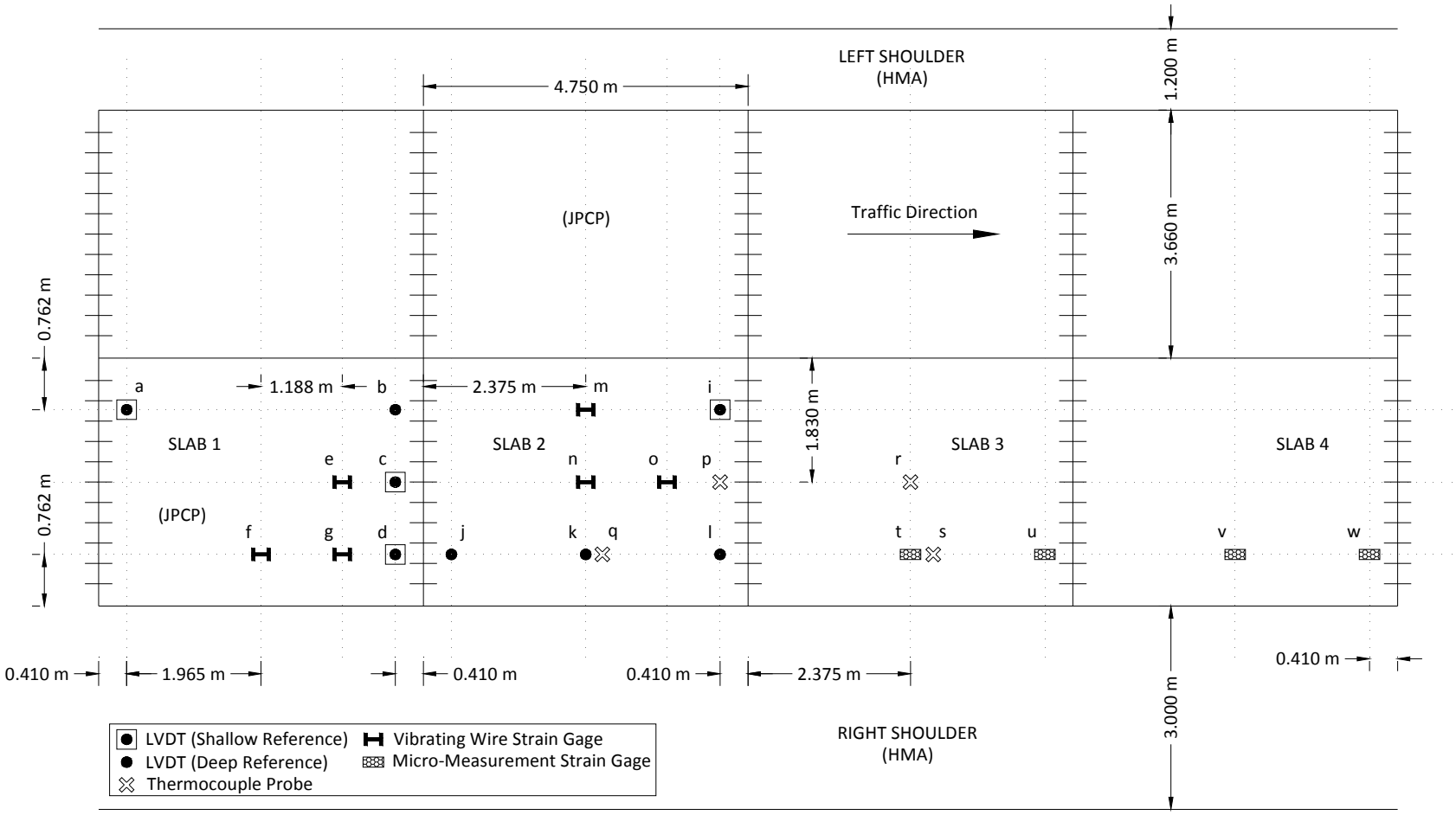

Figure 2. Instrumentation plan and dimensions for a typical section on I86 (1 m = 3.28 ft).

Table 1. As-built dimensions and sensor locations on I86 [Ambrosino, 2007].

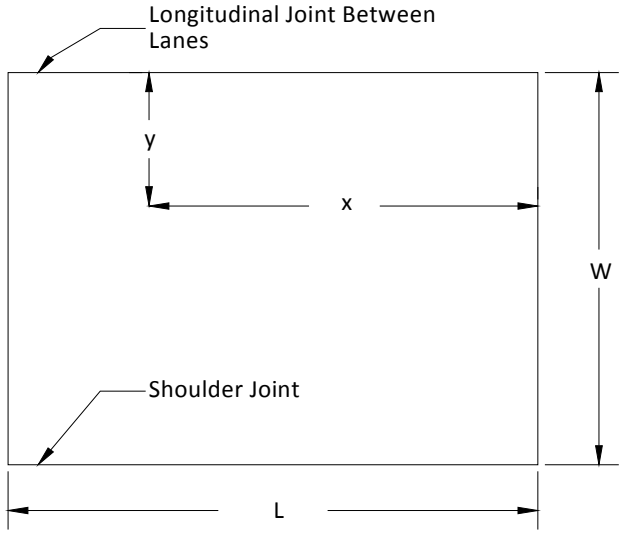

		Untreated		Rubblized		Broken and seated	
		x (cm)	y (cm)	x (cm)	y (cm)	x (cm)	y (cm)
Slab 1	L,W	**480**	366	**475**	366	**464**	366
	LVDT a	**441**	**78**	**436**	**75**	434	76
	LVDT b	**43.5**	**79.2**	**36**	**78.7**	41	76
	LVDT c	**42**	**183**	**42.3**	**183.3**	41	183
	LVDT d	**45**	**289**	**45.2**	**289.5**	41	289
	VW e	119	183	**119**	**183**	119	183
	VW f	238	289	**236**	**292**	238	289
	VW g	119	289	**119**	**292**	119	289
Slab 2	L,W	**485**	366	**478**	366	**468**	366
	LVDT i	**43.5**	**81**	**39**	**79**	41	76
	LVDT j	**446**	**290.6**	**436**	**295**	434	289
	LVDT k	**245.5**	**290.5**	**242**	**291**	238	289
	LVDT l	**40**	**291.8**	**45**	**290**	41	289
	VW m	238	76	**238**	**76**	238	76
	VW n	238	183	**239**	**183**	238	183
	VW o	119	183	**119**	**182**	119	183
	TC p	41	183	41	183	41	183
	TC q	238	289	238	289	238	289
Slab 3	L,W	**486**	366	**476**	266	**466**	366
	MM t	**244**	289	**238**	**291**	238	289
	MM u	**50**	289	**49**	**292**	41	289
	TC r	**241**	183	**233**	**195**	238	283
	TC s	**244**	289	238	289	238	289
Slab 4	L,W	**488**	366	**476**	366	**472**	366
	MM v	**244**	289	**240**	**291**	238	289
	MM w	**50**	289	**50**	**291**	41	289

Measures in **Bold** are **actual measurements**.
Other measurements are nominal values from the instrumentation plan

		Untreated		Rubblized		Broken and seated	
		x (in)	y (in)	x (in)	y (in)	x (in)	y (in)
Slab 1	L,W	**189**	144	**187**	144	**183**	144
	LVDT a	**174**	**31**	**172**	**30**	171	30
	LVDT b	**17**	**31**	**14**	**31**	16	30
	LVDT c	**17**	**72**	**17**	**72**	16	72
	LVDT d	**18**	**114**	**18**	**114**	16	114
	VW e	47	72	**47**	**72**	47	72
	VW f	94	114	**93**	**115**	94	114
	VW g	47	114	**47**	**115**	47	114
Slab 2	L,W	**191**	144	**188**	144	**184**	144
	LVDT i	**17**	**32**	**15**	**31**	16	30
	LVDT j	**176**	**114**	**172**	**116**	171	114
	LVDT k	**97**	**114**	**95**	**115**	94	114
	LVDT l	**16**	**115**	**18**	**114**	16	114
	VW m	94	30	**94**	**30**	94	30
	VW n	94	72	**94**	**72**	94	72
	VW o	47	72	**47**	**72**	47	72
	TC p	16	72	16	72	16	72
	TC q	94	114	94	114	94	114
Slab 3	L,W	**191**	144	**187**	105	**183**	144
	MM t	**96**	114	**94**	**115**	94	114
	MM u	**20**	114	**19**	**115**	16	114
	TC r	**95**	72	**92**	**77**	94	111
	TC s	**96**	114	94	114	94	114
Slab 4	L,W	**192**	144	**187**	144	**186**	144
	MM v	**96**	114	**94**	**115**	94	114
	MM w	**20**	114	**20**	**115**	16	114

4.1.1 Linear Variable Differential Transducer (Honeywell Sensotec S3C Model)

Linear variable differential transducers (LVDT) were installed in order to measure the vertical displacement of the slab at specific points as shown in Figure 2. Eight Honeywell Sensotec LVDTs model S3C were utilized in this project for each section, depicted in Figure 3. These were classified according to point of reference from where the displacement is being measured. Within each section four LVDTs were installed as shallow reference LVDTs given that their reference point is located at the interface of the preexisting pavement structure and the base as shown in Figure 4. The displacement measured from the shallow reference LVDTs is regarded as the displacement of the overlay respect to the subgrade. On the other hand, the

reference point for the deep reference LVDTs is anchored in the subsurface out of the zone of influence of the loads. Thus, the displacement measured by the deep reference LVDTs is considered as the total vertical displacement at the respective point of the slab including the deformation of the soil beneath the pavement structure. The principle and theory behind the operation and measuring deflections using LVDTs can be consulted in the book "*Experimental Stress Analysis*" written by Dally & Riley [2005].

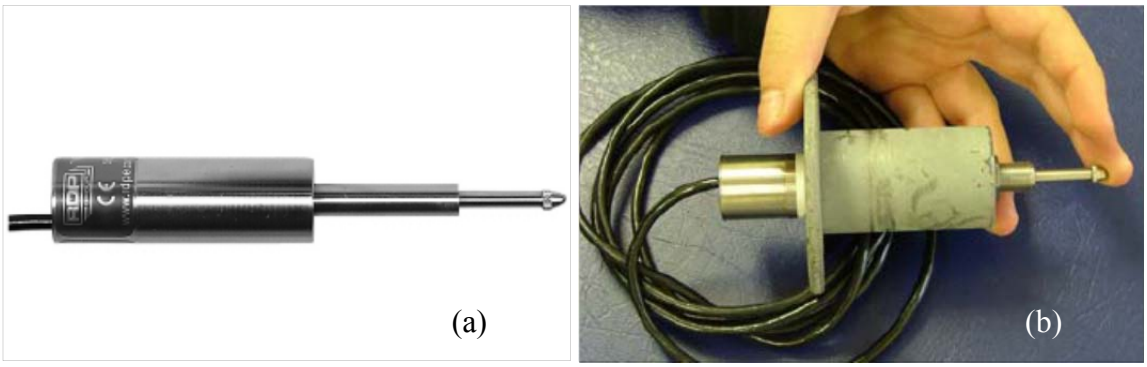

Figure 3. Honeywell Sensotec S3C LVDT: a) LVDT [Honeywell, 2009]; b) LVDT with steel holder [Ambrosino, 2007].

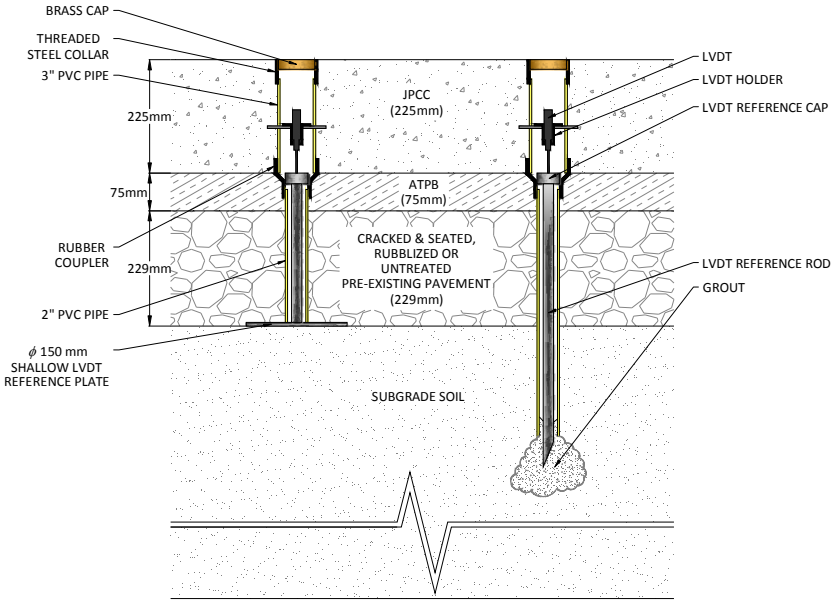

Figure 4. Schematic profile of LVDT installation with reference rods (1" = 2.54 cm, 25.4 mm = 1 in).

4.1.2 Vibrating Wire Strain gauges (Geokon Model 4200)

Vibrating wire strain gauges (VW) were utilized to measure long-term strains at the top and bottom of the concrete slabs due to climatic changes (i.e. strains due to changes in temperature and moisture through the slab's depth) in six different locations indicated in Figure 2. Twelve Geokon VWs model 4200 like the ones shown in Figure 5 were installed in each of the sections. The gauges were mounted on a steel chair such that the bottom gauge was located 31.75mm (1.25 in) from the bottom surface of the slab and the top gauge was located 37.68mm (1.48in) from the top surface as indicated in Figure 6. Each gauge contains a thermistor to measure the

temperatures in the pavement, which are related to the behavior and strains due to climatic changes. The measured temperatures are used in the analysis to correct the read apparent strain isolating the strain component that induces stresses in the slab. The strain readings are measured using the vibrating wire technology which theory is explained in the book *Strain Gauge Technology* [Hornby 1992].

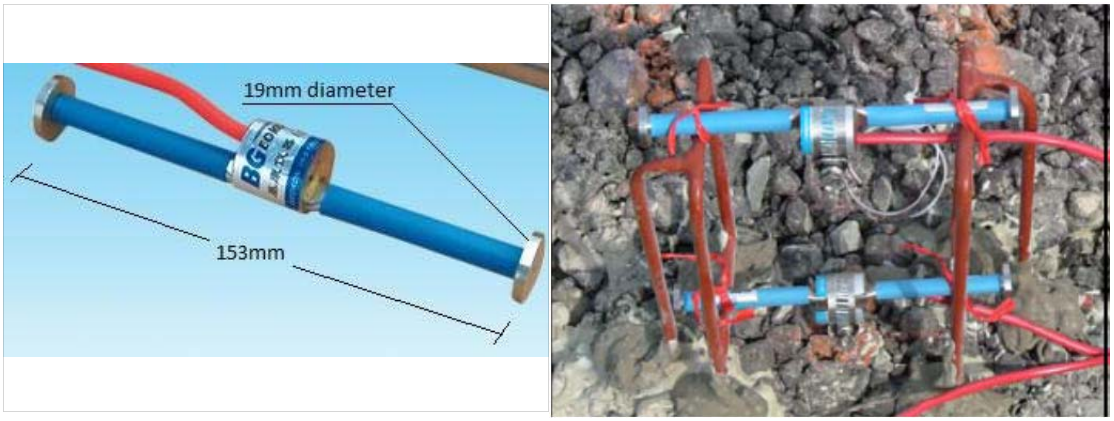

Figure 5. Geokon vibrating wire strain gauge Model 4200. Left: Standard gauge [Geokon, 2008]; Right: Installed gauges [Ambrosino, 2007] (25.4 mm = 1 in).

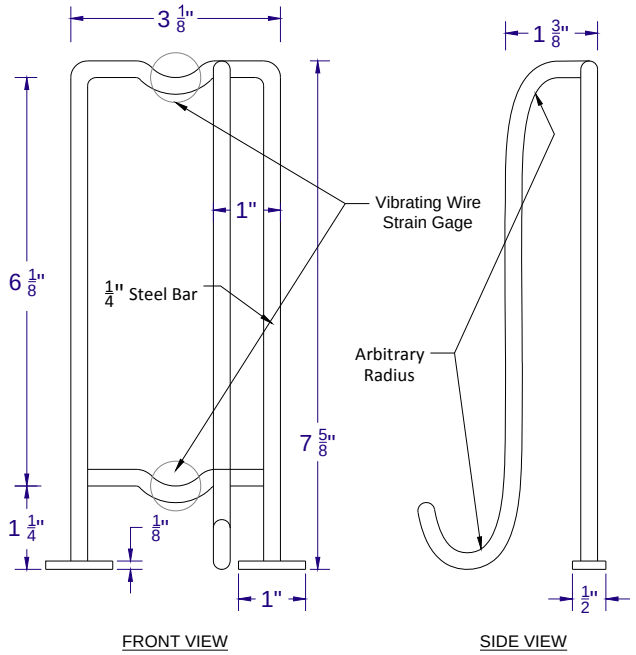

Figure 6. Vibrating wire strain gauge mounting chairs. Adapted from Ambrosino [2007] (1 in = 2.54 cm).

4.1.3 Micro-Measurements Strain gauges (Vishay EGP-5-120)

Micro-measurement (MM) strain gauges were installed to measure the response of the concrete slab induced by traffic or dynamic loads (such as the induced by the FWD test) at four different locations as indicated in Figure 2. Eight self-temperature-compensated Vishay EGP-5-120 Micro-Measurement strain gauges were installed in each section. The gauges were mounted on steel chairs similar to those used for the vibrating wire strain gauges, depicted in Figure 7. The bottom gauges were located 25.4mm (1.0 in) from the bottom surface of the slab and the top

gauges were located 32.91mm (1.3 in) from the top surface of the slab as indicated in Figure 8. Dally & Riley [2005] describe the theory and principles behind the operation of this type of gauge.

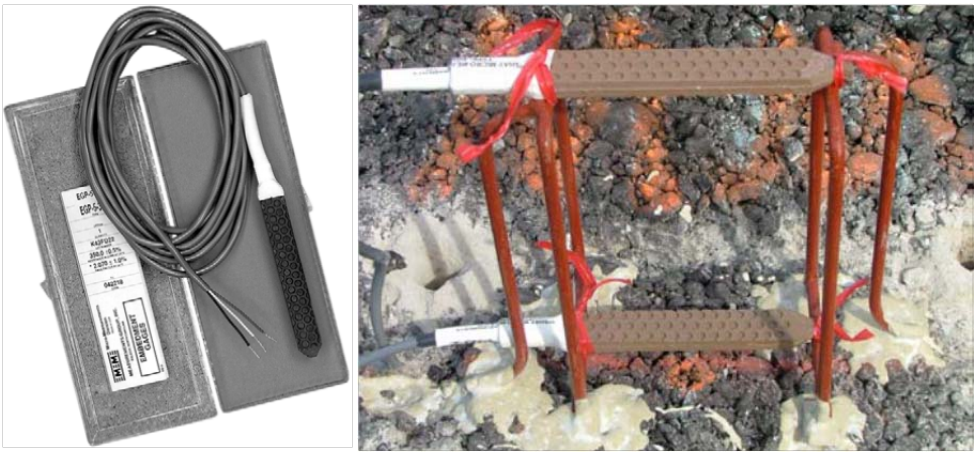

Figure 7. Vishay EGP-5-120 Strain gauge. Left: Standard gauge [Vishay, 2006]; Right: As installed [Ambrosino, 2007].

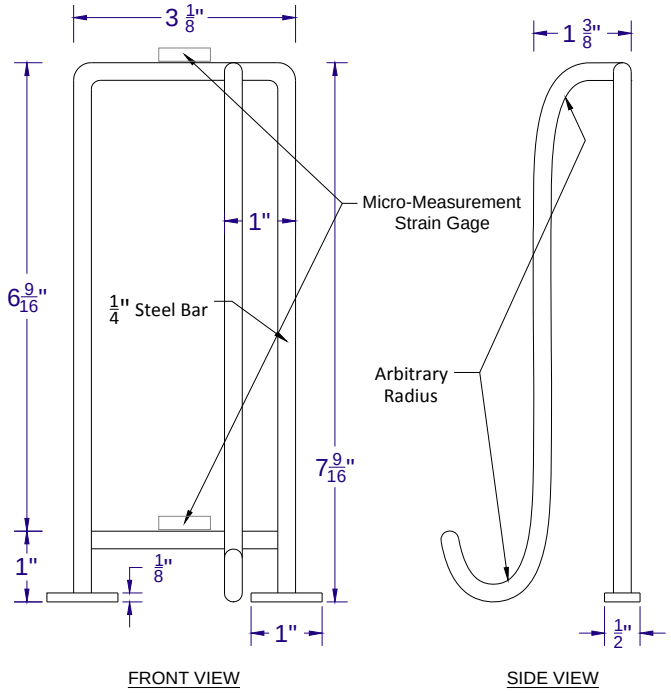

Figure 8. MM mounting chairs. Adapted from Ambrosino [2007] (1 in = 2.54 cm).

4.1.4 Thermocouples (T-type)

Four T-type thermocouple probes were installed in each test section at four different locations indicated in Figure 2. Each probe consisted of four thermocouples equally spaced 55mm (2.16 in) and it was installed such that the first thermocouple was 20 mm (0.79 in) above the bottom surface of the concrete slab. Thus, temperature profiles can be obtained with readings at 20 mm (0.79 in), 75 mm (2.95 in), 130 mm (5.12 in), and 185 mm (7.28 in) from the bottom

surface of the concrete slab. Each thermocouple can measure temperatures from -250°C (-418°F) to 350°C (662°F) with an accuracy of ±1°C (±1.8°F). The principle of operation of the thermocouples is also described by Dally & Riley [2005].

4.2 Testing

Prior to rehabilitation, non-destructive and destructive tests were performed to assess the condition of the existing JRCP pavement structure. Destructive tests included dynamic cone penetrometer (DCP) testing and extraction of concrete cores tested to determine the compressive strength. Non-destructive tests included visual distress surveys, fault measurements using the Georgia Digital Faultmeter, and Falling Weight Deflectometer (FWD) measurements [Ambrosino, 2007; Swart, 2006].

After construction of the JPCP overlay in June 2006, concrete cylinders and beams of the new pavement were tested to determine the compressive and flexural strength respectively. The results obtained were presented by Ambrosino [2007] and are briefly summarized in Section 5.1. Non-destructive testing was performed after construction in regular basis, including FWD tests along the three sections, performed in collaboration with the New York State Department of Transportation (NYSDOT), which included monitoring responses of the MM strain gauges and LVDTs to the FWD loads.

4.2.1 Falling Weight Deflectometer Test

The falling weight deflectometer (FWD) test induces deflections in the pavement structure by applying a load impulse produced by a weight dropping from an adjustable height. The purpose is to simulate the load of a single heavy wheel acting on the pavement structure [Alavi, LeCates, and Tavares, 2008]. The load impulse induces deflections, which are measured by seismometers located at different distances from the point of application of the load including one sensor at the center of the plate. Two models of FWD were used for testing in this project, the KUAB 120 SP1G and the Dynatest 8000 FWD, both shown in Figure 9. The latter was used on the tests conducted on November 2006, March 2007 and August 2011. Both the KUAB model and Dynatest 8000 model have a load range of 7 kN (1.57 kip) to 120kN (27 kip), but the KUAB model includes a segmented load plate to ensure a "uniform pressure distribution over the full area of the plate" [Alavi et al., 2008; ERI Inc., 2003]. The loading sequence consisted of a setting drop and three additional drops from three different heights, and sometimes the sequence included two or three drops from the same height, in which case, only the last drop of each height was considered. The seismometers have a range of 0 to 5.08 mm (0 to 200 mils) and its typical arrangement is depicted in Figure 10. FWD tests conducted were used to estimate load transfer efficiencies (LTE), joint ratio support (JSR), mid-slab spreadability (SPR), and normalized deflections at the load plate location (NDf_0) along the three sections. Averages of these parameters were calculated for each section and season, and results are discussed in the next chapter.

Figure 9. Falling Weight Deflectometer Systems used by NYSDOT: a) KUAB 120 SP1G; b) Dynatest Model 8000.

The load transfer efficiency is defined to be 100% if, when the wheel is approaching the joint or leaving the joint, the loaded slab deflects the same amount as the unloaded slab. Conversely, the LTE is 0% when loaded one of the slabs the deflection of the unloaded slab across the joint is zero. Thus, LTE indicates the pavement's ability on transferring loads across the joints. Values of load transfer efficiency vary depending on the support material, pavement temperatures, aggregate interlock at the joints as well as whether the joints are provided with or without dowel bars [Sargand, Edwards & Kim, 2002]. Figure 11 illustrates the concept for a 0% LTE (a) and 100% LTE (b). Load transfer efficiency can be estimated using the deflections measured from the FWD test. When testing is performed at the joints, the LTE can be calculated using Equations (1) and (2).

$$LTE_a = 100\left(\frac{Df_2}{Df_0}\right) \tag{1}$$

$$LTE_l = 100\left(\frac{Df_1}{Df_0}\right) \tag{2}$$

where Df_0, Df_1 and Df_2 are the measured deflection of sensor 0, 1 and 2 respectively; and the subindexes a and l refers to the position of the load plate (i.e. where the drop takes place) as shown in Figure 10.

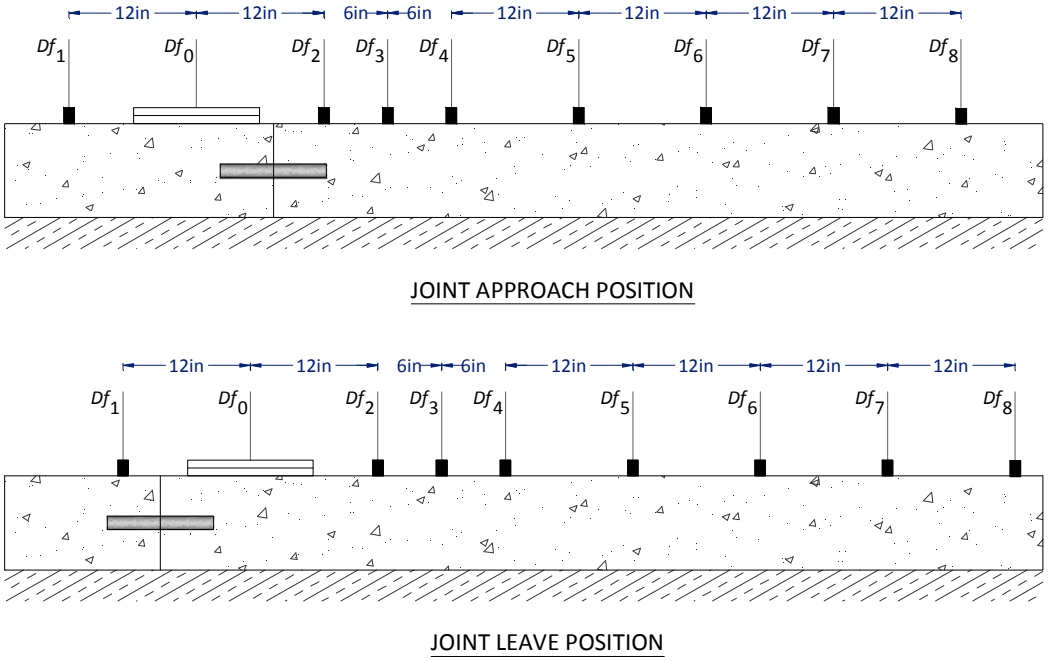

Figure 10. Seismometer arrangement in the FWD system and LTE positions (6 in = 15.24 cm, 12 in = 30.48 cm).

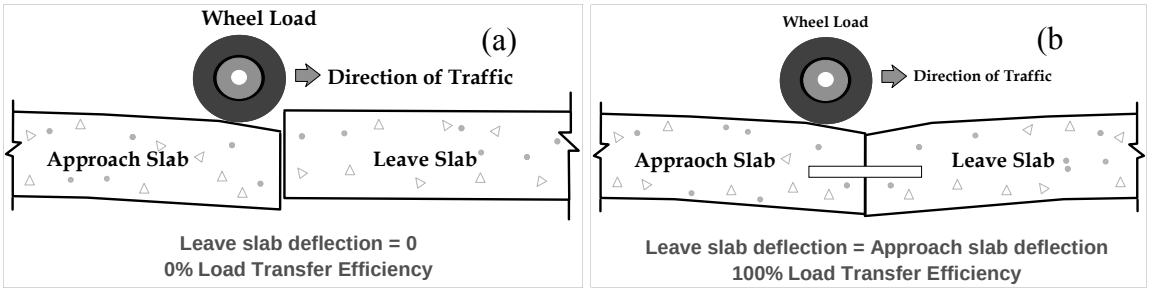

Figure 11. Load Transfer Efficiency concept: a) 0% LTE; b) 100% LTE; Adapted from ERES Consultants Inc. [2002].

The joint support ratio is the ratio between the deflection Df_0 in the leaving position and at the approaching position. This parameter gives an indication of the support condition at each side of the joint, and it can be used to identify voids beneath the slabs at the joint location. For equal support conditions under the slabs at both sides of the joint, the JSR value should be 1.0, and it varies as the conditions become different from one side of the joint to the other [Sargand et al., 2002]. The JSR can be calculated using Equation (3).

$$JSR = \frac{Df_{0-l}}{Df_{0-a}} \tag{3}$$

where the subindexes a and l have the same meaning than in Equations (1) and (2).

Spreadability (SPR) is the average of the deflections measured by all the seismometers normalized to the deflection measured by the seismometer zero. Spreadability is a function of the elastic modulus of the different layers in the structure pavement, geometry of the loaded area, and the arrangement and number of seismometers [Sargand et al., 2002]. SPR values are

indicators of the deflection basin's geometry and bending stiffness of the pavement structure. Spreadability can be calculated as follows,

$$SPR = \frac{\sum_{i=0}^{8} Df_i}{9Df_0} \tag{4}$$

where the average is taken over 9 sensors, which is the number of seismometers of the KUAB and Dynatest FWD models used in this project. Equation (4) should be modified in the case of sensors showing erratic or missing (zero) readings, so that the average includes only the readings from working sensors. However, equal distributions of seismometers and geometry are necessary to obtain valid comparisons [Sargand et al., 2002]. For this reason, the readings where one of the sensors showed erratic or not reading where not included in calculating spreadability.

Deflections measured from the FWD test vary depending on the magnitude of the applied load, geometry of the slab, its flexural stiffness, support conditions and other properties of the pavement structure [Sargand et al., 2002]. Therefore, attempts to compare directly results from the FWD test between the three experimental sections (i.e. comparisons of measured deflections and deflection profiles, deflections basin, etc.) are inappropriate. In order to properly compare results, the deflections are normalized to the load causing them. Thus, for the deflection measured from seismometer zero the normalized deflection is given by

$$NDf_0 = \frac{Df_0}{P} \tag{5}$$

where P is the applied load. Notice that Equations (1), (2) and (4) produce identical results regardless whether normalized deflections or the actual deflections are used.

4.3 Data Types and Reduction

In order to assess the performance of the three experimental sections, data of the response due to environmental effects and the falling weight deflectometer (FWD) test has been collected since the construction day for each of the sections described above. The data recorded were classified as environmental data and dynamic data for those due to changes of temperature and/or moisture (and the related strains and stresses) and those due to the FWD test respectively. MS-Excel worksheets were created to process the raw data and calculate strains and stresses, which were plotted to identify trends. Summary tables for both environmental data and dynamic data were built. In the following sections are briefly described the procedures necessary to reduce and process the different type of data recorded.

4.3.1 Environmental Data

Environmental data comprise pavement temperatures profiles, strains and deflections caused by daily changes in temperature within the pavement as well as air temperature, wind speed, relative humidity, solar radiation and precipitation in the location of the three experimental sections. The analysis presented in this report is limited only to the study of trends and interaction observed for the pavement temperatures, strains and stresses undergone by the slabs from June 6, 2006 to May 11, 2009. The temperatures within the pavement are obtained from the vibrating wire strain gauges and the thermocouple probes from where temperature gradients were

calculated as described below. The strains and stresses are calculated from the output readings of the vibrating wire strain gauges as described below.

4.3.1.1 Pavement Temperatures & Temperature Gradients

Profiles of the temperature distribution through the thickness of the slabs were recorded using the CR7 data acquisition system from Campbell Scientific for each experimental section. The CR7 installed are provided with a resistant temperature detector (RTD) necessary for thermocouple measurements in degrees Celsius (°C). Each system includes only 14 channels for temperature readings with a range of -40°C (-40°F) to 60°C (140°F) and an accuracy of ±0.1°C (±0.18°F) (Campbell Scientific Inc., 1997, p. OV-2). Therefore, only temperatures for the ***p*** and ***q*** locations at 20 mm (0.79 in), 75 mm (2.95 in), 130 mm (5.12 in), and 185 mm (7.28 in) measured from the bottom surface of the slab were recorded from each section. The CR7s were programmed to record temperatures every 30 minutes during the first two days after casting the concrete and every hour for the subsequent days until May 11, 2009. Additionally to the temperatures recorded from the thermocouple probes, temperatures at the locations of each vibrating wire strain gauge were also collected. These correspond to the temperatures at 37.675 mm (1.48 in) from the top surface of the concrete slab and 31.75 mm (1.25 in) from the bottom surface of the concrete slab (see Figure 6). The VW gauge's outputs were recorded using a CR10X from Campbell Scientific every 15 minutes for the first two days following the construction and every hour for the subsequent days for each section until May 11, 2009.

Temperature data from the temperature probes and VW gauges was available in regular basis for different periods between June 6, 2006 and May 11, 2009. Absence of data during some periods was caused by insufficient electrical power or lack of enough memory to store data. The batteries that provide the input voltage to the sensors and keep the data acquisition systems running are charged through solar panels and they deplete proportionally to the sunlight received. Additionally, once all the memory available for data storage is used, the CR7 and CR10X systems will overwrite memory to store succeeding data. Therefore, periods with no data are mainly a consequence of not enough sun exposure in order to keep the power requirements or overwriting of the data because the system's memory was full.

In November of 2009, a vehicle destroyed the cabinet housing the data acquisition system for Section 3 (Untreated section), the data acquisition systems and the data stored since May 2009 were lost. The damaged cabinet and data acquisition systems were not replaced by the NYSDOT and therefore data collection from this section stopped at that time. Data were collected afterwards from the other two sections, but since the data from the control section were not available for comparison, the data analysis stopped with May 2009. The additional data from the other two sections will be made available.

Equivalent Temperature Gradients (ETG) and Linear Temperature Gradients (LTG) were calculated using the temperatures recorded from the thermocouples probes and VW gauges respectively for different periods between June 6, 2009 and May 11, 2009. The equivalent temperature gradient was calculated following a similar procedure to the one proposed by Janssen & Snyder [2000]. Their procedure uses the Temperature-Moment concept discussed before by Timoshenko & Lessells [1925] and other authors. The temperature-moment is defined as the moment produced by the temperature gradient, and "is itself a quantification of the temperature gradient" [Janssen & Snyder, 2000]. In determining the ETG, interpolating cubic splines are used to approach the temperature distribution through the depth. The procedure uses the four temperatures T_{20}, T_{75}, T_{130} and T_{185} measured at 20 mm (0.79 in), 75 mm (2.95 in),

130 mm (5.12 in), and 185 mm (7.28 in) from the bottom surface of the slab respectively to determine four cubic polynomials of the shape

$$s_k(x) = a_k(x - x_k)^3 + b_k(x - x_k)^2 + c_k(x - x_k) + d_k \tag{6}$$

where the index $k = 1,2,3,4$ indicates each of the intervals shown in Figure 12. In order to determine the coefficients for each polynomial, the temperature at the top and bottom surface of the slab need to be extrapolated. In addition, in order to determine completely the 16 unknown coefficients and temperatures at the top and bottom surfaces the following boundary conditions are necessary:

- Linear variation of the temperature between the bottom surface and the temperature T_{20}; thus, $s_1'(0) = s_1'(20)$ and $s_1''(0) = 0$.
- Linear variation of the temperature between the top surface and the temperature T_{185}; thus, $s_5'(185) = s_5'(225)$ and $s_5''(225) = 0$.

From the above conditions and the inherent compatibility conditions imposed by the cubic splines, the 16 unknown coefficients as well as the top and bottom temperature can be expressed in a closed form as follows:

$$a_1 = a_5 = 0,\ b_1 = b_2 = b_5 = 0 \tag{a}$$
$$d_1 = T_0,\ d_2 = T_{20},\ d_3 = T_{75},\ d_4 = T_{130},\ d_5 = T_{185} \tag{b}$$
$$a_2 = \frac{1}{2495625}(-T_{185} + 6T_{130} - 9T_{75} + 4T_{20}) \tag{c}$$
$$a_3 = \frac{1}{499125}(T_{185} - 3T_{130} + 3T_{75} - T_{20}) \tag{d}$$
$$a_4 = \frac{1}{2495625}(-4T_{185} + 9T_{130} - 6T_{75} + T_{20}) \tag{e}$$
$$b_3 = \frac{1}{15125}(-T_{185} + 6T_{130} - 9T_{75} + 4T_{20}) \tag{f}$$
$$b_4 = \frac{1}{15125}(4T_{185} - 9T_{130} + 6T_{75} - T_{20}) \tag{g}$$
$$c_1 = c_2 = \frac{1}{825}(T_{185} - 6T_{130} + 24T_{75} - 19T_{20}) \tag{h}$$
$$c_3 = \frac{1}{825}(-2T_{185} + 12T_{130} - 3T_{75} - 7T_{20}) \tag{i}$$
$$c_4 = \frac{1}{825}(7T_{185} + 3T_{130} - 12T_{75} + 2T_{20}) \tag{j}$$
$$c_5 = \frac{1}{825}(19T_{185} - 24T_{130} + 6T_{75} - T_{20}) \tag{k}$$
$$T_0 = \frac{1}{165}(-4T_{185} + 24T_{130} - 96T_{75} + 241T_{20}) \tag{l}$$
$$T_{225} = \frac{8}{165}(19T_{185} - 24T_{130} + 6T_{75} - T_{20}) \tag{m}$$

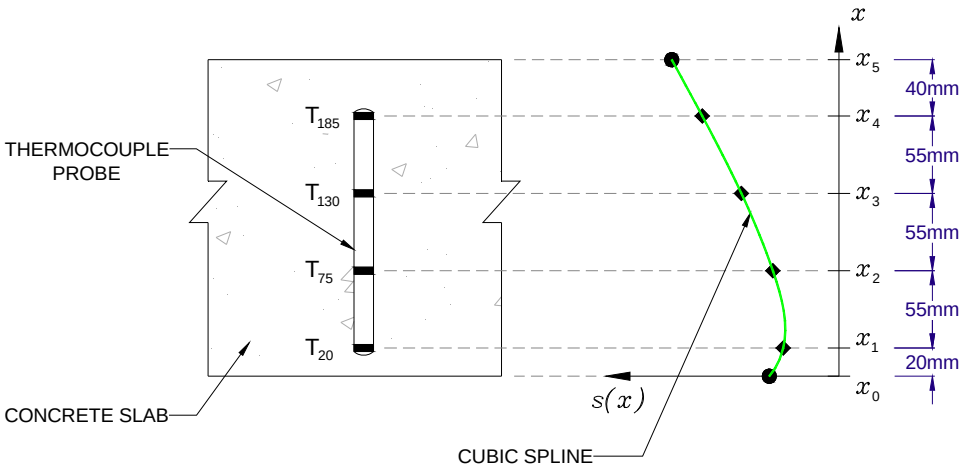

Figure 12. Cubic Approximation for the Nonlinear Gradient of Temperature (25.4 mm = 1 in).

The following step described by Janssen & Snyder [2000] calls for the calculation of the average temperature across the thickness of the slab, which is calculated as the average of the interpolating spline function through the depth of the slab. Thus,

$$T_{ave.} = \frac{1}{225}\sum_{k=1}^{5}\left(\int_{x_{k-1}}^{x_k} s_k(x)dx\right) \tag{7}$$

where the values of x_k are given by Figure 12. This average temperature is subtracted then from each of the measured temperatures to obtain the relative-to-average temperature differences $\bar{T}_{20}$, $\bar{T}_{75}$, $\bar{T}_{130}$, and $\bar{T}_{185}$. The procedure continues by substituting the latest values into Equations a to m and calculating the cubic splines $\bar{s}_k(x)$ for the relative-to-average difference of temperature profile. Once constructed this second set of splines, the equivalent temperature gradient can be calculated as follows:

$$ETG = \frac{12}{h^3}\cdot\sum_{k=1}^{5}\left(\int_{x_{k-1}}^{x_k} x\cdot\bar{s}_k(x)dx\right) \tag{8}$$

Carrying out the integration in Equation (8) using the values of x_k in Figure 12 leads to the following closed-form equation for ETG (in °C/cm):

$$ETG = \frac{3}{110h^3}(69809T_{185} + 15636T_{130} + 22551T_{75} + 3379T_{20}) \tag{9}$$

where h in (8) is the thickness of the concrete slab (22.5cm or 8.86 in).

The linear temperature gradients at the location of each VW gauge were calculated as the arithmetic difference of the top and bottom temperatures divided the distance between the two sensors. Thus,

$$LTG = \frac{T_{top} - T_{bottom}}{d} \tag{10}$$

with T_{top} and T_{bottom} the top and bottom temperatures respectively and d the distance between

sensors from Figure 6 which is equal to 155.575mm (6.125in). The linear temperature gradient at each of the sections was plotted for all the periods of available data. These plots were used later to identify typical periods of time for every season as well as common periods were data was available for each of the experimental sections. The comparisons of the LTG and ETG values for each section are discussed in Section 5.3.

4.3.1.2 Long-Term Strains and Stresses

Strains caused by the daily changes in temperature through the thickness of the slabs were recorded along with the temperatures using the CR10X Campbell System as mentioned above. The VW gauge's output related to strains within the concrete is given by the system in units of frequency-square (kHz^2). These frequencies were converted to strains using the following equation [Geokon Inc., 2005, p. 11]:

$$\Delta\varepsilon = 0.96 * 3304(R - R_0) + (T - T_0)(\alpha_w - \alpha_c) \tag{11}$$

where,

$\Delta\varepsilon =$ The change of strains in micro-strains (με)

$R_0,\ R =$ The initial frequency-square reading and the frequency-square reading at any time respectively (kHz^2)

$T_0,\ T =$ The initial temperature reading and the temperature at any time respectively (°C)

$\alpha_w, \alpha_c =$ Coefficient of thermal expansion of the steel and concrete respectively (με/°C)

Common values reported in the literature were assumed for $\alpha_w = 12.2$ με/°C (6.8 με/°F) and $\alpha_c = 10.4$ με/°C (5.8 με/°F). The strains calculated using Equation (11) are the load related strains or the strains that produces stresses within the concrete. These stresses are caused by the restrictions to expansion given by the joints and subgrade to the slab. Notice that the actual strains in the concrete are given by [Geokon Inc., 2005 p. 11]

$$\Delta\varepsilon_{total} = 0.96 * 3304(R - R_0) + \alpha_w(T - T_0) \tag{12}$$

For a complete explanation of the theory of the vibrating wire technology and deduction of Equation (11) refer to "*Strain Gauge Technology"* p. 325 [Hornby, 1992] or the Instruction Manual for the Geokon VW Model 4200 p. 15 [Geokon Inc., 2005]. The stresses in the pavement due to the environmental effects can be obtained through Equation (11) as follows,

$$\Delta\sigma = E \cdot \Delta\varepsilon \tag{13}$$

where $E = 23.235$ GPa (3370 ksi) is the elastic modulus of the concrete (see Chapter 5.1).

Total strains were calculated using carefully selected values for R_0 and T_0 in Equation (12). Readings were recorded for each section starting some time before the concrete was casted. These readings, at first showed an unstable behavior during the pouring process and stabilized sometime after the sensors were covered by concrete and the surface of the slabs were finalized. The zero-values for R_0 and T_0 chosen correspond then to the time when the readings for each sensor started to show a stable trend. The zero-times for each section were June 6, 2006 at 12:20 for the broken and seated section; June 8, 2006 at 14:20 for the rubblized section; and June 8, 2006 at 18:35 for the untreated section. The total strain plots are provided in an Appendix for further review. In addition to the total strains, the change in strain and stresses were calculated

for each section during selected periods of time. In order to calculate these, the values of R_0 and T_0 were selected for the time when the LTG value from Equation (10) was the closest to zero. Choosing the initial temperature and frequency reading corresponding to almost zero values of LTG minimize the effect on the trends due to accumulative strains such as those caused by shrinkage and creeping of concrete, which are not included in the analysis discussed in Chapter 5.

4.3.1.3 Long-Term Displacements

Displacements of each LVDT at the locations shown in Figure 2 were recorded starting June 6, 2006 for the B&S section and June 8, 2006 for the rubblized and untreated sections. The LVDT displacements of each instrumented slab were recorded using the CR7 Campbell System described before until the LVDTs were removed in 2007. An analysis of the displacements for the period between June 6, 2006 and December 6, 2006 was performed by Ambrosino [2007]). In these, a discussion of the initial curling of the slabs is presented.

4.3.2 Dynamic Data

Dynamic data recorded comprise pavement deflections and strains from the falling weight deflectometer (FWD) test. Strain and displacement responses from all the LVDT's and MM strain gauges were recorded as well as the deflection and applied force from the FWD. Dynamic data is used to evaluate the short-term response of the slab. During testing, each location was impacted with three different loads of nominal values of 40 kN, 53 kN, and 71 kN (9 kip, 12 kip, and 16 kip), and the responses were recorded for each of the MM gauges and LVDTs. Peak values were then obtained and used to calculate normalized deflections, normalized strains and to estimate the amount the neutral axis shifted in the slabs. Normalized deflections are calculated taking the peak of the displacement responses measured from each LVDT and dividing them by the load applied by the FWD. Likewise, the normalized strains are calculated by taking the peak of the strain responses and dividing them by the corresponding applied load. Finally, the amount the neutral axis shifted is estimated using the peak of the strain responses for each pair MM strain gauge as follows,

$$\delta_{NA} = \frac{h}{2} - \left[s + \left(\frac{\varepsilon_{Bottom}}{\varepsilon_{Bottom} - \varepsilon_{Top}} \right) d \right] \tag{14}$$

where $h = 225$mm (8.86in), $s = 25.4$ mm (1 in) and $d = 166.7$mm (6.5625in) are thickness of the slab and the distances (see Figure 8) from the bottom surface to the bottom strain gauge and the distance between the top and bottom gauges respectively. The following chapter discusses the results on the short and long-term performance of the three experimental sections.

5 Results and Discussion

This chapter presents the results from the laboratory tests for the concrete, followed by the results and discussion on the environmental response and dynamic response of each of the three experimental sections. Laboratory testing activities included the compressive strength, maturity test and flexural strength. Ambrosino [2007] discussed the results from these tests, and they are summarized here for convenience. Subsequently the environmental response of the three experimental sections is presented and discussed. The discussion includes pavement temperatures and gradients, curing strains, and the long-term strain/stress responses. To conclude this chapter, the dynamic response of each section is presented and discussed. This discussion includes short-term strain and stress responses of the sensors and deflections measured by the FWD seismometers.

5.1 Compressive & Flexural Strength Results

SJB Services Inc. of Hamburg carried out the compressive strength (f_c') and flexural strength (f_r) testing of field-cured concrete cylinders and beams. Figure 13(a) shows the results of the compressive strength for all the cylinders tested. The f_c' after 28 days averaged 30.50MPa (4.42ksi) and after 90 days the average increased to 32.98MPa (4.78ksi). These values are visibly higher than the design value of 27.58MPa (4.0ksi). Ambrosino [2007] reported values of compressive strength, elastic modulus and Poisson ratio for three cylinders tested at Ohio University after 30 days of pouring. The values for each of the mentioned properties are summarized in Table 2. Observe that the value of the compressive strength obtained by SJB Services is slightly higher than the value obtained at Ohio University.

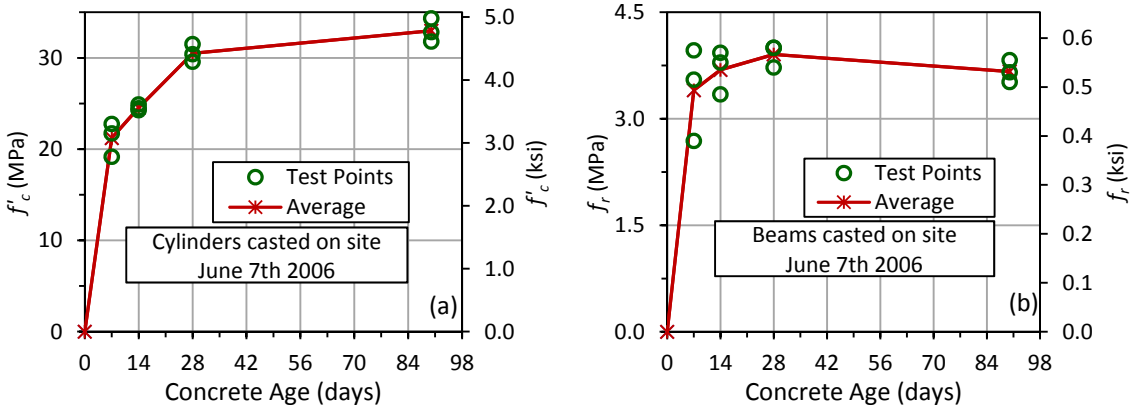

Figure 13. I86 PCC Material Strength: (a) Compressive Strength, (b) Flexural Strength. Adapted from Ambrosino [2007].

The flexural strength values obtained by SJB Services, Inc. are shown in Figure 13(b). The average modulus of rupture reached its maximum at 28 days with a value of 3.91MPa (567psi) and decreased for the test at 90 days. Ambrosino [2007] suggested that the decrement could be the result of inappropriate consolidation of the specimens and suggested as well that a reason for

this could have been that the better-compacted specimens were tested in the first place. Using the measured average compressive strength at 28 days and the expression proposed by ACI 325.12R (2002), $f_r = 0.0135[w\, f_c']^{0.5}$ (in MPa) to approximate the flexural strength gives f_r =3.59MPa (521 psi). This value is only 8.2% less than the average f_r obtained by SJB; therefore, the flexural strength values from testing meet the ACI 2002 specification.

Table 2. Mechanical properties of PCC overlay material on I86.

Property		Value	Measured by
Compressive Strength (28-days)	f_c'	30.50MPa (4.42ksi)	SJB Services, Inc.
		27.94MPa (4.05ksi)	Ohio University
Modulus of Rupture	f_r	3.91MPa (0.567ksi)	SJB Services, Inc.
Elastic Modulus	E	23235.33MPa (3370ksi)	Ohio University
Poisson Ratio	μ	0.181	Ohio University
Unit Weight	w	2315kg/m^3 (144.5lb/ft^3)	Ohio University

5.2 Pavement Response due to Environmental Effects

Section 4.3.1 discussed what variables comprised the environmental data analyzed herein. The following sections present and discuss the response of each of these variables for each experimental section. It starts presenting an analysis of the curing strain and curing temperatures within the pavement and a comparison of the responses between the three sections. Subsequently, the discussion focuses on the long-term strain and stresses as well as temperature gradient variations during the period between June 6, 2006 and May 11, 2009. In this, strain and stress variations with the seasons as well as those variations with the location of the sensor are studied. Additionally, comparisons between the experimental sections are made and discussed.

5.3 Early-Age Pavement Behavior

Defined as the behavior during the first 72 hours after the pavement has been placed, the early-age behavior of the concrete pavements is affected by several factors. Among these are included the climatic conditions at pouring times (i.e. air temperature, wind speed, relative humidity, etc.), temperature of concrete and base at placement, thermal coefficient of the concrete, heat of hydration of the cement paste, shrinkage, creep, restraint in the slab-base interface, lateral restrictions, and others [Ruiz, Rasmussen, Chang, Dick, and Nelson, 2005]. Except for two, all the aforementioned factors affecting the early-age behavior of the concrete pavement are temperature related. The climatic conditions, heat of hydration and the temperature of the base during placement determine the variation of temperatures in the concrete pavement; they change as heat transfers in or out through the surfaces of the slab.

Temperatures within the pavement exhibit oscillate with a period of 24 hours. During a typical day, the temperatures through the pavement rise to a maximum in the early afternoon and then decrease to a minimum in the early morning of next day. Additionally, during a typical day, the temperatures will vary also as a function of depth with maximum and minimum values

occurring generally either at the top surface or at the bottom surface of the slab. In general, the temperature at the top surface will be higher than at the bottom from late morning hours to mid afternoon or evening where the temperature profile reverses, with higher temperatures at the bottom than at the top.

The aforementioned behavior can be observed in Figure 14 for the rubblized section. This figure shows the temperatures on the pavement in location $\boldsymbol{p}$ at 20 mm (0.79 in), 75 mm (2.95 in), 130 mm (5.12 in), and 185 mm (7.28 in) (designated T_{20}, T_{75}, T_{130}, and T_{185} respectively) from the bottom surface of the slab as well as the average hourly air temperature and the solar radiation. In this figure the temperatures in the concrete rise during the first six hours due to the heat of hydration reaching temperatures between 32°C and 36°C (~90°F to 97°F). Temperatures then drop to minimum values between 22°C and 26°C (~72°F to 79°F) for the following 12 or 13 hours. It can be seen that during this first period of 18 to 20 hours the temperature at the bottom, T_{20} is consistently higher than the temperatures at other points closer to the top surface of the slab. Heat from hydration will dissipate faster through the top surface because it is in contact with the surrounding air, which is at a lower temperature than the concrete. Therefore, concrete close to the top surface will experience lower temperatures than at the bottom during the initial 18 to 20 hours after placed. After the first 20 hours, the heat of hydration has dissipated and solar radiation has a greater effect on the temperatures at the top of the slab. This increment leads to a reversed condition where the higher temperatures are now present at the top. In general, high temperatures at the top will be associated with periods of more solar radiation and high values of air temperature. After the first 24 hours, the daily solar cycle will drive changes in the temperature gradients in the slab.

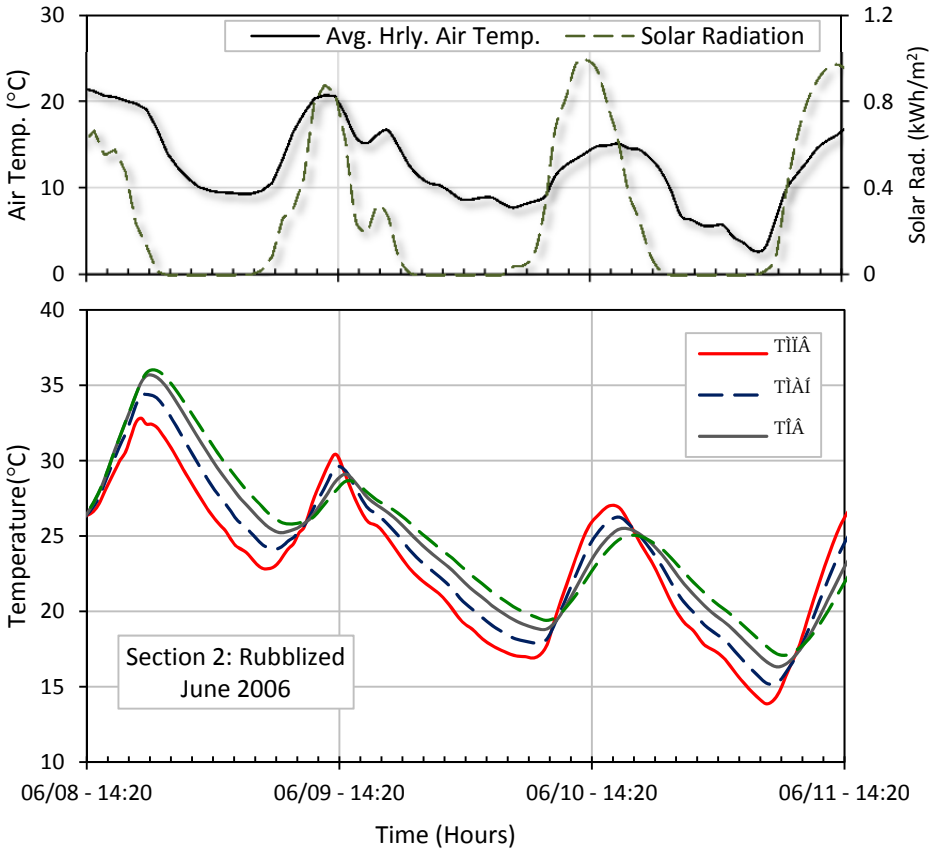

Figure 14. Early-age pavement temperatures in the rubblized section.

The B&S and untreated sections exhibit a similar behavior to the behavior described above for the rubblized section as can be seen in Figure 15 for the B&S section and in Figure 16 for the untreated section. For the B&S section the first five hours of data were not recorded, but notice that the of maximum temperatures in the first six hours for the B&S section are at least between 35°C and 39°C (~95°F to 102°F). This range is higher than the corresponding range experimented by the untreated and rubblized sections being the untreated section the one presenting the lowest range of maximum curing temperatures. Table 3 summarizes these ranges together with the corresponding air temperature.

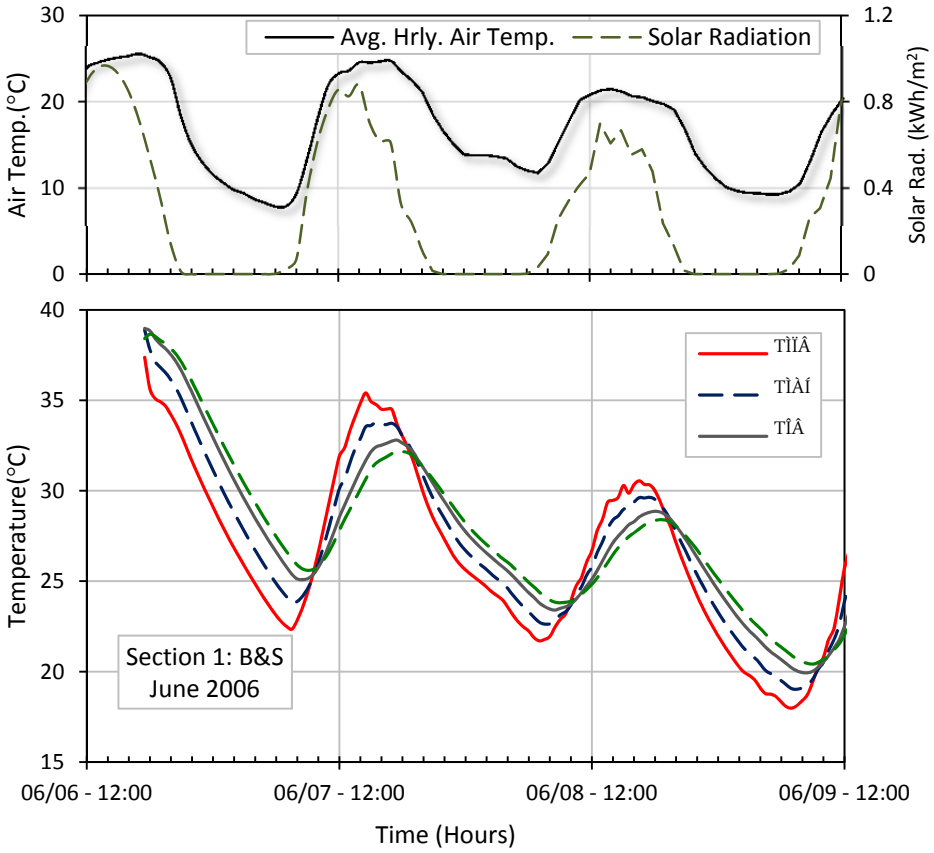

Figure 15. Early-age pavement temperatures in the break and seat section.

Although the value of temperatures that concrete can reach while curing are important, the magnitude of these is less important after the first 18 to 20 hours. Instead, the difference of temperature between the top and bottom of the slab becomes more important since this produces strains of opposite signs [ERES Consultants Inc., 2002; Huang, 2004]. These strains of opposite signs create bending stresses, which combined with the low strength of the concrete at early ages, can lead to cracking of the slab. However, it seems the difference of the top and bottom temperature is the less appropriate parameter since it does not account for either the thickness or the nonlinear variation of the temperatures from top to bottom of the concrete slab. Figure 17 shows temperature profiles for the rubblized section at different times within the first 72 hours after the concrete was placed. Notice that the horizontal axis shows the difference of temperature between each measured temperature minus the temperature measured at the bottom. Additionally, it can be seen that the variation of temperature through the thickness is approximately linear between the first 6 and 18 to 20 hours with T_{20} consistently higher than the other measured temperatures as mentioned before. The temperature profiles are non-linear approximately between zero and six hours after the time of placing. The existence of non-linear temperature profiles during the first six hours obey to the rising temperatures due to the heat of hydration, which as mentioned before, dissipates faster through the top surface of the slab. Similar temperature profiles can be plotted for the B&S and untreated sections, but they present analogous behavior to that evident from Figure 14, Figure 15, and Figure 16; therefore they are not shown here.

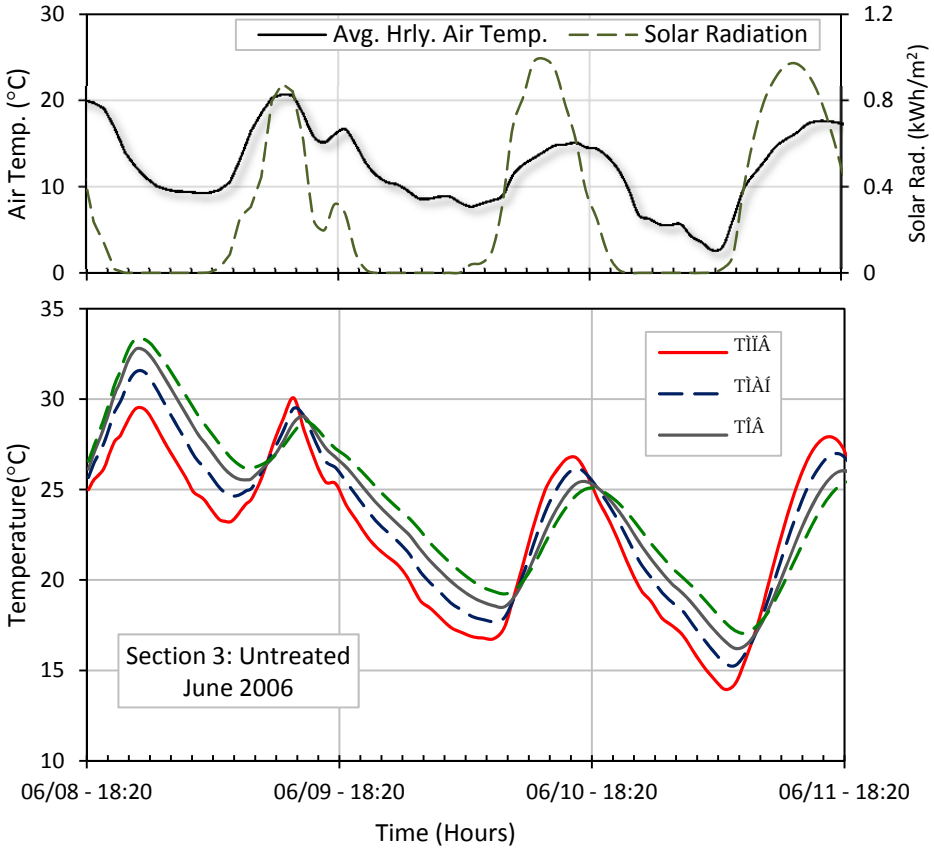

Figure 16. Early-age pavement temperatures in the untreated section.

Table 3. Maximum curing temperatures during the first 24 hours for each section.

Section	Max. Curing Temp. (°C)				Avg. Air Temp. (°C)	Time Range of Maximum
	T_{185}	T_{130}	T_{70}	T_{20}		
Section 1: **B&S**	35.6	37.8	38.9	38.7	25.2	18:00
Section 2: **Rubblized**	32.8	34.4	35.7	36.0	19.5	19:30 – 20:30
Section 3: **Untreated**	29.5	31.6	32.8	33.4	11.8	23:30

Section	Max. Curing Temp. (°F)				Avg. Air Temp. (°F)	Time Range of Maximum
	T_{185}	T_{130}	T_{70}	T_{20}		
Section 1: **B&S**	96.1	100.0	102.0	101.7	77.4	18:00
Section 2: **Rubblized**	91.0	93.9	96.3	96.8	67.1	19:30 – 20:30
Section 3: **Untreated**	85.1	88.9	91.0	92.1	53.2	23:30

In order to account for the nonlinearity of the temperature profiles and the thickness of the slab, temperature gradients could be calculated using either Equation (9) or Equation (10). The first of these accounts for a nonlinear variation of the temperatures by approximating them with cubic splines as described in Section 4.3.1.1. Conversely, Equation (10) only accounts for the

thickness of the slab and assumes a linear variation of the temperatures between the top and bottom surfaces of the slab. Figure 18 shows the equivalent temperature gradient (ETG) for each of the three experimental sections during the first 72 hours. Observe that the values of ETG during the first 20 hours are negative for each of the sections. This agrees with the behavior of temperatures discussed before and the values shown in Figure 14, Figure 15, and Figure 16. Also, notice that after the first 20 hours the gradients of temperature vary periodically with a period of 24 hours as mentioned above.

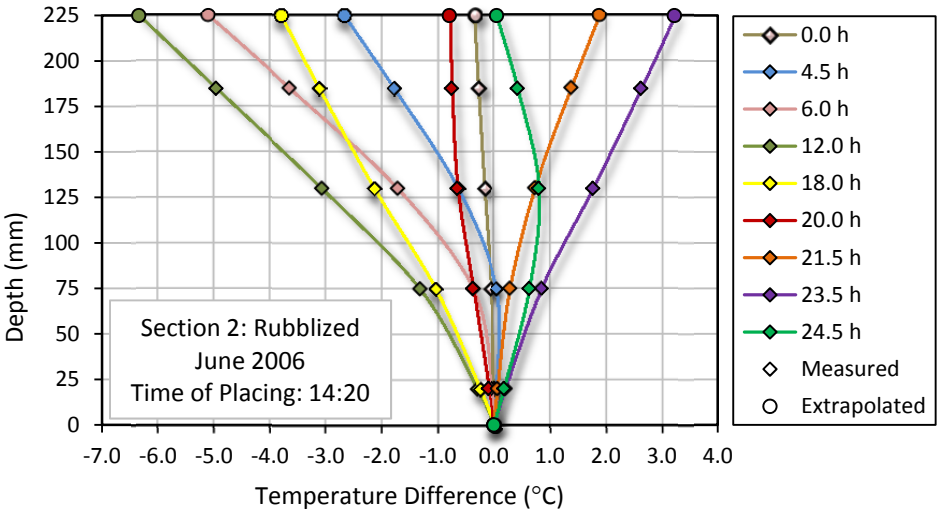

Figure 17. Temperature profiles within the first 24 hours for the rubblized section (25.4 mm = 1 in, 1.8 C° = 1.8°F).

In addition, in Figure 18, it can be seen how the values of ETG for each of the sections are almost equal and show the same trend. Maximum positive ETG values occur in afternoon hours around 14:20 and maximum negative ETG values occur during night hours around 2:20 in the morning. In the following sections, the relationship between strains, stresses and temperature gradients is discussed.

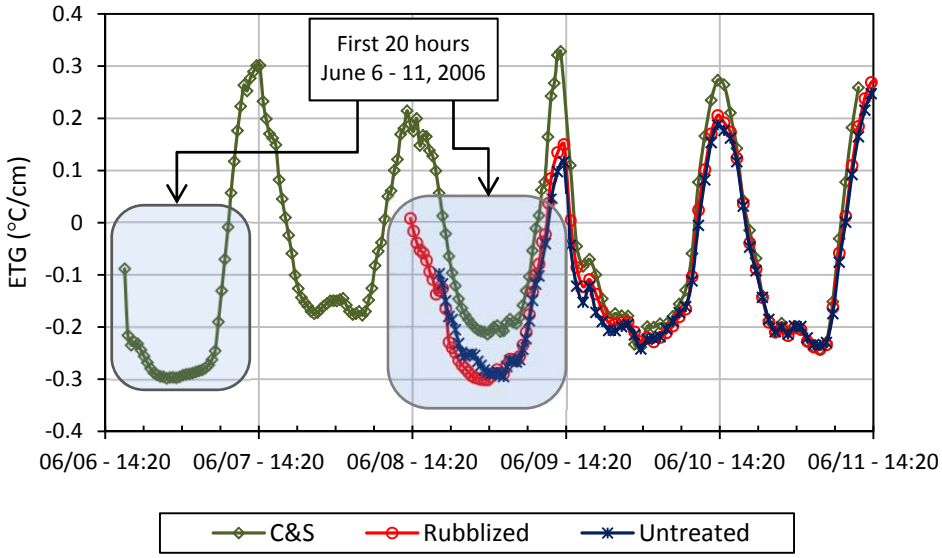

Figure 18. Equivalent temperature gradient during the first 72 hours for each section (1 C°/cm = 4.6 °F/in).

The early-age strains and stresses in the pavement develop as the result of many factors such as expansion or contraction of the slab, shrinkage, creep, curling and warping of the slabs. After it sets, the concrete expands due to the heat of hydration, and as strength increases, compressive stresses develop due to the restraints imposed at the slab-base interface. Once concrete reaches the maximum temperature, the concrete starts cooling; contraction starts and tensile stresses may appear [Ruiz et al., 2005]. Another factor associated with the early stress development is the non-constant variation of temperatures through the thickness of the slab, which induces curling strains. Stresses due to curling are consequence of the slab's self-weight and the restraints at the slab-base interface counteracting the effects of curled shape. If the temperature on the top of the slab is lower than the temperature at the bottom, the slab will curl up and tensile and compressive stresses occur at the top and bottom surface, respectively, as drawn in Figure 19(a). However, in the reversed case when the temperature on the top surface is higher than the temperature at bottom of the slab, this will curl down inducing tensile and compressive stresses at the bottom and top surfaces, respectively, as shown in Figure 19(b) [ERES Consultants Inc., 2002; Ruiz et al., 2005].

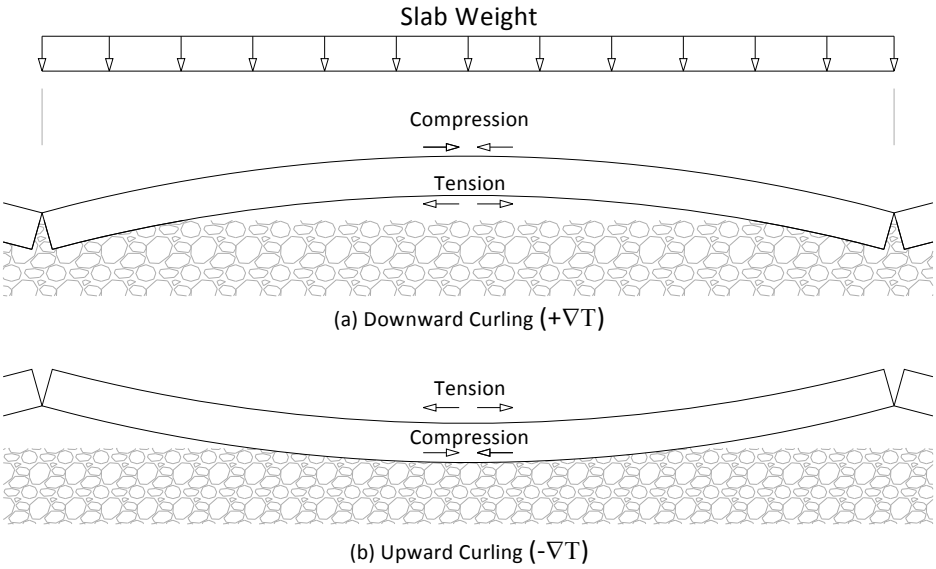

Figure 19. Slab curling caused by temperature gradients.

Similar to curling, warping strains will develop in the slab due to variations of moisture through the depth. If the top surface of the slab is wetter than the bottom surface, the result will be an upward curled slab. On the other hand, if the bottom surface of the slab is wetter, the result will be a downward curled slab like in the case of downward curling. Warping depends on the climate conditions especially rainfall and relative humidity. The stresses induced due to warping are similar to those induced by curling [Ruiz et al., 2005]. The analysis of the strains presented herein does not identify the individual effects of warping or curling, but the overall effect of both phenomena together.

5.3.1Early Age Strains

Early-age strains were recorded at the top and bottom of the slab in six different locations for each of the experimental sections as explained in Section 4.1. Figure 20 shows the total strains undergone by the rubblized section during the first 72 hours after placing the concrete. The figure shows the top and bottom strains corresponding to the mid-slab position along the right and left wheel path as well as the geometric center of the slab. It also shows the linear temperature gradient (LTG) calculated using Equation (10) as well as the equivalent temperature gradient (ETG) calculated using Equation (9). It can be seen that the total strains follow a similar trend of the pavement temperatures at top and bottom of the slab shown in Figure 14. During the first six hours, strains increase due to the heat of hydration and then decrease as this is dissipated. At the same time, the temperature gradient remains negative and after 18 to 20 hours reverses as explained above. After the first 20 hours, the total strain varies periodically exhibiting daily peaks coinciding with the maximum positive temperature gradient, and the minimum daily total strains correspond in general to the periods of maximum negative temperature gradients. However, the rate of variation of the strains is higher from a daily maximum strain to the next daily minimum value than from a minimum daily strain to the next maximum daily strain. Thus, reversal of the strains is faster when the gradient of temperature changes from negative to positive than in the opposite case. Notice that such behavior corresponds to the behavior of the

average air temperature and solar radiation shown in Figure 14. Hence, for a peak in the daily variation of the air temperature, a peak in the temperature gradients and total strains is expected.

The B&S and Untreated section exhibit similar behaviors to the one described for the Rubblized section as is shown in Figure 21 and Figure 22. Notice that the Rubblized section underwent higher strains followed by the B&S section and the untreated section, which experienced smaller strains. However, since the sections were built at different times, and at different air temperature, direct comparisons of the strains values are not suitable. The maximum positive and negative strains for each of the sections are listed in Table 4.

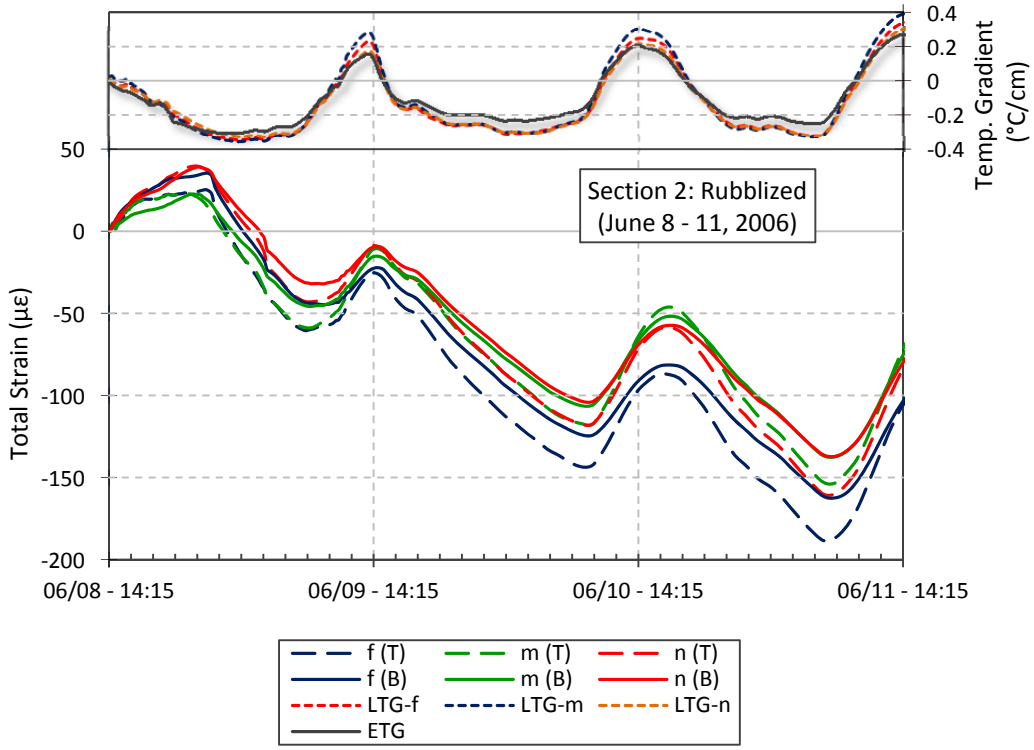

Figure 20. Early-age total strains in the rubblized section. (T: top gauge, B: bottom gauge) (1 C°/cm = 4.6 °F/in).

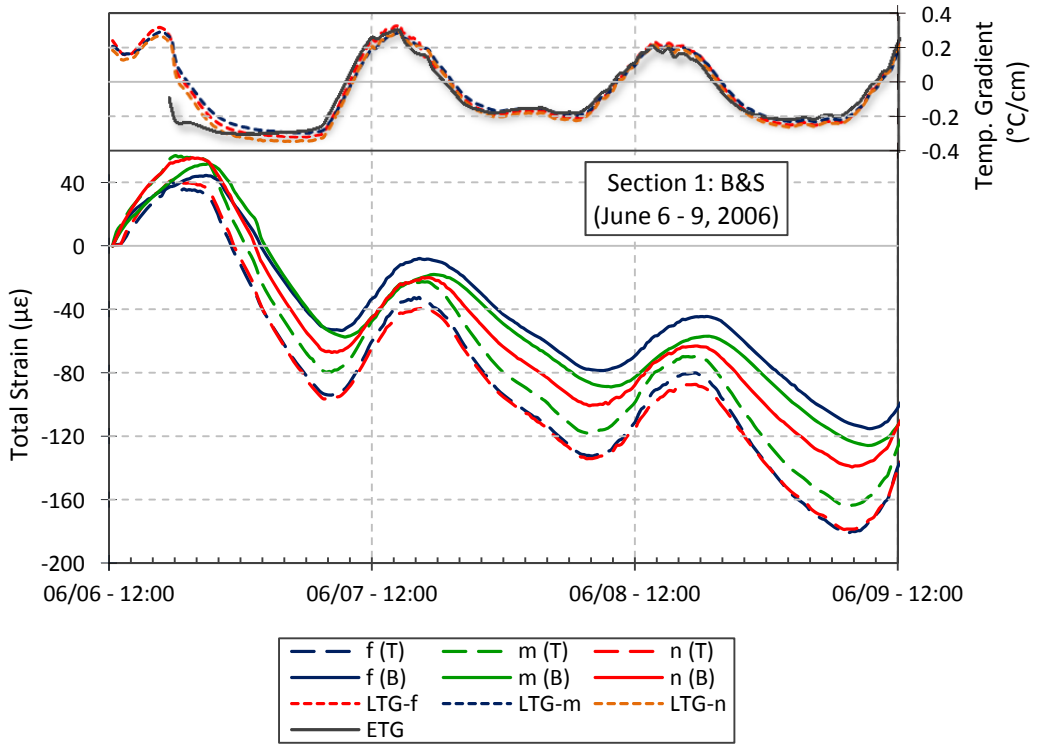

Figure 21. Early-age total strains in the B&S section. (T: top gauge, B: bottom gauge) (1 C°/cm = 4.6 °F/in).

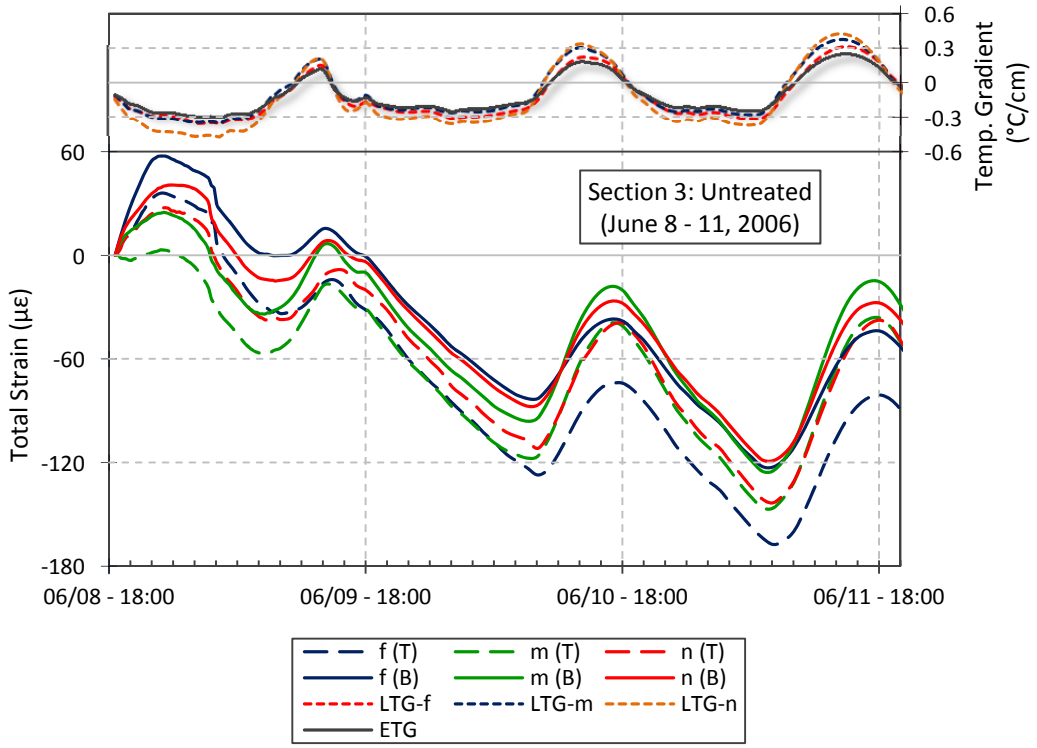

Figure 22. Early-age total strains in the untreated section. (T: top gauge, B: bottom gauge) (1 C°/cm = 4.6 °F/in).

Table 4. Maximum and minimum curing strains for each section.

Section	Max. Contracting Total Strain (με)	Max. Expanding Total Strain (με)
Section 1: **B&S**	-181.05	56.88
Section 2: **Rubblized**	-188.52	39.79
Section 3: **Untreated**	-167.51	57.44

It can be seen also in Figure 20, Figure 21, and Figure 22 that the calculated values of ETG are close to the calculated values of LTG. These values are very similar for the three sections with differences associated to the different separations of the vibrating wire gauges and thermocouples. The agreement between ETG and LTG shows that although the distribution of temperatures through the thickness of the slab is non-linear, the equivalent temperature gradient associated can be replaced by the difference of temperatures measured at the top and bottom normalized to the separation of the sensors.

The total strains discussed above represent the strains produced in the pavement due to expansion and contraction of the slab plus the strains induced by the imposed restraints. Of these, the only component of the strains that induces stress is the component accounting the strains due to the restraints such as adjacent slabs, self-weight and friction between the slab and the base [Huang, 2004; Ruiz et al., 2005]. These load-related strains are derived from the VW strain gauges output using Equation (11). Figure 23 shows the load-related strains during the first 72 hours for the rubblized section as well as the corresponding linear temperature gradients. In this, negative values correspond to strains inducing compression stresses and they are denoted as compressive strains. The opposite applies for positive values, which induces tensile stresses and they are denoted as tensile strains.

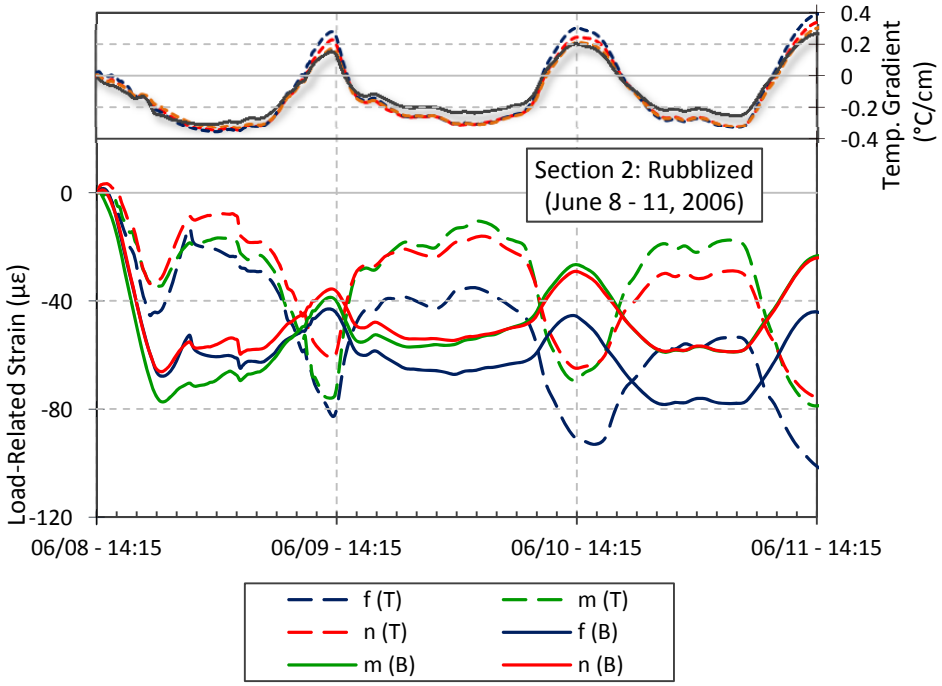

Figure 23. Early-age load-related strains in the rubblized section. (T: top gauge, B: bottom gauge) (1 C°/cm = 4.6 °F/in).

Load-related strains follow a similar trend to those discussed before for the pavement temperatures and total strains. During the first six hours, compressive strains develop as concrete expands due to the heat of hydration reaching a maximum value of about 77.4με in the bottom of the slab at the mid-slab position along the left wheel path. Similarly, a maximum value of 45.4με was reached at the top of the slab occurred along the right wheel path at the mid-slab position. After the first six hours, the compressive strains relax when the pavement temperatures start dropping, as seen in Figure 14. This coincides with the decreasing linear temperature gradient. When the LTG starts increasing, the compressive strains start decreasing at the bottom of the slab and those at the top increase reaching maximum values at the same time that the temperature gradient reaches a maximum positive value. It can be seen that the top strains and bottom strains switch as the LTG changes from positive to negative. Additionally, there is a point where both strains are equal, which usually coincides with the time where the temperature gradient changes from negative to positive (or vice versa). The behavior reverses when the LTG changes from positive to negative values. This behavior repeats periodically with a period of 24 hours analogous to the case of total strains and pavement temperatures described above.

The B&S and Untreated sections experienced similar behavior to the described above for the Rubblized section. The B&S section reached higher compressive strains than the rubblized section after the first six to eight hours for both the top and bottom of the slab. The maximum compressive strains undergone by the B&S section during the first six to eight hours were 93.9με for the bottom VW strain gauge and 78.8με for the top VW strain gauge located at the mid-slab location along the right wheel path, as seen in Figure 24. On the other hand, the compressive strains experienced by the untreated section were lower than the other two sections during the first 20 hours experiencing even tensile strains as shown in Figure 25. The maximum compressive strains experienced by the untreated section during the first six hours were 44.2με and 32.9με for the top VW strain gauge located at the mid-slab location along the left wheel path, while the maximum tensile strains reached values of 14.5με for the center of the slab. Notice that during the first 20 hours the untreated section was exposed to longer times with no solar radiation and low air temperatures. Therefore, the concrete did not expand due to the ambient temperature as much as it did in the rubblized and B&S sections causing lower compressive strains.

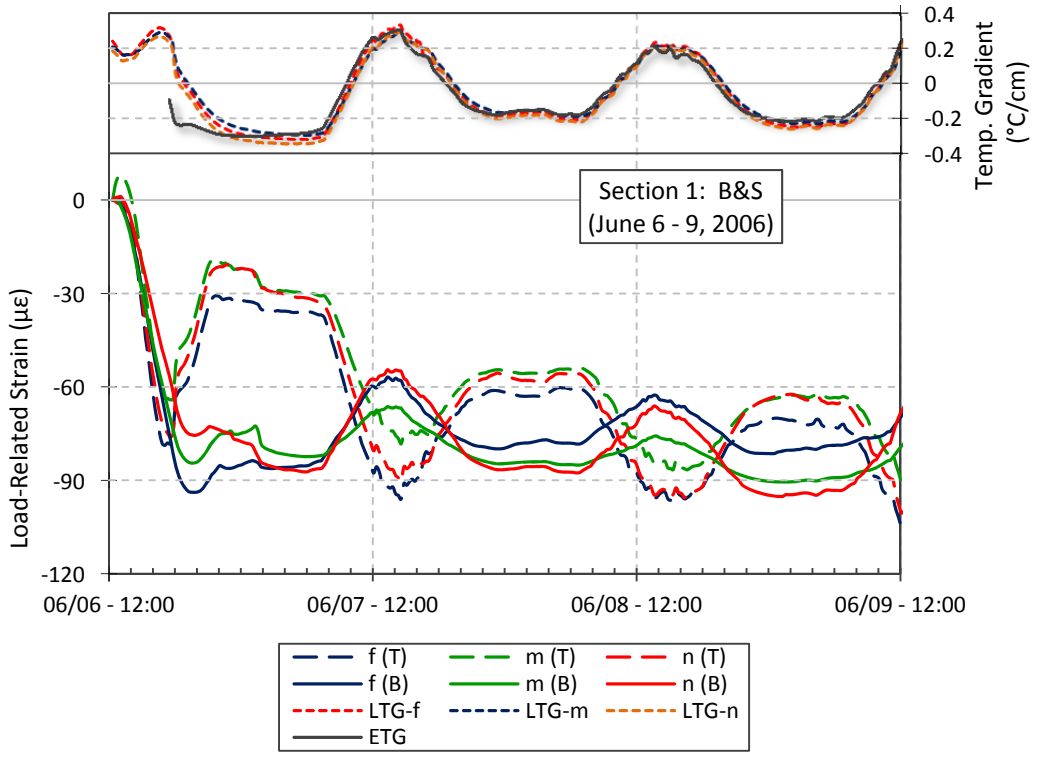

Figure 24. Early-age load-related strains in the B&S section. (T: top gauge, B: bottom gauge) (1 C°/cm = 4.6 °F/in).

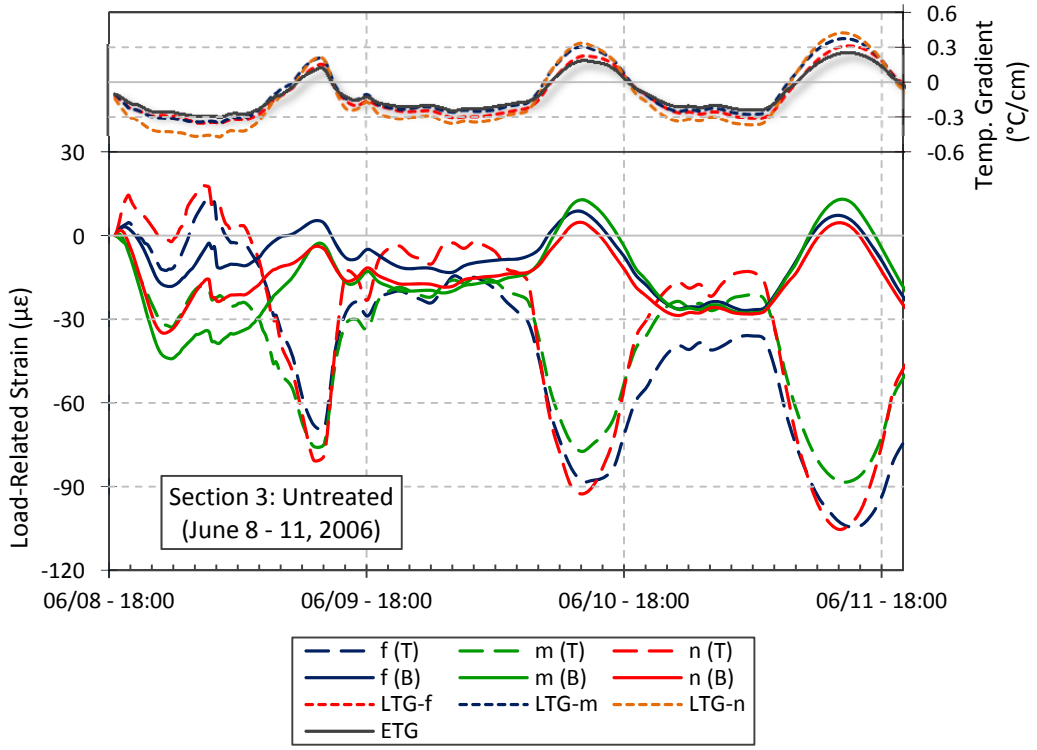

Figure 25. Early-age load-related strains in the untreated section. (T: top gauge, B: bottom gauge) (1 C°/cm = 4.6 °F/in).

Observe in Figure 23, Figure 24, and Figure 25 that during the first 72 hours the general trend followed by the load related strains consists of a constant increase of the compressive strains compared to the initial strain read right after concrete was placed. This trend remains even after the first 72 hours for the rubblized and untreated sections as is shown in Appendix E.

The stress development at early ages depends on several factors such as plastic and drying shrinkage, creep, curling and warping as mentioned above [Ruiz et al., 2005]. Additionally, the concrete strength during the curing period experiences a rapid nonlinear increment from zero to its designed value at 28 days where its rate of change is considered minimum. The interaction of all these factors is complex, and therefore the study of the stresses undergone by the concrete during the first 72 hours becomes a cumbersome task. This requires the prediction of the elastic modulus with time in order to calculate the stresses. Therefore, the analysis of stresses experienced by the experimental sections during the first 72 hours is not addressed in this report and it is left for further research.

5.3.2Slab Displacement Response Profiles for Maximum Positive and Negative Gradients July 2006

Using the same time period for which the strain and stress were examined, the displacements for each LVDT location were plotted in the following figures. Displacement versus time plots for all LVDTs in each section are presented first to show the general daily fluctuations at each slab location. It is important to remember when looking at these figures that LVDTs a, c, d, and i are shallow reference LVDTs, while LVDTs b, j, k, and l are deep reference. The differences between these two types were discussed in the Instrumentation chapter, but to reiterate, shallow reference LVDTs measure the relative displacement of the slab with respect to the subgrade, while deep reference LVDTs measure the absolute displacement of the entire system. Therefore, it is not appropriate to compare the displacement values between a shallow reference LVDT and a deep reference LVDT unless the contribution of the subgrade to the total displacement is desired. Nonetheless, all eight LVDTs are shown in one figure for each section below in Figure 26, Figure 27, and Figure 28.

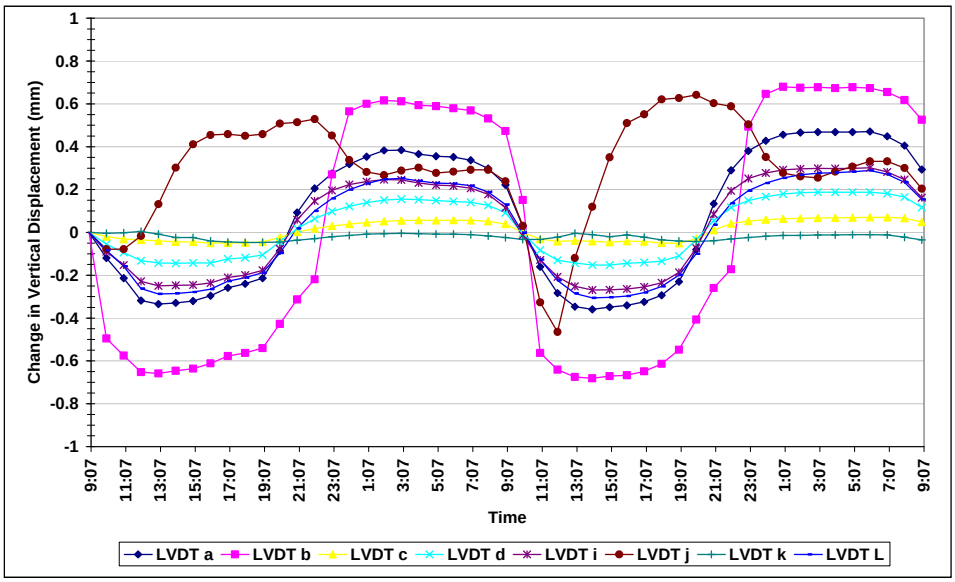

Figure 26. Vertical displacement vs. time, all LVDTs, untreated section: July 18-19, 2006 (1 mm =39.4 mil).

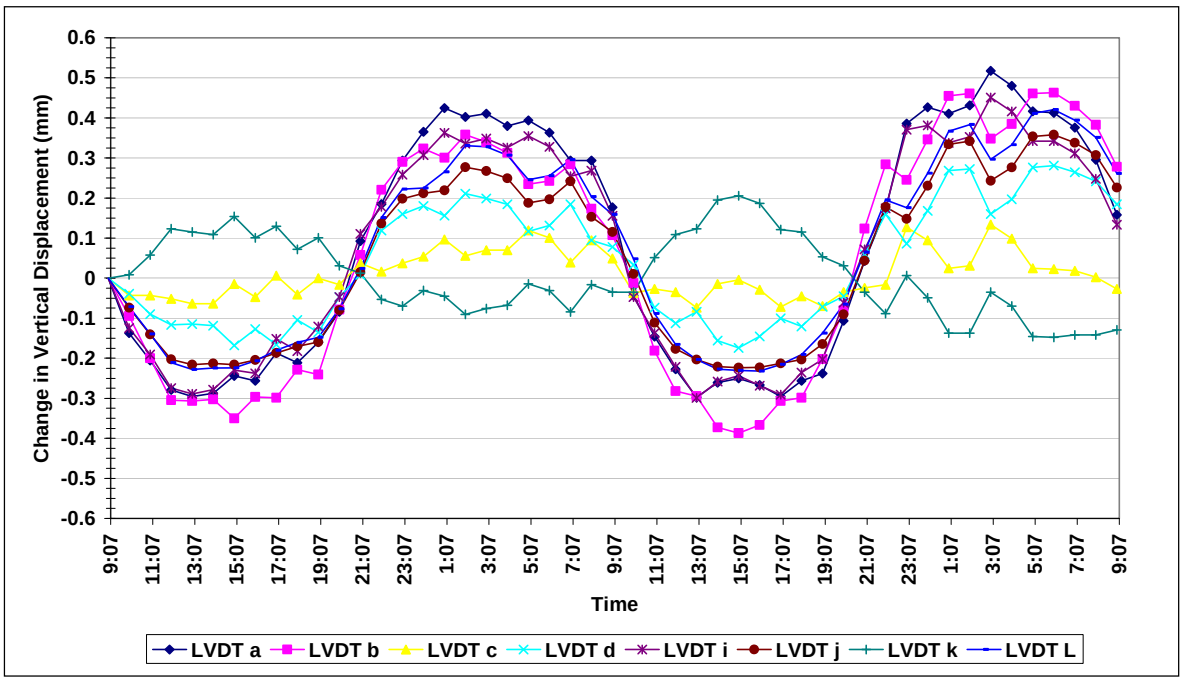

Figure 27. Vertical displacement vs. time, all LVDTs, rubblized section: July 18-19 2006 (1 mm =39.4 mil).

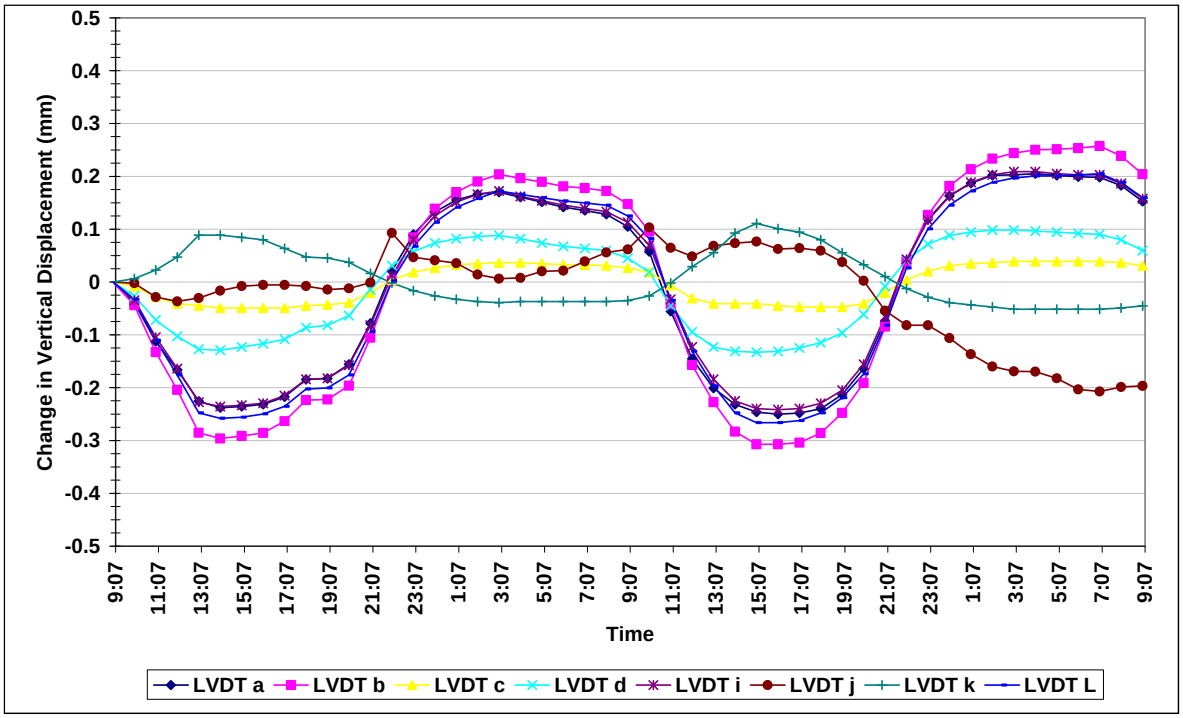

Figure 28. Vertical displacement vs. time, all LVDTs, B&S section: July 18-19 2006 (1 mm =39.4 mil).

While the information given in Figure 26, Figure 27, and Figure 28 is not presented in the best format for detailed comparisons, the overall magnitude of the curl can be estimated from the

figures. Looking at LVDT b, located on the inner wheel path on the leave-end of the slab, the total curl in the untreated section was about 1.2mm (47 mil); in the rubblized section about 0.85 mm (33 mil); and in the B&S section about 0.57 mm (22 mil). Also, there is a clear distinction between the curves for the shallow reference LVDTs and the deep reference LVDTs, most evident in the rubblized and B&S sections. The differences between the readings from the shallow and deep LVDTs in the untreated section are smaller than in the other sections, implying composite action between the overlay and base layers, and that the AC interlayer is not effectively acting as a bond breaker. In general, the magnitudes of the deep LVDT readings were consistently higher than the shallow LVDTs. The data points in the rubblized section have more small fluctuations than the untreated and B&S sections. This phenomenon is likely an issue of inconsistent system power during that time period, but should be further investigated. While the inconsistency may seem to invalidate the data, the values appear to be reasonable, they support the expected trends, and for other time periods the deflection versus time curves in the rubblized section are smooth like those shown for the untreated and B&S sections.

The curled shapes of the slabs are shown in Figure 30 through Figure 35 by plots of displacement values at adjacent LVDTs for specific times on July 19, 2006 selected for each section when the temperature gradient was maximum positive and most negative. The maximum gradients in each section were approximately equal, but did not necessarily occur at the exact same times. The positive maxima occurred between 1:00pm and 4:00pm, and the negative maxima all occurred at 2:00am. Even numbered figures show transverse profiles and odd numbered figures show longitudinal profiles. The changes in displacement from a zero-gradient reference time (about 9:00am July 18 2006) are shown for LVDTs i, c, and d for the transverse profiles, and for LVDTs j, k and l for the longitudinal profiles. While i, c, and d are not all in the same slab, the reading from i is superimposed into Slab 1 from Slab 2, since there are not three consecutive shallow LVDTs in one slab. Looking at the instrumentation plan in Figure 29 helps to visualize the profiles.

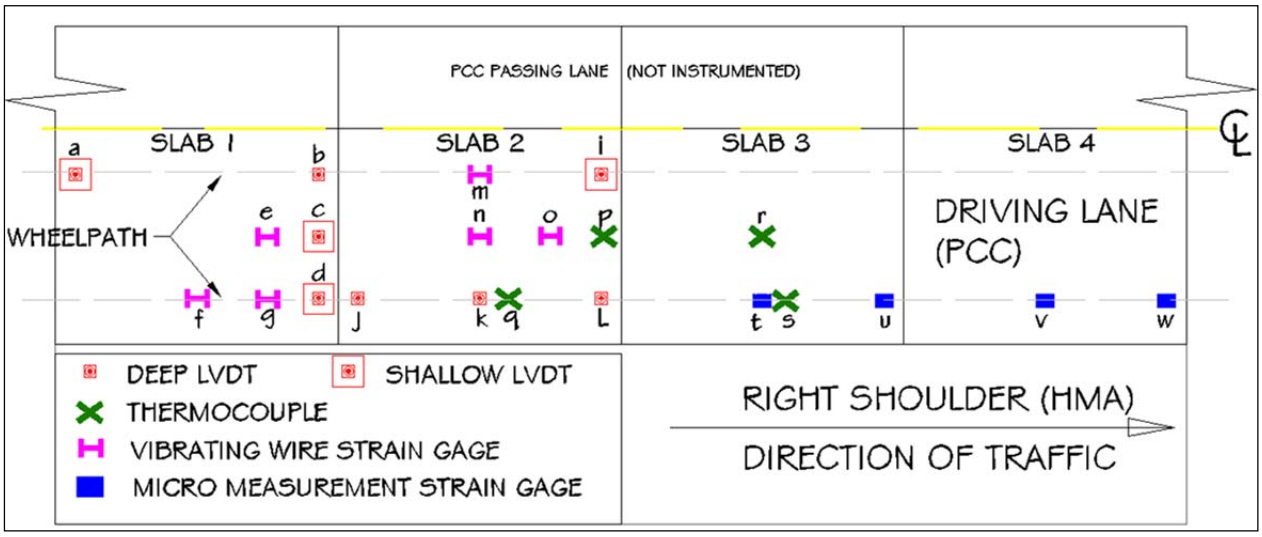

Figure 29. Plan view of instrumentation layout.

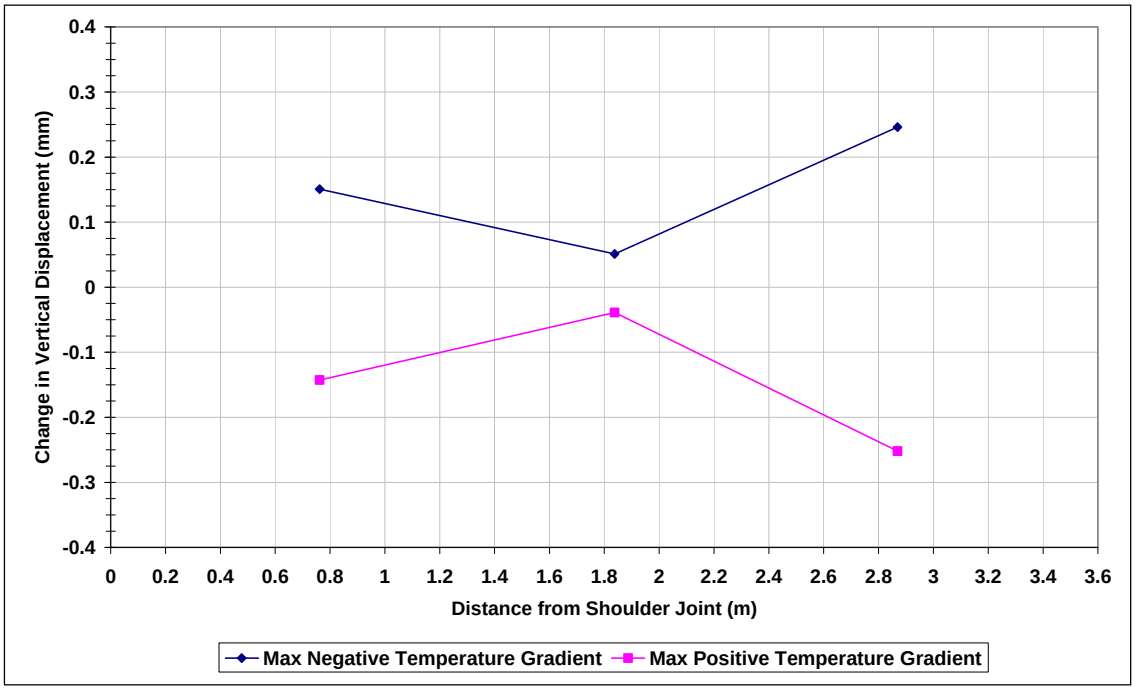

Figure 30. Transverse profile of the slab end in the untreated section July 19, 2006 (1 mm =39.4 mil, 1 m = 3.28 ft).

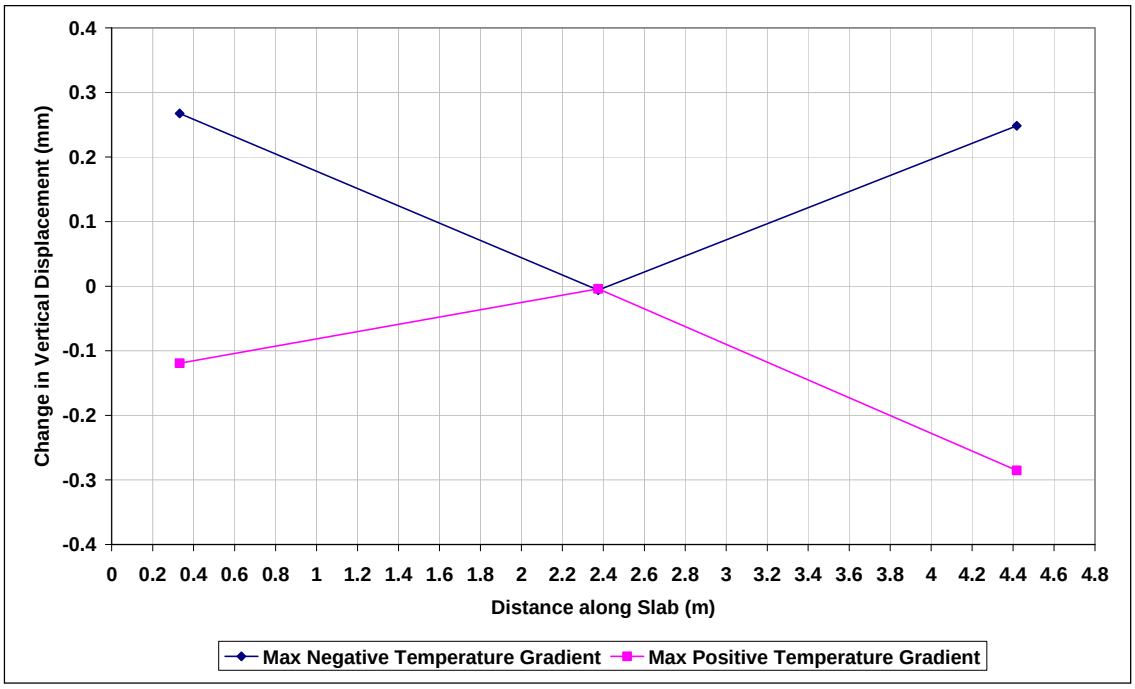

Figure 31. Longitudinal profile of the outer wheel path in the untreated section July 19, 2006 (1 mm =39.4 mil, 1 m = 3.28 ft).

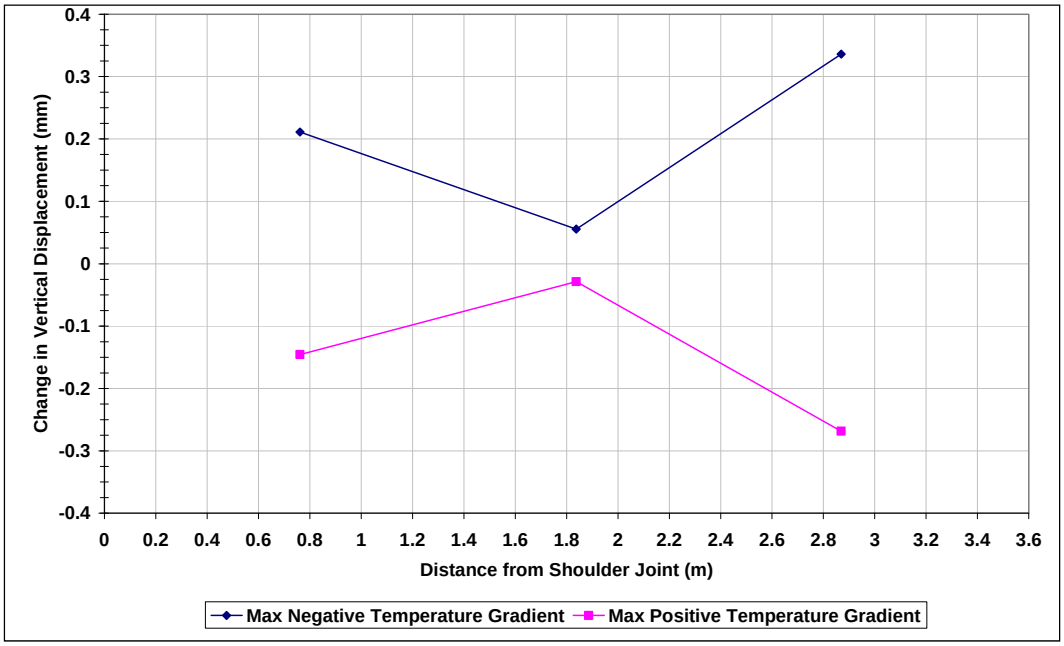

Figure 32. Transverse profile of the slab end in the rubblized section July 19, 2006 (1 mm =39.4 mil, 1 m = 3.28 ft).

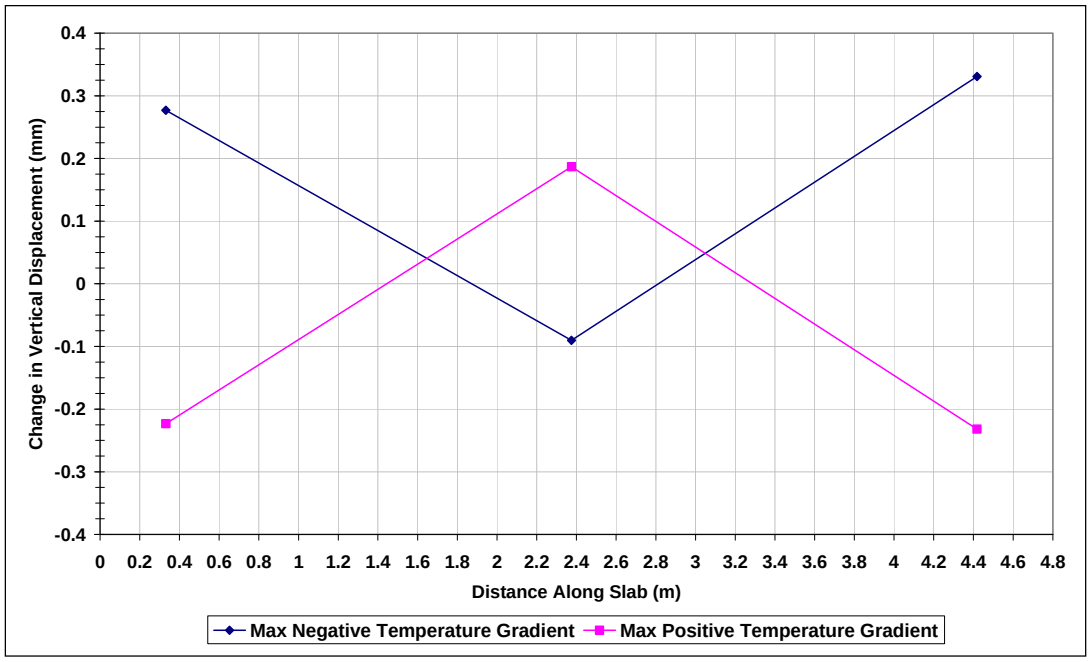

Figure 33. Longitudinal profile of the outer wheel path in the rubblized section July 19, 2006 (1 mm =39.4 mil, 1 m = 3.28 ft).

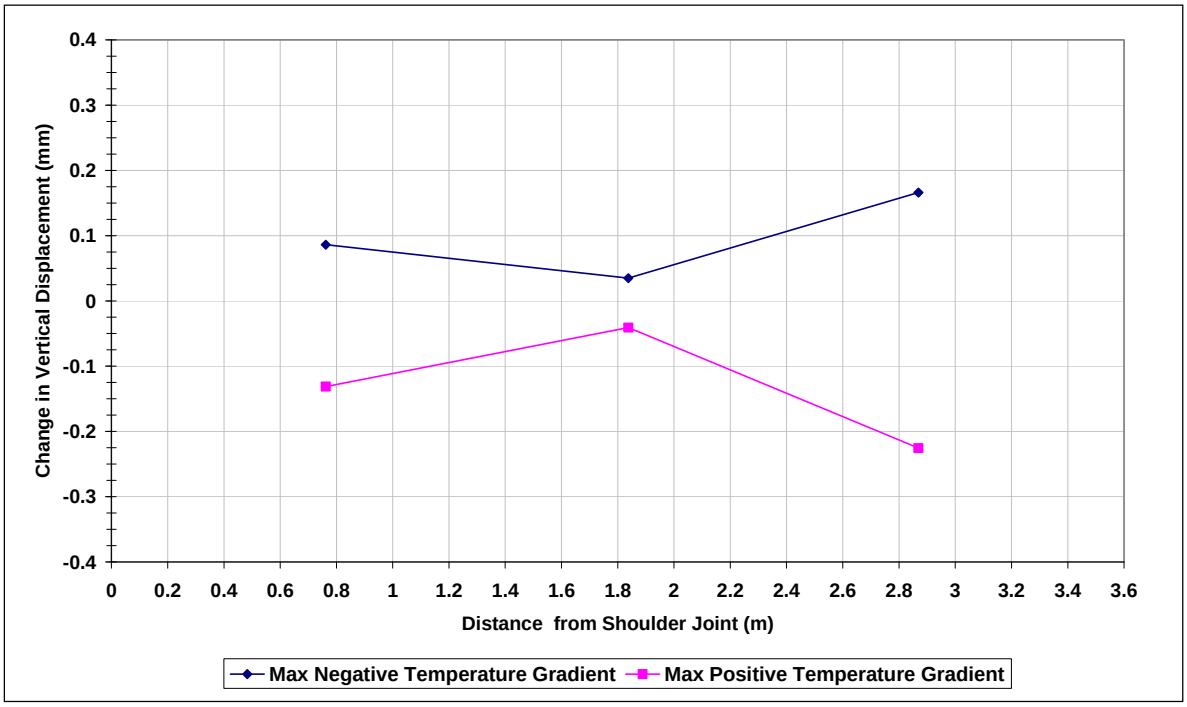

Figure 34. Transverse profile of the slab end in the broken and seated section July 19, 2006 (1 mm =39.4 mil, 1 m = 3.28 ft).

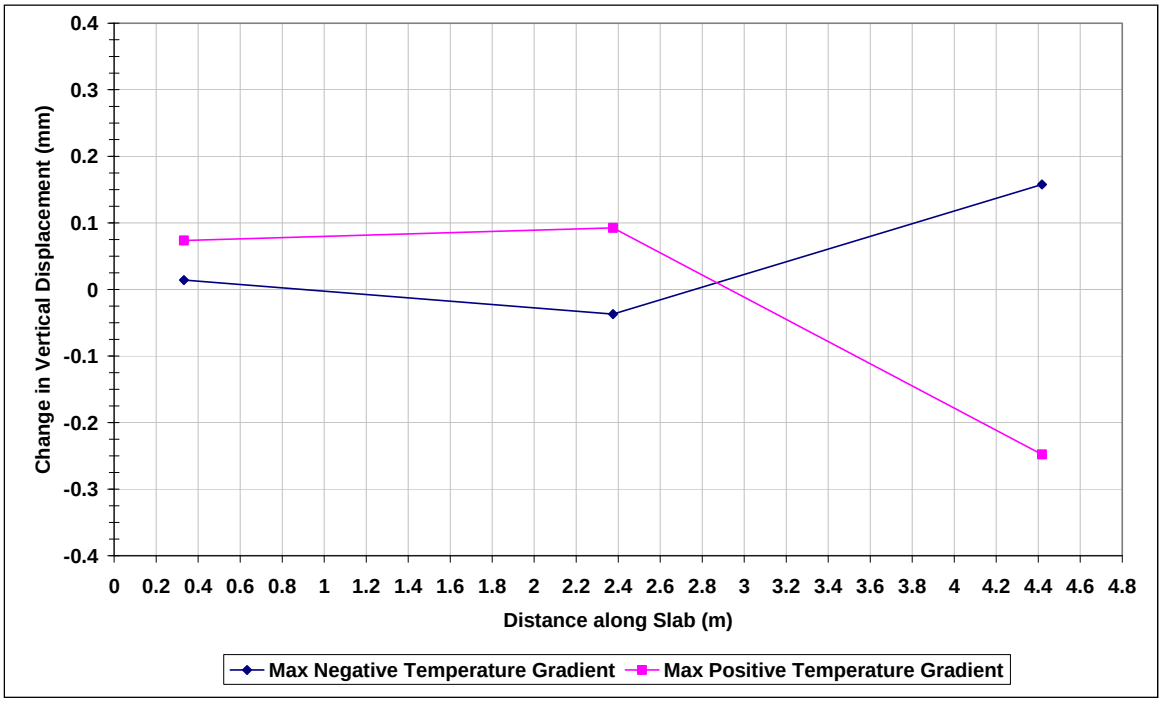

Figure 35. Longitudinal profile of the outer wheel path in the broken and seated section July 19, 2006 (1 mm =39.4 mil, 1 m = 3.28 ft).

For each maximum negative temperature gradient (slab bottoms warmer than tops), both the transverse and longitudinal profiles were concave up in each section. The opposite curvature

was also typical for positive gradients. The *lift* is considered to be the difference between the displacement of the center and the edge. Using the longitudinal profiles, the total curl for the untreated, B&S, and rubblized sections were 0.25 mm (9.8 mil), 0.42 mm (16.5 mil), and 0.2 mm (7.9 mil) concave up, and 0.28 mm (11.0 mil), 0.42 mm (16.5 mil), and 0.34 mm (13.4 mil) concave down, respectively. These results show that the rubblized section had the most severe curling (equal in both directions). The curl of the untreated section was only 60% as severe as the rubblized section concave up and 65% as severe concave down. The B&S section was less than half as severe as the rubblized section concave up and 80% as severe concave down. This sample data suggests that in the rubblized section more curvature typically occurs than in the others, and that the slabs can curl in either direction equally as much. Also, the data suggest that the curl in this particular slab of the B&S section did not curl as much concave up as it did concave down, probably because the negative temperature gradient was not as severe as the positive gradient.

From the longitudinal profiles, it is apparent that during the negative temperature gradient, in the untreated section the center LVDT remained in the same position as during the positive temperature gradient, while in the rubblized and B&S sections, the center lifted during the positive gradient, and dropped during the negative gradient. This effect can be explained by the rigidity of the base material. In the rubblized and B&S sections, the center of the slab was able to depress the base downward, while in the untreated section, the rigid concrete did not appear to give. This effect was largest in the rubblized section, as would be expected.

The curled shapes generally agree with the respective strains and stresses determined for the same time periods in each section. For example, since looking at the longitudinal profile in any section for the positive temperature gradient, there is a concave downward shape in the outer wheel path. Figure 19 suggests the concave down shape would cause tension in the bottom of the slab and compression in the top.

Although the rubblized section exhibited the highest lift, the stresses in the rubblized section were not determined to be greatest. Axial forces induced by differential thermal expansion and contraction of the JRCP layer can explain this effect. Temperature gradients influenced the interaction between the overlay and the existing JRCP differently in each section. In the untreated section especially, the relative expansion or contraction of the original JRCP intensified the bending stresses in the top of the slab. For example, when the slab was curled up, the bottom was warm so the JRCP expanded more than the overlay and added axial tension to the slab, increasing the tension in the top of the slab while reducing the compression in the bottom of the slab. By the same reasoning, this action amplified the compression in the top and reduced the tension in the bottom during negative temperature gradients. This effect was strongest in the untreated section, while moderate in the B&S section, and non-existent in the rubblized section. In the untreated section, the continuous concrete and mesh reinforcement transferred thermally induced forces into the overlay which developed strain and stress. The complete discontinuity of the JRCP in the rubblized section negated this action completely, while still somewhat affecting the B&S section.

5.3.2.1Contribution by the Subgrade

The difference between a deep reference and a shallow reference LVDT in similar locations is the contribution by the subgrade. LVDT b and LVDT i occupy corresponding locations within Slab 1 and Slab 2, respectively. LVDT b is deep reference and LVDT i is shallow reference, so the readings from i were subtracted from b to obtain the subgrade contribution at the inner wheel

path location. The other paired locations are in the outer wheel path at the leave-end of the slab, with LVDT l being a deep reference in Slab 2, and LVDT d a shallow reference in Slab 1. The difference between the two represents the subgrade contribution at this location. For each section, the differences between these two pairs were plotted for the July 18th – 19th 2006 time period in Figure 36, Figure 37, and Figure 38.

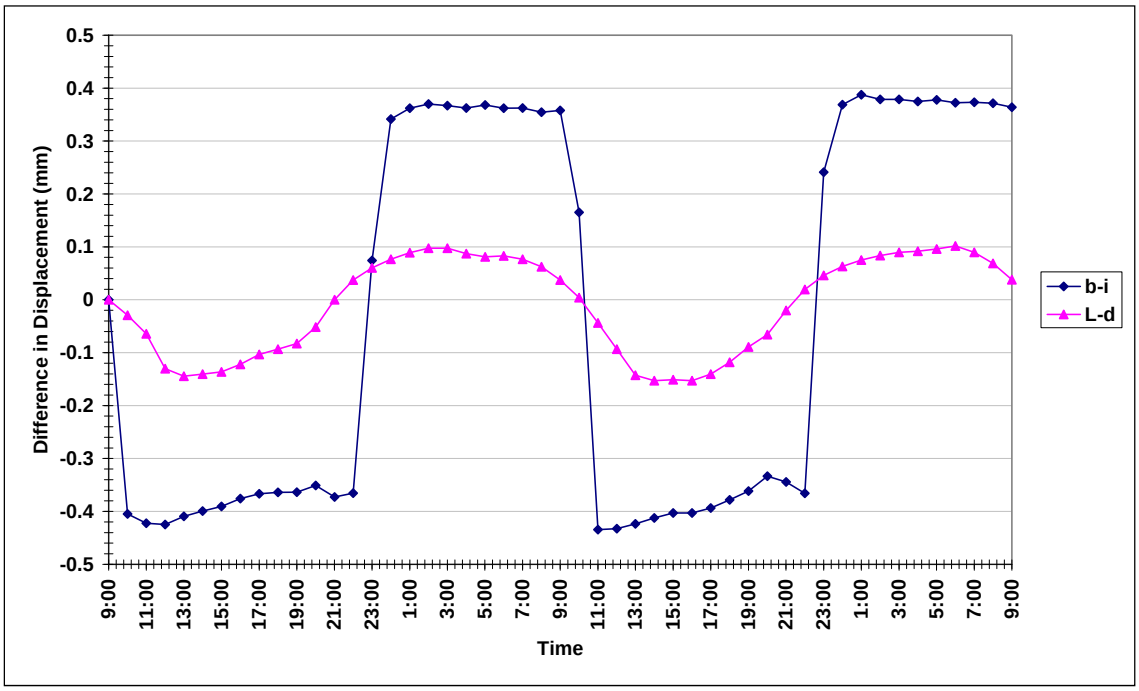

Figure 36. Subgrade contribution to vertical displacement in untreated section, locations b/i and l/d (1 mm =39.4 mil).

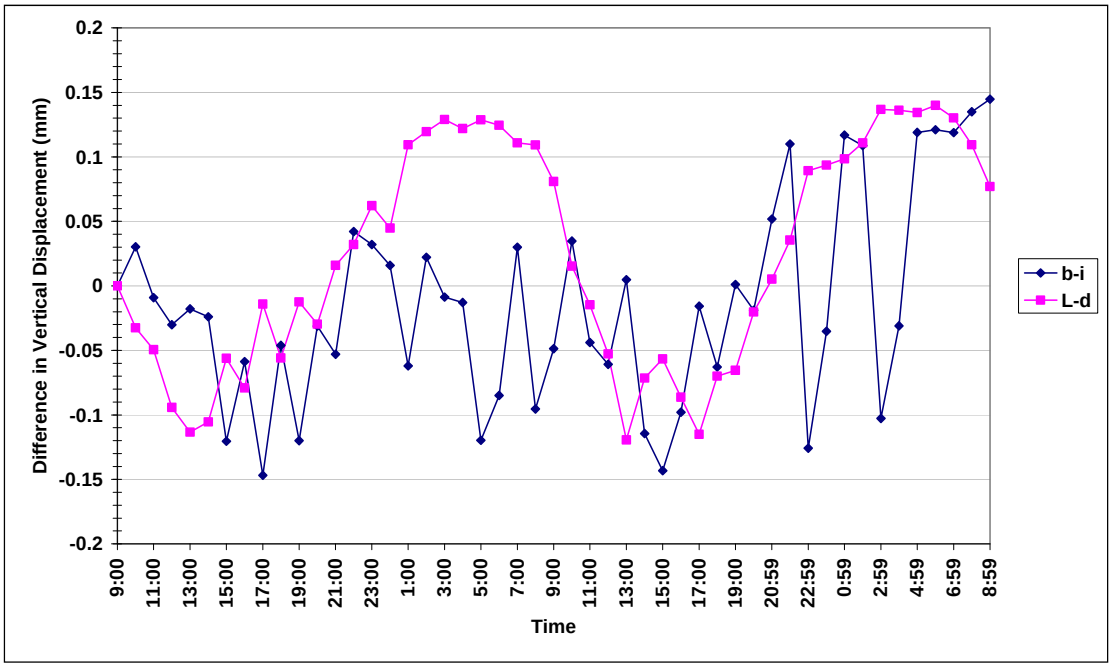

Figure 37. Subgrade contribution to vertical displacement in rubblized section, locations b/i and l/d (1 mm =39.4 mil).

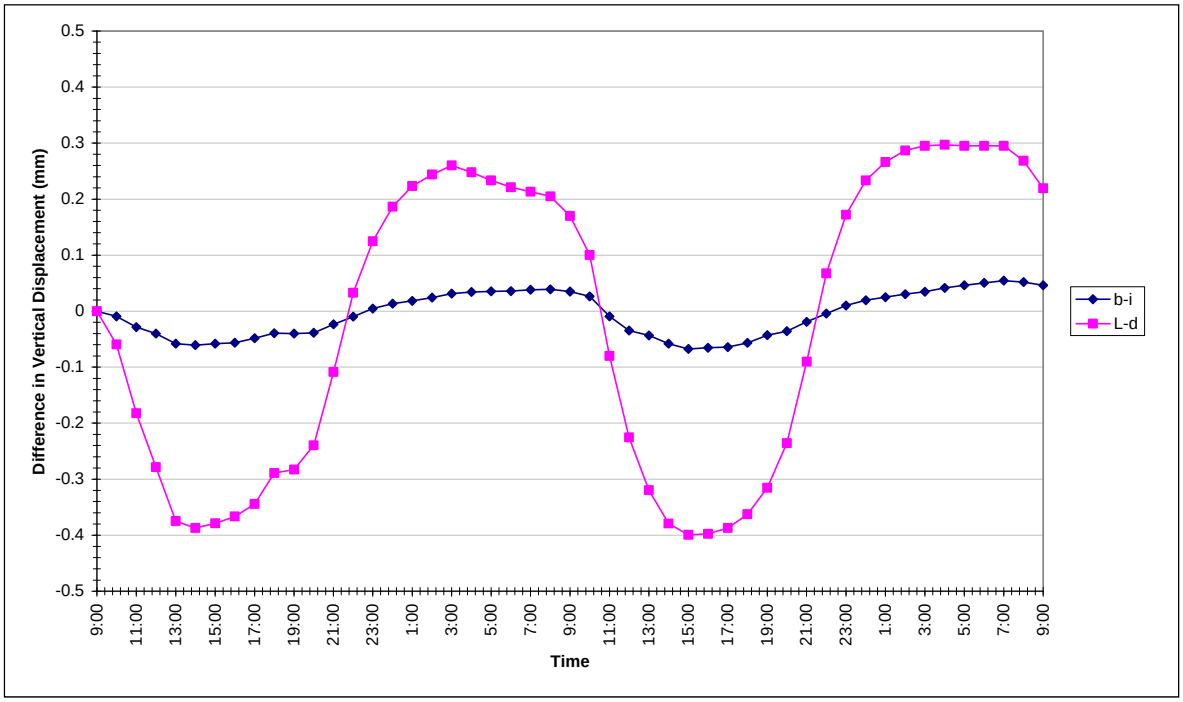

Figure 38. Subgrade contribution to vertical displacement in B&S section, locations b/i and l/d (1 mm =39.4 mil).

The differences between the deep and shallow reference LVDTs in redundant locations are clearly significant. At the points of the maximum displacement, the differences were greatest. In the untreated section, the differences between locations b and i were consistently about 0.4 mm (15.7 mil) (both up and down), while at locations l and d, they varied between 0.1 mm (3.9 mil) and -0.15 mm (-5.9 mil), although the behavior of LVDT b in the untreated section suggests it may have been sticking and responding slowly. The differences in the rubblized section fluctuated in a range of about -0.15 mm (-5.9 mil) and 0.15mm (5.9 mil) in each location, but the data points were sporadic. In the B&S section, the differences were quite similar to those in the untreated section, with somewhat less variance between the shallow and deep reference LVDTs in the outer wheel path. In the untreated and B&S sections, the differences between LVDTs l and d were clearly larger than those between LVDTs b and i. This implies that the subgrade has more influence on the outer edge of the slabs than in the inner wheel path. It is possible the subgrade near the shoulder is more susceptible to temperature and moisture variations, but other causes of this difference should be further investigated. The scattered trends in the rubblized section are due to the irregular readings from this particular time period.

5.4 Long-Term Pavement Response

Strains, pavement temperatures and weather data from each of the experimental sections have been collected since the construction date. This data is used to analyze and compare the performance between the experimental sections. In order to perform the analysis, strains, pavement temperatures and temperature gradients were plotted from all the available data so trends and periods of consistent data could be identified (see Appendix C). Once the consistency of the data was checked, common time periods of at least 72 hours of uninterrupted data were selected. The selected dates were chosen such that they were characteristic of each season from

June 2006 to May 2009. Additionally, representative dates for each section were selected for those seasons where non-common data was available. A list of the selected periods is provided in Table 5. From each of the selected time spans the change in load-related strains (from now on referred just as "*change in strain*") and temperature gradients were analyzed.

Load-related strains can be calculated from the VW strain gauge output using Equation (11) setting as the initial reading the same used for the curing strains. Thus, they would represent the load-related strains undergone by the pavement since the construction day. While the load-related strains were calculated for the selected periods, they are not discussed herein. This is because in order to completely understand the stress/strain response due to environmental effects it is necessary to know the state of strains and temperature gradient in the slab when the concrete sets. Recall that setting of concrete is achieved at early ages and it marks the point where strength, elastic modulus and other mechanical properties start developing [Ruiz et al., 2005]. Estimating the concrete set time is out of the extent of the analysis presented herein and therefore a study of the total strain and stress response undergone by the sections since the construction date is not addressed in this report. However, an assessment of the performance and comparisons between the three sections can be carried out by analyzing the change in strains and stresses due to environmental effects. Whereas the load-related strains are not discussed below, the corresponding plots are provided in Appendix D and Appendix E for further reference.

The change in strain ($\Delta\varepsilon$) for each period was calculated as the relative change between the load-related strain at the beginning of each selected time span and the subsequent strain readings. Therefore, the change of strain is always zero at the beginning of each analyzed period. The starting point of each period was chosen to be a point where the linear temperature gradient was the closest to zero. This selection is supported on the fact that theoretically in an unrestrained slab where the temperature gradient is zero, the temperature induced stresses should be zero. However, in general the strains and stresses are not zero for zero LTG values due to curing stresses, and stresses due to the restraints provided by the base and adjacent slabs. The sign convention for the change of strain is similar to the mentioned before. Thus, negative values correspond to change in strains that induce compressive stresses and they are denoted herein as compressive strains. The opposite applies for positive values, which induce tensile stresses and they are denoted herein as tensile strains. The change in stresses ($\Delta\sigma$) is calculated using Equation (13) and as it can be seen, it follows the same trend with time of the corresponding change in strains. The change in strains and stress responses share the same characteristics mentioned before of the load related strain response at early ages. Hence, $\Delta\varepsilon$ and $\Delta\sigma$ vary periodically with a 24 hour period where the values corresponding to top and bottom gauges commute as the linear temperature gradient changes from positive to negative. Additionally, there is a point where the values for the top and bottom gauge at a particular location are the same. This point coincides with the time when the LTG changes from positive to negative (or vice versa). Moreover, this point generally corresponds to change in strains and stresses close to zero. The following sections present the change in strains/stresses for each of the most representative periods in Table 5. Following this, comparisons of the maximum, minimum, and average of strains and stresses between the three sections are presented. Other periods were considered for the comparisons but they are not discussed herein; however, the plots for those periods are shown in Appendix D.

Table 5. Time periods of common data (*time spans not discussed in this report).

Season	Section		
	B&S	Rubblized	Untreated
Summer 2006	Jul 8-14*, Jul 17-27, Aug 5-9*, Aug 9-15*		
Fall 2006	Dec 1-3*, Dec 3-7		
Winter 2006-2007	Feb 9-15, Feb 15-20*	Feb 26-Mar 5*, Mar 5-9	Mar 9-13*, Mar 13-20
Spring 2007	–	May 27-Jun 7	
Summer 2007	Aug 21-25	–	
Fall 2007	Oct 21-30		
Winter 2007-2008	–		
Spring 2008	Apr 26-May 6		
Summer 2008	Aug 23-Sep 3		
Fall 2008	Oct 6-9		
Winter 2008-2009	–		
Spring 2009	May 1-11		

5.4.1.1 Summer 2006 (July 17-27)

The change in strains of each section during a period of 240 hours (10 days) was recorded between during July 17-27, 2006. The air temperatures and solar radiation at the site during that time is shown in Figure 39. Figure 40, Figure 41, and Figure 42 show the change in strains in the B&S, rubblized, and untreated sections, respectively. In each figure, the values shown correspond to the top and bottom strains at the mid-slab location along the right and left wheel path (i.e. location ***f*** and ***m*** respectively) as well as at the center of the slab (i.e. location ***n***). Other sensors are not included in order to provide a clear view of the behavior of the sections at the most critical locations. The response for the three sections presented similar behaviors with a period of consistently low change in strains compared to the rest of the 10 days. This behavior agrees with a period of low solar radiation (i.e. cloudy day) and a total precipitation of 19.6 mm (0.77 in) during daylight time in July 22, as shown in Figure 39. The minimum and maximum average air temperatures during the analyzed period were 11.9°C (53.4°F) and 30.1°C (86.2°F) respectively. The pavement temperatures during this same period varied from 18.4°C (65.1°F) to 39.1°C (102.4°F).

It is noticeable that in the B&S section consistently experienced higher tensile strains at the center of the slab (i.e. location ***n***) than at the mid-slab location along the wheel paths (i.e. location ***f*** and ***m***). However, the maximum compressive strains were experienced in location ***e*** (not shown in Figure 40) and location ***m*** for the top and bottom of the slab respectively. The rubblized section experienced similar strains to those of the B&S section for the top gauges at the three locations ***f***, ***n***, and ***m***. For this section however, the maximum compressive and tensile strains were at the top and bottom of the slab respectively in the mid-span location ***m***. The untreated section experienced higher strains than the other two sections. The untreated section underwent consistently higher tensile strains at the mid-slab location along the left wheel path,

and it experienced higher compressive strains at the center of the slab than at any of the other sensors. In general, the magnitude of the compressive strains and stresses was higher than the magnitude of the tensile strains. This behavior was characteristic for the three summer periods selected as can be seen in Appendix D.

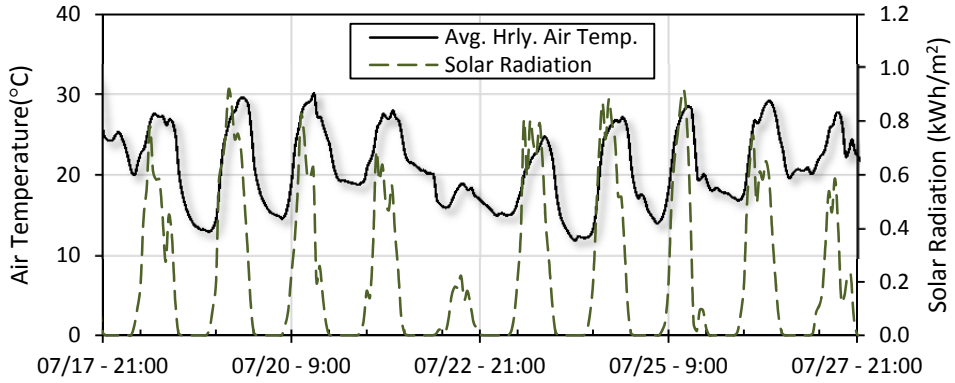

Figure 39. Average air temperature and solar radiation (July 17-27, 2006) (0°C = 32°F, 40°C = 104°F, 1kWh/m^2 = 317.21 Btu/ft^2).

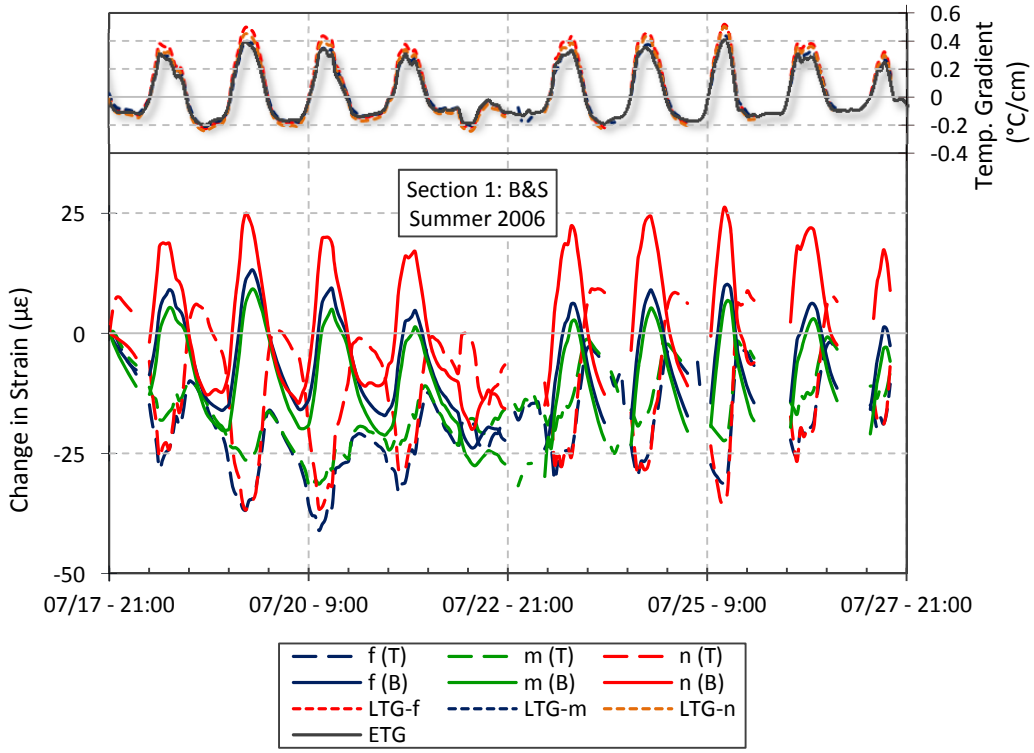

Figure 40. Change in strains over 10 days for the B&S section (July 17-27, 2006) (1 C°/cm = 4.6 °F/in).

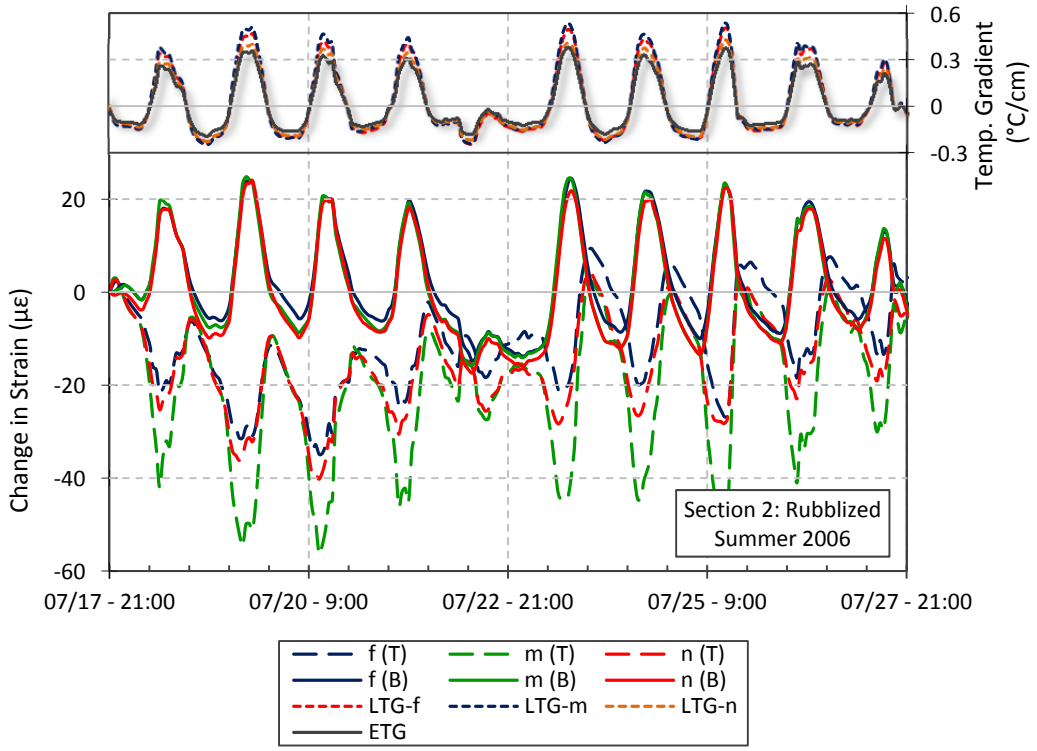

Figure 41. Change in strains over 10 days for the rubblized section (July 17-27, 2006) (1 C°/cm = 4.6 °F/in).

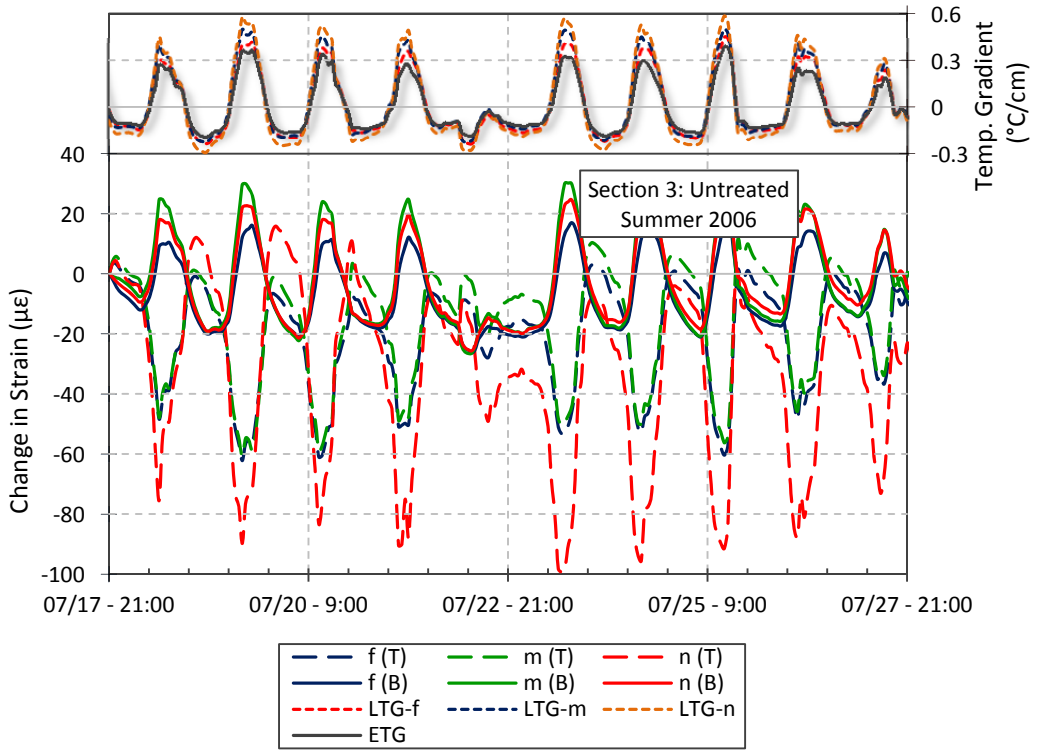

Figure 42. Change in strains over 10 days for the untreated section (July 17-27, 2006) (1 C°/cm = 4.6 °F/in).

The change in stresses within the pavement between July 17 and 27, 2006 showed the same trend shown above for the change in strains. The change in stresses were higher in the untreated section than in the rubblized and B&S sections as expected from the corresponding strain responses. The maximum, minimum and average values of the strains and stresses for each section are discussed in the comparisons section below.

5.4.1.2 Fall 2006 (December 3-7)

The next set of measurements was made in late autumn, December 3-7, 2006. The air temperature and solar radiation is given in Figure 43. Figure 44, Figure 45, and Figure 46 show the change in strains for a period of 108 hours (4.5 days) for the B&S and rubblized section, and 84 hours (3.5 days) for the untreated section, respectively. As before, the values shown correspond to the strains at top and bottom in the center of the slab as well as the mid-slab location along the right and left wheel path (i.e. location ***f*** and ***m*** respectively). Also as before, other sensors were excluded in order to provide a clear view of the behavior of the sections at the most critical locations. The three sections presented similar responses where low daily variations of the strains correspond to low variation of the linear temperature gradient and low solar radiation (see Figure 43). The linear temperature gradients were consistently negative during the period shown here presenting only few short periods of positive LTG values. Additionally, the three sections experienced a period of more than 36 hours where the top of the slab remained under tensile strains while the bottom of the slab remained under compressive strains. The average air temperature varied from -9.6°C (14.7°F) to 5.7°C (42.3°F) while the pavement temperatures for this period varied from -6.4°C (20.5°F) to 4.3°C (39.7°F) (see Appendix E).

The maximum change in strains in the B&S section occurred at the top of the slab in the location ***e*** (not shown in Figure 44). Notice that this coincides with the location of the maximum compressive strain for the summer 2006 period. The slab underwent higher strains at the mid-span on the outer wheel path (i.e. location ***f***) than on the inner wheel path at location ***m***. However, the compressive and tensile strains were consistently higher in the center of the slab (i.e. location ***n***) than those of the wheel path locations. The rubblized section experienced the highest change in strains at the mid-slab along the left wheel path, while the mid-span on the outer wheel path and the center of the slab experienced similar compressive and tensile strain changes. Recall that the rubblized section experienced also the maximum compressive and tensile strains at the left wheel path for both top and bottom during the summer 2006 period. For the untreated section, the maximum compressive strains were experienced at the mid-span location on the inner wheel path (i.e. location ***m***) and the maximum tensile strains were observed at the center of the slab. In general, the three sections experienced higher tensile strains than compressive strains during the analyzed period with the same variation range except for the top sensor in the center of the slab (i.e. location ***n***). Similar behavior was observed for the other fall 2006 period listed in Table 5. However, this was characterized by a period of 36 hours of even smaller variations in the strains and temperature gradient than those shown for the times described here (see Appendix D).

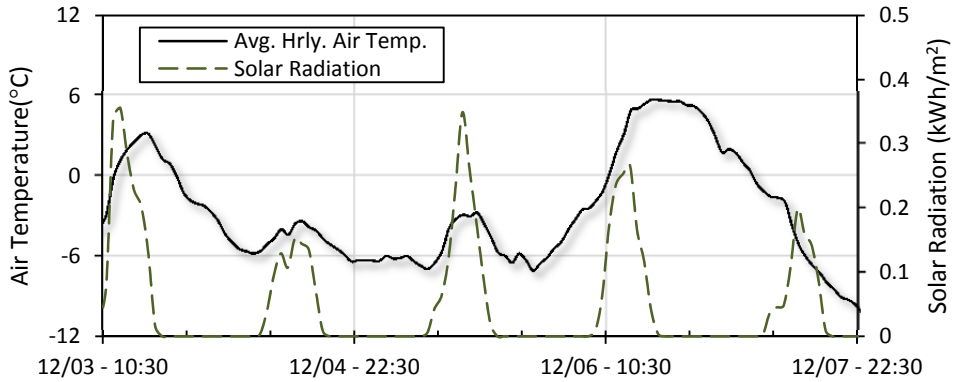

Figure 43. Average air temperature and solar radiation (December 3-7, 2006).

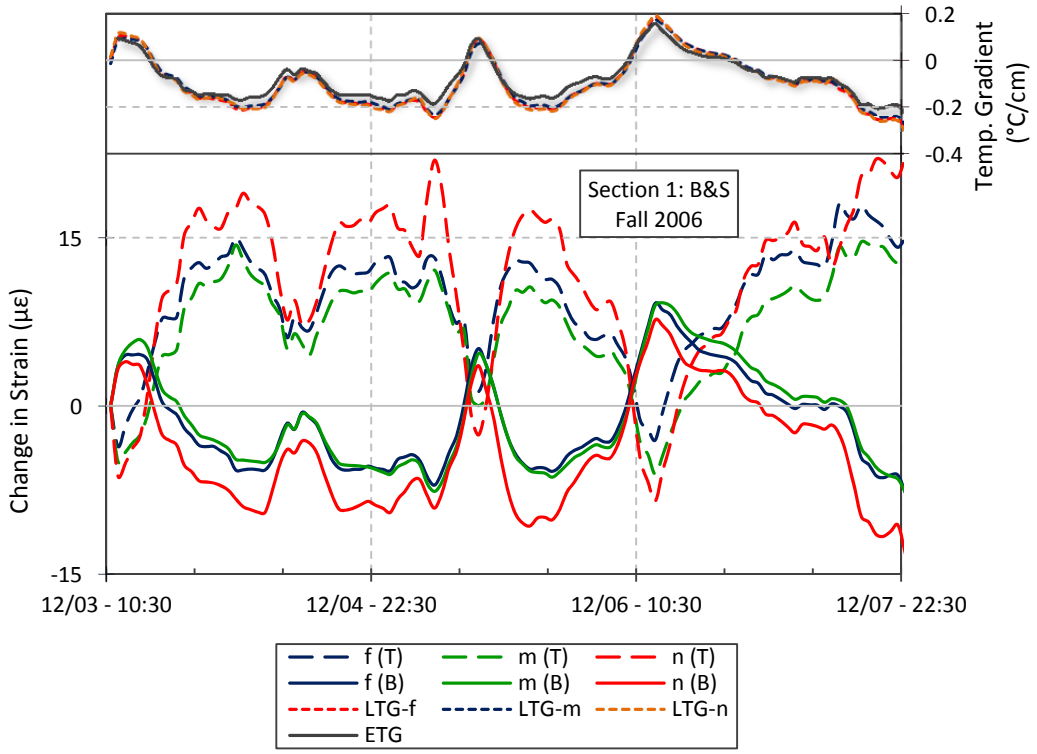

Figure 44. Change in strains over 4.5 days for the B&S section (December 3-7, 2006) (1 C°/cm = 4.6 °F/in).

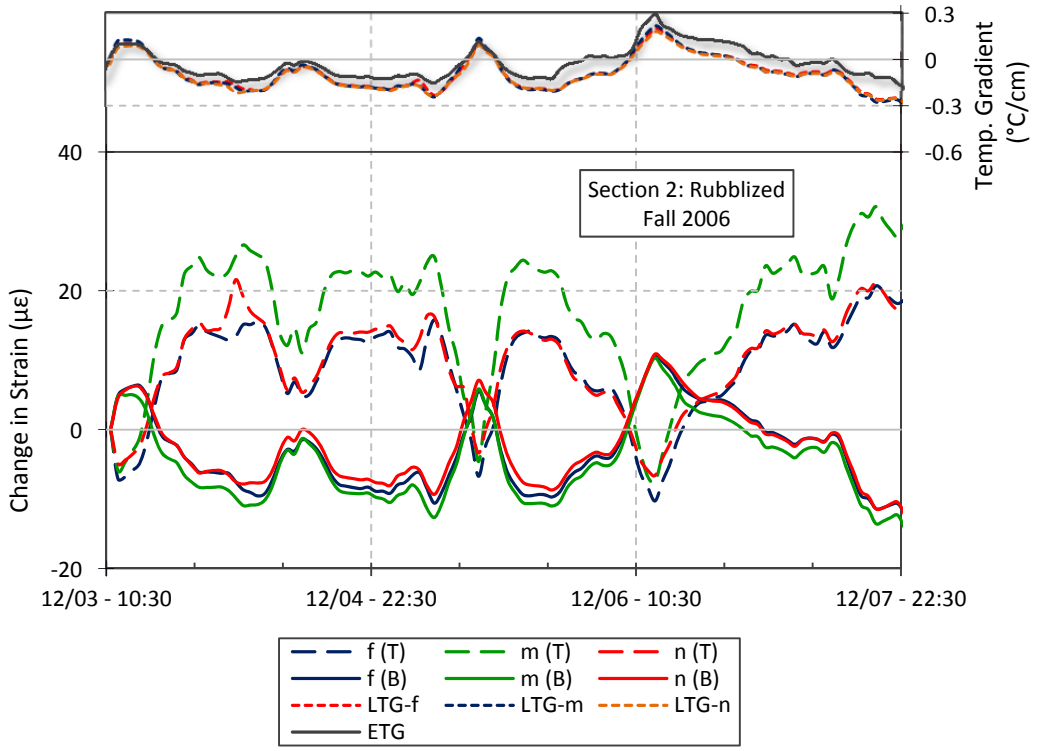

Figure 45. Change in strains over 4.5 days for the rubblized section (December 3-7, 2006) (1 C°/cm = 4.6 °F/in).

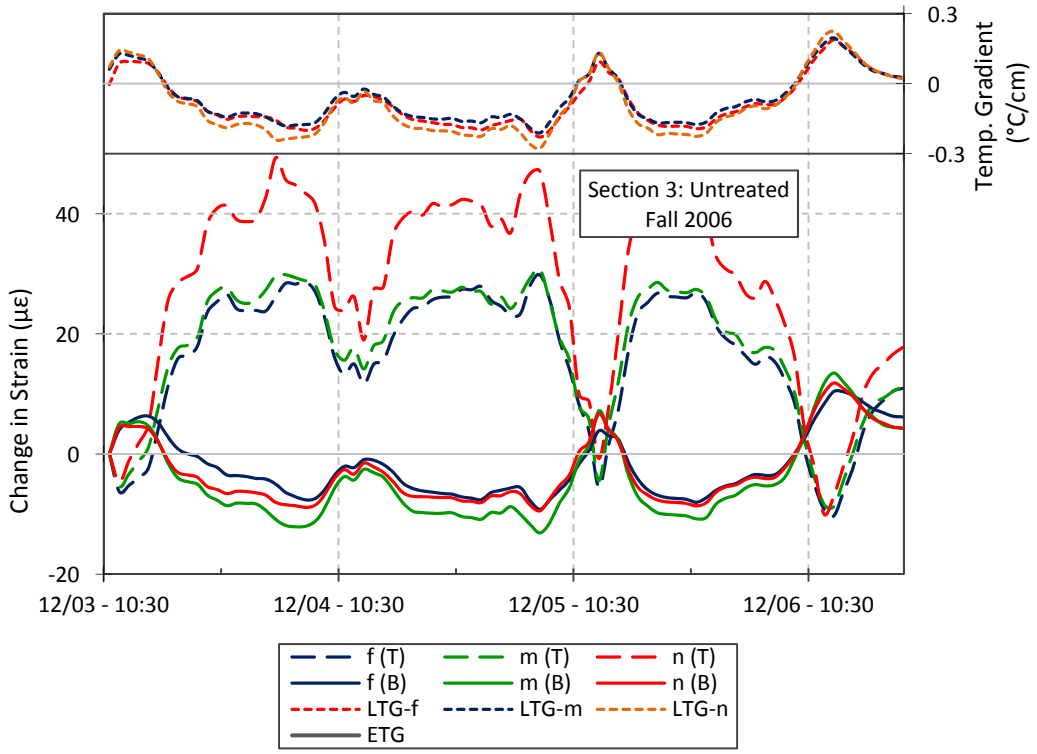

Figure 46. Change in strains over 3.5 days for the untreated section (December 3-7, 2006) (1 C°/cm = 4.6 °F/in).

Since the change of stresses is calculated using Equation (13), it is expected then that it follow the same trend than the change in strains. Thus, the untreated section experienced the higher compressive and tensile stresses followed by the rubblized section and the B&S section which experienced the lowest stresses during the December 3-7, 2006. The maximum, minimum and average values of the strains and stresses for each section are discussed herein below.

5.4.1.3 Winter 2006-2007

Common data to the three experimental sections was not available for the winter period of 2006-2007. However, a characteristic winter period for each section was selected. The average air temperature and solar radiation are shown for the period of February 9-15, 2007 in Figure 47. The corresponding change in strains in the B&S section are shown in Figure 48, while Figure 49 and Figure 50 show the air temperature and the change in strains in the rubblized section during March 5-9, 2007, and Figure 51 and Figure 52 show the air temperature and the change in strains in the untreated section and untreated section during March 13-19, 2007. Each of these periods was selected such that it contained consistent data and the higher change in strains for the existing data corresponding to the winter 2006-2007.

The strain response of the B&S section was characterized by consistent compressive strains at the top of the slab and consistent tensile strains at the bottom of the slab. This behavior in general corresponds to temperature gradients that remained in average positive. However, notice that at the end of the interval shown the strains drop as the temperature gradient varied between -0.3 C° (-0.54°F) and 0.3 C° (0.54°F) which, coincides with a the drop of the average temperature and solar radiation as shown in Figure 47. The average air temperature during the period between the 18:00 hours of February 9th and the 15th varied from -2.3°C (27.9°F) to -17.4°C (0.7°F). The minimum and maximum pavement temperatures during this same period were -4°C (24.8°F) and 20.1°C (68.2°F) respectively (see Appendix E). The B&S section underwent higher compressive and tensile strains at the mid-slab location along the right wheel path than either the left wheel path or center of the slab. However, the maximum change in strains was experienced at the top and bottom of the slab in the location ***e*** (not shown in Figure 48). Recall that the maximum change in strains during the summer and fall 2006 periods was also experienced at the location ***e***.

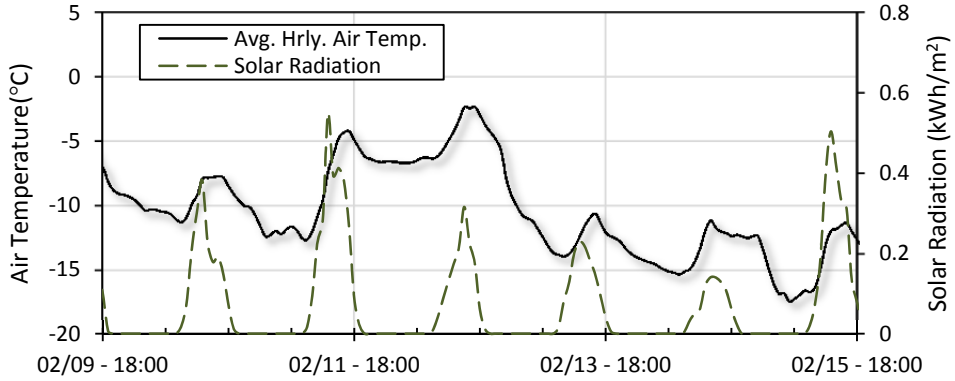

Figure 47. Average air temperature and solar radiation, February 9-15, 2007 (-20°C = -4°F, 5°C = 41°F, 1kWh/m^2 = 317.21 Btu/ft^2).

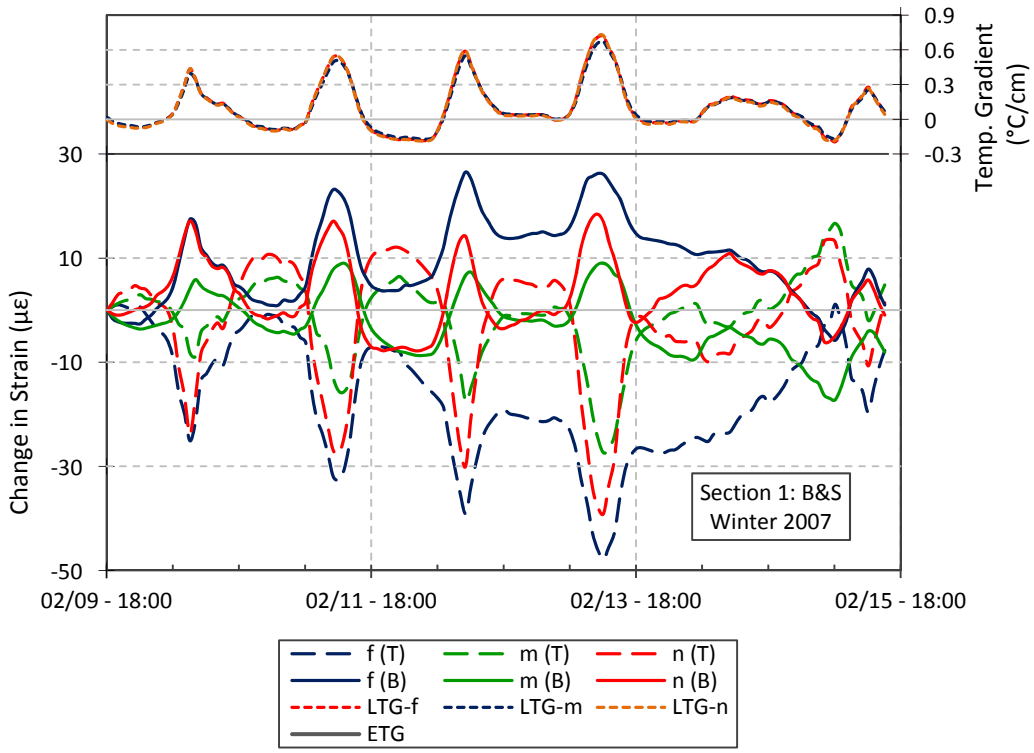

Figure 48. Change in strains over 6 days for the B&S section, February 9-15, 2007 (1 C°/cm = 4.6 °F/in).

The rubblized section experienced similar strains for all the sensors at the bottom of the slab as well as for all the sensors at the top as it is shown in Figure 50. The section experienced higher compressive strains at the top than tensile strains, which coincides with longer periods of the slab subjected to negative temperature gradients. The average air temperature during the period between March 5th and the 9th varied between -20°C (-4°F) and -5.1°C (22.8°F) (see Figure 49) while the pavement temperature varied from -15.1°C (4.8°F) to 5.3°C (22.5°F) (see Appendix E). Although the rubblized section underwent higher strains at the inner wheel path (i.e. location ***m***) most of the time, the center of the slab as well as the outer wheel path (location ***f***) experienced similar strains. This behavior contrasts with the behavior during the summer and fall 2006 periods where the strains at location ***m*** where always higher than at any other sensor's location. It can be seen also that the peak of tensile strains occurs approximately four hours after the peak of compressive strains at the bottom occurs.

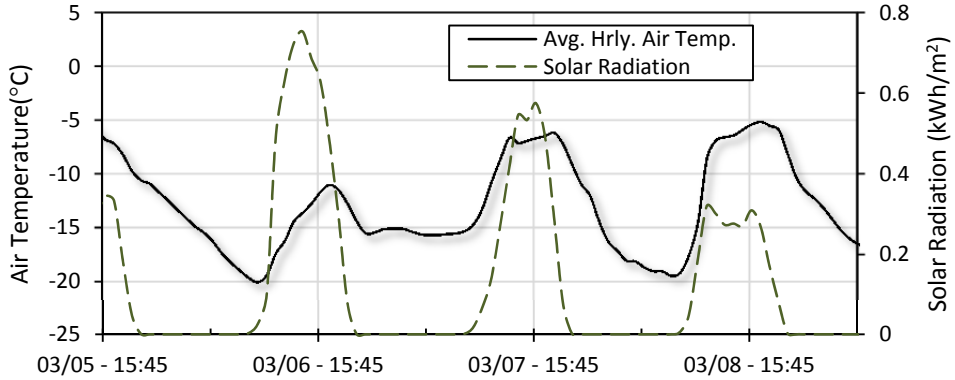

Figure 49. Average air temperature and solar radiation, March 5-9, 2007 (-25°C = -13°F, 5°C = 41°F, 1kWh/m^2 = 317.21 Btu/ft^2).

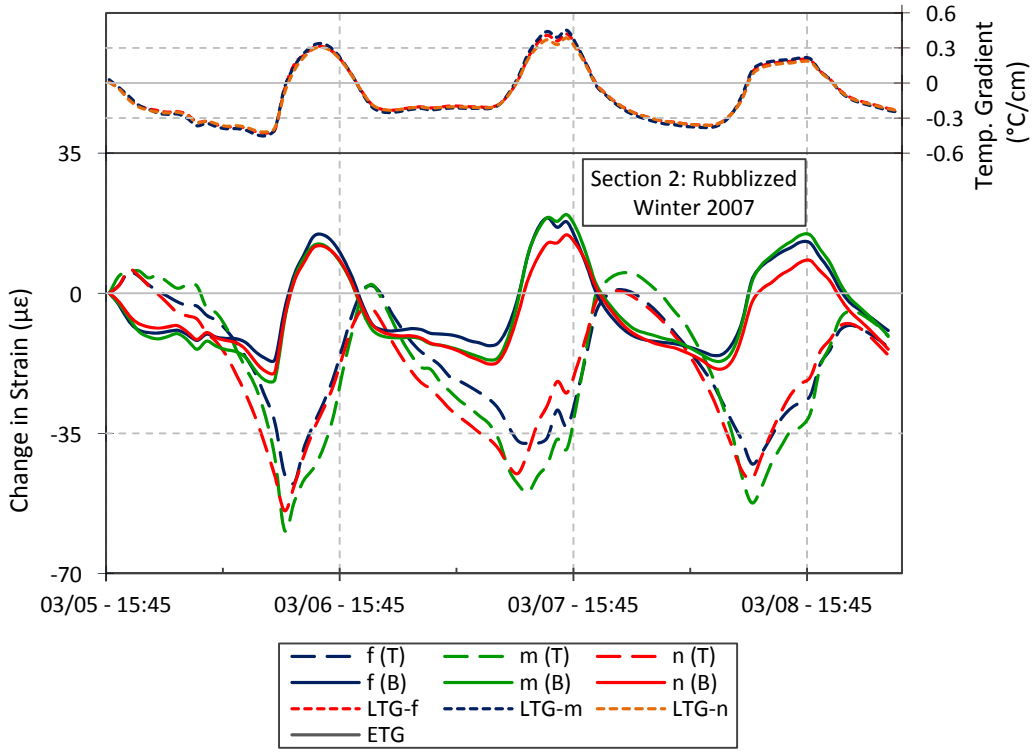

Figure 50. Change in strains over 3.5 days for the rubblized section, March 5-9, 2007 (1 C°/cm = 4.6 °F/in).

The maximum compressive strains in the untreated section were experienced at the top surface in the center of the slab (i.e. location ***n***) while the maximum tensile strains occurred at the mid-slab location along left wheel path (i.e. location ***m***). Notice that in general the compressive strains in general were higher than the tensile strains. Additionally, the section experienced a period of 36 hours with a low variation of strains between the 19:30 March 15 and 7:30 March 17 (see Figure 52). This behavior is related to a period of low solar radiation and a drop in the average air temperature of approximately 15°C (59°F). The minimum and maximum average air temperature during the period shown were –12.3°C (9.9°F) and 14.2°C (57.6°F)

respectively while the pavement temperatures varied from -9°C (-15.8°F) to 12.1°C (53.8°F) (see Appendix E).

Although direct comparisons between the three sections are not suitable for the winter periods described before, it can be seen that the untreated section underwent higher strains compared to the other two sections. However, it also can be seen that the untreated section experienced a maximum daily change in the temperature gradient of maximum ±0.89C°/cm (4.1 °F/in) while the rubblized and B&S section maximum daily change in the temperature gradient were approximately ±0.75C°/cm (3.4°F/in).

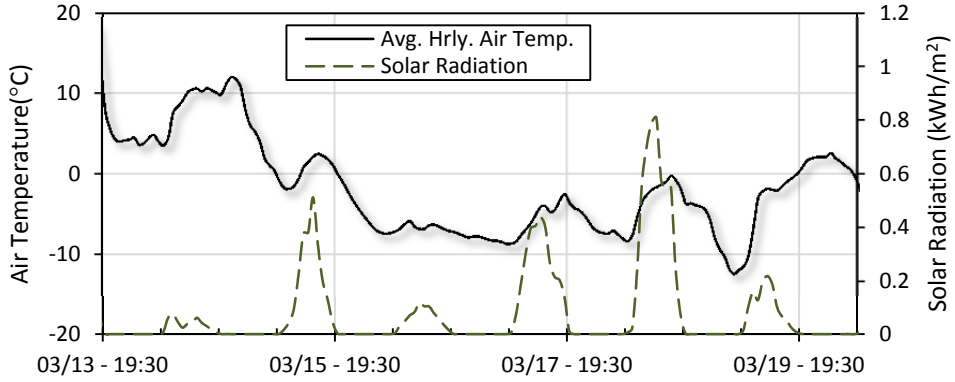

Figure 51. Average air temperature and solar radiation, March 13-19, 2007 (-20°C = 4°F, 20°C = 68°F, 1kWh/m² = 317.21 Btu/ft²).

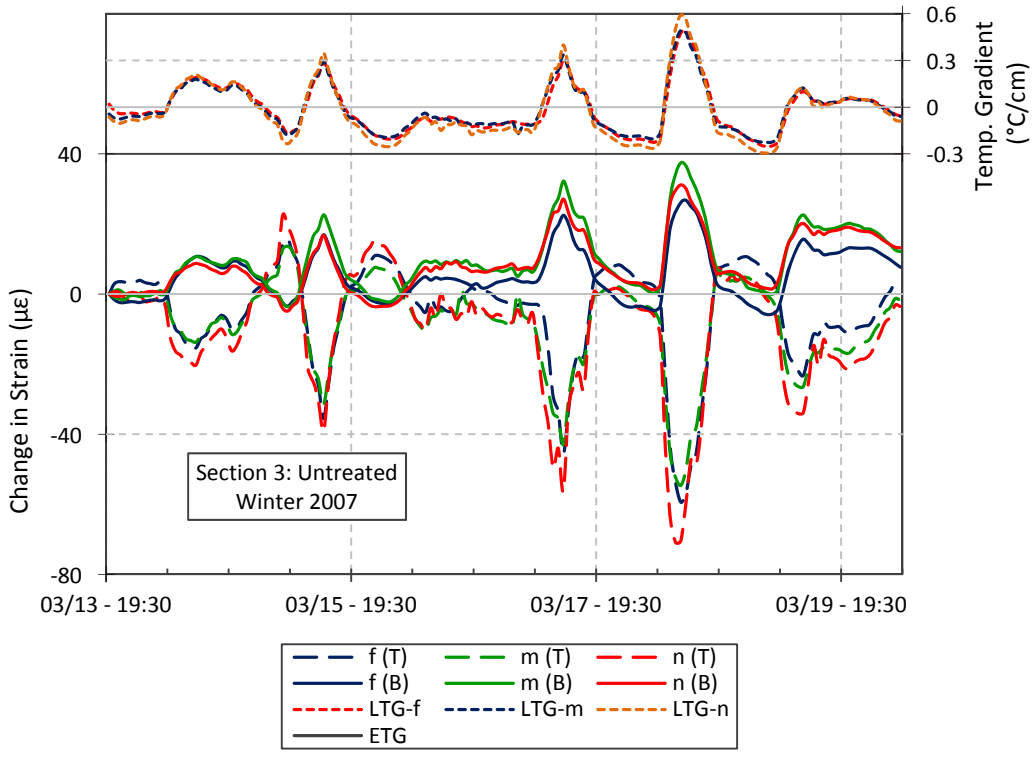

Figure 52. Change in strains over 6.5 days for the untreated section, March 13-19, 2007 (1 C°/cm = 4.6 °F/in).

The change in stresses within the pavement structure during the winter 2006-2007 periods showed the same trend of the corresponding strain responses above described. The maximum, minimum and average values for the strain and stresses for each section are discussed herein below.

5.4.1.4 Spring 2007 (May 27 - June 7, 2007)

The next set of strain observations were made in late spring 2007, during May 27-June 7. The average air temperature and solar radiation are graphed in Figure 53, which shows a period of low solar radiation and a small variation of the average air temperature. The average air temperature between May 27 and June 7 varied between 3.6°C (38.5°F) and 30.1°C (86.2°F) while the pavement temperatures ranged between 11.5°C (52.7°F) and 41.7°C (107.1°F) (see Appendix E). The change of strain of the rubblized and untreated sections during a period of 264 hours (11 days) is shown in Figure 54 and Figure 55 respectively. These figures included the strains in the center of the slab as well as the strains at the mid-span location along the right and left wheel paths as before. The response of the two sections presented similar behavior with a period of three days of low variation of the strains compared to the rest of the time shown. The rubblized section consistently experienced higher compressive and tensile strains at the mid-span along the inner wheel path (i.e. location ***m***) than it did in other locations. On the other hand, the strains in the center of the slab and right wheel path (i.e. locations ***n*** and ***f*** respectively) presented similar values during the analyzed period. It can be seen that the top of the slab experienced high compressive strains most of the time and the tensile strains did not exceed 15με for the period shown. In contrast, the bottom of the slab experienced smaller variations of the strains with a maximum range of 89.8με.

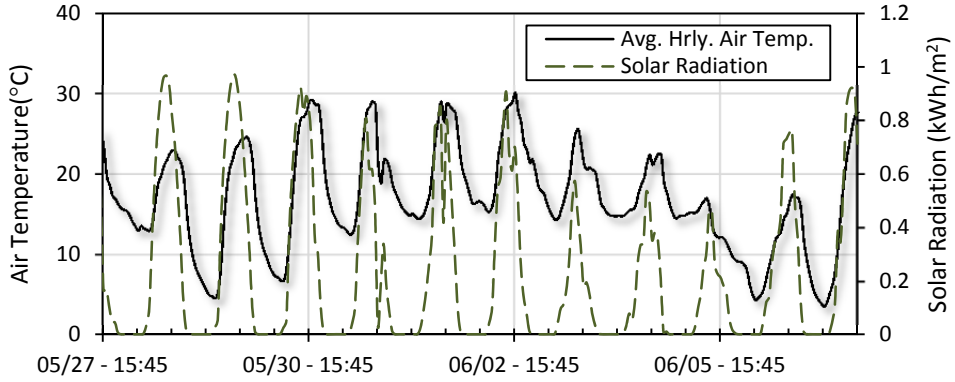

Figure 53. Average air temperature and solar radiation May 27 to June 7, 2007 (0°C = 32°F, 40°C = 104°F, 1kWh/m^2 = 317.21 Btu/ft^2).

In the same way to the rubblized section, the untreated section experienced higher compressive strains at the top of the slab while the range of variation of strains at the bottom was smaller. The top of the slab in the center and mid-span location along of the inner wheel path experienced similar compressive strains while the center of the slab experienced higher tensile strains for almost all the time shown in Figure 54. The maximum tensile strains in the center of the slab occurred during the night time, which stayed below 46με. Notice that this coincides with the discussed in Section 5.3 regarding the upward curling of the slabs. In general, the rubblized and untreated section underwent higher compressive strains than tensile strains during this period. This behavior is characteristic of the spring periods selected as can be seen in Appendix D. Data corresponding to the B&S section for the spring 2007 period were not available.

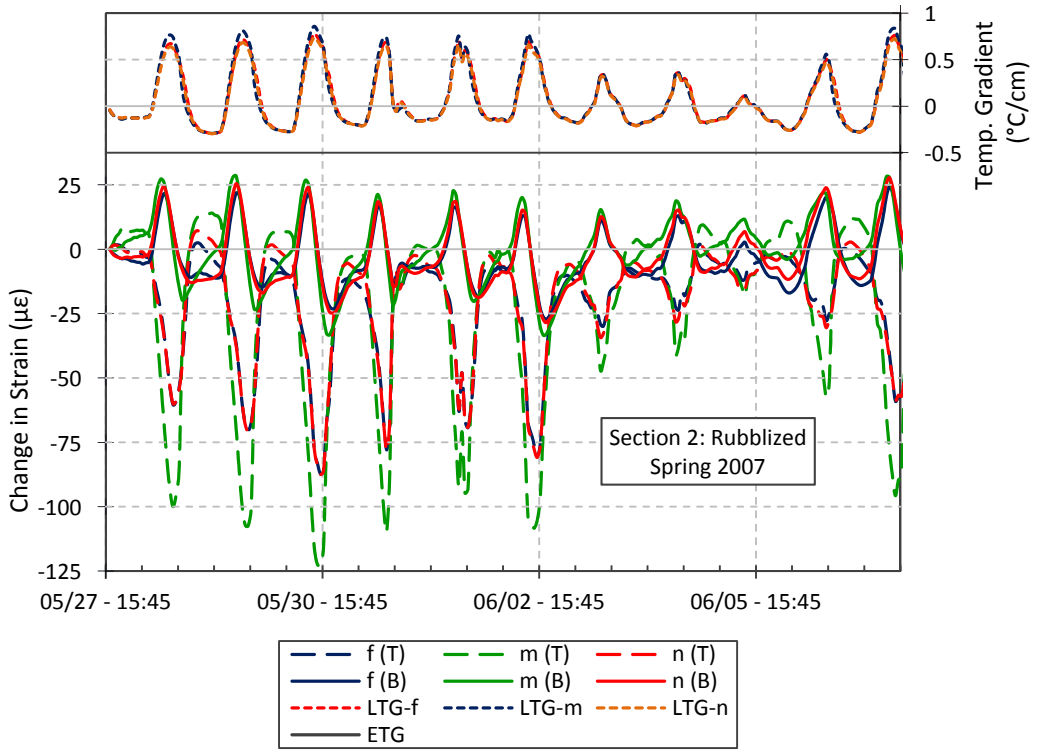

Figure 54. Change in strains over 11 days for the rubblized section, May 27 to June 7, 2007 (1 C°/cm = 4.6 °F/in).

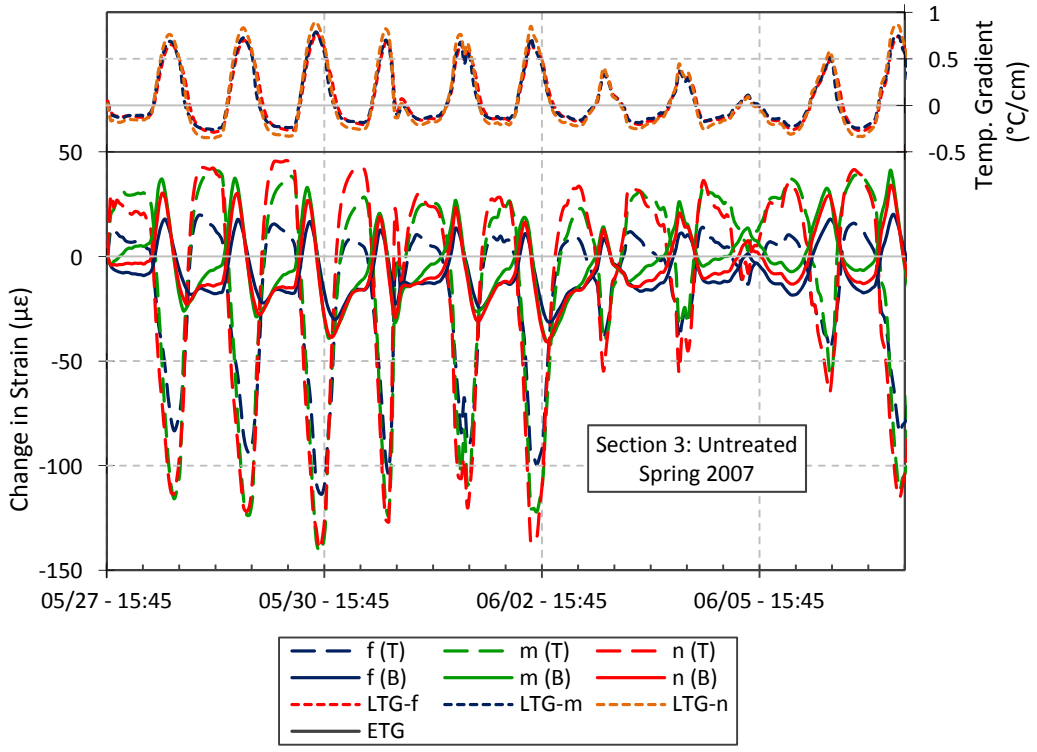

Figure 55. Change in strains over 11 days for the untreated section, May 27 to June 7, 2007 (1 C°/cm = 4.6 °F/in).

The change in stresses within the pavement structure during the spring 2007 period behaves identical to the corresponding strains responses because of Equation (13). The maximum, minimum and average values for the strain and stresses for each section are discussed below.

5.4.1.5 Summer 2007 (August 21-25, 2007)

The next set of strain observations were made in August 21-25, 2007. The average air temperature and solar radiation are graphed in Figure 56. Figure 57 shows the change in strains for the B&S section during the same summer period. Although the integrity of the data shown is low, it can be seen that the section experienced the higher compressive and tensile strains in the center of the slab (i.e. location ***n***). However, the maximum strains occurred in the location ***e*** (not shown in Figure 57) for the top and bottom of the slab. The tensile strains at the mid-span location along the wheel paths (i.e. location ***f*** and ***m***) were similar while the compressive strains at the same locations were slightly different. It can be seen also that the B&S section underwent higher compressive strains than tensile strains for the daylight periods (see Figure 56). Notice that the higher tensile and compressive strains occurred for periods of low solar radiation and low changes in the average air temperature in August 22 and 23 compared to the following two days as it can be seen in Figure 56. This could be a contradictory behavior since it is expected that the higher changes in air temperatures and solar radiation are associated with higher strains. However, notice that the lack of data during the last two days in Figure 57 coincide with the higher drop of temperature during the period shown. Therefore, the slab could have experienced higher compressive strains during the night time in August 24 compared to the strains experienced the two days before. The average air temperature varied from 13.6°C (56.5°F) to 31.6°C (88.9°F) while the pavement temperatures were between 18.5°C (65.3°F) and 33.3°C (91.9°F) (see Appendix E). Strains for the night times were not available. Data corresponding to the rubblized and untreated sections for the summer 2007 period were not available.

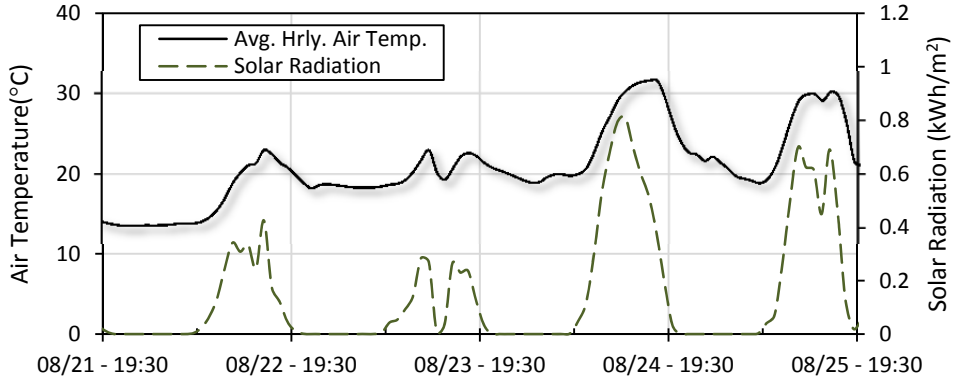

Figure 56. Average air temperature and solar radiation August 21-25, 2007 (0°C = 32°F, 40°C = 104°F, 1kWh/m^2 = 317.21 Btu/ft^2).

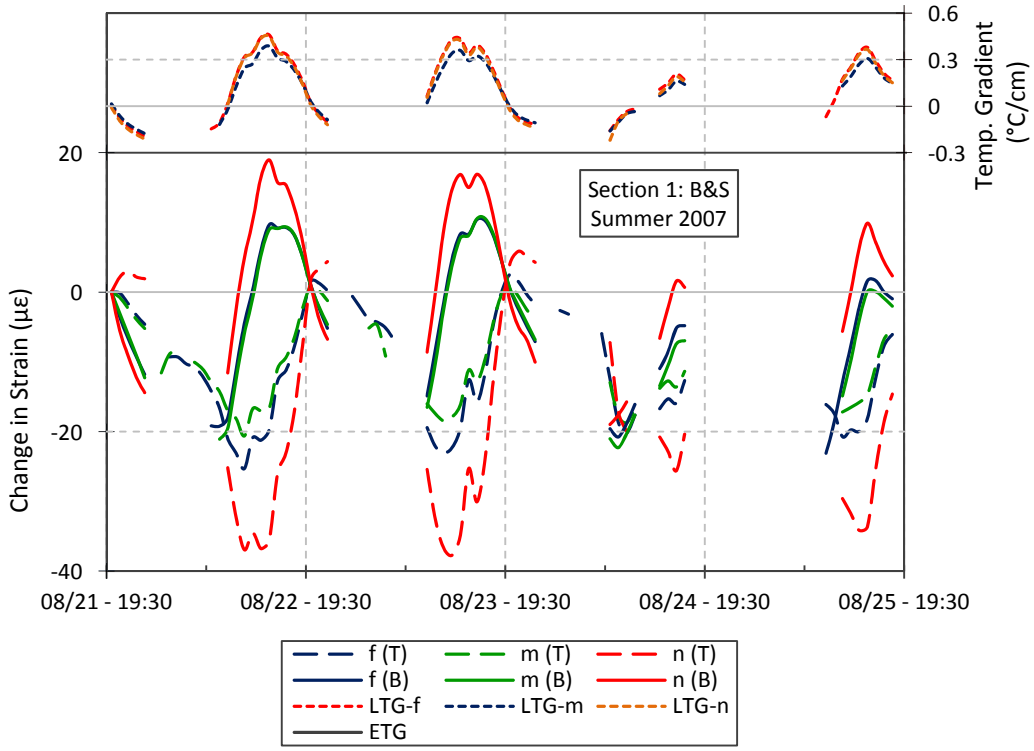

Figure 57. Change in strains over 4 days for the B&S section, August 21-25, 2007 (1 C°/cm = 4.6 °F/in).

5.4.1.6 Fall 2007 (October 21-30, 2007)

This measurement period includes one day of low solar radiation and total precipitation of 46.23mm (1.82 in) on October 22 and another two days of low solar radiation from October 26-27, shown in Figure 58, which both led to small variations in the temperature gradients, shown in Figure 59, Figure 60, and Figure 61 for the break and seat, rubblized, and untreated sections, respectively. Moreover, during these two periods the three sections experienced mostly compressive strains. The average air temperature varied from -3.25°C (26.2°F) to 24°C (75.2°F) while the maximum and minimum pavement temperatures were 1.9°C (35.4°F) and 25.3°C (77.5°F) respectively (see Figure 59 and Appendix E). The change of strains during a period of 216 hours (9 days) for each of the experimental sections is shown in Figure 59, Figure 60, and Figure 61. The strains shown correspond to those at the mid-span location along both wheel paths and the center of the slab. The three sections showed similar behaviors with two periods of about 12 hours with a low variation of strains.

The B&S section consistently experienced higher strains at top and bottom of the slab in location of sensor ***e*** (not shown in Figure 59). Recall that the same occurred during the fall 2006 period as well as for the maximum compressive strains during the summer 2006. The section underwent higher compressive and tensile strains at the center of the slab than the inner and outer wheel paths (i.e. locations ***f*** and ***m*** respectively). Moreover, the strains at the bottom of the slab were similar at locations ***m*** and ***f***, while the strains at the top of the slab for the same locations were different. The rubblized section consistently experienced higher strains at the mid-span location along the left wheel path (i.e. location ***m***). However, the strains values at the bottom in the center of the slab and right wheel path were close to those at the left wheel path. This

behavior is similar to the fall 2006 period described above. The untreated section underwent higher compressive strains at the top surface in the center of the slab and similar tensile strains at the bottom surface at the mid-span location along the inner wheel path and center of the slab. The untreated section experienced higher strains than the rubblized and B&S sections with the B&S section experiencing the lowest range of variation in strains. In general, the three sections experienced higher compressive strains with small values of tensile strains. This behavior contrasts with the trend shown for the other fall periods in Table 5 where the three sections experienced higher tensile strains than compressive strains.

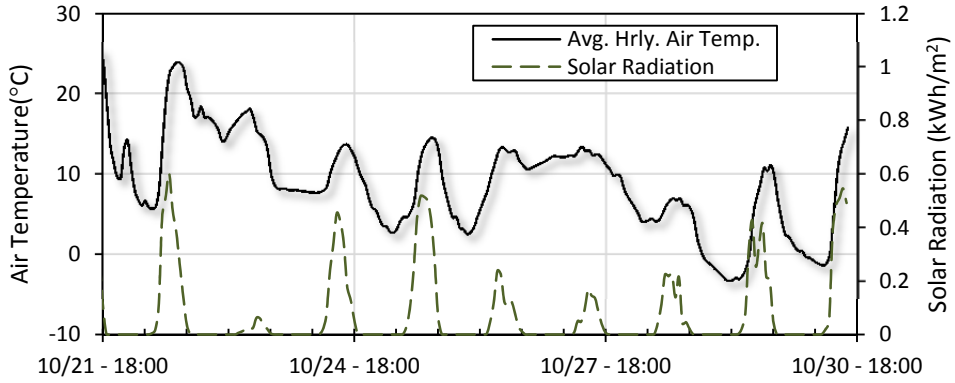

Figure 58. Average air temperature and solar radiation, October 21-30, 2007 (-10°C = 14°F, 30°C = 86°F, 1kWh/m^2 = 317.21 Btu/ft^2).

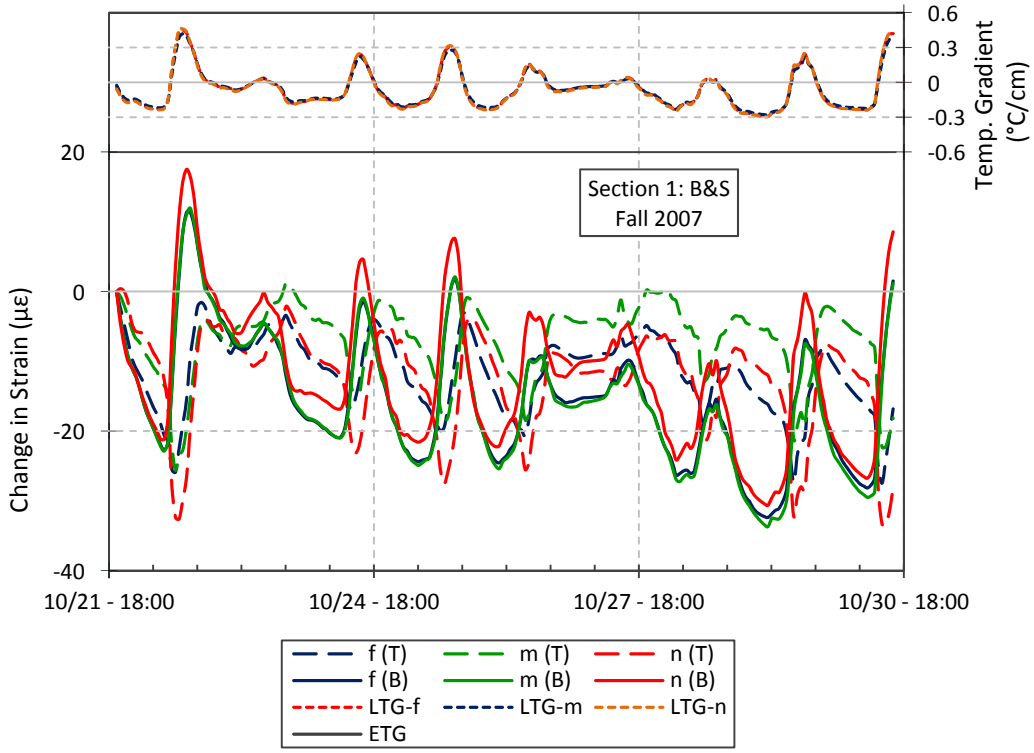

Figure 59. Change in strains over 9 days for the B&S section, October 21-30, 2007 (1 C°/cm = 4.6 °F/in).

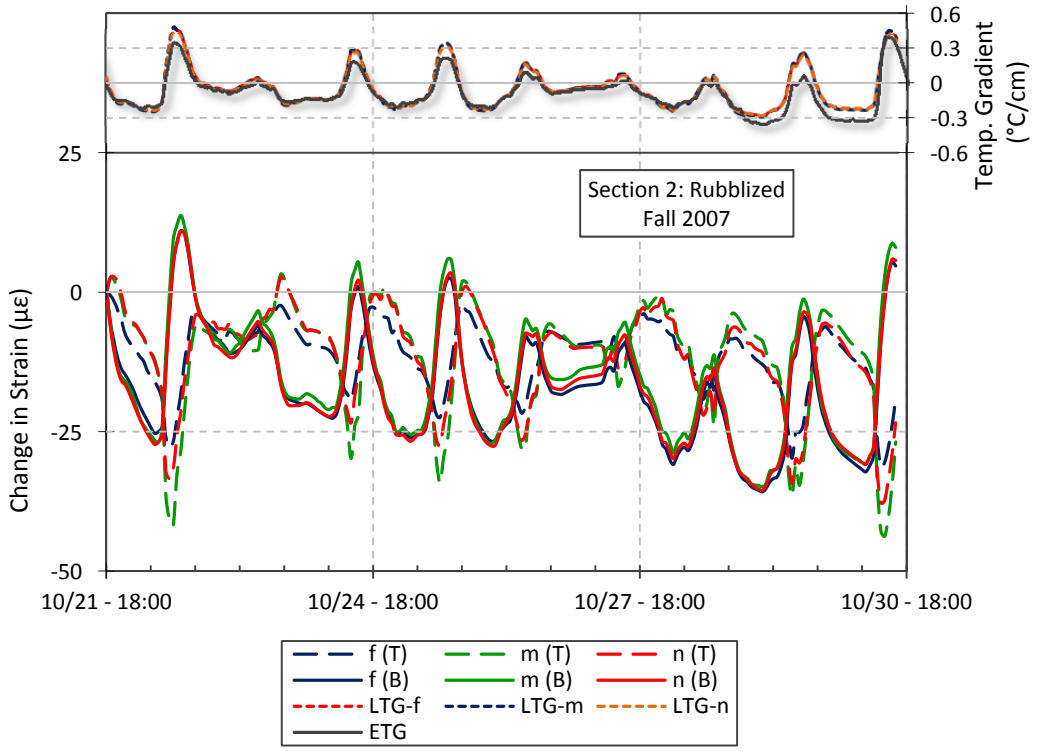

Figure 60. Change in strains over 9 days for the rubblized section, October 21-30, 2007 (1 C°/cm = 4.6 °F/in).

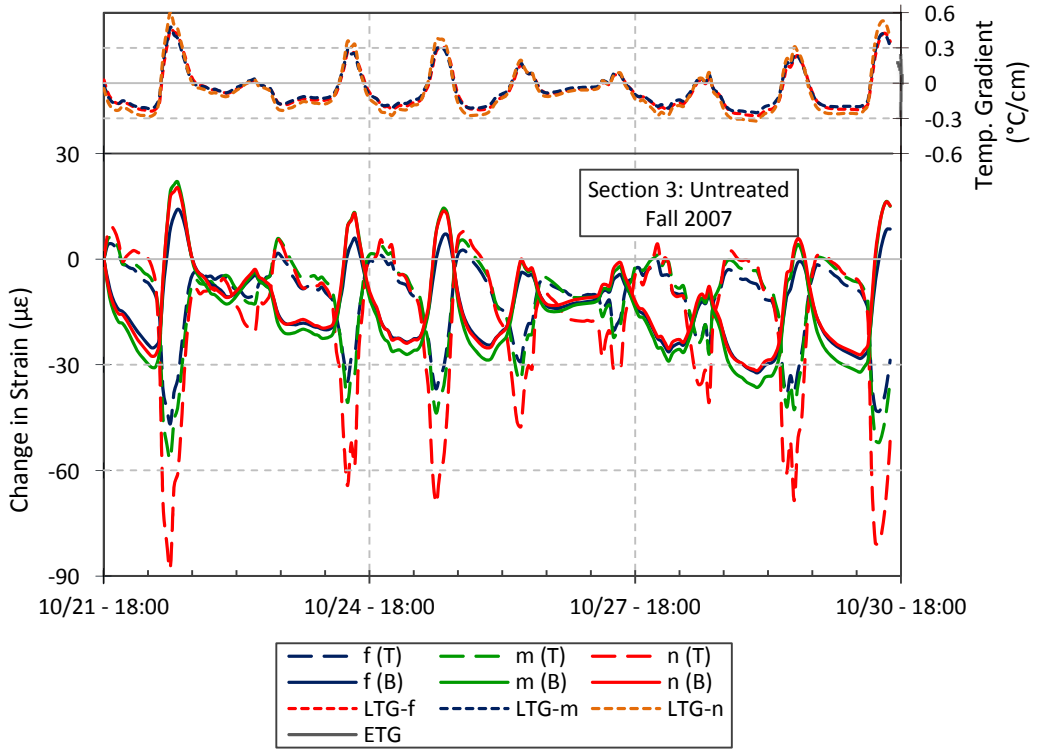

Figure 61. Change in strains over 9 days for the untreated section, October 21-30, 2007 (1 C°/cm = 4.6 °F/in).

5.4.1.7 Spring 2008 (April 26-May 6, 2008)

Figure 62, Figure 63, and Figure 64 show the change of strains during a period of 10 days for the three experimental sections. The response of the three sections was similar and presented a lower variation of the change in strains during a period of 36 hours between April 28th and the 29th. This could have been the result of low solar radiation, low changes of air temperatures, and presence of rain. Unfortunately, weather data for the spring 2008 were not available and therefore the correlation of the weather and strain response cannot be established. The pavement temperatures varied from 3.3°C (37.9°F) to 30.6°C (87.1°F) respectively. The B&S section experienced consistently higher compressive and tensile strains in the center of the slab (i.e. location ***n***) than at the mid-slab location along the inner and outer wheel paths. However, the maximum tensile strains occurred at the location ***e*** (not shown in Figure 62) while similar compressive strains higher than at other sensor's location were experienced at both ***n*** and ***e*** locations. The tensile strains at the bottom surface of the slab were similar for the center and mid-span locations along the right and left wheel paths (i.e. location ***f*** and ***m*** respectively). The rubblized section experienced consistently higher compressive and tensile strains at the mid-slab location ***m*** than any other sensor's location. The center of the slab and mid-span location on the outer wheel path experienced similar compressive and tensile strains. For the untreated section, the maximum compressive strains occurred at the top surface in the center of the slab while the maximum tensile strains consistently occurred at the mid-span location along the left wheel path. Additionally, the untreated section experienced higher strains than the other two sections during the spring 2008 period described here. The change in stresses during this period showed the same trend corresponding to the respective strain responses.

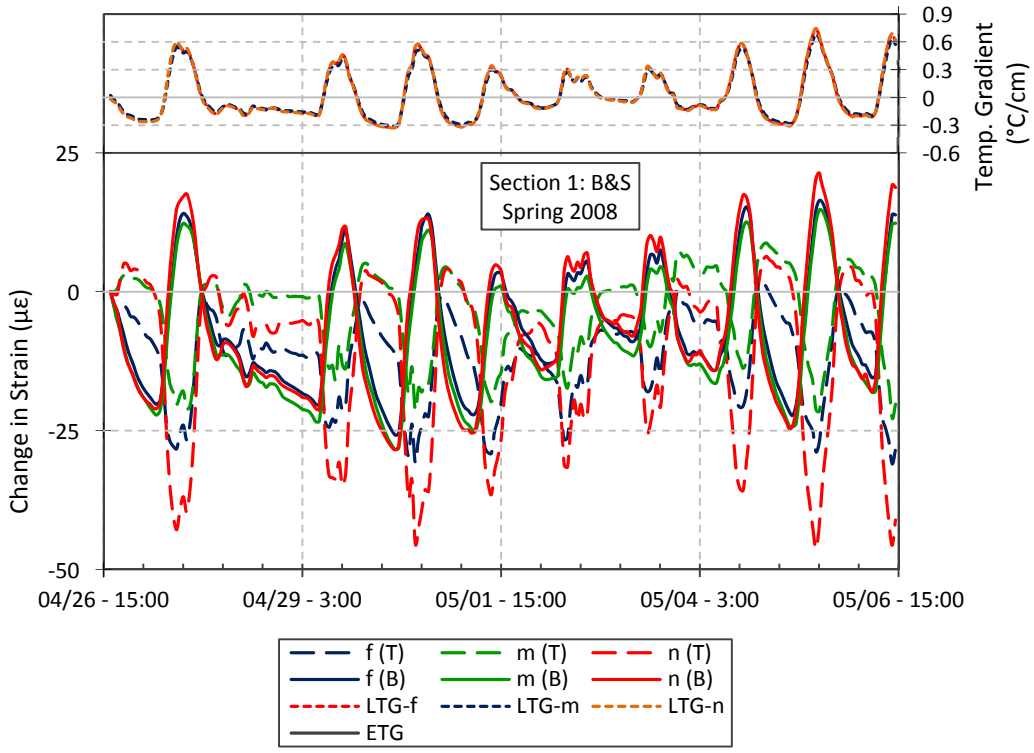

Figure 62. Change in strains over 10 days for the B&S section, April 26-May 6, 2008 (1 C°/cm = 4.6 °F/in).

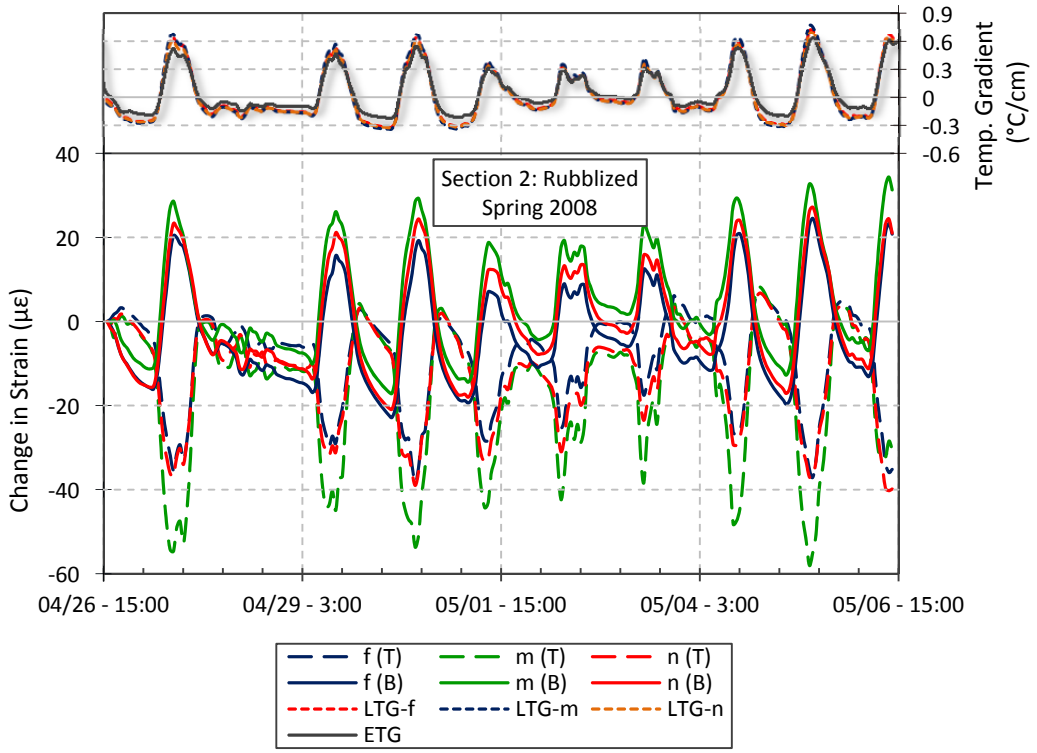

Figure 63. Change in strains over 10 days for the rubblized section, April 26-May 6, 2008.

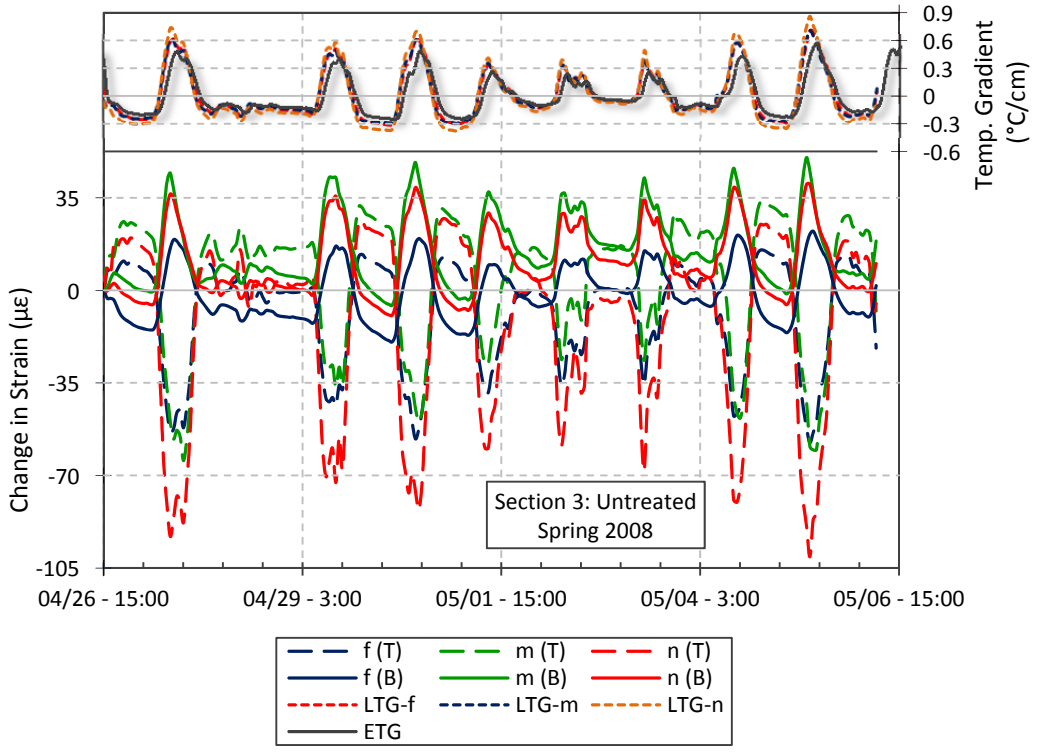

Figure 64. Change in strains over 10 days for the untreated section, April 26-May 6, 2008 (1 C°/cm = 4.6 °F/in).

5.4.1.8 Summer 2008 (August 23-September 3, 2008)

This late summer period includes a period of low solar radiation and small air temperature changes on August 28 as shown in Figure 65. The average air temperature between August 23 and September 3 varied from 7.6°C (45.7°F) to 29.3°C (84.7°F) while the pavement temperatures were between 16.5°C (61.7°F) and 40.5°C (104.9°F) (see Appendix E).The change of strains during a period of 264 hours (11 days) for each of the experimental sections is shown in Figure 66, Figure 67, and Figure 68. The section experienced similar behavior with a common period of about 36 hours where the change in strain was lower than the rest of the 11 days shown. During this period, the sections experienced mostly compressive strains at both top and bottom of the slab with the exception of the untreated section, which experienced consistently compressive and tensile strains at top and bottom of the slab respectively.

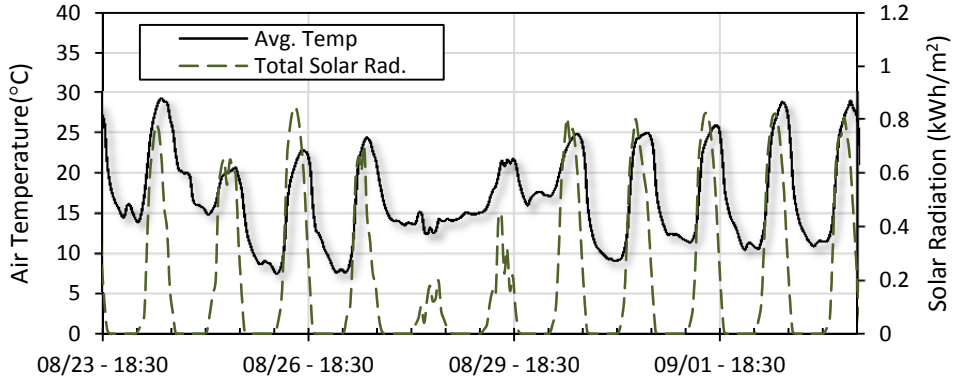

Figure 65. Average air temperature and solar radiation August 23-September 3, 2008 (0°C = 32°F, 40°C = 104°F, 1kWh/m^2 = 317.21 Btu/ft^2).

The B&S section experienced higher tensile strains at the bottom of the slab in location ***e*** (not shown in Figure 66) while the highest compressive strains were experienced at the top in the center of the slab as well as at the bottom in location ***g***. The center of the slab as well as the mid-span location on the right wheel path (i.e. location ***f***) experienced higher tensile strains than the strains experienced in location ***m*** at bottom of the slab. On the other side, the slab underwent higher compressive strains at the top of the slab in the center than in the ***f*** and ***m*** locations. For the rubblized section, the mid-span location along the left wheel path (i.e. location ***m***) experienced higher compressive and tensile strains than at any other sensor's location. This behavior is characteristic of all summer periods in Table 5. The center of the slab experienced similar tensile strains for the bottom of the slab to those of the location ***f*** on the right wheel path. The untreated section experienced higher tensile strains at the bottom of the slab in the mid-span location ***m***, while the higher compressive strains occurred in the center at the top of the slab. In general, the three sections underwent higher compressive strains than tensile strains during the period described. Moreover, the untreated section experienced higher strains than the rubblized and B&S sections. The change in stresses experienced by the experimental sections described the same trend corresponding to the respective strain responses.

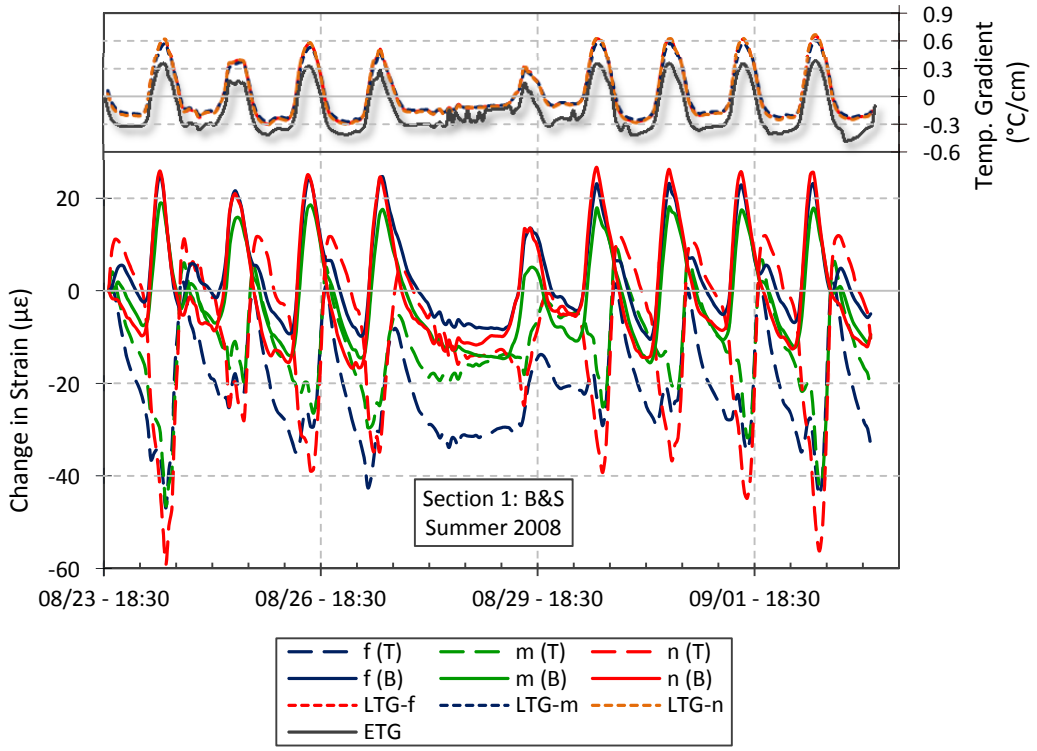

Figure 66. Change in strains over 11 days for the B&S section, August 23-September 3, 2008 (1 C°/cm = 4.6 °F/in).

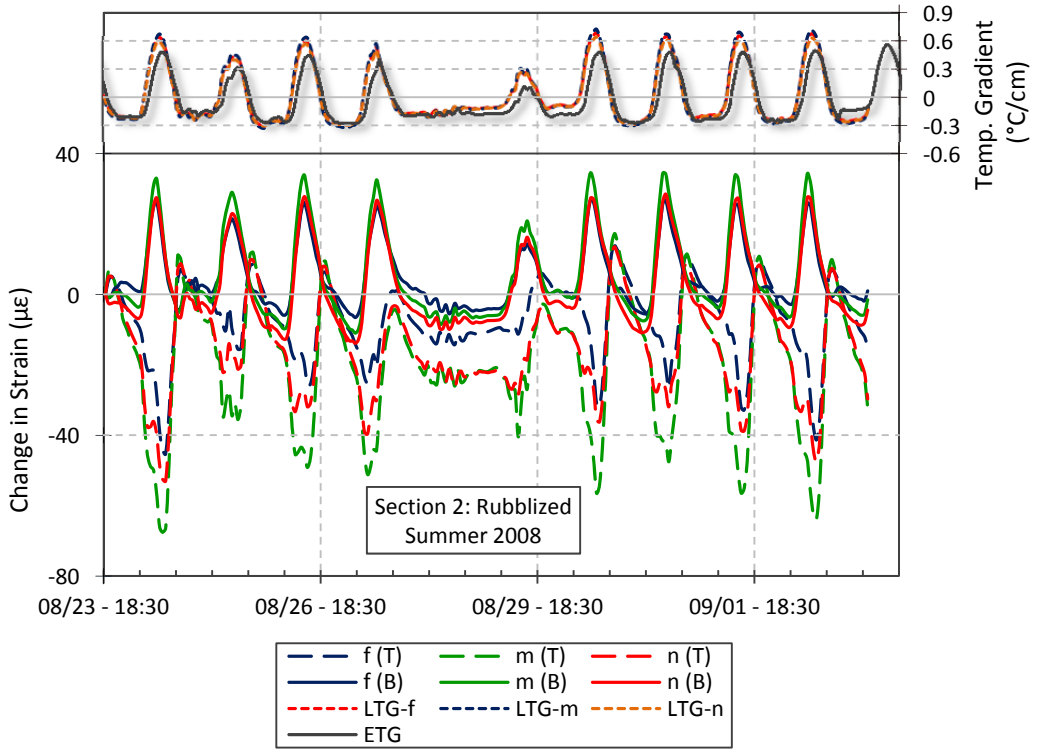

Figure 67. Change in sStrains over 11 days for the rubblized section, August 23-September 3, 2008 (1 C°/cm = 4.6 °F/in).

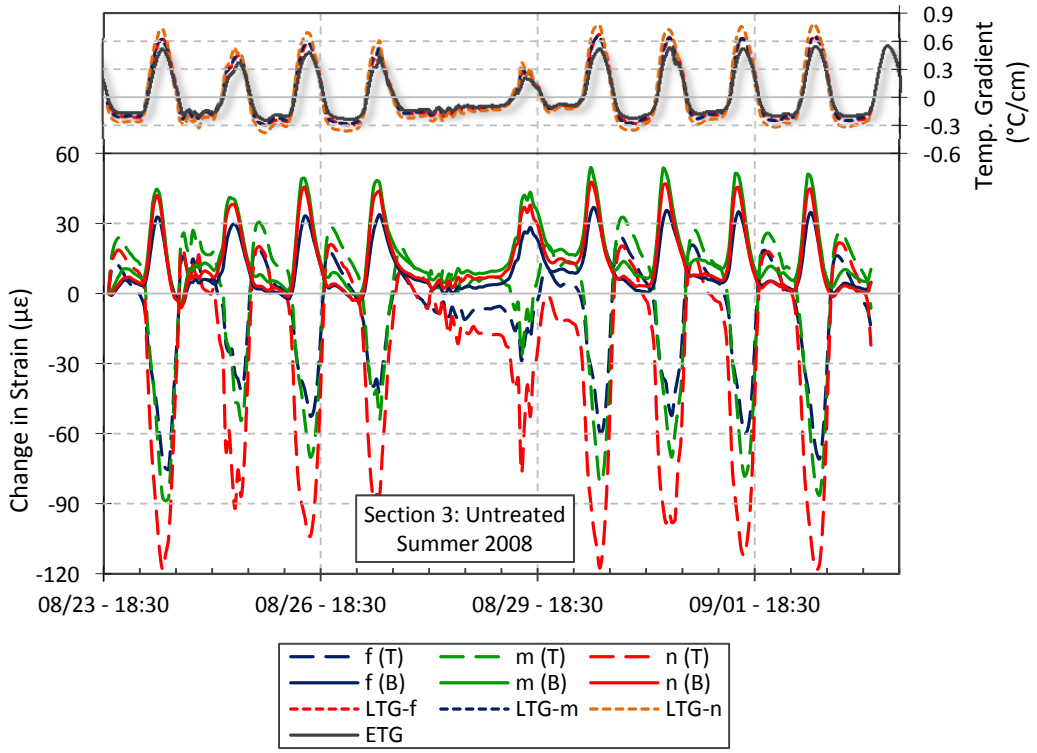

Figure 68. Change in strains over 11 days for the untreated section, August 23-September 3, 2008 (1 C°/cm = 4.6 °F/in).

5.4.1.9 Fall 2008 (October 6-9, 2008)

The next measurement session occurred October 6-9, 2008. This period included two days with only small changes in air temperature and low solar radiation on October 8-9 as can be seen in Figure 69. The average air temperature varied between -1.9°C (28.6°F) and 17.1°C (62.8°F) while the maximum and minimum pavement temperatures were 5.8°C (42.4°F) and 24.6°C (76.3°F) (see Appendix E). Figure 70, Figure 71, and Figure 72 show the change in strains during 72 hours (3 days) for the three experimental sections. The three sections experienced similar responses with small variation of the strains the last day of the period shown.

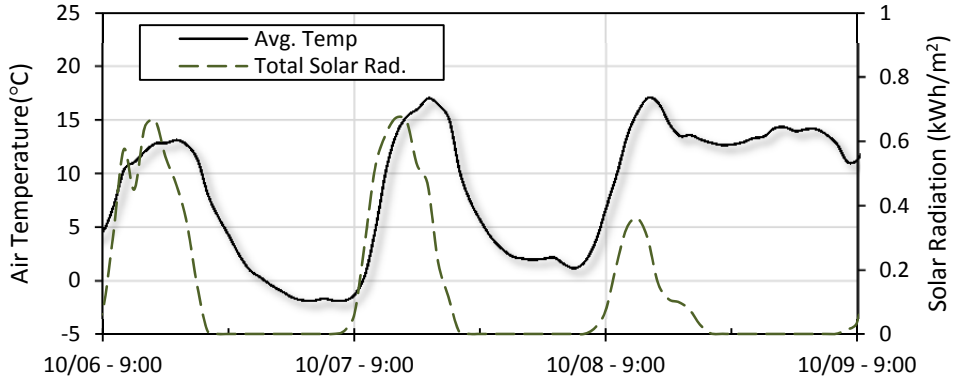

Figure 69. Average air temperature and solar radiation, October 6-9, 2008 (-5°C = 23°F, 25°C = 77°F, 1kWh/m^2 = 317.21 Btu/ft^2).

Change in strains for the B&S section was consistently higher at the corner location ***g*** on the right wheel path and location ***e*** (not shown in Figure 70) than at other location. The tensile strains at the bottom of the slab experienced in the mid-span location along the wheel paths were higher than the strains experienced at the bottom surface in the center of the slab (i.e. location ***n***). Moreover, the tensile strains at locations ***f*** and ***m*** were similar to each other while the compressive strains were consistently higher at the bottom surface in the center of the slab. The top of the slab experienced smaller tensile strains than at the bottom with the highest strains occurring at the center of the slab. For the rubblized section, the maximum tensile and compressive strains occurred consistently in the center and left wheel path for both top and bottom of the slab. However, the strains at the location ***m*** were slightly higher than in the center of the slab. Other locations experienced smaller changes than the location ***m*** and ***n*** experienced. The untreated section underwent higher tensile strains at the bottom of the slab in location ***m*** while the top surface in the center of the slab experienced the highest compressive strains. However, it can be seen that the tensile strains in the center of the slab were also higher than at any other sensor's location. This coincides with the upward curling behavior described above in Section 5.3. Notice that the three sections experienced higher tensile strains than compressive strains, which coincides with the trend shown in the fall 2006 period. Additionally, it can be seen that the untreated section underwent higher change in compressive and tensile strains than the rubblized and B&S sections. The change in stresses experienced by each section described the same trend corresponding to the respective strain responses.

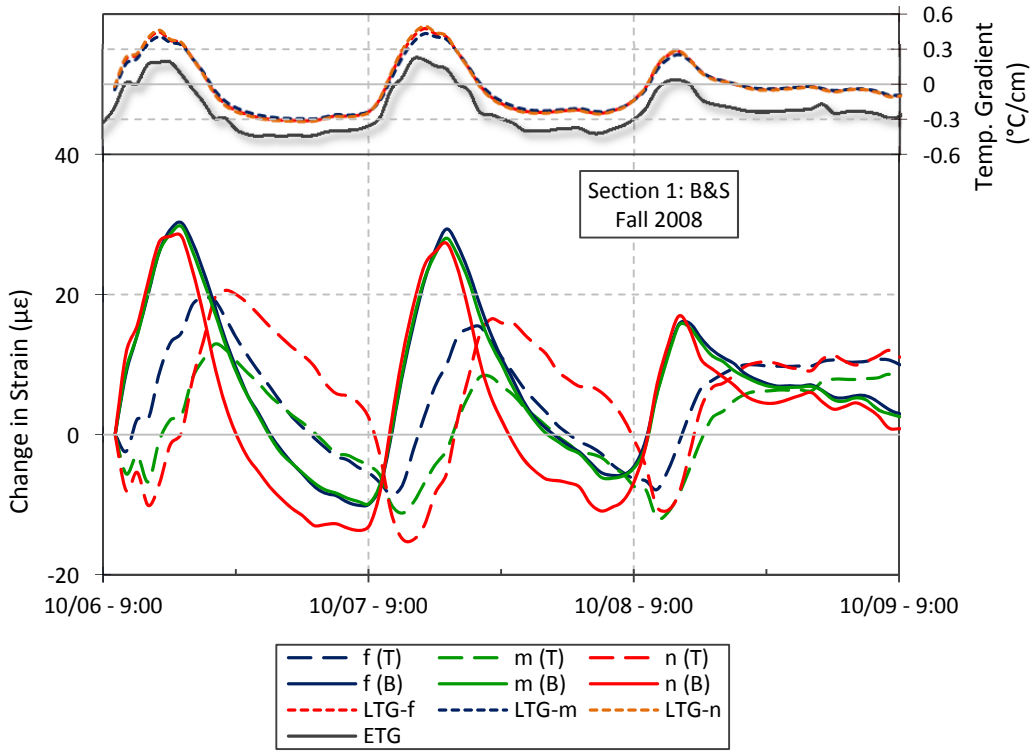

Figure 70. Change in strains over 3 days for the B&S section, October 6-9, 2008 (1 C°/cm = 4.6 °F/in).

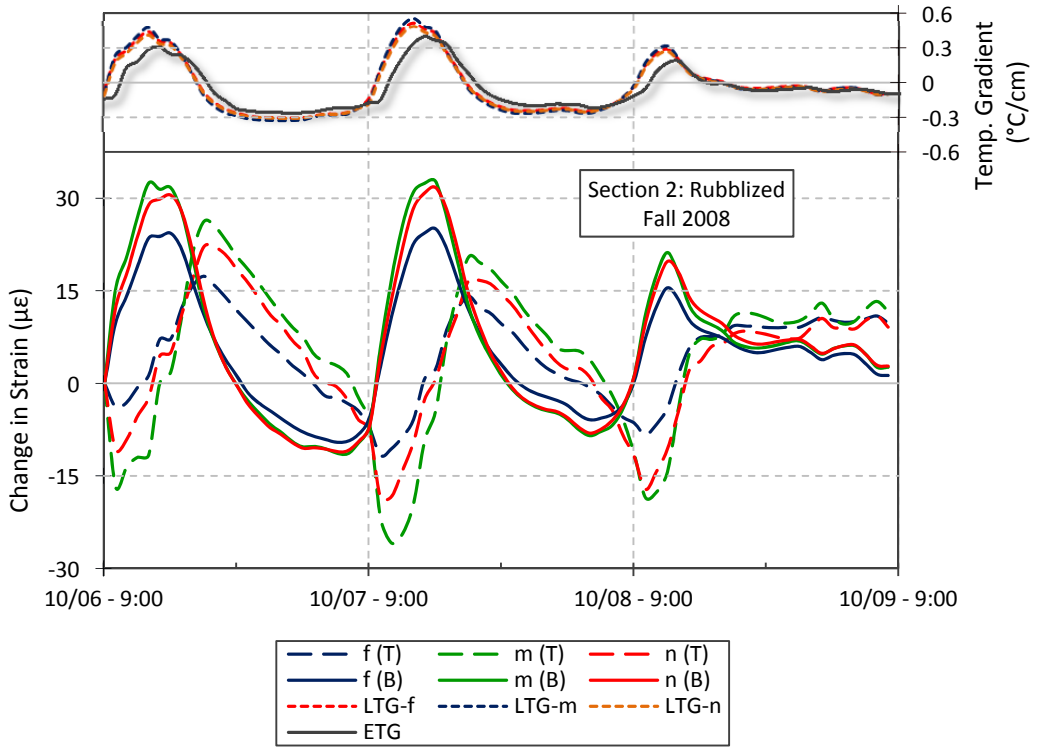

Figure 71. Change in strains over 3 days for the rubblized section, October 6-9, 2008 (1 C°/cm = 4.6 °F/in).

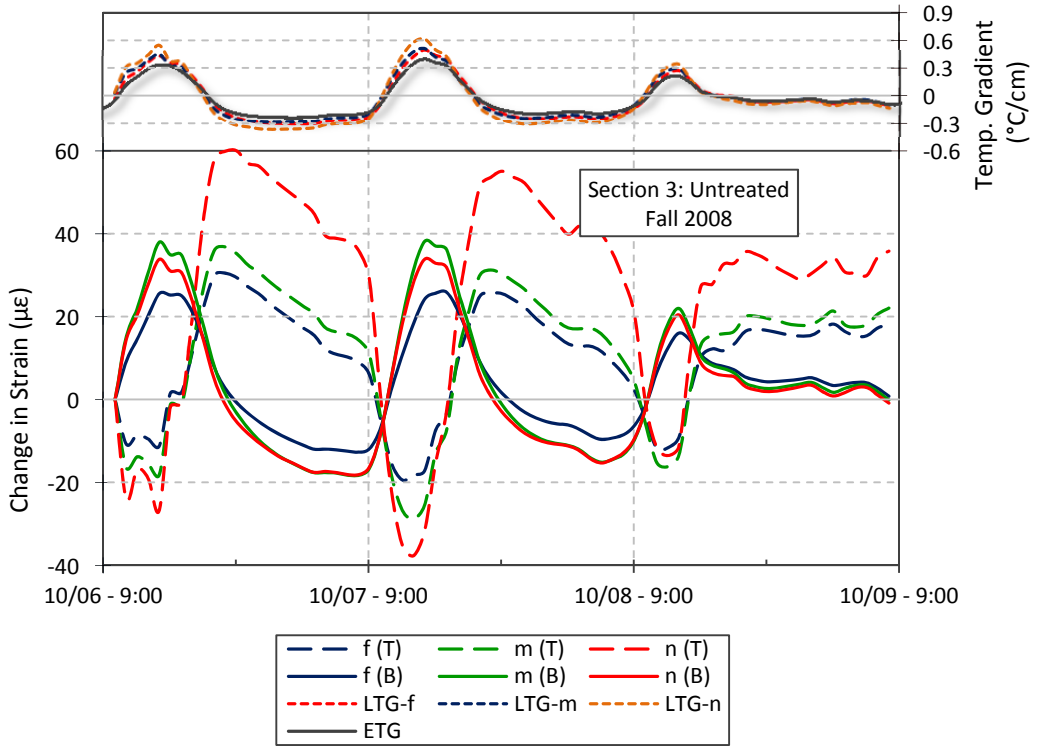

Figure 72. Change in strains over 3 days for the untreated section, October 6-9, 2008 (1 C°/cm = 4.6 °F/in).

5.4.1.10 Spring 2009 (May 1-11, 2009)

Figure 73, Figure 74, and Figure 75 show the change in strains during 264 hours (11 days) for the B&S and rubblized sections, and 240 hours (10 days) for the untreated section. The three sections experienced similar responses with similar daily variations of temperature gradients. Moreover, the temperature gradients as well as the change of the strains presented a regular behavior, suggesting that no particular weather changes such as drop of temperatures or low solar radiation occurred during the period shown here. Unfortunately, weather data for the spring period 2009 were not available and therefore the relationship with the strain response cannot be established. The pavement temperatures during May 1st to the 11th varied between 6.8°C (44.2°F) and 31.5°C (88.7°F) (see Appendix E).

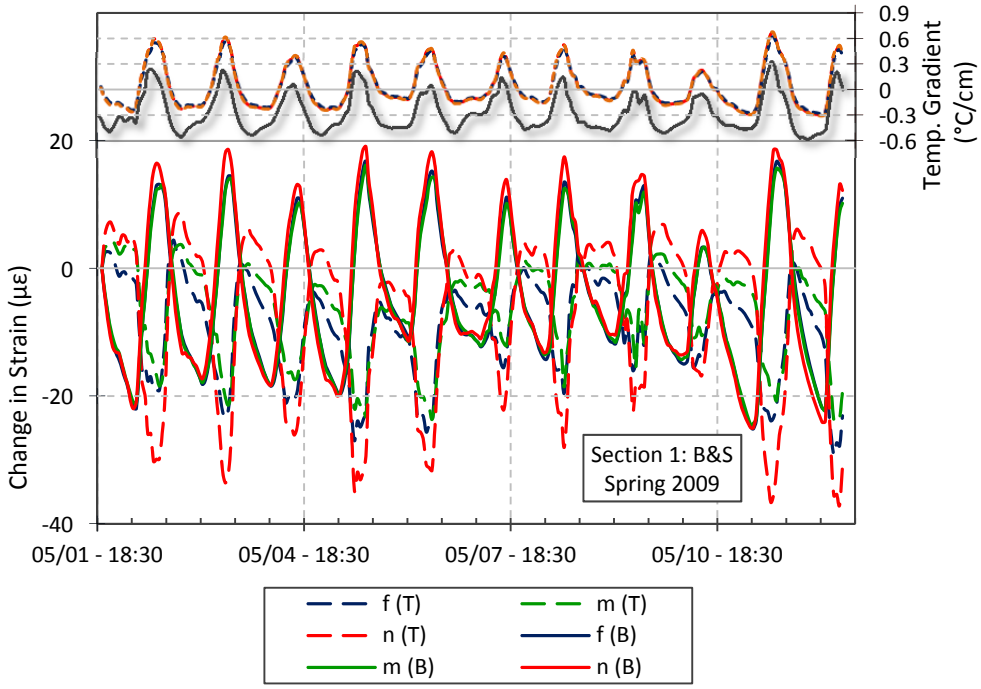

Figure 73. Change in strains over 11 days for the B&S section, May 1-11, 2009 (1 C°/cm = 4.6 °F/in).

The B&S section consistently experienced higher strains at the top and bottom of the slab in location ***e*** (not shown in Figure 73). The center of the slab experienced higher compressive and tensile strains at the top and bottom of the slab respectively than at the mid-span location along the wheel paths (i.e. location ***f*** and ***m***). However, the tensile strains at the bottom of the slab in locations ***f*** and ***m*** were just slightly smaller than at the center of the slab. For the rubblized section, the highest change in strains at top and bottom of the slab occurred in location ***m*** along the inner wheel path. Moreover, while the rubblized section experienced smaller tensile strains at the locations ***m*** and ***f*** for the bottom of the slab, these were close to the values at the location ***n*** (i.e. center of the slab). The compressive strains were similar for both locations at the mid-span along the wheel paths. The untreated section experienced the highest compressive strains in the center of the slab at the top surface while the maximum tensile strains occurred at the bottom of the slab in the mid-span location ***m***. The tensile strains at the mid-span location ***f*** were lower than the strains underwent by the slab in the center and mid-span location ***m*** for both top and bottom surfaces. In general, the three sections underwent higher compressive strains than tensile strains.

Moreover, the untreated section higher experienced higher strains than the rubblized and B&S sections. The change in stresses for each section during the spring 2009 period described the same trends as the corresponding strain responses.

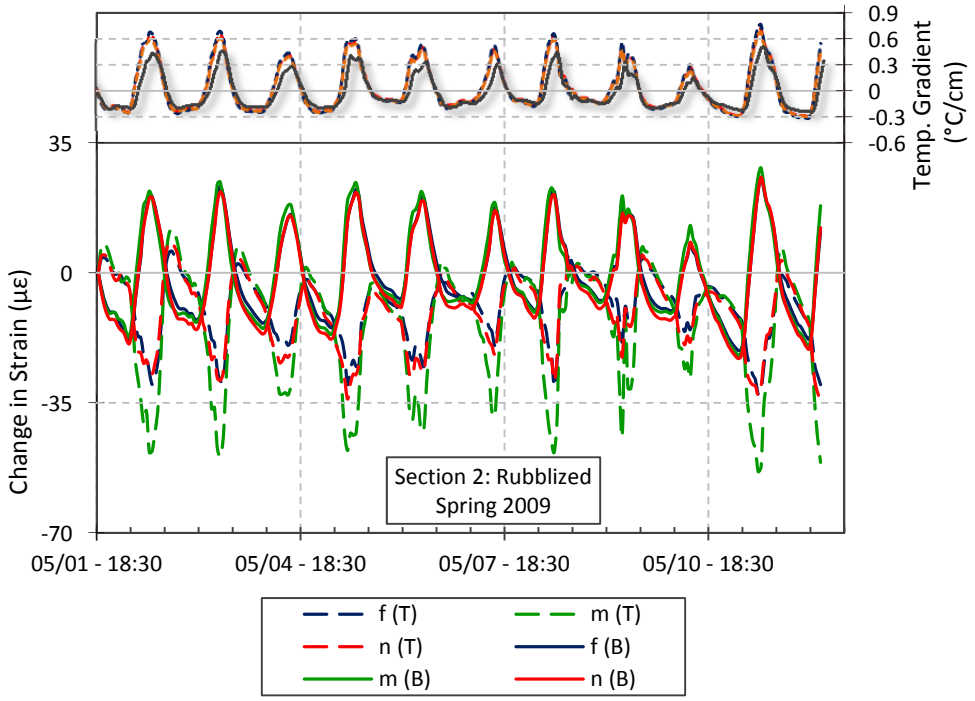

Figure 74. Change in strains over 11 days for the rubblized section, May 1-11, 2009 (1 C°/cm = 4.6 °F/in).

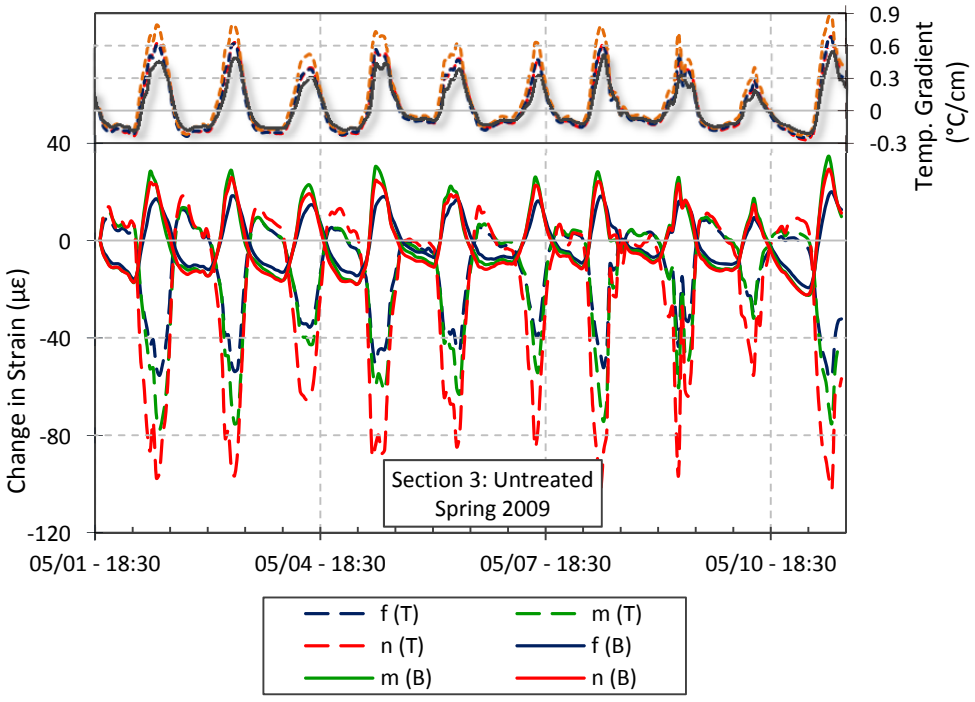

Figure 75. Change in strains over 10 days for the untreated section, May 1-11, 2009 (1 C°/cm = 4.6 °F/in).

5.4.2 Discussion of Long-Term Pavement Behavior

The change in strain responses of each experimental section during the different selected periods in Table 5 were described in the previous section. In this description it was mentioned which sensor location experienced the maximum compressive and tensile change in strains. Moreover, which of those locations consistently showed the highest values for the top and bottom of the slab was described. Additionally, it was highlighted which sensors consistently presented the highest $\Delta\varepsilon$ in the case that it did not correspond to the responses shown for the mid-span locations along the wheel paths and the center of the slab. Showing consistently higher compressive or tensile change in strains means that the sensor experienced in average higher changes compared to the other sensors during the time period analyzed. The selection of what sensor consistently experienced the highest $\Delta\varepsilon$ was based on the average value of the change in strains for positive and negative values separately. Thus, the sensor with the consistently highest positive or negative $\Delta\varepsilon$ was the sensor with highest average of $\Delta\varepsilon$. The average change in strains provides the general picture of the response of the strains for the analyzed period. Thus, it tells whether a specific location within the slab underwent mostly compressive or tensile strains due to environmental effects during a determined period as well as an average of the change in the stresses at that location. The average of the tensile and compressive change in strains was calculated using the following expressions,

$$(T\Delta\varepsilon)_{Aver.} = \frac{1}{(t_f - t_i)} \int_{t_i}^{t_f} [(\Delta\varepsilon)_+]\, dx \tag{15}$$

$$(C\Delta\varepsilon)_{Aver.} = \frac{1}{(t_f - t_i)} \int_{t_i}^{t_f} [(\Delta\varepsilon)_-]\, dx \tag{16}$$

where,

$(\Delta\varepsilon)_+ =$ The change of strain response discarding the negative values (με)

$(\Delta\varepsilon)_- =$ The change of strain response discarding the positive values (με)

$(T\Delta\varepsilon)_{Aver.} =$ The average tensile (positive) change in strains (με)

$(C\Delta\varepsilon)_{Aver.} =$ The average compressive (negative) change in strains (με)

$t_i, t_f =$ The initial and final dates of the period of time analyzed (days)

The average values given by Equations (15) and (16) allow the comparisons of the responses between different locations of the slab as well as the comparisons of the responses between different periods analyzed. Additionally, averaging the change in strains allows for comparisons of the strains response between the different sections. The values of the average positive and negative $\Delta\varepsilon$ were calculated from Equations (15) and (16) using the trapezoidal rule to approximate the integral and they are summarized in Appendix A. After calculating and plotting the average of $\Delta\varepsilon$, the locations that consistently experienced the highest values were identified and summarized in Table 6, Table 7, and Table 8. These tables show the sensors (in blue/bold) among the six locations that consistently experienced the maximum tensile or compressive average change in strains. Additionally, it is listed which of the locations ***f***, ***m*** or ***n*** consistently experienced the maximum compressive and tensile changes in strains. Multiple locations listed for tensile or compressive $\Delta\varepsilon$ indicates that these experienced similar or almost equal values.

Table 6. Locations with highest average Δε in B&S section.

Season		Broken and seated section			
		Top		Bottom	
		Tensile	Compressive	Tensile	Compressive
Summer 2006	July 8-17	f m **o**	**e** n	**e** n	**m**
	July 17-28	**n**	**e** f	**n**	**g** m
	Aug 5-9	**n**	**f**	**e** n	**g** m
	Aug 9-15	**n**	**f**	**e** n	**g** m
Fall 2006	Dec 1-3	**n**	**e** n	**e** n	m **n**
	Dec 3-7	**e** n	**n**	**m**	**e** n
Winter 2006-2007	Feb 9-15	**n**	**f**	**f**	**m**
	Feb 15-20	**m**	**e** n	**e** f	**m**
Summer 2007	Aug 21-25	**n**	**e** n	**e** n	**g** m
Fall 2007	Oct 21-30	**m**	**g** n	**e** n	**m**
Spring 2008	Apr 26-May 6	**e** m	**n**	**e** n	**m**
Summer 2008	Aug 23-Sep 3	**g** n	**f**	**e** f	**g** m n
Fall 2008	Oct 6-9	**e** n	**m**	**f**	**e** n
Spring 2009	May 1-11	**e** n	**e** f	**e** n	f **g** m n

Table 7. Locations with highest average Δε in rubblized section.

Season		Rubblized section			
		Top		Bottom	
		Tensile	Compressive	Tensile	Compressive
Summer 2006	July 8-17	f **o**	**m**	**m**	f **o**
	July 17-28	**f**	**m**	**f**	n **o**
	Aug 5-9	**m**	**e** m	**m**	**n**
	Aug 9-15	**m**	**m**	**f** m	**n**
Fall 2006	Dec 1-3	**m**	**e** n	**m** n	**f**
	Dec 3-7	**m**	**f**	**n**	**m**
Winter 2006-2007	Feb 26-Mar 5	**m**	**f**	**f**	**m**
	Mar 5-9	**m**	**e** n	f **m**	**n**
Spring 2007	May 27-June 7	**m**	**m**	**m**	**e** f n
Fall 2007	Oct 21-30	**m**	**m**	**m**	**e** f
Spring 2008	Apr 26-May 6	**f**	**m**	**m**	**e** f
Summer 2008	Aug 23-Sep 3	**f**	**m**	m **o**	**n**
Fall 2008	Oct 6-9	**m**	**m**	m **o**	**m** n
Spring 2009	May 1-11	**m**	**m**	**m**	**n**

Table 8. Locations with highest average Δε in untreated section.

Season		Untreated section			
		Top		Bottom	
		Tensile	Compressive	Tensile	Compressive
Summer 2006	July 8-17	f o	n	m	f
	July 17-28	n	n o	m	f
	Aug 5-9	n	f o	m	n
	Aug 9-15	n	n o	m	n
Fall 2006	Dec 1-3	n	n	m n	f
	Dec 3-7	n	f	f m	m
Winter 2006-2007	Mar 9-13	m	f	f	m
	Mar 13-20	f o	n	m	e f
Spring 2007	May 27-June 7	n	n	m	f
Fall 2007	Oct 21-30	n o	n	m n	e m
Spring 2008	Apr 26-May 6	m	n	m	f g
Summer 2008	Aug 23-Sep 3	m	n	m o	f g n
Fall 2008	Oct 6-9	n	n o	e m	n
Spring 2009	May 1-11	n	n	m	n

While determining the average of change in strains provides a general picture of the behavior of the strains and stresses within the slab, it does not allow the identification of the maximum change in strains and stresses undergone by the slab. Maximum values of change in strains undergone by the slabs allow identification of critical locations where cracking may occur due to stresses higher than the strength of the slab. Therefore, in order to fully characterize the strain response of the experimental sections, the maximum tensile and compressive $\Delta\varepsilon$ for each of the periods analyzed were identified. Table 9, Table 10, and Table 11 show the locations corresponding to the maximum tensile and compressive $\Delta\varepsilon$ for each of the experimental sections. The following sections discuss the results observed: the maximums and average change in strains as well as the comparisons of the long-term response between the three experimental sections.

Table 9. Locations with maximum Δε in B&S section.

Season		Broken and seated section			
		Top		Bottom	
		Tensile	Compressive	Tensile	Compressive
Summer 2006	July 8-17	f n **o**	**e** n	**e** n	**m**
	July 17-28	**n**	**e** f	**n**	**m**
	Aug 5-9	**n**	**e** f	**e** n	**g** n
	Aug 9-15	**n**	**e** n	**e** n	**g** m
Fall 2006	Dec 1-3	**n**	**e** n	**e** n	**m**
	Dec 3-7	**e** n	**n**	**e** f m	**e** n
Winter 2006-2007	Feb 9-15	m **o**	**e** f	**e** f	m **o**
	Feb 15-20	**m**	**e** n	**e** f	**g** m
Summer 2007	Aug 21-25	**n**	**e** n	**e** n	**m**
Fall 2007	Oct 21-30	**m**	**e** n	**e** n	**m**
Spring 2008	Apr 26-May 6	**e** m	**n**	**e** n	**g** m n
Summer 2008	Aug 23-Sep 3	**g** n	**n**	**e** n	**g** n
Fall 2008	Oct 6-9	**e** n	**g** n	f **g**	**g** n
Spring 2009	May 1-11	**e** n	**e** n	**e** n	f **g** n

Table 10. Locations with maximum Δε in rubblized section.

Season		Rubblized section			
		Top		Bottom	
		Tensile	Compressive	Tensile	Compressive
Summer 2006	July 8-17	f **o**	**m**	**m**	f **o**
	July 17-28	**f**	**m**	f **m**	**n**
	Aug 5-9	**m**	**m**	**m**	**n**
	Aug 9-15	**m**	**m**	**f** m	**n**
Fall 2006	Dec 1-3	**m**	**m**	**m**	**f**
	Dec 3-7	**m**	**f**	f **n**	**m**
Winter 2006-2007	Feb 26-Mar 5	**m**	**m**	**f**	**m**
	Mar 5-9	**e** m n	**m**	**m**	**m**
Spring 2007	May 27-June 7	**m**	**m**	**m**	**e** m
Fall 2007	Oct 21-30	**m**	**m**	**m**	**e** f n
Spring 2008	Apr 26-May 6	**m**	**m**	**m**	**f**
Summer 2008	Aug 23-Sep 3	**m**	**m**	**m**	**n**
Fall 2008	Oct 6-9	**m**	**m**	**m**	**m** n
Spring 2009	May 1-114.2.2	**m**	**m**	**m**	**n**

Table 11. Locations with maximum Δε in untreated section.

Season		Untreated section			
		Top		Bottom	
		Tensile	Compressive	Tensile	Compressive
Summer 2006	July 8-17	f **o**	**n**	**m**	m n **o**
	July 17-28	**n**	**n**	**m**	f **m**
	Aug 5-9	**n**	**n**	**m**	**n**
	Aug 9-15	**n**	**n**	**m**	**m**
Fall 2006	Dec 1-3	n **o**	**n**	**m** n	**f**
	Dec 3-7	**n**	**f** n	**m**	**m**
Winter 2006-2007	Mar 9-13	**n**	f **o**	**f**	**m**
	Mar 13-20	n **o**	**n**	**m**	**e** f
Spring 2007	May 27-June 7	**n**	m **o**	**m**	m n **o**
Fall 2007	Oct 21-30	**n**	**n**	**m**	**m**
Spring 2008	Apr 26-May 6	**m**	**n**	**m**	**f**
Summer 2008	Aug 23-Sep 3	m n **o**	**n**	**m**	**n**
Fall 2008	Oct 6-9	**n**	**n**	**m**	**m** n
Spring 2009	May 1-114.2.2	**n**	**n**	**m**	**m** n

5.4.2.1 Strain/Stress Differences due to Location within the Slab

The variation of the average change in strains for each location in the B&S section is shown in Figure 76 for all the periods in Table 6. It can be seen in this figure that the average tensile $\Delta\varepsilon$ did not exceed 10με for all the analyzed periods except for the fall 2006 period between December 3 and 7 where the average change of strains reached values of about 15με at the location ***e***. Moreover, it can be seen that the top of the slab in general experienced lower average tensile $\Delta\varepsilon$ than the bottom. On the other hand, the average compressive $\Delta\varepsilon$ did not exceed 25με with the higher averages occurring for the summer 2006 period between August 5 and 9. Besides, the average compressive change in strains at the bottom of the slab was in general lower than at the bottom for most of the periods analyzed except for the fall 2006 and 2007 periods where the bottom of the slab experienced the highest averages. Notice that bottom of the slab experienced higher averages for periods when the top of the slab underwent higher average tensile $\Delta\varepsilon$.

The locations that experienced the highest average $\Delta\varepsilon$ in the B&S section for most of the periods in Table 6 correspond to location ***e*** along the centerline of the slab, the corner location ***g*** and the center of the slab (i.e. location ***n***). Among these, location ***e*** experienced the highest positive and negative values for most of the analyzed periods. Location ***n*** and ***g*** on the other hand respectively experienced the highest tensile and compressive average $\Delta\varepsilon$ during six of the periods in Table 6. Despite this, in general, location ***n*** experienced higher average tensile $\Delta\varepsilon$ at the top and bottom of the slab than the mid-span locations on the wheel paths (i.e. locations ***f*** and ***m***). Conversely, the mid-span location ***m*** experienced higher average compressive change in strains than the center of the slab and location ***f*** for most of the analyzed periods. However, notice that the highest positive and negative average $\Delta\varepsilon$ for all the periods in Table 6 were

experienced at locations ***e*** and ***f*** respectively. The change in stresses associated with these values are 345.04 kPa (50.04 psi) in tension and 545.8 kPa (79.2 psi) in compression. Notice that these values are smaller than the modulus of rupture and compressive strength reported in Table 2.

Figure 77 shows the average change in strains of each location in the rubblized section for all the periods in Table 7. It can be seen that the average tensile $\Delta\varepsilon$ did not exceed 10με for all the analyzed periods. However, as in the B&S section the values for the fall 2006 period between December 3 and 7 reached values of 17.1 με at the mid-span location on the inner wheel path (i.e. location ***m***). On the other hand, the average compressive $\Delta\varepsilon$ did not exceed 31 με with the highest averages occurring for the summer 2006 period between August 5 and 9. In general, the top of the slab experienced lower tensile averages than the bottom of the slab but it experienced higher compressive averages than the bottom as can be seen in Figure 77. Additionally, the average compressive $\Delta\varepsilon$ at the top of the slab was in general higher than at the bottom for most of the periods analyzed except for the fall 2006 and 2007 periods when the bottom of the slab experienced higher averages than the top of the slab. The opposite trend is observed for the average tensile change in strains with the bottom of the slab experiencing higher averages than the top of the slab.

In the rubblized section, the locations that experienced the highest average change in strain for most of the periods in Table 7 correspond to the mid-span location on the inner wheel path and the center of the slab (i.e. location ***m*** and ***n*** respectively). Of these, the mid-span location ***m*** experienced the highest average tensile $\Delta\varepsilon$ at top and bottom of the slab for most of the periods. Additionally, the top of the slab in location ***m*** experienced the highest average compressive $\Delta\varepsilon$ for most of the analyzed periods while the center experienced the highest average compressive $\Delta\varepsilon$ at the bottom of the slab for five of the 14 periods. Even though location ***m*** consistently experienced the highest average change in strains for most of the periods, the highest average compressive $\Delta\varepsilon$ of 30.1με occurred at location ***e*** during the summer 2006 time between August 5 and 9. However, the average compressive $\Delta\varepsilon$ at location ***m*** for the same period reached 29.2 με, which is close to the value experienced at location ***e***. The change in stresses associated with the highest average change in strains are 397.3 kPa (57.6 psi) in tension and 699.4 kPa (101.4 psi) in compression. Notice that these values are smaller than the modulus of rupture and compressive strength reported in Table 2.

The average change in strains for the untreated section is shown in Figure 78 for all the periods in Table 8. It can be seen that the average tensile $\Delta\varepsilon$ did not exceed 22 με for all of the analyzed periods except for the fall 2006 and 2008 periods. In these, the average tensile $\Delta\varepsilon$ reached values of 28.2 με and 29.5 με at the top of the slab in location ***n***. On the other hand, the average compressive $\Delta\varepsilon$ was below 32 με for most of the periods except for the summer 2006 period between August 5 and 9 where the values reached 45.7 με at the top of the slab in location ***o***. In general, the bottom of the slab experienced lower compressive averages than the top of the slab while the opposite trend was observed for the average tensile $\Delta\varepsilon$. However, as in the B&S and rubblized sections, the bottom of the slab showed higher average compressive change in strain than the top of the slab for the fall 2006 and 2007 periods.

The locations in the untreated section that experienced the highest average $\Delta\varepsilon$ for most of the periods in Table 8 correspond to the mid-span location on the inner wheel path and center of the slab (i.e. location ***m*** and ***n*** respectively). Of these, the mid-span location ***m*** experienced the highest average tensile change in strain at the bottom of the slab for 11 of the 14 periods

analyzed. Location ***n*** on the other hand, experienced the highest average compressive and tensile $\Delta\varepsilon$ at the top of the slab during eight of the analyzed periods as well as the highest average compressive $\Delta\varepsilon$ at the bottom of the slab for four periods. Although locations ***m*** and ***n*** experienced the highest averages most of the time, the highest compressive average c $\Delta\varepsilon$ occurred in location ***o*** at the top of the slab during the summer 2006 period between August 5 and 9. The change in stresses associated with the highest average $\Delta\varepsilon$ are 685.4 kPa (99.4 psi) in tension and 1061.9 kPa (154 psi) in compression. Notice that these values are smaller than the modulus of rupture and compressive strength reported in Table 2.

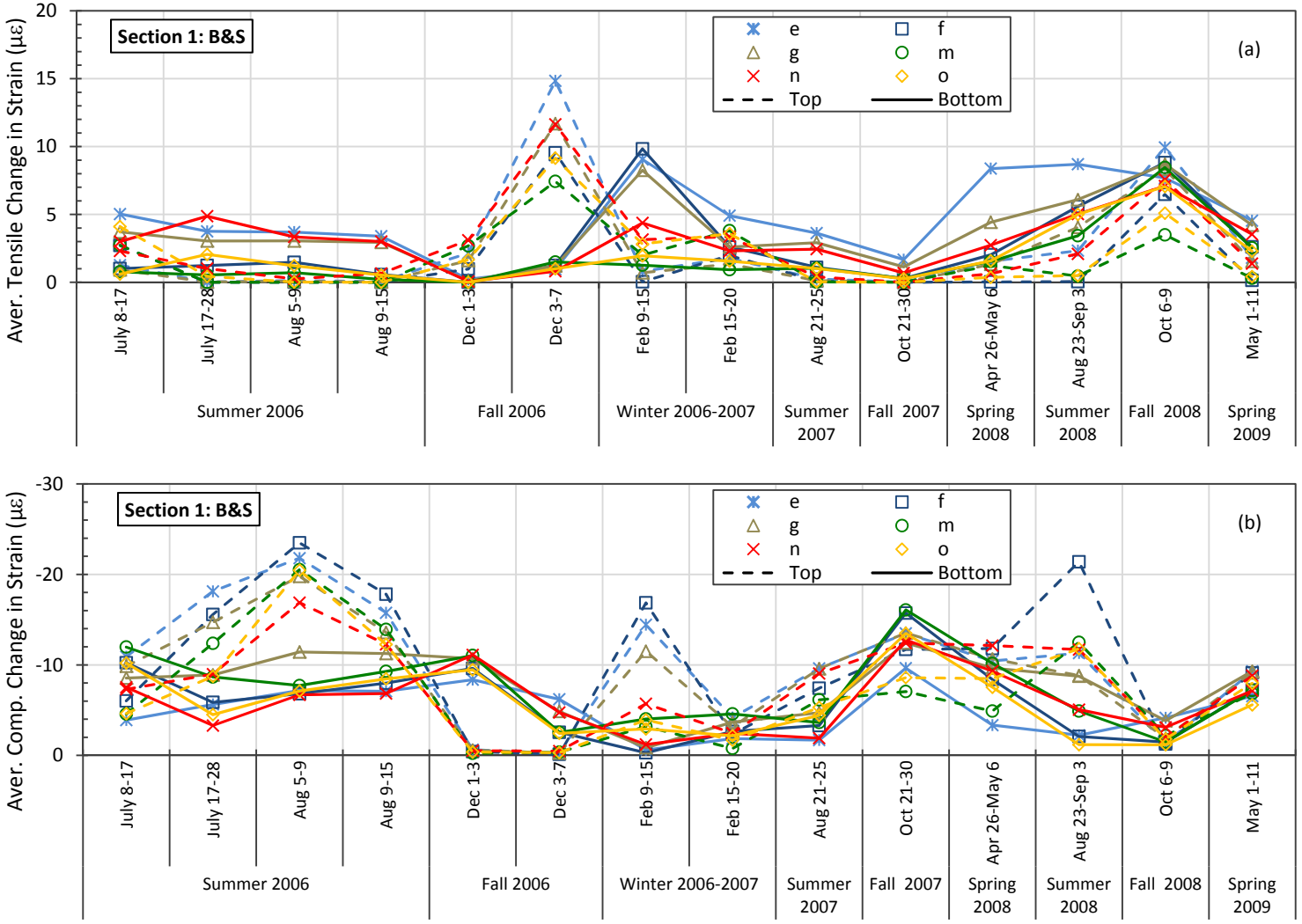

Figure 76. Average Δε for B&S section: a) Tensile change in strains; b) Compressive change in strains.

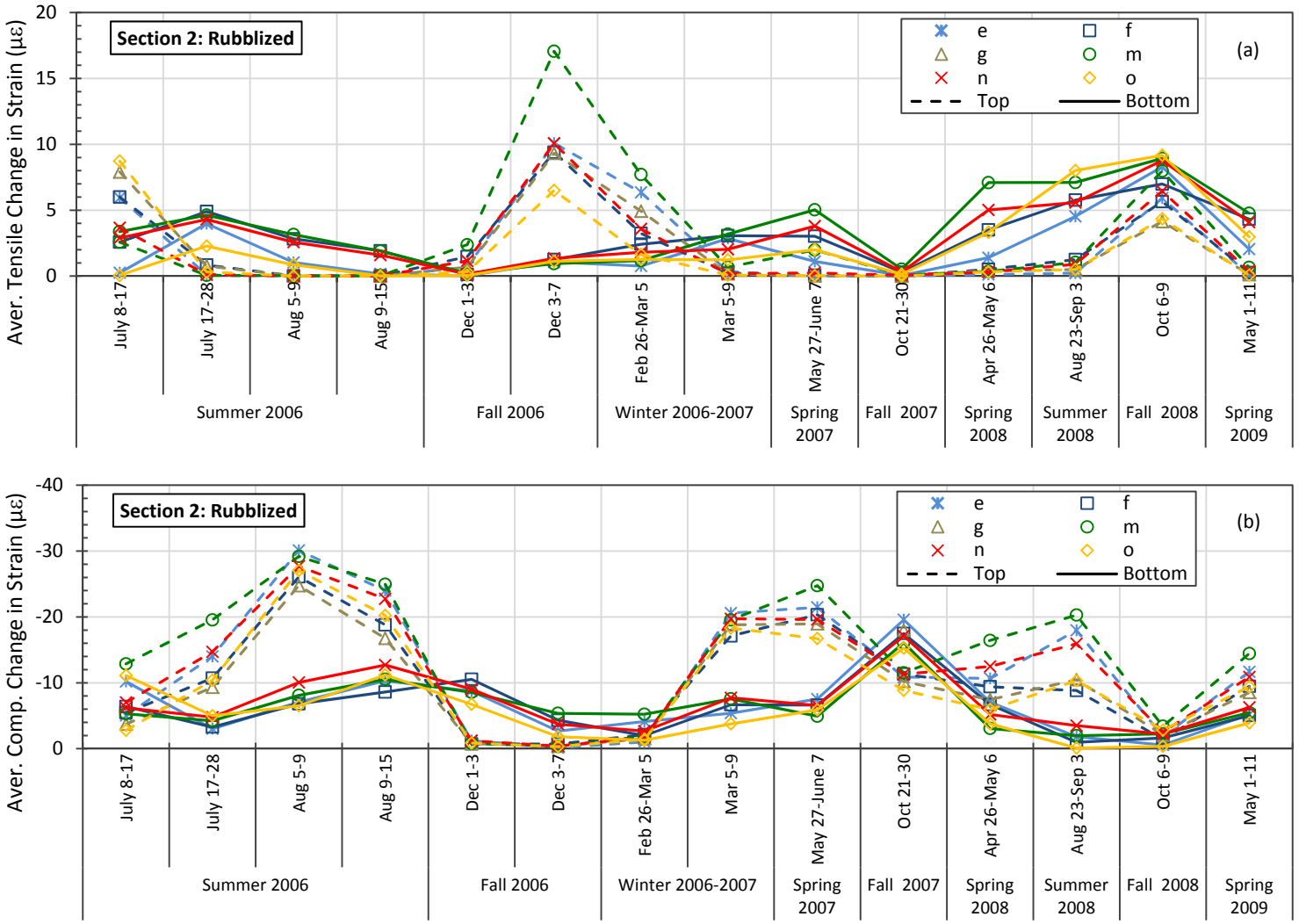

Figure 77. Average Δε for rubblized section: a) Tensile change in strains; b) Compressive change in strains.

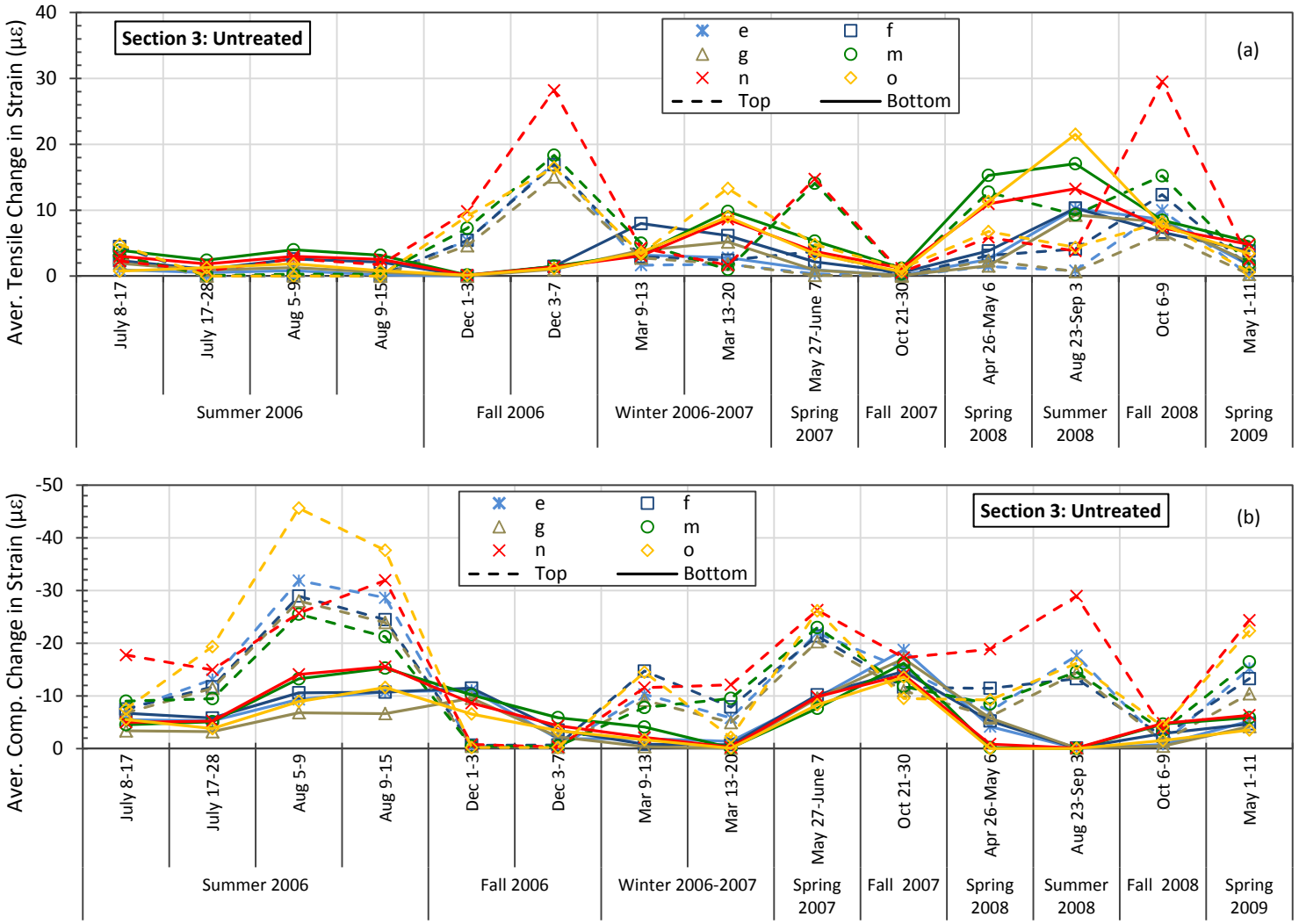

Figure 78. Average Δε for untreated section: a) Tensile change in strains; b) Compressive change in strains.

As mentioned above, the average change in strains only provides a general picture of the behavior of the strains and stresses but it does not allows knowing the maximum changes in strains and stresses which at the end may cause cracking of the slab. Figure 79 shows the maximum tensile and compressive $\Delta\varepsilon$ undergone by the B&S section for all the periods in Table 9. It can be seen that the top of the slab experienced lower tensile $\Delta\varepsilon$ than the bottom with values below 40 με for all the periods analyzed. On the other hand, the maximum compressive $\Delta\varepsilon$ did not exceed 65 με with the top of the slab experiencing higher changes than the bottom of the slab for most of the analyzed periods. Notice that only during the fall 2006 period the bottom of the slab experienced higher compressive $\Delta\varepsilon$ than the top while the opposite occurred for the tensile $\Delta\varepsilon$ during the same period. This behavior is similar to the one shown by the average change in strains discussed above. In general the maximum tensile $\Delta\varepsilon$ occurred at the bottom of the slab in the centerline location ***e*** except for the summer 2006 between July 17 and 28 and the fall 2008 period. For these two periods, the maximum tensile $\Delta\varepsilon$ occurred at the center of the slab (i.e. location ***n***) and at the corner location ***g*** respectively. Similar behavior is shown by the compressive $\Delta\varepsilon$, where the maximum values generally occurred at the top of the slab in location ***e***. Higher values of maximum tensile $\Delta\varepsilon$ are observed for the spring and summer 2008 than any other period in Table 9. On the other hand, the maximum compressive change in strains were higher for the summer 2006 and 2008 periods. However, notice that during the late fall 2008 period between December 3 to 7 and winter 2006-2007 period between February 9 to 15 the change in strains at the top of the slab were comparable to values experienced in other times. This behavior can be explained by the high change in the temperature gradient experienced during those periods where the maximum LTG values varied from about +0.20°C/cm (0.92°F/in) down to –0.31°C/cm (-1.43°F/in) for the fall 2008 period and reached values of +0.75°C/cm (3.45°F/in) for the winter 2006-2007 period within one day. Maximum values of $\Delta\varepsilon$ and LTG in the B&S section can be seen in Appendix A for each sensor and for all the analyzed periods.

Figure 80 shows the maximum tensile and compressive change in strain undergone by the rubblized section for all the periods in Table 10. It can be seen that the bottom of the slab experienced higher tensile $\Delta\varepsilon$ than the top except for the fall 2006 periods and the winter 2006-2007 period between February 26 and March 5. During these, the top of the slab experienced the highest values. Conversely, the top of the slab experienced the highest compressive $\Delta\varepsilon$ for most all the periods analyzed except for the fall 2006 periods where the bottom of the slab reached values slightly higher than those values experienced at the top. Notice that this behavior is similar to the exhibit by the average change in strain above discussed. The tensile change in strains was below the 35 με while the compressive $\Delta\varepsilon$ reached values close to 123 με. In general, the maximum tensile $\Delta\varepsilon$ occurred at the mid-span location ***m*** on the inner wheel path for both top and bottom of the slab while the maximum compressive $\Delta\varepsilon$ occurred generally at location ***m*** for the top of the slab and location ***n*** at the bottom of the slab. Higher maximum tensile values were observed for the spring and summer 2008 periods at the bottom of the slab than any other analyzed period while the higher values at the top of the slab were observed during the Fall 2006 period between December 3 to 7 and Winter 2006-2007 period between February 26 to March 5. On the other hand, the section experienced higher maximum

compressive $\Delta\varepsilon$ at the top of the slab during the spring 2007 period than in any other times. Similar to the B&S section, this behavior is explained by the high change of LTG values from about +0.21°C/cm (0.97°F/in) to –0.31°C/cm (1.43°F/in) for the fall 2006 period and reached a maximum of +0.86°C/cm (2.60°F/in) for the spring 2007 period. Maximum values of $\Delta\varepsilon$ and LTG in the rubblized section can also be seen in Appendix A for each sensor and for all the analyzed periods.

The maximum tensile and compressive changes in strain for the untreated section are shown in Figure 81 for all the periods in Table 11. It can be seen that the bottom of the slab experienced higher maximums values of tensile $\Delta\varepsilon$ than the top except for the fall 2006 periods where the top of the slab experienced the highest values. Conversely, the top of the slab experienced higher maximum values of compressive $\Delta\varepsilon$ than the bottom for all the analyzed periods except for the fall 2006 periods where the bottom of the slab reached values slightly higher than those values experienced at the top. Similar behavior was exhibit by the average change in strain above discussed. The tensile changes in strains were below the 60 με while the compressive change in strains reached values close to 148 με. In general, the highest maximum tensile and compressive $\Delta\varepsilon$ at the top of the slab occurred in the center of the slab (i.e. location ***n***). On the other hand, the highest maximum tensile and compressive $\Delta\varepsilon$ at the bottom of the slab occurred at the mid-span location ***m*** on the inner wheel path. From Figure 81 it can be seen that the maximum tensile values were higher for the 2008 periods analyzed than any other period while the maximum compressive $\Delta\varepsilon$ was higher for the spring 2007 and summer 2008 periods. Similar to the case of the rubblized section, this behavior obeys to high LTG values, which reached a maximum of +0.89°C/cm (4.09°F/in) and –0.36°C/cm (-1.66°F/in) in the center of the slab. Notice that the rubblized section also experienced the highest compressive change in strains at the top of the slab during the spring 2007 period. Maximum values of $\Delta\varepsilon$ and LTG in the untreated section can also be seen in Appendix A for each sensor and for all the analyzed periods.

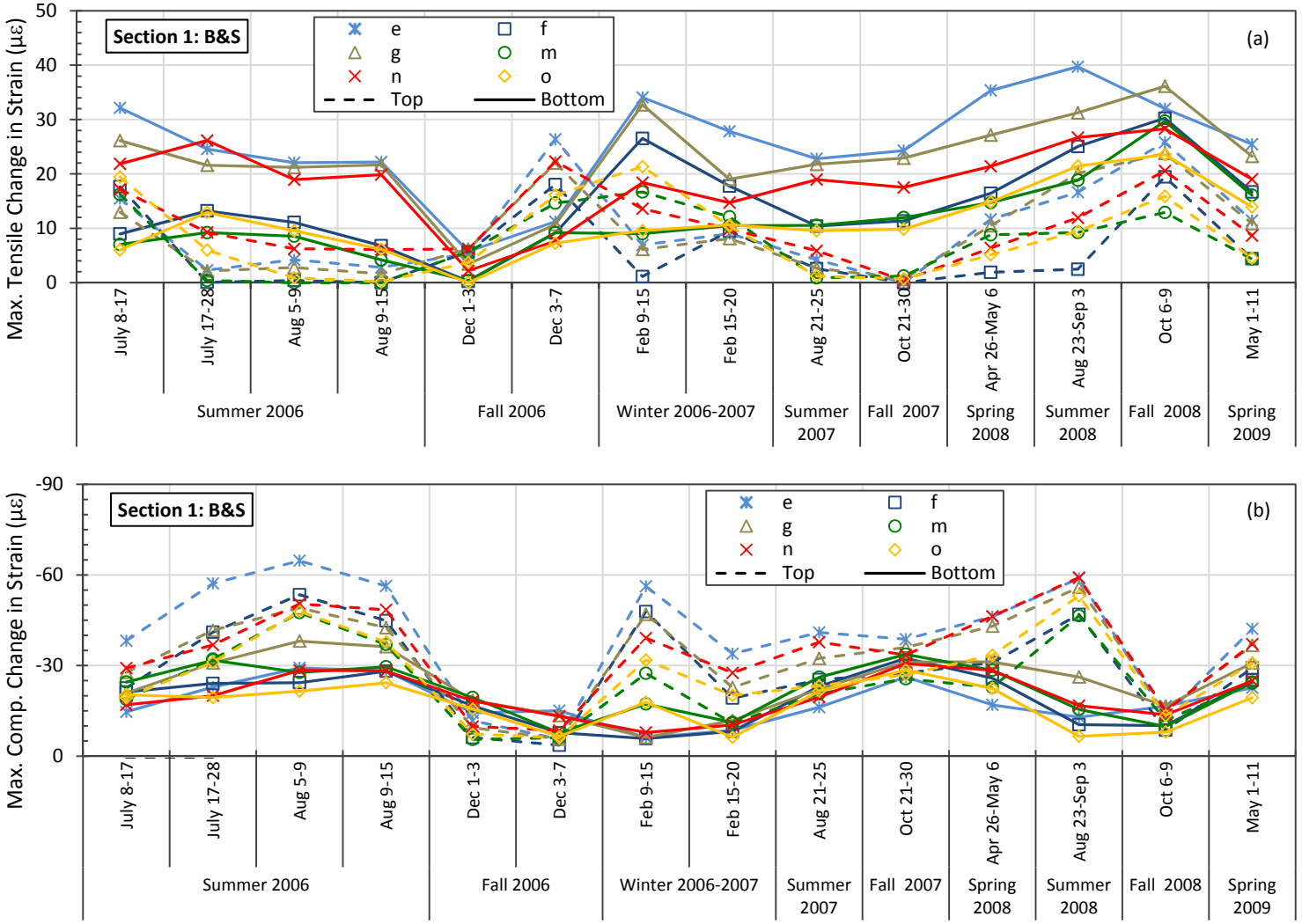

Figure 79. Maximum Δε for B&S section: a) Tensile change in strains; b) Compressive change in strains.

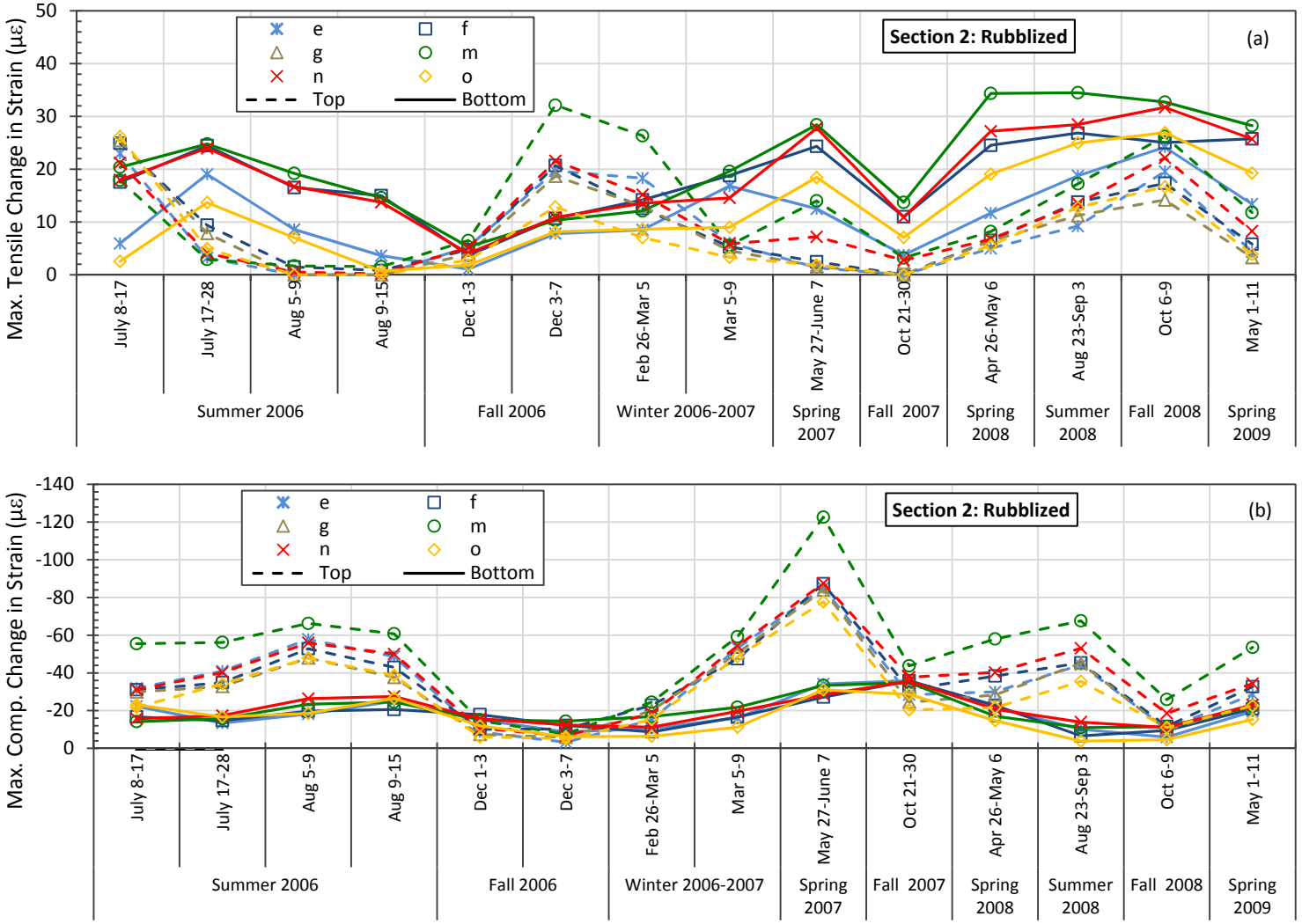

Figure 80. Maximum Δε for rubblized section: a) Tensile change in strains; b) Compressive change in strains.

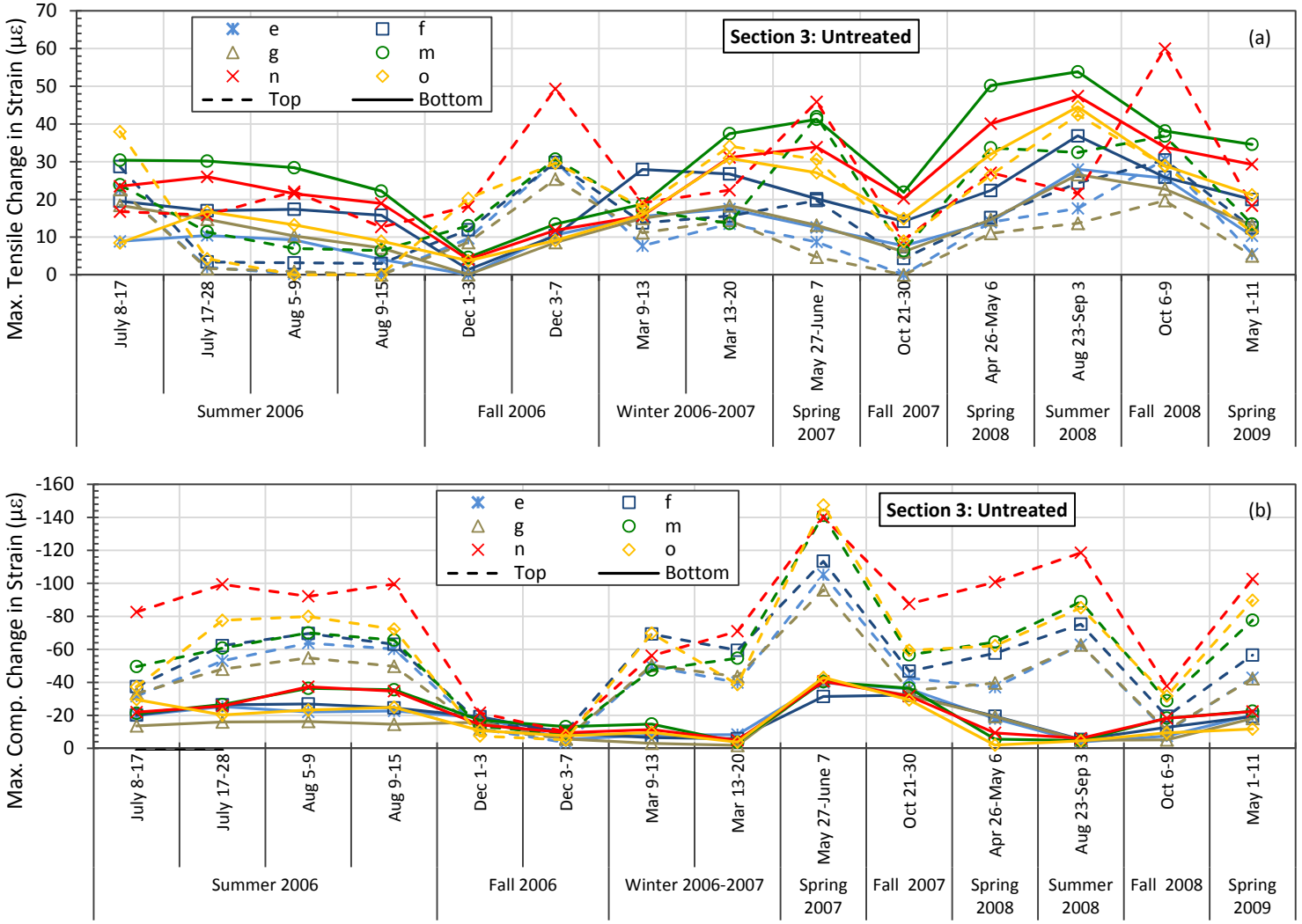

Figure 81. Maximum Δε for untreated section: a) Tensile change in strains; b) Compressive change in strains.

5.4.2.2 Discussion on the Strain/Stress Differences due to Location within the Slab

The discussion presented above indicates a general trend in the three experimental sections where the top of the slab experienced lower tensile average change in strains than the bottom of the slab, and that the converse case occurred for the compressive averages. Similarly, the maximum tensile change in strains was lower at the top of the slab than at the bottom of the slab, and the maximum compressive values showed the opposite behavior. Furthermore, the locations that consistently showed the highest values in each section were identified for all the analyzed periods in Table 5. These locations were identified using the average and the maximum change in strain separately obtaining identical results. This means that the locations that consistently showed the highest average $\Delta\varepsilon$ also consistently showed the maximum $\Delta\varepsilon$ for all the periods analyzed. Table 12 summarizes all these locations for each section. In addition, the location that consistently showed the highest values between the center of the slab and the mid-span locations ***f*** and ***m*** is listed in parenthesis in Table 12.

Table 12. Locations consistently showing the highest average and maximum $\Delta\varepsilon$.

Section	Top		Bottom	
	Tension	Compression	Tension	Compression
B&S	*n* (*n*)	*e* (*n*)	*e* (*n*)	*g* (*m*)
Rubblized	*m* (*m*)	*m* (*m*)	*m* (*m*)	*n* (*m*)
Untreated	*n* (*n*)	*n* (*n*)	*m* (*m*)	*m* (*m*)

Notice that in the B&S section the locations listed correspond to the centerline location ***e***, the center of the slab (i.e. location ***n***) and the corner location ***g***. Moreover, it can be seen that these are different from those locations listed for the rubblized and untreated sections. On the other hand, the locations consistently showing the highest averages and maximum $\Delta\varepsilon$ are the same; however, the correspondence on the faces of the slab (top or bottom) is different. The locations consistently showing the highest values in the rubblized and untreated section correspond to the center of the slab and the mid-span location on the inner wheel path (i.e. locations ***n*** and ***m*** respectively). Although some locations tended to show the highest average and maximum $\Delta\varepsilon$ values, in some sections, the maximum $\Delta\varepsilon$ for all the periods analyzed occurred at a different location. However, this can be classified as a onetime event and it does not reflect the general trend observed during all the periods analyzed. Table 13 lists the locations where the maximum $\Delta\varepsilon$ occurred and its value (together with the corresponding change in stresses) for each of the sections. Refer to Appendix A for the maximum values experienced by each sensor.

Table 13. Maximum values of $\Delta\varepsilon$ and $\Delta\sigma$.

Section	Maximum Change in Strain [με]				Maximum Change in Stresses [psi (kPa)]			
	Top		Bottom		Top		Bottom	
	Tens.	Comp.	Tens.	Comp.	Tens.	Comp.	Tens.	Comp.
B&S	26.4 (*e*)	-64.7 (*e*)	39.7 (*e*)	-38.1 (*g*)	88.9 (612.8)	-218.1 (-1503.6)	133.8 (922.8)	-128.3 (-884.9)
Rubblized	32.1 (*m*)	-122.6 (*m*)	34.5 (*m*)	-35.9 (*e*)	108.3 (746.6)	-413.2 (-2849.1)	116.2 (801.4)	-121.0 (-834.1)
Untreated	60.0 (*n*)	-147.4 (*o*)	53.8 (*m*)	-43.0 (*o*)	202.2 (1394.0)	-496.9 (-3426.0)	181.4 (1250.8)	-144.7 (-998.0)

Notice that the highest value of the maximum tensile and compressive $\Delta\varepsilon$ listed in Table 13 are 60 με and 147.4 με respectively and correspond to changes in stresses of 1394 kPa (202.2 psi) in tension and 3426 kPa (496.9 psi) in compression. If compared to the values reported in Table 4-1, it can be seen that the change in stresses varied up to 35.6% of the modulus of rupture and up to 12.3% of the compressive strength of the concrete. Therefore, considering the hypothesis and premises taken on calculating the change in strains, it can be concluded that the experimental sections did not experience any change in strains that could result in cracking of the slabs during all the periods analyzed. However the latest conclusion could vary if one considers the distribution of stresses after the concrete has set as well as the shrinkage and slab-base friction effects.

5.4.2.3 Strain/Stress Differences between Experimental Sections

The average $\Delta\varepsilon$ was plotted in Figure 82, Figure 83, and Figure 84 to compare the average behavior between the three experimental sections at the mid-span locations ***f*** and ***m*** as well as in the center of the slab (i.e. location ***n***). From Figure 82(a) it can be seen that in location ***n***, the B&S section experienced higher average tensile $\Delta\varepsilon$ at the bottom of the slab than the other two sections during the summer 2006 periods and showed smaller values than the other sections for the rest of the periods analyzed. Conversely, if excluding the summer 2006 and fall 2008 periods, the untreated section experienced higher average tensile $\Delta\varepsilon$ for the majority of the periods analyzed. Likewise, the highest tensile $\Delta\varepsilon$ at the top of the slab were experienced by the untreated section for most of the analyzed periods with exception of two periods of the summer 2006 where the highest values were experienced by the rubblized and B&S sections. The rubblized and B&S sections on the other hand, showed the smallest values at the top and bottom of the slab respectively for the majority of the analyzed periods. Similarly, from Figure 82(b) it can be seen that the top of the slab at location ***n*** of the untreated section experienced the highest compressive average $\Delta\varepsilon$ for almost all the periods analyzed with the exception of the summer 2006 period of August 5-9 and the fall 2006 periods. The top of the slab in the B&S section experienced the smallest compressive averages for the majority of the periods analyzed except for the summer period of July 8-17 and the fall 2007 period where the rubblized section experienced the smallest values. Conversely, the average compressive $\Delta\varepsilon$ at the bottom of the slab was higher in the B&S section than in the other two sections for the majority of the analyzed periods. However, notice that the untreated section experienced the highest values during four of these periods. In general, the rubblized and untreated sections experienced the smallest compressive averages at the bottom of the slab. The highest averages of tensile $\Delta\varepsilon$ at the top and

bottom of the slab for all the periods analyzed were experienced by the untreated section while the corresponding compressive averages were observed in the untreated and rubblized sections at the top and bottom respectively. These values and the corresponding averages at location ***n*** in the rubblized and B&S sections are listed in Table 14.

Figure 83(a) shows the average tensile change in strains in the mid-span location ***f***. In this can be seen that the B&S section in general presented the smallest averages of tensile $\Delta\varepsilon$ at the bottom of the slab while the rubblized and untreated sections both experienced the highest averages during five of the 11 periods of common data. The rubblized section experienced the highest averages during the summer 2006 periods excluding the period of August 9-15 where the untreated section experienced the highest average. In addition, the rubblized section also showed the highest average for the fall 2006 period of December 1-3 and the spring 2009 period. Likewise, the untreated section showed the highest average tensile $\Delta\varepsilon$ at the bottom of the slab for the fall 2006 period of December 3-7, fall 2007, spring and summer 2008 periods. The highest average tensile $\Delta\varepsilon$ at the top of the slab was experienced by the untreated section for the majority of the analyzed periods with the exception of the summer 2006 period of July 8-28. In this, the rubblized section presented the highest averages. Conversely, the B&S section in general presented the smallest average tensile change in strain for the majority of the analyzed periods. Similarly, the B&S section experienced the smallest average compressive $\Delta\varepsilon$ at the top and bottom for five of the periods of common data as shown in Figure 83(b). However, it can be seen also that the B&S section experienced the highest average compressive $\Delta\varepsilon$ at the bottom of the slab for five of the 11 periods of common data while the untreated section showed the highest values for four of the remaining periods. Despite this, the highest average compressive $\Delta\varepsilon$ at the bottom of the slab for all the periods analyzed was experienced by the rubblized section during the fall 2007 period. On the other hand, the untreated and B&S sections experienced the highest average compressive $\Delta\varepsilon$ at the top of the slab during three and four of the analyzed periods respectively. However, the untreated section experienced the highest average compressive $\Delta\varepsilon$ at the top of the slab for all the periods analyzed. Likewise, the untreated section also experienced the highest tensile averages at the top and bottom of the slab for all the analyzed periods. These values and the corresponding averages in the rubblized and B&S sections are also listed in Table 14.

Figure 84(a) shows the average tensile change in strain in the mid-span location ***m***. In this can be seen that the untreated section presented the highest average tensile $\Delta\varepsilon$ at the top of the slab for all the periods of common data. The untreated section also experienced the highest average tensile $\Delta\varepsilon$ at the bottom of the slab for the majority of the analyzed periods with the exception of the summer 2006 period of July 17-28, fall 2006 and the fall 2008 periods where the rubblized and B&S sections showed the highest averages. Conversely, the B&S section in general showed the smallest averages at the top and bottom of the slab for the majority of the periods analyzed. Likewise, the B&S section also experienced the smallest average compressive change in strain at the top of the slab as shown in Figure 84(b). The rubblized section on the other hand, experienced the highest average compressive $\Delta\varepsilon$ during seven of the periods of common data while the untreated section experienced the highest values for the remaining periods. The highest compressive averages at the bottom of the slab were experienced by the B&S section during six of the analyzed periods while the untreated section experienced the highest averages for the remaining periods. The periods where the B&S section showed the highest averages correspond to the summer period of July 8-28, the fall 2006 period of December

1-3, the spring and summer 2008, and spring 2009 periods. However, the highest average compressive $\Delta\varepsilon$ at the bottom of the slab for all the analyzed periods was shown by the untreated section during the fall 2007. The highest average at the top of the slab was shown by the rubblized section during the summer 2006 period of August 5-9. Similarly, the untreated section also showed the highest tensile $\Delta\varepsilon$ at the top and bottom of the slab for all the periods analyzed. These values and the corresponding averages in the B&S and rubblized sections are also listed in Table 14.

Table 14. Highest average Δε (bold/blue values are the highest values among the sections).

	Section / Location	B&S		Rubblized		Untreated	
		Top	Bottom	Top	Bottom	Top	Bottom
Tension (με)	*n*	11.63 (Fall 2006)	7.09 (Fall 2008)	10.07 (Fall 2006)	8.77 (Fall 2008)	**29.49** (Fall 2008)	**13.25** (Summer 2008)
	f	9.54 (Fall 2006)	8.82 (Fall 2008)	9.40 (Fall 2006)	6.99 (Fall 2008)	**16.92** (Fall 2006)	**10.38** (Summer 2008)
	m	7.43 (Fall 2006)	8.46 (Fall 2008)	17.06 (Fall 2006)	8.94 (Fall 2008)	**18.34** (Fall 2006)	**17.06** (Summer 2008)
Compression (με)	*n*	-16.88 (Summer 2006)	-12.76 (Fall 2007)	-27.71 (Summer 2006)	**-17.12** (Fall 2007)	**-31.93** (Summer 2006)	-15.58 (Summer 2006)
	f	-23.49 (Summer 2006)	-15.73 (Fall 2007)	-26.08 (Summer 2006)	**-17.49** (Fall 2007)	**-28.95** (Summer 2006)	-14.65 (Fall 2007)
	m	-20.52 (Summer 2006)	-16.07 (Fall 2007)	**-29.19** (Summer 2006)	-16.07 (Fall 2007)	-25.52 (Summer 2006)	**-16.21** (Fall 2007)

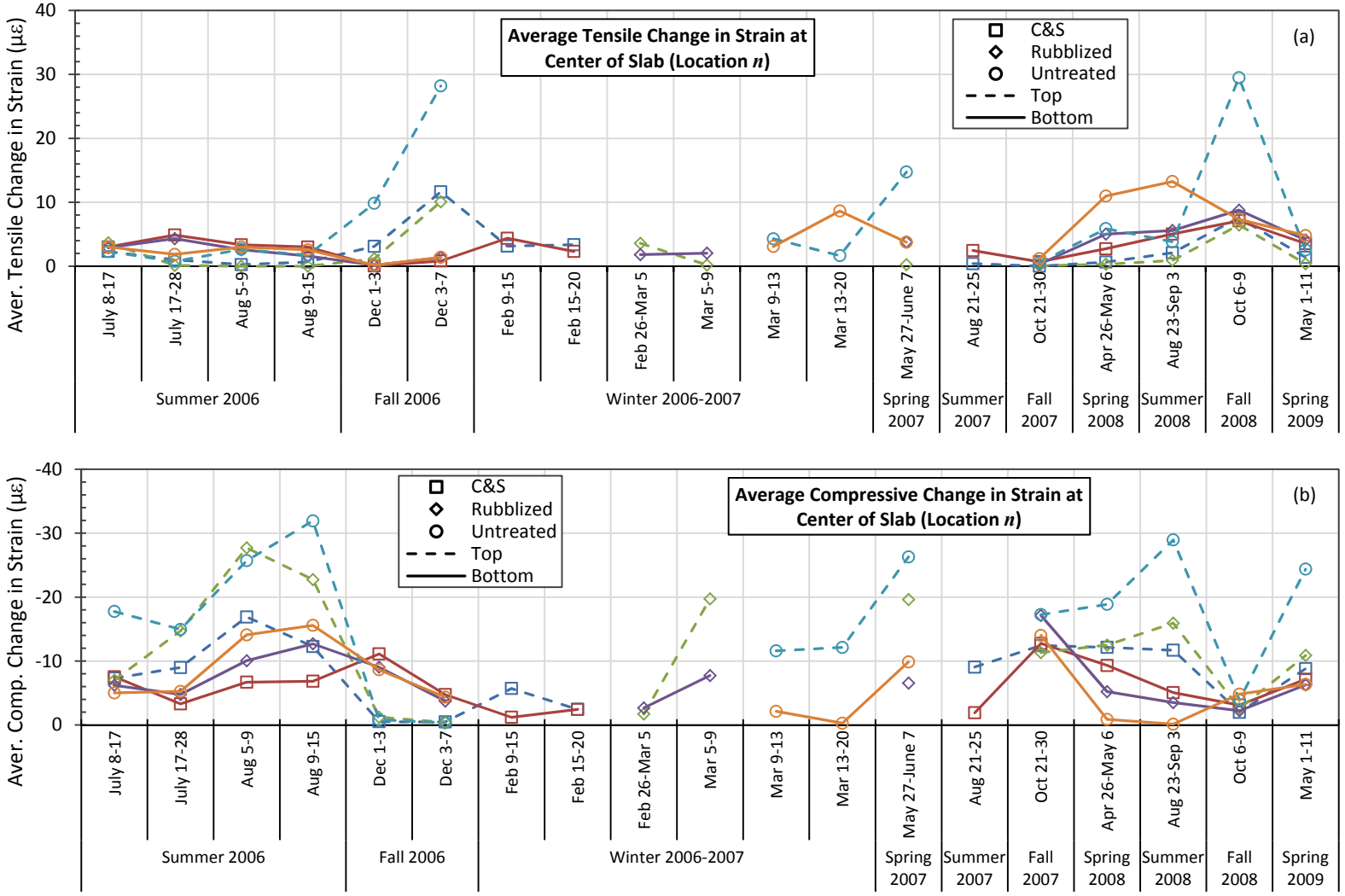

Figure 82. Average Δε at the center of the slab: a) Tensile strains; b) Compressive strains.

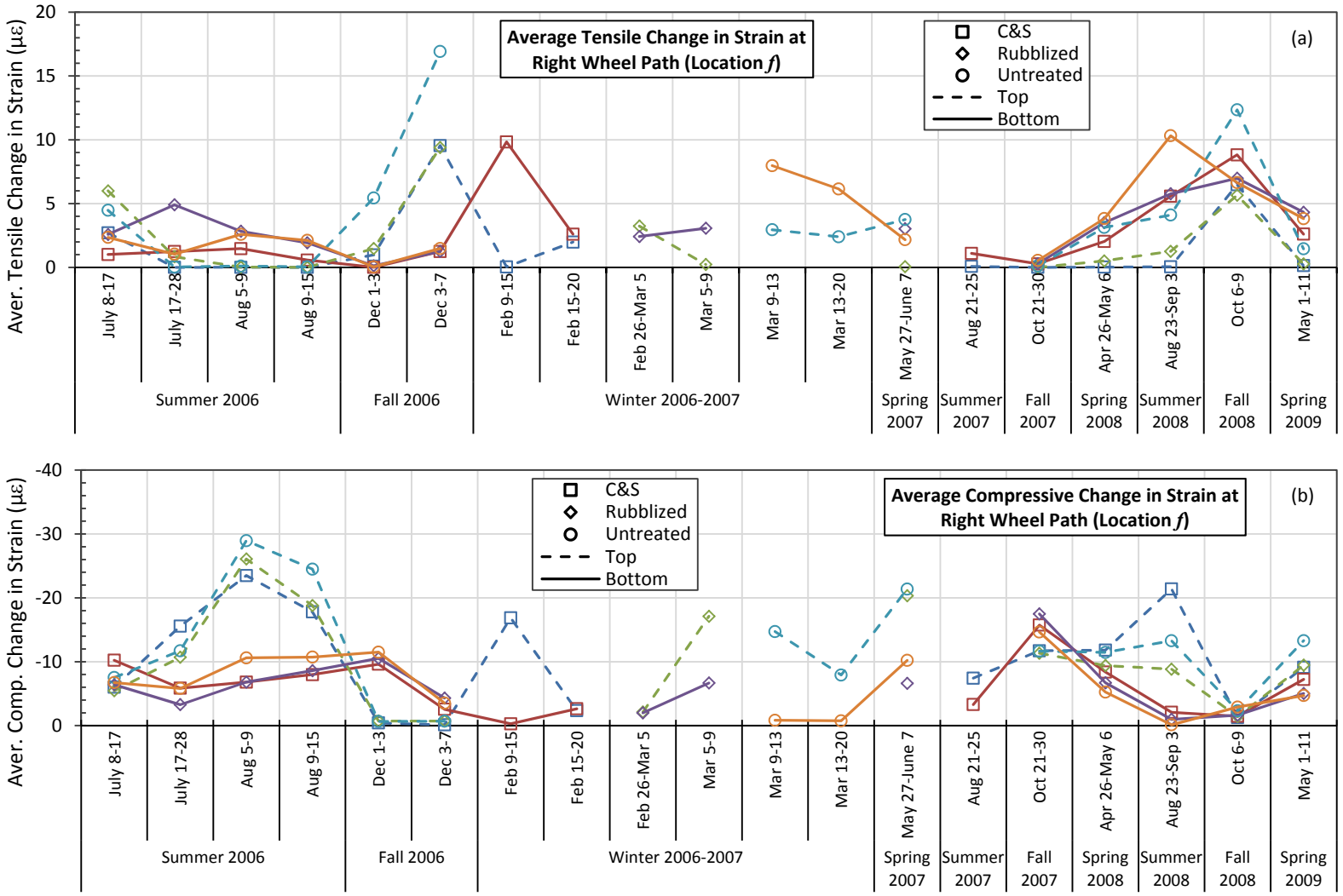

Figure 83. Average Δε at the mid-span location f: a) Tensile strains; b) Compressive strains.

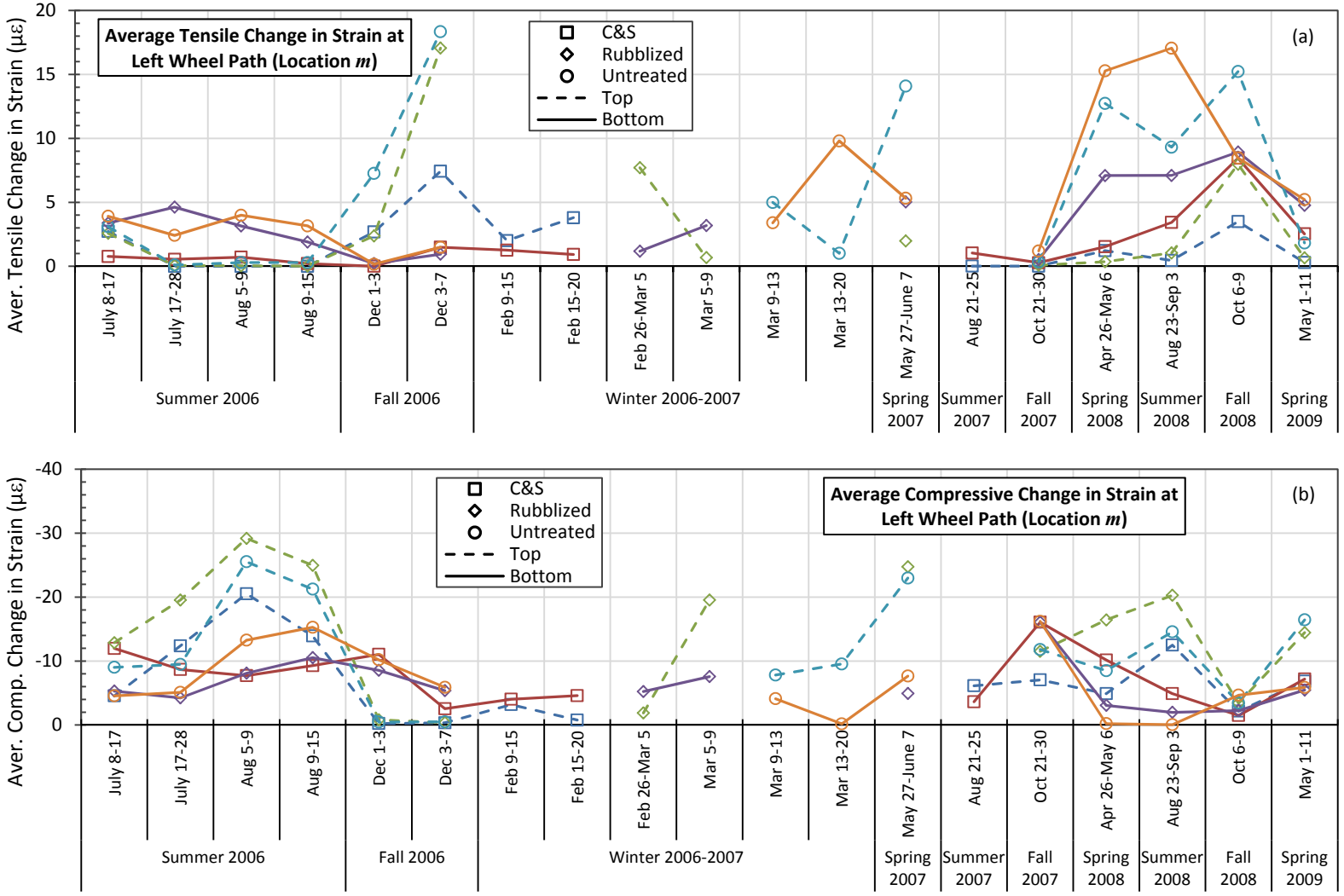

Figure 84. Average Δε at the mid-span location m: a) Tensile strains; b) Compressive strains.

Above, the average change in strain in the center of the slab and mid-span locations ***f*** and ***m*** were compared between the three sections. However, it is necessary also to compare the maximum change in strains in order to describe the differences on the behavior of the three sections. Therefore, the maximum $\Delta\varepsilon$ undergone by the three sections was plotted together for the same locations as before (i.e. locations ***n***, ***f***, and ***m***). Figure 85(a) shows the maximum tensile $\Delta\varepsilon$ experienced by each section at the center of the slab (i.e. location ***n***). In this, it can be seen that the untreated section experienced the highest maximum tensile $\Delta\varepsilon$ at the top and bottom of the slab for the majority of the analyzed periods. Moreover, with the exception of the summer 2006 and fall 2008, the untreated section showed the highest maximum tensile $\Delta\varepsilon$ for all the analyzed periods at the bottom and top respectively. The untreated section did not show the highest maximum values in the summer 2006 period of July 8-17 for the top of the slab and during the summer 2006 periods of July 17-28 and August 9-15 for the bottom of the slab. In these periods, the highest values were experienced by the rubblized section at the top and by the B&S section at the bottom. Conversely, the smallest values at the top of the slab occurred in the rubblized section during six of the 11 periods of common data that correspond to all the periods of 2006 and the spring 2009 period. Likewise, the bottom of the slab in the rubblized section showed the smallest values for the summer 2006 and the fall 2007 period; for the remaining, the B&S section experienced the smallest values. Similarly, the rubblized and B&S sections also experienced the smallest values of maximum compressive change in strain at the top of the slab as it shown in Figure 85(b). The smallest values at the bottom of the slab were shown by the untreated and rubblized sections. On the other hand, the untreated section showed the highest maximum compressive $\Delta\varepsilon$ at the top of the slab for all the analyzed periods while the highest values at the bottom of the slab in general were experienced by the B&S section. The latter showed higher values than those of the rubblized and untreated section during the fall 2006, spring and summer 2008 and spring 2009 periods. For the rest of the analyzed periods, the untreated experienced highest values during the summer 2006 and fall 2008 while the rubblized section showed the highest value during the fall 2007 period. However, the highest maximum compressive $\Delta\varepsilon$ at the bottom as well as the top of the slab for all the analyzed periods was experienced by the untreated section during the spring 2007 period. This value and the corresponding maximum at location ***n*** in the B&S and rubblized sections are listed in Table 15.

The maximum tensile change in strain experienced for each experimental section at location ***f*** is plotted in Figure 86(a). In this can be seen that the highest maximum tensile $\Delta\varepsilon$ at the top of the slab was experienced by the untreated section with the exception of the summer 2006 period of July 17-28 where the rubblized section experienced the highest value. The untreated section also experienced the highest maximum values at the bottom of the slab for five of the 11 periods of common data. These, corresponded to the summer 2006 and 2008 periods as well as the fall 2007 period. Likewise, the rubblized section also experienced the highest values at the top of the slab for five of the 11 analyzed periods. These periods corresponded to the fall 2006 and the spring 2008 and 2009 periods. Conversely, the smallest maximum values in general were shown by the B&S section for both top and bottom of the slab. Similarly, the B&S section also showed the smallest maximum compressive $\Delta\varepsilon$ values at the top of the slab for the majority of the periods of common data while the untreated section experienced the highest values as shown in Figure 86(b). Conversely, the B&S section in general experienced the highest maximum compressive $\Delta\varepsilon$ values at the bottom of the slab while the untreated section showed the smallest values. The highest value of the maximum tensile $\Delta\varepsilon$ for all the analyzed periods were observed

in the untreated section for both top and bottom of the slab. On the other hand, the highest values for the maximum compressive $\Delta\varepsilon$ were observed for the rubblized and untreated sections at the bottom and top of the slab respectively. These values and the corresponding maximum at location ***f*** of the B&S and rubblized sections are listed also in Table 15.

Figure 87 (a) shows the maximum tensile change in strain at the mid-span location ***m*** for the three experimental sections. In this can be seen that the untreated section showed the highest maximum values at the top and bottom of the slab for the majority of the periods analyzed. Moreover, during the spring 2007 and summer 2008, the untreated section showed the highest maximum tensile $\Delta\varepsilon$ for all the analyzed periods at the bottom and top of the slab respectively. The smallest maximum tensile $\Delta\varepsilon$ values on the other hand, were experienced by the B&S for the majority of the periods of common data for both the top and bottom of the slab. This same behavior was observed for the compressive $\Delta\varepsilon$ at the top of the slab as shown in Figure 87(b). Likewise, the B&S section together with the rubblized section showed the smallest values for three of periods analyzed. However, for the bottom of the slab the B&S section showed the highest compressive $\Delta\varepsilon$ for six of the eleven periods of common data while the untreated section showed higher values than the other two sections during four of the remaining periods. The highest compressive $\Delta\varepsilon$ values at the top of the slab in general were experienced by the untreated section. Moreover, the highest maximum compressive $\Delta\varepsilon$ for all the periods analyzed was observed in the untreated section during the spring 2007 for both top and bottom of the slab. These values and the corresponding maximum at location ***m*** of the B&S and rubblized sections are summarized also in Table 15.

Table 15. Highest maximum $\Delta\varepsilon$ (bold/blue values are the highest values among the sections).

Section / Location		B&S		Rubblized		Untreated	
		Top	Bottom	Top	Bottom	Top	Bottom
Tension (με)	***n***	22.27 (Fall 2006)	28.31 (Fall 2008)	22.15 (Fall 2008)	31.72 (Fall 2008)	**59.99** (Fall 2008)	**47.40** (Summer 2008)
	f	19.46 (Fall 2008)	30.24 (Fall 2008)	24.92 (Summer 2006)	26.86 (Summer 2008)	**30.45** (Fall 2008)	**36.86** (Summer 2008)
	m	16.68 (Winter 2007)	29.70 (Fall 2008)	32.13 (Fall 2006)	34.49 (Summer 2008)	**41.92** (Spring 2007)	**53.83** (Summer 2008)
Compression (με)	***n***	-59.14 (Summer 2008)	-30.65 (Fall 2007)	-87.52 (Spring 2007)	-35.57 (Fall 2007)	**-140.13** (Spring 2007)	**-40.61** (Spring 2007)
	f	-53.46 (Summer 2006)	-32.40 (Fall 2007)	-87.31 (Spring 2007)	**-35.81** (Fall 2007)	**-113.39** (Spring 2007)	-32.33 (Fall 2007)
	m	-47.50 (Summer 2006)	-33.71 (Fall 2007)	-122.62 (Spring 2007)	-34.88 (Fall 2007)	**-141.12** (Spring 2007)	**-40.32** (Spring 2007)

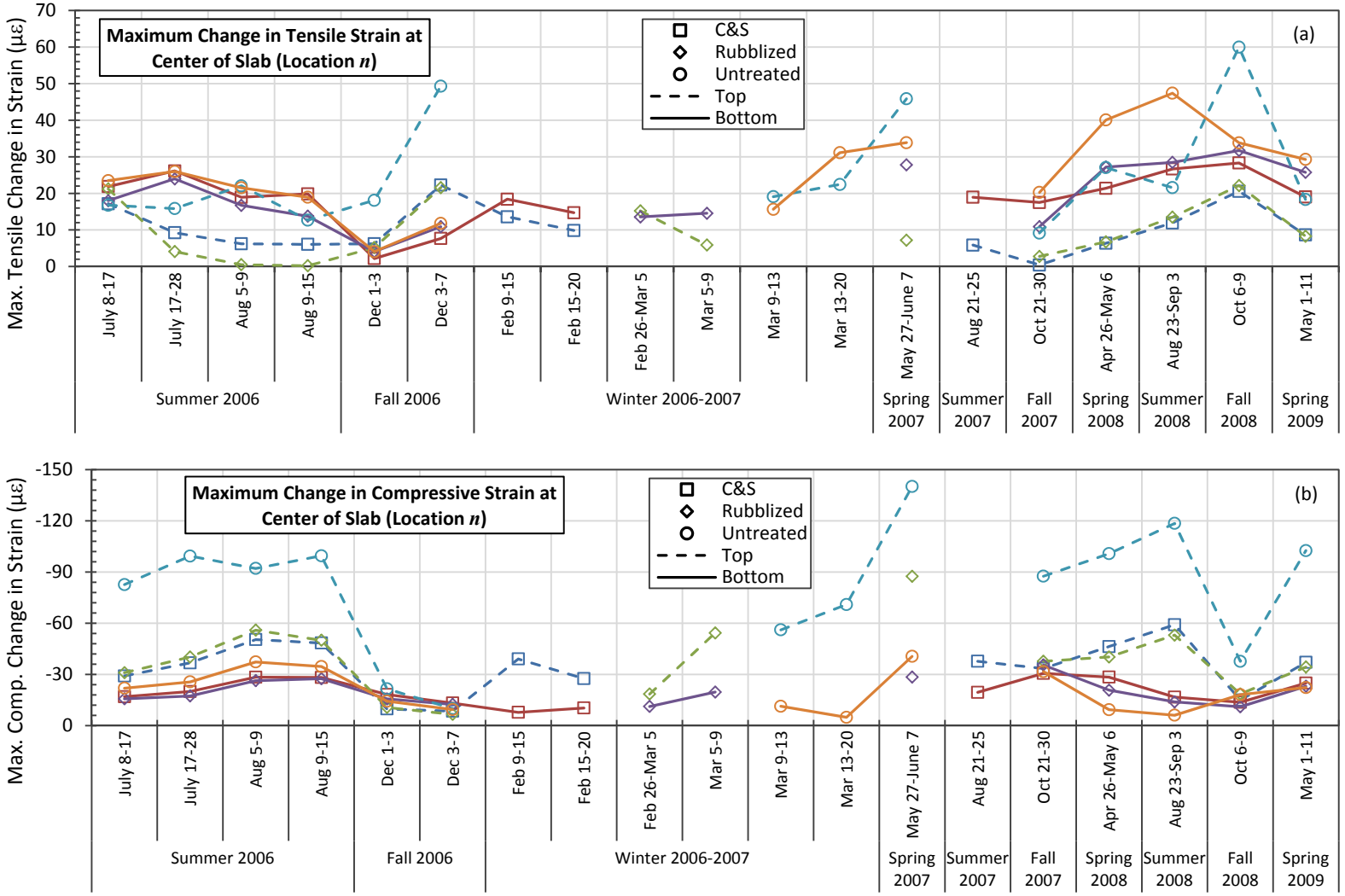

Figure 85. Maximum Δε at the center of slab: a) Tensile strains; b) Compressive strains.

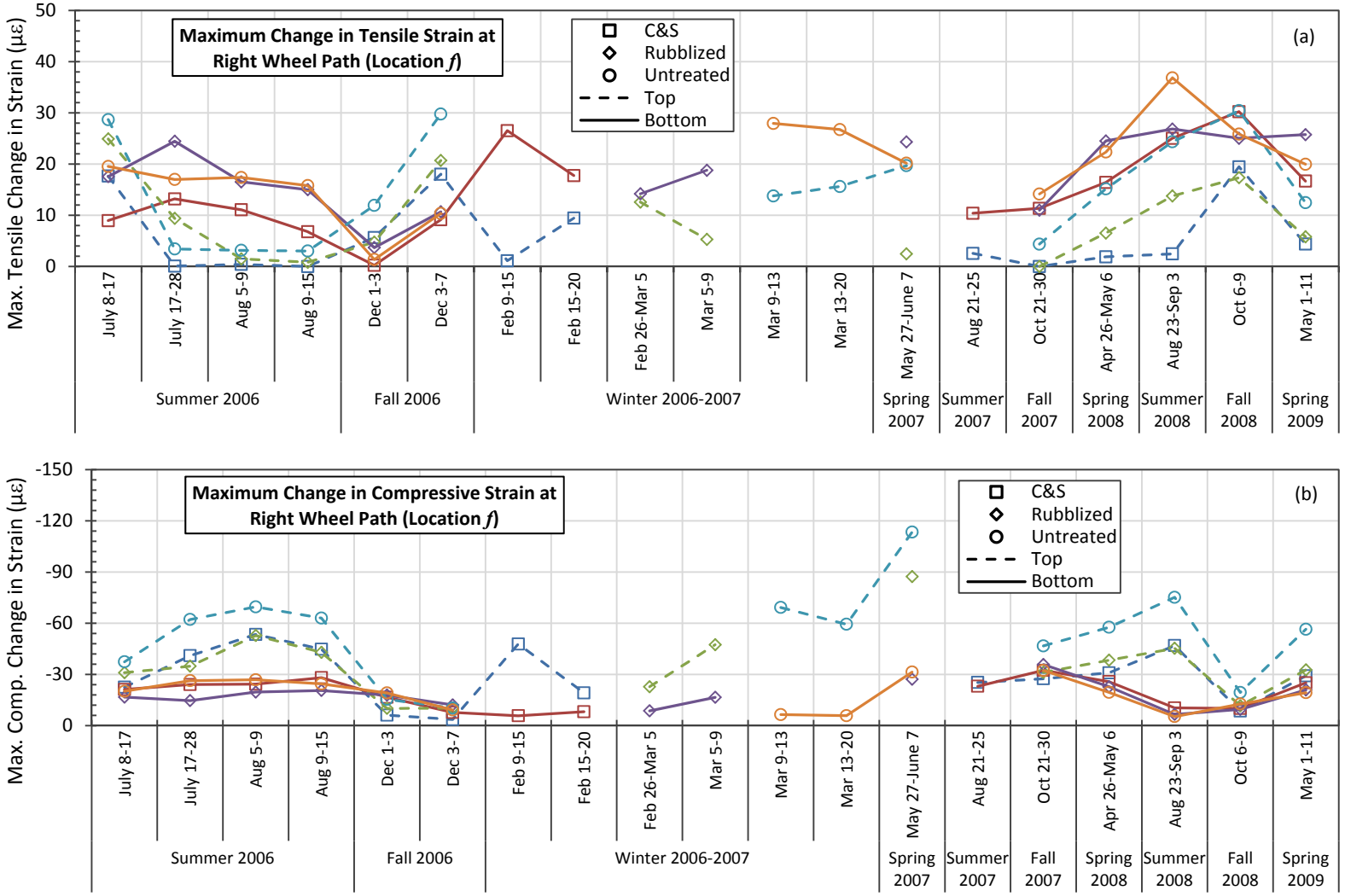

Figure 86. Maximum Δε at mid-span location f: a) Tensile strains; b) Compressive strains.

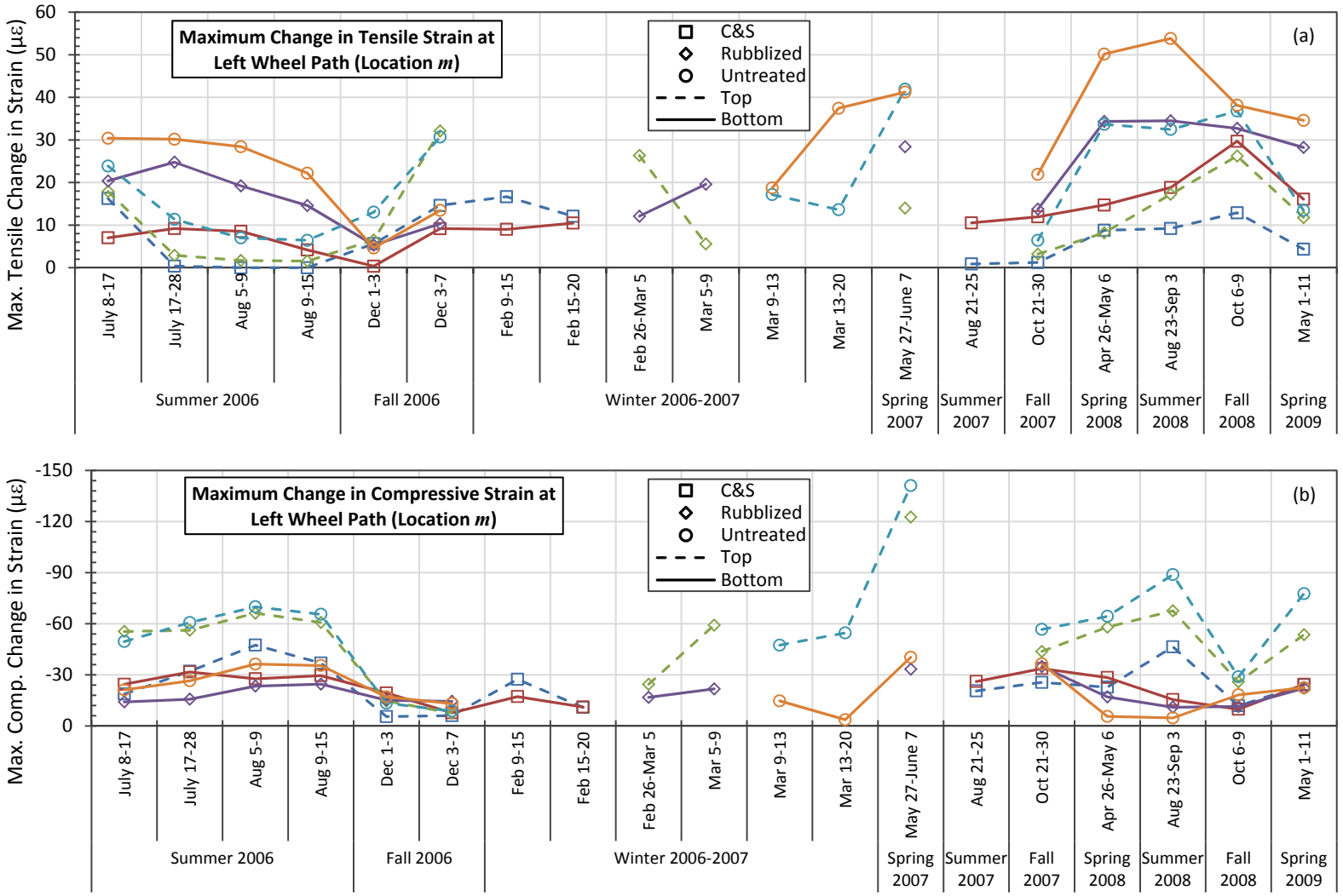

Figure 87. Maximum Δε at mid-span location m: a) Tensile strains; b) Compressive strains.

5.4.2.4 Discussion on the Strain/Stress Differences between Experimental Sections

From the discussion in Section 5.4.2.3, it can be seen that similar results were obtained when using separately the average and maximum values of the $\Delta\varepsilon$ to identify the differences on the environmental response of the experimental sections. Trends were investigated in order to identify which section presented most severe response compared to the other sections. These trends were identified based on the number of periods a section experienced the highest average or maximum values during the 11 periods where data was available for the three sections. However, these 11 periods only involve seven different seasons with four periods during the summer 2006 and two periods during the fall 2006. Therefore, the identification of the section that experienced the highest average or maximum value was based on the times the section showed the highest values. For example, during the summer 2006 the maximum tensile change in strain at the top of the slab in location ***n*** was experienced by the untreated and rubblized sections three and one time respectively, and therefore, the untreated section is selected as the one showing the highest value for the season.

Table 16 lists the occurrence of highest average and maximum values of each section for the seven seasons of common data. This table was constructed using the results in Section 5.4.2.3 and the average and maximum $\Delta\varepsilon$ values listed in Appendix A. From the results, a general trend was observed where the untreated section generally showed the highest average and maximum values at the top of the slab. Additionally, it was observed that the untreated section generally showed the highest tensile average $\Delta\varepsilon$ for the bottom of the slab. In the same way, the untreated section also generally experienced the highest maximum tensile $\Delta\varepsilon$ except at location ***f*** where the maximum values were often observed in the rubblized and untreated section. On the other hand, the highest average and maximum compressive $\Delta\varepsilon$ values at the bottom were observed for the B&S section. Conversely, the lowest tensile maximum values were generally observed in the B&S section at the top and bottom of the slab. Likewise, the B&S section frequently showed the lowest tensile averages at the top and bottom of the slab except at the center of the slab (i.e. location ***n***) where the lowest averages at the top were often observed in the rubblized section. The B&S section also experienced the lowest compressive average and maximum values at the top of the slab except in the center of the slab where both, the rubblized section and the B&S section experienced the lowest values during four season periods. On the other hand, the lowest compressive average and maximum values at the bottom of the slab in locations ***n*** and ***f*** were often observed in the untreated section while the values at the location ***m*** were generally observed in the rubblized and B&S sections.

Table 16. Occurrence of highest average and maximum Δε for each location.

Section			Top						Bottom					
			Max			Min			Max			Min		
			B&S	R	U	B&S	R	U	B&S	R	U	B&S	R	U
Average	Tens.	*n*	0	0	**7**	1	**6**	0	1	2	**5**	**5**	2	0
		f	0	1	**7**	**5**	2	0	1	2	**4**	**6**	0	1
		m	0	0	**7**	**5**	2	0	1	2	**5**	**7**	1	0
	Comp.	*n*	1	1	**6**	**5**	1	1	**4**	1	2	2	**3**	**3**
		f	**3**	1	**3**	**4**	**4**	0	**4**	2	2	3	1	**4**
		m	0	**4**	**4**	**7**	0	0	**4**	0	3	2	**3**	2
Maximum	Tens.	*n*	0	0	**7**	**4**	3	0	1	0	**7**	**5**	2	0
		f	0	0	**7**	**5**	2	0	1	**3**	**3**	**5**	2	0
		m	0	1	**7**	**6**	1	0	0	1	**7**	**7**	0	0
	Comp.	*n*	0	0	**7**	**4**	**4**	0	**4**	1	2	1	2	**4**
		f	0	0	**7**	**5**	2	0	**4**	2	2	1	2	**4**
		m	0	1	**6**	**7**	0	0	**4**	1	3	**3**	**3**	2

In addition to the trends above described, the peak values of the average and maximum $\Delta\varepsilon$ for all the periods analyzed (listed in Table 14 and Table 15) were compared. These values were divided by the smallest peak observed at the specific location, obtaining the ratios of peak average and peak maximum values listed in Table 17 and Table 18, respectively. It can be seen that the untreated section experienced the highest peak value for the tensile average and maximum $\Delta\varepsilon$ at the three studied locations. Furthermore, these values can even triple the smallest peak observed at a specific location. For example, the highest tensile peak average at the top of the slab observed at location ***n*** in the untreated section is 2.9 times the peak value observed in the rubblized section, which was the smallest peak observed.

The highest peak value of the average tensile change in strain occurred in the untreated section for both top and bottom of the slab. The highest peak values corresponding to the compressive averages on the other hand, occurred at the top of the untreated section for locations ***n*** and ***f*** while the top of the slab in the rubblized section showed the highest peak for location ***m***. Conversely, the highest peak of the average compressive $\Delta\varepsilon$ at the bottom of the slab was observed for the rubblized section for locations ***n*** and ***f*** while the untreated section showed the highest peak for location ***m***. Similarly, the highest peak values corresponding to the maximum $\Delta\varepsilon$ at the top and bottom occurred in the untreated section for the three locations with the exception of the bottom of the slab at location ***f*** where the rubblized section experienced the highest peak of compressive $\Delta\varepsilon$.

Table 17. Ratios of peak average $\Delta\varepsilon$ / $\Delta\sigma$.

Location \ Section		B&S		Rubblized		Untreated	
		Top	Bottom	Top	Bottom	Top	Bottom
Tens. (με)	*n*	1.2	**1.0**	**1.0**	1.2	**2.9**	**1.9**
	f	1.0	1.3	**1.0**	**1.0**	**1.8**	**1.5**
	m	**1.0**	**1.0**	2.3	1.1	**2.5**	**2.0**
Comp. (με)	*n*	**1.0**	**1.0**	1.6	**1.3**	**1.9**	1.2
	f	**1.0**	1.1	1.1	**1.2**	**1.2**	**1.0**
	m	**1.0**	1.0	**1.4**	**1.0**	1.2	**1.0**

Table 18. Ratios of peak maximum $\Delta\varepsilon$ / $\Delta\sigma$.

Location \ Section		B&S		Rubblized		Untreated	
		Top	Bottom	Top	Bottom	Top	Bottom
Tens. (με)	*n*	1.0	**1.0**	**1.0**	1.1	**2.7**	**1.7**
	f	**1.0**	1.1	1.3	**1.0**	**1.6**	**1.4**
	m	**1.0**	**1.0**	1.9	1.2	**2.5**	**1.8**
Comp. (με)	*n*	**1.0**	**1.0**	1.5	1.2	**2.4**	**1.3**
	f	**1.0**	1.0	1.6	**1.1**	**2.1**	**1.0**
	m	**1.0**	**1.0**	2.6	1.0	**3.0**	**1.2**

The results obtained and trends described above suggest that the untreated section presented a more severe environmental response when compared with the other two sections at the three chosen locations (i.e. locations ***n***, ***f***, and ***m***). They also suggest that when compared to the other two sections, the B&S section showed the least severe response despite experiencing the highest compressive average and maximum values at the bottom of the slab for most of the periods analyzed. This supported also on the fact that the maximum values of the compressive $\Delta\varepsilon$ at the three studied locations in the untreated section reached a maximum of 147.4 με corresponding to a $\Delta\sigma$ of 3426 kPa (496.9 psi) in compression. This value is less than 12.3% the compressive strength of the concrete reported in Table 2. The following section presents a discussion on the dynamic response of the experimental sections using FWD test results.

5.5 Pavement Response due to Dynamic Loading (FWD Test)

Next, the short-term response of the experimental sections is presented and discussed. As mentioned in Chapter 4, the experimental sections underwent FWD testing and the data collected was used to calculate normalized deflections, normalized strains and to estimate the depth of the effective neutral axis of the pavement structure. FWD testing has taken place at different times of the year since the construction day in June 2006. The analysis presented herein comprises data collected the different dates listed in Table 19. The discussion starts by presenting an analysis of the normalized strains and displacements recorded from the MM strain gauges and LVDTs and their differences due to the location in the slab as well as the difference between sections. Subsequently, the discussion continues comparing the short-term response between the sections. Finally, the results obtained from the FWD test are compared to the strain and displacement responses recorded. Recalling that the LVDTs were removed in early 2007, and despite displacement responses were recorded during the tests in 2006 and March 2007, these will not be discussed herein. A description and analysis of these data was performed by Ambrosino [2007].

Table 19. FWD testing dates on I86 PCC sections.

Date	Strains & Displacements from Sensors Recorded?
June 20, 2006	Yes
November 28, 2006	Yes
March 20, 2007	Yes
October 31, 2007	Yes
May 6, 2008	Yes
May 7, 2008	No
October 21, 2008	Yes
May 13, 2009	No

5.5.1 Short-Term Strain Response

Chapter 4 mentions that the FWD testing consisted of applying an impact load on the slab's top surface that will cause the slab to deform and therefore the MM strain gauges will too. From the gauges then are recorded strain responses like the one shown in Figure 88 for both the top and bottom of the slab at the locations indicated in Figure 2. Figure 88 shows a typical behavior of the strain variation with time due to an impact load. The impact load causes the slab to deflect and bending strains are experienced through the depth of the slab. These strains are represented by the peaks in the strain vs. time chart and each of them corresponds to one of the impact loads applied. Later on, each of those peak values is normalized in order to study relationships between applied loads and strains as well as to compare the responses between the sections. In Table 20 and Table 21 are listed the strains, normalized strains and their respective impact load for the third drop where the positive and negative values correspond to elongation and contraction of the gauge respectively. These data are plotted in Figure 90 and Figure 91 organized by section and by date respectively so the variations and differences between location of sensors, section or season could be easily identified. Although some of the sensors were damaged during paving, the redundancy of gauges allowed collection of significant data. The strains and remaining data corresponding to the first and second drops are provided in Appendix B.

In addition to the strain responses, the deflections caused by the FWD testing were recorded. The FWD test was performed along the centerline of the slabs measuring the deflections for drops at the center of the slab, at the joint-approach and the joint-leave locations. Deflections were then normalized and used to calculate spreadability, load transfer efficiency (LTE) of the joints as well as the joint support ratio. Additionally, FWD testing was performed at the sensors locations and the deflections measured were correlated to the measured strains. In the following sections are discussed the strain responses to FWD testing and their differences between sections followed by a discussion of the FWD test results that includes a view of the relationship of the FWD test results and the strain response.

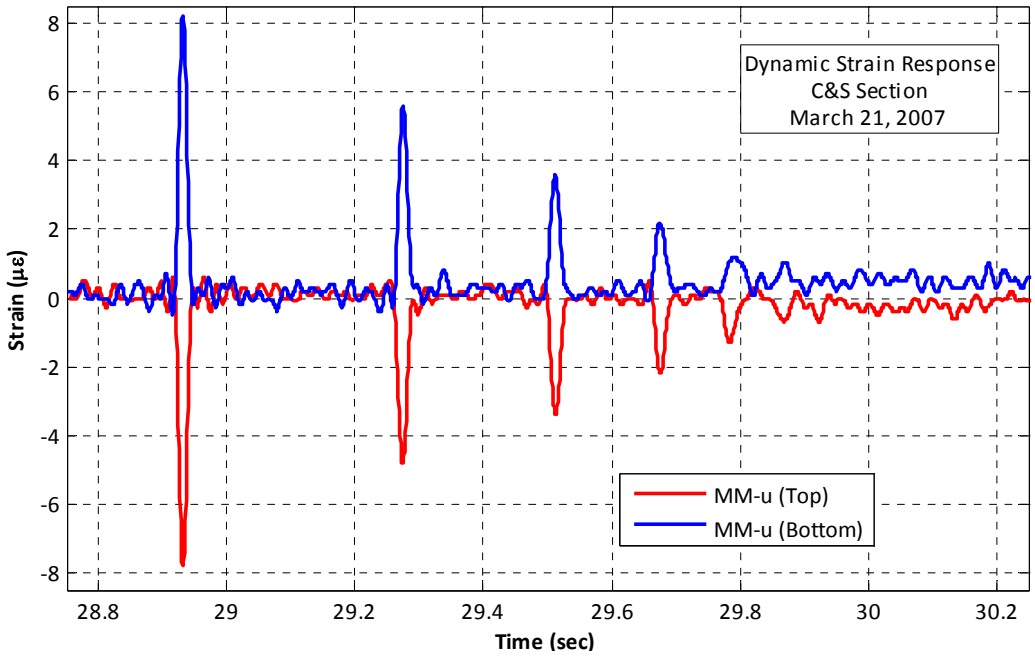

Figure 88. Typical dynamic strain response, in this case on 3rd drop on March 21, 2007, with impact load 71 kN (16 kip).

Table 20. Dynamic strains and normalized strains for 3rd drop of FWD June 2006 through March 2007 (1 kN = 0.225 kip; 1 με/kN = 4.45 με/kip).

Section		B&S			Rubblized			Untreated		
Sensor Location		Load (kN)	Strain (με)	Norm. Strain (με/kN)	Load (kN)	Strain (με)	Norm. Strain (με/kN)	Load (kN)	Strain (με)	Norm. Strain (με/kN)
20-June-2006										
MM-t	Top	71.06	-	-	69.97	-12.30	-0.176	71.03	-	-
	Bottom		6.50	0.091		8.90	0.127		-	-
MM-u	Top	71.12	-9.10	-0.128	72.13	-8.50	-0.118	71.52	-	-
	Bottom		6.50	0.091		7.20	0.100		5.90	0.082
MM-v	Top	70.84	-14.20	-0.200	70.67	-	-	70.52	-9.00	-0.128
	Bottom		7.80	0.110		9.70	0.137		4.00	0.057
MM-w	Top	70.30	-10.90	-0.155	71.96	-10.00	-0.139	71.40	-7.80	-0.109
	Bottom		7.50	0.107		9.10	0.126		5.00	0.070
29-November-2006										
MM-t	Top	73.26	-	-	72.77	-9.50	-0.131	73.65	-	-
	Bottom		-	-		8.80	0.121		4.90	0.296
MM-u	Top	73.36	-9.90	-0.135	72.68	-7.30	-0.100	73.55	-	-
	Bottom		10.50	0.143		7.30	0.100		3.90	0.053
MM-v	Top	73.21	-17.80	-0.243	72.53	-	-	73.45	-10.70	-0.146
	Bottom		10.80	0.148		8.60	0.119		5.90	0.080
MM-w	Top	73.45	-12.10	-0.165	72.34	-7.80	-0.108	73.50	-5.60	-0.076
	Bottom		9.40	0.128		9.40	0.130		7.40	0.101
21-March-2007										
MM-t	Top	67.37	-	-	67.37	-9.70	-0.144	65.38	-	-
	Bottom		11.00	0.163		9.70	0.144		8.50	0.130
MM-u	Top	66.84	-8.00	-0.120	67.52	-5.40	-0.080	65.27	-	-
	Bottom		8.10	0.121		7.80	0.116		6.10	0.093
MM-v	Top	65.18	-22.10	-0.339	67.47	-	-	64.71	-15.40	-0.238
	Bottom		13.40	0.206		9.70	0.144		11.00	0.170
MM-w	Top	66.25	-13.60	-0.205	67.18	-7.20	-0.107	65.78	-7.00	-0.106
	Bottom		9.60	0.145		7.80	0.116		7.80	0.119

Table 21. Dynamic strains and normalized strains for 3rd drop of FWD, October 2007 through October 2008 (1 kN = 0.225 kip; 1 με/kN = 4.45 με/kip).

Section		B&S			Rubblized			Untreated		
Sensor Location		Load (kN)	Strain (με)	Norm. Strain (με/kN)	Load (kN)	Strain (με)	Norm. Strain (με/kN)	Load (kN)	Strain (με)	Norm. Strain (με/kN)
31-October-2007										
MM-t	Top	67.32	-	-	66.55	-11.5	-0.173	66.55	-	-
	Bottom		7.70	0.114		7.7	0.116		4.70	0.071
MM-u	Top	66.16	-7.60	-0.115	66.11	-5.3	-0.080	66.50	-	-
	Bottom		6.00	0.091		4.7	0.071		6.10	0.092
MM-v	Top	66.11	-16.80	-0.254	66.84	-	-	66.40	-6.60	-0.099
	Bottom		10.10	0.153		7.2	0.108		5.00	0.075
MM-w	Top	66.01	-10.10	-0.153	67.03	-6.4	-0.095	66.25	-4.10	-0.062
	Bottom		6.70	0.101		6.1	0.091		7.00	0.106
3-May-2008										
MM-t	Top	70.21	-	-	69.16	-17.3	-0.250	71.57	-	-
	Bottom		-	-		15.9	0.230		11.60	0.162
MM-u	Top	72.10	-	-	73.23	-8.7	-0.119	72.05	-	-
	Bottom		-	-		10.1	0.138		12.70	0.176
MM-v	Top	70.26	-	-	69.97	-	-	70.47	-19.90	-0.282
	Bottom		-	-		24.3	0.347		19.30	0.274
MM-w	Top	71.39	-	-	71.94	-	-	71.49	-11.40	-0.159
	Bottom		-	-		18	0.250		13.10	0.183
18-October-2008										
MM-t	Top	71.65	-	-	71.05	-7.7	-0.108	71.44	-	-
	Bottom		7.20	0.100		8.3	0.117		5.90	0.083
MM-u	Top	71.14	-4.80	-0.067	71.20	-3.8	-0.053	71.04	-	-
	Bottom		5.70	0.080		6.6	0.093		8.20	0.115
MM-v	Top	70.50	-10.00	-0.142	71.03	-	-	71.04	-5.60	-0.079
	Bottom		8.20	0.116		8	0.113		8.50	0.120
MM-w	Top	70.01	-10.40	-0.149	71.02	-5.1	-0.072	70.73	-6.20	-0.088
	Bottom		8.70	0.124		6.8	0.096		8.20	0.116

5.5.1.1 Strain Response Differences due to Location within the Slab

A direct comparison of the strain and normalized strain values in Table 20 and Table 21 shows that the minimum strains (or normalized strains) at top and bottom of the slab for all the sections occurred in general at the joint locations (i.e. locations ***u*** or ***w***) for the majority of the testing sessions. It is only for the untreated section that the minimum values at the bottom of the slab occurred mostly at the mid-span (i.e. locations ***t*** or ***v***). For instance, from Figure 90 it can be seen that in the B&S and Rubblized section, the minimum strains occurred at the joint location ***u*** for the majority of the sessions while in the untreated section, the minimum values were observed mostly for the joint location ***w*** at the top of the slab. The minimum values at the bottom of the slab in the untreated section occurred at locations ***v*** and ***u*** for the summer 2006, fall 2006 and winter 2007 periods respectively; for the rest of the periods the minimum values were observed at the mid-span location ***t***. The maximum strains on the other hand, in general occurred at the mid-span for the three sections. For example, from Figure 90 it can be seen that in the rubblized section and untreated sections, the maximum strains at the top of the slab occurred at locations ***t*** and ***v*** respectively. Conversely, the maximum values at the bottom were observed in

location ***t*** and ***v*** for the rubblized and untreated sections respectively. Finally, in the B&S, the maximum strains occurred at the mid-span location ***v*** for both top and bottom of the slab.

A general trend was also observed from the third-drop normalized strains where the top of the slab at the mid-span (i.e. locations ***t*** and ***v***) generally showed higher values than the bottom of the slab for all the sections whereas for the joint location (i.e. locations ***u*** and ***w***) a clear trend cannot be established. For example, the rubblized and untreated sections experienced in the mid-span higher values at the top than at the bottom of the slab while the opposite occurred at the joint location. In the case of the B&S section, it experienced higher strains at the top than at the bottom for all the periods analyzed for both locations. Figure 91 shows the variation of the normalized strain corresponding to the third drop for all the sections organized by seasons. When comparing by seasons, the three sections experienced higher values at the top than at the bottom of the slab for the summer 2006 and fall 2007 in both mid-span and joint locations except for the untreated section. The latter showed higher values at the bottom in location ***w*** for the fall 2007 session. Similarly, the bottom of the slab showed higher strains during the fall 2008 test in the three sections except for the B&S section, which showed the highest values at the top of the slab in both locations. For the remaining periods, a clear trend between top and bottom cannot be established.

Notice that the comparisons aforementioned described are based on the magnitude of the strain and normalized strains regardless of the sign, which as mentioned before will be negative and positive for top and bottom respectively. Additionally, comparing the magnitude of the strains allows identifying possible composite behavior of the pavement section. In order to do this, the amount of shifting of the neutral axis of the concrete slabs was calculated using Equation (14) and the dynamic strain measured from the MM strain gauges. The amount of shifting of the neutral axis is defined herein as the distance between the theoretical neutral axis (NA) and effective neutral axis (ENA) of the pavement section. The effective neutral axis corresponds to the plane where the dynamic strains are zero assuming a linear distribution of the strains through the thickness of the slab. On the other hand, the theoretical neutral axis is assumed to be located at the centerline of the cross section. Negative shifting values means that the effective neutral axis of the section is located below the centerline of the slab's cross section while positive shifting values indicate that this is located above the centerline. Furthermore, a negative shifting value may indicate either that the actual thickness of the slab at that location is less than the designed thickness (225 mm or 8.86 in) or it can also indicate the presence of a composite behavior of the slab and the ATPB interlayer. Composite behavior is feasible between the concrete slab and the interlayer considering that the latter is a permeable base where "wet concrete undoubtedly seeped" during construction creating a bond between the two layers [Ambrosino, 2007, p. 134]. This can be seen from the shifting values corresponding to the test performed in June 2006, as shown in Figure 89. Additionally, if the amount of negative shifting shows a steady decrement with the time approaching zero it may be an indicator of the loss of this composite behavior. On the other hand, positive shifting values may be an indicator of either the actual thickness of the slab is more than the designed thickness at the particular location. Despite the above described, pointing out the actual case that applies to a specific location has to be decided by determining the in-situ thickness of the pavement. Calculated values of the amount of shifting of the neutral axis for the first and second drop are provided in Appendix B for further review.

Figure 89 shows the amount of shifting of the neutral axis for each section and for all the periods were FWD test was performed. The values plotted correspond to the third drop (i.e. reference impact load of 71 kN (16kips)). It can be seen that the amount of shifting of the neutral axis in the B&S section remained negative at both the mid-slab and joint locations for all the periods shown with the exception of the fall 2008 period. For this period, the ENA seems to have moved upwards at location ***u***. However, it can be seen that the ENA steadily move upwards at the location ***v*** while for the joint locations it moved upwards and then downwards. Similar behavior was observed in the rubblized section where the shifting values showed more variability from test to test even at the mid-span location. In the rubblized section, at the joint locations, the ENA was above the theoretical neutral axis for the fall 2006, winter 2007 and fall 2008 periods while it stayed below the theoretical neutral axis for the summer 2006 and fall 2007 sessions. Conversely, the effective neutral axis at location ***t*** remained below the theoretical neutral axis for all the testing sessions. For the untreated section on the other hand, it can be seen that at the joint location ***w***, the ENA was above the theoretical neutral axis for all the sessions except for the test performed in June 2006. At the mid-span location ***v***, the ENA stayed below the theoretical neutral axis but steadily moved upwards until being above of it for the test performed in the fall 2008.

From the results above discussed, it can be concluded that definitely existed some composite behavior between the concrete slab and the ATPB interlayer. Moreover, this conclusion is supported by the tendency observed of higher strains magnitudes at the top than at the bottom of the slab. Additionally, without discarding the variance of thickness from its design value, the variability of the amount of shifting values from test to test support the case of a composite behavior of the slab-interlayer system. This suggests that the interlayer was not really a total bond breaker.

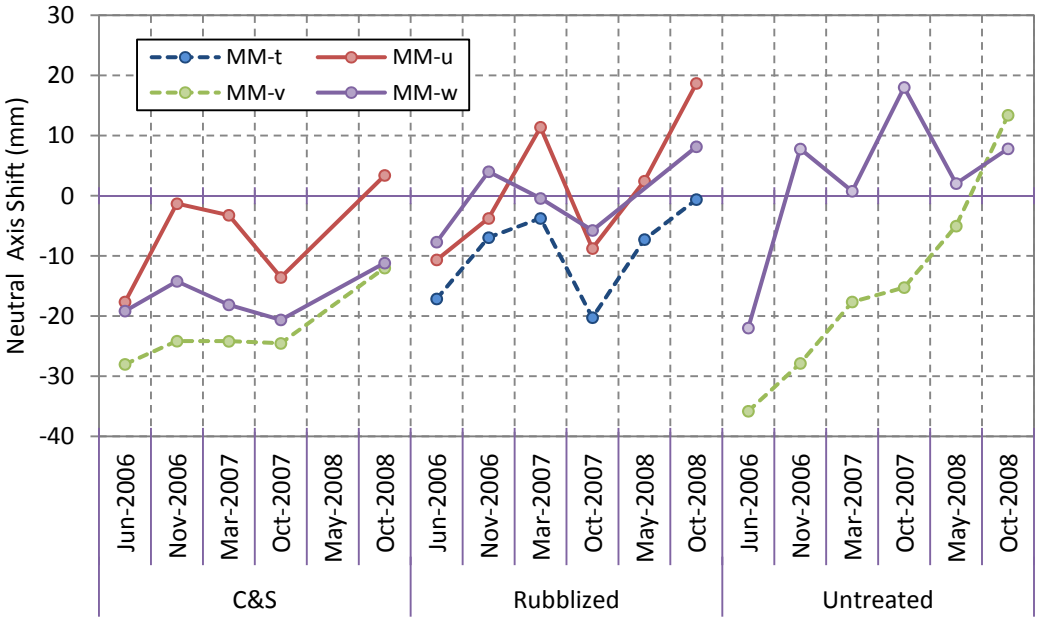

Figure 89. Neutral axis shifting; zero corresponds to the center of the cross-section (25.4 mm = 1 in).

5.5.1.2 Strain Response Differences between Experimental Sections

Regarding the differences of the strain and normalized strain between sections, Table 22 lists the occurrence of maximum strains corresponding to the third drop (as well as normalized strains) for all the dates when FWD testing was performed. It can be seen from this table and from Figure 91 that in general the untreated section at the mid-span (i.e. locations ***t*** and ***v***) experienced the smallest strains than the other two sections for both top and bottom of the slab. Conversely, and despite having available readings only from location ***v***, the B&S section showed the maximum strains at the top of the slab. The rubblized section experienced the maximum strains at the bottom of the slab in location ***t*** for most of the testing dates except for those performed in 2007 where the B&S showed the maximum values. Additionally, the B&S section showed the maximum strains at the bottom in location ***v*** for half of the periods analyzed (Nov 2006 period and 2007 periods); for the other periods, the rubblized followed by the untreated section showed the maximum values. For the joint location (i.e. locations ***u*** and ***w***), the maximum strains at the top occurred in the B&S section for all the periods while the minimum strains were observed in the rubblized and untreated section at locations ***u*** and ***w*** respectively. On the other hand, the maximum strains at the bottom of the slab were observed in the B&S section for three of the testing dates at location ***w*** while the untreated section showed maximum strains at the bottom of the slab in location ***u*** for the October 2007 and 2008 tests.

Table 22. Occurrence of maximum strains/normalized strains for each location on 3rd drop of FWD.

		Top						Bottom					
		Max			Min			Max			Min		
Sensor		B&S	R	U	B&S	R	U	B&S	R	U	B&S	R	U
Mid Span	*t*	-	-	-	-	-	-	2	4	0	1	0	5
	v	5	0	0	0	0	5	3	2	1	0	2	4
Joint	*u*	5	0	0	0	5	0	2	1	3	1	2	3
	w	5	0	0	0	1	4	3	2	1	0	3	3

In addition to the aforementioned trends, the highest values of the strain and normalized strains were compared obtaining equivalent results. Thus, the strains showed the same trends that the normalized strains. Table 23 shows the highest strains and normalized strains observed for each sensor and Table 24 shows the ratios of the strain and normalized strain to the minimum value observed between the three sections for the specific location. From the tables can be seen that the B&S and rubblized sections experienced the highest strains and normalized strains at the top and bottom of the slab respectively. Moreover, the strains at the top of the slab were as high as 36% more the smallest maximum strain. This is the case of the strain at the location ***w*** where the highest value was observed for the B&S section while the smallest value correspond to the rubblized section. Similarly, the strains at the bottom of the slab were as high as 81% more than the smallest maximum strain. This case corresponds to the strains at the location ***v***, where the highest and smallest values were shown by the rubblized and B&S sections respectively.

Table 23. Maximum dynamic strains and normalized strains (bold/blue/red values are extremes (1 με/kN = 4.45 με/kip).

Sensor			B&S Top	B&S Bottom	Rubblized Top	Rubblized Bottom	Untreated Top	Untreated Bottom
Dynamic Strain (με)	Mid Span	*t*	-	11.00 (Winter 2007)	-17.30 (Spring 2008)	**15.90** (Spring 2008)	-	11.60 (Spring 2008)
		v	**-22.10** (Winter 2007)	13.40 (Winter 2007)	-	**24.30** (Spring 2008)	-19.90 (Spring 2008)	19.30 (Spring 2008)
	Joint	*u*	**-9.90** (Fall 2006)	10.50 (Fall 2006)	-8.70 (Spring 2008)	10.10 (Spring 2008)	-	**12.70** (Spring 2008)
		w	**-13.60** (Winter 2007)	9.60 (Winter 2007)	-10.00 (Summer 2006)	**18.00** (Spring 2008)	-11.40 (Spring 2008)	13.10 (Spring 2008)
Normalized Strain (με/kN)	Mid Span	*t*	-	0.163 (Winter 2007)	-0.250 (Spring 2008)	**0.230** (Spring 2008)	-	0.162 (Spring 2008)
		v	**-0.339** (Winter 2007)	0.206 (Winter 2007)	-	**0.347** (Spring 2008)	-0.282 (Spring 2008)	0.274 (Spring 2008)
	Joint	*u*	**-0.135** (Fall 2006)	0.143 (Fall 2006)	-0.119 (Spring 2008)	0.138 (Spring 2008)	-	**0.176** (Spring 2008)
		w	**-0.205** (Winter 2007)	0.145 (Winter 2007)	-0.139 (Summer 2006)	**0.250** (Spring 2008)	-0.159 (Spring 2008)	0.183 (Spring 2008)

Based on the results and trends of the strain response discussed above, it can be inferred that the B&S section followed by the rubblized section presented the most critical dynamic strain response among the three sections for both the mid-span and joint locations. In addition, the results suggest that the untreated section can be considered the section with the least critical dynamic strain response. However, notice that the strain responses discussed above do not totally describe the behavior of each section due to the FWD testing and therefore, a conclusion of which is the most critical section based on the FWD test results cannot be provided yet. In the following section, the deflections measured from the FWD and relationships with the measured strains are discussed.

Table 24. Ratios of maximum strains and normalized strains.

Sensor			B&S Top	B&S Bottom	Rubblized Top	Rubblized Bottom	Untreated Top	Untreated Bottom
Dynamic Strain	Mid Span	*t*	-	**1.000**	1.000	**1.445**	-	1.055
		v	**1.111**	**1.000**	-	**1.813**	**1.000**	1.440
	Joint	*u*	**1.138**	1.040	**1.000**	**1.000**	-	**1.257**
		w	**1.360**	**1.000**	**1.000**	**1.875**	1.140	1.365
Normalized Strain	Mid Span	*t*	-	**1.007**	**1.000**	**1.418**	-	**1.000**
		v	**1.201**	**1.000**	-	**1.689**	**1.000**	1.332
	Joint	*u*	**1.136**	**1.038**	**1.000**	**1.000**	-	**1.278**
		w	**1.477**	**1.000**	**1.000**	**1.727**	1.148	1.265

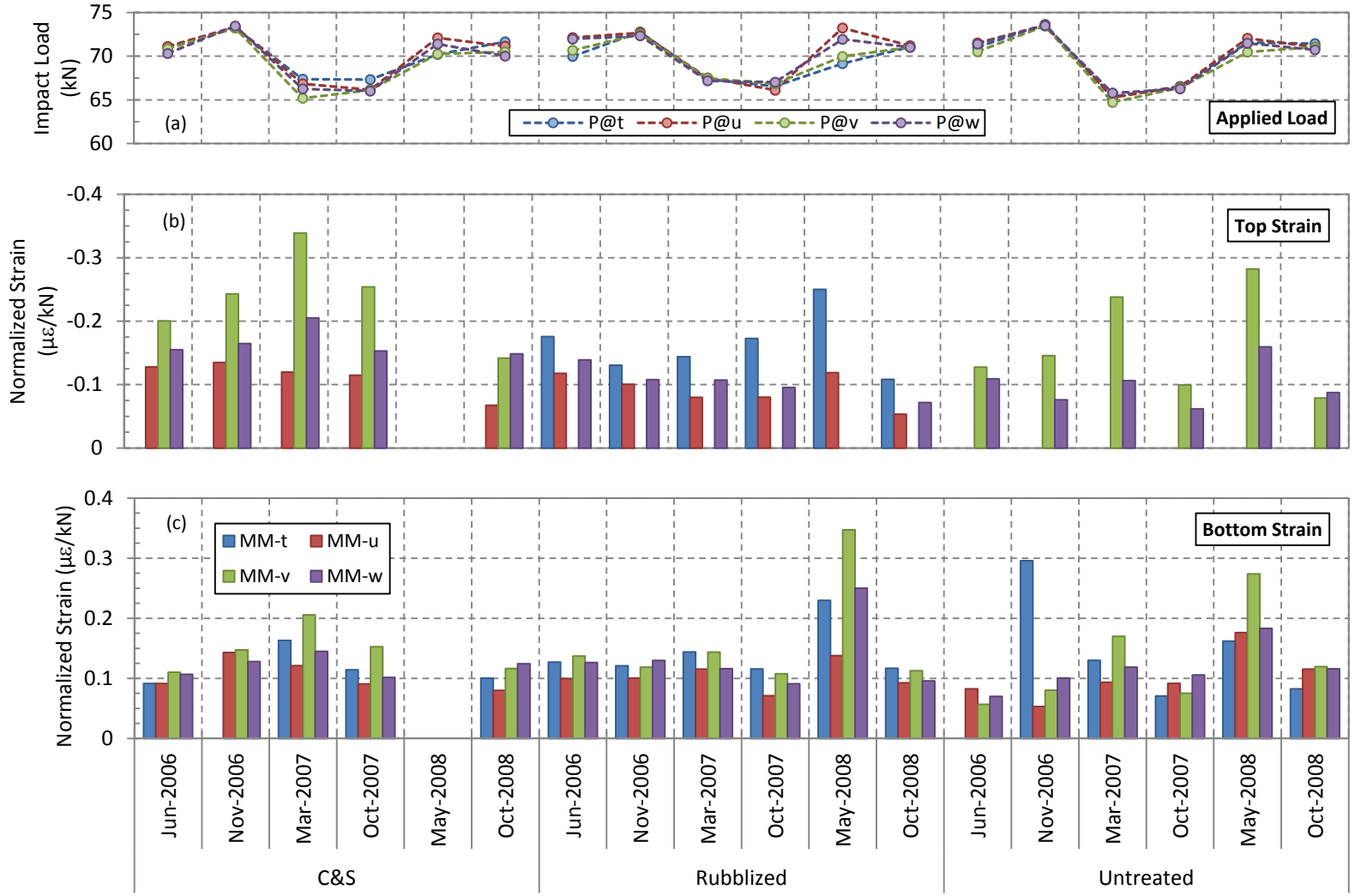

Figure 90. Normalized strain and applied load by section for 3rd drop of FWD: a) Applied load, b) Top strain, c) Bottom strain (1 kN = 0.225 kip; 1 με/kN = 4.45 με/kip).

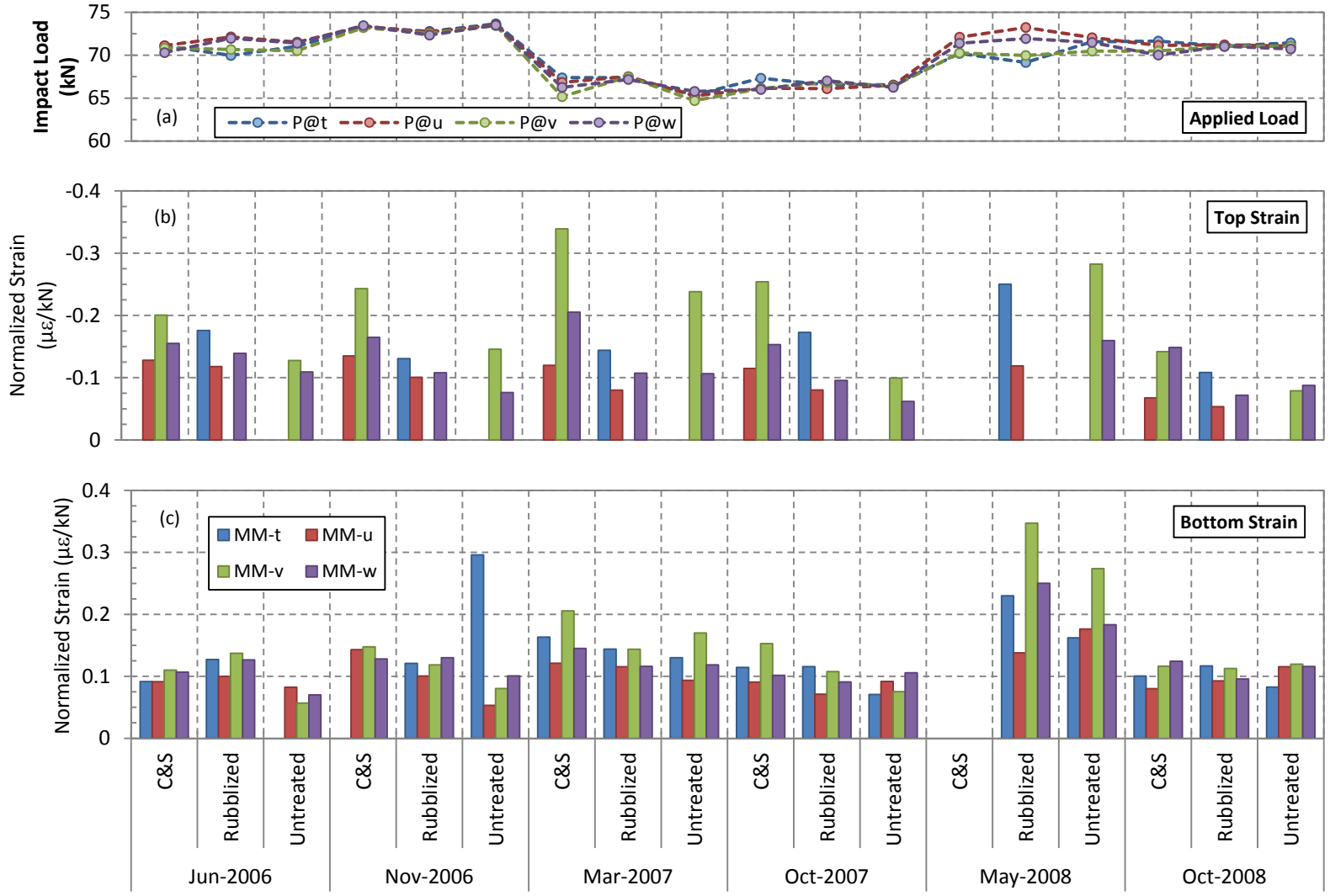

Figure 91. Normalized strain and applied load by date for 3rd drop of FWD: a) Applied load, b) Top strain, c) Bottom strain (1 kN = 0.225 kip; 1 με/kN = 4.45 με/kip).

5.5.2 FWD Testing Results

As mentioned above the deflections were measured at the center of the slabs and load transfer testing was performed at the joints along the centerline of the slabs. The data collected was plotted to identify trends or inconsistency within the data. Subsequently, values corresponding to the third drop of the normalized deflection measured by seismometer zero (i.e. at the loading location), the joint load transfer efficiencies (LTE), joint support ratio and spreadability were averaged. The averages and standard deviations for each measurement data are listed in Table 31, Table 32, and Table 33 respectively for break and seat, rubblized, and untreated experimental sections. In addition, FWD testing was performed also at the sensor locations with the purpose of establishing relationships between these and the strain and displacement responses discussed above. The FWD data corresponding to the first and second drops are provided in Appendix C for further reviews.

5.5.2.1LVDT Deflections due to FWD loads

Sample plots of vertical deflection versus time at location b on June 20, 2006 are presented in Figure 92, Figure 93, and Figure 94 for the three sections. Table 25 was constructed with the peak values from plots of all collected data. Only the load-normalized deflections are shown in Table 26. In the subsequent tables the normalized results from the LVDTs and FWD device are shown separately. Both sets are organized in the same manner as the peak strain data: by section and by month.

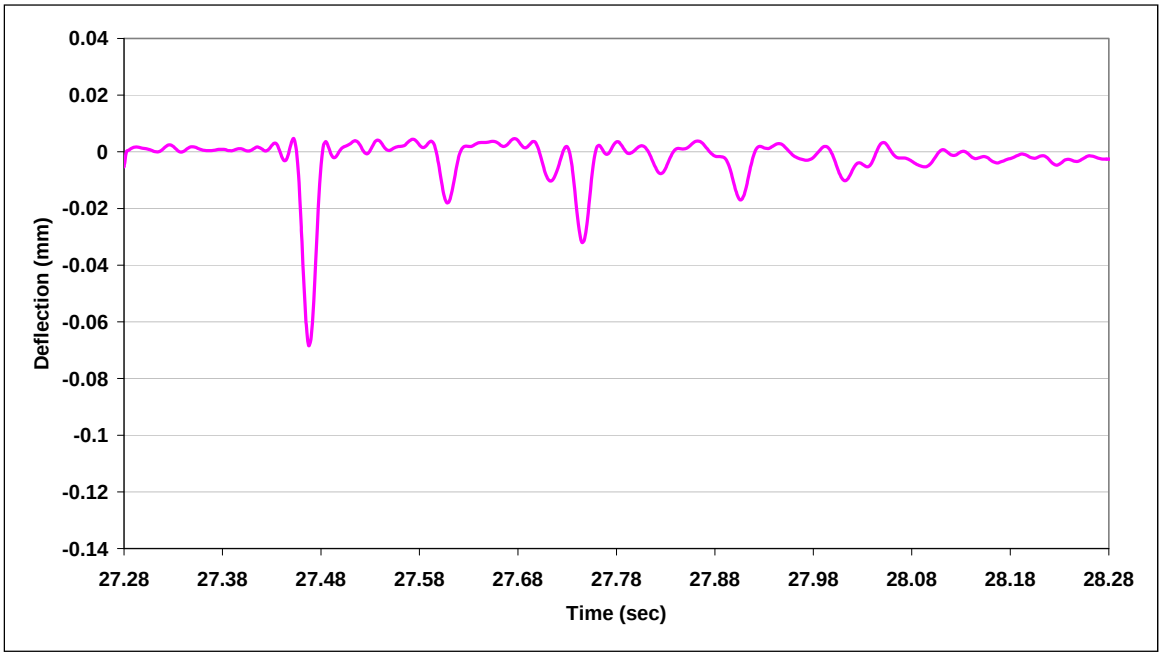

Figure 92. Dynamic deflection response, untreated section, location b, June 20, 2006 (1 mm = 39.4 mil).

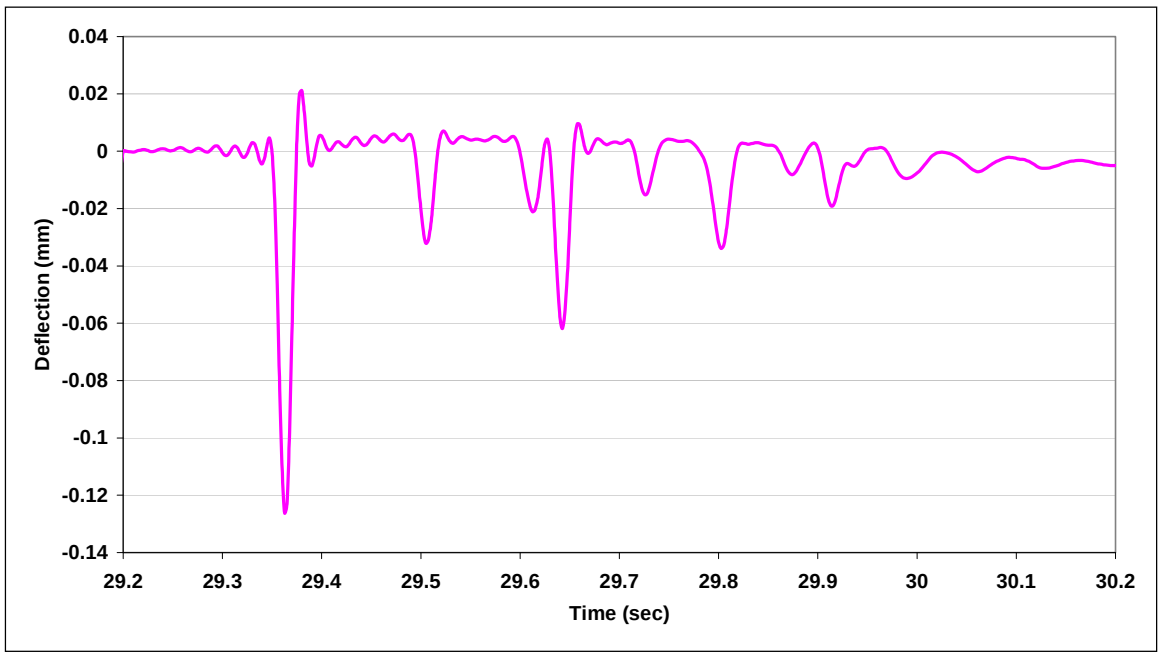

Figure 93. Dynamic deflection response, rubblized section, location b, June 20, 2006 (1 mm = 39.4 mil).

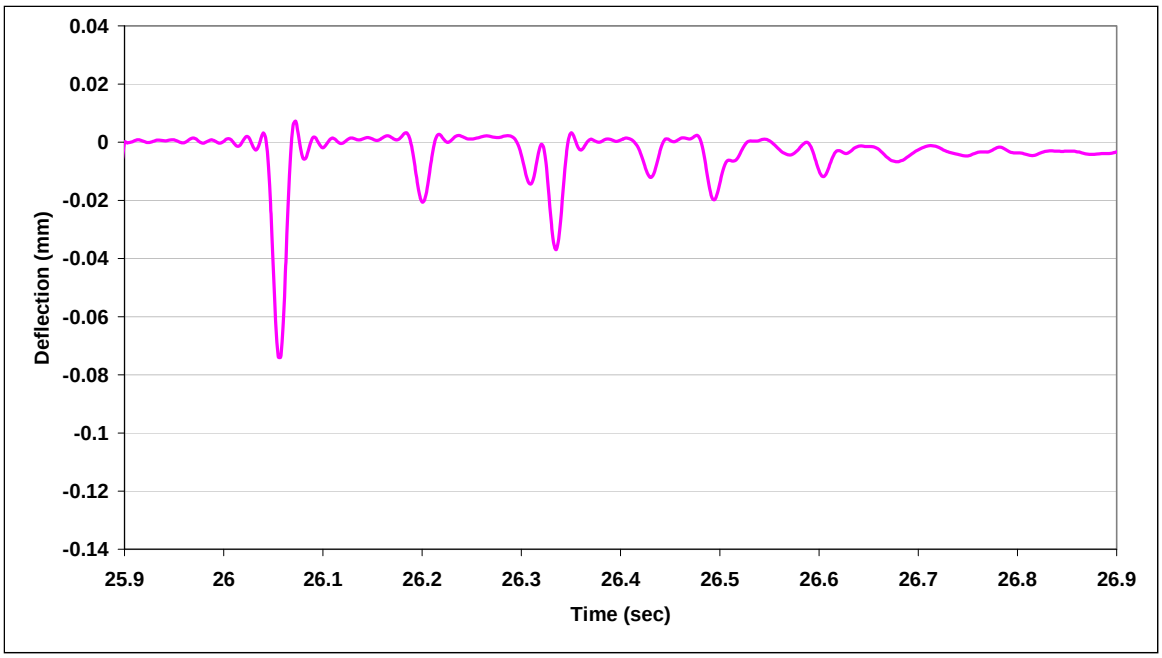

Figure 94. Dynamic deflection response, broken and seated section, location b, June 20, 2006 (1 mm = 39.4 mil).

From the June 20, 2006 FWD testing series, the rubblized section clearly experienced higher displacement at LVDT b than the B&S or untreated section, with a peak magnitude of 0.126 mm (4.96 mil), while B&S was only 0.074 mm (2.91 mil), and untreated just 0.068 mm (2.68 mil). LVDT b is a deep reference instrument, meaning that it reads the total deflection of the pavement and the subgrade combined. The deflections occurring at this location show that the rubblized section has less stiff support than B&S or untreated slabs. To identify the source of the differences in displacement between the sections, the responses from shallow LVDTs were

examined. From the June 20, 2006 section of Table 25, shallow LVDTs a, c, d, and i also exhibit significantly higher displacements in the rubblized section, again suggesting that the rubblized base is significantly less stiff than the B&S or untreated concrete. Furthermore, with the minor exception of the readings by LVDT i, the rubblized displaced the most in every shallow location, the B&S section displaced next most, and the untreated section displaced the lease, according to both the LVDTs and the FWD device. In November 2006 and March 2007, the B&S section typically displaced as much or more than the rubblized section, while the untreated section still exhibited the smallest displacements.

The magnitudes of displacement, however, are also dependent on the load. When the displacements are normalized by the load acting, a more equal comparison of the responses may be made. While the largest deflections occurred in the rubblized section, this section also incurred the highest load of the three sections of 71.89kN (16.16 kip). The load from drop 3 on LVDT b in the B&S section was 71.32kN (16.03 kip), and in the untreated section it was 71.17kN (16.00 kip). When the displacements were normalized by the loads, the rank remained the same, just in slightly different ratios: rubblized, 1.754 μm/kN (0.307 mil/kip); B&S, 1.035 μm/kN (0.181 mil/kip); untreated, 0.961μm/kN (0.168 mil/kip). When using the vertical displacement values to calculate relationships directly, the rubblized section deflected 1.853 times more than the untreated section. When comparing the normalized deflections, the ratio reduces to 1.825, which is 2.5% less. The difference is small but normalized quantities are more appropriate and more informative than making direct comparisons. Table 25 includes all available data from LVDTs and from the FWD device to March 2007, before the LVDTs were removed. Table 27 and Table 28 show the peak FWD and LVDT load response displacements, respectively. In each table, the data are organized by section on the left and by date on the right.

Table 25. Peak dynamic deflections and normalized deflections from FWD testing – all data (1 µm/kN = 0.17526 mil/kip; 1 kN = 0.225 kip; 1 mm = 39.4 mil).

June 20th 2006		Untreated			Rubbilized			C/S		
LVDT	micron/kN	Load (kN)	d (mm)	Norm. Disp. (micron/kN)	Load (kN)	d (mm)	Norm. Disp. (micron/kN)	Load (kN)	d (mm)	Norm. Disp. (micron/kN)
a	d_{FWD}	71.07	0.100	1.404	70.72	0.144	2.040	71.14	0.136	1.910
	d_{LVDT}		0.019	0.270		0.032	0.447		0.027	0.385
b	d_{FWD}	71.17	0.098	1.374	71.89	0.162	2.254	71.32	0.126	1.774
	d_{LVDT}		0.068	0.961		0.126	1.754		0.074	1.035
c	d_{FWD}	71.17	0.083	1.171	71.01	0.140	1.978	68.30	0.099	1.443
	d_{LVDT}		ND	ND		0.026	0.362		0.020	0.288
d	d_{FWD}	71.38	0.086	1.199	71.00	0.131	1.839	71.46	0.107	1.500
	d_{LVDT}		ND	ND		ND	ND		ND	ND
i	d_{FWD}	71.07	0.103	1.447	70.79	0.175	2.476	71.32	0.121	1.699
	d_{LVDT}		0.025	0.355		0.055	0.770		0.020	0.280
J	d_{FWD}	71.85	0.088	1.223	71.11	0.131	1.839	70.60	0.112	1.587
	d_{LVDT}		ND	ND		0.087	1.221		0.068	0.969
k	d_{FWD}	70.94	0.087	1.225	71.36	0.130	1.819	71.93	0.061	0.855
	d_{LVDT}		0.214	3.018		0.087	1.225		0.068	0.951
L	d_{FWD}	71.35	0.087	1.225	71.31	0.136	1.913	71.57	0.116	1.622
	d_{LVDT}		0.058	0.813		0.093	1.301		0.085	1.182
November 28th 2006		Untreated			Rubbilized			C/S		
LVDT		Load (kN)	d (mm)	Norm. Disp. (micron/kN)	Load (kN)	d (mm)	Norm. Disp. (micron/kN)	Load (kN)	d (mm)	Norm. Disp. (micron/kN)
a	d_{FWD}	ND	ND	ND	ND	ND	ND	ND	ND	ND
	d_{LVDT}		ND	ND		ND	ND		ND	ND
b	d_{FWD}	ND	ND	ND	ND	ND	ND	ND	ND	ND
	d_{LVDT}		ND	ND		ND	ND		ND	ND
c	d_{FWD}	73.77	0.073	0.988	74.60	0.105	1.410	73.53	0.107	1.451
	d_{LVDT}		0.013	0.182		0.021	0.279		0.017	0.231
d	d_{FWD}	77.38	0.086	1.106	73.77	0.098	1.322	73.92	0.135	1.821
	d_{LVDT}		ND	ND		ND	ND		0.013	0.173
i	d_{FWD}	ND	ND	ND	ND	ND	ND	ND	ND	ND
	d_{LVDT}		ND	ND		ND	ND		ND	ND
J	d_{FWD}	74.89	0.084	1.123	73.04	0.109	1.488	73.68	0.167	2.262
	d_{LVDT}		ND	ND		ND	ND		ND	ND
k	d_{FWD}	74.46	ND	ND	73.63	0.101	1.366	75.14	0.152	2.028
	d_{LVDT}		0.057	0.764		ND	ND		0.058	0.765
L	d_{FWD}	73.92	0.066	0.887	74.07	0.103	1.396	73.34	0.269	3.668
	d_{LVDT}		0.067	0.909		ND	ND		0.098	1.334
March 21st 2007		Untreated			Rubbilized			C/S		
LVDT		Load (kN)	d (mm)	Norm. Disp. (micron/kN)	Load (kN)	d (mm)	Norm. Disp. (micron/kN)	Load (kN)	d (mm)	Norm. Disp. (micron/kN)
a	d_{FWD}	ND	ND	ND	ND	ND	ND	ND	ND	ND
	d_{LVDT}		ND	ND		ND	ND		ND	ND
b	d_{FWD}	ND	ND	ND	ND	ND	ND	ND	ND	ND
	d_{LVDT}		ND	ND		ND	ND		ND	ND
c	d_{FWD}	65.85	0.098	1.492	67.93	0.168	2.479	68.32	0.164	2.398
	d_{LVDT}		ND	ND		ND	ND		ND	ND
d	d_{FWD}	65.15	0.128	1.968	68.41	0.124	1.819	66.66	0.142	2.138
	d_{LVDT}		ND	ND		ND	ND		ND	ND
i	d_{FWD}	ND	ND	ND	ND	ND	ND	ND	ND	ND
	d_{LVDT}		ND	ND		ND	ND		ND	ND
J	d_{FWD}	65.51	0.091	1.393	68.07	0.120	1.761	66.22	0.133	2.006
	d_{LVDT}		ND	ND		ND	ND		ND	ND
k	d_{FWD}	64.95	0.204	3.143	67.83	0.137	2.015	65.93	0.237	3.591
	d_{LVDT}		ND	ND		ND	ND		ND	ND
L	d_{FWD}	66.04	0.105	1.586	67.78	0.098	1.443	67.20	0.143	2.128
	d_{LVDT}		ND	ND		ND	ND		ND	ND

Shaded rows represent deep reference LVDTs

*ND indicates no usable data

Table 26. Peak dynamic normalized deflection response data (1 µm/kN = 0.17526 mil/kip).

micron/kN		Untreated			Rubbilized			Crack & Seat		
Location		June	Nov	Mar	June	Nov	Mar	June	Nov	Mar
a	d_{FWD}	1.40	ND	ND	2.04	ND	ND	1.91	ND	ND
	d_{LVDT}	0.27	ND	ND	0.45	ND	ND	0.39	ND	ND
b	d_{FWD}	1.37	ND	ND	2.25	ND	ND	1.77	ND	ND
	d_{LVDT}	0.96	ND	ND	1.75	ND	ND	1.03	ND	ND
c	d_{FWD}	1.17	0.99	1.49	1.98	1.41	2.48	1.44	1.45	2.40
	d_{LVDT}	ND	0.18	ND	0.36	0.28	ND	0.29	0.23	ND
d	d_{FWD}	1.20	1.11	1.97	1.84	1.32	1.82	1.50	1.82	2.14
	d_{LVDT}	ND	ND	ND	ND	ND	ND	ND	0.17	ND
i	d_{FWD}	1.45	ND	ND	2.48	ND	ND	1.70	ND	ND
	d_{LVDT}	0.35	ND	ND	0.77	ND	ND	0.28	ND	ND
j	d_{FWD}	1.22	1.12	1.39	1.84	1.49	1.76	1.59	2.26	2.01
	d_{LVDT}	ND	ND	ND	1.22	ND	ND	0.97	ND	ND
k	d_{FWD}	1.22	ND	3.14	1.82	1.37	2.01	0.85	2.03	3.59
	d_{LVDT}	3.02	0.76	ND	1.22	ND	ND	0.95	0.77	ND
l	d_{FWD}	1.22	0.89	1.59	1.91	1.40	1.44	1.62	3.67	2.13
	d_{LVDT}	0.81	0.91	ND	1.30	ND	ND	1.18	1.33	ND

*ND indicates no usable data

Table 27. Peak dynamic deflection LVDT data. Left: organized by section; Right: organized by date (1 µm/kN = 0.17526 mil/kip).

micron/kN		Untreated		Rubbilized		Crack & Seat	
Location		June	Nov	June	Nov	June	Nov
a	LVDT	0.27	ND	0.45	ND	0.39	ND
b	LVDT	0.96	ND	1.75	ND	1.03	ND
c	LVDT	ND	0.18	0.36	0.28	0.29	0.23
d	LVDT	ND	ND	ND	ND	ND	0.17
i	LVDT	0.35	ND	0.77	ND	0.28	ND
J	LVDT	ND	ND	1.22	ND	0.97	ND
k	LVDT	3.02	0.76	1.22	ND	0.95	0.77
L	LVDT	0.81	0.91	1.30	ND	1.18	1.33

*ND indicates no usable data

micron/kN		June			Nov		
Location		Untreated	Rubbilized	C/S	Untreated	Rubbilized	C/S
a	LVDT	0.27	0.45	0.39	ND	ND	ND
b	LVDT	0.96	1.75	1.03	ND	ND	ND
c	LVDT	ND	0.36	0.29	0.18	0.28	0.23
d	LVDT	ND	ND	ND	ND	ND	0.17
i	LVDT	0.35	0.77	0.28	ND	ND	ND
J	LVDT	ND	1.22	0.97	ND	ND	ND
k	LVDT	3.02	1.22	0.95	0.76	ND	0.77
L	LVDT	0.81	1.30	1.18	0.91	ND	1.33

*ND indicates no usable data

Table 28. Peak dynamic deflection FWD data. Left: organized by section; Right: organized by date (1 µm/kN = 0.17526 mil/kip).

micron/kN		Untreated			Rubbilized			Crack & Seat		
Location		June	Nov	Mar	June	Nov	Mar	June	Nov	Mar
a	FWD	1.40	ND	ND	2.04	ND	ND	1.91	ND	ND
b	FWD	1.37	ND	ND	2.25	ND	ND	1.77	ND	ND
c	FWD	1.17	0.99	1.49	1.98	1.41	2.48	1.44	1.45	2.40
d	FWD	1.20	1.11	1.97	1.84	1.32	1.82	1.50	1.82	2.14
i	FWD	1.45	ND	ND	2.48	ND	ND	1.70	ND	ND
J	FWD	1.22	1.12	1.39	1.84	1.49	1.76	1.59	2.26	2.01
k	FWD	1.22	ND	3.14	1.82	1.37	2.01	0.85	2.03	3.59
L	FWD	1.22	0.89	1.59	1.91	1.40	1.44	1.62	3.67	2.13

*ND indicates no usable data

micron/kN		June			Nov			Mar		
Location		Untreated	Rubbilized	C/S	Untreated	Rubbilized	C/S	Untreated	Rubbilized	C/S
a	FWD	1.40	2.04	1.91	ND	ND	ND	ND	ND	ND
b	FWD	1.37	2.25	1.77	ND	ND	ND	ND	ND	ND
c	FWD	1.17	1.98	1.44	0.99	1.41	1.45	1.49	2.48	2.40
d	FWD	1.20	1.84	1.50	1.11	1.32	1.82	1.97	1.82	2.14
i	FWD	1.45	2.48	1.70	ND	ND	ND	ND	ND	ND
J	FWD	1.22	1.84	1.59	1.12	1.49	2.26	1.39	1.76	2.01
k	FWD	1.22	1.82	0.85	ND	1.37	2.03	3.14	2.01	3.59
L	FWD	1.22	1.91	1.62	0.89	1.40	3.67	1.59	1.44	2.13

*ND indicates no usable data

The dynamic deflection data from the above tables are shown graphically in the following figures. Inadequate amounts of data were collected from the LVDTs in the November 2006 and March 2007 testing periods due to equipment weathering and traffic control constraints. Despite the shortfalls from the LVDTs, sufficient data were obtained to deduce general relationships between the sections and the seasons. Figure 95 and Figure 96 show the data organized by date

and by section, respectively. In general the rubblized section experienced the largest displacements in June 2006 (with the notable exception of LVDT k in the untreated section, which is discussed subsequently). The data from November 2006, however, are inconclusive.

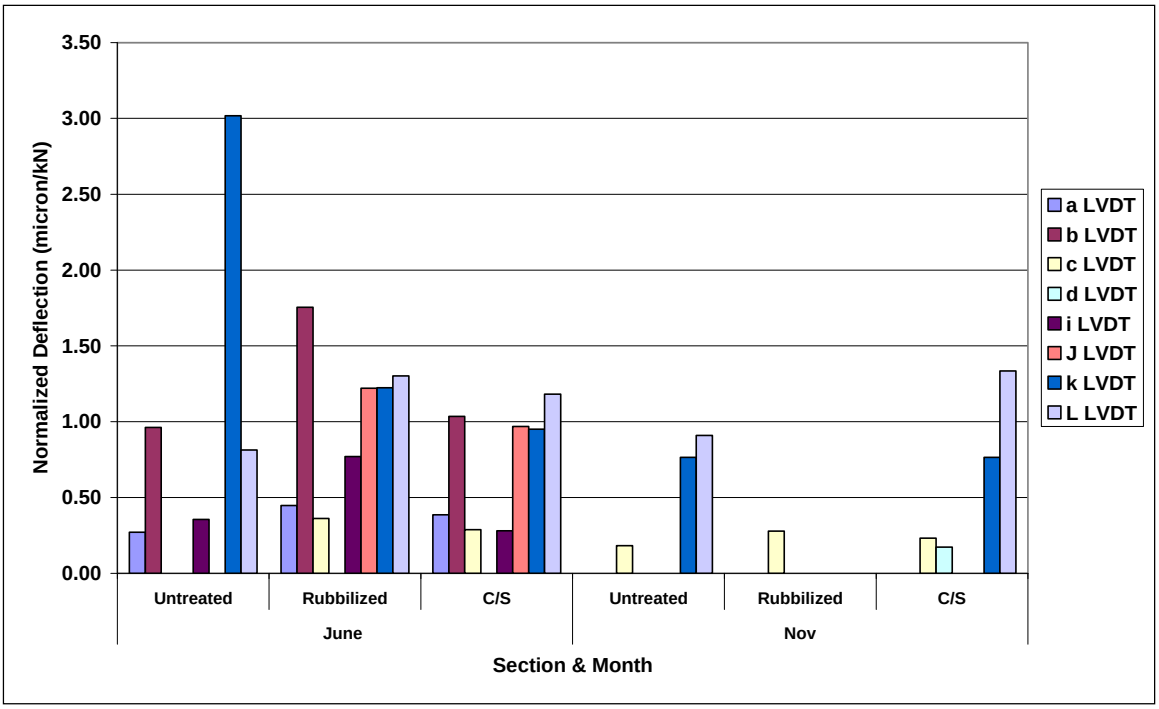

Figure 95. Peak dynamic deflection responses from LVDTs organized by date (1 µm/kN = 0.17526 mil/kip).

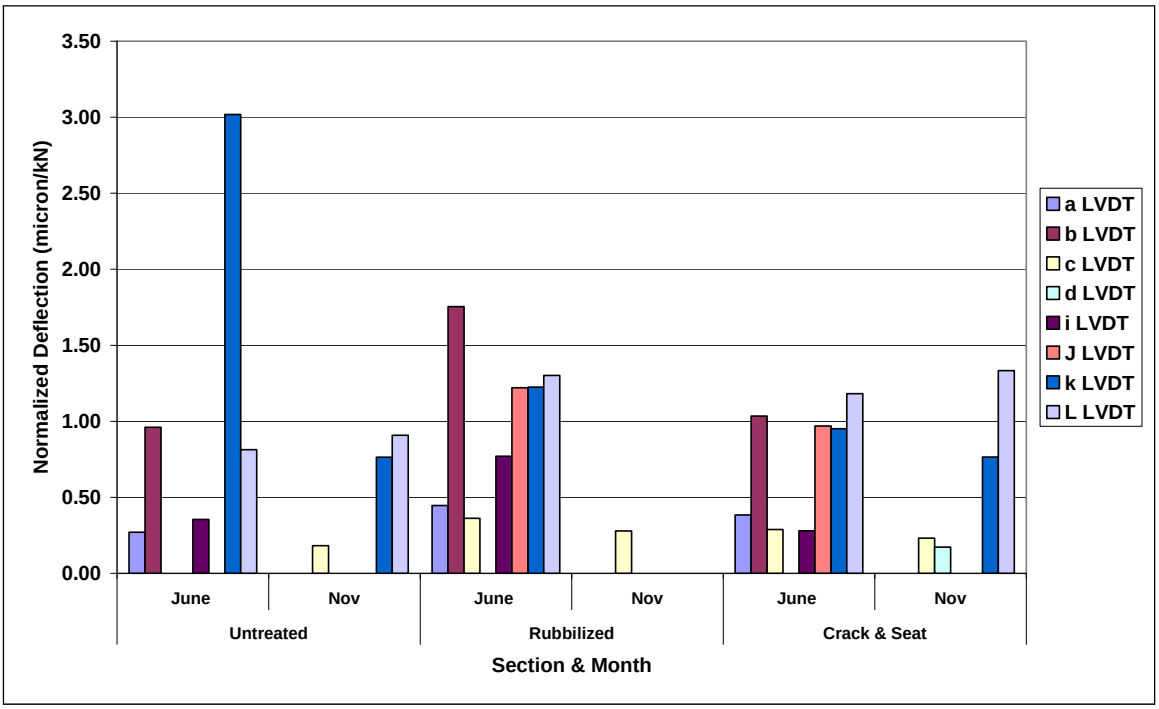

Figure 96. Peak dynamic deflection response from LVDTs organized by section (1 µm/kN = 0.17526 mil/kip).

Due to limited data, relationships in Figure 96 are more elusive when comparing the response of any section between seasons. From the untreated and B&S sections, the data show that midslab deflections (LVDT k – outer wheel path midslab) were higher in June than in November, while at the joint, the deflections were greater in November, albeit only slightly. In June, the very high displacement measured in the untreated section by LVDT k may be justified by the temperature gradient at the time of testing. The drop occurred at about 6:00pm, when the temperature gradient in the concrete was at a high positive value, meaning that the top of the slab was several degrees warmer than the bottom. This induced a concave down curled shape, causing the center of the slab to lift. In the untreated section, this lift was not supported while in the rubblized and C/S sections, more support was maintained by the base and the AC interlayer.

For comparisons at specific locations, Figure 97 and Figure 98 were organized by sensor location. This allows for the normalized deflections at matching locations to be compared by section.

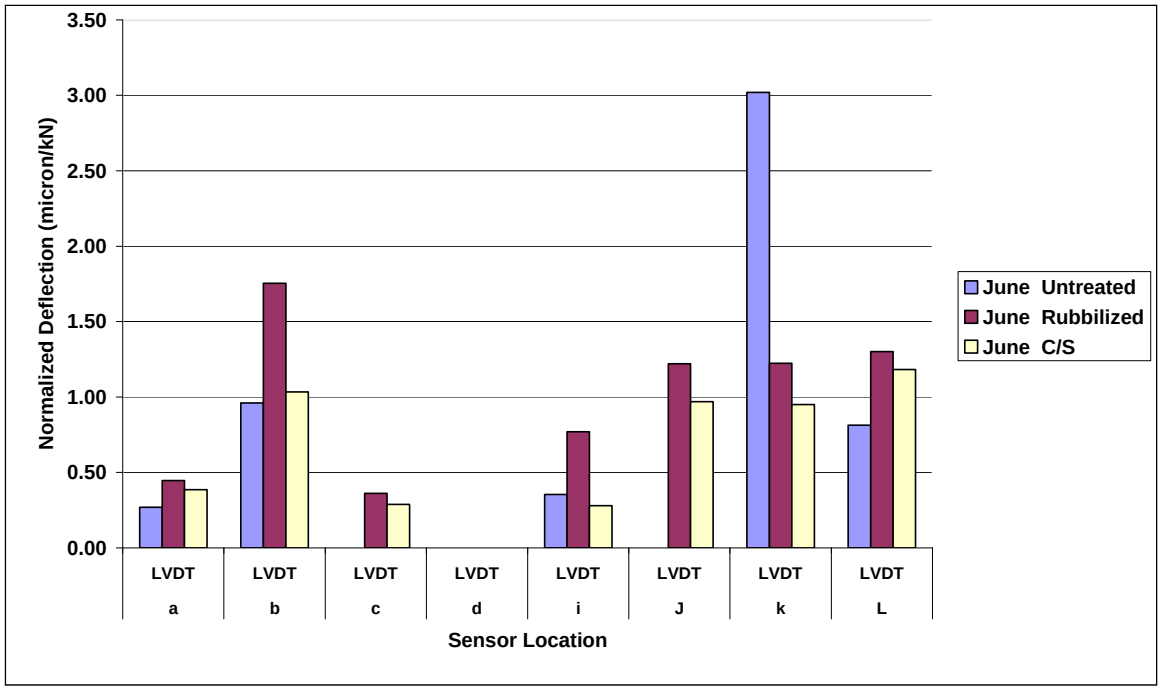

Figure 97. Peak normalized deflection responses from LVDTs by sensor location, June 20, 2006 (1 µm/kN = 0.17526 mil/kip).

Figure 97 shows the readings from LVDTs in each section for June 20, 2006. With the exception of location k, the rubblized section exhibited the largest displacements at each LVDT location. The differences are quantified in Table 29 by dividing the normalized displacement values of the untreated and B&S sections into those of the rubblized section for each LVDT location.

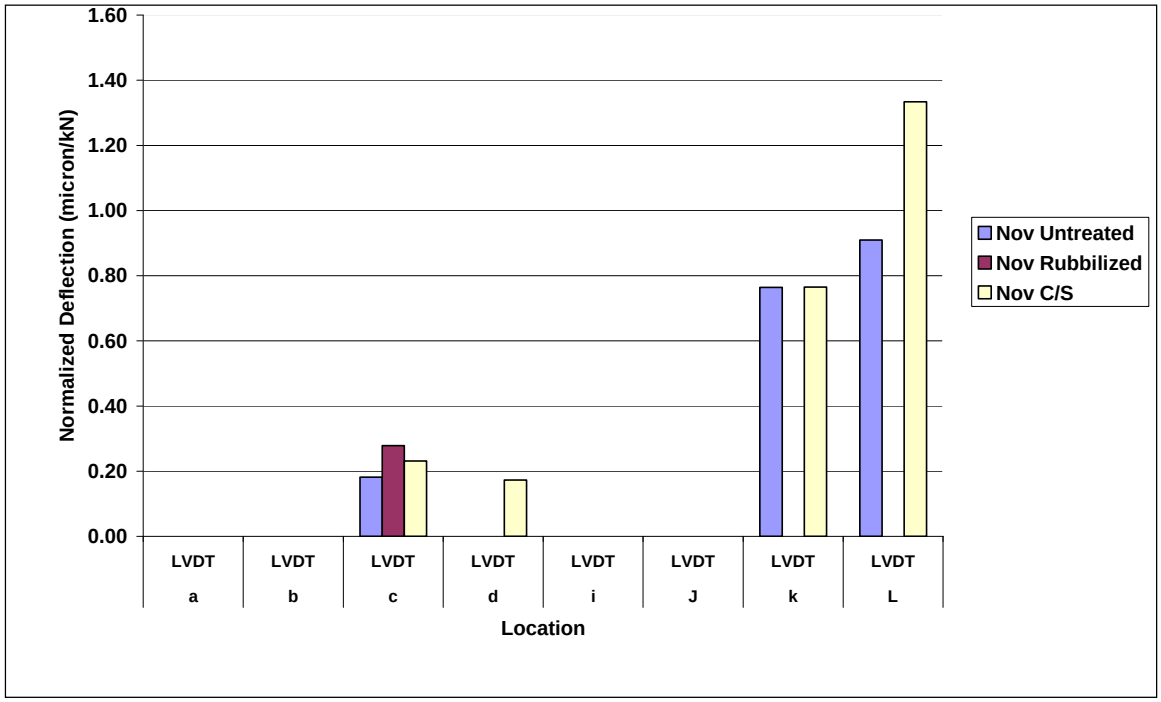

Figure 98. Peak normalized deflection responses from LVDTs by sensor location, November 28, 2006 (1 µm/kN = 0.17526 mil/kip).

Table 29. Ratios of LVDT displacements in rubblized section to untreated and B&S sections, June 20, 2006.

June 20th, 2006

	Ratio of Rubblized to	
LVDT	Untreated	B&S
a	1.65	1.16
b	1.83	1.7
c	ND	1.25
d	ND	ND
i	2.17	2.75
j	ND	1.26
k	0.41	1.29
l	1.6	1.1

Aside from the relative rank of the rubblized section typically having highest deflections, the differences were variable. From the shallow reference LVDTs, only LVDT a and LVDT i have data in all three sections. At LVDT a, the deflection in the rubblized section was 1.65 times greater than the untreated section, and 1.16 times more than B&S. At LVDT i (also in the inner wheel path, but at the opposite end of the slab), the rubblized section values were 2.17 and 2.75 times greater than the untreated or B&S sections, respectively. The vertical displacement readings from the shallow LVDTs represent the deflection in the pavement-subbase system only. The data show that the rubblized JRCP deflected significantly more than the untreated or B&S JRCP, but the amount of difference to expect in this system is inconclusive.

With very limited data from the LVDTs in November 2006, few conclusions can be drawn about the differences between the sections. In location c, however, it can be observed that the shallow displacement in the rubblized section was again greater than in the other two sections.

5.5.2.2 FWD Data

To verify the relationships observed from the LVDTs and to better describe the dynamic deflection responses, the data recorded by the FWD device are presented below. In the same manner as before, Figure 99 shows the deflection data from the FWD at the LVDT locations, organized by date, and Figure 100 shows the same data organized by section.

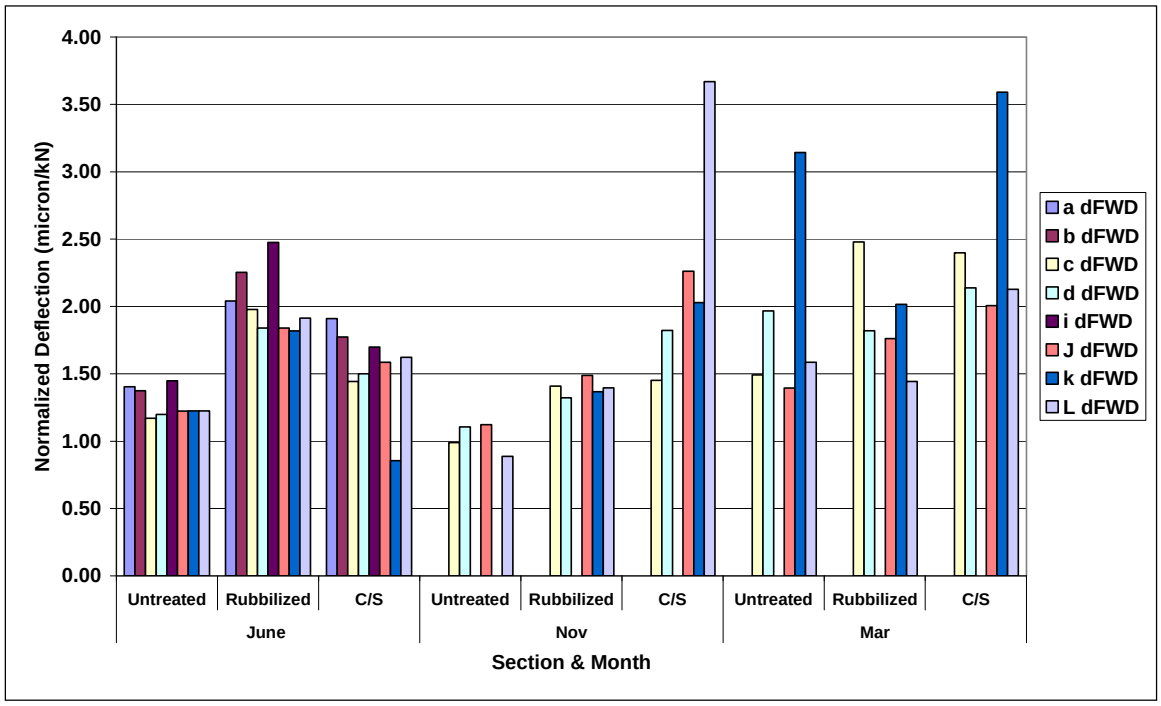

Figure 99. Peak dynamic deflection responses from FWD organized by date (1 µm/kN = 0.17526 mil/kip).

Overall, the following observations can be made from Figure 99: In June, the rubblized section experienced larger displacements than the other two sections, at all locations. In November, the displacements at all locations in the B&S section exceeded those in the other sections. In March 2007 the trend between the sections is less clear, but it is notable that between June 2006 and March 2007 the relationship between the three adjacent deep reference LVDTs was inverted. In June, the total displacements at the joints were equal to the midslab displacements in the untreated and rubblized sections, and in the B&S section, joint displacements exceeded the midslab displacement by nearly double. In November, the rubblized and B&S sections behaved similarly, but there was not a successful reading from LVDT k in the untreated section. The behavior was inverted in March 2007, when the midslab deflections were larger than the joint displacements in each section.

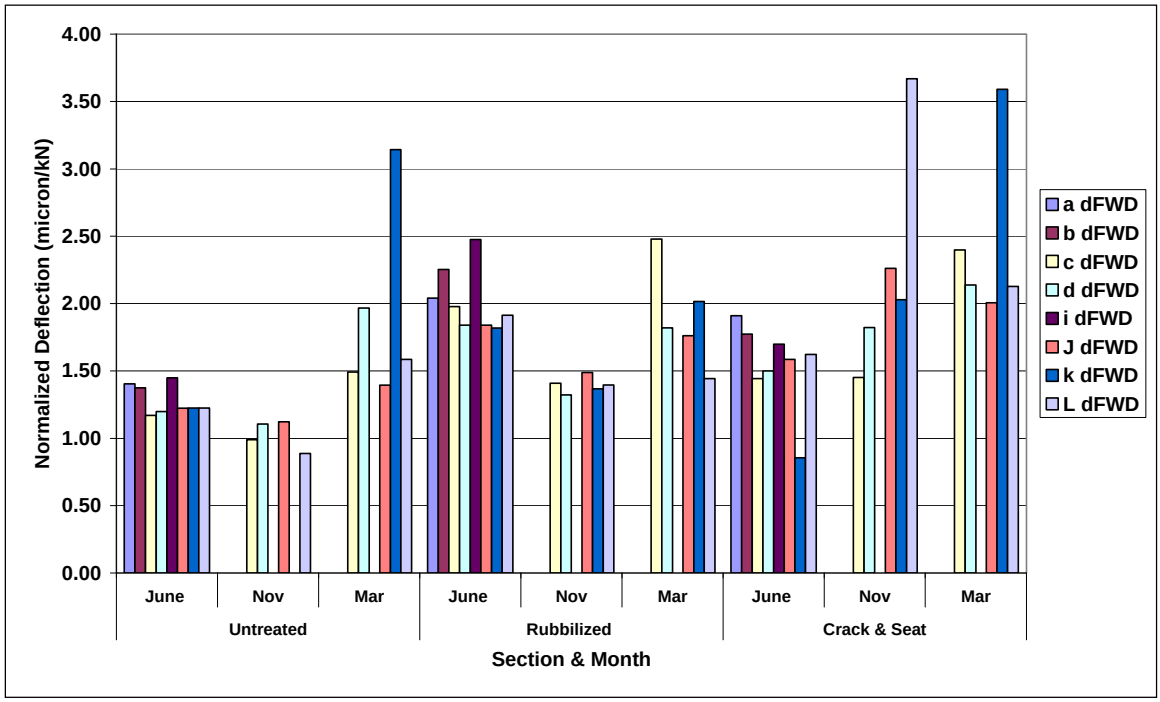

Figure 100. Peak dynamic responses from FWD organized by section (1 µm/kN = 0.17526 mil/kip).

Generally supporting the observations of the data from the LVDTs, Figure 100 shows that displacements were highest in March 2007 for the untreated and B&S sections, but that the rubblized section deflected more in June 2006 than other months. In March, FWD readings at location k exhibited higher displacements in the untreated and B&S sections than in the rubblized section, probably due to loss of support. In November this did not occur since the temperature gradients were opposite.

In Figure 101, Figure 102, and Figure 103, comparisons of deflections at each LVDT location from the FWD device are shown separately for each season. Visual comparisons can be made from the column charts. Ratios of the peak displacements are shown in Table 30. Generally, the FWD device recorded higher deflections in the rubblized section in all locations in June 2006. In November 2006, the deflections in the B&S section were higher in each location than the other sections. In March 2007, the trends between the sections are less identifiable, but the B&S section still generally displaced more than the others. In each location, the deflections in the B&S section were greater than the untreated section. In four of the five locations, the B&S section exhibited higher displacements than the rubblized section.

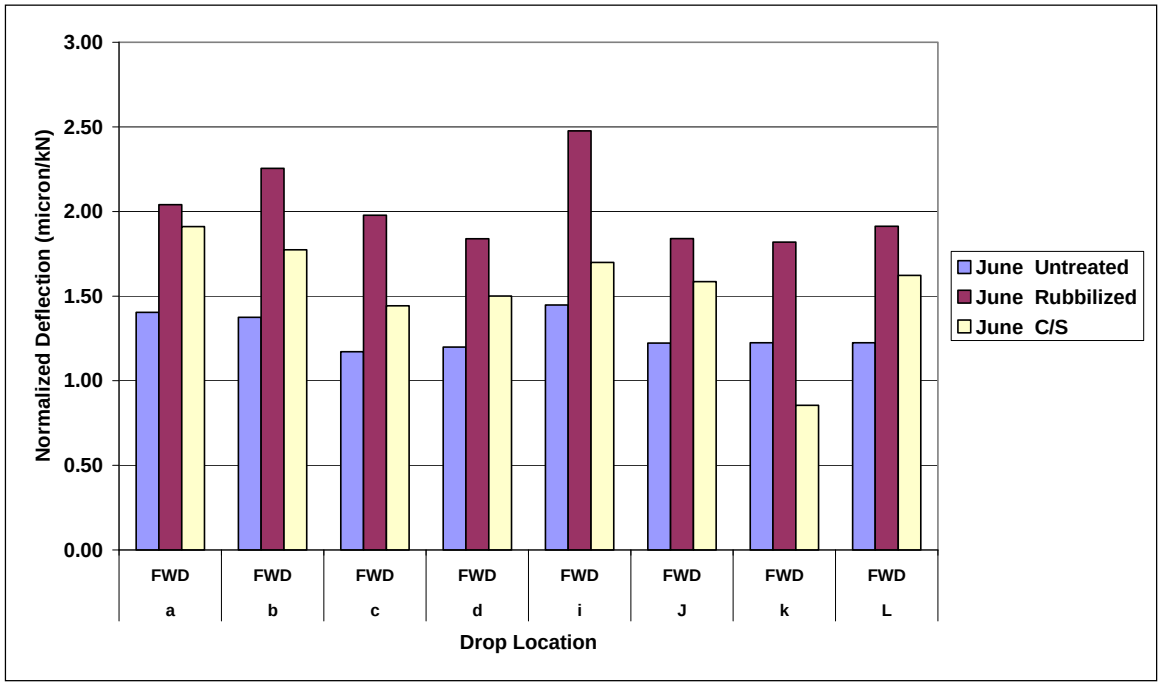

Figure 101. Peak normalized deflection responses from FWD by sensor location, June 20, 2006 (1 µm/kN = 0.17526 mil/kip).

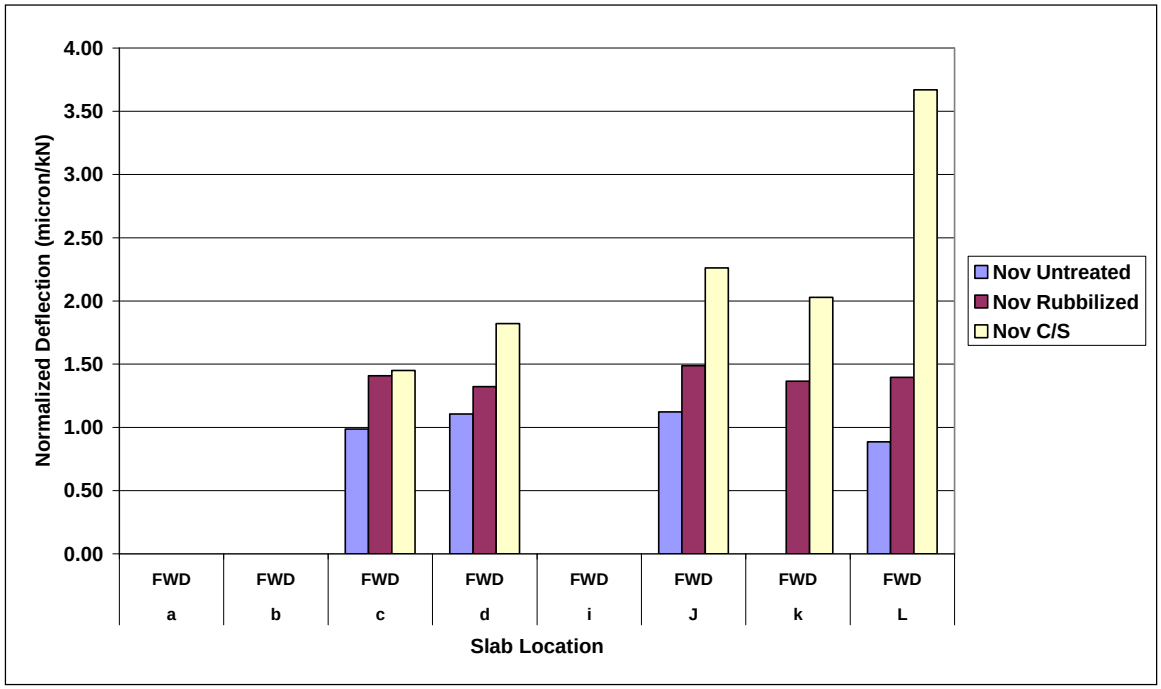

Figure 102. Peak normalized deflection responses from FWD by sensor location, November 28, 2006 (1 µm/kN = 0.17526 mil/kip).

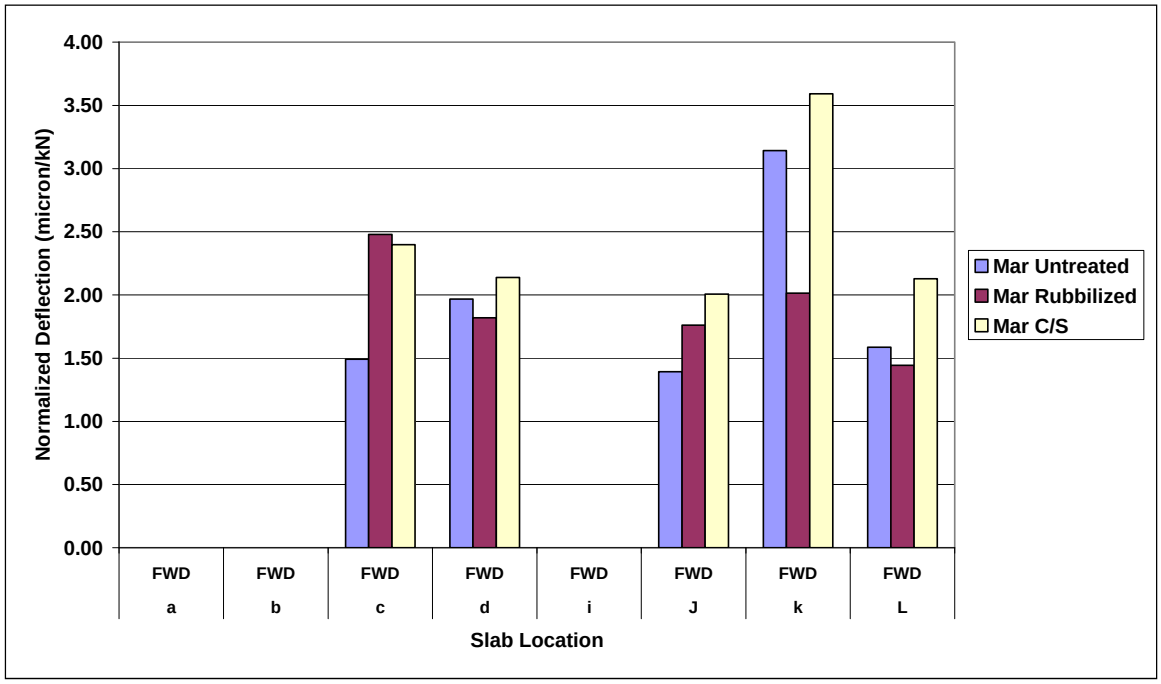

Figure 103. Peak normalized deflection responses from FWD by sensor location, March 21, 2007 (1 µm/kN = 0.17526 mil/kip).

Table 30 summarizes the relationships between the FWD displacements in the three sections at each LVDT location. While other valuable information can be taken from the LVDT readings themselves, the FWD device tended to be more consistent, and more complete data sets were obtained. From the table, it can be generalized that in June, the displacements in the rubblized section were distinctively greatest in the rubblized section, and distinctively smallest in the untreated section. In November, the B&S section exhibited larger displacements in each location than the rubblized section, but the untreated section still tended to displace the least. In March 2007, the data were more scattered, but the B&S section and the untreated section tended to displace more than the rubblized section, and the B&S section again had the highest normalized displacements.

Table 30. Ratios of FWD displacements in rubblized section to untreated and B&S sections.

	June		November		March	
	Ratio of Rubblized to		Ratio of Rubblized to		Ratio of Rubblized to	
LVDT	Untreated	B&S	Untreated	B&S	Untreated	B&S
a	1.45	1.07	ND	ND	ND	ND
b	1.64	1.27	ND	ND	ND	ND
c	1.69	1.37	1.43	0.97	1.66	1.03
d	1.53	1.23	1.2	0.73	0.92	0.85
i	1.71	1.46	ND	ND	ND	ND
j	1.5	1.16	1.33	0.66	1.26	0.88
k	1.49	2.13	ND	0.67	0.64	0.56
l	1.56	1.18	1.57	0.38	0.91	0.68

The underlying trends in the data suggest that the rubblized section is more flexible in warm weather. However, the warm weather condition coincided with very young concrete (only about 2 weeks old). When the concrete was young, only possessing about 75% of its ultimate strength, the displacements were more dependent on the base support itself, rather than the rigidity of the slab. Very low deflection spreadabilities (around 50% to 60%) at this time were calculated based on FWD data. Therefore, with less rigid concrete, the structural support of the system was mostly dependent on the subbase, which is obviously the most flexible in the rubblized section. As the concrete matured, and coincidently the weather cooled, the trends shifted. The B&S section tended to displace more than the rubblized section. The relatively higher displacements occurring in the B&S section may be due to loss of support under thermally curled concrete slabs. While the loss of support theory does not necessarily extend to the untreated section (since it did exhibit the smallest displacements in all three seasons), it may be because the untreated base was left undisturbed during construction, or that the thermal curling of the base mirrored that of the overlay and support was maintained in some conditions.

Deflections measured by the FWD device along the centerline of the slab were greatest in the rubblized section in each season, except for at the midslab location in March 2007. Since some discrepancies exist between the relationships of the C&B&SS and rubblized sections depending on the drop locations, more data is necessary to conclude which fracturing technique consistently experiences larger displacements at the center of the slab. The average values for the rubblized section were over twice those in the untreated section, and the averages from the B&S section were only slightly lower than the rubblized.

The dynamic deflections measured in the wheel path completely correspond with the trends in dynamic strain previously discussed. The summarized data show that while in November and March the rubblized section still tended to experience the highest displacements along the centerline of the lane, in the wheel path the deflections were highest in the B&S section.

5.5.2.3FWD Deflections, Load Transfer Efficiency, Joint Support Ratio and Spreadability

Figure 104(a) shows the average of the normalized deflection measured under the loading plate for each of the dates where FWD testing was performed. It can be seen that the NDf_0 values at the approach and leave positions are close together with differences no more than 7%. In addition, the normalized deflection varied between 0.89 μm/kN (0.156 mil/kip) and 2.34 μm/kN (0.410 mil/kip) showing the maximum values for the winter 2007 and fall testing sessions which are the coldest periods. In the case of the B&S section, the maximum normalized deflection occurred during the winter 2007 and fall 2008 and the minimum occurred for the fall 2006 period. The rubblized section on the other hand, experienced more steady averages of NDf_0 showing the maximum values for the summer 2006 and winter 2007 sessions while the minimum values were observed for the fall 2006 and 2007 tests. Finally, the untreated section showed highest normalized deflections for the fall 2007 and 2008 periods while the minimum NDf_0 was observed for the summer 2006 test. In general, the rubblized section showed the highest normalized deflections, which is the expected trend since it has the most flexible base among the three sections. The normalized deflection average at the center of the slab showed a higher variability than those at the joints specially in the B&S section which experienced the highest values reaching an average NDf_0 of 4.77 μm/kN (0.836 mil/kip) for the winter 2007 test. Moreover, the highest NDf_0 averages in each section were observed for the testing sessions of

winter 2007, spring 2008 and spring 2009. This coincides with a lower compressive stiffness of the base and subgrade due to the thawing process of the subgrade and/or base materials. The lowest values on the other hand, were observed in general for the fall testing sessions. Notice that the March 2007 periods correspond to late winter periods or early spring period, which will explain the similar averages measured in this period compared to those for the spring 2008 and 2009 values.

The load transfer efficiency averages for each section is plotted in Figure 104(b). It can be seen that for the three sections, the LTE values were in general higher compared to the adjacent points for the warmer seasons (i.e. summer and spring periods) which is the expected behavior. Moreover, a direct relationship can be inferred when comparing the LTE values to the corresponding values of the normalized deflections at the joints where an increment in the load transfer efficiency is associated to a decrement in the NDf_0 values. However, a decreasing tendency of the LTE values since soon after paving is observed for the three sections. The LTE values observed for the summer 2006 test were above 80% and dropped to averages of about 75% for the B&S section, and 70% for the rubblized and untreated sections. According to Sargand et al. [2002], these values are considering to be in the fair range (50% to 80%), but notice that a decrement of about 10% in the LTE values in three years is a higher than average rate of deterioration of the load transfer mechanism with time.

The average of the joint support ratio was calculated for each section and shown in Figure 105(a). It can be seen that the variance of the average JSR values is small despite the tendency of JSR values higher than one for most of the testing sessions in the three sections. The JSR ratio values were between 0.9 and 1.1, a range that is considered acceptable according to Sargand et al. [2002]. However, notice that B&S section showed JSR values higher than one for the majority of the testing sessions which indicates unequal support conditions (i.e. weaker) at the leave location for some of the slabs. Likewise, the rubblized section showed JSR values higher than one, but closer to the unit than those observed in the B&S and untreated section. The untreated section on the other hand, showed the most variations from test to test with JSR values between those showed by the other two sections.

Average spreadability at the mid-slab was plotted for each section in Figure 105(b). It can be seen that the average SPR was between 60% and 70% where the B&S section tended to show highest values. Moreover, the average SPR in the B&S section showed less variation between testing sessions than the other two sections followed by the rubblized section. Lower values of the spreadability compared to the adjacent values were observed during the fall 2006 and spring 2009 testing sessions for all three sections. In addition, SPR values decreased in the rubblized and untreated sections for the spring 2008 and fall 2007 sessions respectively. It seems from the SPR values that the B&S section showed the highest values for the majority of testing session with the exception of the winter 2007 and spring 2009 sessions.

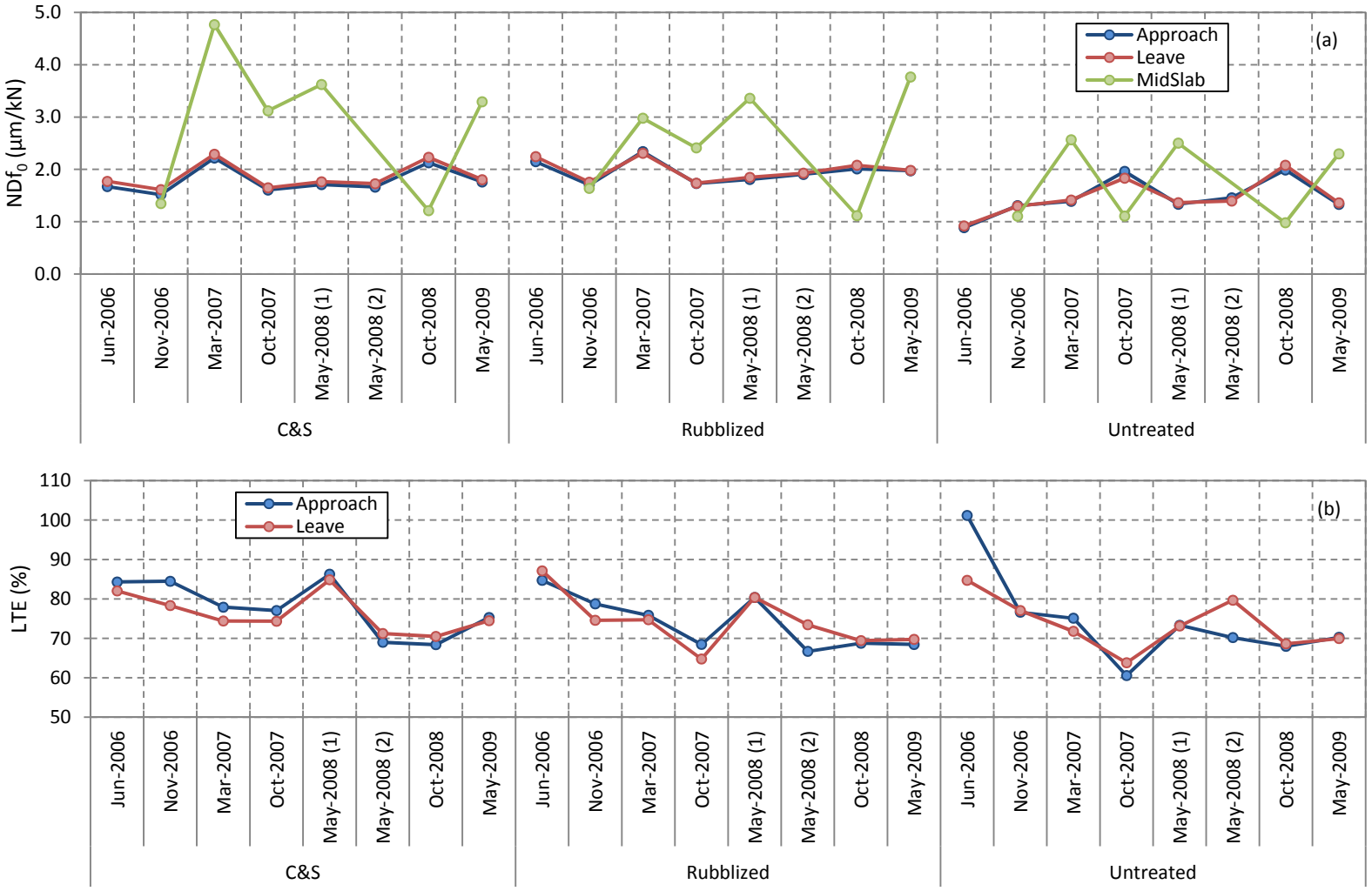

Figure 104. Normalized deflection (a) and load transfer efficiency (b) averaged for all sections (1 µm/kN = 0.17526 mil/kip).

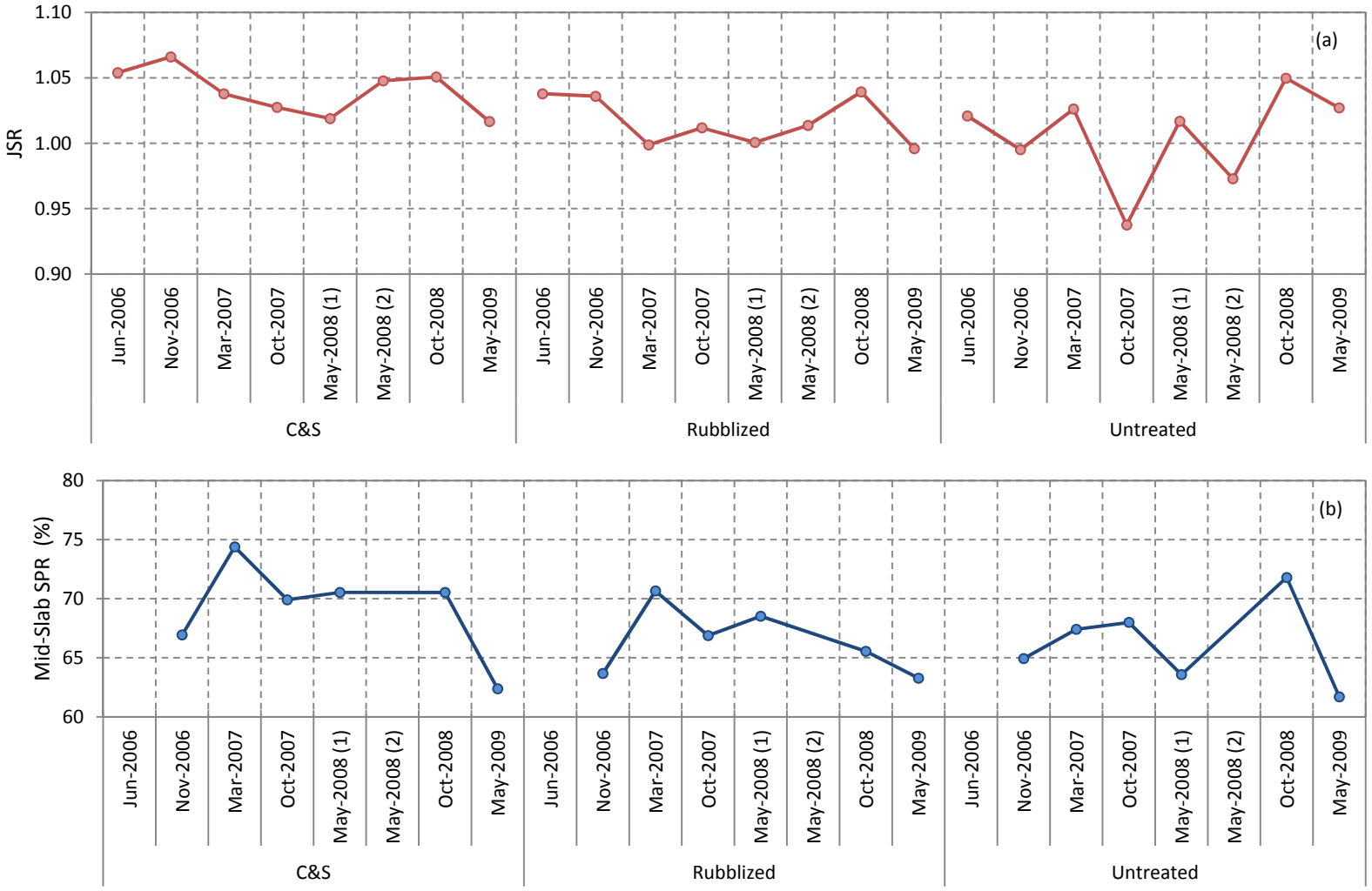

Figure 105. Joint support ratio (a) and mid-slab spreadability (b) averaged for all sections.

Table 31. Summary 3rd drop FWD data averages and standard deviations for B&S section (1 µm/kN = 0.17526 mil/kip).

Section 1: Broken & Seated							
Load Transfer Averages							
Date	**NDf-0 (µm/kN)**			**LTE (%)**		**JSR**	**MidSlab SPR (%)**
	Approach	**Leave**	**MidSlab**	**Approach**	**Leave**		
Jun-2006	1.671	1.772	-	84.3	82.0	1.054	-
Nov-2006	1.518	1.613	1.348	84.5	78.3	1.066	66.9
Mar-2007	2.219	2.291	4.768	77.9	74.4	1.038	74.4
Oct-2007	1.607	1.648	3.120	77.0	74.3	1.027	69.9
May-2008 (1)	1.709	1.764	3.622	86.2	84.8	1.019	70.5
May-2008 (2)	1.662	1.726	-	69.0	71.2	1.048	-
Oct-2008	2.128	2.231	1.213	68.4	70.5	1.051	70.5
May-2009	1.760	1.803	3.294	75.3	74.5	1.017	62.4
Load Transfer Standard Deviation							
Jun-2006	0.174	0.205	-	4.0	5.9	0.034	-
Nov-2006	0.176	0.194	0.169	6.4	6.7	0.081	4.2
Mar-2007	0.367	0.317	1.091	4.4	3.9	0.070	4.0
Oct-2007	0.149	0.151	0.520	4.5	3.4	0.047	3.2
May-2008 (1)	0.094	0.086	0.457	5.3	2.4	0.040	3.1
May-2008 (2)	0.218	0.159	-	9.7	4.2	0.108	-
Oct-2008	0.254	0.230	0.179	5.9	4.6	0.046	3.2
May-2009	0.184	0.215	0.585	3.9	4.6	0.054	1.2

Table 32. Summary of 3rd drop FWD data averages and standard deviations for rubblized section (1 µm/kN = 0.17526 mil/kip).

Section 2: Rubblized							
Load Transfer Averages							
Date	**NDf-0 (µm/kN)**			**LTE (%)**		**JSR**	**MidSlab SPR (%)**
	Approach	**Leave**	**MidSlab**	**Approach**	**Leave**		
Jun-2006	2.148	2.244	-	84.7	87.1	1.038	-
Nov-2006	1.703	1.756	1.637	78.7	74.6	1.036	63.7
Mar-2007	2.340	2.309	2.979	75.8	74.7	0.999	70.7
Oct-2007	1.731	1.737	2.412	68.5	64.7	1.012	66.9
May-2008 (1)	1.808	1.849	3.361	80.4	80.4	1.001	68.5
May-2008 (2)	1.904	1.927	-	66.7	73.4	1.014	-
Oct-2008	2.009	2.079	1.117	68.8	69.4	1.039	65.5
May-2009	1.974	1.981	3.768	68.4	69.7	0.996	63.3
Load Transfer Standard Deviation							
Jun-2006	0.130	0.103	-	5.9	5.2	0.020	-
Nov-2006	0.160	0.137	0.138	4.0	2.8	0.025	1.5
Mar-2007	0.432	0.368	1.154	6.8	4.9	0.086	5.7
Oct-2007	0.130	0.134	0.601	6.3	4.7	0.036	2.9
May-2008 (1)	0.143	0.141	0.695	4.7	2.8	0.052	5.8
May-2008 (2)	0.224	0.153	-	8.6	7.6	0.038	-
Oct-2008	0.348	0.324	0.088	8.3	5.7	0.047	1.1
May-2009	0.166	0.166	0.781	5.4	4.9	0.036	2.4

Table 33. Summary of 3rd drop FWD data averages and standard deviations for untreated section (1 μm/kN = 0.17526 mil/kip).

Section 3: Untreated							
Load Transfer Averages							
Date	**NDf-0 (μm/kN)**			**LTE (%)**		**JSR**	**MidSlab SPR (%)**
	Approach	**Leave**	**MidSlab**	**Approach**	**Leave**		
Jun-2006	0.886	0.918	-	101.2	84.7	1.021	-
Nov-2006	1.306	1.297	1.106	76.6	77.1	0.995	64.9
Mar-2007	1.389	1.415	2.566	75.1	71.8	1.026	67.4
Oct-2007	1.962	1.833	1.109	60.5	63.8	0.938	68.0
May-2008 (1)	1.335	1.363	2.503	73.3	73.1	1.017	63.6
May-2008 (2)	1.457	1.395	-	70.2	79.7	0.973	-
Oct-2008	1.990	2.080	0.980	68.0	68.6	1.050	71.8
May-2009	1.331	1.360	2.297	70.2	69.9	1.027	61.7
Load Transfer Standard Deviation							
Jun-2006	0.071	0.115	-	16.6	7.9	0.043	-
Nov-2006	0.155	0.134	0.078	6.1	11.9	0.045	2.1
Mar-2007	0.246	0.201	1.658	8.7	5.9	0.081	4.3
Oct-2007	0.502	0.426	0.085	15.4	14.1	0.050	2.6
May-2008 (1)	0.126	0.120	1.128	6.6	3.3	0.048	3.4
May-2008 (2)	0.155	0.119	-	6.7	3.3	0.032	-
Oct-2008	0.236	0.202	0.089	6.5	6.1	0.058	2.3
May-2009	0.171	0.173	0.951	6.6	5.7	0.076	4.6

5.5.2.4 FWD Deflections at the Sensor Locations

FWD testing was also performed at the location of the LVDTs and MM strain gauges in order to corroborate the results obtained from the analysis of the strain and deflection responses. Therefore, deflections were recorded from the FWD and normalized deflections were calculated as well as the spreadability at the locations of those sensors along the right wheel path. Table 34 summarizes these values for the third drop and for all the section and testing sessions. Additionally, this data was plotted in order to identify trends and compare the behavior between the experimental sections. The remaining data corresponding to the first and second drop is provided in Appendix C.

Figure 107(a) shows the FWD normalized deflection organized by sections for all the sensor locations. It can be seen that the B&S section experienced higher deflections during the winter 2007 test than during any other session. It also experienced considerable higher displacement at the mid-span locations ***k***, ***t***, and ***v***, than at any other location for the winter 2007, fall 2007, and spring 2008 sessions. This behavior could be attributed to loss of support since the mentioned sessions correspond to cold seasons with the exception of the spring 2008 session. Similarly, the high deflection experienced at the corner location ***l*** during the Nov-2006 session can be attributed to loss of support at the corner of the slab caused by a curled-up slab. In general, the B&S section experienced higher normalized displacements in the outer right edge at the mid-span than at any other location reaching a maximum of 4.58 μm/kN (0.802 mil/kip) at location ***v*** during the winter 2007 session. The rubblized section showed a similar behavior to the B&S section but the normalized displacements in this case were lower. The maximum normalized deflections were observed also at the wheel path locations ***k***, ***t***, and ***v*** reaching a maximum value of 2.64 μm/kN (0.463 mil/kip) at the location ***t*** during the winter 2007 session. Additionally, the

rubblized section experienced the highest deflections for the summer 2006 session. Notice that unlike the B&S section the differences of normalized displacements between each location are lower, suggesting that the loss of support in the rubblized section was milder than in the B&S section. The untreated section on the other hand, experienced in general smaller displacement than the B&S and rubblized section with the exception of those measured at locations ***k***, ***t***, and ***v***. For these the differences with the displacements at the other locations were higher than the ones observed in the rubblized section but lower than the ones observed for the B&S section. The maximum normalized displacement for the untreated section was 3.22 μm/kN (0.564 mil/kip) at the location ***t***.

Figure 107(b) shows the normalized deflections organized by date. The B&S section in general experienced higher displacements for four of the testing sessions whereas showing similar values to those of the untreated section for the rest of the sessions. These sessions corresponded to the Nov-2006, 2007 sessions, and May-2009 session. The untreated section on the other hand, experienced the smaller displacements for the 2006, 2007 and 2009 sessions but it experienced higher displacements for the 2008 testing sessions. In the case of the rubblized section, it showed higher displacements than the other two sections only during the June-2006 sessions.

Table 34. Normalized strain and mid-slab spreadability at sensor locations on 3rd drop (1 μm/kN = 0.17526 mil/kip).

Date	Normalized Deflection (μm/kN)												Spreadability (%)		
	A	B	C	D	I	J	K	L	T	U	V	W	K	T	V
Section 1: Broken and seated															
Jun-2006	1.785	1.699	1.443	1.500	1.690	1.587	1.483	1.622	1.494	1.546	1.728	1.770	57.4	57.0	55.9
Nov-2006			1.453	1.824		2.265	2.032	3.674	1.539	1.378	1.801	1.701	49.4	64.0	62.1
Mar-2007			2.402	2.141		2.009	3.597	2.132	3.800	2.033	4.575	2.565	72.3	72.5	77.1
Oct-2007			2.147	1.532		1.567	2.735	1.593	2.747	1.778	3.274	1.947	66.6	69.1	67.8
May-2008				1.531		1.667	2.853	1.597	2.478	1.501	2.903	1.896	65.2	59.7	61.6
Oct-2008			1.230	1.487		1.583	1.223	2.148	1.273	1.857	1.513	2.507	72.2	70.6	73.2
May-2009			1.253	1.607		1.671	1.571	1.903					61.1		
Section 2: Rubblized															
Jun-2006	2.040	2.254	1.978	1.839	2.476	1.975	1.833	1.913	1.844	1.764	1.858	1.888	56.4	59.2	54.9
Nov-2006			1.412	1.324		1.491	1.368	1.398	1.361	1.279	1.348	1.440	62.0	60.8	61.2
Mar-2007			2.483	1.822		1.764	2.018	1.445	2.639	1.554	1.882	1.838	67.1	64.4	62.3
Oct-2007			1.852	1.533		1.536	2.201	1.315	2.298	1.310	1.893	1.436	66.9	63.8	63.5
May-2008				1.589		1.487	2.143	1.587	2.391	1.384	2.312	1.525	67.1	68.7	58.4
Oct-2008			1.564	1.906		1.983	1.106	1.985	1.108	1.798	1.134	1.863	64.1	65.0	64.6
May-2009			1.888	1.564		1.518	2.139	1.536					65.3		
Section 3: Untreated															
Jun-2006	1.404	1.374	1.171	1.199	1.447	1.223	1.225	1.225	1.155	1.119	1.138	1.163	55.7	57.0	55.2
Nov-2006			0.990	1.108		1.124		0.888	3.221	0.963	1.604	1.030		29.3	47.2
Mar-2007			1.494	1.971		1.396	3.148	1.589	1.810	1.409	2.165	1.494	60.9	64.3	66.4
Oct-2007			1.227	1.935		1.328	1.268	1.349	1.256	1.276	1.266	1.415	68.8	70.3	68.7
May-2008				1.528		1.559	2.913	1.610	2.889	1.375	3.085	1.482	69.8	71.8	60.3
Oct-2008			1.565	2.171		2.220	1.324	2.480	1.440	2.342	1.430	2.550	74.2	75.6	72.9
May-2009			1.442	1.458		1.475	1.762	1.479					67.0		

The spreadability at the mid-span locations ***k***, ***t***, and ***v*** was calculated and the values are shown in Figure 106. It can be seen that the SPR values were between 45% and 80% with the exception of the untreated section where values below 30% were observed at the location ***t***. Moreover, the untreated section showed the most variation of the SPR with the sessions while

the rubblized section showed the least variation. This behavior coincides with that observed for the spreadability values at the center of the slab where the untreated section also showed the highest variations. The spreadability in general tended to increase for the three sections experiencing decrements only for the fall 2006 and spring 2008 testing sessions in the B&S and untreated sections. For the rubblized section on the other hand, the SPR decreased for the spring and fall 2008 testing sessions. In general, it can be said that the rubblized section showed the lowest SPR values for the last testing sessions while the untreated section showed higher values than the other two sections.

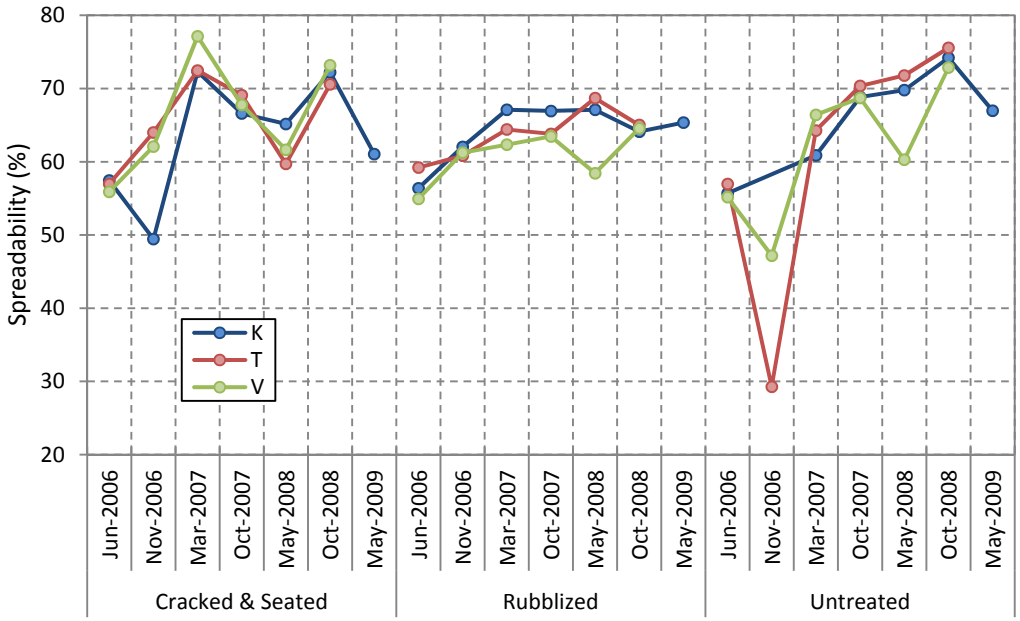

Figure 106. Spreadability at sensor locations.

From the FWD testing results can be concluded that the rubblized section in general experienced the highest displacements at the joints along the centerline as well as the best joint support ratios (i.e. JSR values closer to the unity) while the B&S section experienced the highest values at the center of the slab. This trend did not uphold for the displacements measured along the right wheel path where the B&S section in general showed the highest displacements for both, mid-span and joint locations as well as the worst joint support ratios. However, the B&S section showed the highest load transfer efficiencies for the majority of the testing sessions. The B&S section also experienced the higher spreadability in the center of the slab while at the mid-span locations on the right wheel path, the untreated section tended to show the highest values. Additionally, the untreated section can be considered the one showing the least critical deflections along the centerline as well as along the right wheel path but it showed the lowest load transfer efficiency among the three sections for most of the sessions.

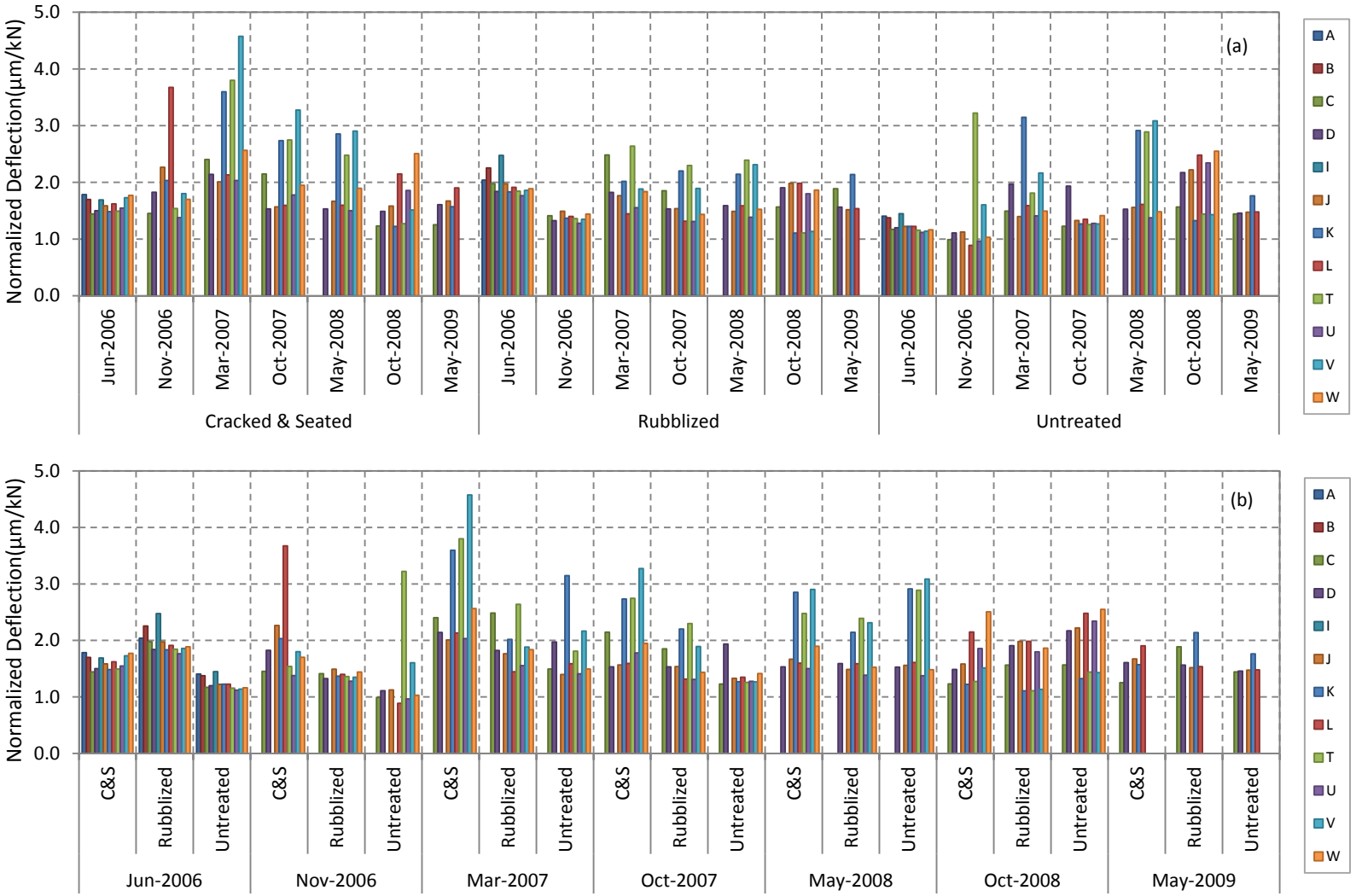

Figure 107. Deflections at sensor locations: a) by section; b) by date (1 µm/kN = 0.17526 mil/kip).

5.5.3 Relationship Between Strain Responses and FWD Deflections

Since strains and displacements were recorded for the FWD testing performed at the strain gauges locations, and known that the strains and displacements are a response to the same load acting on the pavement structure, it seems reasonable to study the correlation between the two of them. First, the normalized strains and normalized displacements were plotted together vs. the impact load recorded by the falling weight deflectometer in order to identify their relationship. Figure 108 shows the normalized strain vs. the applied load for each drop and all the FWD testing sessions. It can be seen that the normalized strains were between -0.053με/kN (-0.236 με/kip) and -0.35με/kN (-1.56 με/kip) for all the three drops at the top of the slab. Moreover, the normalized strains are mostly concentrated in the interval (-0.053με/kN, -0.2με/kN) (or (-0.236 με/kip, -0.890 με/kip)). Likewise, the normalized strains at the bottom of the slab were between 0.053με/kN (0.236 με/kip) and 0.38με/kN (1.69 με/kip) with the majority of the values concentrated in the interval (0.053με/kN, 0.17με/kN) (or (0.236 με/kip, 0.756 με/kip)). Consider now the case where the applied load for each point has been normalized to the reference load of the respective drop. Thus, the measured load of each point corresponding to the first drop was divided by 40.03 kN (9 kip); the loads corresponding to the second drop were divided by 53.4 kN (12 kip), and finally those loads corresponding to the third drop were divided by 71.2 kN (16 kip). The result is shown in Figure 109, where all the normalized strains for the three drops concentrated around a normalized load of 1 kN/kN. Therefore, it can be said that any normalized strain measured in any of the three experimental sections can be expected to fall within the interval (±0.05με/kN, ±0.2με/kN) (or (± 0.222 με/kip, ±0.890 με/kip)) for any applied load within a ±10% deviation of the reference load. In the same way as described for the normalized strains, the normalized deflections were plotted vs. the applied load and the normalized applied load. From Figure 110 it can be seen that the majority of the normalized deflections are concentrated between 1μm/kN (0.175 mil/kip) and 2μm/kN (0.351 mil/kip). Therefore as in the case of the normalized strains, it can be said that any normalized deflection measured in any of the three experimental sections can be expected to fall within the interval (1μm/kN, 2μm/kN) (or (0.175 mil/kip, 0.351 mil/kip)) for any applied load within a ±10% deviation of the reference load.

Additionally to the relationships aforementioned, the relationship between the normalized strains and normalized deflections was considered. In Figure 111 are shown the normalized strains vs. the normalized displacements of all the sections for all the drops and all the FWD testing sessions. From the figures it is clear that the higher concentration of data points is within the intervals described above. Thus, for the top strains the data points are enclosed in the region [1, 2]μm/kN×[0.053, 0.2]με/kN (or [0.175, 0.351]mil/kip × [0.236, 0.890]με/kip) whereas for the bottom strains the values are enclosed in the region [1, 2]μm/kN × [-0.053, -0.2]με/kN (or [0.175, 0.351]mil/kip × [-0.236, -0.890]με/kip). However, notice that the variability of the data is higher for the top strains while the bottom strains are more concentrated within the mentioned intervals. This variability can be explained by the variations on the thickness of the slabs or more precisely the variations on the distance of the strain gauge to the top surface of the slab. These variations on the thickness will affect the strains at the top more than at the bottom

since the bottom gauges were fixed to the chairs 25 mm (1 in) above the ATPB. From the figures can be seen also a trend within the distribution of data points. Therefore, a power regression adjusted to the data in an attempt to obtain an equation that relates both the normalized strains and normalized deflection. This regression resulted in the following expressions for the normalized strains as a function of NDf_0.

$$\varepsilon_{Top} = -0.03765(NDf_0)^{1.389} - 0.05306 \quad (17)$$

$$\varepsilon_{Bottom} = 0.03283(NDf_0)^{0.9264} + 0.05757 \quad (18)$$

where NDf_0 is the normalized deflections given in μm/kN. The regression parameters and goodness of the regression are listed in Table 35 and the plots of the data together with the 95% confidence bounds are shown in Figure 112. Notice that this regression does not include as independent variables other parameters that influence the strain response of the slabs such as the thickness, joint spacing, width of the slab and the applied load itself. Additionally, the R^2 value of the regression equation for the top is low and that corresponding to the bottom although higher, is below 90%. This implies that based on the regression model the variability observed in the measured strains is not totally due to the variability on the measured displacements or for instance due directly to the impacting load. Moreover, this implies that the strains depend on more parameters than just the direct response to the impacting load (i.e. the normalized deflection NDf_0). Therefore, this regression model needs to be improved by including more data, modifying the regression model equation, and/or including parameters such as the dimensions of the slab and its use is recommended only for guidance purposes in the I86 project discussed herein or pavement with similar characteristics.

Table 35. Parameters of regression between strain and FWD measurements.

Parameter		Top	Bottom
Model		$\varepsilon = a(NDf_0)^b + c$	
Coefficients	**a**	-0.03765	0.03283
	b	1.389	0.9264
	c	-0.05306	0.05757
Confidence Bounds (95%)	**a**	(–0.08228, 0.006977)	(–0.02687, 0.09252)
	b	(0.6671, 2.111)	(–0.03312, 1.886)
	c	(–0.1147, 0.008593)	(–0.01081, 0.126)
Sum of Squared Error (SSE)		0.2635	0.1559
R^2		0.5328	0.7219
DFE		128	194
Adjusted R^2		0.5255	0.719
Standard Error (RMSE)		0.0454	0.0283

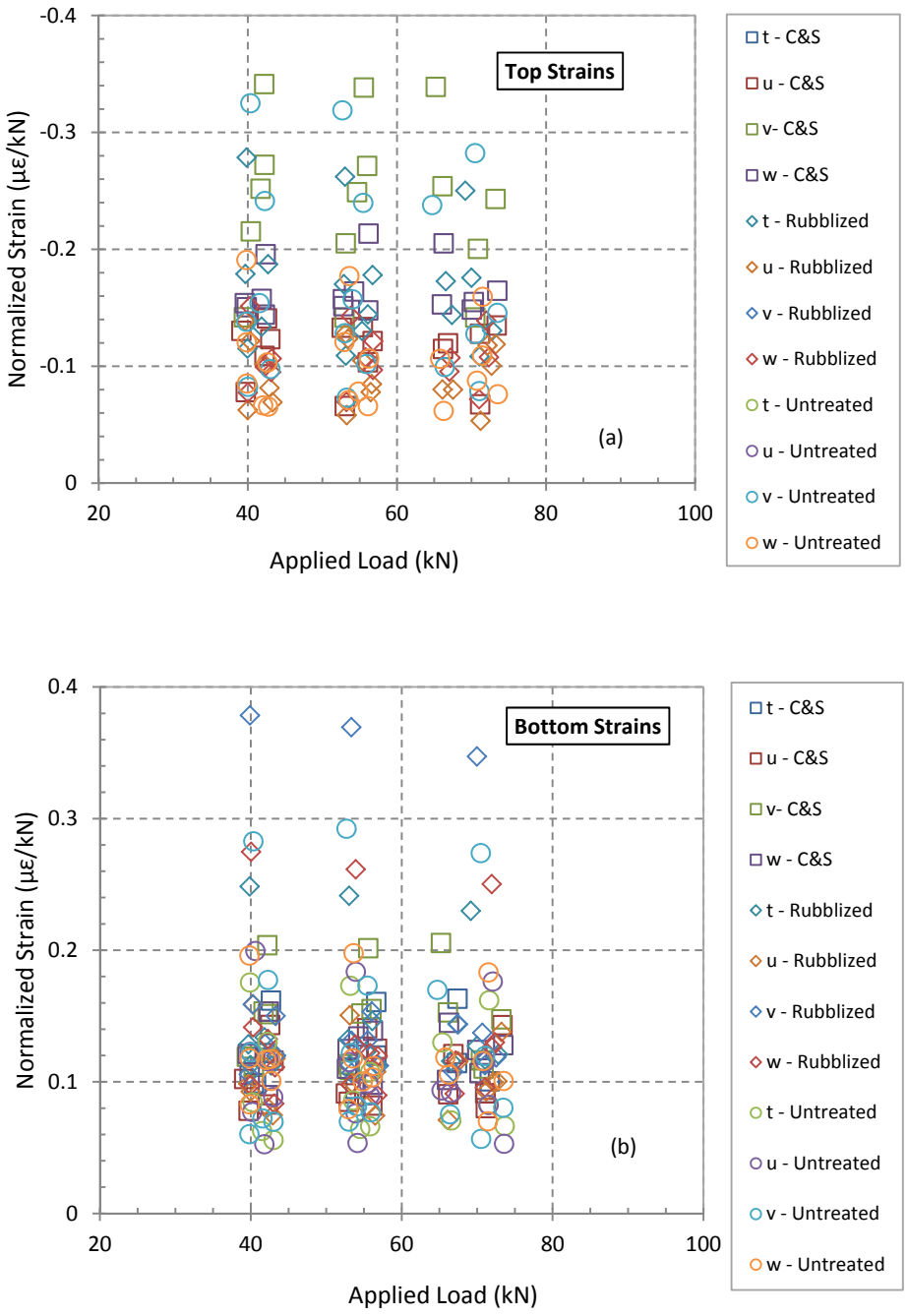

Figure 108. Normalized strain vs. applied load: a) Top; b) Bottom. (Reference Loads: 40 kN (9kip), 53.4 kN (12 kip), and 71.2 kN (16kip)) (1 kN = 0.225 kip; 1 με/kN = 4.448 με/kip).

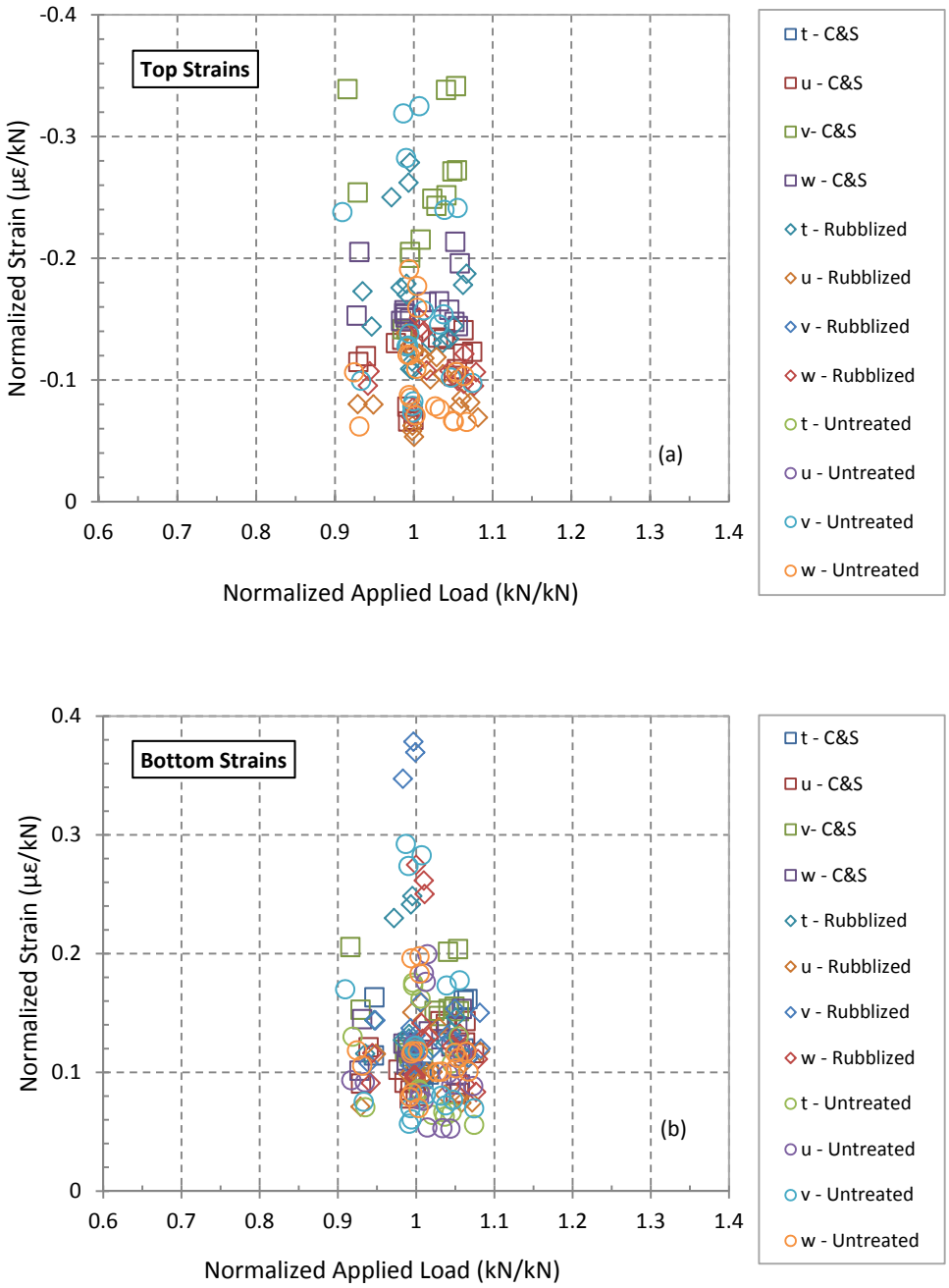

Figure 109. Normalized strain vs. normalized applied load: a) Top; b) Bottom (1 με/kN = 4.448 με/kip).

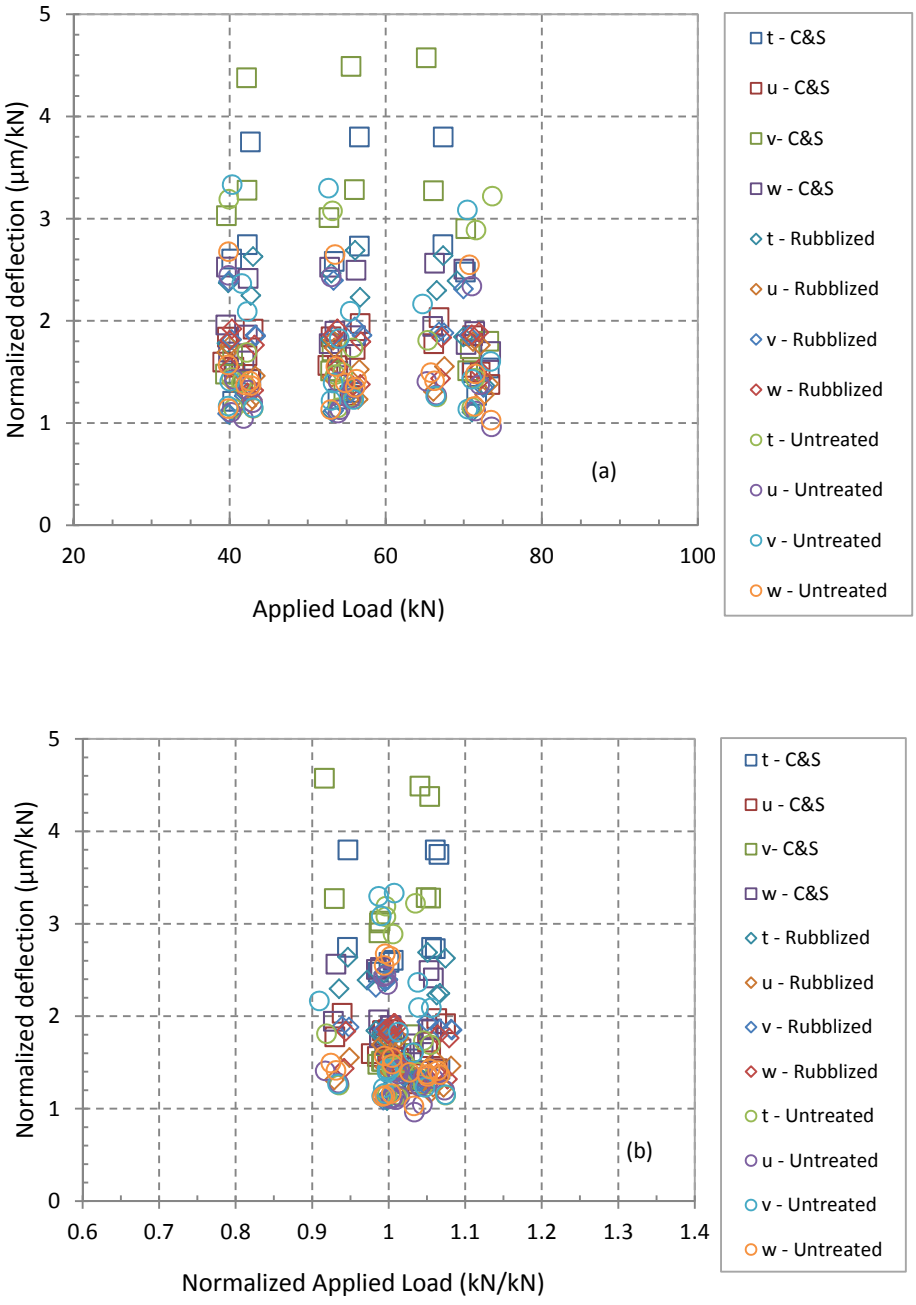

Figure 110. Normalized deflections vs. a) Applied load; b) Normalized applied load. (Reference loads: 40 kN (9kip), 53.4 kN (12 kip), and 71.2 kN (16kip)) (1 kN = 0.225 kip; 1 με/kN = 4.448 με/kip).

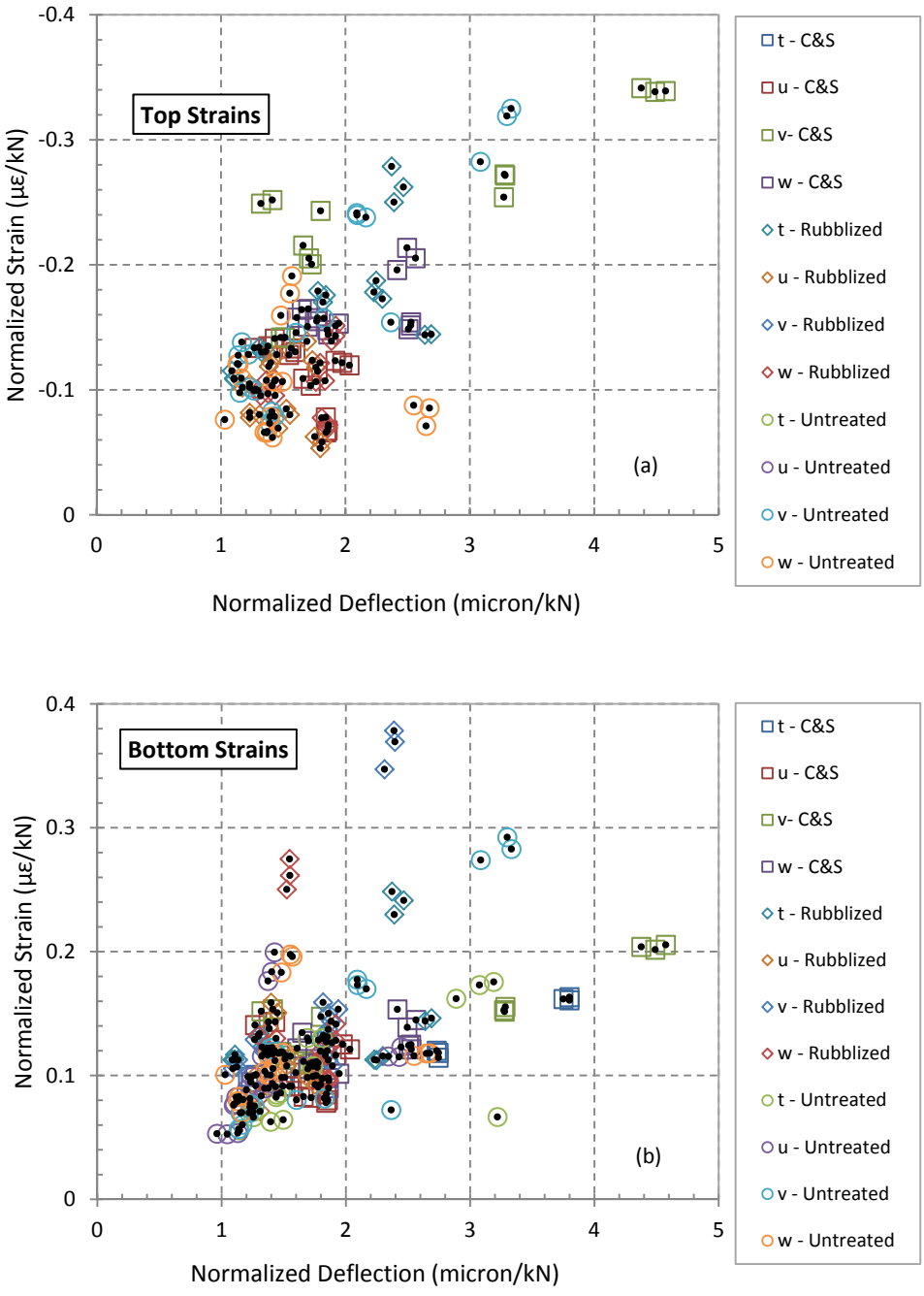

Figure 111. Normalized strain vs. normalized deflections: a) Top; b) Bottom (1 μm/kN = 0.175 mil/kip; 1 με/kN = 4.448 με/kip).

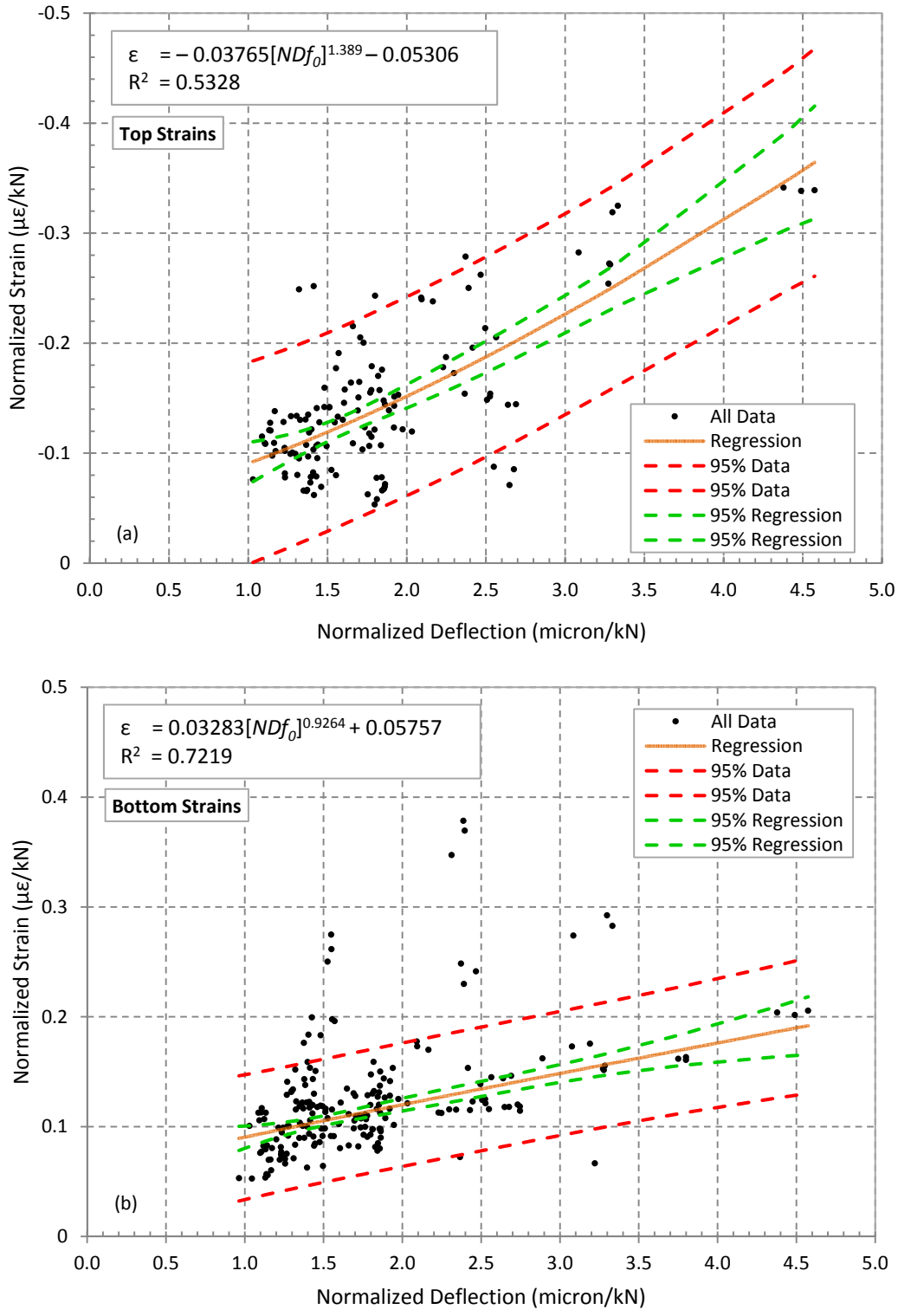

Figure 112. Regression of normalized strains and normalized deflections: a) Top; b) Bottom (1 μm/kN = 0.175 mil/kip; 1 με/kN = 4.448 με/kip).

6Summary and Conclusions

This report presents an analysis and discussion of the behavior of three experimental sections located in Cattaraugus County, southwest New York State. The sections comprised a 225 mm (8.86 in) JPCP concrete overlay over preexisting JRCP that was broken and seated in the first section, rubblized in the second section, and untreated in the third section. Data collected since the construction in June 2006 was analyzed and discussed. The discussion focused on the sections' response to environmental effects, the short-term response to the FWD testing, FWD test results and comparisons of these responses and results between the experimental sections. The environmental response analysis was addressed using the average change in strains and maximum strains undergone by each section at the different instrumented locations. Likewise, the short-term response to the FWD testing was addressed using the peak strains from the dynamic strain response at each strain gage location. Finally, the analysis of FWD testing data comprises normalized FWD deflections at each sensor location as well as load transfer efficiency, JSR and spreadability averages. The seasonal variations were also discussed. Next, the main findings and conclusions for each section are highlighted, as well as the comparisons of the performance between sections.

6.1 Conclusions on the Environmental Response

When comparing the experimental sections, it was found that the untreated section experienced a more severe environmental response for most of the periods analyzed. The B&S section on the other hand, showed the least severe response compared to the other two sections. Moreover, on average, the peak average tensile $\Delta\varepsilon$ and $\Delta\sigma$ at the center of the slab in the untreated section reached values up to 190% and 90% higher than the peak averages in the other two sections for top and bottom of the slab respectively. In the same way, the maximum peak tensile values at the center of the slab in the untreated section were up to 170% and 70% higher than the other two sections for top and bottom respectively. Less drastic values were observed for the wheel paths. However, the maximum stresses observed within the slabs for the three sections were between 15% and 36% of f_r in tension and 3% and 12.3% f_c' in compression; and therefore, the sections did not experienced change in strains and stresses that could result in cracking during the test period. Yet, this does not consider the built-in curling strains, shrinkage, and stresses due to the slab-base friction effects.

The differences in the change in strain and stresses between sections are explained when looking at the temperature gradients experienced at each section. It was found that at the center of the slab, the untreated section experienced the maximum positive and negative linear temperature gradients for the majority of the analyzed periods. At the mid-span on the inner wheel path, maximum positive and negative LTG were consistently observed in the rubblized section while the B&S section consistently showed the maximum values at the quarter-length location along the centerline. These locations are the same as those that tended to show the highest average and maximum $\Delta\varepsilon$. Additionally, the temperature distribution also affects the material underneath of the concrete slab. Therefore, for the experimental sections, the temperature effects are more critical for the untreated section where the base material consists of JRCP slabs that will curl and warp due to changes of temperature and moisture inducing strains to the overlying slabs. These effects are less pronounced for the B&S section where the dimensions of the preexisting JRCP are reduced but it still preserves some structural capacity to undertake thermal strains and stresses. In the rubblized section on the other hand, the dimensions of the base material are reduced such that they are unable to take any considerable thermal

strains and stresses that will transfer to the overlying slabs. Moreover, the flexibility of the rubblized base provides better support to the slabs and therefore reduces the strains and stresses due to loss of support, which are more likely in the B&S section untreated sections.

In conclusion, a JPCP overlay over untreated preexisting JRCP would experience a more severe response to environmental factors compared to an overlay placed over broken and seated or rubblized preexisting pavement. Additionally, it can be concluded that at the center of the slab and mid-span along the wheel paths, the breaking and seating of the preexisting concrete would lower the change in strains and stress to values comparable to those experienced using a rubblized base. The results support the initial expectations about the performance of the untreated section and the early conclusions drawn by Ambrosino [2007] and Bendaña et al. [2008] regarding the environmental response. Based on the results and analysis presented, it is recommended to use one of these fracturing techniques, rubblization or breaking and seating, before placing a JPCP overlay.

6.2 Conclusions on the Dynamic Response and FWD Test

The analysis of the dynamic response to the FWD testing showed that the experimental sections experienced a composite behavior with the bond-breaker interlayer to some degree. Composite behavior was consistently observed in the B&S where its degree varied for the different testing sessions. The same happened in the rubblized and untreated sections; however, positive shifting of the neutral axis was observed as well as higher variations between sessions. In the case of the untreated section on the other hand, it was determined that in the summer 2006 session at the mid-span the neutral axis shifted about 35 mm (1.4 in) downwards, which is equivalent to an effective slab thickness of 295 mm (1.6 in). The positive shifting values observed may be an indicator of loss of support at the particular location. Despite this fact, it should not be discarded the possibility that of a thinner or thicker slab than designed (225 mm or 8.8 in) and determining the in-situ thickness of the pavement is advised.

The untreated section generally experienced a slightly smaller dynamic response compared to the other two sections, but results were comparable for all treatments. The FWD test results showed that the untreated section typically experienced the lowest deflections while the B&S and rubblized sections showed the highest values at the right wheel path and slab's centerline respectively. These results are sensitive to the location and placement of the FWD. The dynamic responses are also considerably smaller in magnitude than the environmental responses.

6.3 General Conclusions

The analysis performed showed that the environmental effects on concrete pavements are more critical than the effects due to dynamic loading of the slab. It should be noted that the strain values corresponding to the dynamic response to the FWD testing are much lower than the values corresponding to the environmental response, as shown in Table 36. The maximum strains recorded from the FWD test were 22.1με in compression and 24.3με in tension corresponding to 513kPa in compression and 564kPa in tension respectively. In contrast, the maximum environmental strains observed were 60.0με in tension and 147.4με in compression, which correspond to 1394kPa in tension and 3426kPa in compression respectively. Moreover, it can be seen that the maximum dynamic strains are 14.4% of the modulus of rupture and 2% of the compressive strength whereas the maximum environmental strains are 36% of f_r and 12.3% of f_c'. This shows that the sections did not experience change in strains and stresses that could result in cracking during the period between the construction day in June 2006 and May 2009.

Yet, this does not consider the built-in curling strains, shrinkage, and stresses due to the slab-base friction effects.

Based on the results and analysis presented, the use of fracturing techniques is recommended before laying down a JPCP overlay. The results showed that rubblizing the preexisting JRCP before overlaying reduced the environmental strains and stresses in the new concrete pavement by providing a better support than that obtained by using the other techniques. Additionally, it also provided a better performance during the FWD test with good load transfer efficiencies despite the high level of tensile strains experienced near the bottom surface and the low compressive stiffness of the base when compared to the other sections. The breaking and seating technique significantly reduced the strains and stresses due to environmental effects as well, and provided the joints with higher capability to transfer loads compared to the other two sections. Despite this, the results from the FWD test suggest that loss of support in the B&S section was more pronounced than in the other two sections. Finally, not treating the existing concrete allowed the overlaying pavement to experience the highest level of strain and stresses due to environmental effects.

The change in strain ($\Delta\varepsilon$) was used to compare the performance of the sections. However, $\Delta\varepsilon$ is not the actual strains underwent by the slabs since this is defined as relative change between the strains corresponding to a LTG value closest to zero and subsequent strains. Moreover, the actual strains depend on the slab conditions at set and the built-in curing strains, and shrinkage. Thus, the actual strains in the concrete can shift upwards compared to the values of $\Delta\varepsilon$ discussed here.

From the results and as Ambrosino [2007] mentioned, the order in magnitude of $\Delta\varepsilon$ due to environmental effects in the untreated section could lead to failure of this section in the form of top-down cracks. In a distress survey completed during November 2009 as part of this research, mid-panel top-down cracks were observed in the 90% of the slabs of the untreated section. Mid-panel cracks also were observed in the rubblized and B&S sections but these were considered localized cases given the percentage of cracked slabs. The percentages of cracks observed for each section are listed in Table 37. Additionally, hairline cracks like those in Figure 113 were observed at the tie-bar locations in all three sections. These top-down cracks, however, are believed to be a consequence of the tie-bar installation procedure used during paving. The tie-bar holes were drilled in the concrete slabs of the passing lane, which was constructed first, and then these were glued with epoxy into the holes before paving the driving lane. The results presented support the initial expectations about the performance of the untreated section and the early conclusions drawn by Bendaña et al. [2008]. Additional surveys conducted in 2010 and 2011 did not show any increase in the number of cracks found in November 2009.

Table 36. Maximum environmental and dynamic strains.

Section	Maximum Change in Strain [με]			
	Environmental Strains		Dynamic Strains	
	Tension	Compression	Tension	Compression
Broken and seated	-122.6 (Top)	-64.7 (Top)	13.4 (Bottom)	-22.1 (Top)
Rubblized	-147.4 (Top)	-	24.3 (Bottom)	-17.3 (Top)
Untreated	60.0 (Top)	-	19.3 (Bottom)	-19.9 (Top)

Table 37. Percentage of cracked slabs observed in distress survey of November 2009.

Section	Mid-Panel	Hairline	
	% Slabs Cracked	% Slabs Cracked	Cracks per Slab
Broken and seated	5%	40%	0 – 2
Rubblized	5%	50%	1 – 3
Untreated	90%	90%	3 – 6

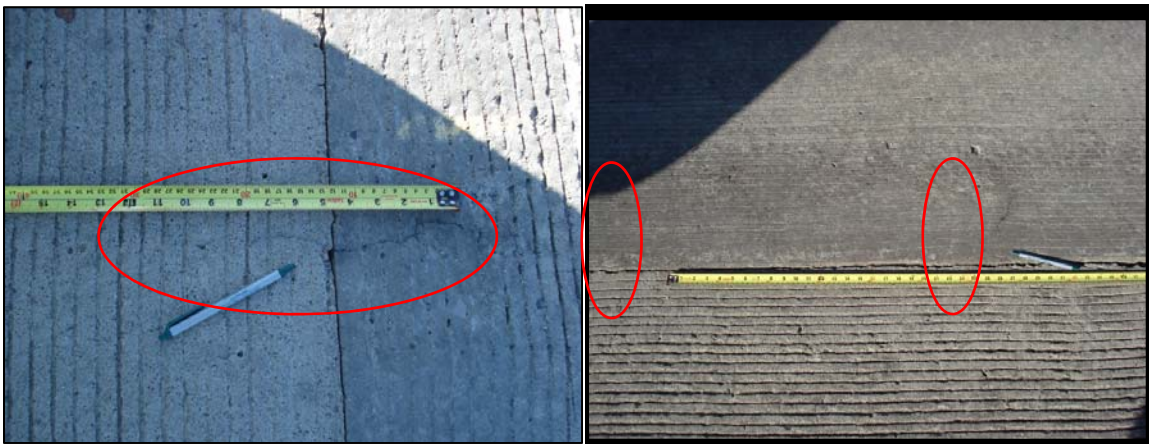

Figure 113. Hairline cracks at tie-bar locations in the untreated section.

6.4Recommendations

Based on the conclusions above, the following recommendations are offered. Existing PCC pavement should not be left untreated before applying an overlay. If the subgrade is weak, the break and seat approach is recommended. If the subgrade is strong, the rubblization method is better. The treatment cost should also be considered.

6.5Implementation

The New York State Department of Transportation should make sure specifications are in place for break and seat and rubblization procedures. Then one of these procedures, as recommended above based on the strength of the subgrade, should be incorporated into the design and construction of any PCC pavement overlay project.

7References

AASHTO. (2008). *Mechanistic-Empirical pavement guide: A manual of practice* (Interim edition). Washington, D.C.: American Association of State Highway and Transportation Officials (AASHTO).

ACI Committee 325. (2002). *ACI 325.12R-02: Guide for the design of jointed concrete pavements for streets and local roads*. American Concrete Institute (ACI).

Alavi, S., LeCates, J. F., & Tavares, M. P. (2008). *Falling weight deflectometer usage* (NCHRP Synthesis No. 381). Washington, D.C.: Transportation Research Board.

Ambrosino, J. D. (2007). *Evaluation of rigid pavement rehabilitation methods using an unbonded concrete overlay* (Master's thesis, Ohio University).

ASTM. (2003). *Standard practice for roads and parking lots pavement condition index surveys* [ASTM historical standard d6433-03]. West Conshohocken, PA: American Society for Testing and Materials. DOI: 10.1520/C0033-03

Bendaña, L. J., Ambrosino, J., & Sargand, S. (2008, August 21). *Evaluation of rigid pavement rehabilitation methods on I-86.* Paper presented at the 9th International conference on concrete pavements, San Francisco, CA.

Campbell Scientific Inc. (1997). *CR7 Measurement and control system: Instruction manual.* Logan, UT: Author.

Dally, J. W., & Riley, W. F. (2005). *Experimental stress analysis* (4th ed.). Knoxville, TN: College House Enterprises, LLC.

Darter, M. I., Mallela, J., & Titus-Glover, L. (2009, April 24). *Impact of existing pavement on jointed plain concrete overlay design and performance.* Paper presented at the National conference on preservation, repair, and rehabilitation of concrete pavements, St. Louis, MO. Retrieved April 17, 2009, from http://www.ecst.csuchico.edu/__depts/cp2c/documents/PCC_St_Louis/1B-Darter.pdf

ERES Consultants Inc. (1999). *Evaluation of unbonded concrete portland cement concrete overlays* (NCHRP Report No. 415). Washington, D.C.: Transportation Research Board.

ERES Consultants Inc. (2002). *Introduction to mechanistic-empirical design of new and rehabilitated pavements: Reference manual* [NHI course 131064]. Champaign, IL: National Highway Institute.

ERI Inc. (2003). *KUAB falling weight deflectometer*. Retrieved October 5, 2009, from http://www.erikuab.com/kuab.htm

Geokon Inc. (2005). *Instruction manual: Model 4200/4202/4204/4210 vibrating wire strain gages.* Lebanon, NH: Author.

Geokon Inc. (2008). *Concrete embedment strain gages* [Data sheet]. Retrieved June 24, 2009, from http://www.geokon.com/products/datasheets/4200.pdf

Hall, K. T., Correa, C. E., Carpenter, S. H., & Elliot, R. P. (2001). *Rehabilitation strategies for highway pavements* (NCHRP Web Document No. 35). Transportation Research Board. Retrieved April 17, 2009, from http://onlinepubs.trb.org/onlinepubs/nchrp/nchrp_w35-a.pdf

Harrington, D. (2008). *Guide to concrete overlays: Sustainable solutions for resurfacing and rehabilitation existing pavements* (2nd ed.). NCPTC. Retrieved April 16, 2009, from http://www.cptechcenter.org/publications/overlays/guide_concrete_overlays_2nd_ed.pdf

Honeywell International Inc. (2009). *Model S3C DC-DC: Miniature displacement transducer* [Data sheet]. Retrieved January 5, 2010, from http://content.honeywell.com/sensing/sensotec/pdf_catalog08/008757-2-EN_Model_S3C_DC-DC.pdf

Hornby, I. W. (1992). The vibrating wire strain gauge. In A. L. Window (Ed.), *Strain gauge technology* (pp. 325-347). London, UK: Elsevier Applied Science.

Huang, Y. H. (2004). *Pavement analysis and design* (2nd ed.). Upper Saddle River, NJ: Prentice Hall.

Janssen, D. J., & Snyder, M. B. (2000). Temperature-Moment concept for evaluating pavement temperature data. *Journal of Infrastructure Systems,* ASCE*, 6*(2), 81-83.

Kazmierowski, T. J., & Chan, S. (2005, September 21). *CPR techniques in Ontario – 15 years experience.* Paper presented at the 2005 Annual Conference of the Transportation Association of Canada (TAC), Calgary, Alberta, Canada. Retrieved June 10, 2009, from http://www.tac-atc.ca/english/resourcecentre/readingroom/conference/conf2005/docs/s19/kazmie.pdf

Kazmierowski, T. J., & Sturm, H. (1994). Performance of unbonded concrete overlay project in Canada. *Transportation Research Record, 1449,* 169-173.

Morian, D. A., Sadasivam, S., Mack, J. W., & Stoffels, S. M. (2006). Pavement rehabilitation using fractured concrete pavement techniques. In I. L. Al-Qadi (Ed.), *Proceedings of 2006 airfield and highway pavements specialty conference: Vol. 191. Airfield and highway pavement: Meeting today's challenges with emerging technologies* (pp. 836-847). Atlanta, GA, US: ASCE.

Quality Engineering Solutions Inc. (2008, June). *Improved overlay design parameters for concrete airfield pavements* (IPRF Project FAA-01-G-002-04-2, Final Report). Conneaut Lake, PA: Innovative Pavement Research Foundation. Retrieved April 19, 2009, from http://iprf.org/products/IPRF%20Project%2004-2%20Final%20Report.pdf

Ruiz, J. M., Rasmussen, R. O., Chang, G. K., Dick, J. C., & Nelson, P. K. (2005). *Computer-based guidelines for concrete pavements volume II - Design and construction guidelines and HIPERPAV II user's manual* (Final Report No. FHWA–HRT–04–122). McLean, VA: Federal Highway Administration. Retrieved October 21, 2009, from http://www.tfhrc.gov/pavement/pccp/pubs/04122/04122.pdf

Sargand, S. M., Edwards, W., & Kim, H. (2002, October). *Determination of pavement layer stiffness on the Ohio SHRP test road using non-destructive testing techniques* (ORITE Final Report No. FHWA/OH-2002/031). Columbus, OH: Ohio Department of Transportation.

Shad Sargand and J. Ludwig Figueroa, 2010, *Monitoring and Modeling of Pavement Response and Performance Task A: Ohio*, Technical Report No. FHWA/OH-2010/03A for the Ohio Department of Transportation, Pooled Fund Project TPF-5(121), State Job No. 134287, June 2010.

Swart, C. S. (2006). *A forensic investigation of pavement performance on Interstate 86 in Olean, New York* (Master's thesis, Ohio University).

Tenison, J. H., & Hanson, D. I. (2009). *Pre-overlay treatment of existing pavements* (NCHRP Synthesis No. 388). Washington, D.C.: Transportation Research Board.

Timoshenko, S., & Lessells, J. M. (1925). *Applied elasticity.* East Pittsburgh, PA: Westinghouse technical night school press.

Vishay Intertechnology Inc. (2006). *Concrete embedment strain gages: Vishay micro-measurements* [Data sheet]. Retrieved October 11, 2009, from http://www.vishay.com/docs/11526/emgages.pdf

Appendices

Appendix A: SUPPLEMENTAL ENVIRONMENTAL RESPONSE DATA

Section 1: B&S													
Season		*e*		*f*		*g*		*m*		*n*		*o*	
		Top	Bottom	Top	Bottom	Top	Bottom	Top	Bottom	Top	Bottom	Top	Bottom
Average Tensile Change in Strains (με)													
Summer 2006	July 8-17	1.26	5.03	2.71	1.01	0.92	3.71	2.72	0.77	2.31	3.00	4.10	0.61
	July 17-28	0.02	3.76	0.00	1.24	0.02	3.04	0.00	0.54	1.01	4.87	0.43	2.05
	Aug 5-9	0.13	3.70	0.00	1.47	0.08	3.05	0.00	0.71	0.25	3.34	0.02	1.22
	Aug 9-15	0.05	3.39	0.00	0.57	0.02	2.94	0.00	0.21	0.65	3.00	0.00	0.53
Fall 2006	Dec 1-3	2.15	0.23	0.98	0.00	1.60	0.11	2.69	0.01	3.10	0.06	1.66	0.00
	Dec 3-7	14.85	0.96	9.54	1.24	11.69	1.21	7.43	1.49	11.63	0.81	9.14	1.00
Winter 2007	Feb 9-15	0.80	9.06	0.04	9.83	0.70	8.25	2.01	1.26	3.15	4.37	2.82	1.95
	Feb 15-20	1.77	4.91	1.98	2.60	1.34	2.60	3.80	0.93	3.35	2.31	3.58	1.56
Summer 2007	Aug 21-25	0.24	3.63	0.07	1.10	0.13	2.92	0.02	1.04	0.39	2.44	0.03	1.02
Fall 2007	Oct 21-30	0.00	1.67	0.00	0.27	0.01	1.13	0.01	0.28	0.00	0.68	0.00	0.25
Spring 2008	Apr 26-May 6	1.54	8.38	0.02	2.03	1.32	4.43	1.22	1.53	0.64	2.73	0.37	1.57
Summer 2008	Aug 23-Sep 3	2.33	8.70	0.05	5.58	4.05	6.09	0.46	3.43	2.09	5.03	0.50	5.00
Fall 2008	Oct 6-9	9.93	7.69	6.48	8.82	8.33	8.70	3.50	8.46	7.57	7.09	5.09	7.06
Spring 2009	May 1-11	1.80	4.54	0.14	2.61	1.55	4.21	0.30	2.54	1.38	3.53	0.42	2.29
Average Compressive Change in Strains (με)													
Summer 2006	July 8-17	-10.91	-3.90	-6.02	-10.23	-9.86	-8.55	-4.56	-11.97	-7.31	-7.53	-4.62	-10.20
	July 17-28	-18.13	-5.63	-15.57	-5.86	-14.71	-8.89	-12.37	-8.67	-8.98	-3.29	-8.73	-4.50
	Aug 5-9	-21.80	-7.17	-23.49	-6.81	-19.79	-11.43	-20.52	-7.72	-16.88	-6.69	-20.45	-7.11
	Aug 9-15	-15.77	-7.09	-17.81	-7.98	-13.59	-11.26	-13.93	-9.28	-12.27	-6.84	-12.26	-8.46
Fall 2006	Dec 1-3	-0.63	-8.36	-0.42	-9.61	-0.58	-10.69	-0.22	-11.04	-0.52	-11.11	-0.36	-9.46
	Dec 3-7	-0.21	-6.20	-0.12	-2.55	-0.25	-4.86	-0.35	-2.54	-0.47	-4.74	-0.30	-2.43
Winter 2007	Feb 9-15	-14.43	-0.60	-16.86	-0.28	-11.51	-0.85	-3.19	-4.02	-5.70	-1.20	-3.92	-2.92
	Feb 15-20	-4.18	-1.86	-2.34	-2.64	-3.15	-3.67	-0.77	-4.58	-2.44	-2.42	-1.68	-2.17
Summer 2007	Aug 21-25	-9.61	-1.68	-7.42	-3.30	-9.58	-4.72	-6.14	-3.63	-9.04	-1.90	-5.30	-4.42
Fall 2007	Oct 21-30	-13.48	-9.65	-11.71	-15.73	-13.52	-12.43	-7.06	-16.07	-12.42	-12.76	-8.59	-13.48
Spring 2008	Apr 26-May 6	-10.43	-3.34	-11.81	-8.39	-10.66	-9.65	-4.89	-10.16	-12.14	-9.31	-8.48	-7.53
Summer 2008	Aug 23-Sep 3	-11.30	-2.22	-21.39	-2.09	-8.82	-8.75	-12.50	-4.90	-11.69	-5.06	-11.79	-1.18
Fall 2008	Oct 6-9	-1.32	-4.15	-1.25	-1.46	-1.90	-3.84	-2.17	-1.49	-1.98	-3.10	-1.80	-1.18
Spring 2009	May 1-11	-9.30	-6.54	-9.12	-7.24	-9.22	-9.31	-6.85	-7.18	-8.80	-7.15	-7.98	-5.58

Table A-2. Average Change in Strains (All Sensors, B&S Section).

Section 2: Rubblized													
Season		*e*		*f*		*g*		*m*		*n*		*o*	
		Top	Bottom	Top	Bottom	Top	Bottom	Top	Bottom	Top	Bottom	Top	Bottom
Average Tensile Change in Strains (με)													
Summer 2006	July 8-17	5.94	0.25	6.00	2.58	7.90		2.58	3.38	3.67	2.90	8.73	0.05
	July 17-28	0.09	3.98	0.84	4.90	0.77		0.06	4.62	0.12	4.30	0.31	2.28
	Aug 5-9	0.00	1.04	0.02	2.83	0.00		0.03	3.16	0.01	2.58	0.00	0.86
	Aug 9-15	0.00	0.16	0.01	1.92	0.00		0.02	1.90	0.00	1.59	0.00	0.01
Fall 2006	Dec 1-3	0.68	0.02	1.48	0.12	0.68		2.38	0.21	1.15	0.15	0.31	0.05
	Dec 3-7	10.08	1.07	9.40	1.25	9.32		17.06	0.94	10.07	1.35	6.50	1.12
Winter 2007	Feb 26-Mar 5	6.35	0.76	3.24	2.42	4.93		7.71	1.18	3.58	1.80	1.64	1.27
	Mar 5-9	0.34	2.86	0.22	3.07	0.18		0.68	3.19	0.18	2.03	0.07	1.24
Spring 2007	May 27-June 7	0.01	1.11	0.06	3.03	0.02		1.98	5.03	0.24	3.79	0.03	2.00
Fall 2007	Oct 21-30	0.00	0.05	0.00	0.29	0.00	0.03	0.08	0.52	0.07	0.32	0.00	0.14
Spring 2008	Apr 26-May 6	0.12	1.40	0.51	3.51	0.40		0.36	7.09	0.30	5.02	0.32	3.32
Summer 2008	Aug 23-Sep 3	0.22	4.53	1.26	5.77	0.50		1.04	7.11	0.90	5.58	0.51	8.01
Fall 2008	Oct 6-9	5.92	8.29	5.65	6.99	4.14		7.98	8.94	6.45	8.77	4.35	9.17
Spring 2009	May 1-11	0.09	2.04	0.27	4.32	0.12		0.66	4.77	0.38	4.10	0.07	2.98
Average Compressive Change in Strains (με)													
Summer 2006	July 8-17	-5.04	-10.20	-5.45	-6.41	-3.73		-12.86	-5.30	-7.01	-6.20	-2.79	-11.13
	July 17-28	-14.00	-3.02	-10.70	-3.28	-9.32		-19.55	-4.24	-14.70	-4.78	-10.38	-5.00
	Aug 5-9	-30.10	-7.07	-26.08	-6.81	-24.75		-29.19	-8.10	-27.71	-10.05	-27.04	-6.52
	Aug 9-15	-23.99	-10.32	-18.80	-8.60	-16.75		-24.96	-10.53	-22.74	-12.69	-20.22	-11.20
Fall 2006	Dec 1-3	-1.23	-8.74	-0.71	-10.53	-0.77		-0.80	-8.55	-1.21	-9.04	-0.86	-6.73
	Dec 3-7	-0.15	-2.68	-0.72	-4.31	-0.35		-0.37	-5.37	-0.40	-3.73	-0.31	-1.81
Winter 2007	Feb 26-Mar 5	-1.03	-4.12	-2.13	-1.99	-1.54		-1.88	-5.23	-1.72	-2.67	-1.42	-1.28
	Mar 5-9	-20.59	-5.38	-17.11	-6.67	-18.79		-19.55	-7.57	-19.71	-7.72	-18.32	-3.77
Spring 2007	May 27-June 7	-21.46	-7.53	-20.33	-6.61	-18.95		-24.75	-4.93	-19.61	-6.55	-16.72	-5.90
Fall 2007	Oct 21-30	-10.89	-19.57	-11.33	-17.49	-10.21	-17.97	-11.53	-16.07	-11.31	-17.12	-8.84	-15.27
Spring 2008	Apr 26-May 6	-10.66	-7.07	-9.40	-6.70	-7.44		-16.43	-3.06	-12.48	-5.20	-5.94	-3.78
Summer 2008	Aug 23-Sep 3	-17.95	-1.81	-8.83	-0.97	-10.48		-20.28	-1.97	-15.93	-3.50	-10.33	-0.10
Fall 2008	Oct 6-9	-1.86	-0.56	-1.42	-1.64	-2.07		-3.41	-2.25	-2.55	-2.23	-2.82	-0.35
Spring 2009	May 1-11	-11.67	-5.19	-9.47	-5.02	-8.53		-14.44	-5.47	-10.88	-6.26	-9.41	-3.92

Table A-3. Average Change in Strains (All Sensors, Rubblized Section).

Section 3: Untreated													
Season		*e*		*f*		*g*		*m*		*n*		*o*	
		Top	Bottom	Top	Bottom	Top	Bottom	Top	Bottom	Top	Bottom	Top	Bottom
Average Tensile Change in Strains (με)													
Summer 2006	July 8-17	2.40	0.95	4.48	2.35	2.82	1.93	3.10	3.91	2.29	3.00	4.79	0.76
	July 17-28	0.00	0.54	0.04	1.03	0.01	0.93	0.10	2.42	0.75	1.85	0.00	1.28
	Aug 5-9	0.00	0.82	0.10	2.59	0.01	1.29	0.29	3.99	2.62	3.00	0.00	1.86
	Aug 9-15	0.00	0.17	0.04	2.11	0.00	0.58	0.29	3.16	1.72	2.56	0.00	0.81
Fall 2006	Dec 1-3	5.41	0.00	5.44	0.04	4.62	0.00	7.26	0.16	9.83	0.14	9.12	0.14
	Dec 3-7	17.17	1.48	16.92	1.48	15.06	1.03	18.34	1.49	28.20	1.39	16.49	1.16
Winter 2007	Mar 9-13	1.66	3.18	2.95	7.98	2.75	3.89	4.99	3.40	4.28	3.08	3.35	3.61
	Mar 13-20	1.81	2.80	2.40	6.15	1.82	5.17	1.02	9.81	1.65	8.63	13.31	9.00
Spring 2007	May 27-June 7	0.35	0.95	3.75	2.17	0.12	0.90	14.09	5.32	14.74	3.74	4.78	3.37
Fall 2007	Oct 21-30	0.00	0.13	0.11	0.54	0.00	0.10	0.34	1.20	0.54	1.18	1.14	0.65
Spring 2008	Apr 26-May 6	1.46	2.53	3.13	3.82	2.35	1.56	12.73	15.28	5.88	10.97	6.77	11.32
Summer 2008	Aug 23-Sep 3	0.83	10.23	4.10	10.32	0.70	9.26	9.31	17.06	3.81	13.25	4.35	21.52
Fall 2008	Oct 6-9	10.00	8.60	12.35	6.64	6.37	8.23	15.23	8.47	29.49	7.33	8.20	7.65
Spring 2009	May 1-11	0.13	1.67	1.45	3.82	0.27	2.11	1.82	5.21	2.52	4.80	0.59	3.41
Average Compressive Change in Strains (με)													
Summer 2006	July 8-17	-7.29	-5.51	-7.53	-6.73	-6.78	-3.39	-9.02	-4.55	-17.76	-5.01	-7.53	-5.54
	July 17-28	-13.14	-5.29	-11.72	-5.82	-11.46	-3.24	-9.48	-5.10	-14.95	-5.25	-19.36	-3.82
	Aug 5-9	-31.90	-9.36	-28.95	-10.61	-28.03	-6.81	-25.52	-13.26	-25.71	-14.09	-45.65	-8.95
	Aug 9-15	-28.64	-10.78	-24.49	-10.72	-23.94	-6.65	-21.24	-15.28	-31.93	-15.58	-37.64	-11.62
Fall 2006	Dec 1-3	-0.44	-11.09	-0.65	-11.50	-0.45	-9.57	-0.46	-10.19	-0.80	-8.64	-0.22	-6.58
	Dec 3-7	-0.12	-1.88	-0.69	-3.52	-0.29	-2.24	-0.49	-5.89	-0.34	-4.35	-0.21	-3.43
Winter 2007	Mar 9-13	-10.30	-1.91	-14.73	-0.83	-9.19	-0.38	-7.81	-4.11	-11.59	-2.13	-14.51	-1.68
	Mar 13-20	-5.85	-1.41	-7.91	-0.75	-4.95	-0.09	-9.53	-0.17	-12.12	-0.27	-2.14	-0.10
Spring 2007	May 27-June 7	-21.97	-9.69	-21.38	-10.21	-20.30	-9.57	-22.98	-7.66	-26.29	-9.86	-26.16	-8.34
Fall 2007	Oct 21-30	-15.15	-18.75	-11.65	-14.65	-11.01	-17.07	-11.80	-16.21	-17.27	-14.01	-9.53	-13.58
Spring 2008	Apr 26-May 6	-7.08	-4.19	-11.46	-5.25	-6.10	-5.83	-8.49	-0.20	-18.86	-0.87	-9.25	-0.03
Summer 2008	Aug 23-Sep 3	-17.66	-0.05	-13.28	-0.12	-14.37	-0.13	-14.56	-0.05	-28.95	-0.12	-16.19	-0.04
Fall 2008	Oct 6-9	-0.96	-0.78	-2.33	-2.90	-1.37	-0.48	-3.44	-4.67	-3.88	-4.81	-4.19	-1.56
Spring 2009	May 1-11	-15.21	-5.23	-13.29	-4.71	-10.42	-4.20	-16.44	-5.87	-24.38	-6.34	-22.34	-3.54

Table A-4. Average Change in Strains (All Sensors, Rubblized Section).

Section 1: B&S													
Season		*e*		*f*		*g*		*m*		*n*		*o*	
		Top	Bottom	Top	Bottom	Top	Bottom	Top	Bottom	Top	Bottom	Top	Bottom
Maximum Tensile Change in Strains (με)													
Summer 2006	July 8-17	15.45	32.15	17.67	8.96	12.96	26.14	16.24	7.03	17.18	21.86	19.44	6.03
	July 17-28	2.29	24.57	0.08	13.20	2.13	21.60	0.39	9.21	9.25	26.14	5.98	12.92
	Aug 5-9	4.21	22.07	0.41	11.08	2.78	21.20	0.00	8.54	6.22	18.94	0.87	9.55
	Aug 9-15	2.80	22.19	0.00	6.79	1.61	21.67	0.00	4.18	6.07	19.86	0.18	6.14
Fall 2006	Dec 1-3	5.34	5.73	5.66	0.24	6.18	3.41	5.65	0.36	6.21	2.18	3.70	0.00
	Dec 3-7	26.38	11.23	18.02	9.15	21.98	10.71	14.63	9.19	22.27	7.68	16.11	7.26
Winter 2007	Feb 9-15	6.92	34.08	1.12	26.54	6.11	32.73	16.68	9.01	13.59	18.41	21.35	9.56
	Feb 15-20	8.99	27.85	9.46	17.77	8.10	19.02	12.10	10.49	9.86	14.71	10.37	10.63
Summer 2007	Aug 21-25	4.22	22.79	2.56	10.40	2.68	21.77	0.89	10.54	5.86	18.96	1.21	9.54
Fall 2007	Oct 21-30	0.00	24.30	0.00	11.36	0.65	22.91	1.22	11.96	0.41	17.52	0.69	9.83
Spring 2008	Apr 26-May 6	11.65	35.35	1.90	16.43	10.46	27.14	8.78	14.72	6.37	21.40	5.12	14.83
Summer 2008	Aug 23-Sep 3	16.62	39.71	2.47	25.04	20.11	31.25	9.22	18.83	11.92	26.68	9.44	21.45
Fall 2008	Oct 6-9	25.80	32.01	19.46	30.24	23.77	36.13	12.90	29.70	20.58	28.31	15.89	23.56
Spring 2009	May 1-11	11.42	25.46	4.41	16.68	10.88	23.23	4.35	16.09	8.66	19.02	4.54	13.93
Maximum Compressive Change in Strains (με)													
Summer 2006	July 8-17	-38.21	-14.66	-22.54	-21.23	-27.72	-20.89	-18.78	-24.51	-29.13	-16.98	-19.31	-20.31
	July 17-28	-57.16	-22.86	-41.02	-24.08	-41.65	-30.84	-32.12	-31.74	-36.81	-20.00	-31.08	-19.40
	Aug 5-9	-64.71	-29.22	-53.46	-24.34	-49.06	-38.08	-47.50	-27.71	-50.44	-28.42	-47.91	-21.52
	Aug 9-15	-56.32	-28.24	-44.82	-28.11	-42.53	-36.21	-36.97	-29.58	-48.44	-28.24	-37.78	-24.30
Fall 2006	Dec 1-3	-11.73	-14.34	-6.18	-16.63	-9.43	-18.43	-5.51	-19.39	-9.81	-18.25	-7.29	-15.59
	Dec 3-7	-5.61	-15.06	-3.61	-7.77	-5.62	-13.43	-6.10	-7.71	-8.50	-13.23	-6.08	-6.49
Winter 2007	Feb 9-15	-56.23	-6.13	-47.84	-5.81	-46.96	-6.20	-27.41	-17.25	-39.09	-7.83	-31.82	-17.82
	Feb 15-20	-33.91	-8.58	-19.21	-8.17	-22.73	-11.81	-10.87	-11.15	-27.56	-10.35	-20.12	-6.21
Summer 2007	Aug 21-25	-40.95	-16.18	-25.32	-23.10	-32.37	-22.21	-20.62	-26.14	-37.73	-19.53	-23.29	-21.52
Fall 2007	Oct 21-30	-38.72	-26.19	-27.49	-32.40	-36.02	-31.20	-25.62	-33.71	-33.50	-30.65	-26.93	-28.50
Spring 2008	Apr 26-May 6	-46.17	-16.96	-30.99	-25.82	-43.02	-31.23	-22.76	-28.43	-46.31	-28.43	-33.40	-22.41
Summer 2008	Aug 23-Sep 3	-58.85	-12.89	-46.92	-10.42	-55.88	-26.20	-46.48	-15.48	-59.14	-16.72	-53.05	-6.54
Fall 2008	Oct 6-9	-13.30	-16.55	-8.59	-10.08	-15.45	-16.56	-11.87	-9.80	-14.99	-13.68	-13.39	-7.96
Spring 2009	May 1-11	-42.15	-22.64	-29.20	-25.12	-36.65	-30.83	-24.13	-24.46	-37.08	-24.95	-30.79	-19.34

Table A-5. Maximum Change in Strains (All Sensors, B&S Section).

Section 2: Rubblized													
Season		*e*		*f*		*g*		*m*		*n*		*o*	
		Top	Bottom	Top	Bottom	Top	Bottom	Top	Bottom	Top	Bottom	Top	Bottom
Maximum Tensile Change in Strains (με)													
Summer 2006	July 8-17	22.99	5.94	24.92	17.56	25.43		17.90	20.39	21.23	18.00	26.17	2.54
	July 17-28	3.23	19.04	9.41	24.47	7.86		2.92	24.79	4.09	23.97	4.96	13.70
	Aug 5-9	0.00	8.60	1.49	16.54	0.00		1.69	19.22	0.52	16.73	0.00	7.05
	Aug 9-15	0.00	3.64	0.83	15.00	0.00		1.55	14.60	0.22	13.75	0.00	0.70
Fall 2006	Dec 1-3	5.29	1.09	4.76	3.69	3.92		6.50	5.31	5.18	4.05	2.83	1.84
	Dec 3-7	19.68	7.80	20.71	10.69	18.70		32.13	10.32	21.59	10.88	12.87	8.17
Winter 2007	Feb 26-Mar 5	18.32	8.52	12.59	14.20	13.03		26.35	12.11	15.21	13.55	7.06	8.65
	Mar 5-9	6.06	16.83	5.32	18.80	4.56		5.60	19.60	5.88	14.57	3.32	9.00
Spring 2007	May 27-June 7	1.35	12.51	2.48	24.34	1.60		14.01	28.41	7.21	27.80	1.83	18.46
Fall 2007	Oct 21-30	0.00	3.75	0.00	11.00	0.00	2.26	3.20	13.74	2.76	10.91	0.00	7.09
Spring 2008	Apr 26-May 6	5.01	11.71	6.54	24.54	6.45		8.20	34.36	6.75	27.20	5.55	19.08
Summer 2008	Aug 23-Sep 3	9.23	18.76	13.77	26.86	11.22		17.24	34.49	13.50	28.48	12.79	24.97
Fall 2008	Oct 6-9	19.57	24.17	17.35	25.04	14.19		26.22	32.72	22.15	31.72	16.67	26.94
Spring 2009	May 1-11	4.37	13.40	5.81	25.76	3.28		11.79	28.24	8.28	25.74	3.90	19.29
Maximum Compressive Change in Strains (με)													
Summer 2006	July 8-17	-31.88	-22.30	-31.05	-16.71	-29.89		-55.47	-14.14	-31.04	-15.71	-21.78	-23.13
	July 17-28	-40.95	-13.41	-34.84	-14.68	-32.84		-56.21	-15.74	-40.23	-17.40	-34.24	-16.64
	Aug 5-9	-57.85	-18.20	-52.83	-19.71	-47.91		-66.24	-23.42	-55.98	-26.37	-47.87	-18.52
	Aug 9-15	-48.65	-25.02	-42.95	-20.61	-37.63		-60.76	-24.58	-50.05	-27.52	-38.69	-26.56
Fall 2006	Dec 1-3	-8.72	-15.22	-10.14	-17.90	-7.35		-14.64	-15.18	-10.68	-15.70	-6.04	-11.89
	Dec 3-7	-3.25	-8.66	-10.28	-12.19	-5.88		-7.57	-14.43	-6.60	-12.44	-5.11	-6.19
Winter 2007	Feb 26-Mar 5	-15.12	-10.55	-22.82	-8.69	-20.06		-24.48	-16.82	-18.54	-11.25	-15.25	-6.41
	Mar 5-9	-53.13	-16.13	-47.44	-16.60	-50.51		-59.19	-21.77	-54.32	-19.69	-48.57	-11.20
Spring 2007	May 27-June 7	-85.08	-34.15	-87.31	-27.17	-84.00		-122.62	-33.33	-87.52	-28.50	-77.72	-31.07
Fall 2007	Oct 21-30	-28.43	-35.90	-31.23	-35.81	-24.44	-32.64	-43.78	-34.88	-37.75	-35.57	-20.37	-28.66
Spring 2008	Apr 26-May 6	-29.93	-21.60	-38.35	-22.82	-28.31		-57.99	-17.06	-40.24	-20.82	-21.63	-14.73
Summer 2008	Aug 23-Sep 3	-44.32	-10.08	-45.31	-6.59	-45.14		-67.61	-11.02	-53.05	-13.92	-35.53	-3.87
Fall 2008	Oct 6-9	-10.32	-5.94	-11.67	-9.54	-9.90		-25.88	-11.45	-18.58	-11.04	-11.02	-4.58
Spring 2009	May 1-11	-28.54	-19.61	-32.68	-20.93	-23.08		-53.55	-22.23	-34.37	-23.09	-22.57	-15.36

Table A-6. Maximum Change in Strains (All Sensors, Rubblized Section).

Section 3: Untreated													
Season		*e*		*f*		*g*		*m*		*n*		*o*	
		Top	Bottom	Top	Bottom	Top	Bottom	Top	Bottom	Top	Bottom	Top	Bottom
Maximum Tensile Change in Strains (με)													
Summer 2006	July 8-17	22.65	8.88	28.69	19.55	22.60	18.43	23.88	30.41	16.76	23.49	37.97	8.47
	July 17-28	2.01	10.45	3.43	17.01	1.70	14.74	11.36	30.17	15.85	25.99	4.26	16.76
	Aug 5-9	0.24	9.26	3.17	17.39	0.87	10.30	7.00	28.42	22.07	21.52	0.00	13.25
	Aug 9-15	0.00	4.14	3.03	15.80	0.00	7.14	6.44	22.21	12.67	18.96	0.00	8.93
Fall 2006	Dec 1-3	9.66	0.00	11.93	1.38	8.59	0.08	13.04	4.64	18.11	4.07	20.27	3.73
	Dec 3-7	30.04	10.60	29.79	10.38	25.37	8.58	30.69	13.47	49.32	11.80	29.61	9.11
Winter 2007	Mar 9-13	7.69	15.49	13.78	27.96	11.15	14.99	17.16	18.75	19.11	15.64	17.98	15.83
	Mar 13-20	13.53	17.48	15.63	26.75	14.44	18.34	13.62	37.44	22.45	31.12	34.10	30.90
Spring 2007	May 27-June 7	8.73	12.56	19.69	20.17	4.69	13.17	41.92	41.24	45.86	33.86	30.59	27.08
Fall 2007	Oct 21-30	0.00	7.71	4.38	14.17	0.00	6.15	6.43	21.90	9.14	20.26	8.92	14.89
Spring 2008	Apr 26-May 6	13.97	14.07	15.17	22.36	11.02	14.63	33.66	50.18	27.06	40.09	26.45	31.98
Summer 2008	Aug 23-Sep 3	17.60	27.97	24.36	36.86	13.67	26.59	32.47	53.83	21.56	47.40	42.43	44.55
Fall 2008	Oct 6-9	30.60	25.66	30.45	25.87	19.71	22.76	36.79	38.14	59.99	33.83	28.86	28.92
Spring 2009	May 1-11	5.52	10.34	12.48	19.97	5.02	13.15	13.46	34.59	18.33	29.29	11.32	21.18
Maximum Compressive Change in Strains (με)													
Summer 2006	July 8-17	-31.58	-19.94	-37.39	-20.17	-33.32	-13.64	-49.56	-21.22	-82.63	-21.95	-37.31	-29.58
	July 17-28	-53.06	-25.25	-62.22	-26.39	-47.95	-15.96	-60.72	-26.54	-99.38	-25.66	-77.56	-20.29
	Aug 5-9	-63.75	-22.06	-69.59	-26.91	-54.77	-16.27	-69.96	-36.35	-92.13	-37.33	-79.93	-23.24
	Aug 9-15	-60.18	-22.65	-63.06	-24.49	-49.73	-14.59	-65.57	-35.50	-99.53	-34.65	-72.26	-24.88
Fall 2006	Dec 1-3	-11.72	-18.60	-15.45	-19.17	-11.58	-15.79	-13.35	-17.08	-21.57	-14.32	-7.47	-10.77
	Dec 3-7	-3.53	-5.51	-10.34	-9.23	-5.93	-5.63	-8.75	-13.15	-10.00	-9.46	-5.12	-7.65
Winter 2007	Mar 9-13	-49.80	-8.07	-69.25	-6.49	-50.27	-3.05	-47.43	-14.73	-56.13	-11.36	-69.79	-9.55
	Mar 13-20	-39.87	-8.35	-59.41	-5.86	-43.50	-1.82	-54.64	-3.68	-70.96	-4.89	-38.65	-3.75
Spring 2007	May 27-June 7	-105.17	-39.78	-113.39	-31.40	-96.01	-41.23	-141.12	-40.32	-140.13	-40.61	-147.45	-42.95
Fall 2007	Oct 21-30	-42.62	-36.04	-46.75	-32.33	-34.98	-31.95	-56.69	-36.47	-87.56	-31.68	-59.34	-29.36
Spring 2008	Apr 26-May 6	-36.99	-17.93	-57.67	-19.49	-39.57	-19.26	-64.38	-5.62	-100.76	-9.37	-62.18	-2.03
Summer 2008	Aug 23-Sep 3	-62.68	-3.88	-75.22	-5.32	-62.66	-4.87	-88.83	-4.73	-118.52	-6.12	-85.23	-4.53
Fall 2008	Oct 6-9	-10.21	-7.44	-19.44	-12.70	-10.93	-5.15	-28.84	-18.30	-37.71	-18.17	-31.71	-9.40
Spring 2009	May 1-11	-42.74	-20.14	-56.51	-19.31	-42.24	-18.10	-77.68	-22.49	-102.58	-22.35	-89.67	-11.68

Table A-7. Maximum Change in Strains (All Sensors, Untreated Section).

Linear Temperature Gradient LTG (°C/cm)													
Section 1: B&S													
Season		***e***		***f***		***g***		***m***		***n***		***o***	
		Max	**Min**	**Max**	**Min**	**Max**	**Min**	**Max**	**Min**	**Max**	**Min**	**Max**	**Min**
Summer 2006	July 8-17	0.54	-0.20	0.55	-0.18	0.46	-0.16	0.45	-0.16	0.51	-0.20	0.46	-0.17
	July 17-28	0.52	-0.25	0.52	-0.23	0.44	-0.20	0.43	-0.21	0.50	-0.24	0.45	-0.22
	Aug 5-9	0.52	-0.33	0.51	-0.31	0.43	-0.28	0.42	-0.29	0.50	-0.33	0.44	-0.29
	Aug 9-15	0.53	-0.30	0.53	-0.29	0.44	-0.29	0.44	-0.31	0.51	-0.33	0.46	-0.28
Fall 2006	Dec 1-3	0.09	-0.24	0.09	-0.23	0.10	-0.21	0.09	-0.22	0.09	-0.24	0.09	-0.22
	Dec 3-7	0.20	-0.31	0.18	-0.29	0.19	-0.27	0.17	-0.28	0.19	-0.31	0.18	-0.27
Winter 2007	Feb 9-15	0.75	-0.20	0.71	-0.19	0.70	-0.17	0.67	-0.17	0.72	-0.19	0.66	-0.17
	Feb 15-20	0.57	-0.27	0.51	-0.26	0.50	-0.23	0.47	-0.24	0.51	-0.26	0.46	-0.24
Summer 2007	Aug 21-25	0.46	-0.22	0.46	-0.19	0.40	-0.20	0.39	-0.18	0.45	-0.22	0.41	-0.18
Fall 2007	Oct 21-30	0.47	-0.30	0.45	-0.29	0.44	-0.27	0.42	-0.28	0.46	-0.30	0.42	-0.27
Spring 2008	Apr 26-May 6	0.79	-0.34	0.74	-0.32	0.72	-0.30	0.68	-0.31	0.75	-0.33	0.69	-0.30
Summer 2008	Aug 23-Sep 3	0.70	-0.33	0.65	-0.30	0.63	-0.28	0.60	-0.28	0.66	-0.31	0.61	-0.28
Fall 2008	Oct 6-9	0.53	-0.33	0.48	-0.31	0.46	-0.29	0.43	-0.29	0.50	-0.32	0.45	-0.29
Spring 2009	May 1-11	0.72	-0.32	0.66	-0.30	0.65	-0.27	0.62	-0.28	0.67	-0.30	0.62	-0.27
Section 2: Rubblized													
Summer 2006	July 8-17	0.50	-0.18	0.55	-0.19			0.60	-0.20	0.47	-0.18	0.51	-0.19
	July 17-28	0.45	-0.23	0.50	-0.25			0.54	-0.25	0.42	-0.23	0.47	-0.24
	Aug 5-9	0.44	-0.30	0.53	-0.31			0.55	-0.33	0.41	-0.30	0.45	-0.32
	Aug 9-15	0.45	-0.30	0.53	-0.32			0.56	-0.33	0.42	-0.30	0.46	-0.32
Fall 2006	Dec 1-3	0.08	-0.22	0.09	-0.22			0.10	-0.23	0.08	-0.23	0.09	-0.24
	Dec 3-7	0.18	-0.28	0.20	-0.28			0.21	-0.30	0.18	-0.29	0.20	-0.31
Winter 2007	Feb 26-Mar 5	0.39	-0.15	0.44	-0.14			0.47	-0.15	0.41	-0.15	0.47	-0.15
	Mar 5-9	0.37	-0.42	0.42	-0.43			0.45	-0.45	0.38	-0.42	0.42	-0.46
Spring 2007	May 27-June 7	0.73	-0.29	0.78	-0.30			0.86	-0.29	0.74	-0.30	0.81	-0.32
Fall 2007	Oct 21-30	0.42	-0.28	0.46	-0.28	0.45	-0.29	0.48	-0.30	0.43	-0.28	0.48	-0.30
Spring 2008	Apr 26-May 6	0.65	-0.32	0.71	-0.32			0.77	-0.34	0.68	-0.33	0.74	-0.35
Summer 2008	Aug 23-Sep 3	0.61	-0.30	0.68	-0.30	0.68	-0.26	0.72	-0.33	0.64	-0.31	0.71	-0.32
Fall 2008	Oct 6-9	0.46	-0.30	0.51	-0.31	0.14	-0.24	0.55	-0.33	0.48	-0.31	0.53	-0.33
Spring 2009	May 1-11	0.64	-0.29	0.71	-0.29	0.57	-0.18	0.76	-0.32	0.67	-0.30	0.74	-0.32
Section 3: Untreated													
Summer 2006	July 8-17	0.49	-0.17	0.47	-0.22	0.46	-0.19	0.55	-0.18	0.62	-0.23	0.49	-0.18
	July 17-28	0.44	-0.22	0.45	-0.24	0.44	-0.25	0.50	-0.23	0.58	-0.29	0.46	-0.24
	Aug 5-9	0.44	-0.29	0.44	-0.31	0.44	-0.32	0.52	-0.29	0.58	-0.38	0.45	-0.31
	Aug 9-15	0.45	-0.29	0.46	-0.31	0.46	-0.32	0.52	-0.29	0.59	-0.37	0.46	-0.31
Fall 2006	Dec 1-3	0.10	-0.21	0.09	-0.22	0.08	-0.23	0.11	-0.20	0.12	-0.25	0.10	-0.23
	Dec 3-7	0.20	-0.23	0.19	-0.23	0.18	-0.24	0.20	-0.21	0.22	-0.28	0.20	-0.24
Winter 2007	Mar 9-13	0.72	-0.18	0.71	-0.18	0.71	-0.20	0.67	-0.18	0.81	-0.23	0.74	-0.19
	Mar 13-20	0.51	-0.24	0.49	-0.25	0.49	-0.25	0.49	-0.23	0.59	-0.30	0.52	-0.26
Spring 2007	May 27-June 7	0.81	-0.29	0.77	-0.29	0.78	-0.30	0.79	-0.26	0.89	-0.36	0.82	-0.30
Fall 2007	Oct 21-30	0.48	-0.28	0.45	-0.28	0.46	-0.29	0.48	-0.25	0.61	-0.32	0.49	-0.30
Spring 2008	Apr 26-May 6	0.73	-0.31	0.70	-0.31	0.71	-0.32	0.71	-0.30	0.86	-0.38	0.74	-0.33
Summer 2008	Aug 23-Sep 3	0.68	-0.30	0.67	-0.30	0.67	-0.31	0.65	-0.30	0.79	-0.38	0.70	-0.32
Fall 2008	Oct 6-9	0.52	-0.31	0.49	-0.30	0.49	-0.31	0.51	-0.29	0.61	-0.37	0.53	-0.32
Spring 2009	May 1-11	0.70	-0.27	0.68	-0.27	0.69	-0.28	0.68	-0.25	0.87	-0.23	0.72	-0.29

Table A-8. Maximum and Minimum Linear Temperature Gradient (LTG) (1°C/cm = 4.6°F/in).

Appendix B: SUPPLEMENTAL DYNAMIC RESPONSE DATA

Dynamic Strains (με)																								
Sensor Location		Drop 1	Drop 2	Drop 3	Time	Drop 1	Drop 2	Drop 3	Time	Drop 1	Drop 2	Drop 3	Time	Drop 1	Drop 2	Drop 3	Time	Drop 1	Drop 2	Drop 3	Time	Drop 1	Drop 2	Drop 3	Time
Section 1: B&S																								
Date		**20-June-2006**				**29-November-2006**				**21-March-2007**				**31-October-2007**				**6-May-2008**				**18-October-2008**			
t	Top	-	-	-	15:53	-	-	-	-	-	-	-	12:38	-	-	-	14:59	-	-	-	-	-	-	-	14:02
	Bottom	4.0	5.3	6.5		-	-	-		6.9	9.1	11.0		5.0	6.8	7.7		-	-	-		4.0	5.1	7.2	
u	Top	-5.1	-7.0	-9.1	15:52	-6.0	-7.4	-9.9	14:01	-5.3	-6.9	-8.0	12:39	-4.6	-5.8	-7.6	15:00	-	-	-	-	-3.1	-3.5	-4.8	14:03
	Bottom	4.0	4.8	6.5		6.1	7.8	10.5		5.0	7.1	8.1		3.5	4.6	6.0		-	-	-		3.1	4.5	5.7	
v	Top	-8.7	-10.9	-14.2	15:50	-10.5	-13.6	-17.8	14:03	-14.4	-18.8	-22.1	12:40	-11.5	-15.2	-16.8	15:01	-	-	-	-	-5.6	-7.5	-10.0	14:05
	Bottom	4.5	5.8	7.8		6.4	8.3	10.8		8.6	11.2	13.4		6.4	8.7	10.1		-	-	-		4.7	6.0	8.2	
w	Top	-6.0	-8.3	-10.9	15:26	-6.6	-8.9	-12.1	14:04	-8.3	-12.0	-13.6	12:42	-6.1	-8.3	-10.1	15:02	-	-	-	-	-6.1	-8.0	-10.4	14:06
	Bottom	4.2	5.8	7.5		5.1	7.3	9.4		6.5	7.8	9.6		3.8	5.5	6.7		-	-	-		4.8	6.6	8.7	
Section 2: Rubblized																								
Date		**20-June-2006**				**28-November-2006**				**21-March-2007**				**31-October-2007**				**6-May-2008**				**18-October-2008**			
t	Top	-7.1	-9.0	-12.3	16:59	-5.6	-7.2	-9.5	14:48	-	-8.1	-9.7	10:24	-8.0	-10.1	-11.5	13:26	-11.1	-13.9	-17.3	15:17	-4.6	-5.8	-7.7	12:06
	Bottom	5.1	7.0	8.9		5.6	6.8	8.8		-	8.2	9.7		4.8	6.4	7.7		9.9	12.8	15.9		4.5	6.0	8.3	
u	Top	-5.5	-6.6	-8.5	16:57	-4.3	-5.8	-7.3	14:49	-3.0	-4.8	-5.4	10:25	-3.5	-4.4	-5.3	13:27	-4.9	-6.8	-8.7	15:18	-2.5	-3.1	-3.8	12:07
	Bottom	3.9	5.3	7.2		3.4	4.5	7.3		5.1	6.1	7.8		3.2	4.2	4.7		6.4	8.0	10.1		3.7	5.2	6.6	
v	Top	-	-	-	16:55	-	-	-	14:51	-	-	-	10:26	-	-	-	13:29	-	-	-	15:19	-	-	-	12:08
	Bottom	6.4	7.0	9.7		5.4	7.3	8.6		6.5	8.6	9.7		5.2	6.4	7.2		15.1	19.7	24.3		4.2	5.7	8.0	
w	Top	-6.1	-7.7	-10.0	16:52	-4.2	-6.0	-7.8	14:52	-4.6	-6.9	-7.2	10:27	-4.1	-5.5	-6.4	13:30	-	-	-	15:20	-3.1	-3.7	-5.1	12:09
	Bottom	5.7	6.9	9.1		5.6	6.8	9.4		4.8	6.8	7.8		3.6	5.1	6.1		11.0	14.1	18.0		3.9	5.2	6.8	
Section 3: Untreated																								
Date		**20-June-2006**				**28-November-2006**				**20-March-2007**				**31-October-2007**				**6-May-2008**				**18-October-2008**			
t	Top	-	-	-	-	-	-	-	15:42	-	-	-	15:54	-	-	-	11:40	-	-	-	12:42	-	-	-	11:26
	Bottom	-	-	-		2.6	3.5	4.9		5.5	6.0	8.5		2.4	3.7	4.7		7.0	9.2	11.6		3.4	4.6	5.9	
u	Top	-	-	-	18:04	-	-	-	15:44	-	-	-	15:56	-	-	-	11:41	-	-	-	12:43	-	-	-	11:28
	Bottom	3.1	4.1	5.9		2.2	2.9	3.9		4.9	5.0	6.1		3.8	5.5	6.1		8.1	9.9	12.7		4.9	6.1	8.2	
v	Top	-5.5	-6.8	-9.0	18:02	-6.4	-8.5	-10.7	15:46	-10.2	-13.3	-15.4	15:59	-4.2	-5.7	-6.6	11:42	-13.1	-16.8	-19.9	12:45	-3.3	-3.9	-5.6	11:29
	Bottom	2.4	3.7	4.0		3.0	4.4	5.9		7.5	9.6	11.0		3.0	4.3	5.0		11.4	15.4	19.3		4.9	6.5	8.5	
w	Top	-4.8	-6.4	-7.8	18:00	-2.8	-4.3	-5.6	15:47	-4.4	-6.0	-7.0	16:01	-2.8	-3.7	-4.1	11:44	-7.6	-9.5	-11.4	12:46	-3.4	-3.8	-6.2	11:30
	Bottom	3.3	4.2	5.0		4.9	5.5	7.4		5.0	6.3	7.8		4.3	5.8	7.0		7.8	10.6	13.1		4.7	6.3	8.2	

Table B-1. Dynamic Strain Peaks from FWD Testing.

Impact Load (kN)																								
Sensor Location	Drop			Time	Drop			Time	Drop			Time	Drop			Time	Drop			Time	Drop			Time
	1	2	3		1	2	3		1	2	3		1	2	3		1	2	3		1	2	3	
Section 1: B&S																								
Date	**20-June-2006**				**29-November-2006**				**21-March-2007**				**31-October-2007**				**6-May-2008**				**18-October-2008**			
t	40.7	53.9	71.1	15:53	42.7	55.7	73.3	-	42.7	56.6	67.4	12:38	42.3	56.6	67.3	14:59	40.3	53.4	70.2	-	40.4	53.9	71.6	14:02
u	39.1	52.6	71.1	15:52	42.6	55.4	73.4	14:01	43.0	56.7	66.8	12:39	42.2	56.1	66.2	15:00	40.5	53.8	72.1	-	39.7	53.0	71.1	14:03
v	40.4	53.1	70.8	15:50	41.7	54.6	73.2	14:03	42.2	55.6	65.2	12:40	42.2	56.0	66.1	15:01	39.6	52.7	70.3	-	39.5	52.9	70.5	14:05
w	39.8	52.7	70.3	15:26	41.8	54.2	73.5	14:04	42.4	56.2	66.3	12:42	42.3	56.1	66.0	15:02	39.5	53.5	71.4	-	39.6	52.8	70.0	14:06
Section 2: Rubblized																								
Date	**20-June-2006**				**28-November-2006**				**21-March-2007**				**31-October-2007**				**6-May-2008**				**18-October-2008**			
t	39.7	52.9	70.0	16:59	41.8	55.3	72.8	14:48	43.0	56.1	67.4	10:24	42.7	56.7	66.5	13:26	39.8	53.0	69.2	15:17	39.9	53.1	71.1	12:06
u	39.6	53.4	72.1	16:57	42.2	55.4	72.7	14:49	43.3	56.6	67.5	10:25	42.9	56.5	66.1	13:27	40.3	53.1	73.2	15:18	40.0	53.3	71.2	12:07
v	40.3	53.3	70.7	16:55	41.9	55.5	72.5	14:51	43.3	56.0	67.5	10:26	43.3	57.0	66.8	13:29	39.9	53.3	70.0	15:19	39.7	53.3	71.0	12:08
w	40.3	53.8	72.0	16:52	42.3	55.8	72.3	14:52	43.2	56.8	67.2	10:27	43.1	56.8	67.0	13:30	40.0	53.9	71.9	15:20	40.0	53.2	71.0	12:09
Section 3: Untreated																								
Date	**20-June-2006**				**28-November-2006**				**20-March-2007**				**31-October-2007**				**6-May-2008**				**18-October-2008**			
t	40.5	53.9	71.0	-	41.5	54.5	73.6	15:42	42.2	55.8	65.4	15:54	43.0	55.8	66.5	11:40	39.9	53.2	71.6	12:42	40.2	53.6	71.4	11:26
u	40.2	53.9	71.5	18:04	41.8	54.1	73.6	15:44	42.4	55.8	65.3	15:56	43.0	55.6	66.5	11:41	40.6	53.9	72.0	12:43	39.9	53.0	71.0	11:28
v	39.8	53.0	70.5	18:02	41.5	54.0	73.5	15:46	42.3	55.5	64.7	15:59	43.0	55.9	66.4	11:42	40.3	52.7	70.5	12:45	40.0	53.3	71.0	11:29
w	39.8	52.9	71.4	18:00	42.0	54.8	73.5	15:47	42.6	56.2	65.8	16:01	42.7	56.1	66.3	11:44	39.8	53.6	71.5	12:46	39.9	53.5	70.7	11:30

Table B-2. Impact Load (FWD Test) (1 kN = 0.225 kip).

Dynamic Deflections (μm)																								
LVDT Location		Drop 1	Drop 2	Drop 3	Time	Drop 1	Drop 2	Drop 3	Time	Drop 1	Drop 2	Drop 3	Time	Drop 1	Drop 2	Drop 3	Time	Drop 1	Drop 2	Drop 3	Time	Drop 1	Drop 2	Drop 3	Time
Section 1: B&S																								
Date		**20-June-2006**				**29-November-2006**				**21-March-2007**				**31-October-2007**				**6-May-2008**				**18-October-2008**			
a	Shallow	-16.2	-21.4	-28.0	16:27	-	-	-	-	-	-	-	-	-	-	-	-	-	-	-	-	-	-	-	-
b	Deep	-42.9	-56.7	-75.5	16:22	-	-	-	-	-	-	-	-	-	-	-	-	-	-	-	-	-	-	-	-
c	Shallow	-10.4	-14.8	-17.9	16:13	-10.6	-14.5	-17.4	14:08	-	-	-	-	-	-	-	-	-	-	-	-	-	-	-	-
d	Shallow	-6.4	-8.4	-10.1	16:06	-7.1	-9.2	-13.2	13:54	-	-	-	-	-	-	-	-	-	-	-	-	-	-	-	-
i	Shallow	-12.2	-16.6	-21.0	16:20	-	-	-	-	-	-	-	-	-	-	-	-	-	-	-	-	-	-	-	-
j	Deep	-37.7	-51.3	-69.3	16:05	-	-	-	-	-	-	-	-	-	-	-	-	-	-	-	-	-	-	-	-
k	Deep	-38.7	-52.6	-67.5	16:03	-23.0	-37.1	-58.8	13:56	-	-	-	-	-	-	-	-	-	-	-	-	-	-	-	-
l	Deep	-48.9	-66.8	-85.3	15:56	-52.9	-71.9	-98.1	13:58	-	-	-	-	-	-	-	-	-	-	-	-	-	-	-	-
Section 2: Rubblized																								
Date		**20-June-2006**				**28-November-2006**				**21-March-2007**				**31-October-2007**				**6-May-2008**				**18-October-2008**			
a	Shallow	-18.5	-26.3	-31.9	17:37	-	-	-	-	-	-	-	-	-	-	-	-	-	-	-	-	-	-	-	-
b	Deep	-73.5	-98.0	-128.7	17:33	-	-	-	-	-	-	-	-	-	-	-	-	-	-	-	-	-	-	-	-
c	Shallow	-17.0	-21.4	-26.1	17:24	-12.9	-15.4	-20.9	14:57	-	-	-	-	-	-	-	-	-	-	-	-	-	-	-	-
d	Shallow	-5.8	-7.1	-8.8	17:09	-	-	-	-	-	-	-	-	-	-	-	-	-	-	-	-	-	-	-	-
i	Shallow	-37.0	-44.2	-55.7	17:31	-	-	-	-	-	-	-	-	-	-	-	-	-	-	-	-	-	-	-	-
j	Deep	-47.0	-65.5	-94.9	17:08	-	-	-	-	-	-	-	-	-	-	-	-	-	-	-	-	-	-	-	-
k	Deep	-47.9	-64.8	-87.7	17:06	-	-	-	-	-	-	-	-	-	-	-	-	-	-	-	-	-	-	-	-
l	Deep	-52.9	-70.1	-93.9	17:00	-	-	-	-	-	-	-	-	-	-	-	-	-	-	-	-	-	-	-	-
Section 3: Untreated																								
Date		**20-June-2006**				**28-November-2006**				**20-March-2007**				**31-October-2007**				**6-May-2008**				**18-October-2008**			
a	Shallow	-12.9	-16.5	-20.0	18:26	-	-	-	-	-	-	-	-	-	-	-	-	-	-	-	-	-	-	-	-
b	Deep	-37.7	-53.5	-68.5	18:24	-	-	-	-	-	-	-	-	-	-	-	-	-	-	-	-	-	-	-	-
c	Shallow	-	-	-	-	-8.2	-10.3	-13.5	15:52	-	-	-	-	-25.1	-33.1	-40.3	11:47	-	-	-	-	-	-	-	-
d	Shallow	-	-	-	-	-	-	-	-	-	-	-	-	-	-	-	-	-	-	-	-	-	-	-	-
i	Shallow	-20.2	-20.9	-25.5	18:22	-	-	-	-	-	-	-	-	-	-	-	-	-	-	-	-	-	-	-	-
j	Deep	-	-	-	-	-	-	-	-	-	-	-	-	-	-	-	-	-	-	-	-	-	-	-	-
k	Deep	-140.7	-183.8	-213.8	18:11	-31.9	-43.1	-57.2	15:37	-	-	-	-	-	-	-	-	-	-	-	-	-	-	-	-
l	Deep	-32.1	-42.9	-56.8	18:09	-37.1	-50.4	-69.2	15:39	-	-	-	-	-	-	-	-	-	-	-	-	-	-	-	-

Table B-3. Dynamic Deflection Peaks from FWD Testing (25.4 μm = 1 mil).

Neutral Axis Shift (mm)																								
Sensor Location	Drop			Time	Drop			Time	Drop			Time	Drop			Time	Drop			Time	Drop			Time
	1	2	3		1	2	3		1	2	3		1	2	3		1	2	3		1	2	3	
Section 1: B&S																								
Date	**20-June-2006**				**29-November-2006**				**21-March-2007**				**31-October-2007**				**6-May-2008**				**18-October-2008**			
t	-	-	-	-	-	-	-	-	-	-	-	-	-	-	-	-	-	-	-	-	-	-	-	-
u	-13.8	-19.3	-17.6	15:52	-3.1	-1.6	-1.3	14:01	-6.2	-2.6	-3.2	12:39	-15.1	-13.4	-13.6	15:00	-	-	-	-	-3.8	6.7	3.4	14:03
v	-30.3	-29.2	-28.0	15:50	-24.0	-23.9	-24.2	14:03	-24.8	-24.9	-24.2	12:40	-27.5	-26.4	-24.5	15:01	-	-	-	-	-11.0	-13.0	-12.0	14:05
w	-18.5	-18.5	-19.2	15:26	-14.4	-12.0	-14.2	14:04	-13.9	-21.4	-18.1	12:42	-23.1	-20.7	-20.6	15:02	-	-	-	-	-13.7	-11.7	-11.2	14:06
Section 2: Rubblized																								
Date	**20-June-2006**				**28-November-2006**				**21-March-2007**				**31-October-2007**				**6-May-2008**				**18-October-2008**			
t	-17.4	-14.2	-17.1	16:59	-3.8	-6.1	-6.9	14:48	-	-3.2	-3.8	10:24	-24.6	-22.4	-20.3	13:26	-8.5	-7.2	-7.3	15:17	-4.7	-2.3	-0.6	12:06
u	-17.9	-12.9	-10.7	16:57	-13.5	-14.3	-3.8	14:49	17.9	6.2	11.4	10:25	-7.5	-5.7	-8.8	13:27	7.3	3.0	2.5	15:18	12.4	17.3	18.7	12:07
v	-	-	-	-	-	-	-	-	-	-	-	-	-	-	-	-	-	-	-	-	-	-	-	-
w	-6.6	-8.3	-7.7	16:52	8.1	1.5	4.0	14:52	-2.0	-4.4	-0.4	10:27	-9.2	-6.9	-5.8	13:30	-	-	-	-	5.8	10.3	8.1	12:09
Section 3: Untreated																								
Date	**20-June-2006**				**28-November-2006**				**20-March-2007**				**31-October-2007**				**6-May-2008**				**18-October-2008**			
t	-	-	-	-	-	-	-	-	-	-	-	-	-	-	-	-	-	-	-	-	-	-	-	-
u	-	-	-	-	-	-	-	-	-	-	-	-	-	-	-	-	-	-	-	-	-	-	-	-
v	-36.5	-28.4	-35.8	18:02	-33.9	-30.2	-27.9	15:46	-16.5	-17.2	-17.6	15:59	-17.6	-15.4	-15.3	11:42	-9.5	-7.4	-5.0	12:45	12.5	17.1	13.4	11:29
w	-19.2	-21.1	-22.0	18:00	19.0	6.4	7.8	15:47	1.6	-1.7	0.7	16:01	13.9	14.7	18.0	11:44	-2.7	0.8	2.0	12:46	9.6	16.9	7.8	11:30

Table B-4. Neutral Axis Shift (1 mm = 39.4 mil).

Appendix C: SUPPLEMENTAL FALLING WEIGHT TESTING DATA

Date	Drop 1							Drop 2							Drop 3						
	NDf-0 (µm/kN)			LTE (%)		JSR	MidSlab SPR (%)	NDf-0 (µm/kN)			LTE		JSR	MidSlab SPR (%)	NDf-0 (µm/kN)			LTE		JSR	MidSlab SPR (%)
	Approach	Leave	MidSlab	Approach	Leave			Approach	Leave	MidSlab	Approach	Leave			Approach	Leave	MidSlab	Approach	Leave		
Section 1: Broken and seated																					
Jun-2006	1.631	1.769		80.0	79.9	1.076		1.663	1.779		86.3	81.2	1.069		1.671	1.772		84.3	82.0	1.054	
Nov-2006	1.493	1.545	1.363	78.1	74.3	1.038	62.3	1.402	1.458	1.147	87.6	82.8	1.050	75.6	1.518	1.613	1.348	84.5	78.3	1.066	66.9
Mar-2007	2.113	2.195	4.623	76.8	72.9	1.043	74.1	2.174	2.250	4.720	77.4	73.8	1.040	74.2	2.219	2.291	4.768	77.9	74.4	1.038	74.4
Oct-2007	1.494	1.545	3.097	76.6	72.3	1.034	69.4	1.556	1.601	3.114	76.8	73.8	1.030	69.8	1.607	1.648	3.120	77.0	74.3	1.027	69.9
May-2008 (1)	1.609	1.683	3.805	87.9	84.7	1.027	70.0	1.750	1.808	3.785	87.0	84.4	1.028	70.1	1.709	1.764	3.622	86.2	84.8	1.019	70.5
May-2008 (2)	1.609	1.683		67.9	67.3	1.031		1.657	1.741		67.1	68.4	1.064		1.662	1.726		69.0	71.2	1.048	
Oct-2008	2.146	2.277	1.156	65.7	66.2	1.065	70.8	2.163	2.281	1.188	67.0	68.1	1.060	70.5	2.128	2.231	1.213	68.4	70.5	1.051	70.5
May-2009	1.750	1.797	3.394	72.4	72.2	1.023	62.0	1.773	1.824	3.387	74.5	73.2	1.025	62.2	1.760	1.803	3.294	75.3	74.5	1.017	62.4
Section 2: Rubblized																					
Jun-2006	2.090	2.220	-	85.1	84.7	1.056	-	2.151	2.234	-	84.8	86.6	1.023	-	2.148	2.244	-	84.7	87.1	1.038	-
Nov-2006	1.571	1.635	1.595	76.6	72.3	1.041	62.8	1.632	1.687	1.606	77.3	73.8	1.036	63.3	1.703	1.756	1.637	78.7	74.6	1.036	63.7
Mar-2007	2.270	2.279	2.918	74.6	73.3	1.012	70.3	2.315	2.302	2.968	75.3	74.2	1.005	70.5	2.340	2.309	2.979	75.8	74.7	0.999	70.7
Oct-2007	1.604	1.626	2.403	65.5	64.2	1.014	66.5	1.673	1.686	2.400	67.1	62.8	1.011	66.8	1.731	1.737	2.412	68.5	64.7	1.012	66.9
May-2008 (1)	1.831	1.873	3.482	77.9	78.0	1.017	68.0	1.863	1.896	3.481	79.8	79.3	1.012	68.8	1.808	1.849	3.361	80.4	80.4	1.001	68.5
May-2008 (2)	1.917	1.946	-	61.4	67.9	1.020	-	1.937	1.968	-	64.1	71.1	1.020	-	1.904	1.927	-	66.7	73.4	1.014	-
Oct-2008	2.023	2.114	1.075	65.5	65.8	1.049	64.1	2.042	2.120	1.109	66.8	67.5	1.043	64.9	2.009	2.079	1.117	68.8	69.4	1.039	65.5
May-2009	1.972	1.990	3.853	65.9	65.7	1.001	62.7	1.991	2.012	3.868	66.3	67.5	1.005	62.3	1.974	1.981	3.768	68.4	69.7	0.996	63.3
Section 3: Untreated																					
Jun-2006	0.876	0.920	-	73.4	81.1	1.032	-	0.883	0.932	-	96.2	82.3	1.045	-	0.886	0.918	-	101.2	84.7	1.021	-
Nov-2006	1.226	1.215	1.027	74.6	73.3	0.995	64.4	1.275	1.261	1.071	75.1	73.8	0.995	64.4	1.306	1.297	1.106	76.6	77.1	0.995	64.9
Mar-2007	1.335	1.360	2.600	73.4	69.8	1.029	66.9	1.366	1.387	2.545	74.5	71.2	1.026	67.2	1.389	1.415	2.566	75.1	71.8	1.026	67.4
Oct-2007	1.942	1.809	1.021	57.7	63.1	0.939	68.0	1.969	1.828	1.080	59.6	63.8	0.936	67.8	1.962	1.833	1.109	60.5	63.8	0.938	68.0
May-2008 (1)	1.325	1.362	2.652	71.2	70.4	1.028	63.0	1.345	1.379	2.616	72.3	71.5	1.024	63.3	1.335	1.363	2.503	73.3	73.1	1.017	63.6
May-2008 (2)	1.446	1.406	-	67.1	76.3	0.986	-	1.469	1.402	-	67.9	78.5	0.972	-	1.457	1.395	-	70.2	79.7	0.973	-
Oct-2008	2.065	2.146	0.940	64.4	64.6	1.051	71.8	2.050	2.139	0.973	66.2	66.3	1.053	71.1	1.990	2.080	0.980	68.0	68.6	1.050	71.8
May-2009	1.307	1.332	2.439	68.6	67.5	1.031	61.2	1.326	1.361	2.417	69.8	68.2	1.039	61.0	1.331	1.360	2.297	70.2	69.9	1.027	61.7

Table C-1. Summarized FWD Test Data Averages (1 µm/kN = 0.175 mil/kip).

20-June-2006																	
Joint		NDf-0 (mils/kip)						LTE (%)						JSR			
		Approach			Leave			Approach			Leave						
N°	Type	Drop 1	Drop 2	Drop 3	Drop 1	Drop 2	Drop 3	Drop 1	Drop 2	Drop 3	Drop 1	Drop 2	Drop 3	Drop 1	Drop 2	Drop 3	
Section 3: **Untreated**																	
1	RJ	0.147	0.147	0.150	0.156	0.163	0.157	52.5	102.3	107.0	88.8	86.3	89.3	1.019	1.090	1.023	
2	RJ	0.157	0.154	0.150	0.149	0.148	0.148	73.0	84.6	85.9	83.8	87.6	89.7	0.945	0.952	0.983	
3	RJ	0.167	0.172	0.176	0.184	0.190	0.196	72.6	81.2	81.3	71.3	72.1	70.9	1.074	1.088	1.090	
4	RJ	0.142	0.146	0.144	0.149	0.149	0.147	88.2	99.5	113.1	81.8	84.4	85.7	1.028	1.024	1.018	
5	RJ	0.153	0.154	0.155	0.167	0.166	0.156	80.5	113.3	118.5	79.8	81.3	88.0	1.094	1.071	0.990	
6	SJ	0.201	0.207	0.207	0.198	0.194	0.190	119.9	87.3	107.8	80.0	71.2	73.0	0.941	0.907	0.914	
7	SJ	0.175	0.180	0.172	0.172	0.179	0.175	82.6	91.3	88.5	83.3	80.6	83.1	1.006	1.025	1.054	
8	SJ	0.155	0.144	0.151	0.144	0.146	0.146	108.3	75.0	110.1	84.4	82.2	81.5	0.987	1.033	1.000	
9	SJ	0.156	0.204	0.203	0.191	0.204	0.203	88.3	115.9	111.8	83.5	85.3	82.4	0.903	1.018	1.034	
10	SJ	0.201	0.203	0.203	0.189	0.193	0.196	90.9	84.3	86.3	84.0	84.5	83.0	0.988	0.983	1.352	
Section 2: **Rubblized**																	
1	SJ	0.413	0.418	0.411	0.420	0.437	0.422	94.1	89.8	94.7	90.4	87.3	88.5	0.995	1.031	1.038	
2	SJ	0.481	0.479	0.475	0.531	0.534	0.521	87.9	85.0	90.0	93.1	94.5	94.4	1.116	1.099	1.084	
3	SJ	0.444	0.446	0.442	0.459	0.461	0.451	98.3	106.9	105.8	88.5	88.9	90.6	1.020	1.020	1.023	
4	SJ	0.406	0.425	0.418	0.452	0.468	0.453	89.5	92.0	94.3	93.3	93.3	93.0	1.084	1.082	1.088	
5	SJ	0.380	0.391	0.382	0.399	0.410	0.406	90.7	89.0	89.5	85.2	85.0	85.6	1.044	1.038	1.076	
6	RJ	0.400	0.404	0.413	0.417	0.428	0.422	81.6	83.8	78.6	76.8	80.0	81.5	1.005	1.055	1.012	
7	RJ	0.347	0.369	0.364	0.366	0.366	0.377	90.3	87.8	93.2	90.1	91.3	90.2	1.071	0.986	1.027	
8	RJ	0.367	0.379	0.373	0.434	0.400	0.398	81.3	78.4	81.4	74.0	80.7	82.5	1.172	1.015	1.057	
9	RJ	0.341	0.354	0.353	0.359	0.371	0.379	85.7	84.4	82.3	88.9	89.2	87.4	1.052	1.050	1.060	
10	RJ	0.375	0.377	0.378	0.369	0.391	0.389	86.7	89.7	88.0	94.0	91.8	93.9	0.979	1.011	1.033	
Section 1: **Broken and seated**																	
1	RJ	0.281	0.297	0.298	0.302	0.306	0.306	90.2	83.5	86.8	90.0	91.0	92.0	1.063	1.022	1.023	
2	RJ	0.292	0.274	0.279	0.310	0.320	0.313	94.3	97.3	88.4	72.7	73.7	75.2	1.053	1.164	1.118	
3	RJ	0.279	0.287	0.285	0.317	0.302	0.308	71.7	87.5	83.9	77.4	83.7	83.3	1.114	1.049	1.072	
4	RJ	0.282	0.278	0.289	0.295	0.291	0.291	80.2	87.6	83.2	86.4	86.2	86.9	1.052	1.055	1.015	
5	RJ	0.346	0.353	0.358	0.380	0.385	0.387	58.9	78.4	77.1	72.2	74.2	76.2	1.094	1.086	1.052	
6	SJ	0.273	0.277	0.274	0.261	0.271	0.265	83.9	85.5	86.8	84.6	85.8	86.2	0.944	0.961	0.968	
7	SJ	0.268	0.267	0.263	0.270	0.274	0.275	70.9	85.1	92.9	85.7	86.7	86.0	1.000	1.028	1.038	
8	SJ	0.334	0.337	0.337	0.365	0.379	0.376	75.7	72.3	72.2	73.7	73.3	74.0	1.090	1.119	1.119	
9	RJ	0.272	0.282	0.276	0.280	0.290	0.284	76.3	86.7	88.2	81.6	79.5	80.5	1.020	1.024	1.041	
10	RJ	0.248	0.268	0.265	0.284	0.288	0.283	88.8	83.2	82.5	79.1	80.1	79.9	1.139	1.081	1.057	

Table C-2. FWD Test Data (20-June-2006) (1 µm/kN = 0.175 mil/kip).

Section 1: **Broken and seated**																							
28-November-2006																							
Joint		**NDf-0 (mils/kip)**									**LTE (%)**						**JSR**			**Mid-Slab SPR (%)**			
		Approach			**Leave**			**Mid-Slab**			**Approach**			**Leave**										
N°	**Type**	**Drop**			**Drop**			**Drop**			**Drop**			**Drop**			**Drop**			**Drop**			
		1	**2**	**3**	**1**	**2**	**3**	**1**	**2**	**3**	**1**	**2**	**3**	**1**	**2**	**3**	**1**	**2**	**3**	**1**	**2**	**3**	
1	RJ	0.263	0.298	0.296	0.301	0.261	0.308	0.232	0.192	0.221	91.4	83.4	85.9	80.4	92.5	78.9	1.141	0.876	1.045	66.2	81.4	73.3	
2	RJ	0.299	0.276	0.293	0.301	0.292	0.307	0.244	0.176	0.225	76.4	85.9	82.1	75.6	80.4	77.6	1.010	1.057	1.039	63.0	86.3	70.0	
3	RJ	0.269	0.246	0.266	0.288	0.288	0.304	0.227	0.211	0.230	86.4	97.4	92.0	78.9	80.7	78.3	1.070	1.175	1.149	65.6	72.2	68.8	
4	RJ	0.284	0.249	0.292	0.303	0.251	0.289	0.228	0.174	0.227	82.0	96.2	84.3	72.9	91.8	81.5	1.070	1.006	0.996	61.5	80.4	64.9	
5	RJ	0.294	0.251	0.299	0.301	0.287	0.307	0.223	0.189	0.222	70.8	85.6	74.3	67.9	73.8	71.0	1.021	1.138	1.024	61.7	73.1	65.6	
6	RJ	0.239	0.210	0.251	0.269	0.253	0.275	0.192	0.192	0.203	84.6	98.9	85.3	72.0	80.2	75.9	1.127	1.204	1.097	67.6	70.1	69.4	
7	RJ	0.261	0.254	0.274	0.278	0.268	0.280	0.214	0.190	0.224	79.7	84.6	81.6	73.1	78.0	77.8	1.052	1.052	1.024	61.8	70.3	63.6	
8	RJ	0.266	0.297	0.292	0.324	0.316	0.353	0.249	0.232	0.267	86.9	80.7	85.7	68.0	73.1	68.0	1.226	1.061	1.215	64.3	69.9	64.4	
9	RJ	0.294	0.308	0.331	0.344	0.329	0.369	0.273	0.250	0.279	82.9	83.1	81.2	69.4	76.5	70.8	1.168	1.069	1.121	63.5	70.1	65.7	
10	RJ	0.316	0.308	0.335	0.306	0.315	0.335	0.249	0.206	0.275	80.7	85.7	82.0	82.0	82.5	79.8	0.963	1.023	1.005	64.6	77.4	63.0	
11	RJ	0.298	0.256	0.311	0.236	0.277	0.316	0.239	0.174	0.269	79.6	97.5	83.9	97.3	86.6	79.8	0.789	1.087	1.014	60.3	82.1	60.1	
12	RJ	0.253	0.293	0.301	0.284	0.324	0.331	0.240	0.180	0.246	73.6	66.7	68.5	67.8	63.8	66.2	1.130	1.108	1.106	57.7	76.3	61.5	
13	RJ	0.292	0.240	0.294	0.283	0.232	0.316	0.202	0.187	0.235	75.6	95.1	81.6	77.4	98.3	74.9	0.967	0.964	1.071	66.4	73.9	63.2	
14	RJ	0.260	0.213	0.286	0.255	0.266	0.258	0.210	0.184	0.237	76.8	98.5	77.8	75.1	78.0	83.8	0.980	1.244	0.904	65.8	76.2	64.2	
15	RJ	0.280	0.225	0.261	0.278	0.280	0.289	0.225	0.190	0.202	73.6	95.4	87.0	72.5	75.9	77.7	0.989	1.244	1.104	61.0	73.1	71.6	
16	RJ	0.230	0.259	0.261	0.237	0.241	0.256	0.238	0.182	0.231	87.6	81.4	84.7	83.5	85.0	84.7	1.032	0.933	0.984	59.5	77.4	65.5	
17	RJ	0.302	0.216	0.278	0.263	0.271	0.310	0.287	0.108	0.280	59.6	89.7	75.7	68.3	70.6	67.1	0.874	1.250	1.107	53.2	129.7	59.4	
18	RJ	0.216	0.234	0.257	0.212	0.280	0.281	0.179	0.161	0.194	95.1	89.8	89.2	94.0	75.4	79.4	0.980	1.197	1.094	68.0	76.9	68.6	
19	RJ	0.248	0.215	0.247	0.238	0.239	0.267	0.194	0.174	0.202	77.8	94.8	87.4	79.0	82.8	78.2	0.957	1.118	1.090	64.2	72.9	66.9	
20	RJ	0.262	0.247	0.275	0.247	0.294	0.299	0.219	0.188	0.221	78.6	87.3	82.5	83.6	74.1	75.7	0.935	1.191	1.093	65.0	76.1	68.2	
21	RJ	0.297	0.237	0.254	0.303	0.249	0.282	0.226	0.192	0.209	69.4	91.0	89.1	65.3	85.4	78.8	1.025	1.047	1.107	63.3	75.1	72.0	
22	RJ	0.248	0.218	0.260	0.244	0.212	0.276	0.236	0.217	0.233	82.0	98.6	86.7	83.0	99.6	80.6	0.987	0.971	1.064	61.4	67.9	65.6	
23	RJ	0.249	0.235	0.270	0.267	0.241	0.250	0.204	0.194	0.197	76.8	86.5	79.5	71.9	84.0	86.5	1.069	1.034	0.927	65.0	70.6	72.5	
24	RJ	0.270	0.243	0.250	0.288	0.218	0.252	0.238	0.160	0.238	76.0	89.8	91.5	69.4	98.9	88.7	1.067	0.898	1.007	61.7	89.3	65.8	
25	RJ	0.235	0.232	0.238	0.282	0.239	0.266	0.219	0.251	0.226	89.6	94.9	97.0	73.4	90.1	84.9	1.203	1.031	1.121	70.8	64.4	72.0	
26	RJ	0.257	0.222	0.237	0.244	0.253	0.260	0.228	0.198	0.193	74.4	90.7	89.2	77.0	78.1	80.3	0.950	1.143	1.101	62.3	71.9	75.4	
27	RJ	0.209	0.181	0.205	0.254	0.219	0.211	0.233	0.124	0.242	91.4	110.9	102.3	74.1	88.8	97.2	1.207	1.210	1.023	57.1	101.7	60.7	
28	RJ	0.270	0.232	0.261	0.306	0.229	0.287	0.285	0.261	0.230	75.0	92.5	87.8	65.6	94.8	80.0	1.125	0.983	1.097	54.4	60.7	69.8	
29	RJ	0.239	0.269	0.272	0.245	0.255	0.271				77.0	73.4	76.8	75.1	77.0	75.6	1.032	0.946	0.998				
30	SJ	0.288	0.220	0.258	0.275	0.219	0.253	0.249	0.202	0.210	71.6	97.8	87.0	72.8	95.6	85.6	0.959	0.996	0.988	61.0	74.0	73.3	
31	SJ	0.263	0.223	0.263	0.292	0.221	0.223	0.227	0.198	0.213	74.6	92.5	82.6	64.9	90.6	94.1	1.113	0.989	0.851	61.2	73.3	71.1	
32	SJ	0.308	0.250	0.290	0.295	0.235	0.287	0.205	0.229	0.237	68.4	88.3	80.2	69.8	91.6	79.7	0.966	0.943	0.985	69.0	64.1	64.7	
33	SJ	0.260	0.249	0.288	0.284	0.231	0.245	0.255	0.229	0.252	77.6	85.1	77.4	67.9	86.5	88.5	1.094	0.935	0.851	58.5	65.8	63.0	
34	RJ	0.265	0.217	0.227	0.231	0.250	0.249	0.230	0.185	0.211	58.8	76.8	78.8	65.8	64.1	69.7	0.876	1.158	1.107	56.8	69.6	64.6	
35	RJ	0.294	0.258	0.254	0.316	0.270	0.286	0.185	0.116	0.168	66.4	78.6	83.0	61.1	74.3	72.9	1.076	1.046	1.116	55.4	85.8	66.2	
36	RJ	0.252	0.216	0.215	0.285	0.246	0.268				74.5	89.8	95.5	69.5	82.6	79.5	1.126	1.135	1.248				
37	RJ	0.231	0.194	0.211	0.235	0.187	0.221	0.306	0.247	0.265	73.6	90.7	87.6	71.3	93.7	83.2	1.014	0.967	1.042	56.2	67.9	65.6	
38	RJ	0.252	0.224	0.244	0.233	0.227	0.257	0.213	0.226	0.211	69.5	82.8	80.5	75.0	79.6	74.5	0.921	1.014	1.051	69.3	66.9	74.1	
39	RJ	0.262	0.197	0.247	0.234	0.206	0.246	0.266	0.211	0.265	73.0	101.2	84.8	78.7	93.5	82.1	0.891	1.044	1.002	60.2	75.7	65.3	
40	RJ	0.212	0.216	0.209	0.220	0.181	0.231	0.284	0.216	0.225	76.6	80.7	88.5	74.2	94.3	78.8	1.040	0.839	1.109	59.3	78.1	77.3	

Section 1: **Broken and seated**																					
28-November-2006																					
Joint		**NDf-0 (mils/kip)**									**LTE (%)**						**JSR**			**Mid-Slab SPR (%)**		
		Approach			**Leave**			**Mid-Slab**			**Approach**			**Leave**								
N°	**Type**	**Drop**			**Drop**			**Drop**			**Drop**			**Drop**			**Drop**			**Drop**		
		1	**2**	**3**	**1**	**2**	**3**	**1**	**2**	**3**	**1**	**2**	**3**	**1**	**2**	**3**	**1**	**2**	**3**	**1**	**2**	**3**
41	RJ	0.271	0.224	0.271	0.250	0.265	0.254	0.251	0.180	0.250	72.3	91.5	79.3	77.5	76.1	82.7	0.922	1.184	0.940	61.6	83.9	65.3
42	RJ	0.259	0.242	0.250	0.257	0.223	0.250	0.249	0.217	0.249	74.8	84.0	86.2	73.8	88.7	84.6	0.992	0.925	1.005	60.9	69.8	64.3
43	RJ	0.249	0.244	0.263	0.302	0.244	0.315	0.233	0.257	0.283	83.0	88.0	87.6	68.3	89.6	73.8	1.221	0.994	1.196	68.7	65.8	63.0
44	RJ	0.260	0.236	0.258	0.322	0.265	0.261	0.281	0.243	0.255	78.9	91.6	90.0	63.6	81.3	88.9	1.240	1.114	1.000	59.7	69.6	69.9
45	RJ	0.212	0.408	0.288	0.264	0.266	0.306	0.297	0.279	0.301	97.0	53.6	81.2	74.7	80.2	74.4	1.245	0.658	1.062	64.1	68.8	66.6
46	RJ	0.328	0.297	0.322	0.305	0.279	0.306	0.260	0.247	0.260	63.0	72.3	71.7	66.6	76.7	75.2	0.923	0.936	0.946	63.4	66.3	65.2
47	RJ	0.237	0.229	0.239	0.251	0.251	0.251	0.300	0.270	0.277	80.8	87.2	88.6	75.1	80.4	85.1	1.058	1.093	1.048	59.6	65.2	64.8
48	RJ	0.220	0.239	0.249	0.219	0.198	0.322				82.1	78.7	80.5	80.2	93.2	60.3	1.000	0.833	1.307			

Table C-3. FWD Test Data (B&S Section, 28-Novemeber-2006) (1 µm/kN = 0.175 mil/kip).

Section 2: **Rubblized**																					
28-November-2006																					
Joint		**NDf-0 (mils/kip)**									**LTE (%)**						**JSR**			**Mid-Slab SPR (%)**		
		Approach			**Leave**			**Mid-Slab**			**Approach**			**Leave**								
N°	**Type**	**Drop**			**Drop**			**Drop**			**Drop**			**Drop**			**Drop**			**Drop**		
		1	**2**	**3**	**1**	**2**	**3**	**1**	**2**	**3**	**1**	**2**	**3**	**1**	**2**	**3**	**1**	**2**	**3**	**1**	**2**	**3**
1	RJ	0.267	0.276	0.292	0.275	0.288	0.304	0.312	0.311	0.316	76.9	78.2	79.1	72.6	73.4	74.3	1.031	1.046	1.037	65.5	65.7	65.8
2	RJ	0.294	0.307	0.323	0.306	0.320	0.332	0.320	0.319	0.322	81.9	82.5	83.5	77.7	79.0	79.1	1.035	1.041	1.040	62.4	62.9	63.8
3	RJ	0.316	0.331	0.348	0.324	0.335	0.346	0.285	0.285	0.291	67.3	66.9	69.0	69.3	72.0	73.2	1.020	1.012	0.995	62.0	62.9	63.4
4	SJ	0.303	0.313	0.325	0.307	0.317	0.328	0.314	0.317	0.319	81.2	81.7	82.7	76.6	78.0	78.7	1.014	1.015	1.011	62.7	63.1	63.7
5	SJ	0.290	0.301	0.314	0.283	0.294	0.306	0.284	0.288	0.297	76.4	77.8	79.0	75.6	76.7	78.4	0.982	0.977	0.964	64.9	65.4	65.6
6	SJ	0.306	0.313	0.328	0.301	0.314	0.328	0.233	0.239	0.248	74.3	76.5	76.9	72.6	73.5	75.0	0.976	0.995	0.998	62.2	63.0	63.4
7	SJ	0.267	0.281	0.291	0.288	0.297	0.312	0.242	0.247	0.258	82.1	79.9	81.9	72.3	74.5	75.7	1.075	1.051	1.054	61.4	62.0	62.4
8	SJ	0.302	0.316	0.330	0.285	0.297	0.308	0.258	0.266	0.272	70.1	69.8	72.5	72.1	73.0	74.8	0.947	0.940	0.945	61.5	61.7	62.7
9	RJ	0.267	0.280	0.294	0.276	0.285	0.296	0.281	0.280	0.282	73.9	74.1	76.1	69.6	71.4	72.1	1.028	1.014	1.010	65.0	65.6	65.5
10	RJ	0.248	0.260	0.267	0.262	0.268	0.282	0.282	0.282	0.284	82.0	81.2	83.2	75.2	77.1	77.1	1.073	1.033	1.056	61.0	60.8	61.6
11	RJ	0.252	0.261	0.269	0.270	0.279	0.288	0.243	0.239	0.251	77.6	77.6	78.9	70.9	72.4	73.6	1.072	1.063	1.057	60.9	63.3	62.6
12	RJ	0.237	0.244	0.255	0.259	0.265	0.275	0.252	0.258	0.265	79.4	80.3	81.5	71.6	73.2	74.2	1.090	1.087	1.082	60.0	60.5	61.1
13	RJ	0.269	0.278	0.291	0.282	0.288	0.301	0.263	0.270	0.276	76.7	78.1	79.5	71.3	74.1	75.0	1.047	1.031	1.041	62.5	62.7	63.7
14	RJ	0.315	0.323	0.335	0.322	0.331	0.341	0.322	0.321	0.323	69.3	71.7	73.9	64.0	65.7	67.5	1.024	1.027	1.027	64.1	64.8	65.0
15	RJ	0.304	0.314	0.327	0.323	0.331	0.339	0.251	0.260	0.269	76.3	77.3	78.4	72.0	73.1	74.5	1.059	1.053	1.044	65.4	64.6	65.3
16	RJ	0.277	0.288	0.300	0.280	0.290	0.302	0.300	0.305	0.306	79.6	78.8	79.8	76.0	76.2	76.8	1.012	1.008	1.010	64.4	64.2	64.6
17	RJ	0.278	0.287	0.299	0.273	0.284	0.300	0.245	0.248	0.255	75.1	77.2	78.7	74.1	75.1	75.9	0.992	0.994	1.006	61.1	62.0	62.6
18	RJ	0.253	0.265	0.278	0.268	0.278	0.292	0.276	0.279	0.285	80.3	80.8	81.8	75.8	76.3	76.1	1.054	1.051	1.061	61.9	62.1	62.7

Table C-4. FWD Test Data (Rubblized Section, 28-Novemeber-2006) (1 µm/kN = 0.175 mil/kip).

Section 3: **Untreated**																							
28-November-2006																							
Joint		**NDf-0 (mils/kip)**									**LTE (%)**						**JSR**			**Mid-Slab SPR (%)**			
		Approach			**Leave**			**Mid-Slab**			**Approach**			**Leave**									
N°	**Type**	**Drop**			**Drop**			**Drop**			**Drop**			**Drop**			**Drop**			**Drop**			
		1	**2**	**3**	**1**	**2**	**3**	**1**	**2**	**3**	**1**	**2**	**3**	**1**	**2**	**3**	**1**	**2**	**3**	**1**	**2**	**3**	
1	RJ	0.283	0.296	0.283	0.274	0.283	0.279	0.188	0.202	0.204	83.8	85.8	85.1	84.8	84.4	84.9	0.966	0.964	0.973	66.9	66.2	66.4	
2	RJ	0.249	0.255	0.251	0.246	0.254	0.248	0.169	0.176	0.185	84.4	84.7	85.5	83.0	83.5	84.4	0.996	1.003	0.991	68.2	68.6	68.2	
3	RJ	0.245	0.250	0.247	0.232	0.241	0.240	0.176	0.185	0.189	80.2	82.1	83.1	82.4	83.3	84.4	0.952	0.974	0.976	67.3	67.0	66.6	
4	RJ	0.252	0.258	0.254	0.258	0.264	0.264	0.191	0.200	0.201	78.7	79.9	81.3	73.3	75.8	76.4	1.021	1.022	1.028	65.5	64.9	65.2	
5	RJ	0.254	0.259	0.257	0.246	0.253	0.254	0.186	0.192	0.198	81.7	81.1	82.4	80.5	81.1	81.6	0.983	0.984	0.981	65.6	65.6	66.2	
6	RJ	0.227	0.231	0.237	0.233	0.240	0.242	0.163	0.175	0.183	76.3	77.2	78.6	73.6	73.9	75.9	1.024	1.035	1.023	69.1	68.6	69.1	
7	RJ	0.248	0.253	0.252	0.259	0.266	0.268	0.179	0.186	0.193	81.0	82.7	82.5	75.4	75.0	76.8	1.056	1.064	1.047	68.0	68.2	68.1	
8	RJ	0.221	0.230	0.235	0.228	0.235	0.242	0.166	0.172	0.181	77.0	76.8	78.4	74.5	75.1	76.3	1.033	1.028	1.031	69.8	68.9	68.0	
9	RJ	0.247	0.253	0.257	0.241	0.249	0.253	0.169	0.178	0.186	75.5	76.4	78.2	74.9	75.4	76.8	0.991	0.997	0.991	67.6	67.9	68.2	
10	RJ	0.221	0.228	0.237	0.239	0.245	0.252	0.163	0.171	0.180	84.0	84.5	85.8	78.9	79.1	80.4	1.071	1.072	1.063	68.4	68.3	68.4	
11	RJ	0.225	0.232	0.238	0.227	0.235	0.240	0.162	0.170	0.178	76.1	77.0	78.4	72.9	74.1	74.2	1.005	1.007	1.008	69.0	67.9	67.6	
12	RJ	0.214	0.223	0.228	0.214	0.221	0.225	0.174	0.179	0.185	75.0	74.6	75.9	75.9	75.1	77.2	0.995	0.993	0.990	66.5	66.7	66.4	
13	RJ	0.234	0.253	0.246	0.233	0.240	0.245	0.193	0.201	0.207	73.4	71.2	75.7	71.6	72.8	74.9	1.000	0.955	0.988	62.1	62.8	63.3	
14	RJ	0.276	0.282	0.288	0.256	0.269	0.270	0.168	0.180	0.185	74.8	74.9	76.5	77.3	75.7	79.1	0.922	0.949	0.939	63.9	63.8	64.8	
15	RJ	0.218	0.227	0.235	0.230	0.240	0.244	0.183	0.191	0.197	74.4	75.2	76.5	71.2	71.0	73.5	1.058	1.049	1.034	64.4	64.4	66.0	
16	RJ	0.228	0.241	0.240	0.219	0.233	0.239	0.162	0.166	0.175	72.6	70.9	74.0	70.8	70.3	72.0	0.986	0.990	1.000	63.1	64.7	64.4	
17	RJ	0.187	0.193	0.200	0.203	0.208	0.213	0.168	0.181	0.186	82.6	82.9	83.6	75.6	75.5	77.2	1.084	1.077	1.075	64.6	63.7	65.1	
18	RJ	0.236	0.244	0.251	0.215	0.223	0.231	0.175	0.197	0.202	62.1	63.7	66.2	63.7	64.4	66.9	0.911	0.918	0.927	67.9	64.9	66.3	
19	RJ	0.237	0.250	0.248	0.221	0.231	0.232	0.195	0.215	0.213	69.4	69.6	72.4	73.4	74.2	75.3	0.932	0.925	0.937	63.9	61.5	65.5	
20	RJ	0.228	0.239	0.243	0.223	0.238	0.238	0.196	0.207	0.219	75.6	75.3	77.6	75.6	74.7	77.7	0.981	1.000	0.982	64.0	63.9	64.4	
21	RJ	0.259	0.272	0.279	0.256	0.266	0.275	0.196	0.208	0.216	70.0	70.9	74.7	69.7	71.6	73.8	0.992	0.982	0.991	66.2	65.9	66.9	
22	RJ	0.256	0.265	0.268	0.242	0.253	0.256	0.176	0.188	0.198	70.1	70.9	72.7	74.6	74.9	77.1	0.946	0.955	0.955	64.6	64.8	65.1	
23	RJ	0.219	0.230	0.241	0.215	0.224	0.231	0.174	0.183	0.190	70.5	70.8	71.5	74.3	74.4	76.3	0.976	0.976	0.955	66.1	66.3	66.5	
24	RJ	0.232	0.241	0.247	0.217	0.227	0.235	0.178	0.193	0.197	72.9	72.2	74.6	76.0	77.1	77.9	0.936	0.940	0.948	64.0	62.1	63.8	
25	RJ	0.222	0.231	0.237	0.205	0.213	0.221	0.185	0.192	0.199	76.2	75.6	77.9	80.9	81.6	82.3	0.924	0.918	0.931	63.0	63.5	63.6	
26	RJ	0.207	0.216	0.225	0.213	0.224	0.233	0.168	0.182	0.183	75.9	76.6	77.4	72.6	73.1	74.2	1.031	1.037	1.033	65.2	63.3	66.3	
27	RJ	0.209	0.218	0.227	0.216	0.220	0.230	0.175	0.189	0.197	79.3	79.9	80.9	77.2	79.1	78.8	1.020	1.000	1.013	65.7	63.2	64.5	
28	RJ	0.219	0.228	0.240	0.217	0.231	0.243	0.191	0.200	0.204	69.1	69.3	71.0	67.2	65.9	67.6	0.986	1.010	1.013	60.9	61.4	62.8	
29	RJ	0.216	0.226	0.226	0.220	0.228	0.234	0.169	0.181	0.188	78.7	79.1	82.0	75.5	76.3	77.7	1.030	1.018	1.027	62.9	61.8	63.2	
30	RJ	0.207	0.220	0.224	0.212	0.219	0.224	0.162	0.167	0.173	68.6	68.2	71.5	65.0	65.0	66.8	1.031	1.000	1.008	62.3	63.7	63.9	
31	RJ	0.205	0.214	0.224	0.202	0.210	0.221	0.167	0.175	0.183	74.6	75.2	77.4	73.3	74.6	76.2	0.990	0.978	0.992	63.4	63.4	64.1	
32	RJ	0.224	0.229	0.239	0.197	0.208	0.215	0.169	0.178	0.188	62.2	64.4	66.7	66.8	67.2	69.3	0.880	0.912	0.903	64.9	64.9	65.4	
33	RJ	0.189	0.201	0.208	0.194	0.203	0.213	0.162	0.174	0.178	78.7	77.6	79.8	74.2	75.4	76.1	1.022	1.008	1.018	62.3	62.1	63.2	
34	RJ	0.184	0.194	0.197	0.192	0.196	0.207	0.153	0.158	0.171	76.7	76.2	79.0	71.8	73.3	73.9	1.052	1.033	1.052	66.4	67.5	67.0	
35	RJ	0.181	0.188	0.196	0.187	0.192	0.199	0.150	0.159	0.163	78.4	79.5	80.8	72.7	74.1	76.0	1.029	1.017	1.012	62.7	63.4	63.6	
36	RJ	0.190	0.196	0.203	0.191	0.198	0.205	0.160	0.165	0.171	71.9	72.6	74.5	68.7	69.6	71.5	1.006	1.008	1.009	63.8	64.4	65.5	
37	RJ	0.193	0.200	0.207	0.203	0.203	0.212	0.162	0.174	0.180	72.9	73.5	75.1	66.8	69.4	156.9	1.050	1.012	1.027	66.5	65.6	67.5	

Section 3: **Untreated**																						
28-November-2006																						
Joint		**NDf-0 (mils/kip)**									**LTE (%)**						**JSR**			**Mid-Slab SPR (%)**		
		Approach			**Leave**			**Mid-Slab**			**Approach**			**Leave**								
N°	**Type**	**Drop**			**Drop**			**Drop**			**Drop**			**Drop**			**Drop**			**Drop**		
		1	**2**	**3**	**1**	**2**	**3**	**1**	**2**	**3**	**1**	**2**	**3**	**1**	**2**	**3**	**1**	**2**	**3**	**1**	**2**	**3**
38	RJ	0.199	0.210	0.217	0.192	0.198	0.203	0.183	0.188	0.195	71.9	71.0	73.2	71.9	72.1	74.6	0.962	0.942	0.932	62.5	62.0	61.8
39	RJ	0.191	0.201	0.204	0.192	0.199	0.206	0.187	0.196	0.207	78.0	77.7	78.7	75.8	75.6	76.7	1.006	0.996	1.003	64.4	64.1	64.6
40	RJ	0.201	0.208	0.218	0.197	0.203	0.212	0.198	0.204	0.211	75.0	74.7	76.0	73.0	73.7	75.1	0.984	0.977	0.972	60.5	61.5	62.3
41	RJ	0.184	0.190	0.200	0.196	0.204	0.210	0.204	0.203	0.213	75.4	75.9	77.8	70.3	69.9	71.0	1.057	1.075	1.057	68.4	69.6	69.0
42	RJ	0.205	0.210	0.219	0.196	0.203	0.212	0.165	0.166	0.174	74.4	76.3	77.8	77.4	77.8	79.2	0.954	0.966	0.975	61.7	62.7	62.9
43	RJ	0.202	0.211	0.216	0.207	0.212	0.217	0.197	0.201	0.206	71.2	70.9	73.2	67.5	68.0	69.3	1.016	1.004	1.008	64.8	66.0	66.3
44	RJ	0.194	0.202	0.211	0.194	0.200	0.207	0.191	0.194	0.197	76.9	76.7	79.1	75.3	76.3	78.5	1.000	1.000	1.000	63.3	63.0	64.0
45	RJ	0.182	0.176	0.186	0.184	0.191	0.194	0.198	0.193	0.193	73.7	76.8	76.5	68.8	69.9	71.9	1.012	1.086	1.042	60.3	61.7	62.6
46	RJ	0.185	0.194	0.203	0.175	0.179	0.189	0.186	0.188	0.192	69.1	70.0	71.6	73.3	74.2	74.4	0.943	0.926	0.937	60.9	61.7	62.0
47	RJ	0.173	0.182	0.189	0.181	0.188	0.194	0.202	0.202	0.206	72.6	73.0	73.8	66.5	66.8	69.0	1.037	1.022	1.019	61.1	62.6	62.6
48	RJ	0.182	0.187	0.194	0.191	0.194	0.205	0.211	0.216	0.212	75.4	75.8	76.5	70.6	71.6	100.3	1.035	1.030	1.043	58.5	58.4	60.0
49	RJ	0.177	0.189	0.193	0.164	0.177	0.184	0.210	0.213	0.214	71.1	70.0	72.2	72.9	71.9	73.8	0.934	0.933	0.954	61.8	60.8	61.6
50	RJ	0.200	0.203	0.212	0.204	0.211	0.216	0.185	0.188	0.192	72.7	74.6	74.4	69.3	70.7	72.3	1.027	1.039	1.025	63.3	63.6	63.9
51	RJ	0.193	0.200	0.210	0.192	0.199	0.207	0.204	0.209	0.215	76.0	76.1	76.8	74.2	75.1	76.9	0.995	0.992	0.977	65.6	65.2	65.2
52	RJ	0.261	0.270	0.275	0.213	0.223	0.231	0.178	0.185	0.191	59.5	60.1	61.7	68.2	68.5	69.2	0.818	0.834	0.840	62.9	62.7	63.2
53	RJ	0.199	0.207	0.215	0.190	0.206	0.209	0.182	0.186	0.199	79.9	80.7	82.0	79.0	78.3	79.8	0.957	0.996	0.977	63.8	65.5	65.5
54	RJ	0.207	0.217	0.227	0.207	0.213	0.222	0.179	0.176	0.182	70.1	69.6	71.1	64.4	64.9	65.2	1.000	0.981	0.978	61.9	63.6	63.7
55	RJ	0.175	0.177	0.188	0.190	0.197	0.205	0.185	0.189	0.198	80.5	82.8	82.7	73.0	72.5	73.9	1.085	1.104	1.088	63.6	64.6	64.7
56	RJ	0.171	0.176	0.185	0.175	0.177	0.186	0.182	0.186	0.193	77.4	78.5	80.1	76.1	77.6	76.9	1.025	1.000	1.003	64.6	64.6	64.6
57	RJ	0.203	0.215	0.223	0.210	0.215	0.226	0.169	0.178	0.187	77.2	77.0	78.5	73.3	75.2	76.3	1.032	1.004	1.014	64.5	64.7	64.8
58	RJ	0.185	0.193	0.202	0.193	0.204	0.216	0.200	0.217	0.227	83.9	85.8	86.7	77.3	76.8	77.4	1.040	1.063	1.057	58.9	58.1	59.2
59	RJ	0.273	0.294	0.306	0.249	0.268	0.283	0.186	0.194	0.203	49.6	48.9	48.5	63.8	63.8	63.3	0.913	0.912	0.928	63.9	65.0	65.3
60	RJ	0.201	0.210	0.219	0.202	0.209	0.220				80.2	81.5	82.6	77.9	79.6	79.9	1.016	1.004	1.006			
61	SJ	0.202	0.211	0.217	0.192	0.199	0.207	0.201	0.199	0.208	71.4	70.8	72.6	75.4	72.4	72.6	0.947	0.946	0.958	60.0	61.1	60.5
62	SJ	0.186	0.189	0.197	0.194	0.200	0.202	0.159	0.167	0.168	76.4	79.6	79.8	71.3	74.0	75.8	1.040	1.047	1.028	63.4	62.6	63.6
63	SJ	0.190	0.198	0.198	0.189	0.193	0.198	0.177	0.181	0.187	73.9	74.1	75.2	73.4	72.4	73.4	1.006	0.984	0.991	65.0	64.7	64.1
64	SJ	0.183	0.187	0.193	0.176	0.182	0.188	0.197	0.201	0.209	73.7	73.0	75.2	72.1	73.5	73.5	0.965	0.983	0.981	60.6	60.4	60.3
65	SJ	0.169	0.177	0.183	0.159	0.168	0.174	0.189	0.192	0.194	79.0	78.3	78.3	79.1	78.6	78.4	0.943	0.949	0.943	60.3	59.9	59.7

Table C-5. FWD Test Data (Untreated Section, 28-Novemeber-2006) (1 µm/kN = 0.175 mil/kip).

Section 1: **Broken and seated**																						
20-March-2007																						
Joint		**NDf-0 (mils/kip)**									**LTE (%)**						**JSR**			**Mid-Slab SPR (%)**		
		Approach			**Leave**			**Mid-Slab**			**Approach**			**Leave**								
N°	**Type**	**Drop**			**Drop**			**Drop**			**Drop**			**Drop**			**Drop**			**Drop**		
		1	**2**	**3**	**1**	**2**	**3**	**1**	**2**	**3**	**1**	**2**	**3**	**1**	**2**	**3**	**1**	**2**	**3**	**1**	**2**	**3**
1	RJ	0.306	0.319	0.326	0.361	0.373	0.378	0.782	0.799	0.803	80.5	81.8	82.3	69.6	71.5	72.9	1.169	1.151	1.147	76.1	76.3	76.6
2	RJ	0.392	0.399	0.404	0.390	0.400	0.406	0.594	0.607	0.614	70.3	72.0	73.1	66.3	67.6	68.5	0.990	1.002	1.002	65.8	66.0	66.3
3	RJ	0.289	0.299	0.308	0.336	0.345	0.351	0.520	0.524	0.518	84.3	85.6	86.1	74.4	75.5	75.7	1.157	1.151	1.141	67.4	67.2	67.4
4	RJ	0.364	0.372	0.379	0.385	0.395	0.403	0.725	0.733	0.736	72.8	74.2	74.7	69.0	71.0	71.8	1.058	1.062	1.058	68.3	68.4	68.4
5	RJ	0.380	0.392	0.399	0.408	0.416	0.422	0.737	0.745	0.748	75.5	77.0	77.6	72.4	73.8	74.3	1.070	1.060	1.058	69.7	69.9	69.9
6	RJ	0.264	0.279	0.290	0.288	0.297	0.302	0.354	0.365	0.371	77.9	78.2	79.0	71.0	72.5	73.4	1.080	1.063	1.048	66.6	66.8	66.8
7	RJ	0.260	0.268	0.273	0.293	0.299	0.303	0.571	0.573	0.576	82.6	83.4	83.8	73.0	74.9	75.2	1.120	1.109	1.102	69.8	69.7	69.8
8	RJ	0.364	0.374	0.382	0.384	0.396	0.404	0.723	0.737	0.742	71.1	73.0	73.6	67.0	67.6	68.2	1.053	1.062	1.061	75.8	76.0	76.2
9	RJ	0.352	0.364	0.369	0.361	0.369	0.374	0.737	0.752	0.755	85.6	85.4	85.8	82.6	82.5	82.8	1.023	1.013	1.011	74.7	74.8	75.1
10	RJ	0.319	0.333	0.342	0.301	0.316	0.326	0.625	0.643	0.653	76.4	76.7	76.9	76.6	76.2	76.7	0.942	0.949	0.951	77.4	77.7	78.0
11	RJ	0.349	0.363	0.371	0.408	0.418	0.421	0.803	0.820	0.832	80.5	81.2	81.6	72.4	73.2	74.4	1.160	1.146	1.135	74.6	74.4	74.4
12	RJ	0.383	0.392	0.397	0.440	0.448	0.453	0.778	0.795	0.805	83.4	83.2	83.6	73.8	74.4	74.9	1.155	1.148	1.140	75.7	75.8	75.9
13	RJ	0.338	0.357	0.365	0.335	0.352	0.362	0.695	0.710	0.719	77.3	77.7	78.6	77.7	77.6	78.6	0.988	0.987	0.989	76.7	77.1	77.2
14	RJ	0.339	0.352	0.359	0.378	0.387	0.391	0.685	0.705	0.711	84.1	82.9	82.9	73.7	74.6	75.0	1.108	1.096	1.091	69.7	69.9	70.0
15	RJ	0.375	0.389	0.399	0.384	0.398	0.407	0.767	0.779	0.789	77.8	78.3	79.0	74.3	75.0	75.6	1.025	1.020	1.025	74.5	74.9	75.2
16	RJ	0.339	0.346	0.356	0.336	0.343	0.351	0.881	0.902	0.915	78.0	80.2	79.8	74.7	76.6	77.8	0.988	0.993	0.983	77.3	77.7	78.1
17	RJ	0.412	0.432	0.448	0.376	0.393	0.409	0.771	0.791	0.793	71.5	72.7	73.9	72.7	72.4	72.7	0.912	0.917	0.926	78.6	78.3	78.8
18	SJ	0.348	0.360	0.372	0.318	0.333	0.339	0.860	0.875	0.878	80.8	81.0	81.0	84.4	84.0	84.5	0.922	0.932	0.926	72.6	72.6	72.8
19	SJ	0.351	0.361	0.368	0.358	0.370	0.378	0.812	0.819	0.823	79.4	79.8	80.3	77.7	77.7	78.1	1.018	1.022	1.021	85.9	86.1	86.3
20	SJ	0.405	0.416	0.422	0.423	0.433	0.440	0.949	0.954	0.957	79.9	80.9	80.8	77.0	77.1	77.7	1.038	1.037	1.039	77.1	77.2	77.4
21	SJ	0.460	0.468	0.475	0.406	0.411	0.415	0.863	0.865	0.879	75.5	75.7	76.3	85.2	86.0	86.1	0.885	0.880	0.880	67.3	67.1	67.1
22	SJ	0.347	0.363	0.377	0.344	0.356	0.369	0.931	0.954	0.966	77.9	78.6	78.8	77.2	77.9	78.5	0.997	0.987	0.984	75.4	75.5	75.9
23	RJ	0.367	0.375	0.381	0.386	0.396	0.404	0.966	0.985	0.994	72.3	73.3	73.9	70.0	70.1	70.4	1.054	1.060	1.062	75.8	76.0	76.1
24	RJ	0.381	0.394	0.399	0.383	0.393	0.398	1.005	1.027	1.042	70.3	69.9	70.7	67.5	67.7	68.2	1.005	0.998	0.992	77.0	77.1	77.3
25	RJ	0.335	0.351	0.361	0.385	0.398	0.407	1.006	1.026	1.042	79.8	79.6	80.1	69.6	70.9	71.8	1.141	1.131	1.126	77.3	77.7	78.0
26	RJ	0.380	0.389	0.397	0.385	0.390	0.396	0.999	1.021	1.036	77.8	77.7	78.3	76.5	77.0	77.3	1.005	1.002	1.002	72.9	73.0	73.1
27	RJ	0.345	0.353	0.359	0.394	0.400	0.403	1.068	1.083	1.092	70.9	70.2	70.1	63.9	66.0	67.0	1.128	1.127	1.128	76.4	76.5	76.8
28	RJ	0.393	0.398	0.407	0.365	0.370	0.379	1.002	1.033	1.050	76.1	77.0	76.9	79.9	81.0	81.3	0.932	0.926	0.922	78.8	79.1	79.4
29	RJ	0.501	0.509	0.515	0.516	0.523	0.528	1.054	1.080	1.101	74.3	74.1	74.1	70.3	70.7	71.3	1.025	1.026	1.034	76.4	76.2	76.5
30	RJ	0.344	0.357	0.367	0.371	0.380	0.389	0.998	1.023	1.015	80.2	80.0	80.3	73.7	74.4	75.2	1.072	1.064	1.054	72.8	72.3	71.5
31	RJ	0.551	0.551	0.557	0.539	0.541	0.549	0.842	0.861	0.877	73.6	74.3	74.9	73.1	74.0	74.7	0.979	0.981	0.978	75.3	75.2	75.5
32	RJ	0.512	0.515	0.523	0.464	0.475	0.482	1.047	1.071	1.084	71.0	72.8	73.7	78.3	78.6	78.9	0.917	0.923	0.926	77.1	77.2	77.6
33	RJ	0.428	0.439	0.447	0.408	0.423	0.435	0.936	0.955	0.967	74.5	74.9	75.4	77.7	77.7	77.9	0.959	0.961	0.966	76.5	76.5	76.8

Table C-6. FWD Test Data (B&S Section, 20-March-2007) (1 µm/kN = 0.175 mil/kip).

Section 2: **Rubblized**																							
20-March-2007																							
Joint		**NDf-0 (mils/kip)**									**LTE (%)**						**JSR**			**Mid-Slab SPR (%)**			
		Approach			**Leave**			**Mid-Slab**			**Approach**			**Leave**										
N°	**Type**	**Drop**			**Drop**			**Drop**			**Drop**			**Drop**			**Drop**			**Drop**			
		1	**2**	**3**	**1**	**2**	**3**	**1**	**2**	**3**	**1**	**2**	**3**	**1**	**2**	**3**	**1**	**2**	**3**	**1**	**2**	**3**	
1	RJ	0.401	0.403	0.396	0.441	0.440	0.435	0.290	0.298	0.299	70.8	72.3	74.4	69.2	73.2	74.6	1.106	1.091	1.096	61.0	61.8	61.9	
2	RJ	0.490	0.501	0.505	0.550	0.547	0.539	0.254	0.258	0.261	84.9	83.4	82.8	70.4	71.9	71.6	1.121	1.094	1.077	64.7	66.5	66.7	
3	SJ	0.334	0.347	0.351	0.321	0.328	0.332	0.284	0.290	0.291	81.9	81.7	81.8	82.8	84.2	84.2	0.961	0.947	0.945	62.8	63.6	63.9	
4	SJ	0.340	0.350	0.354	0.320	0.328	0.331	0.329	0.332	0.332	79.6	80.0	80.2	83.0	83.3	83.2	0.938	0.937	0.932	66.0	67.0	67.5	
5	SJ	0.617	0.614	0.604	0.628	0.609	0.590	0.240	0.250	0.254	71.1	71.2	71.2	56.7	60.0	61.1	1.022	0.995	0.982	66.6	66.6	67.3	
6	SJ	0.392	0.398	0.398	0.356	0.362	0.362	0.232	0.239	0.242	79.5	79.6	79.9	86.6	86.4	86.3	0.909	0.917	0.907	62.8	63.6	63.9	
7	SJ	0.410	0.417	0.421	0.353	0.361	0.364	0.234	0.241	0.245	67.1	68.1	68.1	78.6	79.2	79.0	0.869	0.871	0.867	64.0	64.3	64.7	
8	RJ	0.401	0.407	0.413	0.384	0.388	0.389	0.280	0.282	0.284	67.7	69.2	70.2	69.9	69.9	70.7	0.957	0.955	0.948	69.9	70.3	70.3	
9*	RJ	0.405	0.412	0.413	0.400	0.397	0.396	0.323	0.323	0.325	79.9	80.4	80.5	79.7	80.4	80.2	0.980	0.972	0.969	61.8	62.5	62.7	
10*	RJ	0.363	0.370	0.376	0.359	0.363	0.364	0.294	0.294	0.294	71.6	71.9	71.7	71.5	72.3	72.9	0.986	0.977	0.966	61.0	61.4	61.3	
11*	RJ	0.420	0.427	0.436	0.437	0.434	0.431	0.276	0.285	0.288	80.5	79.9	79.9	72.3	73.1	74.2	1.034	1.018	0.997	61.8	62.8	63.1	
12*	RJ	0.573	0.568	0.569	0.443	0.451	0.456	0.428	0.418	0.410	57.1	60.1	61.7	80.3	80.8	81.0	0.772	0.795	0.806	67.3	67.6	67.6	
13	RJ	0.395	0.402	0.411	0.421	0.428	0.429	1.024	1.038	1.033	73.4	74.4	74.2	62.4	64.6	65.7	1.072	1.069	1.059	79.2	79.2	79.3	
14	RJ	0.542	0.548	0.551	0.392	0.410	0.407	0.191	0.196	0.196	65.6	66.4	66.7	88.4	87.7	86.3	0.731	0.762	0.748	64.7	64.9	65.3	
15	RJ	0.436	0.449	0.453	0.491	0.488	0.489	0.717	0.721	0.705	86.2	85.8	85.6	73.1	74.3	74.4	1.131	1.110	1.097	71.8	71.0	70.9	
16	RJ	0.388	0.399	0.407	0.370	0.377	0.379	0.290	0.293	0.294	73.3	73.4	73.6	72.5	72.9	73.4	0.953	0.948	0.939	66.9	67.7	67.4	
17	RJ	0.312	0.329	0.336	0.306	0.312	0.317	0.619	0.619	0.611	72.5	72.9	73.0	70.9	72.4	73.7	0.977	0.965	0.959	69.9	69.5	69.5	
18	RJ	0.370	0.380	0.381	0.379	0.385	0.386	0.486	0.494	0.495	57.4	59.4	61.1	57.1	60.6	62.4	1.025	1.006	1.008	70.7	70.8	70.8	
19	RJ	0.414	0.420	0.419	0.422	0.420	0.419	0.421	0.422	0.420	77.5	78.0	78.4	77.1	77.0	77.7	1.015	0.998	0.997	65.1	65.2	65.3	
20	RJ	0.417	0.427	0.434	0.477	0.478	0.472	0.604	0.619	0.623	81.6	81.7	81.9	76.2	77.3	77.6	1.131	1.113	1.088	70.6	71.0	71.2	
21	RJ	0.313	0.323	0.325	0.322	0.333	0.337	0.714	0.729	0.735	78.8	79.2	80.0	74.3	74.5	75.5	1.029	1.029	1.028	76.0	75.9	76.0	
22	RJ	0.438	0.442	0.437	0.411	0.416	0.419	0.561	0.561	0.564	64.8	66.0	68.6	69.3	70.4	70.5	0.941	0.935	0.952	70.5	70.8	70.8	
23	RJ	0.274	0.288	0.295	0.279	0.290	0.298	0.516	0.530	0.536	77.7	77.6	78.2	73.7	75.9	76.9	1.019	1.008	1.009	68.5	68.3	68.3	
24	RJ	0.378	0.390	0.402	0.437	0.444	0.447	0.612	0.629	0.637	83.4	83.3	83.3	74.4	74.6	74.4	1.155	1.137	1.115	74.1	74.1	74.3	
25	RJ	0.287	0.301	0.309	0.324	0.333	0.340	0.622	0.642	0.651	86.5	86.8	87.2	77.6	78.4	78.2	1.124	1.114	1.111	76.3	76.3	76.5	
26	RJ	0.298	0.309	0.316	0.299	0.309	0.317	0.614	0.634	0.639	66.9	69.0	70.1	67.7	69.7	69.8	1.003	1.008	1.004	75.5	75.3	75.5	
27	RJ	0.359	0.366	0.367	0.349	0.353	0.355	0.507	0.507	0.509	70.9	72.4	72.8	71.1	71.3	72.0	0.977	0.978	0.977	69.0	69.0	69.1	
28	RJ	0.275	0.281	0.293	0.298	0.307	0.314	0.650	0.671	0.680	78.4	80.8	81.0	72.1	73.0	74.4	1.078	1.092	1.077	78.8	78.7	79.2	
29	RJ	0.400	0.408	0.414	0.389	0.390	0.396	0.669	0.688	0.698	74.7	75.3	76.1	75.5	76.4	76.6	0.969	0.960	0.960	79.9	80.0	80.4	
30	RJ	0.550	0.550	0.556	0.549	0.538	0.530	0.702	0.724	0.729	76.6	76.7	76.9	78.2	78.0	78.1	0.989	0.980	0.963	77.7	77.7	78.0	
31	RJ	0.436	0.442	0.445	0.452	0.453	0.453	0.623	0.638	0.649	81.4	81.0	81.8	80.6	79.6	79.5	1.035	1.027	1.019	75.3	75.4	75.6	

Table C-7. FWD Test Data (Rubblized Section, 20-March-2007) (1 µm/kN = 0.175 mil/kip).

Section 3: **Untreated**																							
20-March-2007																							
Joint		**NDf-0 (mils/kip)**									**LTE (%)**						**JSR**			**Mid-Slab SPR (%)**			
		Approach			**Leave**			**Mid-Slab**			**Approach**			**Leave**										
N°	**Type**	**Drop**			**Drop**			**Drop**			**Drop**			**Drop**			**Drop**			**Drop**			
		1	**2**	**3**	**1**	**2**	**3**	**1**	**2**	**3**	**1**	**2**	**3**	**1**	**2**	**3**	**1**	**2**	**3**	**1**	**2**	**3**	
1	RJ	0.268	0.264	0.265	0.266	0.267	0.268	0.172	0.178	0.182	50.5	54.2	56.7	53.6	56.9	58.6	0.999	1.012	1.014	65.4	65.7	65.8	
2	RJ	0.199	0.204	0.207	0.222	0.227	0.230	0.184	0.193	0.199	76.5	75.8	76.1	73.1	74.5	75.2	1.117	1.110	1.110	68.3	68.4	68.7	
3	RJ	0.251	0.257	0.262	0.243	0.248	0.253	0.158	0.167	0.173	52.8	51.1	50.9	65.5	67.2	68.4	0.963	0.968	0.971	67.8	67.7	67.5	
4	RJ	0.225	0.230	0.235	0.239	0.239	0.242	0.176	0.182	0.187	74.7	75.8	76.4	69.1	70.6	71.6	1.059	1.039	1.034	66.9	67.4	67.7	
5	RJ	0.233	0.240	0.246	0.237	0.241	0.245	0.203	0.206	0.208	60.9	61.2	61.8	57.8	60.9	62.5	1.018	1.001	0.992	59.7	60.9	61.5	
6	RJ	0.193	0.199	0.203	0.248	0.255	0.259	0.216	0.219	0.222	82.5	82.1	82.4	65.0	66.4	67.1	1.284	1.274	1.274	61.4	62.3	62.6	
7	RJ	0.191	0.193	0.193	0.208	0.212	0.215	0.182	0.184	0.186	68.4	69.4	70.7	63.0	65.1	65.1	1.090	1.098	1.119	63.9	65.0	65.4	
8	RJ	0.175	0.178	0.180	0.181	0.184	0.186	0.196	0.197	0.198	80.8	81.2	81.6	77.7	77.9	79.0	1.032	1.036	1.032	59.2	60.1	61.0	
9	RJ	0.178	0.184	0.188	0.203	0.210	0.215	0.176	0.178	0.180	82.2	81.8	82.1	70.1	71.7	71.7	1.141	1.136	1.134	63.3	64.4	65.1	
10	RJ	0.181	0.185	0.190	0.190	0.195	0.197	0.223	0.224	0.223	78.9	80.0	79.6	75.5	76.1	77.1	1.050	1.056	1.038	63.0	64.1	64.9	
11	RJ	0.209	0.210	0.214	0.232	0.235	0.240	0.186	0.189	0.192	93.0	95.3	95.5	66.4	67.2	67.9	1.114	1.125	1.123	61.8	62.3	62.8	
12	RJ	0.168	0.174	0.180	0.181	0.185	0.186	0.179	0.182	0.187	83.2	82.1	81.1	72.4	74.0	74.9	1.075	1.063	1.037	67.0	68.2	68.1	
13	RJ	0.242	0.247	0.251	0.222	0.229	0.235	0.198	0.200	0.201	59.8	61.2	62.8	63.1	63.1	64.0	0.920	0.925	0.935	61.1	61.5	61.8	
14	RJ	0.200	0.205	0.211	0.215	0.220	0.224	0.211	0.218	0.223	68.3	69.6	70.8	64.1	65.8	67.0	1.071	1.067	1.061	68.2	68.0	67.9	
15	RJ	0.178	0.184	0.189	0.179	0.186	0.191	0.207	0.211	0.210	77.3	78.2	79.0	74.9	75.2	75.4	1.006	1.008	1.013	63.8	64.1	65.2	
16	RJ	0.290	0.297	0.286	0.262	0.267	0.265	0.819	0.775	0.744	71.5	73.6	73.7	76.0	77.3	76.6	0.902	0.912	0.917	77.6	77.8	77.8	
17	RJ	0.339	0.343	0.331	0.285	0.291	0.290	1.090	1.114	1.116	72.8	74.8	75.9	76.2	77.4	77.5	0.844	0.857	0.872	76.4	76.4	76.5	
18	RJ	0.322	0.329	0.329	0.289	0.297	0.303	0.998	0.924	0.895	64.2	66.2	67.8	69.1	70.5	71.6	0.903	0.911	0.919	72.7	71.5	71.6	
19	RJ	0.264	0.275	0.281	0.288	0.290	0.299	0.916	0.860	0.852	73.3	74.1	75.0	65.4	67.9	68.4	1.090	1.058	1.062	69.7	69.7	69.9	
20	RJ	0.270	0.278	0.282	0.275	0.276	0.284	0.940	0.893	0.884	73.8	75.3	75.9	70.9	73.0	72.9	1.013	0.993	0.998	66.5	65.8	65.9	
21*	RJ	0.273	0.277	0.284	0.266	0.269	0.277	0.497	0.477	0.485	72.5	73.6	74.1	72.4	73.3	73.0	0.971	0.972	0.979	63.7	63.8	63.5	
22*	RJ	0.222	0.224	0.230	0.235	0.237	0.241	0.900	0.880	0.891	73.0	74.6	75.1	69.6	70.6	71.4	1.063	1.055	1.043	71.2	70.4	70.3	
23*	RJ	0.268	0.274	0.282	0.288	0.293	0.302	0.591	0.576	0.598	77.7	78.9	79.2	70.2	71.0	71.8	1.072	1.070	1.065	67.1	67.0	67.1	
24*	RJ	0.239	0.240	0.244	0.236	0.238	0.244	0.769	0.725	0.728	73.2	74.9	75.8	71.8	73.5	73.5	0.990	0.993	1.002	65.8	65.7	65.7	
25	RJ	0.226	0.232	0.240	0.227	0.228	0.237	0.723	0.687	0.695	78.0	78.7	78.9	74.3	76.1	76.7	1.006	0.985	0.982	77.1	76.8	76.9	
26	SJ	0.323	0.325	0.329	0.271	0.275	0.286	0.493	0.484	0.495	63.9	66.1	67.9	76.0	76.9	76.5	0.843	0.848	0.868	65.1	65.4	65.4	
27	SJ	0.286	0.285	0.290	0.299	0.302	0.312	0.431	0.431	0.445	81.2	83.1	83.5	78.9	79.7	78.4	1.042	1.059	1.069	64.0	64.4	64.9	
28	SJ	0.242	0.249	0.257	0.251	0.253	0.259	0.544	0.532	0.533	80.5	80.0	80.8	75.3	76.7	76.5	1.036	1.020	1.025	68.4	68.3	68.1	
29	SJ	0.224	0.229	0.235	0.204	0.213	0.220	0.535	0.520	0.516	75.4	76.9	76.8	80.0	80.1	79.4	0.913	0.936	0.941	70.3	70.1	70.1	
30	SJ	0.245	0.249	0.257	0.235	0.238	0.245	0.413	0.410	0.425	77.5	77.7	77.5	77.7	78.3	78.1	0.955	0.959	0.963	59.7	60.5	60.5	
31	RJ	0.235	0.241	0.249	0.240	0.244	0.252	0.561	0.564	0.590	76.5	77.8	78.3	74.9	75.3	75.7	1.018	1.013	1.012	70.3	70.6	70.8	
32	RJ	0.221	0.229	0.236	0.212	0.219	0.226	0.569	0.561	0.582	78.0	78.3	79.0	78.7	79.2	79.7	0.962	0.958	0.959	68.1	68.5	69.0	
33	RJ	0.248	0.259	0.267	0.233	0.243	0.251	0.549	0.536	0.543	79.5	80.0	80.5	82.8	83.7	83.0	0.940	0.939	0.940	68.0	67.9	68.0	
34	RJ	0.292	0.299	0.312	0.299	0.308	0.319	0.369	0.370	0.382	65.9	68.8	69.8	57.2	59.5	60.3	1.018	1.033	1.035	63.8	64.2	64.5	
35	RJ	0.216	0.225	0.233	0.245	0.252	0.259	0.502	0.502	0.523	83.8	85.0	86.3	71.7	74.0	75.3	1.136	1.121	1.115	68.4	68.6	68.7	

Table C-8. FWD Test Data (Untreated Section, 20-March-2007) (1 µm/kN = 0.175 mil/kip).

31-October-2007																							
Joint		NDf-0 (mils/kip)									LTE (%)						JSR			Mid-Slab SPR (%)			
		Approach			Leave			Mid-Slab			Approach			Leave									
N°	Type	Drop			Drop			Drop			Drop			Drop			Drop			Drop			
		1	2	3	1	2	3	1	2	3	1	2	3	1	2	3	1	2	3	1	2	3	
Section 1: **Broken and seated**																							
1	RJ	0.293	0.302	0.313	0.286	0.295	0.309	0.537	0.545	0.560	72.6	74.4	74.7	69.8	72.6	72.1	0.975	0.974	0.981	68.0	68.7	68.3	
2	RJ	0.234	0.246	0.254	0.259	0.273	0.281	0.486	0.489	0.487	79.1	80.3	81.2	70.4	71.9	72.4	1.111	1.108	1.101	68.3	68.4	68.4	
3	RJ	0.261	0.272	0.283	0.272	0.284	0.290	0.591	0.590	0.584	71.3	72.2	72.5	70.4	70.5	71.2	1.036	1.040	1.028	69.4	70.0	69.7	
4	RJ	0.274	0.289	0.297	0.281	0.294	0.303	0.528	0.520	0.509	71.9	71.5	72.4	70.4	71.3	71.9	1.027	1.022	1.022	67.2	66.8	67.0	
5	RJ	0.218	0.228	0.236	0.227	0.236	0.241	0.393	0.395	0.396	76.3	77.1	77.7	72.0	75.2	77.6	1.033	1.034	1.019	68.2	68.3	68.2	
6	RJ	0.223	0.226	0.232	0.226	0.231	0.235	0.400	0.391	0.386	82.3	84.5	84.2	77.3	79.0	80.0	1.005	1.017	1.017	64.9	65.4	65.5	
7	RJ	0.277	0.287	0.296	0.290	0.300	0.309	0.622	0.626	0.636	68.3	68.9	69.7	65.2	67.1	68.0	1.042	1.046	1.045	75.0	76.2	76.5	
8	RJ	0.282	0.290	0.295	0.278	0.282	0.291	0.634	0.647	0.660	77.4	77.8	77.4	75.9	77.4	77.4	0.985	0.973	0.991	72.0	72.8	73.0	
9	RJ	0.273	0.285	0.294	0.257	0.269	0.278	0.588	0.608	0.619	74.5	73.3	73.0	75.4	75.1	74.8	0.943	0.940	0.940	67.2	67.5	67.8	
10	RJ	0.269	0.281	0.293	0.299	0.309	0.316	0.633	0.643	0.644	82.1	80.7	80.4	70.6	73.7	74.3	1.125	1.103	1.090	68.3	69.0	69.0	
11	RJ	0.264	0.277	0.288	0.295	0.303	0.311	0.556	0.540	0.522	80.6	80.8	80.8	73.3	73.6	74.9	1.115	1.093	1.082	73.0	73.8	73.7	
12	RJ	0.271	0.286	0.296	0.276	0.289	0.300	0.540	0.549	0.554	82.2	80.0	80.5	76.8	77.7	77.5	1.015	1.008	1.013	70.7	71.3	71.6	
13	SJ	0.316	0.321	0.331	0.279	0.293	0.301	0.679	0.692	0.698	80.7	81.6	81.8	78.9	75.0	76.9	0.880	0.914	0.908	75.0	74.8	74.9	
14	SJ	0.256	0.264	0.271	0.271	0.281	0.288	0.687	0.662	0.632	77.0	76.9	77.1	70.0	69.5	69.6	1.058	1.059	1.055	69.0	68.3	68.2	
15	SJ	0.287	0.301	0.310	0.317	0.323	0.330	0.681	0.637	0.598	74.3	73.5	73.2	71.1	64.4	66.3	1.107	1.065	1.061	70.5	69.9	69.7	
16	SJ	0.311	0.317	0.322	0.296	0.299	0.306	0.680	0.685	0.693	71.1	72.2	73.1	74.5	76.4	77.1	0.959	0.945	0.951	68.6	68.9	68.6	
17	SJ	0.271	0.281	0.290	0.275	0.286	0.297	0.605	0.588	0.576	73.3	73.6	74.1	70.5	70.6	71.1	1.023	1.022	1.023	70.7	70.2	70.0	
Section 2: **Rubblized**																							
1	RJ	0.286	0.299	0.311	0.287	0.302	0.311	0.342	0.346	0.352	62.1	64.1	66.2	63.0	60.7	60.5	1.004	1.013	1.002	64.2	65.5	65.4	
2	RJ	0.286	0.308	0.317	0.293	0.310	0.318	0.309	0.316	0.320	76.4	77.0	78.5	72.8	75.6	75.4	1.025	1.008	1.004	61.0	61.3	62.0	
3	RJ	0.319	0.335	0.348	0.320	0.329	0.337	0.286	0.290	0.296	53.4	54.4	55.2	56.7	61.0	63.5	1.010	0.988	0.981	61.5	62.4	62.9	
4	SJ	0.331	0.344	0.359	0.337	0.344	0.357	0.336	0.342	0.346	59.1	60.9	61.8	56.5	59.7	61.1	1.013	1.000	0.996	64.8	65.3	65.7	
5	SJ	0.302	0.318	0.324	0.330	0.339	0.348	0.355	0.360	0.363	68.3	68.3	69.5	59.0	59.7	61.2	1.082	1.059	1.060	67.6	67.6	67.6	
6	SJ	0.352	0.368	0.380	0.446	0.456	0.470	0.287	0.291	0.294	104.1	103.8	104.4	70.6	73.0	72.4	1.259	1.232	1.230	64.3	64.6	65.0	
7	SJ	0.340	0.351	0.360	0.289	0.297	0.310	0.262	0.266	0.273	54.1	56.7	57.9	58.6	60.8	61.9	0.850	0.848	0.860	63.4	63.7	64.2	
8	SJ	0.371	0.384	0.396	0.335	0.341	0.353	0.351	0.356	0.357	35.8	38.4	40.3	36.9	41.7	43.2	0.908	0.895	0.902	66.8	66.2	66.0	
9	RJ	0.262	0.273	0.283	0.269	0.276	0.286	0.417	0.404	0.403	64.5	66.9	68.1	60.2	61.7	62.4	1.020	1.014	1.016	68.8	69.9	69.5	
10	RJ	0.267	0.282	0.291	0.267	0.278	0.289	0.449	0.454	0.458	75.6	76.3	77.6	70.2	71.9	72.5	1.000	0.994	1.016	67.2	67.3	67.3	
11	RJ	0.266	0.277	0.285	0.270	0.277	0.287	0.506	0.509	0.512	67.7	68.3	69.5	68.6	66.4	67.0	1.016	1.003	1.007	68.3	67.8	67.7	
12	RJ	0.248	0.260	0.268	0.251	0.263	0.270	0.349	0.347	0.351	63.4	65.0	66.0	71.4	55.7	62.1	1.013	1.006	1.007	63.9	64.8	64.8	
13	RJ	0.282	0.288	0.297	0.266	0.276	0.284	0.310	0.312	0.316	58.3	60.9	63.3	59.6	61.0	63.0	0.941	0.962	0.967	64.6	64.3	64.5	
14	RJ	0.283	0.295	0.305	0.314	0.325	0.333	0.645	0.642	0.639	68.1	71.1	71.9	60.1	53.3	59.3	1.103	1.110	1.105	68.8	68.7	68.4	
15	RJ	0.314	0.321	0.336	0.321	0.329	0.342	0.529	0.517	0.510	63.2	66.3	67.1	59.9	63.1	63.6	1.023	1.034	1.032	70.1	70.2	69.9	
16	RJ	0.271	0.282	0.291	0.284	0.289	0.298	0.517	0.515	0.517	69.9	71.0	72.2	67.0	61.1	64.5	1.054	1.031	1.034	71.3	71.7	71.5	
17	RJ	0.286	0.296	0.304	0.275	0.288	0.296	0.391	0.392	0.396	63.4	64.5	65.9	60.8	62.1	63.0	0.963	0.973	0.970	68.2	67.9	68.4	

Table C-9. FWD Test Data (B&S and Rubblized Sections, 31-October-2007) (1 µm/kN = 0.175 mil/kip).

Section 3: **Untreated**																					
31-October-2007																					
Joint		**NDf-0 (mils/kip)**									**LTE (%)**						**JSR**			**Mid-Slab SPR**		
		Approach			**Leave**			**Mid-Slab**			**Approach**			**Leave**						**(%)**		
N°	**Type**	**Drop**			**Drop**			**Drop**			**Drop**			**Drop**			**Drop**			**Drop**		
		1	**2**	**3**	**1**	**2**	**3**	**1**	**2**	**3**	**1**	**2**	**3**	**1**	**2**	**3**	**1**	**2**	**3**	**1**	**2**	**3**
1	RJ	0.402	0.404	0.398	0.319	0.323	0.326	0.200	0.212	0.215	47.7	49.8	51.3	73.3	75.1	75.8	0.795	0.804	0.817	74.0	74.1	74.3
2	RJ	0.585	0.578	0.558	0.540	0.528	0.510	0.193	0.204	0.208	28.2	30.8	32.5	26.1	27.3	28.6	0.936	0.920	0.912	71.4	70.1	70.0
3	RJ	0.322	0.329	0.325	0.333	0.336	0.333	0.176	0.189	0.193	77.3	78.2	79.2	73.9	74.2	73.6	1.042	1.022	1.016	68.5	68.2	68.6
4	RJ	0.275	0.287	0.291	0.271	0.279	0.279	0.165	0.176	0.180	62.2	63.5	63.8	64.3	62.6	60.9	0.985	0.970	0.962	67.5	66.5	66.1
5	RJ	0.326	0.334	0.335	0.313	0.316	0.318	0.162	0.173	0.179	60.2	61.0	61.5	66.0	66.7	67.6	0.959	0.946	0.945	67.2	66.3	66.9
6	RJ	0.263	0.270	0.273	0.253	0.259	0.263	0.160	0.167	0.173	73.2	74.7	74.6	73.7	74.2	73.7	0.961	0.959	0.964	65.7	66.4	66.4
7	RJ	0.300	0.301	0.302	0.284	0.287	0.289	0.165	0.174	0.180	63.5	66.0	67.1	65.0	66.7	68.2	0.945	0.951	0.952	69.9	69.9	69.9
8	RJ	0.364	0.357	0.351	0.323	0.328	0.332	0.185	0.197	0.203	53.1	57.9	59.8	65.3	67.7	68.8	0.895	0.927	0.942	65.7	66.7	67.1
9	RJ	0.394	0.410	0.418	0.367	0.374	0.379	0.181	0.190	0.196	32.8	34.0	34.9	45.9	46.2	47.3	0.924	0.910	0.902	65.3	65.3	65.5
10	RJ	0.250	0.255	0.254	0.233	0.235	0.241	0.201	0.208	0.215	71.6	73.9	74.5	73.5	73.3	72.5	0.930	0.932	0.943	65.3	65.8	66.2
11	RJ	0.259	0.269	0.273	0.249	0.256	0.261	0.179	0.189	0.194	64.8	65.7	66.7	67.4	67.9	64.7	0.957	0.959	0.959	67.2	66.9	67.0
12	SJ	0.254	0.258	0.264	0.267	0.276	0.279	0.182	0.193	0.194	57.7	59.6	59.5	51.7	51.7	53.2	1.053	1.064	1.053	61.2	61.3	62.1
13	SJ	0.231	0.241	0.249	0.218	0.232	0.237	0.168	0.176	0.178	71.4	70.8	70.2	70.4	70.6	71.1	0.951	0.961	0.949	61.8	62.8	63.7
14	SJ	0.260	0.268	0.273	0.247	0.249	0.254	0.176	0.179	0.185	55.6	56.8	57.4	55.4	56.5	56.4	0.960	0.926	0.927	64.2	66.4	66.1
15	SJ	0.213	0.223	0.226	0.232	0.237	0.239	0.192	0.196	0.201	63.3	63.8	64.9	53.7	56.0	56.0	1.097	1.071	1.065	64.6	65.3	65.7
16	SJ	0.185	0.193	0.199	0.172	0.183	0.188	0.197	0.202	0.205	76.0	75.8	76.5	71.9	76.0	69.6	0.933	0.955	0.950	61.8	62.0	61.9

Table C-10. FWD Test Data (Untreated Section, 31-October-2007) (1 µm/kN = 0.175 mil/kip).

Section 1: **Broken and seated**																					
6-May-2008																					
Joint		**NDf-0 (mils/kip)**									**LTE (%)**						**JSR**			**Mid-Slab SPR (%)**		
		Approach			**Leave**			**Mid-Slab**			**Approach**			**Leave**								
N°	**Type**	**Drop**			**Drop**			**Drop**			**Drop**			**Drop**			**Drop**			**Drop**		
		1	**2**	**3**	**1**	**2**	**3**	**1**	**2**	**3**	**1**	**2**	**3**	**1**	**2**	**3**	**1**	**2**	**3**	**1**	**2**	**3**
1	R	0.297	0.308	0.310	0.320	0.324	0.318	0.648	0.637	0.609	90.0	89.5	90.2	85.1	85.6		1.067	1.049	1.039	69.2	69.4	70.1
2	R	0.305	0.319	0.308	0.336	0.343	0.337	0.613	0.618	0.600	89.9	90.6	91.0	81.0	82.9	82.0	1.101	1.078	1.078	72.2	72.8	72.9
3	R	0.296	0.308	0.293	0.300	0.310	0.301	0.596	0.592	0.574	87.5	84.9	91.5	85.9	83.3	86.8	1.019	1.003	0.992	67.3	67.2	67.6
4	R	0.284	0.284	0.279	0.295	0.301	0.295	0.685	0.692	0.679	85.3	88.9	87.9	83.8	83.5		1.027	1.061	1.040	70.1	71.1	70.8
5	R	0.298	0.298	0.293	0.310	0.316	0.311	0.715	0.712	0.683	85.3	85.6	79.2	82.8	81.7	83.1	1.026	1.055	1.046	71.9	71.8	72.1
6	R	0.327	0.323	0.312	0.325	0.321	0.312	0.817	0.807	0.766	83.5	87.1	85.4	84.1	85.5	84.1	0.997	0.979	0.980	73.7	74.1	74.5
7	R	0.323	0.325	0.323	0.315	0.321	0.310	0.590	0.581	0.528	95.0	83.8	77.6	89.7	89.9	88.4	0.946	0.975	0.954	65.5	64.5	65.7
8	S	0.329	0.329	0.314	0.331	0.333	0.319	0.632	0.605	0.561	90.8	87.0	83.7	84.4	85.3	86.5	1.027	1.018	1.004	67.3	67.5	
9	S	0.280	0.279	0.278	0.289	0.298	0.290	0.504	0.486	0.450	85.9	88.4	95.8	84.6	85.5	83.0	1.020	1.020	1.026	66.3	67.1	67.5
10	S	0.331	0.338	0.325	0.372	0.370	0.359	0.540	0.527	0.491	98.0	87.9	95.0	83.1	81.8	81.7	1.122	1.099	1.124	68.6	67.6	
11	S	0.390	0.388	0.369	0.402	0.394	0.382	0.548	0.537	0.508	84.2	86.9	86.0	83.3	87.1	85.4	1.028	1.017	1.020	65.7	66.0	66.2
12	S	0.347	0.346	0.335	0.383	0.389	0.379	0.640	0.637	0.586	94.9	92.8	90.9	85.3	84.4	83.9	1.112	1.128	1.115	69.4	67.6	68.3
13	R	0.285	0.286	0.277	0.299	0.296	0.287				86.8	85.3	87.3	85.4	83.1	84.5	1.035	1.023	1.022			

Table C-11. FWD Test Data (B&S Section, 6-May-2008) (1 µm/kN = 0.175 mil/kip).

Section 2: **Rubblized**																							
6-May-2008																							
Joint		**NDf-0 (mils/kip)**									**LTE (%)**						**JSR**			**Mid-Slab SPR (%)**			
		Approach			**Leave**			**Mid-Slab**			**Approach**			**Leave**										
N°	**Type**	**Drop**			**Drop**			**Drop**			**Drop**			**Drop**			**Drop**			**Drop**			
		1	**2**	**3**	**1**	**2**	**3**	**1**	**2**	**3**	**1**	**2**	**3**	**1**	**2**	**3**	**1**	**2**	**3**	**1**	**2**	**3**	
1	R	0.330	0.337	0.329	0.315	0.325	0.321	0.571	0.576	0.557	68.5	72.9	72.4	80.4	79.8	79.6	0.953	0.925	0.874	62.6	62.4	62.7	
2	R	0.360	0.369	0.360	0.388	0.387	0.380	0.412	0.413	0.399	79.0	86.5	83.9	78.4	80.0	81.9	1.073	1.058	1.029	59.2	60.0	60.5	
3	R	0.313	0.326	0.316	0.339	0.347	0.339	0.411	0.405	0.391	83.2	82.9	84.2	74.5	81.2	80.8	1.082	1.061	1.075	62.4	63.0	63.5	
4	S	0.314	0.319	0.312	0.346	0.347	0.333	0.403	0.395	0.379	86.1	88.2	89.0	81.1	82.7	82.8	1.110	1.097	1.078	60.9	61.7	62.3	
5	S	0.305	0.313	0.306	0.321	0.327	0.323	0.529	0.531	0.512	89.2	89.4	89.6	83.6	85.9	84.3	1.032	1.034	1.051		59.5	60.9	
6	S	0.345	0.355	0.348	0.347	0.348	0.345	0.416	0.407	0.389	80.8	81.7	80.4	79.4	81.3	81.5	0.981	0.977	0.974	60.7	61.0	61.1	
7	S	0.339	0.343	0.332	0.342	0.334	0.334	0.469	0.467	0.452	84.2	80.9	83.0	82.8	83.5	82.2	1.017	0.993	1.029	62.9	62.3	62.1	
8	S	0.323	0.334	0.322	0.313	0.313	0.307	0.428	0.427	0.412	80.5	79.4	81.0	83.2	83.6	83.1	1.004	1.030	0.980	59.4	59.0	59.8	
9	R	0.311	0.301	0.296	0.291	0.292	0.288	0.507	0.503	0.494	76.6	84.1	82.5	86.7	84.9	82.3	0.933	0.964	0.963	60.4		62.3	
10	R	0.311	0.315	0.305	0.303	0.305	0.301	0.454	0.456	0.441	83.3	82.0	85.8	85.7	88.1	84.8	0.943	0.943	0.960	60.3	60.6	61.1	
11	R	0.290	0.295	0.292	0.307	0.309	0.309	0.482	0.482	0.470	84.3	85.2	84.8	77.7	81.1	81.3	1.022	1.039	1.034	59.5		60.0	
12	R	0.288	0.302	0.290	0.300	0.309	0.298	0.453	0.451	0.434	87.4	84.3	82.6	74.4	76.1	80.1	1.031	1.025	1.023	57.8	58.1	58.7	
13	R	0.323	0.332	0.322	0.315	0.315	0.312	0.739	0.739	0.707	71.5	71.8	76.1	76.7	81.2	79.9	0.973	0.945	0.950	70.2	70.1	70.3	
14	R	0.374	0.384	0.372	0.382	0.388	0.371	0.860	0.851	0.824	81.8	76.4	80.6	83.8	81.2	80.7	1.030	1.026	1.031	68.8	70.3	70.2	
15	R	0.345	0.351	0.341	0.365	0.371	0.359	0.780	0.771	0.744	78.8	80.4	79.2	76.2	75.7	78.2	1.068	1.050	1.027	69.6	70.1	70.1	
16	R	0.316	0.324	0.325	0.330		0.325	0.726	0.725	0.711	78.2	83.8	82.6	74.9		78.2	1.035		0.968	73.5	74.2	74.4	
17	R	0.359	0.364	0.349	0.331	0.336	0.329	0.624	0.616	0.594	70.1	73.0	70.3	75.2	77.6		0.909	0.914	0.913	71.2	72.1	71.7	
18	R	0.307	0.316	0.306	0.323	0.326	0.320	0.732	0.731	0.702	83.2	83.0	86.0	82.3	80.1	85.6	1.050	1.023	0.998	73.5	73.2	73.3	
19	R	0.341	0.334	0.323	0.342	0.347	0.339	0.637	0.628	0.607	72.3	79.0	73.3	77.0	77.0	77.2	0.984	1.020	1.008	73.5	73.9	74.0	
20	R	0.323	0.326	0.311	0.331	0.328	0.316	0.606	0.617	0.593	80.7	79.3	77.4	77.6	78.1		1.024	1.003	1.016	74.0	72.9	74.0	
21	R	0.319	0.320	0.310	0.346	0.339	0.324	0.650	0.654	0.631	74.6	75.3	76.2	71.3	70.8	74.2	1.092	1.060	1.022	73.5	73.2	73.1	
22	R	0.301	0.310	0.296	0.303	0.310	0.300	0.717	0.722	0.698	73.9	83.0	80.8	81.0	83.1	82.3	0.989	0.992	0.998	74.1		74.6	
23	R	0.334	0.341	0.324	0.342	0.345	0.335	0.625	0.636	0.604	75.3	75.1	84.0	76.8	77.9		1.033	1.015	0.996	70.9	69.6	70.4	
24	R	0.283	0.283	0.273	0.293	0.302	0.294	0.594	0.591	0.564	78.4	80.6	85.7	77.4	78.8	78.8	1.039	1.067	1.033	70.4	70.4	70.2	
25	R	0.288	0.295	0.290	0.317	0.328	0.317	0.616	0.624	0.608	77.7	77.6	78.8	72.2	74.0		1.072	1.101	1.095	75.3	75.2	75.3	

Table C-12. FWD Test Data (Rubblized Section, 6-May-2008) (1 µm/kN = 0.175 mil/kip).

Section 3: **Untreated**																							
6-May-2008																							
Joint		**NDf-0 (mils/kip)**									**LTE (%)**						**JSR**			**Mid-Slab SPR (%)**			
		Approach			**Leave**			**Mid-Slab**			**Approach**			**Leave**									
N°	**Type**	**Drop**			**Drop**			**Drop**			**Drop**			**Drop**			**Drop**			**Drop**			
		1	**2**	**3**	**1**	**2**	**3**	**1**	**2**	**3**	**1**	**2**	**3**	**1**	**2**	**3**	**1**	**2**	**3**	**1**	**2**	**3**	
1	R	0.302	0.293	0.303	0.290	0.281	0.282	0.203	0.200	0.208	48.0	53.5	53.3	60.9	67.2	69.2	0.956	0.930	0.890	67.7	71.5	70.0	
2	R	0.271	0.268	0.260	0.297	0.298	0.278	0.202	0.215	0.206	56.1	60.2	67.8	62.5	66.0	72.2	1.094	1.125	1.063	69.2	65.6	68.3	
3	R	0.294	0.292	0.303	0.302	0.315	0.314	0.203	0.208	0.209	74.2	77.8	78.1	72.0	72.4	73.0	1.027	1.074	1.058	72.0	72.1	72.5	
4	R	0.299	0.309	0.295	0.282	0.280	0.284	0.176	0.193	0.193	51.7	47.1	51.2	70.6	72.7	72.7	0.944	0.923	0.968	66.9	64.0	65.2	
5	R	0.229	0.257	0.247	0.259	0.253	0.258	0.162	0.173	0.174	49.0	50.8	50.4	61.6	66.6	68.1	1.115	0.965	1.023	67.0	67.9	69.0	
6	R	0.247	0.235	0.250	0.257	0.268	0.255	0.188	0.205	0.199	66.2	74.4	70.6	69.1	69.2	75.4	1.050	1.142	1.023	59.4	61.4	64.2	
7	R	0.233	0.247	0.245	0.238	0.227	0.233	0.210	0.218	0.218	67.0	64.3	65.3	71.4	76.8	76.1	1.038	0.925	0.969	64.6	64.8	64.0	
8	R	0.227	0.232	0.232	0.232	0.231	0.240	0.190	0.197	0.196	72.9	73.2	74.7	67.6	72.2	69.6	1.034	0.989	1.038	64.7	65.3	66.1	
9	R	0.227	0.256	0.245	0.236	0.255	0.247	0.176	0.194	0.187	60.0	52.4	57.3	74.9	70.6	74.7	1.029	0.997	0.995	69.1	60.6	68.3	
10	R	0.239	0.236	0.235	0.220	0.235	0.236	0.199	0.197	0.190	63.1	70.5	72.8	72.7	74.1	76.6	0.925	1.000	1.003	53.7	63.0	64.9	
11	R	0.219	0.238	0.245	0.234	0.239	0.237	0.191	0.200	0.204	75.0	69.2	69.0	66.7	69.9		1.056	0.990	0.947	64.8	63.9	64.0	
12	R	0.222	0.236	0.234	0.251	0.236	0.244	0.185	0.203	0.198	60.3		67.5	53.7	55.5		1.141	0.989	1.043	67.1	63.4	66.2	
13	R	0.213	0.214	0.217	0.234	0.245	0.231	0.194	0.225	0.208	71.5	73.0	71.2	66.7	67.8	72.4	1.073	1.141	1.074	68.7	61.6	64.9	
14	R	0.232	0.218	0.230	0.238	0.220	0.230	0.202	0.191	0.206	68.8	72.3	70.3	63.0	70.4		1.068	1.027	1.033	65.0	69.1	66.8	
15	R	0.234	0.244	0.240	0.244	0.243	0.249	0.189	0.194	0.197	73.2	66.6	66.9	70.0	71.5	71.6	1.053	1.028	1.044	65.6	64.3	63.6	
16	R	0.216	0.205	0.213	0.208	0.225	0.215	0.182	0.194	0.200	62.8	68.6	71.0	74.6	67.2	74.3	0.964	1.118	1.036	70.2	69.1	68.2	
17	R	0.237	0.231	0.238	0.216	0.225	0.221	0.191	0.185	0.182	63.0	65.0	66.1	75.9	70.7	76.0	0.903	0.964	0.924	46.5	62.9	63.9	
18	R	0.228	0.228	0.215	0.231	0.233	0.233	0.215	0.207	0.205	67.0	71.4	74.3	64.1	67.5	68.0	1.030	1.026	1.093	61.1	64.0	64.6	
19	R	0.209	0.224	0.219	0.234	0.248	0.240	0.214	0.216	0.213	71.1	71.6	77.5	67.8	67.0	70.3	1.128	1.136	1.127	67.0	67.3	67.8	
20	R	0.241	0.219	0.226	0.230	0.220	0.220	0.260	0.259	0.248	69.4	73.1	69.7	68.3	74.9	76.8	0.949	0.981	0.983	61.3	62.6	63.1	
21	R	0.211	0.212	0.219	0.222	0.217	0.213	0.352	0.328	0.309	72.2	80.5	78.5	71.6	77.4	79.8	1.036	1.000	0.966	62.3	64.5	64.8	
22	R	0.234	0.228	0.239	0.244	0.245	0.242	0.367	0.343	0.315	77.1	76.8	74.8	68.0	69.5	72.0	1.043	1.069	1.000	58.8	58.8	60.1	
23	R	0.212	0.205	0.206	0.204	0.222	0.226	0.470	0.419	0.380	71.4	77.7	79.5	72.3	70.2	69.9	0.958	1.073	1.076	61.5	63.3	63.5	
24	R	0.233	0.243	0.241	0.255	0.251	0.254	0.301	0.286	0.262	74.3	72.2	72.7	65.4	69.1	69.7	1.086	1.045	1.064	61.2	61.1	63.5	
25	R	0.234	0.237	0.237	0.236	0.234	0.225	0.490	0.454	0.416	70.1	72.3	71.6	64.6	68.6	71.5	1.005	0.993	0.935	61.4	63.5	62.1	
26	R	0.221	0.244	0.233	0.244	0.254	0.256	0.476	0.430	0.389	82.4	75.7	79.1	67.1	70.7	71.7	1.116	1.051	1.119	60.3	60.4	63.0	
27	R	0.213	0.212	0.200	0.207	0.216	0.212	0.465	0.412	0.365	66.7	66.0	69.8	66.7	66.0	67.4	0.969	1.000	1.040	60.2	62.0	62.1	
28	R	0.212	0.208	0.216	0.219	0.226	0.221	0.411	0.386	0.349	72.7	75.7	76.8	74.9	71.0	72.4	1.026	1.055	1.029	59.3	58.3	59.1	
29	R	0.201	0.218	0.207	0.217	0.214	0.212	0.485	0.474	0.430	68.0	69.6	72.7	65.8	68.1	68.7	1.066	0.966	0.985	62.9	61.7	61.6	
30	R	0.222	0.216	0.218	0.207	0.214	0.212	0.494	0.461	0.411	70.0	73.4	73.5	70.6	73.9	73.5	0.935	0.992	0.968	59.0	59.1	59.5	
31	R	0.217	0.221	0.220	0.233	0.236	0.226	0.547	0.523	0.466	69.7	73.9	75.2	69.2	70.7	75.9	1.082	1.087	1.051	63.1	63.0	63.4	
32	R	0.217	0.220	0.229	0.243	0.245	0.246	0.389	0.358	0.329	66.0	71.6	68.8	66.2	66.4	67.4	1.129	1.117	1.076	62.6	62.9	63.8	
33	R	0.224	0.223	0.236	0.239	0.231	0.240	0.546	0.542	0.484	79.7	79.0	75.0	71.4	76.9	75.7	1.074	1.033	1.008	61.9	61.0	61.8	
34	R	0.247	0.259	0.254	0.265	0.264	0.262	0.396	0.361	0.322	71.6	73.6	76.2	69.4	71.0	72.6	1.090	1.046	1.029	60.8	61.8	60.6	
35	R	0.227	0.236	0.239	0.210	0.217	0.228	0.553	0.547	0.509	63.7	66.5	67.7	73.6	72.9	70.1	0.905	0.907	0.940	55.5	57.1	57.7	
36	R	0.204	0.216	0.215	0.212	0.225	0.215	0.595	0.596	0.590	72.4	76.9	75.2	73.3	69.9	73.9	1.032	1.035	0.972	63.6	62.9	62.2	
37	R	0.226	0.226	0.229	0.243	0.259	0.246	0.582	0.583	0.553	80.3	80.1	80.1	69.9	68.8	72.8	1.053	1.123	1.045	63.2	62.4	62.2	
38	R	0.203	0.211	0.194	0.212	0.216	0.209	0.662	0.659	0.630	76.8	77.6	79.8	72.8	68.8	74.7	1.032	1.035	1.077	68.0	69.0	68.4	
39	R	0.271	0.276	0.268	0.272	0.278	0.271	0.538	0.509	0.465	73.3	72.8	74.4	72.0	70.0	72.4	0.996	1.027	1.000	65.7	65.9	54.5	

Section 3: **Untreated**																						
6-May-2008																						
Joint		**NDf-0 (mils/kip)**									**LTE (%)**						**JSR**			**Mid-Slab SPR**		
		Approach			**Leave**			**Mid-Slab**			**Approach**			**Leave**						**(%)**		
N°	**Type**	**Drop**			**Drop**			**Drop**			**Drop**			**Drop**			**Drop**			**Drop**		
		1	**2**	**3**	**1**	**2**	**3**	**1**	**2**	**3**	**1**	**2**	**3**	**1**	**2**	**3**	**1**	**2**	**3**	**1**	**2**	**3**
40	R	0.222	0.234	0.219	0.223	0.239	0.232				75.0	75.0	80.4	76.7	72.6	76.7	1.010	1.029	1.031			
41	R	0.206	0.210	0.214	0.221	0.227	0.227	0.498	0.497	0.484	78.6	80.9	76.8	71.4	71.1	74.2	1.064	1.066	1.055	64.7	64.8	64.9
42	R	0.252	0.255	0.253	0.262	0.277	0.271	0.597	0.592	0.583	77.5	77.5	77.9	77.5	75.1	73.9	1.040	1.058	1.077	64.4	64.7	64.9
43	R	0.228	0.233	0.233	0.240	0.243	0.243	0.623	0.612	0.597	63.1	68.6	76.3	72.4	74.6		1.039	1.025	1.029	60.5		60.5
44	R	0.224	0.224	0.218	0.233	0.237	0.239	0.661	0.651	0.631	68.9	75.8	72.3	65.9	67.0	67.2	1.024	1.044	1.056	62.5	63.0	63.6
45	R	0.223	0.238	0.229	0.231	0.227	0.226	0.644	0.654	0.641		79.6	74.6	76.0	78.0	78.2	1.030	0.958	0.978	64.1	63.6	63.4
46	R	0.212	0.213	0.209	0.220	0.234	0.228	0.675	0.689	0.663	69.7	68.1	76.3	67.3	67.7	67.1	1.036	1.096	1.058	66.1	65.6	66.1
47	R	0.220	0.220	0.215	0.218	0.213	0.217	0.600	0.592	0.566	78.4	77.4	81.3	80.5	78.0	78.6	0.980	0.974	1.023	62.6	63.6	63.5
48	R	0.209	0.217	0.209	0.227	0.229	0.229	0.549	0.542	0.526	67.4	66.3	71.8	64.2	66.2	67.7	1.074	1.042	1.062	64.7	64.7	64.7
49	R	0.212	0.210	0.212	0.227	0.221	0.220	0.213	0.223	0.216	77.1	81.4	78.7	71.2	75.2	75.6	1.068	1.051	1.038	66.0	63.9	65.4
50	R	0.237	0.244	0.237	0.235	0.238	0.233	0.674	0.676	0.637	66.2	73.9	71.3	70.3	71.1	70.6	1.024	1.000	1.003	65.8	64.9	66.0
51	R	0.232	0.241	0.242	0.234	0.238	0.231	0.683	0.689	0.659	71.6	72.4	73.2	69.0	71.7	72.7	1.009	0.973	0.972	61.8	60.7	60.7
52	R	0.223	0.229	0.225	0.235	0.230	0.231	0.724	0.723	0.702	71.3	69.2	74.9	70.4	77.5	75.1	1.054	0.989	1.028	64.9	64.7	65.2
53	R	0.235	0.235	0.228	0.227	0.233	0.229	0.643	0.636	0.612	74.2	75.7	73.2	73.5	72.9	75.2	0.940	0.972	0.963	61.9	61.8	62.0
54	R	0.252	0.253	0.250	0.254	0.251	0.246	0.551	0.559	0.538	69.4	71.2	71.7	69.3	67.2	69.3	0.983	0.968	0.978	65.3	64.0	
55	R	0.225	0.232	0.234	0.235	0.241	0.234	0.580	0.582	0.558	81.7	69.7	70.4	70.4	70.4	73.1	1.054	1.000	0.989	64.3	63.1	63.9
56	R	0.221	0.210	0.212	0.224	0.225	0.220	0.512	0.508	0.491	76.6	78.0	78.2	66.8	77.2	71.9	1.005	1.035	1.011	63.4	63.1	63.5
57	R	0.215	0.214	0.211	0.203	0.207	0.203	0.510	0.506	0.485	76.6	78.8	80.5	82.7	81.9	79.6	0.964	0.961	0.956	64.0	64.3	64.7
58	R	0.207	0.208	0.209	0.223	0.217	0.211	0.624	0.616	0.608	72.6	79.6	81.9	69.3	73.1		1.086	1.056	1.030	66.4	66.9	66.7
59	R	0.259	0.270	0.257	0.266	0.270	0.263	0.577	0.574	0.548	79.1	67.6	74.8	73.8	71.7	72.3	1.021	0.982	0.988	59.3	59.7	59.7
60	R	0.209	0.211	0.214	0.218	0.220	0.220	0.653	0.655	0.628	78.6	76.7	74.4	73.0	75.3	74.1	1.021	1.035	0.991	65.9	65.5	65.0
61	R	0.250	0.251	0.248	0.238	0.238	0.238	0.741	0.741	0.724	78.5	77.8	79.1	77.4	79.0	79.1	0.973	0.960	0.985	67.6	67.3	67.2
62	R	0.263	0.271	0.272	0.249	0.255	0.256	0.635	0.622	0.603	69.5	70.1	70.2	79.7	75.4	74.2	0.950	0.954	0.928	56.9	57.0	57.4
63	R	0.254	0.257	0.249	0.273	0.273	0.266	0.705	0.699	0.675	79.2	75.8	78.1	69.0	70.6	72.2	1.061	1.078	1.075	57.7	57.3	57.8
64	R	0.258	0.260	0.250	0.271	0.269	0.265	0.744	0.738	0.710	79.3	79.5	80.0	73.0	75.4	75.2	1.030	1.013	1.027	55.9	56.4	56.3
65	R	0.234	0.230	0.225	0.243	0.240	0.233	0.588	0.581	0.559	70.3	72.9	73.7	69.9	72.2	70.2	1.048	1.039	1.022	57.0	57.7	57.4
66	R	0.262	0.269	0.256	0.261	0.251	0.253	0.723	0.707	0.690	82.9	73.6	80.0	72.0	79.9	77.8	0.983	0.944	0.966	58.7	59.6	59.5
67	R	0.256	0.258	0.255	0.269	0.284	0.273	0.812	0.792	0.759	80.8	80.6	80.2	76.7	72.3	75.6	1.047	1.092	1.045		62.2	62.6
68	R	0.229	0.229	0.224	0.249	0.249	0.238	0.942	0.925	0.887	80.0	81.4	81.2	75.0	70.6	77.0	1.067	1.086	1.054	66.1	65.6	65.8
69	R	0.235	0.234	0.228	0.240	0.246	0.232	0.849	0.832	0.812	77.6	75.4	77.7	75.3	72.7	75.7	1.023	1.028	1.027	61.9	62.2	61.9
70	S	0.302	0.293	0.282	0.243	0.242	0.235	0.660	0.661	0.632	69.6	70.7	71.3	82.5	84.5	84.9	1.032	1.007	0.997	61.9	61.8	61.8
71	S	0.295	0.294	0.283	0.290	0.283	0.274	0.556	0.549	0.526	80.4	76.6	79.7	80.6	81.2	82.7	0.956	0.963	0.967	61.9	62.2	61.8
72	S	0.246	0.247	0.241	0.242	0.245	0.238	0.519	0.523	0.499	83.0	83.6	81.4	84.5	85.2	81.1	0.978	0.997	0.997	57.7	58.8	58.4
73	S	0.223	0.221	0.218	0.213	0.215	0.210	0.697	0.693	0.667	81.6	79.5	77.8	82.0	82.2	81.4	0.965	0.963	0.963	63.8	64.4	64.2
74	S	0.337	0.325	0.308	0.318	0.310	0.292	0.503	0.514	0.495	81.4	81.0	79.2	83.6	80.2	81.8	0.973	0.966	0.996	55.4	55.6	56.0

Table C-13. FWD Test Data (Untreated Section, 6-May-2008) (1 µm/kN = 0.175 mil/kip).

7-May-2008																	
Joint		NDf-0 (mils/kip)						LTE (%)						JSR			
		Approach			Leave			Approach			Leave						
N°	Type	Drop1	Drop 2	Drop 3	Drop1	Drop 2	Drop 3	Drop1	Drop 2	Drop 3	Drop1	Drop 2	Drop 3	Drop1	Drop 2	Drop 3
Section 3: **Untreated**																	
1	R	0.281	0.292	0.283	0.270	0.268	0.267	50.7	56.3	60.4	75.0	77.1	77.8	1.051	0.981	1.007
2	R	0.285	0.285	0.286	0.264	0.260	0.259	63.7	66.3	66.1	80.8	83.5	83.7	0.932	0.922	0.918
3	R	0.268	0.262	0.258	0.256	0.254	0.251		64.0	68.0	71.8	75.2	77.1	0.946	0.974	0.980
4	S	0.267	0.273	0.271	0.293	0.302	0.295	74.9	73.9	74.7	64.9	65.6	67.5	1.091	1.094	1.085
5	S	0.242	0.241	0.241	0.268	0.268	0.265	80.3	82.1	79.8	68.6	68.2	71.4	1.096	1.117	1.093
6	S	0.262	0.264	0.259	0.279	0.282	0.281	71.2	73.9	74.9	65.7	68.0	65.3	1.090	1.076	1.085
7	S	0.233	0.234	0.234	0.276	0.275	0.270	72.0	73.5	77.2	54.7	60.4	58.7	1.193	1.186	1.161
8	S	0.208	0.211	0.210	0.191	0.197	0.201	86.0	83.3	81.8	80.5	82.1	82.4	0.935	0.929	0.967
9	R	0.223	0.233	0.231	0.220	0.223	0.222	69.0	65.9	71.7	70.8	74.4	75.6	0.975	0.953	0.959
10	R	0.213	0.220	0.218	0.217	0.212	0.215	77.1	79.7	79.0	81.0	82.5	82.8	1.016	0.966	0.977
11	R	0.250	0.252	0.256	0.250	0.256	0.252	75.2	75.0	75.7	78.2	78.1	80.8	0.996	1.033	0.995
Section 2: **Rubblized**																	
1	R	0.351	0.350	0.345	0.370	0.367	0.359	69.5	66.7	70.9	60.1	63.3	63.9	1.051	1.058	1.051
2	R	0.361	0.364	0.358	0.358	0.359	0.349	53.5	62.0	63.0	73.1	76.8	81.3	0.991	0.995	0.982
3	R	0.384	0.386	0.389	0.363	0.366	0.369	51.5	51.3	54.3	71.5	74.5	77.0	0.965	0.948	0.959
4	S	0.353	0.358	0.357	0.367	0.368	0.367	66.9	68.6	69.6	68.2	70.1	72.9	1.061	1.043	1.046
5	S	0.350	0.343	0.351	0.371	0.379	0.372	70.3	72.3	72.5	69.7	70.9	72.5	1.050	1.040	1.039
6	S	0.467	0.479	0.469	0.495	0.496	0.488	21.6	24.6	23.0	23.9	24.1	26.6	1.043	1.035	1.041
7	S	0.332	0.338	0.333	0.352	0.353	0.356	61.8	62.2	64.4	64.5	67.3	67.6	1.023	1.017	1.031
8	S	0.423	0.426	0.417	0.419	0.427	0.415	34.8	35.6	40.2	41.2	42.1	44.5	0.971	1.008	1.008
9	R	0.309	0.311	0.303	0.327	0.337	0.325	64.7	66.4	70.1	57.6	60.5	64.4	1.068	1.075	1.053
10	R	0.288	0.295	0.281	0.296	0.298	0.295	73.1	78.0	79.1	75.8	79.1	79.9	1.015	1.011	1.009
11	R	0.321	0.329	0.324	0.331	0.341	0.328	56.1	59.8	62.8	69.4	72.1	74.0	1.028	1.030	1.027
Section 1: **Broken and seated**																	
1	R	0.289	0.301	0.295	0.327	0.336	0.331	74.2	71.5	76.5	63.4	64.6	66.4	1.123	1.116	1.121
2	R	0.289	0.296	0.294	0.276	0.295	0.290		64.1	65.8	66.8	69.5	74.3	0.938	0.983	0.983
3	R	0.326	0.333	0.336	0.326	0.336	0.340	74.8	77.2	76.0	71.2	71.8	73.0	0.993	1.025	1.000
4	S	0.245	0.254	0.258	0.247	0.256	0.260	82.4	82.1	82.3	80.4	82.0	80.4	1.014	0.997	1.015
5	S	0.235	0.242	0.241	0.257	0.268	0.268	79.4	79.9	81.8	73.2	72.9	73.3	1.079	1.092	1.100
6	S	0.268	0.282	0.281	0.316	0.323	0.324	73.3	73.8	74.8	65.7	65.9	66.4	1.177	1.138	1.134
7	S	0.261	0.279	0.282	0.249	0.252	0.256	76.4	79.3	80.8	74.8	75.2	76.2	1.017	1.051	1.031
8	S	0.250	0.254	0.258	0.284	0.290	0.295	83.6	79.3	82.2	69.0	72.2	72.7	1.198	1.196	1.202
9	R	0.254	0.256	0.258	0.266	0.268	0.267	57.5	61.3	63.3	63.9	65.2	68.1	1.044	1.066	1.049
10	R	0.321	0.324	0.326	0.292	0.304	0.301	55.5	50.1	53.8	74.3	72.9	77.1	0.914	0.929	0.916
11	R	0.211	0.231	0.237	0.281	0.289	0.285	77.5	78.2	78.5	64.4	66.1	68.3	1.172	1.265	1.218

Table C-14. FWD Test Data (7-May-2008) (1 µm/kN = 0.175 mil/kip).

Section 1: **Broken and seated**																						
21-October-2008																						
Joint		**NDf-0 (mils/kip)**									**LTE (%)**						**JSR**			**Mid-Slab SPR (%)**		
		Approach			**Leave**			**Mid-Slab**			**Approach**			**Leave**								
N°	**Type**	**Drop**			**Drop**			**Drop**			**Drop**			**Drop**			**Drop**			**Drop**		
		1	**2**	**3**	**1**	**2**	**3**	**1**	**2**	**3**	**1**	**2**	**3**	**1**	**2**	**3**	**1**	**2**	**3**	**1**	**2**	**3**
1	R	0.295	0.304	0.302	0.347	0.344	0.340	0.197	0.197	0.204	80.3	82.6	81.1	72.7	74.7	76.1	1.156	1.131	1.119		71.2	69.7
2	R	0.369	0.374	0.368	0.390	0.388	0.383	0.192	0.199	0.202	64.8	63.9	66.0	64.1	65.9	68.1	1.057	1.045	1.029	70.8	71.8	71.8
3	R	0.352	0.359	0.356	0.367	0.368	0.364	0.192	0.207	0.210	68.3	62.6	66.7	68.0	71.6	72.4	1.041	1.023	1.035	78.9	76.6	76.7
4	R	0.358	0.370	0.366	0.368	0.381	0.377	0.257	0.267	0.266	70.6	69.9	72.8	77.7	77.5	79.7	1.015	1.025	1.012	78.4	77.5	77.2
5	R	0.378	0.373	0.371	0.398	0.396	0.390	0.228	0.233	0.240	72.0	77.0	74.8	74.7	75.7	76.7	1.062	1.076	1.057	73.3	74.0	72.6
6	R	0.398	0.405	0.395	0.418	0.417	0.407	0.254	0.258	0.260	66.3	68.0	69.2	68.8	70.0	71.7	1.062	1.033	1.029		69.8	69.4
7	R	0.350	0.349	0.352	0.395	0.403	0.391	0.204	0.211	0.216	70.5	72.7	74.6	66.1	66.9	70.0	1.124	1.151	1.110	71.7	73.0	72.4
8	R	0.400	0.406	0.399	0.433	0.437	0.426	0.198	0.208	0.210	70.5	71.7	73.1	67.9	69.1	71.0	1.084	1.083	1.069	71.8	71.2	72.0
9	R	0.398	0.394	0.385	0.395	0.391	0.389	0.199	0.203	0.207	60.8	63.5	66.5	65.1	67.7	70.5	1.009	0.998	1.005	70.1	69.3	70.5
10	R	0.283	0.290	0.293	0.308	0.311	0.314	0.183	0.186	0.193	66.4	67.7	69.3	64.3	66.8	68.6	1.082	1.066	1.072	68.4	70.2	70.1
11	R	0.356	0.361	0.364	0.379	0.388	0.384	0.209	0.204	0.210	67.8	68.4	68.7	63.6	64.3	66.0	1.072	1.079	1.059		72.6	71.6
12	R	0.361	0.368	0.365	0.366	0.382	0.373	0.241	0.248	0.257	67.4	68.5	69.2	69.3	70.0	73.8	0.982	1.021	1.010	71.6	73.2	72.7
13	R	0.479	0.479	0.470	0.506	0.504	0.493	0.252	0.265	0.267	67.0	68.9	71.3	63.4	66.2	69.0	1.056	1.054	1.051	69.4	68.3	69.2
14	S	0.368	0.372	0.372	0.383	0.390	0.385	0.213	0.221	0.226	73.1	72.8	74.9	70.8	69.9	69.7	1.036	1.045	1.034	66.1	68.2	67.7
15	S	0.349	0.352	0.352	0.393	0.395	0.389	0.203	0.210	0.212	68.9	69.4	69.9	63.1	62.7	63.8	1.101	1.123	1.113		66.1	66.9
16	S	0.386	0.393	0.392	0.420	0.427	0.418	0.187	0.195	0.199	51.7	53.1	53.8	52.0	53.6	54.7	1.071	1.075	1.067		66.7	67.7
17	S	0.341	0.356	0.351	0.397	0.400	0.388	0.201	0.212	0.216	67.8	66.9	67.9	58.8	59.9	62.0	1.174	1.124	1.098	63.4	63.4	63.9
18	S	0.349	0.356	0.357	0.365	0.376	0.375	0.199	0.204	0.207	65.8	66.2	67.5	66.4	65.9	65.2	1.054	1.068	1.047		61.7	62.5
19	R	0.352	0.352	0.349	0.371	0.369	0.357	0.169	0.176	0.180	54.4	55.9	58.4	58.5	61.0	64.6	1.060	1.047	1.034	65.7	66.0	66.8
20	R	0.477	0.480	0.459	0.448	0.447	0.434	0.160	0.158	0.161	59.9	60.2	60.7	74.3	74.6	77.2	0.942	0.937	0.947	66.0	67.5	69.3
21	R	0.354	0.353	0.344	0.410	0.403	0.390	0.187	0.192	0.197	61.5	61.6	63.4	60.1	61.8	63.9	1.161	1.143	1.137		68.6	68.3
22	R	0.349	0.344	0.334	0.378	0.368	0.352	0.178	0.182	0.186	68.2	69.8	71.9	59.9	65.7	68.5	1.090	1.078	1.054	64.8	65.2	64.7
23	R	0.394	0.398	0.391	0.462	0.454	0.435	0.173	0.174	0.181	58.0	62.8	61.0	60.2	61.8	64.5	1.169	1.139	1.105		69.0	69.1
24	R	0.439	0.438	0.418	0.440	0.436	0.424	0.174	0.187	0.190	54.2	57.1	60.6	60.0	62.7	66.6	1.010	1.020	1.026		64.9	65.9

Table C-15. FWD Test Data (B&S Section, 21-October-2008) (1 µm/kN = 0.175 mil/kip).

Section 2: **Rubblized**																					
21-October-2008																					
Joint		**NDf-0 (mils/kip)**									**LTE (%)**						**JSR**			**Mid-Slab SPR (%)**		
		Approach			**Leave**			**Mid-Slab**			**Approach**			**Leave**								
N°	**Type**	**Drop**			**Drop**			**Drop**			**Drop**			**Drop**			**Drop**			**Drop**		
		1	**2**	**3**	**1**	**2**	**3**	**1**	**2**	**3**	**1**	**2**	**3**	**1**	**2**	**3**	**1**	**2**	**3**	**1**	**2**	**3**
1	R	0.394	0.399	0.387	0.420	0.417	0.404	0.215	0.222	0.222	59.1	59.4	64.2	56.4	59.2	62.4	1.069	1.046	1.059	64.7	65.1	65.7
2	R	0.401	0.404	0.393	0.399	0.399	0.391	0.201	0.207	0.209	53.9	57.5	62.1	65.2	68.7		1.003	0.998	0.997	62.8	63.7	64.9
3	R	0.435	0.435	0.429	0.435	0.434	0.422	0.196	0.200	0.204	50.1	51.0	53.8	62.6	65.7	67.6	0.985	0.973	0.977	64.7	65.3	65.3
4	S	0.463	0.457	0.446	0.480	0.473	0.462	0.210	0.212	0.216	55.2	56.8	57.9	62.6	64.2	65.9	1.041	1.042	1.040	69.6	71.0	70.8
5	S	0.481	0.478	0.470	0.541	0.534	0.521	0.216	0.225	0.229	64.2	64.7	65.6	60.3	61.4	62.3	1.103	1.108	1.100	69.2	69.1	69.5
6	S	0.607	0.602	0.587	0.653	0.639	0.614	0.188	0.196	0.199	17.1	19.8	21.7	18.6	21.1	23.0	1.087	1.069	1.044		68.2	68.3
7	S	0.487	0.482	0.469	0.476	0.471	0.459	0.176	0.184	0.189	51.4	51.6	52.8	60.6	63.7	65.3	0.972	0.971	0.985	70.7	69.2	69.7
8	S	0.659	0.646	0.615	0.694	0.669	0.637	0.189	0.188	0.194	34.0	37.0	40.0	30.8	33.7	36.6	1.061	1.052	1.054	63.5	67.5	66.7
9	R	0.396	0.394	0.383	0.398	0.403	0.390	0.185	0.186	0.189	62.5	64.2	66.5	63.0	63.9	66.2	1.011	1.021	1.021	63.5	64.9	65.1
10	R	0.350	0.353	0.352	0.354	0.361	0.358	0.174	0.181	0.184	72.5	74.1	74.9	72.9	74.4	74.6	1.003	1.021	1.016	63.2	64.1	64.7
11	R	0.422	0.418	0.410	0.456	0.452	0.437	0.165	0.172	0.175	69.9	71.7	72.8	66.2	68.1	70.3	1.093	1.088	1.063	63.6	65.0	64.7
12	R	0.393	0.394	0.385	0.407	0.403	0.390	0.189	0.193	0.196	61.9	61.8	66.0	61.9	64.6	67.9	1.017	1.030	1.013	58.1	65.1	66.0
13	R	0.457	0.456	0.445	0.439	0.439	0.430	0.195	0.203	0.203	52.3	53.5	56.5	63.7	66.5	68.3	0.963	0.967	0.961	67.2	66.4	68.4
14	R	0.382	0.385	0.377	0.405	0.397	0.392	0.211	0.216	0.219	64.8	66.2	69.1	62.2	65.5	67.7	1.061	1.030	1.045	65.0		65.9
15	R	0.461	0.460	0.444	0.461	0.459	0.443	0.192	0.203	0.203	48.0	53.3	56.0	61.2	64.9	68.6	1.005	1.000	1.000	66.7	67.6	67.5
16	R	0.415	0.407	0.399	0.474	0.465	0.447	0.209	0.214	0.215	57.8	61.8	66.1	53.2	57.3	61.1	1.148	1.146	1.121	63.2	62.7	66.3
17	R	0.357	0.358	0.356	0.396	0.391	0.385	0.189	0.198	0.199	65.9	66.7	69.0	52.9	54.6	57.7	1.126	1.096	1.081	66.2	65.5	66.5
18	R	0.349	0.351	0.352	0.334	0.339	0.338	0.206	0.209	0.212	64.5	65.5	67.9	71.1	72.3	74.0	0.962	0.957	0.963		66.8	66.4
19	R	0.274	0.281	0.281	0.297	0.302	0.301	0.194	0.204	0.207	81.0	80.5	81.1	77.7	77.1	77.0	1.067	1.071	1.055	64.6	63.2	64.5
20	R	0.307	0.316	0.314	0.334	0.340	0.342	0.172	0.181	0.184	64.8	67.1	68.2	64.2	64.1	64.2	1.084	1.072	1.090	63.4	63.5	64.4
21	R	0.261	0.266	0.267	0.287	0.289	0.292	0.164	0.167	0.169	78.0	79.8	80.8	73.5	74.6	75.4	1.089	1.091	1.096			65.2
22	R	0.310	0.324	0.318	0.310	0.317	0.313	0.171	0.180	0.182	63.6	62.8	62.5	66.7	68.2	70.5	0.996	0.982	0.984	62.1	63.3	63.3
23	R	0.253	0.257	0.256	0.283	0.290	0.285			0.179	75.8	80.8	79.1	74.5	74.4	75.3	1.123	1.134	1.102			64.5
24	R	0.254	0.265	0.263	0.268	0.280	0.277	0.168	0.175	0.177	78.6	77.3	78.3	75.1	72.0	75.3	1.076	1.073	1.075	64.4	63.8	65.1
25	R	0.291	0.300	0.292	0.316	0.316	0.310	0.184	0.188	0.192	70.0	67.9	68.1	61.3	63.9	65.7	1.080	1.050	1.049	65.8	66.7	65.9
26	R	0.277	0.285	0.285	0.299	0.302	0.301	0.184	0.185	0.189	81.4	80.2	81.3	75.8	76.9	78.4	1.063	1.050	1.057	63.8	65.5	65.8

Table C-16. FWD Test Data (Rubblized Section, 21-October-2008) (1 µm/kN = 0.175 mil/kip).

Section 3: **Untreated**																							
21-October-2008																							
Joint		**NDf-0 (mils/kip)**									**LTE (%)**						**JSR**			**Mid-Slab SPR (%)**			
		Approach			**Leave**			**Mid-Slab**			**Approach**			**Leave**										
N°	**Type**	**Drop**			**Drop**			**Drop**			**Drop**			**Drop**			**Drop**			**Drop**			
		1	**2**	**3**	**1**	**2**	**3**	**1**	**2**	**3**	**1**	**2**	**3**	**1**	**2**	**3**	**1**	**2**	**3**	**1**	**2**	**3**	
1	R	0.455	0.448	0.419	0.430	0.422	0.400	0.185	0.190	0.193	58.6	63.6	67.8	64.5	67.9	71.5	0.953	0.948	0.939				
2	R	0.387	0.387	0.374	0.408	0.425	0.406	0.164	0.175	0.173	51.5	54.8	57.2	51.1	55.9	60.2	1.064	1.100	1.093	76.3		77.5	
3	R	0.449	0.438	0.419	0.462	0.457	0.441	0.156	0.159	0.162	62.2	65.1	66.0	62.8	65.1	67.0	1.017	1.042	1.049		72.2	71.2	
4	R	0.357	0.352	0.339	0.363	0.358	0.348	0.158	0.168	0.170	60.8	65.4	68.4	61.7	65.0	68.9	1.032	1.024	1.035	71.4	69.5	69.7	
5	R	0.317	0.316	0.314	0.345	0.339	0.335	0.182	0.192	0.192	57.4	57.9	60.0	54.8	56.0	60.0	1.113	1.077	1.070	75.6	73.1	72.3	
6	R	0.330	0.329	0.328	0.372	0.372	0.369	0.153	0.163	0.165	71.9	71.9	72.3	59.2	59.5	60.6	1.140	1.133	1.129				
7	R	0.405	0.401	0.386	0.424	0.417	0.401	0.144	0.152	0.154	57.9	59.7	62.0	61.6	64.0	65.8	1.055	1.044	1.041	72.9	72.4	72.9	
8	R	0.382	0.376	0.362	0.373	0.362	0.352	0.160	0.152	0.158	59.9	61.3	63.5	65.8	69.2	70.9	0.991	0.971	0.976	68.9	71.8	71.3	
9	R	0.396	0.389	0.372	0.395	0.384	0.368	0.160	0.170	0.164	64.2	61.9	66.7	64.6	67.9	70.6	1.011	0.991	0.995	67.8	66.1	68.4	
10	S	0.565	0.544	0.519	0.786	0.723	0.654	0.163	0.166	0.166	35.3	38.1	40.7	26.0	29.4	32.8	1.373	1.320	1.267	76.7	76.9	76.7	
11	S	0.490	0.484	0.463	0.497	0.477	0.451	0.164	0.168	0.172	57.8	60.0	59.9	59.1	62.0	63.6	1.021	0.984	0.972	75.1	75.8	75.2	
12	S	0.829	0.782	0.702	0.880	0.806	0.715	0.207	0.204	0.205	57.5	58.8	60.6	51.7	53.4	55.2	1.066	1.042	1.024				
13	S	0.804	0.755	0.685	0.763	0.712	0.652	0.195	0.205	0.203	53.7	54.5	55.3	68.5	70.0	71.3	0.957	0.954	0.961				
14	S	0.368	0.359	0.346	0.391	0.390	0.373	0.186	0.189	0.189	68.7	70.3	71.1	73.3	72.9	74.1	1.082	1.096	1.085		73.3	74.1	
15	R	0.331	0.331	0.321	0.325	0.331	0.322	0.163	0.170	0.172	61.5	64.1	65.3	67.5	66.5	69.8	0.986	1.005	1.008		70.2	69.4	
16	R	0.293	0.291	0.286	0.325	0.326	0.325	0.156	0.161	0.158	75.5	74.4	76.6	76.8	76.6	77.7	1.091	1.135	1.138	70.8	70.7	72.6	
17	R	0.294	0.303	0.299	0.337	0.340	0.334	0.148	0.153	0.154	70.7	71.1	69.8	63.0	62.3	63.9	1.128	1.118	1.108	70.7	71.6	72.7	
18	R	0.334	0.335	0.328	0.359	0.361	0.353	0.192	0.197	0.200	80.7	80.3	80.0	77.1	78.3	78.5	1.077	1.085	1.074	70.5	71.7	71.2	
19	R	0.330	0.332	0.332	0.344	0.350	0.346	0.182	0.183	0.188	69.4	75.7	76.2	74.4	73.5	74.8	1.061	1.068	1.042	72.7	72.7	72.4	

Table C-17. FWD Test Data (Untreated Section, 21-October-2008) (1 µm/kN = 0.175 mil/kip).

Section 1: **Broken and seated**																						
13-May-2009																						
Joint		**NDf-0 (mils/kip)**									**LTE (%)**						**JSR**			**Mid-Slab SPR (%)**		
		Approach			**Leave**			**Mid-Slab**			**Approach**			**Leave**								
N°	**Type**	**Drop**			**Drop**			**Drop**			**Drop**			**Drop**			**Drop**			**Drop**		
		1	**2**	**3**	**1**	**2**	**3**	**1**	**2**	**3**	**1**	**2**	**3**	**1**	**2**	**3**	**1**	**2**	**3**	**1**	**2**	**3**
1	R	0.348	0.359	0.360	0.386	0.382	0.373	0.533	0.525	0.506	69.1	64.1	65.6	58.3	62.5	66.6	1.088	1.043	1.029	60.3	60.0	
2	S	0.316	0.323	0.324	0.341	0.352	0.353	0.587	0.581	0.553	71.1	73.7	73.3	66.7	65.0	67.7	1.088	1.082	1.085	61.7	62.4	
3	S	0.342	0.350	0.349	0.422	0.420	0.414	0.752	0.750	0.731		66.7	69.2	50.1	53.8	54.0	1.203	1.191	1.170	64.8	64.3	64.7
4	S	0.419	0.428	0.426	0.444	0.451	0.442	0.631	0.628	0.603	53.1	47.8	47.8	45.7	48.0	50.3	1.056	1.047	1.020	62.3		
5	S	0.316	0.318	0.319	0.320	0.330	0.329	0.660	0.662	0.644	68.8	71.9	73.4		67.8		0.990	1.023	1.017	64.3	64.7	65.0
6	S	0.381	0.387	0.386	0.398	0.399	0.396	0.656	0.658	0.641	55.5	52.6	51.4	47.8	50.0	52.5	1.035	1.030	1.002	63.5		
7	R	0.311	0.320	0.316	0.312	0.317	0.314	0.666	0.662	0.649	69.1	68.5	70.8	63.7	67.1		0.986	0.980	0.973	63.5		
8	R	0.316	0.321	0.320	0.334	0.342	0.336	0.577	0.584	0.567	76.2	73.7	76.2	67.2	68.4	70.6	1.056	1.062	1.046	61.4	61.4	61.3
9	R	0.335	0.340	0.336	0.344	0.345	0.341	0.643	0.644	0.630	60.6	64.4	65.5	66.3	66.9	69.2	1.033	1.002	1.011	61.7	62.0	
10	R	0.308	0.312	0.314	0.301	0.309	0.306	0.703	0.698	0.680	59.7	63.6	65.6	65.8	68.0	68.8	0.951	0.974	0.967	62.0	62.4	
11	R	0.341	0.347	0.348	0.330	0.340	0.335	0.848	0.851	0.830	73.1	70.5	71.9	73.2	73.4	74.4	0.968	0.976	0.973	65.7		
12	R	0.410	0.403	0.395	0.397	0.403	0.397	0.979	0.985	0.971	69.0	70.6	73.0	73.7	73.0	73.5	0.957	1.004	0.989	66.7		66.4
13	R	0.389	0.389	0.386	0.396	0.397	0.391	0.771	0.785	0.760	71.2	68.4	71.0	70.6	71.4	73.3	1.017	0.994	0.990	63.8	63.2	64.1
14	R	0.357	0.357	0.354	0.368	0.371	0.361	0.758	0.759	0.738	65.1	64.6	66.3	61.1	61.0	65.8	1.015	1.014	1.005	63.3	62.4	63.0
15	R	0.386	0.387	0.378	0.347	0.358	0.353	0.567	0.567	0.549	57.1	58.0	62.1	66.7	67.4	69.2	0.900	0.942	0.909	58.9	58.6	
16	R	0.338	0.340	0.336	0.354	0.359	0.359	0.781	0.783	0.763	63.9	67.8	70.8	61.4	61.7	64.9	1.036	1.056	1.063	66.4	66.0	66.0
17	R	0.371	0.371	0.369	0.376	0.375	0.370	0.685	0.692	0.678	58.8	57.0	62.8	57.7	60.6	62.0	1.003	1.011	1.000	67.2	67.0	
18	R	0.364	0.364	0.355	0.358	0.353	0.346	0.460	0.461	0.454	57.0	61.3	65.0	63.8	65.4	68.2	0.985	0.973	0.982	60.0	60.1	60.1
19	R	0.316	0.322	0.324	0.327	0.330	0.320	0.543	0.545	0.539	58.5	61.2	60.5	59.5	63.8	68.1	1.014	1.028	0.996	61.1	61.8	61.9
20	R	0.288	0.297	0.294	0.296	0.303	0.302	0.606	0.619	0.584	79.3	81.2	79.5	77.2	81.3	81.7	1.008	1.020	1.004	58.3		

Table C-18. FWD Test Data (B&S Section, 13-May-2009) (1 µm/kN = 0.175 mil/kip).

Section 2: **Rubblized**																					
13-May-2009																					
Joint		**NDf-0 (mils/kip)**									**LTE (%)**						**JSR**			**Mid-Slab SPR (%)**		
		Approach			**Leave**			**Mid-Slab**			**Approach**			**Leave**								
N°	**Type**	**Drop**			**Drop**			**Drop**			**Drop**			**Drop**			**Drop**			**Drop**		
		1	**2**	**3**	**1**	**2**	**3**	**1**	**2**	**3**	**1**	**2**	**3**	**1**	**2**	**3**	**1**	**2**	**3**	**1**	**2**	**3**
1	RJ	0.286	0.299	0.311	0.287	0.302	0.311	0.342	0.346	0.352	62.1	64.1	66.2	63.0	60.7	60.5	1.004	1.013	1.002	64.2	65.5	65.4
2	RJ	0.286	0.308	0.317	0.293	0.310	0.318	0.309	0.316	0.320	76.4	77.0	78.5	72.8	75.6	75.4	1.025	1.008	1.004	61.0	61.3	62.0
3	RJ	0.319	0.335	0.348	0.320	0.329	0.337	0.286	0.290	0.296	53.4	54.4	55.2	56.7	61.0	63.5	1.010	0.988	0.981	61.5	62.4	62.9
4	SJ	0.331	0.344	0.359	0.337	0.344	0.357	0.336	0.342	0.346	59.1	60.9	61.8	56.5	59.7	61.1	1.013	1.000	0.996	64.8	65.3	65.7
5	SJ	0.302	0.318	0.324	0.330	0.339	0.348	0.355	0.360	0.363	68.3	68.3	69.5	59.0	59.7	61.2	1.082	1.059	1.060	67.6	67.6	67.6
6	SJ	0.352	0.368	0.380	0.446	0.456	0.470	0.287	0.291	0.294	104.1	103.8	104.4	70.6	73.0	72.4	1.259	1.232	1.230	64.3	64.6	65.0
7	SJ	0.340	0.351	0.360	0.289	0.297	0.310	0.262	0.266	0.273	54.1	56.7	57.9	58.6	60.8	61.9	0.850	0.848	0.860	63.4	63.7	64.2
8	SJ	0.371	0.384	0.396	0.335	0.341	0.353	0.351	0.356	0.357	35.8	38.4	40.3	36.9	41.7	43.2	0.908	0.895	0.902	66.8	66.2	66.0
9	RJ	0.262	0.273	0.283	0.269	0.276	0.286	0.417	0.404	0.403	64.5	66.9	68.1	60.2	61.7	62.4	1.020	1.014	1.016	68.8	69.9	69.5
10	RJ	0.267	0.282	0.291	0.267	0.278	0.289	0.449	0.454	0.458	75.6	76.3	77.6	70.2	71.9	72.5	1.000	0.994	1.016	67.2	67.3	67.3
11	RJ	0.266	0.277	0.285	0.270	0.277	0.287	0.506	0.509	0.512	67.7	68.3	69.5	68.6	66.4	67.0	1.016	1.003	1.007	68.3	67.8	67.7
12	RJ	0.248	0.260	0.268	0.251	0.263	0.270	0.349	0.347	0.351	63.4	65.0	66.0	71.4	55.7	62.1	1.013	1.006	1.007	63.9	64.8	64.8
13	RJ	0.282	0.288	0.297	0.266	0.276	0.284	0.310	0.312	0.316	58.3	60.9	63.3	59.6	61.0	63.0	0.941	0.962	0.967	64.6	64.3	64.5
14	RJ	0.283	0.295	0.305	0.314	0.325	0.333	0.645	0.642	0.639	68.1	71.1	71.9	60.1	53.3	59.3	1.103	1.110	1.105	68.8	68.7	68.4
15	RJ	0.314	0.321	0.336	0.321	0.329	0.342	0.529	0.517	0.510	63.2	66.3	67.1	59.9	63.1	63.6	1.023	1.034	1.032	70.1	70.2	69.9
16	RJ	0.271	0.282	0.291	0.284	0.289	0.298	0.517	0.515	0.517	69.9	71.0	72.2	67.0	61.1	64.5	1.054	1.031	1.034	71.3	71.7	71.5
17	RJ	0.286	0.296	0.304	0.275	0.288	0.296	0.391	0.392	0.396	63.4	64.5	65.9	60.8	62.1	63.0	0.963	0.973	0.970	68.2	67.9	68.4

Table C-19. FWD Test Data (Rubblized Section, 13-May-2009) (1 µm/kN = 0.175 mil/kip).

Section 3: **Untreated**																						
13-May-2009																						
Joint		**NDf-0 (mils/kip)**									**LTE (%)**						**JSR**			**Mid-Slab SPR (%)**		
		Approach			**Leave**			**Mid-Slab**			**Approach**			**Leave**								
N°	**Type**	**Drop**			**Drop**			**Drop**			**Drop**			**Drop**			**Drop**			**Drop**		
		1	**2**	**3**	**1**	**2**	**3**	**1**	**2**	**3**	**1**	**2**	**3**	**1**	**2**	**3**	**1**	**2**	**3**	**1**	**2**	**3**
1	R	0.210	0.218	0.219	0.233	0.240	0.240	0.216	0.218	0.217	61.9	64.4	66.8	60.6	61.2	64.2	1.101	1.096	1.097	63.7	64.4	65.3
2	R	0.221	0.230	0.220	0.199	0.207	0.213	0.174	0.169	0.166	52.4	51.9	53.1	69.0	64.7	68.6	0.962	0.958	0.917	64.8	65.2	65.5
3	R	0.240	0.244	0.244	0.226	0.231		0.205	0.178	0.179	65.0	65.2	67.0	64.0	67.8		1.000	1.011		66.4	65.2	67.1
4	R	0.201	0.204	0.207	0.209	0.214	0.211	0.146	0.147	0.147	61.7	64.5	66.1	55.2	57.6	58.8	0.939	1.034	0.916	63.7	64.4	65.3
5	R	0.157	0.161	0.167	0.188	0.191	0.191	0.153	0.161	0.159	61.3	72.3	69.7	63.5	63.6	66.3	1.181	1.165	1.123	62.5	63.7	64.6
6	R		0.190	0.199	0.212	0.221	0.219	0.200	0.204	0.204		69.7	69.4	61.4	61.3	63.4		1.217	1.168	65.2	65.3	66.2
7	R	0.223	0.231	0.233	0.239	0.232	0.231	0.423	0.395	0.366	66.1	68.9	70.7	69.5	68.7	68.3	1.183	1.096	1.121	58.0	58.5	59.1
8	R	0.230	0.238	0.238	0.260	0.266	0.265	0.207	0.210	0.204	75.5	73.7	73.9	64.4	64.8	67.1	1.197	1.172	1.160	63.5	63.2	64.7
9	R	0.231	0.230	0.232	0.232	0.233	0.235	0.338	0.321	0.304	68.8	68.8	69.9	70.0	72.6	74.4	1.010	1.033	1.016	61.6	62.3	63.0
10	R	0.244	0.248	0.250	0.239	0.252	0.252	0.566	0.491	0.426	65.4	65.3	65.9	64.2	66.7	65.7	0.991	1.020	1.015	65.8	65.7	65.9
11	R	0.267	0.276	0.275	0.238	0.246	0.248	0.384	0.355	0.330	73.0	72.7	73.7	78.3	77.4	79.1	0.869	0.889	0.902	58.9	59.5	60.3
12	R	0.239	0.247	0.246	0.223	0.234	0.233	0.323		0.283	66.5	63.4	63.9	62.5	59.8	57.8	0.917	0.943	0.939	59.8		61.5
13	R	0.227	0.229	0.226	0.219	0.222	0.222	0.490	0.475	0.441	66.0	70.3	68.7	69.7	71.1	72.5	0.961	0.964	0.978	65.3	65.3	65.4
14	R	0.203	0.206	0.206	0.197	0.201	0.201	0.549	0.554	0.542	71.3	70.6	73.4	70.8	73.6	74.3	0.983	0.976	0.988	62.5	62.9	62.8
15	R	0.219	0.223	0.228	0.223	0.226	0.227	0.535	0.483	0.422	73.2	76.8	74.6	72.0	71.0	72.9	1.010	1.019	0.986	64.8	65.2	65.5
16	R	0.247	0.255	0.257	0.257	0.262	0.260	0.406	0.402	0.396	72.4	72.0	73.4	70.3	68.7	70.9	1.031	1.020	1.022	54.5	54.8	55.7
17	R	0.256	0.262	0.260	0.293	0.297	0.299	0.384	0.376	0.361	67.1	68.4	69.1	58.8	60.7	62.5	1.134	1.127	1.141	51.0	52.0	53.1
18	R	0.329	0.334	0.338	0.333	0.338	0.339	0.509	0.510	0.496	50.2	50.0	48.6	57.9	58.3		1.014	1.013	1.009	57.6	57.0	
19	R	0.224	0.229	0.228	0.229	0.236	0.235	0.688	0.701	0.682	72.1	74.4	75.9	75.1	71.7	73.1	1.005	1.022	1.014	63.8		
20	R	0.250	0.254	0.253	0.248	0.253	0.251	0.565	0.562	0.528	70.4	68.1	72.2	68.2	68.4	70.0	0.987	0.990	0.976	64.2	63.9	
21	R	0.233	0.239	0.240	0.235	0.241	0.239	0.560	0.560	0.533	76.9	75.8	77.6	75.0	77.2	78.6	1.000	1.000	0.987	60.0	60.2	
22	R	0.232	0.235	0.235	0.245	0.246	0.244	0.722	0.723	0.702	75.6	77.5	74.9	70.6	73.0	73.9	1.057	1.039	1.032		60.2	
23	R	0.199	0.202	0.205	0.212	0.216	0.216	0.537	0.545	0.537	71.4	72.4	72.2	66.1	70.0	71.6	1.055	1.057	1.042	61.9	61.5	61.7
24	R	0.235	0.235	0.239	0.231	0.238	0.235	0.392	0.390	0.376	74.6	78.2	76.0	77.3	78.1	77.1	0.972	1.011	0.990	58.0	57.9	58.4
25	R	0.227	0.233	0.232	0.263	0.267	0.265	0.464	0.467	0.454	74.5	75.9	74.6	64.9	64.8	66.5	1.172	1.155	1.154	56.7	57.0	57.1
26	R	0.207	0.213	0.211	0.217	0.221	0.219	0.585	0.588	0.576	76.8	77.8	77.9	69.4	70.4	70.8	1.059	1.039	1.038	57.6		
27	R	0.205	0.207	0.208	0.210	0.216	0.213	0.615	0.619	0.620	72.3	72.1	74.6	71.3	73.1	74.1	1.022	1.036	1.015	58.7		58.3
28	S	0.260	0.264	0.260	0.233	0.243	0.241	0.503	0.502	0.473	67.8	74.1	69.7	73.3	71.8	72.7	0.890	0.907	0.919	60.3	60.1	
29	S	0.225	0.225	0.229	0.224	0.228	0.229	0.443	0.425	0.397	78.2	77.6	77.0	81.2	77.7	76.7	1.000	1.007	0.986	60.2	60.4	
30	S	0.234	0.239	0.236	0.232	0.240	0.243	0.436	0.428	0.404	67.3	73.9	75.0	69.2	72.0	70.4	1.000	1.007	1.024		58.0	58.5
31	S	0.211	0.217	0.218	0.219	0.221	0.225	0.619	0.617	0.603	75.8	71.8	72.0	74.7	69.6	67.7	1.042	1.004	1.034	62.8	63.0	
32	S	0.233	0.232	0.231	0.200	0.207	0.206	0.412	0.411	0.409	73.0	69.3	69.3	74.7	76.4	76.8	0.863	0.893	0.888	54.4	55.7	
33	R	0.225	0.227	0.231	0.223	0.227	0.227	0.624	0.623	0.608		74.8	73.0	71.1	74.7	75.8	1.015	0.996	0.984	61.3	49.8	50.4

Table C-20. FWD Test Data (Untreated Section, 13-May-2009) (1 µm/kN = 0.175 mil/kip).

Drop	Date	Normalized Deflection (μm/kN)												Spreadability (%)		
		A	B	C	D	I	J	K	L	T	U	V	W	K	T	V
Drop 1	**Section 1: Broken and seated**															
	Jun-2006	1.760	1.671	1.418	1.458	1.600	1.550	1.443	1.574	1.486	1.597	1.660	1.696	55.3	58.4	55.1
	Nov-2006			1.350	1.326		1.437	2.332	3.591	1.427	1.432	1.414	1.609	42.8	63.7	72.5
	Mar-2007			2.297	2.021		1.878	3.424	2.005	3.751	1.920	4.378	2.416	72.3	72.2	76.7
	Oct-2007			2.018	1.432		1.442	2.703	1.497	2.746	1.660	3.278	1.863	66.4	68.2	67.4
	May-2008				1.539		1.634	2.994	1.618	2.605	1.547	3.029	1.961	64.1	69.1	70.6
	Oct-2008			1.164	1.430		1.555	1.148	2.158	1.214	1.842	1.480	2.528	72.8	69.1	71.1
	May-2009			1.207	1.530		1.650	1.607	1.820					57.9		
	Section 2: Rubblized															
	Jun-2006	1.976	2.195	1.937	1.826	2.421	1.890	1.820	1.893	1.780	1.691	1.817	1.922	54.6	55.5	52.8
	Nov-2006			1.368	1.218		1.352	1.301	1.304	1.305	1.173	1.267	1.298	61.1	59.2	60.4
	Mar-2007			2.484	1.750		1.504	1.970	1.335	2.628	1.461	1.860	1.764	66.9	64.0	61.4
	Oct-2007			1.770	1.439		1.383	2.123	1.212	2.248	1.231	1.852	1.320	66.0	62.4	62.7
	May-2008				1.600		1.489	2.204	1.599	2.372	1.399	2.387	1.548	66.3	69.3	67.1
	Oct-2008			1.546	1.895		1.978	1.024	1.948	1.087	1.754	1.093	1.810			
	May-2009			1.882			1.547	2.131	1.535					66.0		
	Section 3: Untreated															
	Jun-2006	1.373	1.333	1.223	1.164	1.478	1.219	1.235	1.240	1.142	1.106	1.168	1.141	59.5	57.5	55.3
	Nov-2006			1.384	1.085		1.148		1.075	1.396	1.046	2.366	1.372		50.8	34.7
	Mar-2007			1.444	2.045		1.339	3.147	1.460	1.691	1.324	2.092	1.411	59.0	63.8	65.6
	Oct-2007			1.194	1.888		1.274	1.228	1.238	1.146	1.200	1.152	1.368	67.3	70.7	69.1
	May-2008				1.630		1.344	3.134	1.652	3.191	1.426	3.333	1.570	67.4	71.1	69.4
	Oct-2008			1.644	2.175		2.212	1.259	2.581	1.446	2.446	1.409	2.677	75.9	75.6	72.7
	May-2009			1.466	1.462		1.498	1.747	1.468					65.7		
Drop 2	**Section 1: Broken and seated**															
	Jun-2006	1.762	1.740	1.399	1.509	1.650	1.536	1.461	1.643	1.509	1.565	1.707	1.777	58.8	55.7	55.7
	Nov-2006			1.212	1.465		1.263	2.240	2.783	1.300	1.270	1.320	1.648	45.4	71.5	79.9
	Mar-2007			2.371	2.095		1.962	3.538	2.072	3.799	1.975	4.490	2.495	72.1	72.3	76.9
	Oct-2007			2.043	1.486		1.486	2.759	1.527	2.732	1.721	3.284	1.855	66.3	69.0	67.9
	May-2008				1.544		1.679	2.958	1.657	2.583	1.563	3.011	1.899	64.3	69.1	71.4
	Oct-2008			1.195	1.505		1.579	1.205	2.197	1.235	1.845	1.511	2.525	71.5	70.9	72.1
	May-2009			1.237	1.580		1.666	1.585	1.878					60.0		
	Section 2: Rubblized															
	Jun-2006	2.043	2.280	2.001	1.837	2.508	1.979	1.834	1.903	1.820	1.735	1.852	1.921	57.1	57.4	54.6
	Nov-2006			1.443	1.276		1.444	1.336	1.377	1.327	1.230	1.295	1.366	62.1	60.2	60.2
	Mar-2007			2.540	1.835		1.668	2.040	1.404	2.690	1.525	1.940	1.797	66.9	63.8	60.8
	Oct-2007			1.803	1.457		1.462	2.152	1.257	2.230	1.232	1.859	1.378	66.6	63.9	63.4
	May-2008				1.608		1.494	2.215	1.659	2.467	1.449	2.396	1.550	66.8	68.4	67.8
	Oct-2008			1.552	1.930		2.007	1.066	1.990	1.104	1.812	1.124	1.861	64.9	62.6	62.9
	May-2009			1.919			1.526	2.148	1.552					65.7		
	Section 3: Untreated															
	Jun-2006	1.433	1.422	1.213	1.208	1.460	1.303	1.217	1.246	1.150	1.098	1.222	1.132	56.3	57.8	53.6
	Nov-2006			1.289	1.228		1.163		1.387	1.497	1.131	1.828	1.395		50.1	43.7
	Mar-2007			1.474	1.983		1.359	3.027	1.528	1.737	1.346	2.095	1.430	60.7	64.2	66.1
	Oct-2007			1.257	1.964		1.324	1.242	1.314	1.256	1.244	1.232	1.350	69.1	69.0	68.4
	May-2008				1.606		1.502	3.056	1.662	3.076	1.404	3.299	1.554	70.0	71.2	69.9
	Oct-2008			1.609	2.188		2.242	1.317	2.563	1.475	2.430	1.392	2.649	74.6	74.8	72.6
	May-2009			1.480	1.486		1.495	1.761	1.492					65.3		

Table C-21. Normalized Strain and Mid-Slab Spreadability at Sensor Locations (1st and 2nd Drop) (1 μm/kN = 0.175 mil/kip).

Pavement Strains (Common Periods) (1°C/cm = 4.6°F/in)

B&S Section

Load-Related Strain

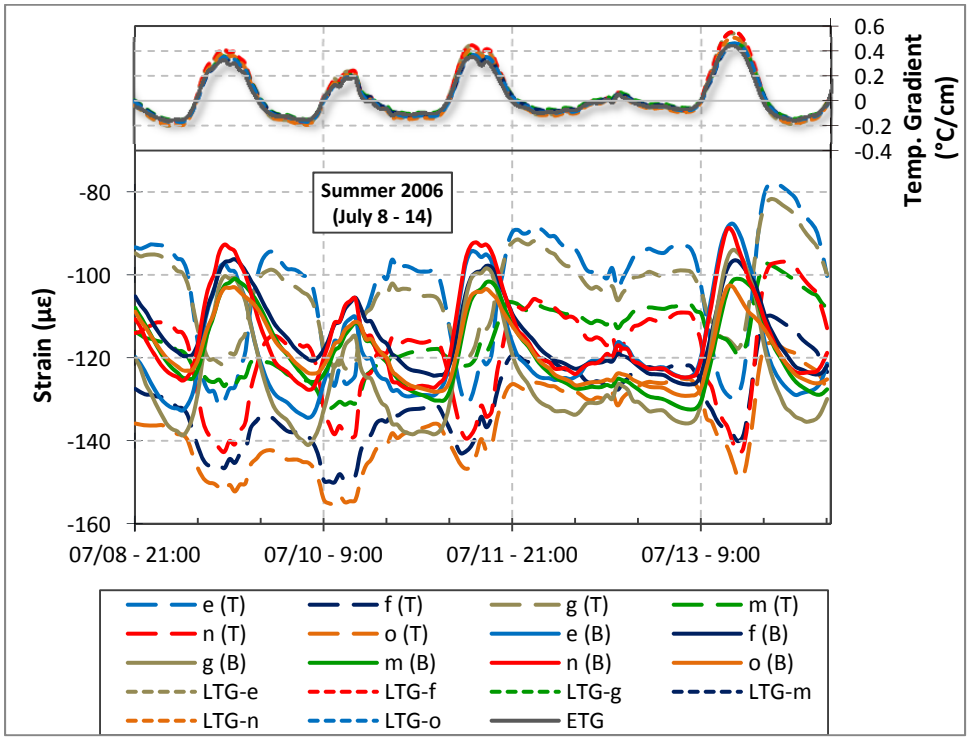

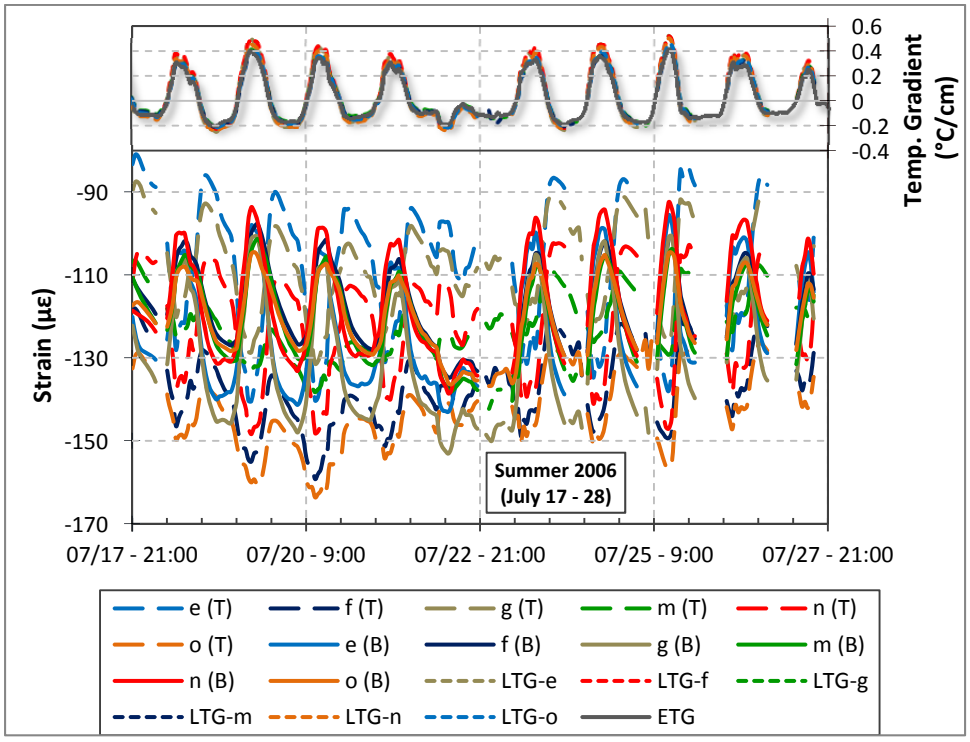

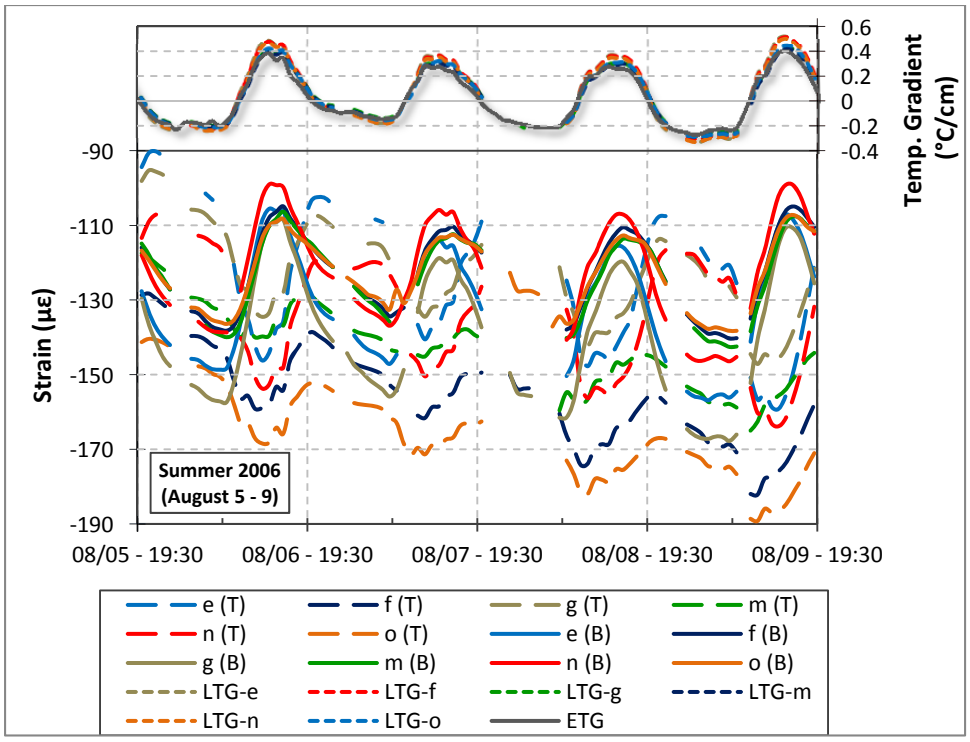
0.6
0.4
0.2
0
-0.2
-0.4
Temp. Gradient (°C/cm)
-90
-110
-130
-150
-170
-190
Strain (με)
Summer 2006 (August 5 - 9)
08/05 - 19:30
08/06 - 19:30
08/07 - 19:30
08/08 - 19:30
08/09 - 19:30
e (T)
f (T)
g (T)
m (T)
n (T)
o (T)
e (B)
f (B)
g (B)
m (B)
n (B)
o (B)
LTG-e
LTG-f
LTG-g
LTG-m
LTG-n
LTG-o
ETG

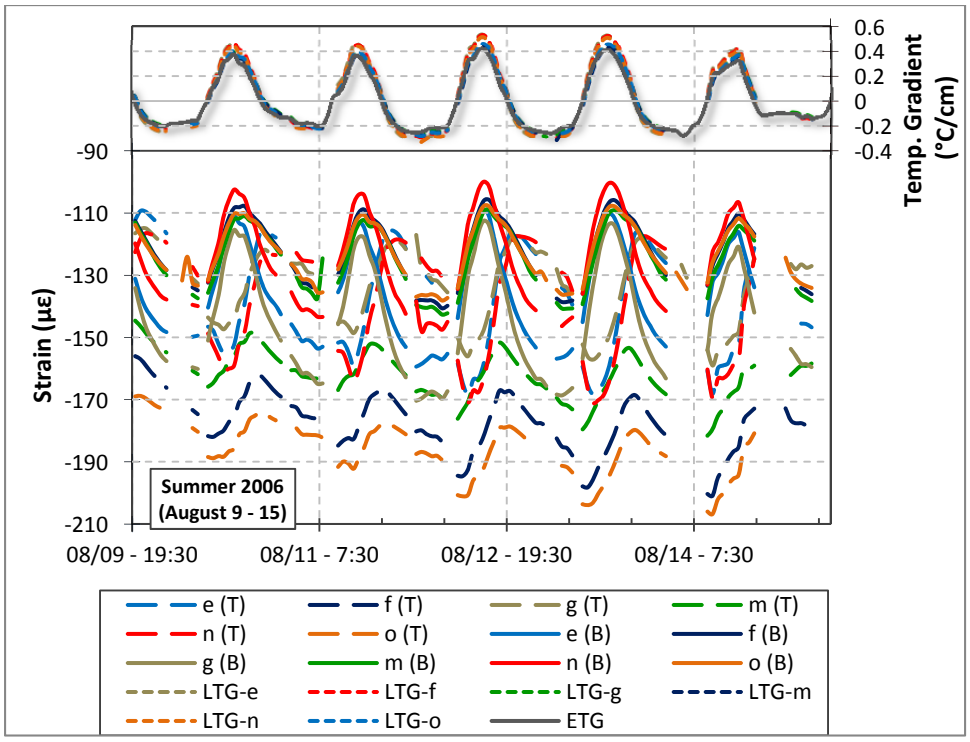
0.6
0.4
0.2
0
-0.2
-0.4
Temp. Gradient (°C/cm)
-90
-110
-130
-150
-170
-190
-210
Strain (με)
Summer 2006 (August 9 - 15)
08/09 - 19:30
08/11 - 7:30
08/12 - 19:30
08/14 - 7:30
e (T)
f (T)
g (T)
m (T)
n (T)
o (T)
e (B)
f (B)
g (B)
m (B)
n (B)
o (B)
LTG-e
LTG-f
LTG-g
LTG-m
LTG-n
LTG-o
ETG

(1°C/cm = 4.6°F/in)

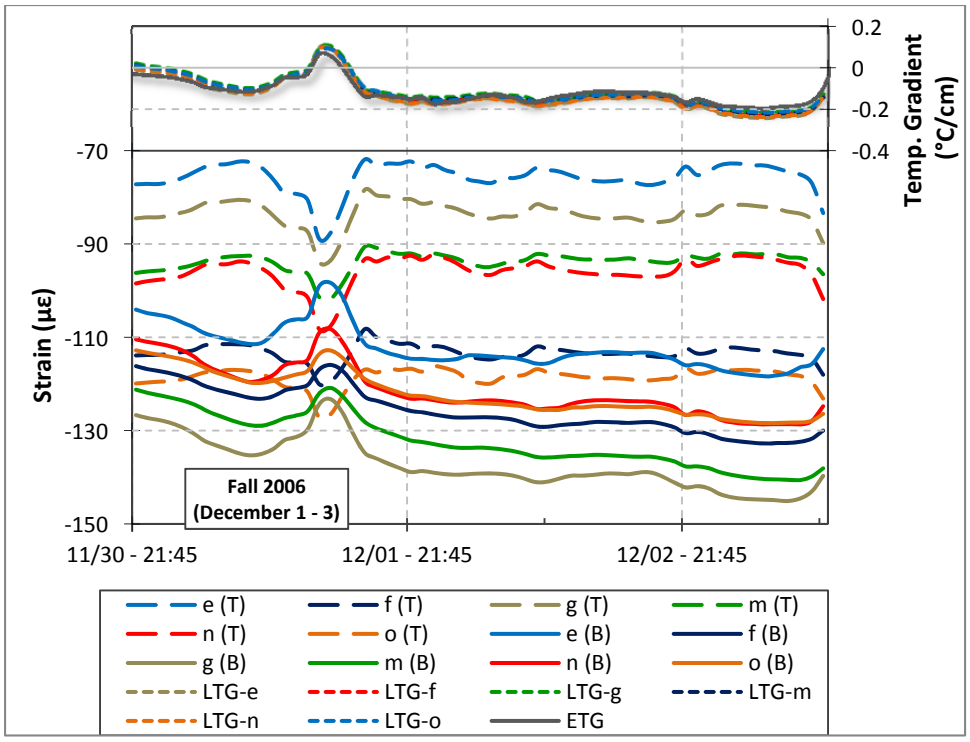
Strain (με)
Temp. Gradient (°C/cm)
0.2
0
-0.2
-0.4
-70
-90
-110
-130
-150
Fall 2006
(December 1 - 3)
11/30 - 21:45
12/01 - 21:45
12/02 - 21:45
e (T)
f (T)
g (T)
m (T)
n (T)
o (T)
e (B)
f (B)
g (B)
m (B)
n (B)
o (B)
LTG-e
LTG-f
LTG-g
LTG-m
LTG-n
LTG-o
ETG

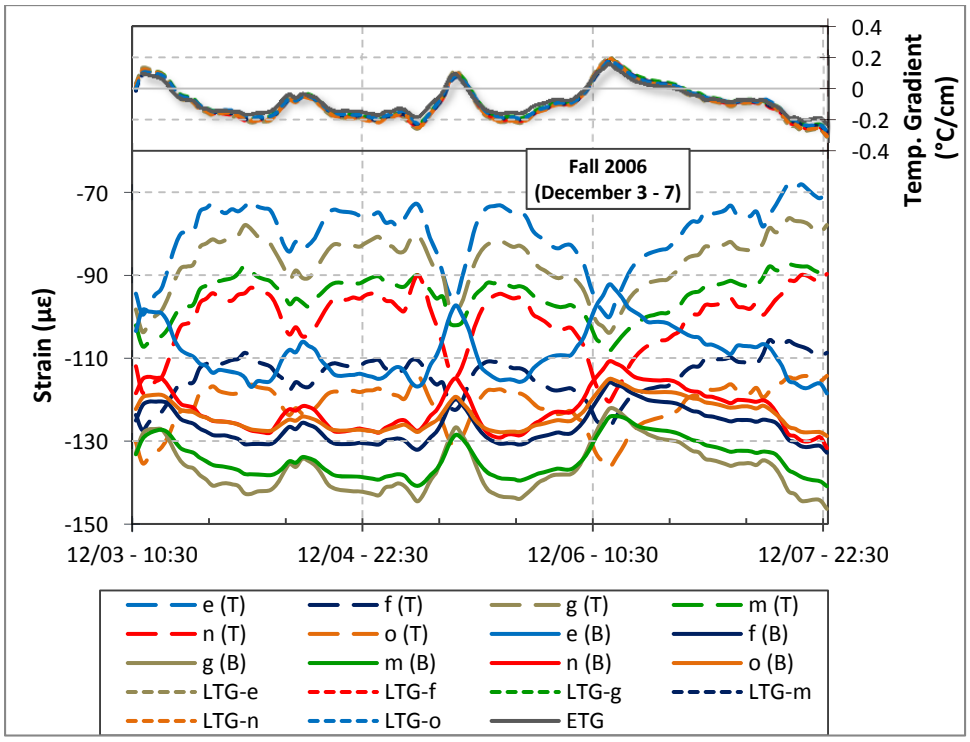
Strain (με)
Temp. Gradient (°C/cm)
0.4
0.2
0
-0.2
-0.4
-70
-90
-110
-130
-150
Fall 2006
(December 3 - 7)
12/03 - 10:30
12/04 - 22:30
12/06 - 10:30
12/07 - 22:30
e (T)
f (T)
g (T)
m (T)
n (T)
o (T)
e (B)
f (B)
g (B)
m (B)
n (B)
o (B)
LTG-e
LTG-f
LTG-g
LTG-m
LTG-n
LTG-o
ETG

(1°C/cm = 4.6°F/in)

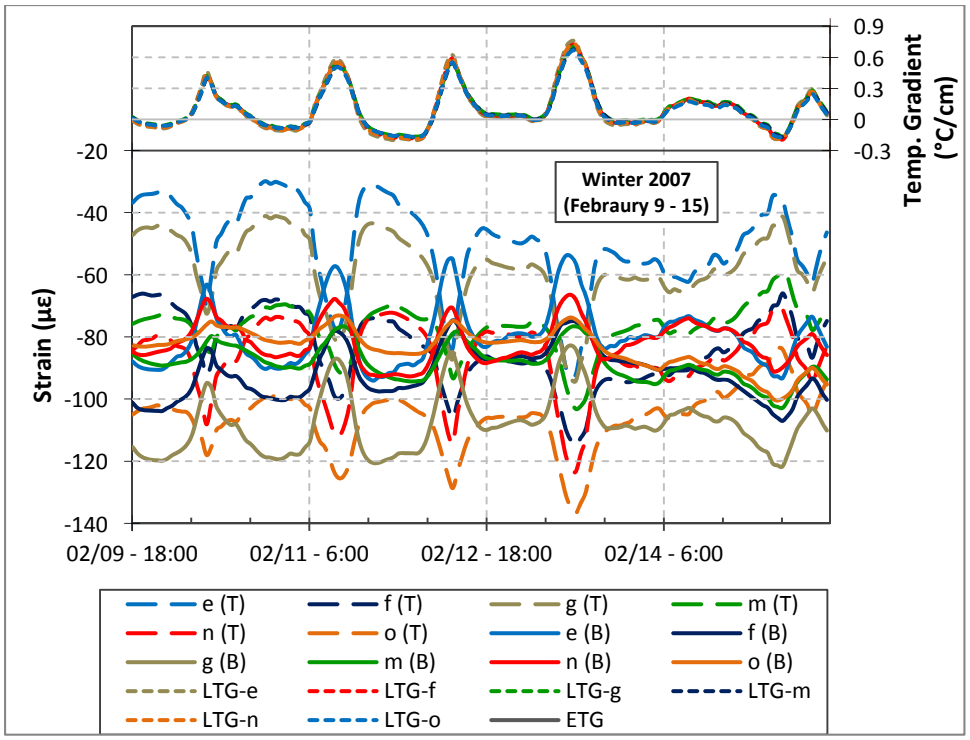
Winter 2007
(Febraury 9 - 15)
Strain (με)
Temp. Gradient (°C/cm)
0.9
0.6
0.3
0
-0.3
-20
-40
-60
-80
-100
-120
-140
02/09 - 18:00
02/11 - 6:00
02/12 - 18:00
02/14 - 6:00
e (T)
f (T)
g (T)
m (T)
n (T)
o (T)
e (B)
f (B)
g (B)
m (B)
n (B)
o (B)
LTG-e
LTG-f
LTG-g
LTG-m
LTG-n
LTG-o
ETG

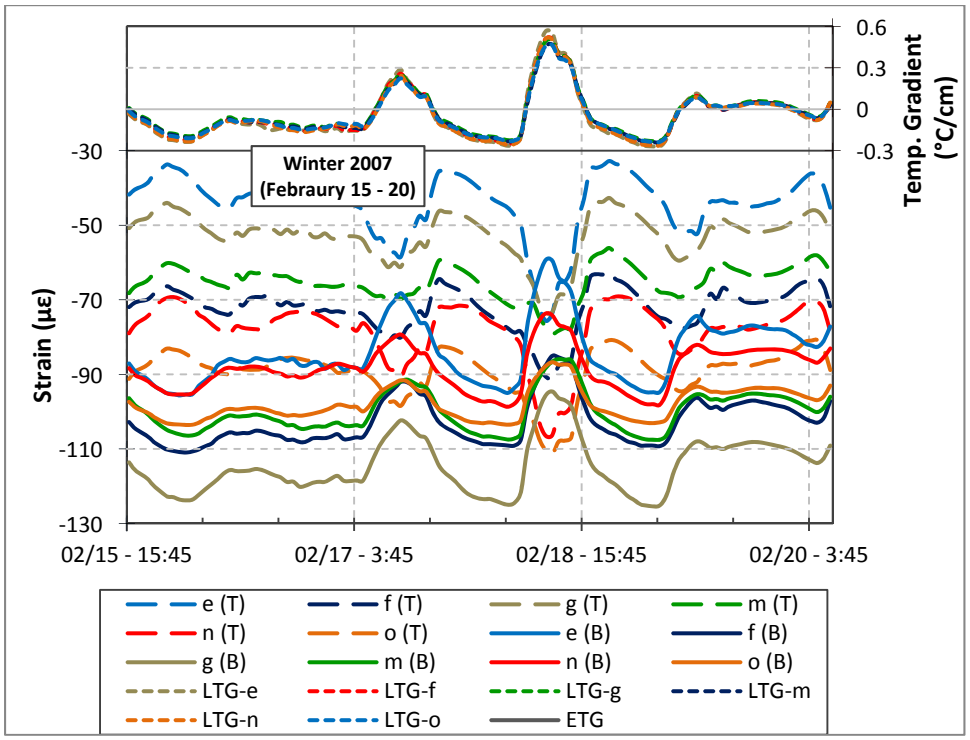
Winter 2007
(Febraury 15 - 20)
Strain (με)
Temp. Gradient (°C/cm)
0.6
0.3
0
-0.3
-30
-50
-70
-90
-110
-130
02/15 - 15:45
02/17 - 3:45
02/18 - 15:45
02/20 - 3:45
e (T)
f (T)
g (T)
m (T)
n (T)
o (T)
e (B)
f (B)
g (B)
m (B)
n (B)
o (B)
LTG-e
LTG-f
LTG-g
LTG-m
LTG-n
LTG-o
ETG

(1°C/cm = 4.6°F/in)

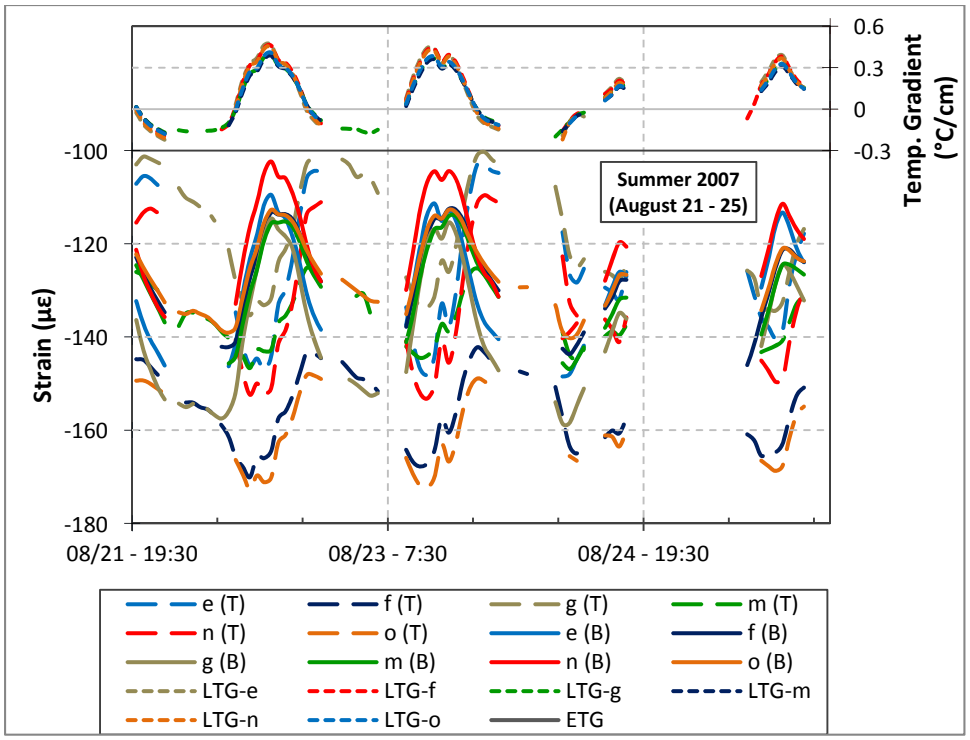
Summer 2007
(August 21 - 25)
Strain (με)
Temp. Gradient (°C/cm)
-100
-120
-140
-160
-180
0.6
0.3
0
-0.3
08/21 - 19:30
08/23 - 7:30
08/24 - 19:30
e (T)
f (T)
g (T)
m (T)
n (T)
o (T)
e (B)
f (B)
g (B)
m (B)
n (B)
o (B)
LTG-e
LTG-f
LTG-g
LTG-m
LTG-n
LTG-o
ETG

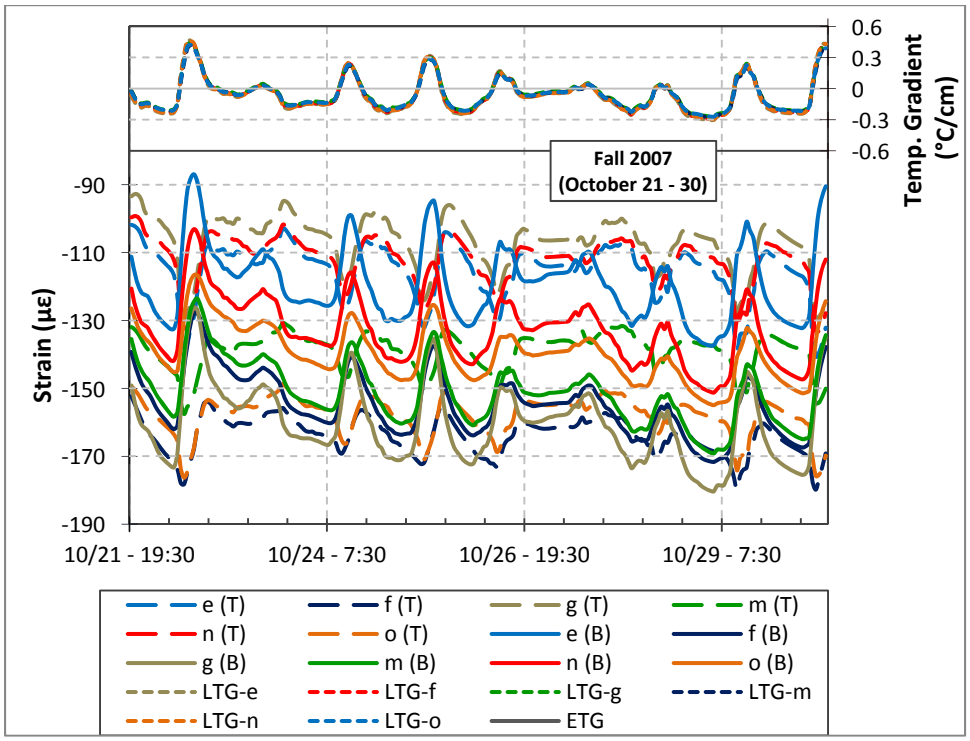
Fall 2007
(October 21 - 30)
Strain (με)
Temp. Gradient (°C/cm)
-90
-110
-130
-150
-170
-190
0.6
0.3
0
-0.3
-0.6
10/21 - 19:30
10/24 - 7:30
10/26 - 19:30
10/29 - 7:30
e (T)
f (T)
g (T)
m (T)
n (T)
o (T)
e (B)
f (B)
g (B)
m (B)
n (B)
o (B)
LTG-e
LTG-f
LTG-g
LTG-m
LTG-n
LTG-o
ETG

(1°C/cm = 4.6°F/in)

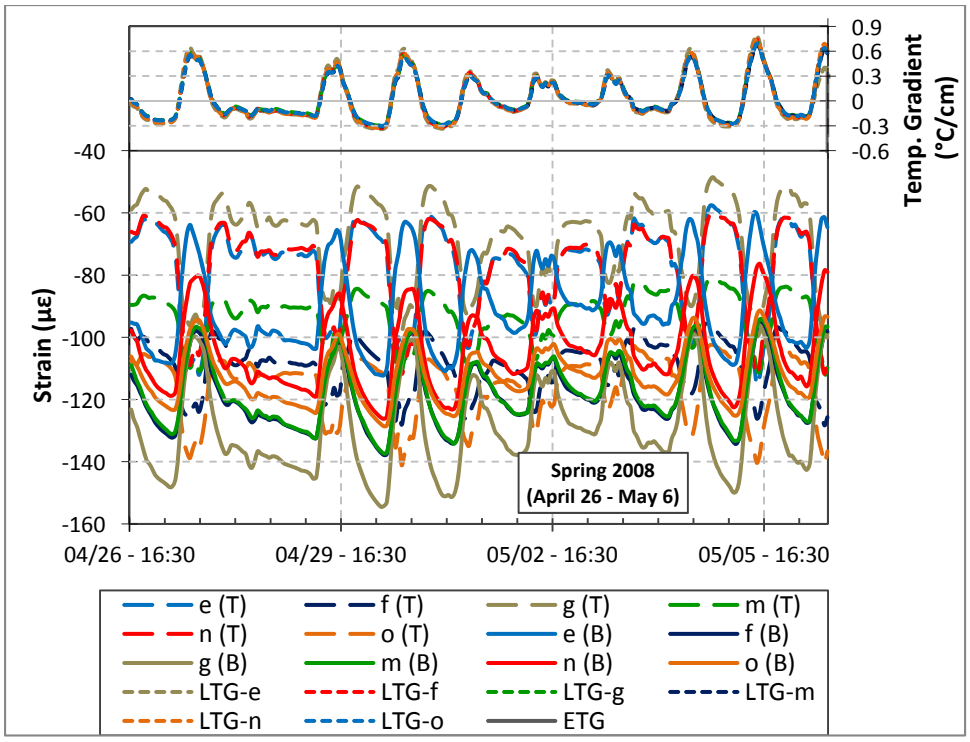
Temp. Gradient (°C/cm)
0.9
0.6
0.3
0
-0.3
-0.6
Strain (με)
-40
-60
-80
-100
-120
-140
-160
Spring 2008
(April 26 - May 6)
04/26 - 16:30
04/29 - 16:30
05/02 - 16:30
05/05 - 16:30
e (T)
f (T)
g (T)
m (T)
n (T)
o (T)
e (B)
f (B)
g (B)
m (B)
n (B)
o (B)
LTG-e
LTG-f
LTG-g
LTG-m
LTG-n
LTG-o
ETG

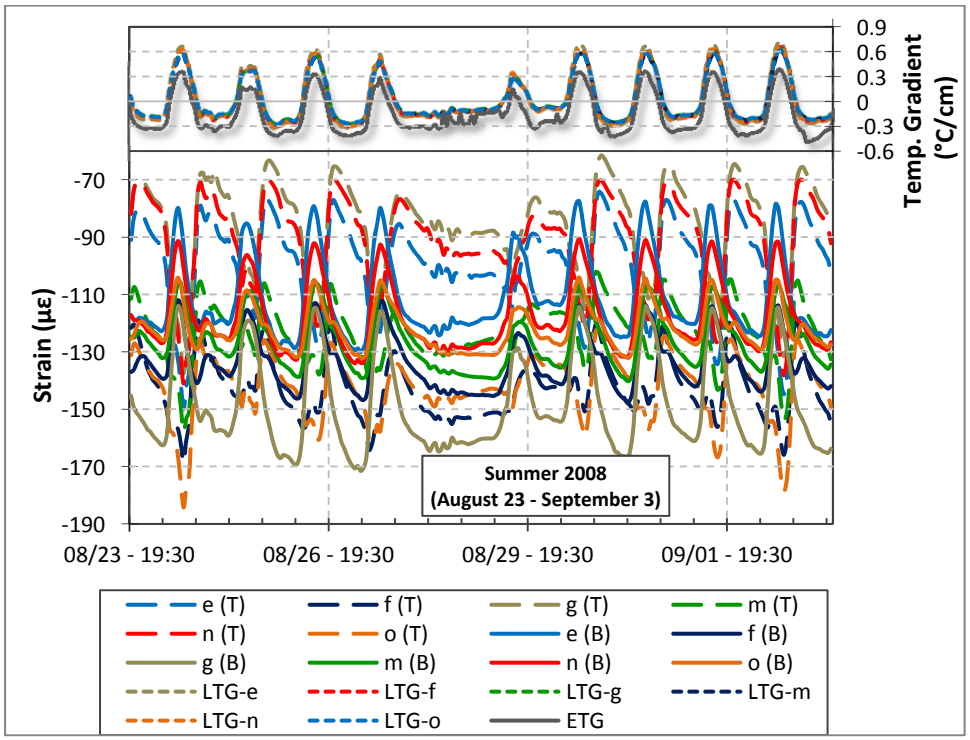
Temp. Gradient (°C/cm)
0.9
0.6
0.3
0
-0.3
-0.6
Strain (με)
-70
-90
-110
-130
-150
-170
-190
Summer 2008
(August 23 - September 3)
08/23 - 19:30
08/26 - 19:30
08/29 - 19:30
09/01 - 19:30
e (T)
f (T)
g (T)
m (T)
n (T)
o (T)
e (B)
f (B)
g (B)
m (B)
n (B)
o (B)
LTG-e
LTG-f
LTG-g
LTG-m
LTG-n
LTG-o
ETG

(1°C/cm = 4.6°F/in)

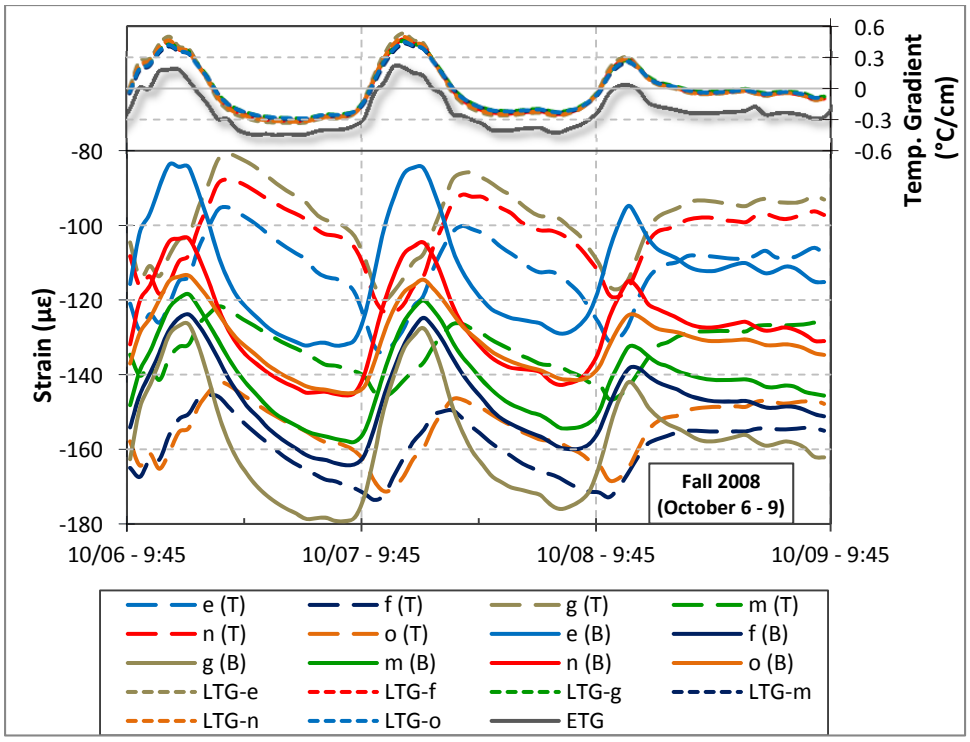
0.6
0.3
0
-0.3
-0.6
Temp. Gradient (°C/cm)
-80
-100
-120
-140
-160
-180
Strain (με)
Fall 2008
(October 6 - 9)
10/06 - 9:45
10/07 - 9:45
10/08 - 9:45
10/09 - 9:45
e (T)
f (T)
g (T)
m (T)
n (T)
o (T)
e (B)
f (B)
g (B)
m (B)
n (B)
o (B)
LTG-e
LTG-f
LTG-g
LTG-m
LTG-n
LTG-o
ETG

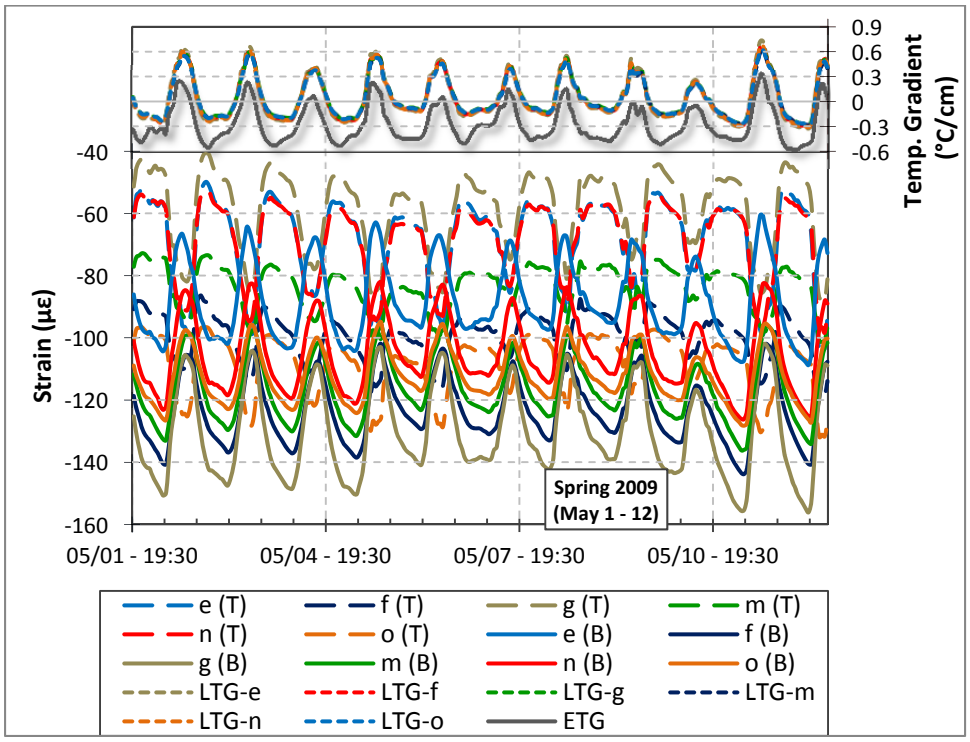
0.9
0.6
0.3
0
-0.3
-0.6
Temp. Gradient (°C/cm)
-40
-60
-80
-100
-120
-140
-160
Strain (με)
Spring 2009
(May 1 - 12)
05/01 - 19:30
05/04 - 19:30
05/07 - 19:30
05/10 - 19:30
e (T)
f (T)
g (T)
m (T)
n (T)
o (T)
e (B)
f (B)
g (B)
m (B)
n (B)
o (B)
LTG-e
LTG-f
LTG-g
LTG-m
LTG-n
LTG-o
ETG

(1°C/cm = 4.6°F/in)

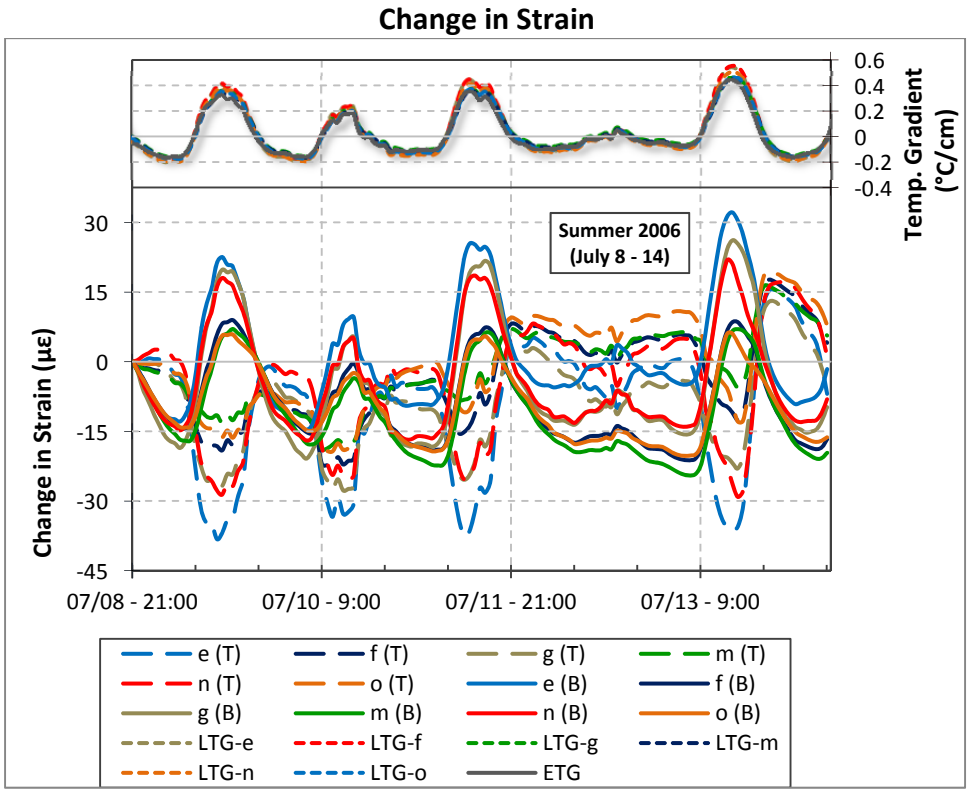
Change in Strain
Summer 2006
(July 8 - 14)
Change in Strain (με)
Temp. Gradient (°C/cm)
0.6
0.4
0.2
0
-0.2
-0.4
30
15
0
-15
-30
-45
07/08 - 21:00
07/10 - 9:00
07/11 - 21:00
07/13 - 9:00
e (T)
f (T)
g (T)
m (T)
n (T)
o (T)
e (B)
f (B)
g (B)
m (B)
n (B)
o (B)
LTG-e
LTG-f
LTG-g
LTG-m
LTG-n
LTG-o
ETG

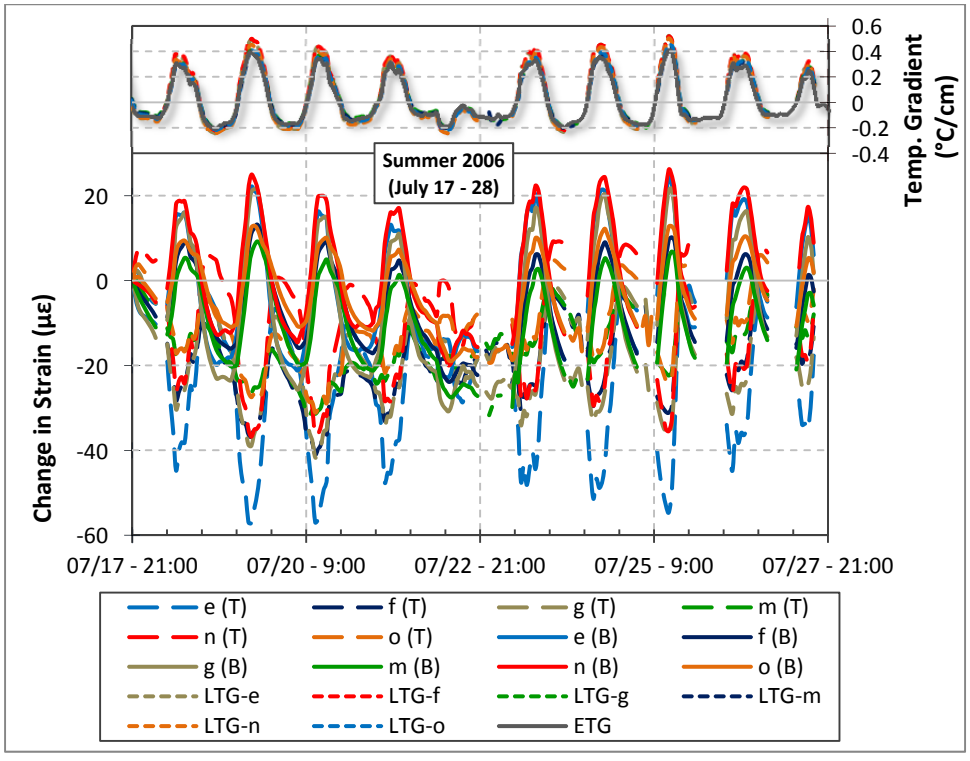
Summer 2006
(July 17 - 28)
Change in Strain (με)
Temp. Gradient (°C/cm)
0.6
0.4
0.2
0
-0.2
-0.4
20
0
-20
-40
-60
07/17 - 21:00
07/20 - 9:00
07/22 - 21:00
07/25 - 9:00
07/27 - 21:00
e (T)
f (T)
g (T)
m (T)
n (T)
o (T)
e (B)
f (B)
g (B)
m (B)
n (B)
o (B)
LTG-e
LTG-f
LTG-g
LTG-m
LTG-n
LTG-o
ETG

(1°C/cm = 4.6°F/in)

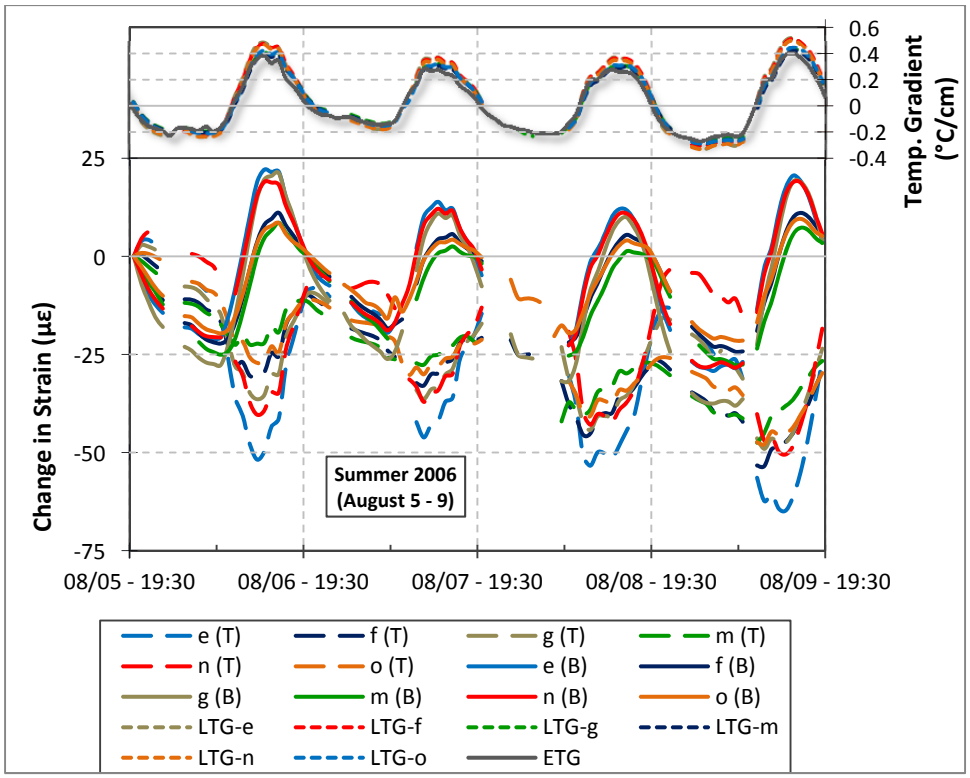
Temp. Gradient (°C/cm)
0.6
0.4
0.2
0
-0.2
-0.4
Change in Strain (με)
25
0
-25
-50
-75
Summer 2006
(August 5 - 9)
08/05 - 19:30
08/06 - 19:30
08/07 - 19:30
08/08 - 19:30
08/09 - 19:30
e (T)
f (T)
g (T)
m (T)
n (T)
o (T)
e (B)
f (B)
g (B)
m (B)
n (B)
o (B)
LTG-e
LTG-f
LTG-g
LTG-m
LTG-n
LTG-o
ETG

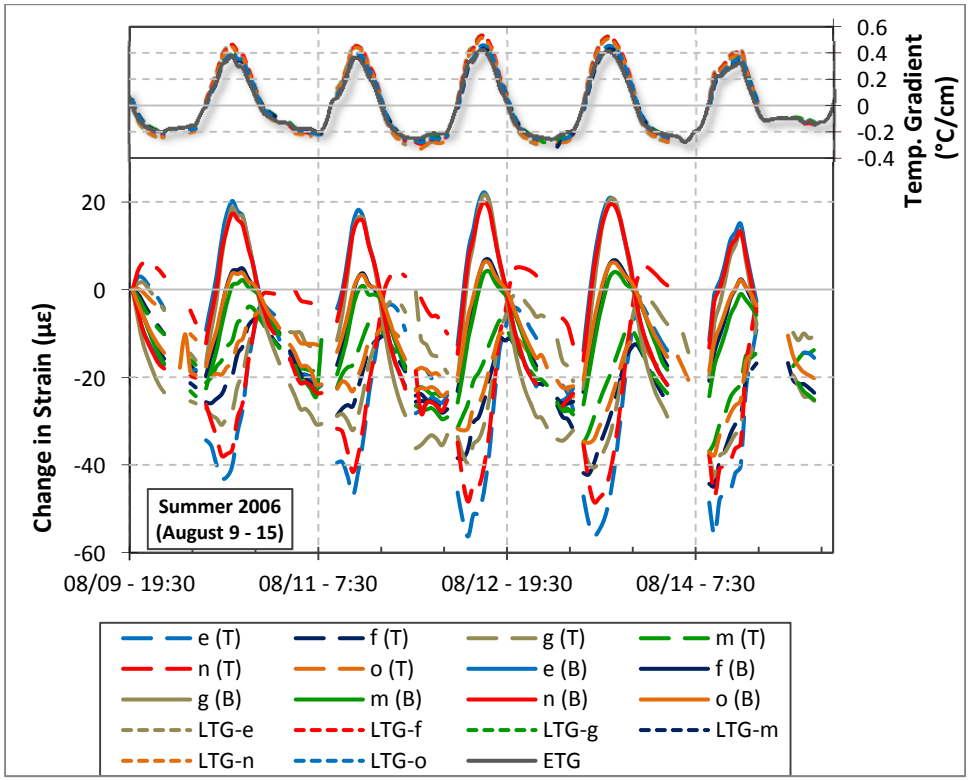
Temp. Gradient (°C/cm)
0.6
0.4
0.2
0
-0.2
-0.4
Change in Strain (με)
20
0
-20
-40
-60
Summer 2006
(August 9 - 15)
08/09 - 19:30
08/11 - 7:30
08/12 - 19:30
08/14 - 7:30
e (T)
f (T)
g (T)
m (T)
n (T)
o (T)
e (B)
f (B)
g (B)
m (B)
n (B)
o (B)
LTG-e
LTG-f
LTG-g
LTG-m
LTG-n
LTG-o
ETG

(1°C/cm = 4.6°F/in)

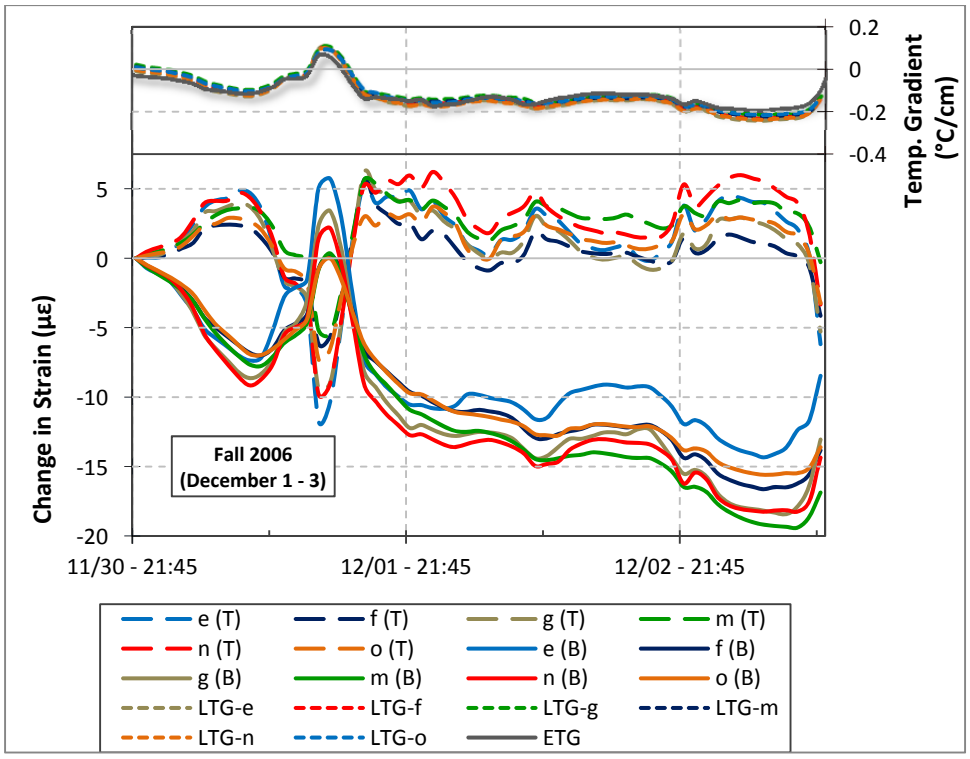
Temp. Gradient (°C/cm)
0.2
0
-0.2
-0.4
Change in Strain (με)
5
0
-5
-10
-15
-20
Fall 2006
(December 1 - 3)
11/30 - 21:45
12/01 - 21:45
12/02 - 21:45
e (T)
f (T)
g (T)
m (T)
n (T)
o (T)
e (B)
f (B)
g (B)
m (B)
n (B)
o (B)
LTG-e
LTG-f
LTG-g
LTG-m
LTG-n
LTG-o
ETG

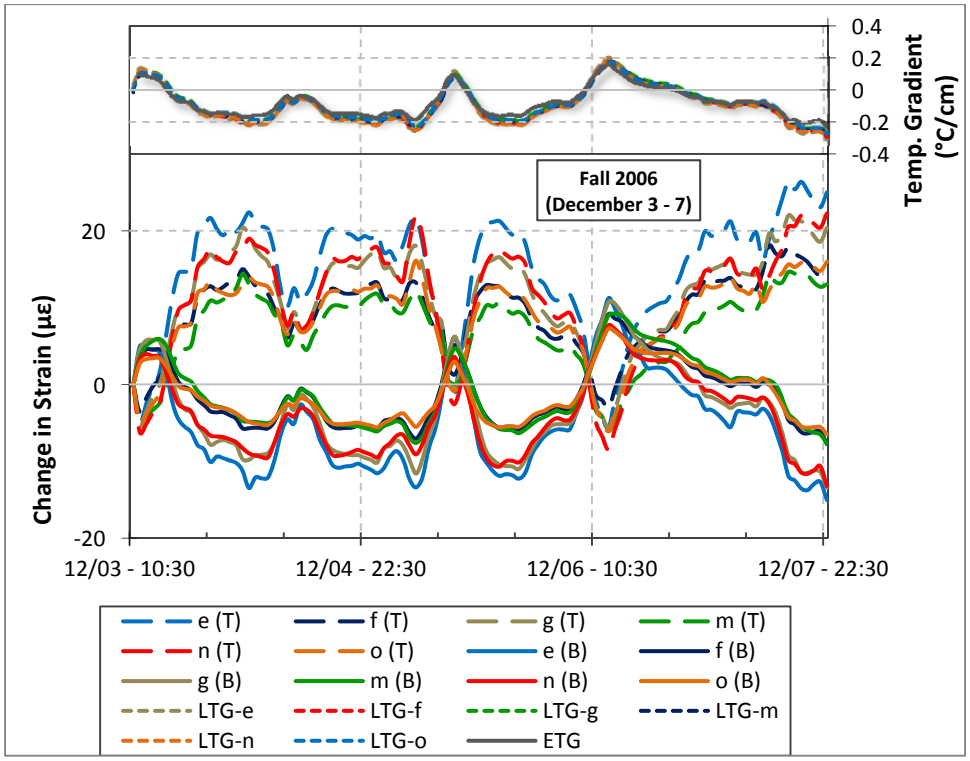
Temp. Gradient (°C/cm)
0.4
0.2
0
-0.2
-0.4
Change in Strain (με)
20
0
-20
Fall 2006
(December 3 - 7)
12/03 - 10:30
12/04 - 22:30
12/06 - 10:30
12/07 - 22:30
e (T)
f (T)
g (T)
m (T)
n (T)
o (T)
e (B)
f (B)
g (B)
m (B)
n (B)
o (B)
LTG-e
LTG-f
LTG-g
LTG-m
LTG-n
LTG-o
ETG

(1°C/cm = 4.6°F/in)

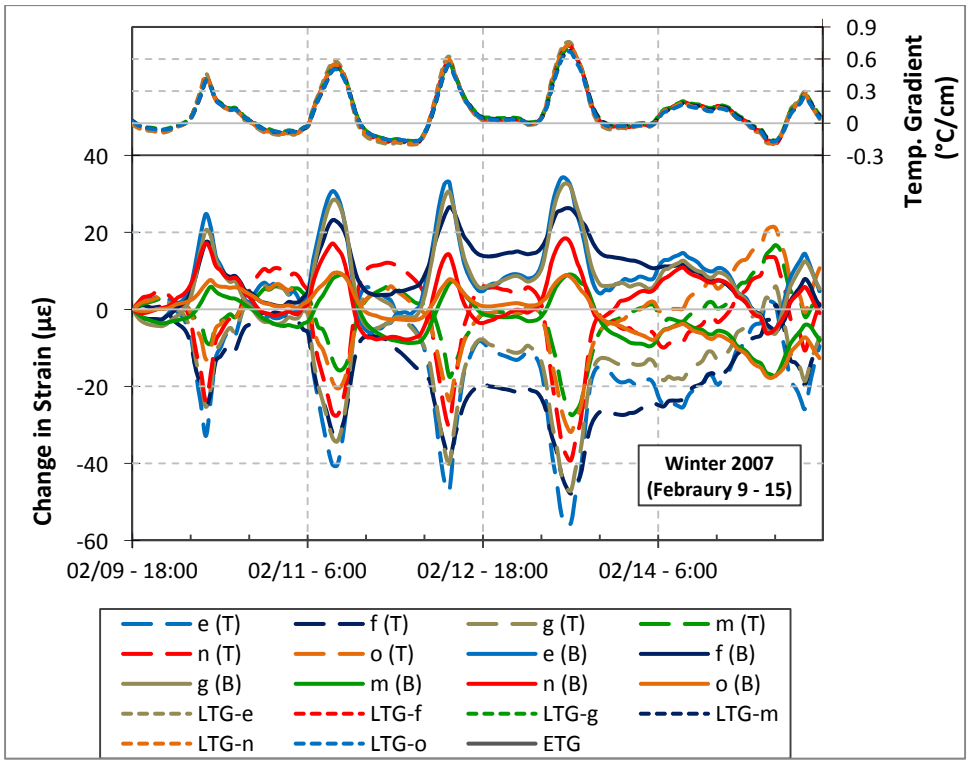
Temp. Gradient (°C/cm)
0.9
0.6
0.3
0
-0.3
Change in Strain (με)
40
20
0
-20
-40
-60
Winter 2007
(Febraury 9 - 15)
02/09 - 18:00
02/11 - 6:00
02/12 - 18:00
02/14 - 6:00
e (T)
f (T)
g (T)
m (T)
n (T)
o (T)
e (B)
f (B)
g (B)
m (B)
n (B)
o (B)
LTG-e
LTG-f
LTG-g
LTG-m
LTG-n
LTG-o
ETG

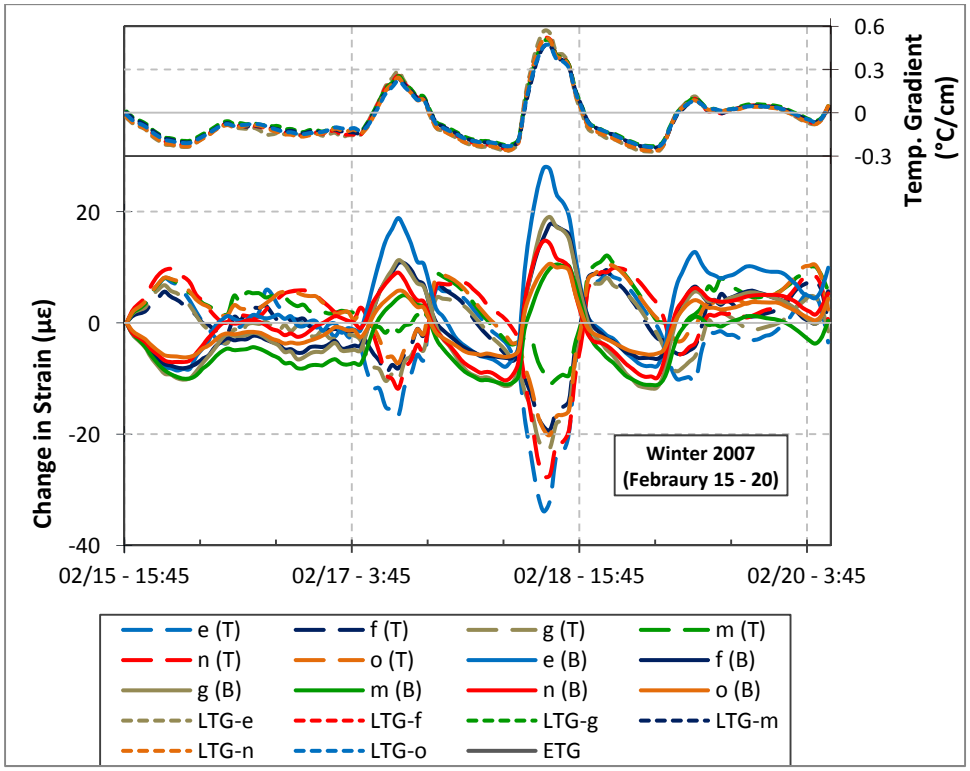
Temp. Gradient (°C/cm)
0.6
0.3
0
-0.3
Change in Strain (με)
20
0
-20
-40
Winter 2007
(Febraury 15 - 20)
02/15 - 15:45
02/17 - 3:45
02/18 - 15:45
02/20 - 3:45
e (T)
f (T)
g (T)
m (T)
n (T)
o (T)
e (B)
f (B)
g (B)
m (B)
n (B)
o (B)
LTG-e
LTG-f
LTG-g
LTG-m
LTG-n
LTG-o
ETG

(1°C/cm = 4.6°F/in)

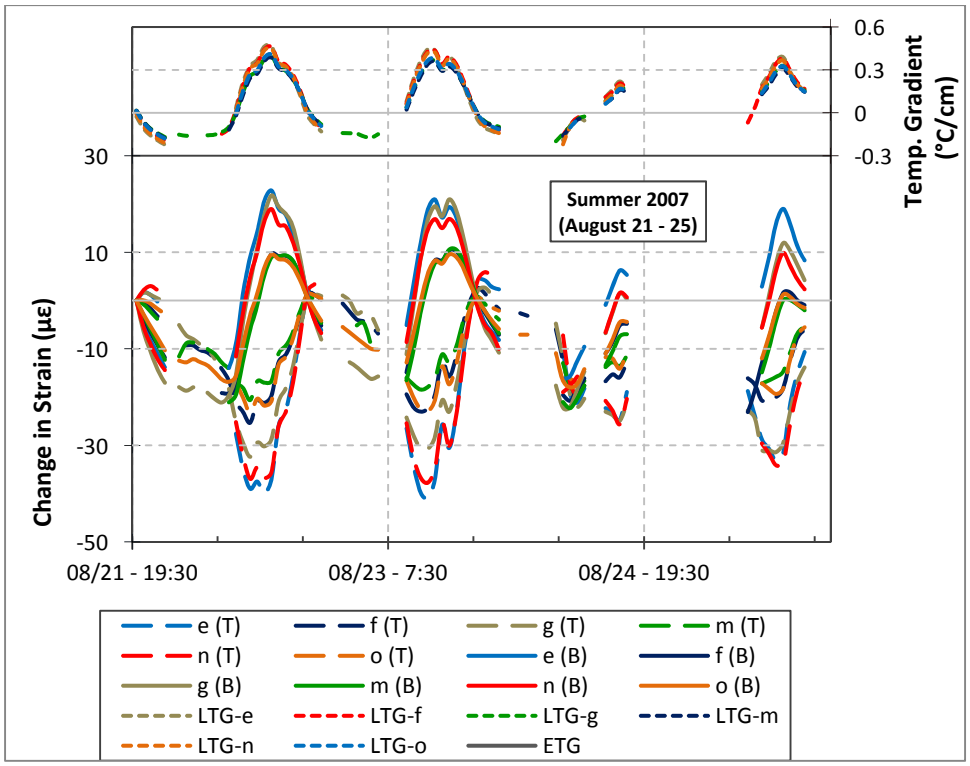
Summer 2007
(August 21 - 25)
Change in Strain (με)
Temp. Gradient (°C/cm)
30
10
-10
-30
-50
0.6
0.3
0
-0.3
08/21 - 19:30
08/23 - 7:30
08/24 - 19:30
e (T)
f (T)
g (T)
m (T)
n (T)
o (T)
e (B)
f (B)
g (B)
m (B)
n (B)
o (B)
LTG-e
LTG-f
LTG-g
LTG-m
LTG-n
LTG-o
ETG

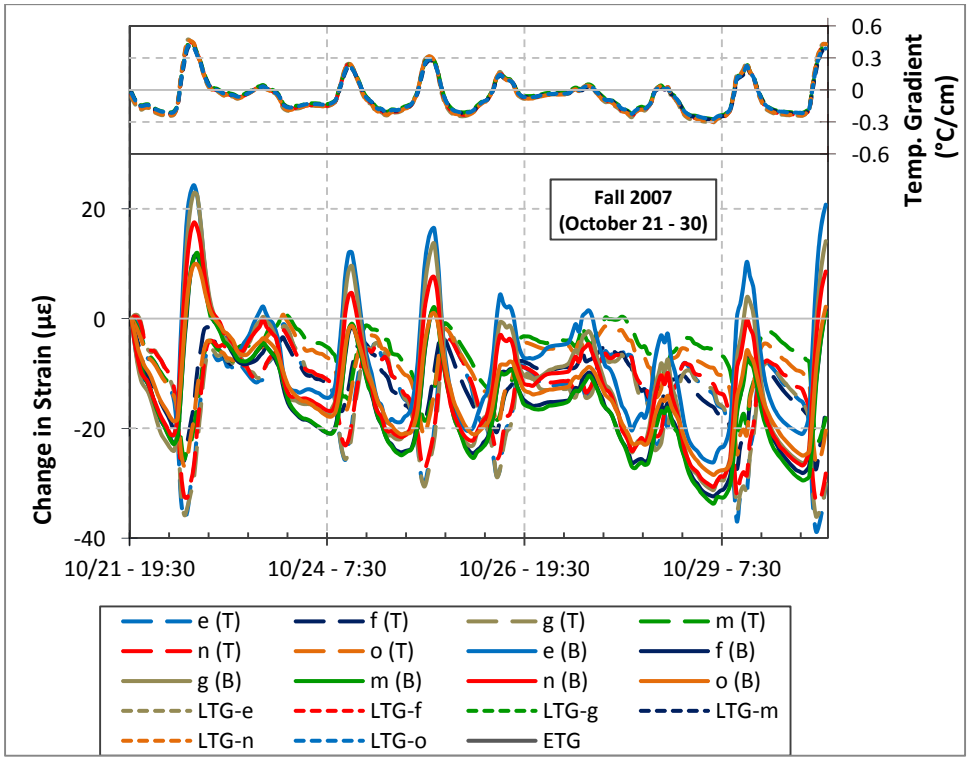
Fall 2007
(October 21 - 30)
Change in Strain (με)
Temp. Gradient (°C/cm)
20
0
-20
-40
0.6
0.3
0
-0.3
-0.6
10/21 - 19:30
10/24 - 7:30
10/26 - 19:30
10/29 - 7:30
e (T)
f (T)
g (T)
m (T)
n (T)
o (T)
e (B)
f (B)
g (B)
m (B)
n (B)
o (B)
LTG-e
LTG-f
LTG-g
LTG-m
LTG-n
LTG-o
ETG

(1°C/cm = 4.6°F/in)

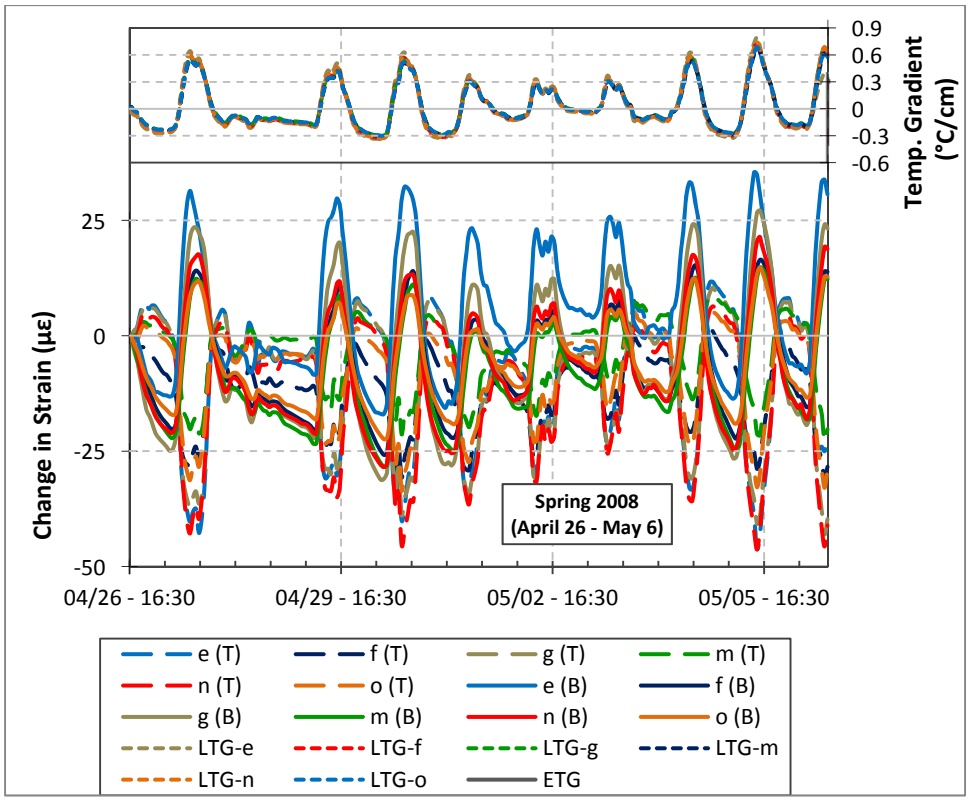
Temp. Gradient (°C/cm)
0.9
0.6
0.3
0
-0.3
-0.6
Change in Strain (με)
25
0
-25
-50
Spring 2008
(April 26 - May 6)
04/26 - 16:30
04/29 - 16:30
05/02 - 16:30
05/05 - 16:30
e (T)
f (T)
g (T)
m (T)
n (T)
o (T)
e (B)
f (B)
g (B)
m (B)
n (B)
o (B)
LTG-e
LTG-f
LTG-g
LTG-m
LTG-n
LTG-o
ETG

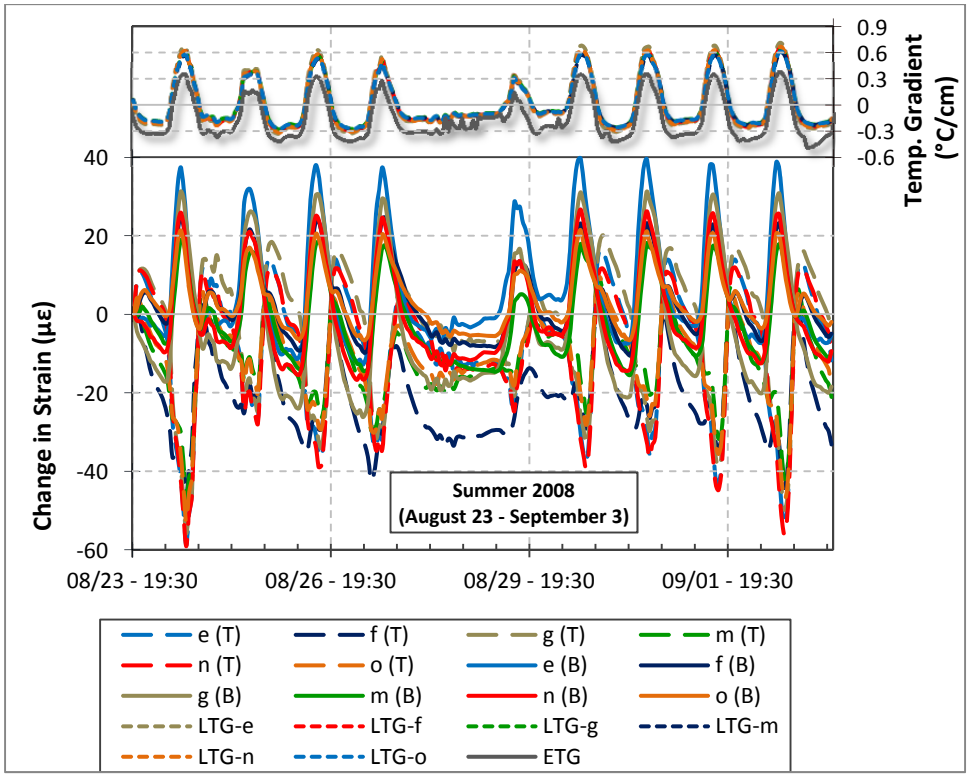
Temp. Gradient (°C/cm)
0.9
0.6
0.3
0
-0.3
-0.6
Change in Strain (με)
40
20
0
-20
-40
-60
Summer 2008
(August 23 - September 3)
08/23 - 19:30
08/26 - 19:30
08/29 - 19:30
09/01 - 19:30
e (T)
f (T)
g (T)
m (T)
n (T)
o (T)
e (B)
f (B)
g (B)
m (B)
n (B)
o (B)
LTG-e
LTG-f
LTG-g
LTG-m
LTG-n
LTG-o
ETG

(1°C/cm = 4.6°F/in)

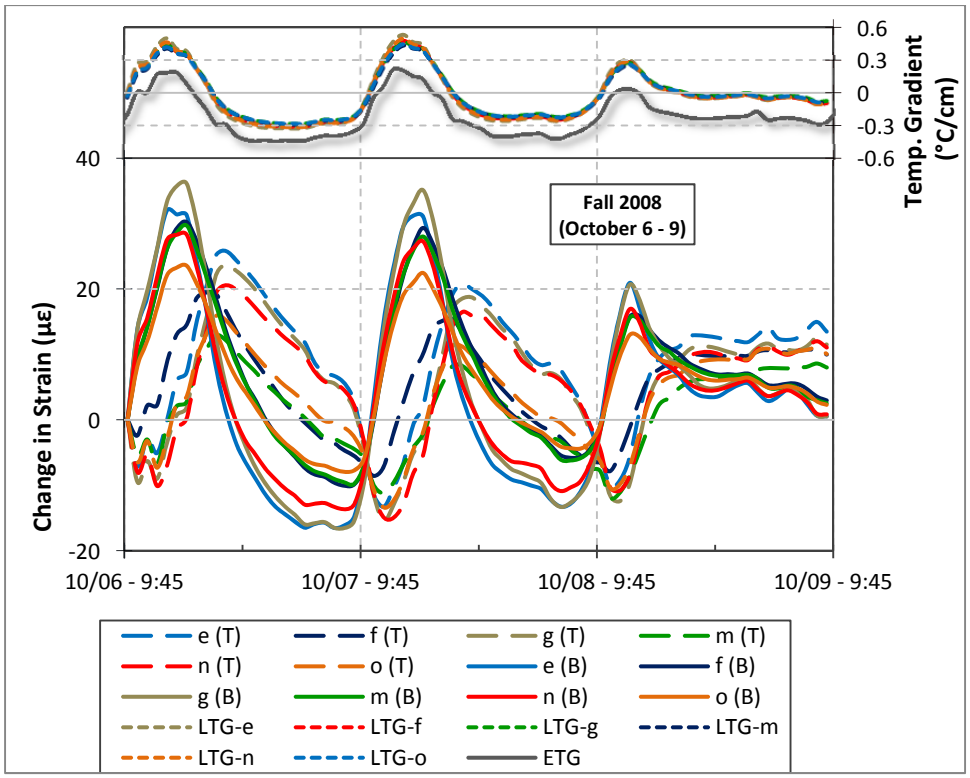
Fall 2008
(October 6 - 9)
Change in Strain (με)
Temp. Gradient (°C/cm)
40
20
0
-20
0.6
0.3
0
-0.3
-0.6
10/06 - 9:45
10/07 - 9:45
10/08 - 9:45
10/09 - 9:45
e (T)
f (T)
g (T)
m (T)
n (T)
o (T)
e (B)
f (B)
g (B)
m (B)
n (B)
o (B)
LTG-e
LTG-f
LTG-g
LTG-m
LTG-n
LTG-o
ETG

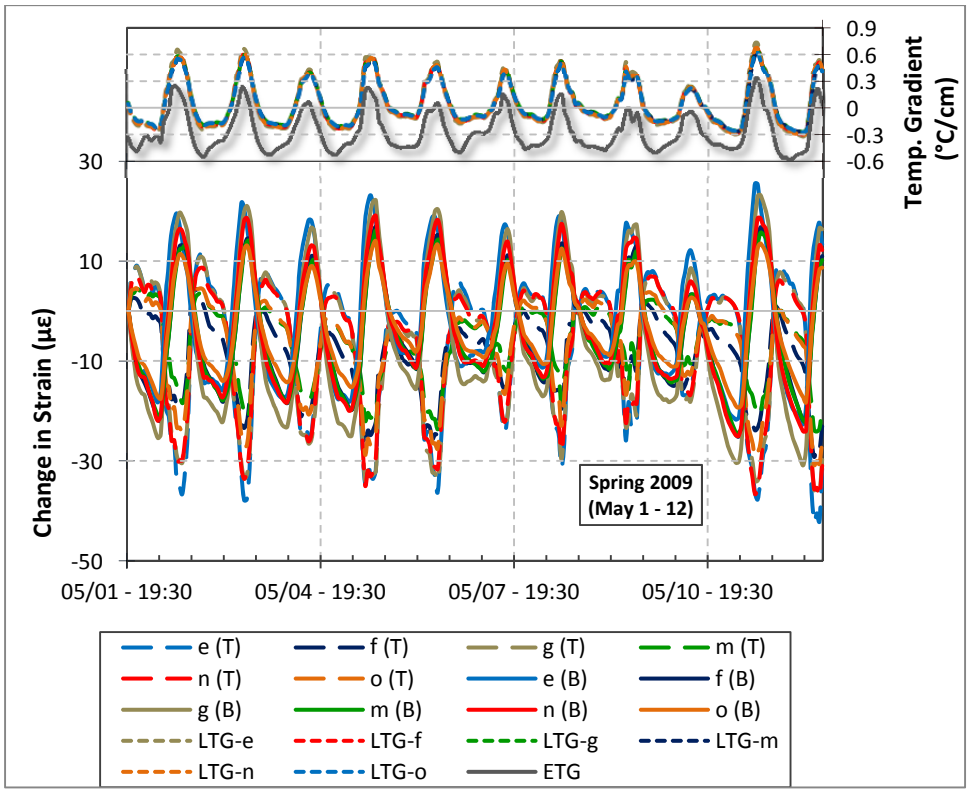
Spring 2009
(May 1 - 12)
Change in Strain (με)
Temp. Gradient (°C/cm)
30
10
-10
-30
-50
0.9
0.6
0.3
0
-0.3
-0.6
05/01 - 19:30
05/04 - 19:30
05/07 - 19:30
05/10 - 19:30
e (T)
f (T)
g (T)
m (T)
n (T)
o (T)
e (B)
f (B)
g (B)
m (B)
n (B)
o (B)
LTG-e
LTG-f
LTG-g
LTG-m
LTG-n
LTG-o
ETG

(1°C/cm = 4.6°F/in)

Pavement Strains (Common Periods)

Rubblized Section

Load-Related Strain

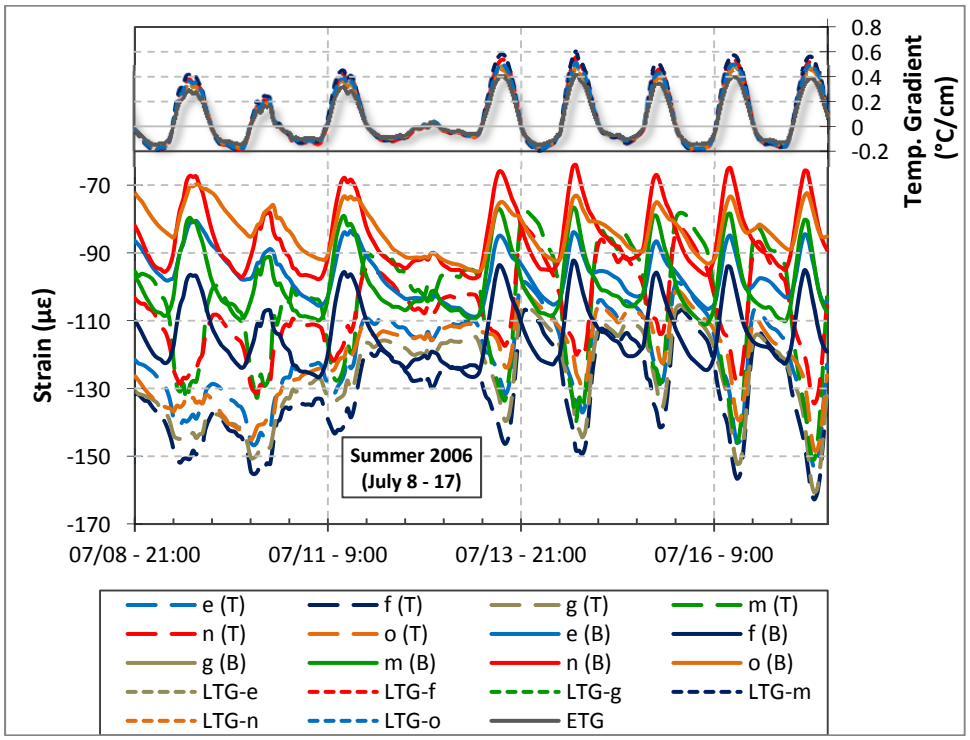

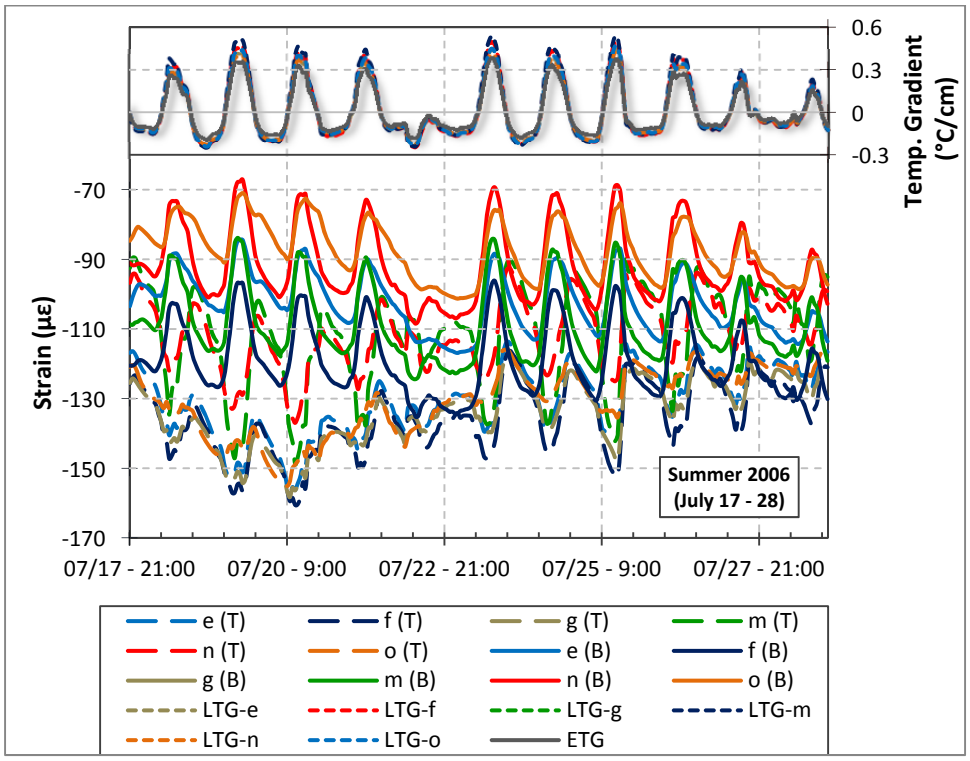

(1°C/cm = 4.6°F/in)

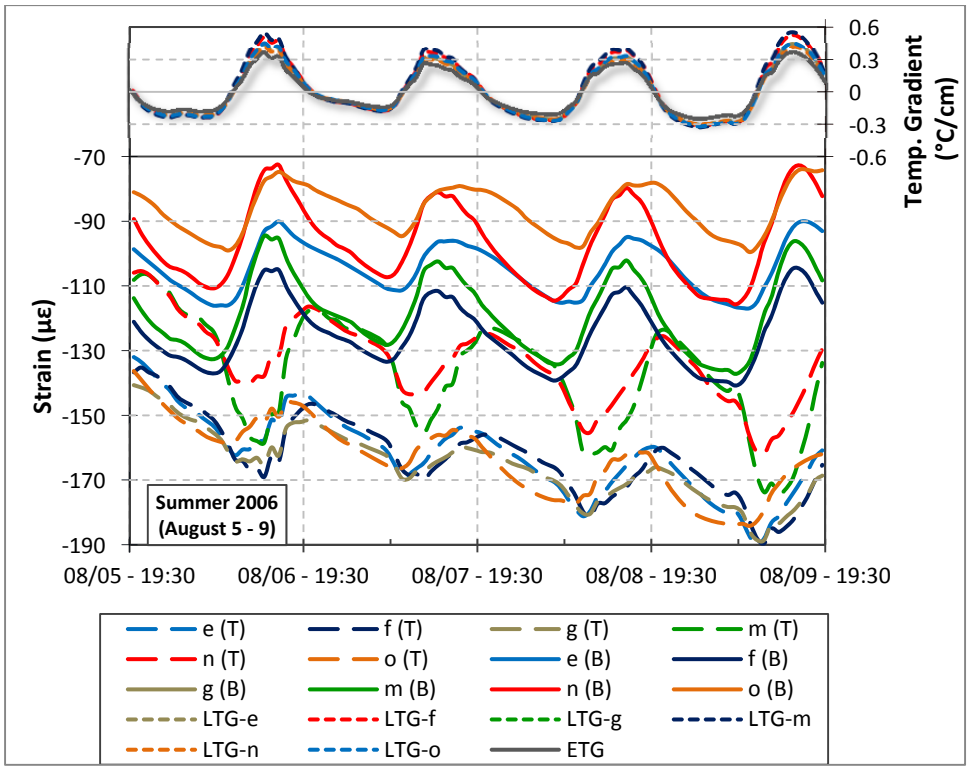
Temp. Gradient (°C/cm)
0.6
0.3
0
-0.3
-0.6
Strain (με)
-70
-90
-110
-130
-150
-170
-190
Summer 2006
(August 5 - 9)
08/05 - 19:30
08/06 - 19:30
08/07 - 19:30
08/08 - 19:30
08/09 - 19:30
e (T)
f (T)
g (T)
m (T)
n (T)
o (T)
e (B)
f (B)
g (B)
m (B)
n (B)
o (B)
LTG-e
LTG-f
LTG-g
LTG-m
LTG-n
LTG-o
ETG

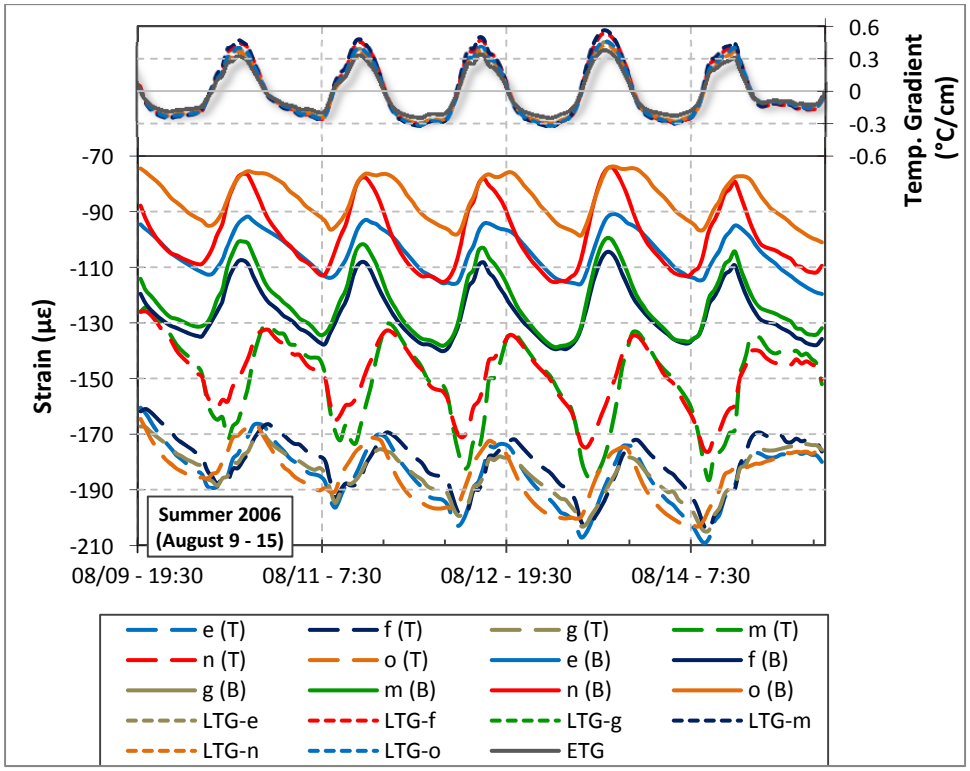
Temp. Gradient (°C/cm)
0.6
0.3
0
-0.3
-0.6
Strain (με)
-70
-90
-110
-130
-150
-170
-190
-210
Summer 2006
(August 9 - 15)
08/09 - 19:30
08/11 - 7:30
08/12 - 19:30
08/14 - 7:30
e (T)
f (T)
g (T)
m (T)
n (T)
o (T)
e (B)
f (B)
g (B)
m (B)
n (B)
o (B)
LTG-e
LTG-f
LTG-g
LTG-m
LTG-n
LTG-o
ETG

(1°C/cm = 4.6°F/in)

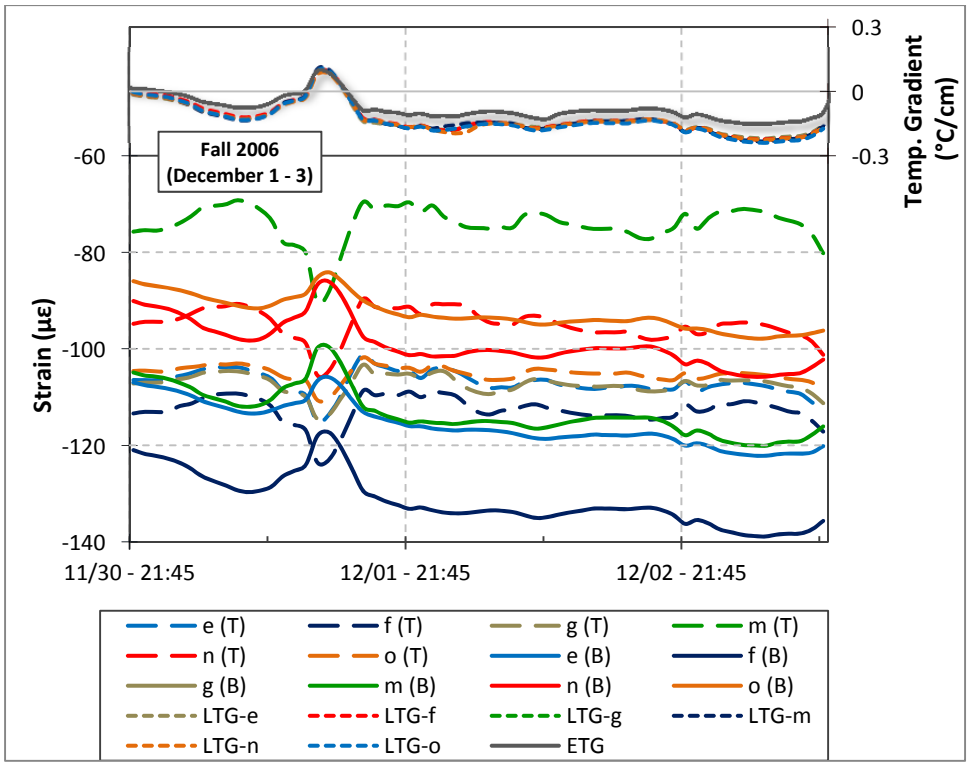
Fall 2006
(December 1 - 3)
Strain (με)
-60
-80
-100
-120
-140
11/30 - 21:45
12/01 - 21:45
12/02 - 21:45
0.3
0
-0.3
Temp. Gradient (°C/cm)
e (T)
f (T)
g (T)
m (T)
n (T)
o (T)
e (B)
f (B)
g (B)
m (B)
n (B)
o (B)
LTG-e
LTG-f
LTG-g
LTG-m
LTG-n
LTG-o
ETG

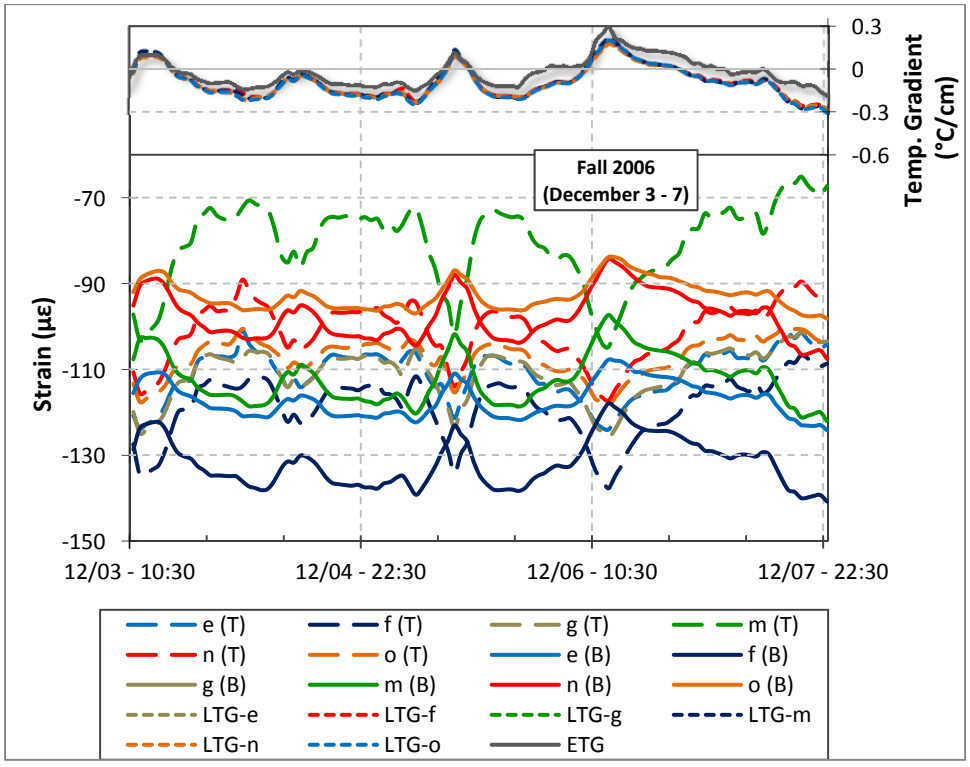
Fall 2006
(December 3 - 7)
Strain (με)
-70
-90
-110
-130
-150
12/03 - 10:30
12/04 - 22:30
12/06 - 10:30
12/07 - 22:30
0.3
0
-0.3
-0.6
Temp. Gradient (°C/cm)
e (T)
f (T)
g (T)
m (T)
n (T)
o (T)
e (B)
f (B)
g (B)
m (B)
n (B)
o (B)
LTG-e
LTG-f
LTG-g
LTG-m
LTG-n
LTG-o
ETG

(1°C/cm = 4.6°F/in)

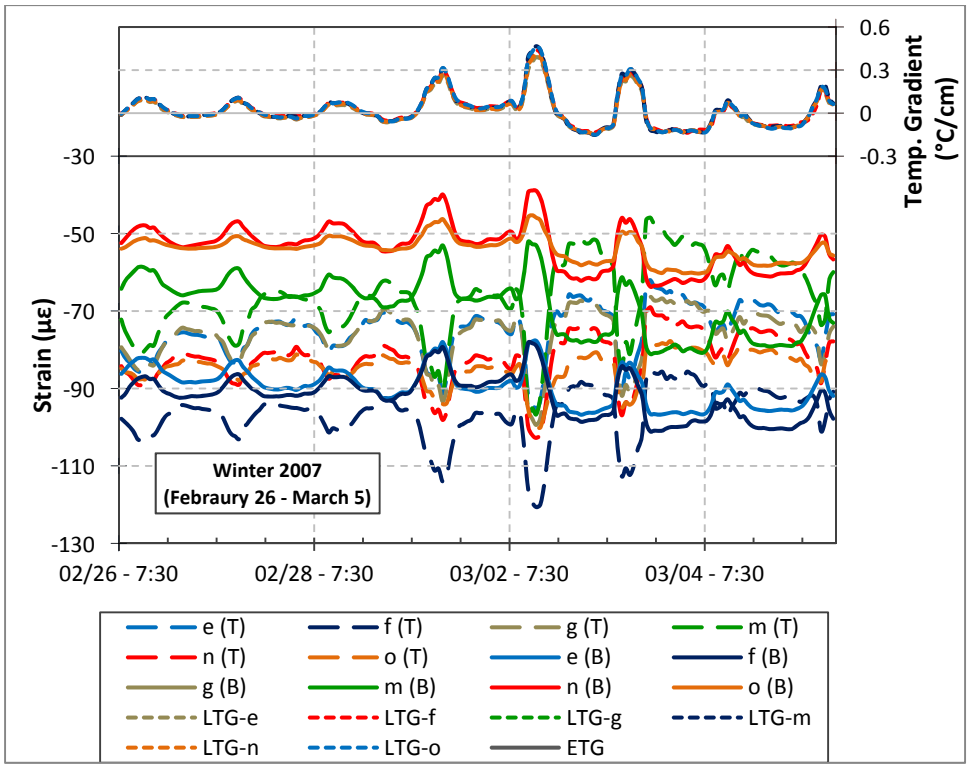
0.6
0.3
0
-0.3
Temp. Gradient (°C/cm)
-30
-50
-70
-90
-110
-130
Strain (με)
Winter 2007
(Febraury 26 - March 5)
02/26 - 7:30
02/28 - 7:30
03/02 - 7:30
03/04 - 7:30
e (T)
f (T)
g (T)
m (T)
n (T)
o (T)
e (B)
f (B)
g (B)
m (B)
n (B)
o (B)
LTG-e
LTG-f
LTG-g
LTG-m
LTG-n
LTG-o
ETG

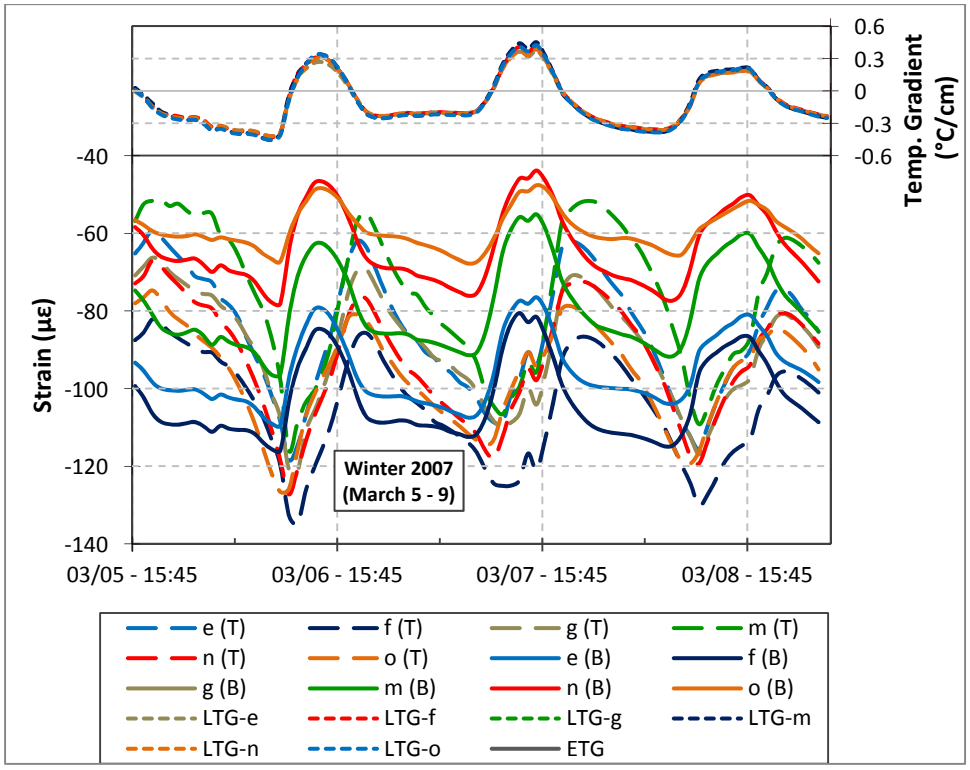
0.6
0.3
0
-0.3
-0.6
Temp. Gradient (°C/cm)
-40
-60
-80
-100
-120
-140
Strain (με)
Winter 2007
(March 5 - 9)
03/05 - 15:45
03/06 - 15:45
03/07 - 15:45
03/08 - 15:45
e (T)
f (T)
g (T)
m (T)
n (T)
o (T)
e (B)
f (B)
g (B)
m (B)
n (B)
o (B)
LTG-e
LTG-f
LTG-g
LTG-m
LTG-n
LTG-o
ETG

(1°C/cm = 4.6°F/in)

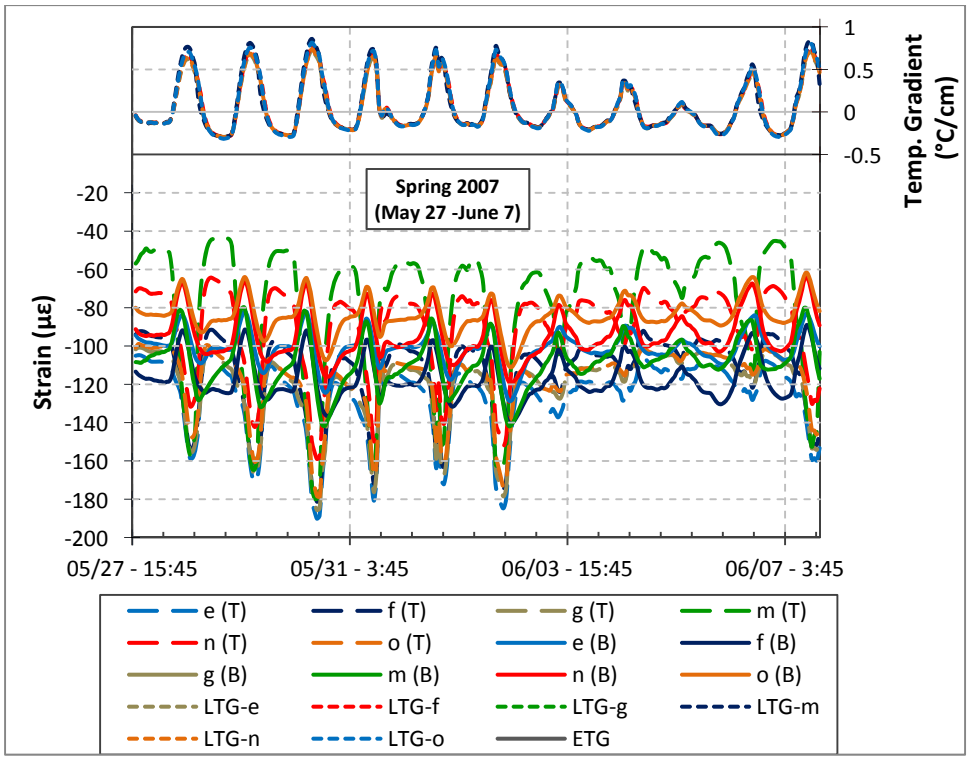
Spring 2007
(May 27 -June 7)
Strain (με)
Temp. Gradient (°C/cm)
1
0.5
0
-0.5
-20
-40
-60
-80
-100
-120
-140
-160
-180
-200
05/27 - 15:45
05/31 - 3:45
06/03 - 15:45
06/07 - 3:45
e (T)
f (T)
g (T)
m (T)
n (T)
o (T)
e (B)
f (B)
g (B)
m (B)
n (B)
o (B)
LTG-e
LTG-f
LTG-g
LTG-m
LTG-n
LTG-o
ETG

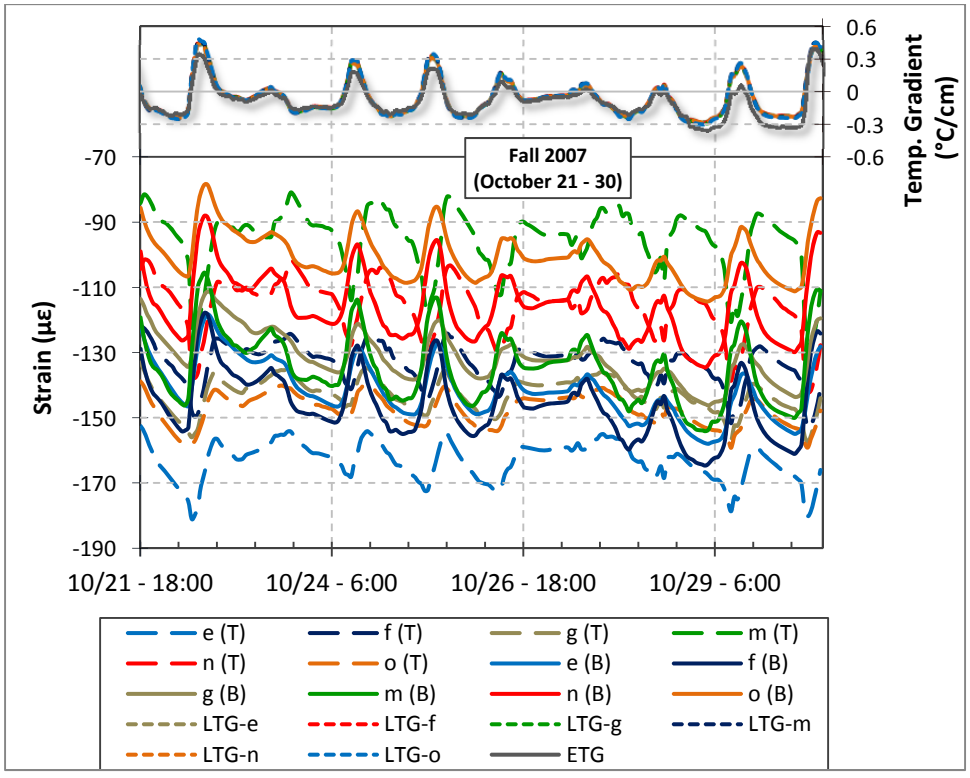
Fall 2007
(October 21 - 30)
Strain (με)
Temp. Gradient (°C/cm)
0.6
0.3
0
-0.3
-0.6
-70
-90
-110
-130
-150
-170
-190
10/21 - 18:00
10/24 - 6:00
10/26 - 18:00
10/29 - 6:00
e (T)
f (T)
g (T)
m (T)
n (T)
o (T)
e (B)
f (B)
g (B)
m (B)
n (B)
o (B)
LTG-e
LTG-f
LTG-g
LTG-m
LTG-n
LTG-o
ETG

(1°C/cm = 4.6°F/in)

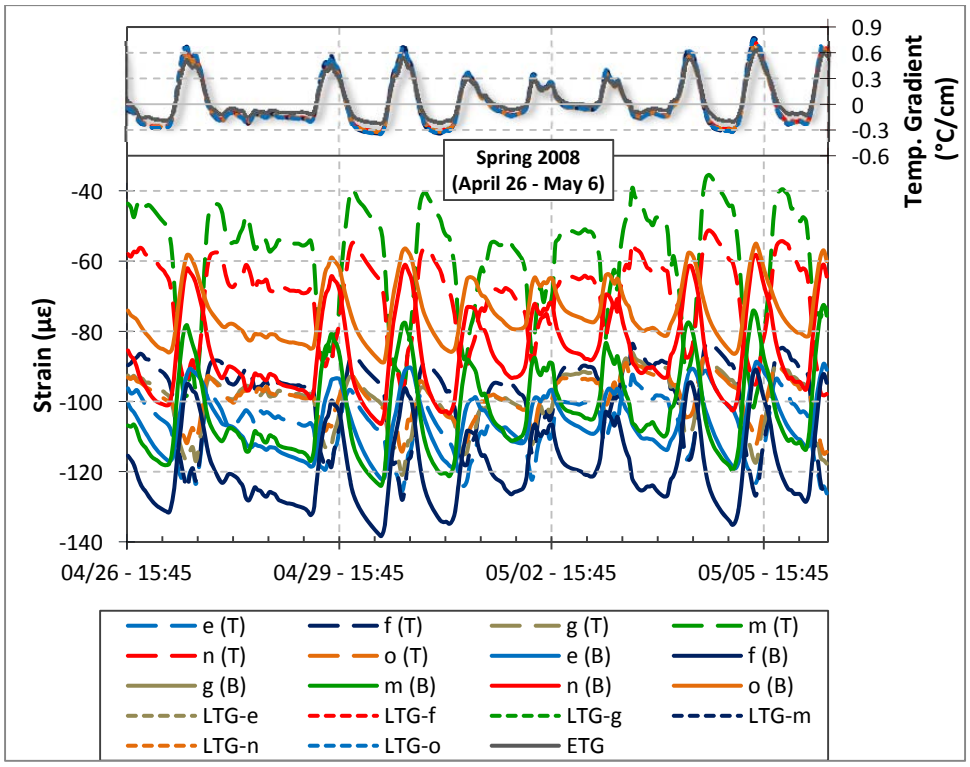
Spring 2008
(April 26 - May 6)
Strain (με)
Temp. Gradient (°C/cm)
0.9
0.6
0.3
0
-0.3
-0.6
-40
-60
-80
-100
-120
-140
04/26 - 15:45
04/29 - 15:45
05/02 - 15:45
05/05 - 15:45
e (T)
f (T)
g (T)
m (T)
n (T)
o (T)
e (B)
f (B)
g (B)
m (B)
n (B)
o (B)
LTG-e
LTG-f
LTG-g
LTG-m
LTG-n
LTG-o
ETG

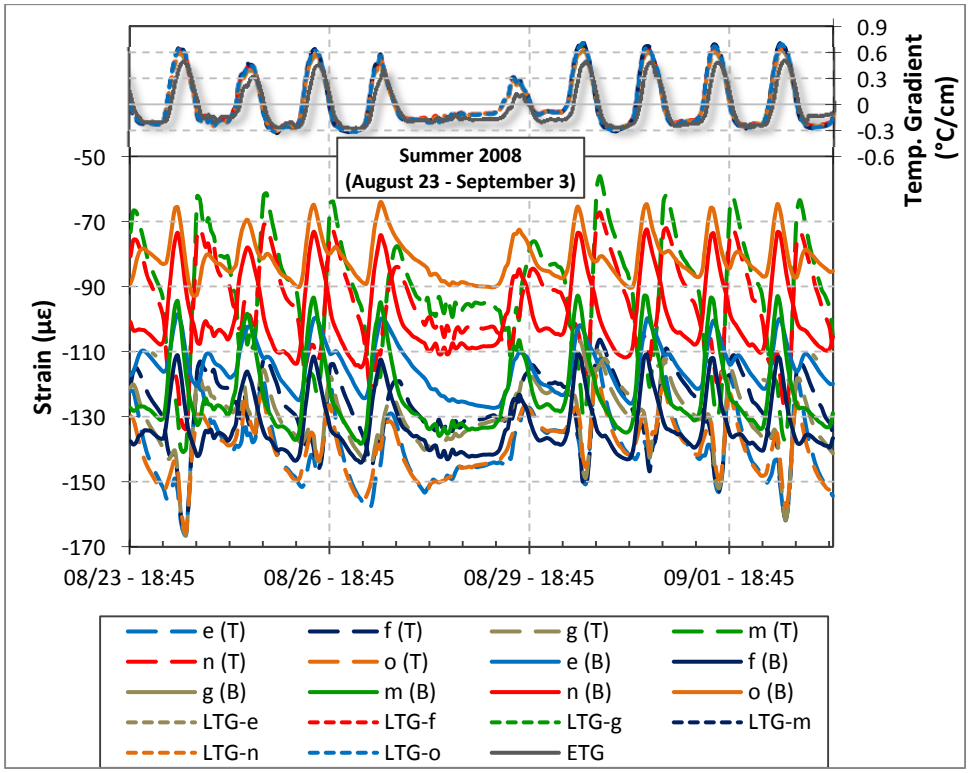
Summer 2008
(August 23 - September 3)
Strain (με)
Temp. Gradient (°C/cm)
0.9
0.6
0.3
0
-0.3
-0.6
-50
-70
-90
-110
-130
-150
-170
08/23 - 18:45
08/26 - 18:45
08/29 - 18:45
09/01 - 18:45
e (T)
f (T)
g (T)
m (T)
n (T)
o (T)
e (B)
f (B)
g (B)
m (B)
n (B)
o (B)
LTG-e
LTG-f
LTG-g
LTG-m
LTG-n
LTG-o
ETG

(1°C/cm = 4.6°F/in)

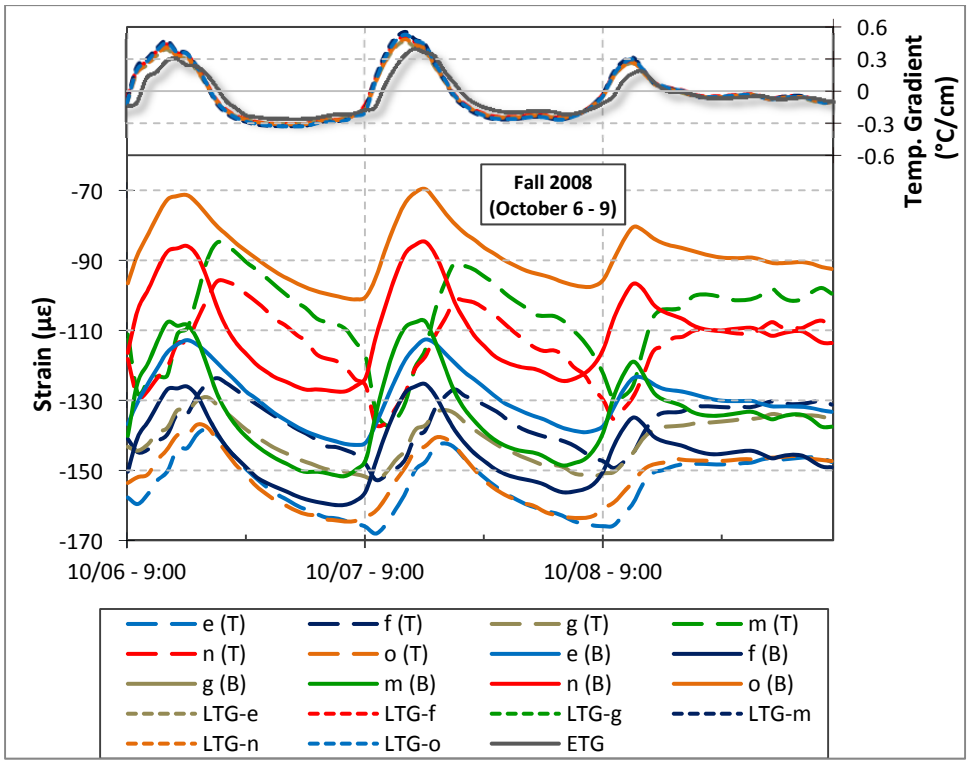
Fall 2008
(October 6 - 9)
Strain (με)
Temp. Gradient (°C/cm)
0.6
0.3
0
-0.3
-0.6
-70
-90
-110
-130
-150
-170
10/06 - 9:00
10/07 - 9:00
10/08 - 9:00
e (T)
f (T)
g (T)
m (T)
n (T)
o (T)
e (B)
f (B)
g (B)
m (B)
n (B)
o (B)
LTG-e
LTG-f
LTG-g
LTG-m
LTG-n
LTG-o
ETG

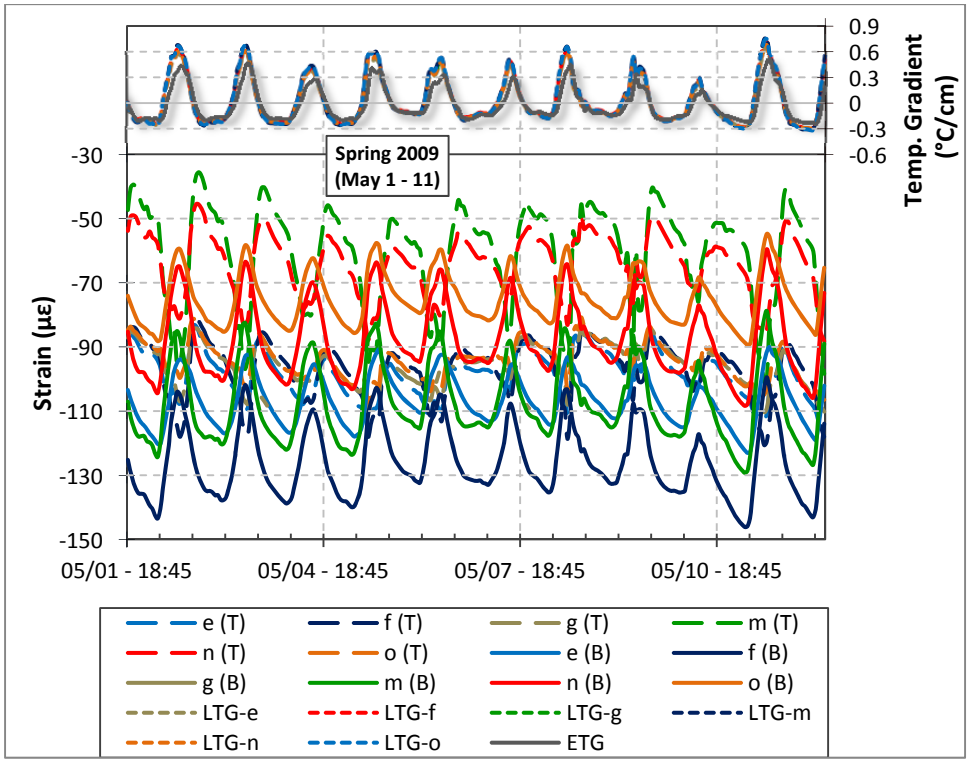
Spring 2009
(May 1 - 11)
Strain (με)
Temp. Gradient (°C/cm)
0.9
0.6
0.3
0
-0.3
-0.6
-30
-50
-70
-90
-110
-130
-150
05/01 - 18:45
05/04 - 18:45
05/07 - 18:45
05/10 - 18:45
e (T)
f (T)
g (T)
m (T)
n (T)
o (T)
e (B)
f (B)
g (B)
m (B)
n (B)
o (B)
LTG-e
LTG-f
LTG-g
LTG-m
LTG-n
LTG-o
ETG

(1°C/cm = 4.6°F/in)

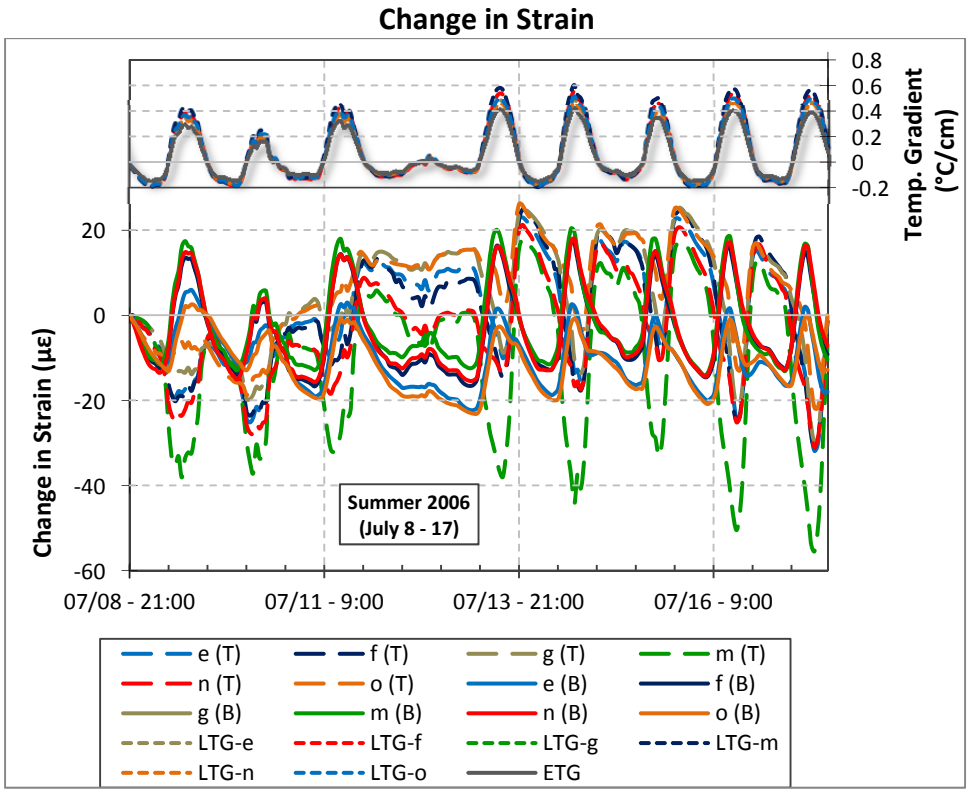
Change in Strain
Temp. Gradient (°C/cm)
0.8
0.6
0.4
0.2
0
-0.2
Change in Strain (με)
20
0
-20
-40
-60
Summer 2006
(July 8 - 17)
07/08 - 21:00
07/11 - 9:00
07/13 - 21:00
07/16 - 9:00
e (T)
f (T)
g (T)
m (T)
n (T)
o (T)
e (B)
f (B)
g (B)
m (B)
n (B)
o (B)
LTG-e
LTG-f
LTG-g
LTG-m
LTG-n
LTG-o
ETG

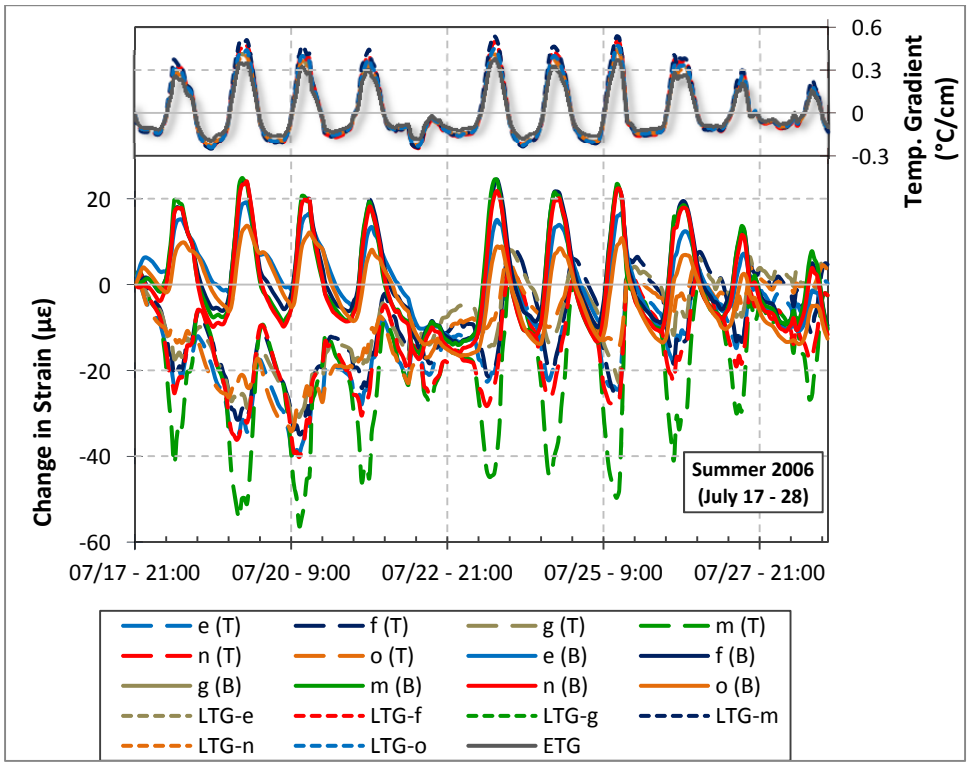
Temp. Gradient (°C/cm)
0.6
0.3
0
-0.3
Change in Strain (με)
20
0
-20
-40
-60
Summer 2006
(July 17 - 28)
07/17 - 21:00
07/20 - 9:00
07/22 - 21:00
07/25 - 9:00
07/27 - 21:00
e (T)
f (T)
g (T)
m (T)
n (T)
o (T)
e (B)
f (B)
g (B)
m (B)
n (B)
o (B)
LTG-e
LTG-f
LTG-g
LTG-m
LTG-n
LTG-o
ETG

(1°C/cm = 4.6°F/in)

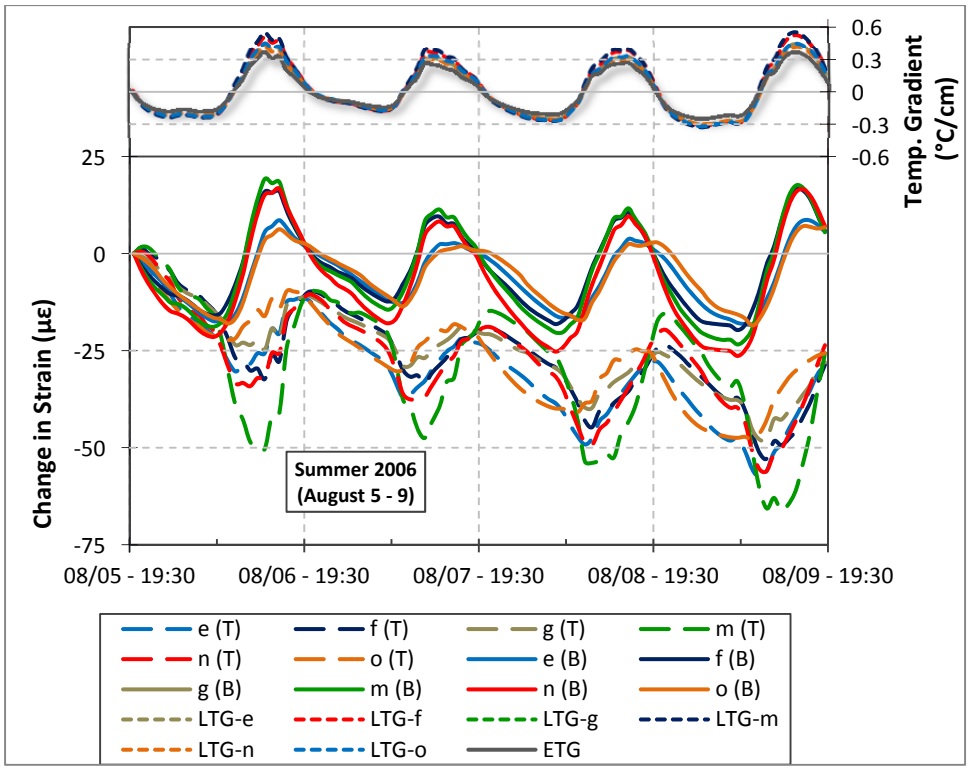
Temp. Gradient (°C/cm)
0.6
0.3
0
-0.3
-0.6
Change in Strain (με)
25
0
-25
-50
-75
Summer 2006
(August 5 - 9)
08/05 - 19:30
08/06 - 19:30
08/07 - 19:30
08/08 - 19:30
08/09 - 19:30
e (T)
f (T)
g (T)
m (T)
n (T)
o (T)
e (B)
f (B)
g (B)
m (B)
n (B)
o (B)
LTG-e
LTG-f
LTG-g
LTG-m
LTG-n
LTG-o
ETG

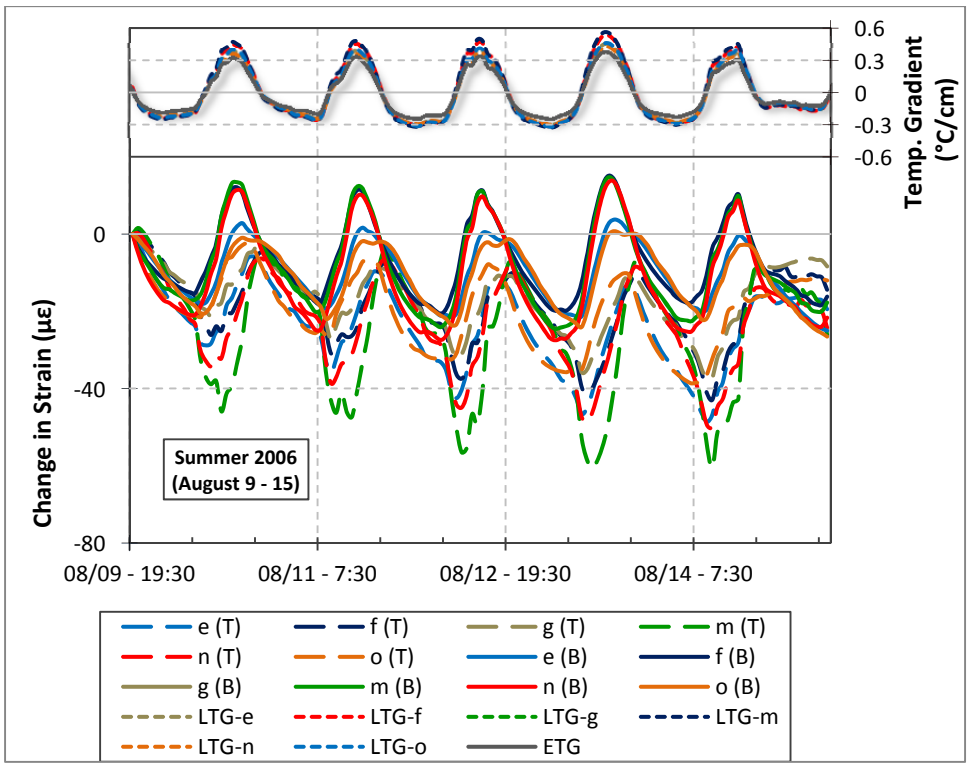
Temp. Gradient (°C/cm)
0.6
0.3
0
-0.3
-0.6
Change in Strain (με)
0
-40
-80
Summer 2006
(August 9 - 15)
08/09 - 19:30
08/11 - 7:30
08/12 - 19:30
08/14 - 7:30
e (T)
f (T)
g (T)
m (T)
n (T)
o (T)
e (B)
f (B)
g (B)
m (B)
n (B)
o (B)
LTG-e
LTG-f
LTG-g
LTG-m
LTG-n
LTG-o
ETG

(1°C/cm = 4.6°F/in)

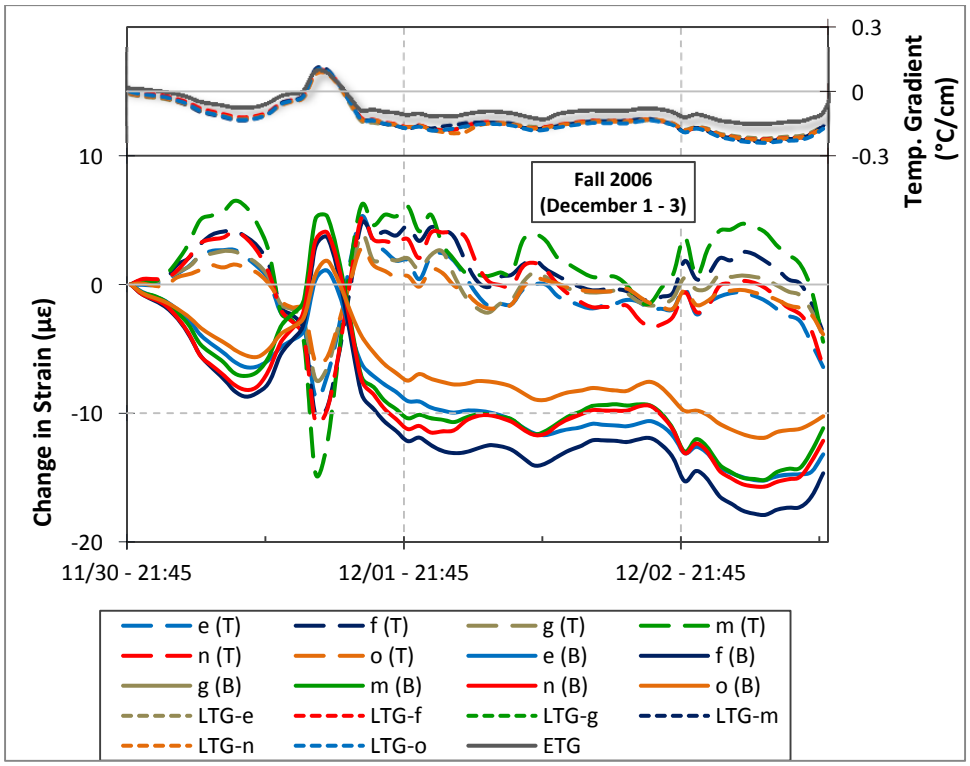
Fall 2006
(December 1 - 3)
Change in Strain (με)
Temp. Gradient (°C/cm)
0.3
0
-0.3
10
0
-10
-20
11/30 - 21:45
12/01 - 21:45
12/02 - 21:45
e (T)
f (T)
g (T)
m (T)
n (T)
o (T)
e (B)
f (B)
g (B)
m (B)
n (B)
o (B)
LTG-e
LTG-f
LTG-g
LTG-m
LTG-n
LTG-o
ETG

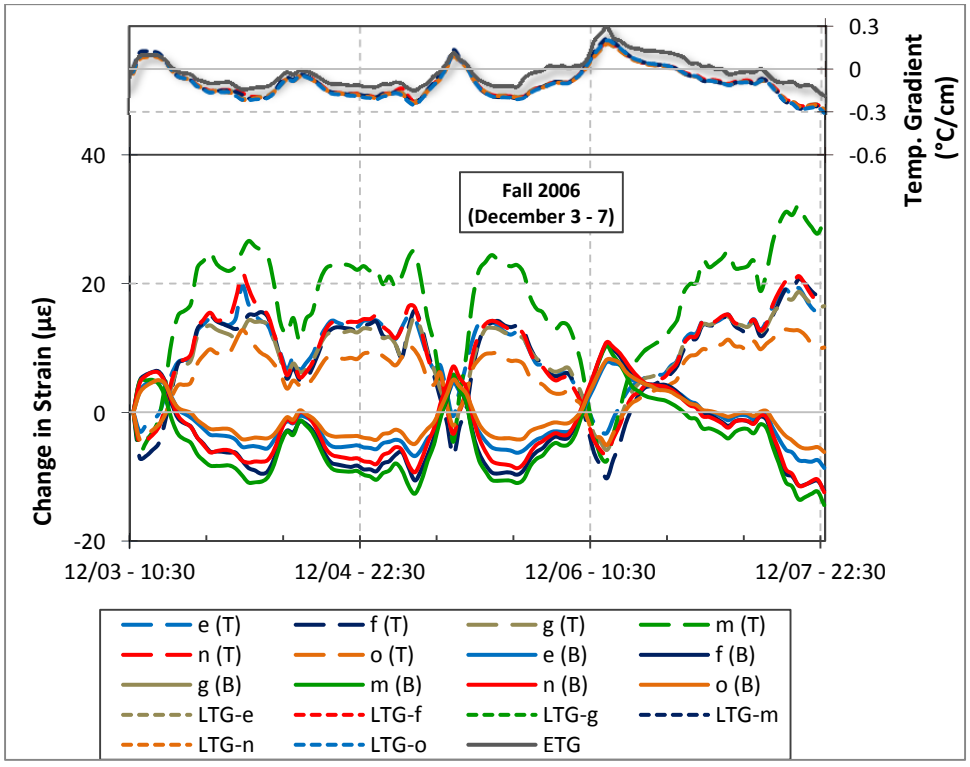
Fall 2006
(December 3 - 7)
Change in Strain (με)
Temp. Gradient (°C/cm)
0.3
0
-0.3
-0.6
40
20
0
-20
12/03 - 10:30
12/04 - 22:30
12/06 - 10:30
12/07 - 22:30
e (T)
f (T)
g (T)
m (T)
n (T)
o (T)
e (B)
f (B)
g (B)
m (B)
n (B)
o (B)
LTG-e
LTG-f
LTG-g
LTG-m
LTG-n
LTG-o
ETG

(1°C/cm = 4.6°F/in)

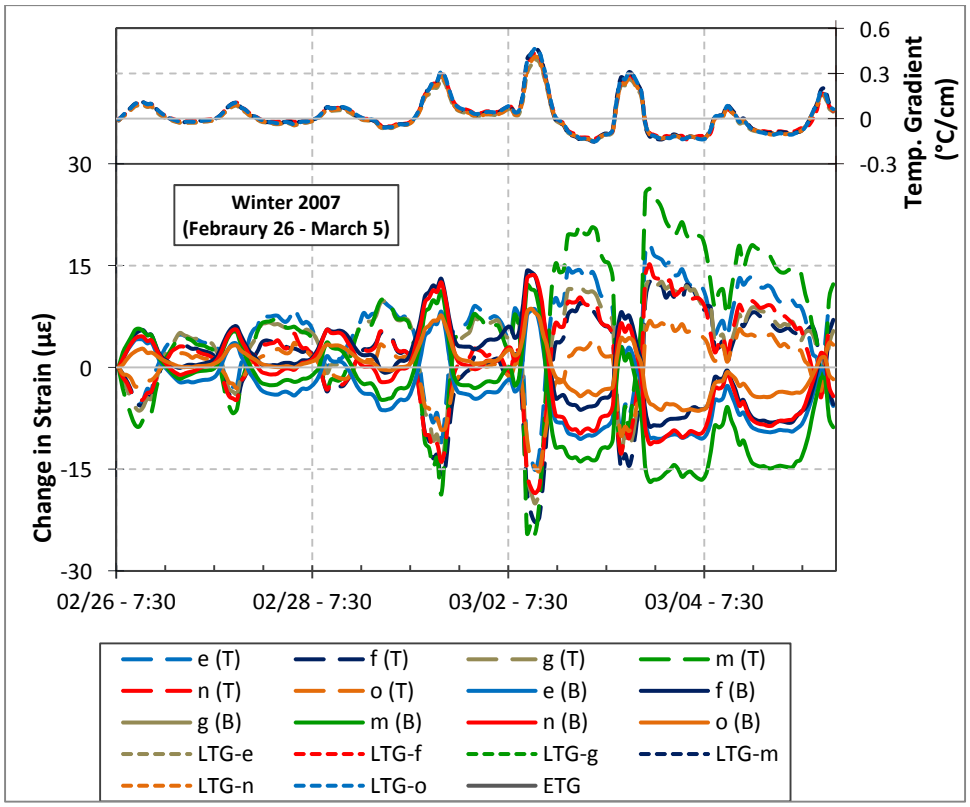
Winter 2007
(Febraury 26 - March 5)
Change in Strain (με)
Temp. Gradient (°C/cm)
0.6
0.3
0
-0.3
30
15
0
-15
-30
02/26 - 7:30
02/28 - 7:30
03/02 - 7:30
03/04 - 7:30
e (T)
f (T)
g (T)
m (T)
n (T)
o (T)
e (B)
f (B)
g (B)
m (B)
n (B)
o (B)
LTG-e
LTG-f
LTG-g
LTG-m
LTG-n
LTG-o
ETG

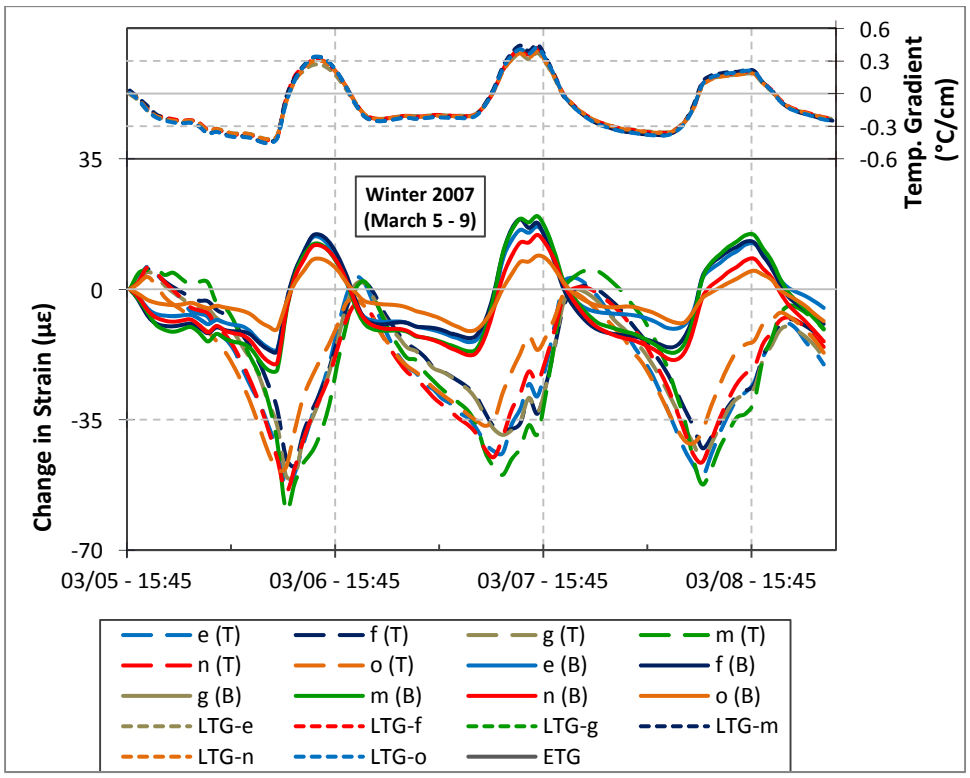
Winter 2007
(March 5 - 9)
Change in Strain (με)
Temp. Gradient (°C/cm)
0.6
0.3
0
-0.3
-0.6
35
0
-35
-70
03/05 - 15:45
03/06 - 15:45
03/07 - 15:45
03/08 - 15:45
e (T)
f (T)
g (T)
m (T)
n (T)
o (T)
e (B)
f (B)
g (B)
m (B)
n (B)
o (B)
LTG-e
LTG-f
LTG-g
LTG-m
LTG-n
LTG-o
ETG

(1°C/cm = 4.6°F/in)

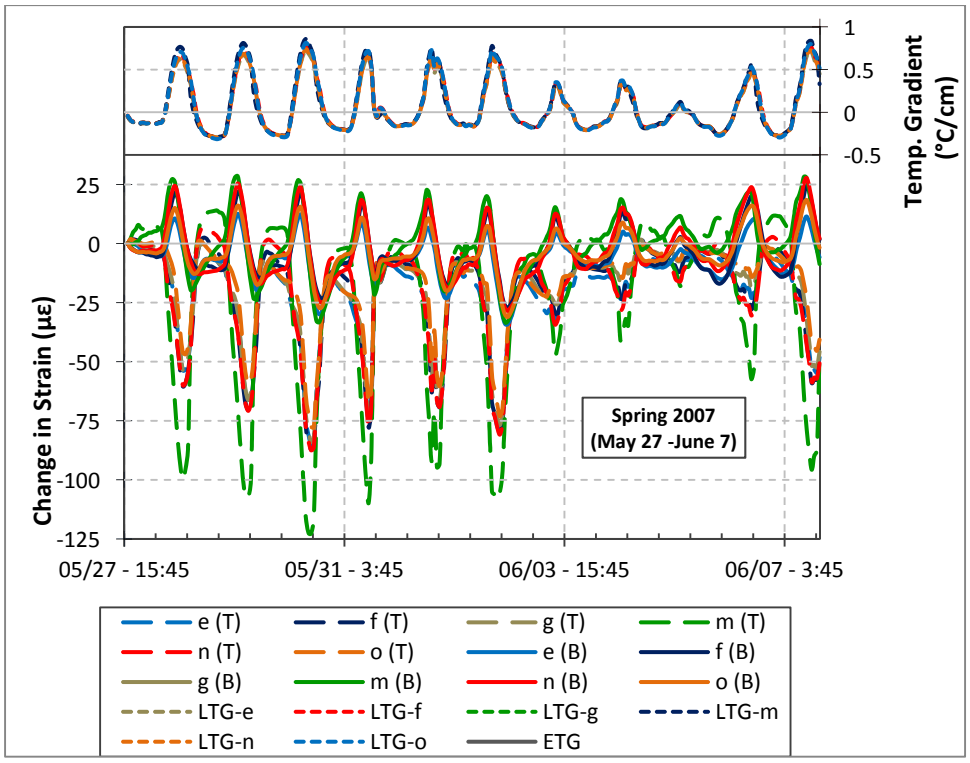
Temp. Gradient (°C/cm)
1
0.5
0
-0.5
Change in Strain (με)
25
0
-25
-50
-75
-100
-125
Spring 2007
(May 27 -June 7)
05/27 - 15:45
05/31 - 3:45
06/03 - 15:45
06/07 - 3:45
e (T)
f (T)
g (T)
m (T)
n (T)
o (T)
e (B)
f (B)
g (B)
m (B)
n (B)
o (B)
LTG-e
LTG-f
LTG-g
LTG-m
LTG-n
LTG-o
ETG

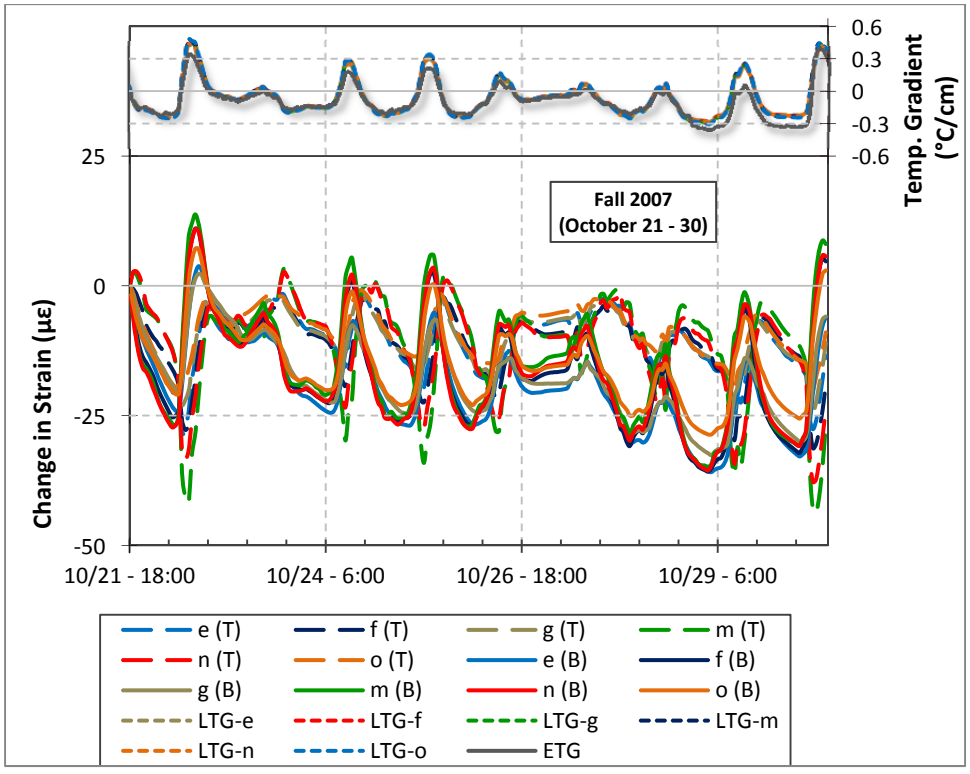
Temp. Gradient (°C/cm)
0.6
0.3
0
-0.3
-0.6
Change in Strain (με)
25
0
-25
-50
Fall 2007
(October 21 - 30)
10/21 - 18:00
10/24 - 6:00
10/26 - 18:00
10/29 - 6:00
e (T)
f (T)
g (T)
m (T)
n (T)
o (T)
e (B)
f (B)
g (B)
m (B)
n (B)
o (B)
LTG-e
LTG-f
LTG-g
LTG-m
LTG-n
LTG-o
ETG

(1°C/cm = 4.6°F/in)

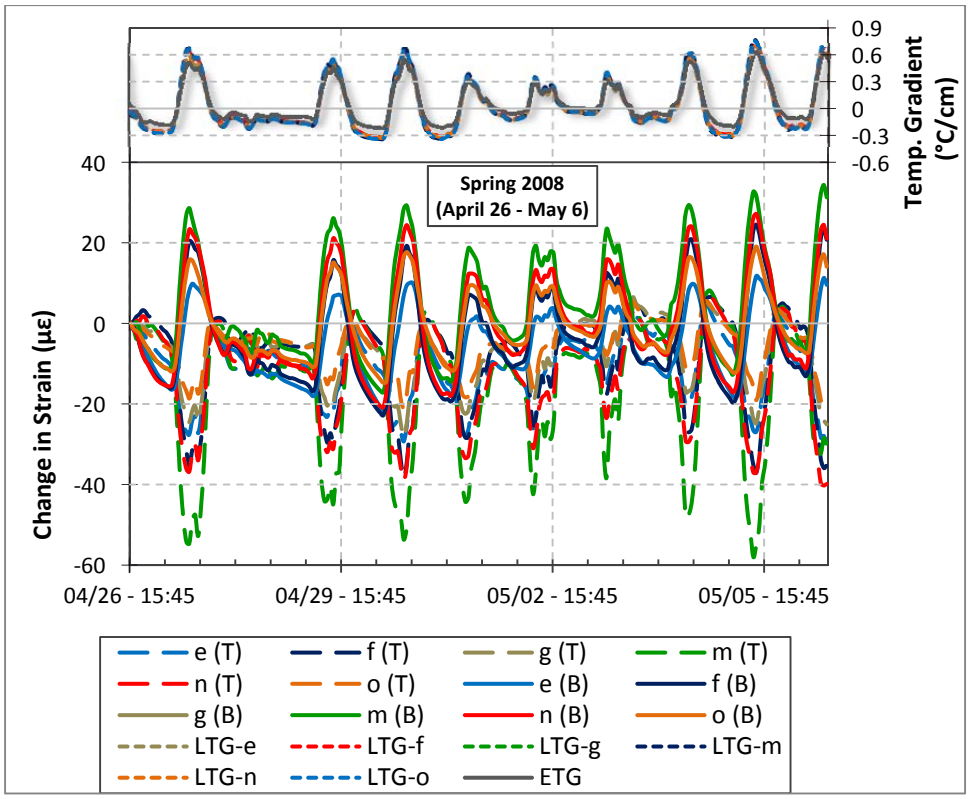
Spring 2008
(April 26 - May 6)
Change in Strain (με)
Temp. Gradient (°C/cm)
0.9
0.6
0.3
0
-0.3
-0.6
40
20
0
-20
-40
-60
04/26 - 15:45
04/29 - 15:45
05/02 - 15:45
05/05 - 15:45
e (T)
f (T)
g (T)
m (T)
n (T)
o (T)
e (B)
f (B)
g (B)
m (B)
n (B)
o (B)
LTG-e
LTG-f
LTG-g
LTG-m
LTG-n
LTG-o
ETG

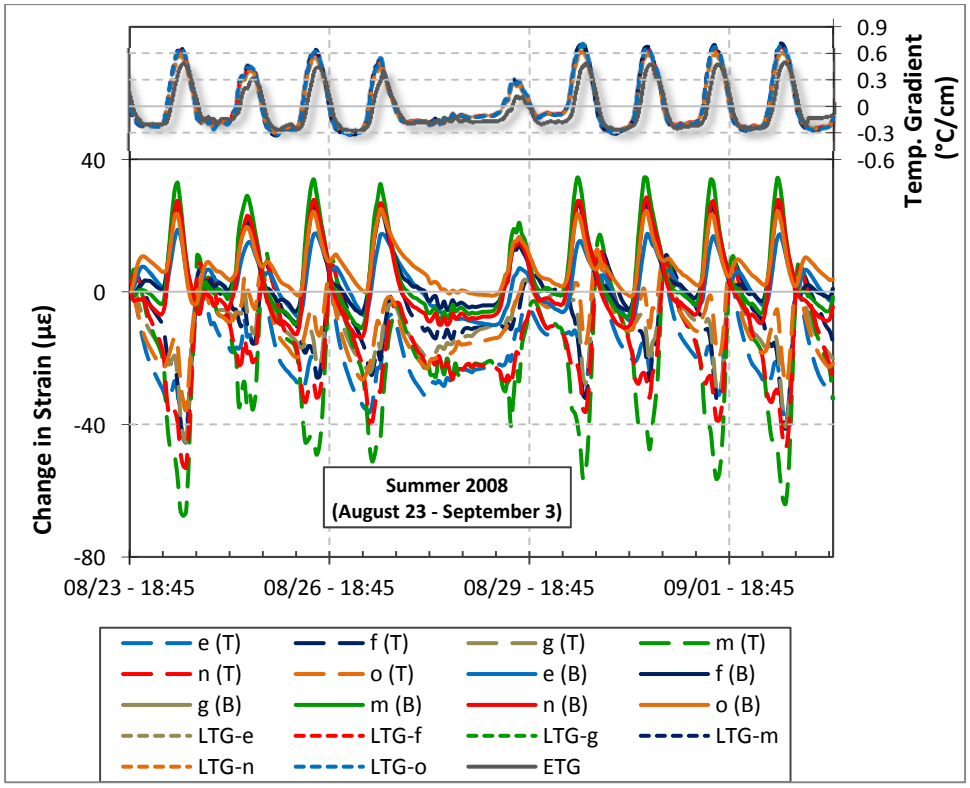
Summer 2008
(August 23 - September 3)
Change in Strain (με)
Temp. Gradient (°C/cm)
0.9
0.6
0.3
0
-0.3
-0.6
40
0
-40
-80
08/23 - 18:45
08/26 - 18:45
08/29 - 18:45
09/01 - 18:45
e (T)
f (T)
g (T)
m (T)
n (T)
o (T)
e (B)
f (B)
g (B)
m (B)
n (B)
o (B)
LTG-e
LTG-f
LTG-g
LTG-m
LTG-n
LTG-o
ETG

(1°C/cm = 4.6°F/in)

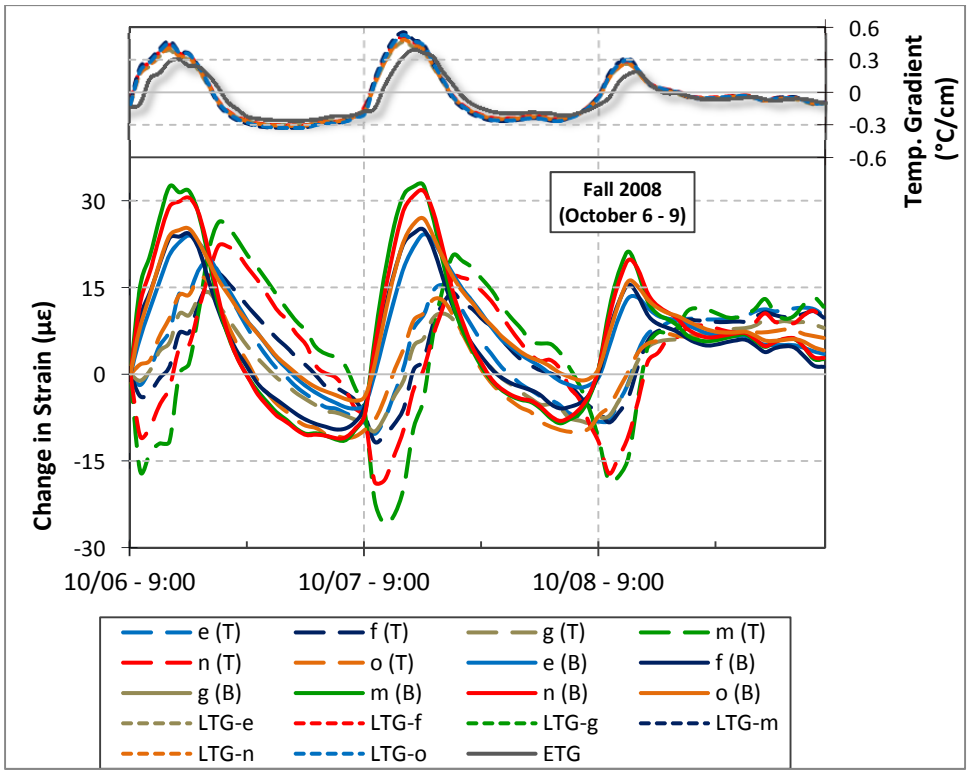
Fall 2008
(October 6 - 9)
Change in Strain (με)
Temp. Gradient (°C/cm)
0.6
0.3
0
-0.3
-0.6
30
15
0
-15
-30
10/06 - 9:00
10/07 - 9:00
10/08 - 9:00
e (T)
f (T)
g (T)
m (T)
n (T)
o (T)
e (B)
f (B)
g (B)
m (B)
n (B)
o (B)
LTG-e
LTG-f
LTG-g
LTG-m
LTG-n
LTG-o
ETG

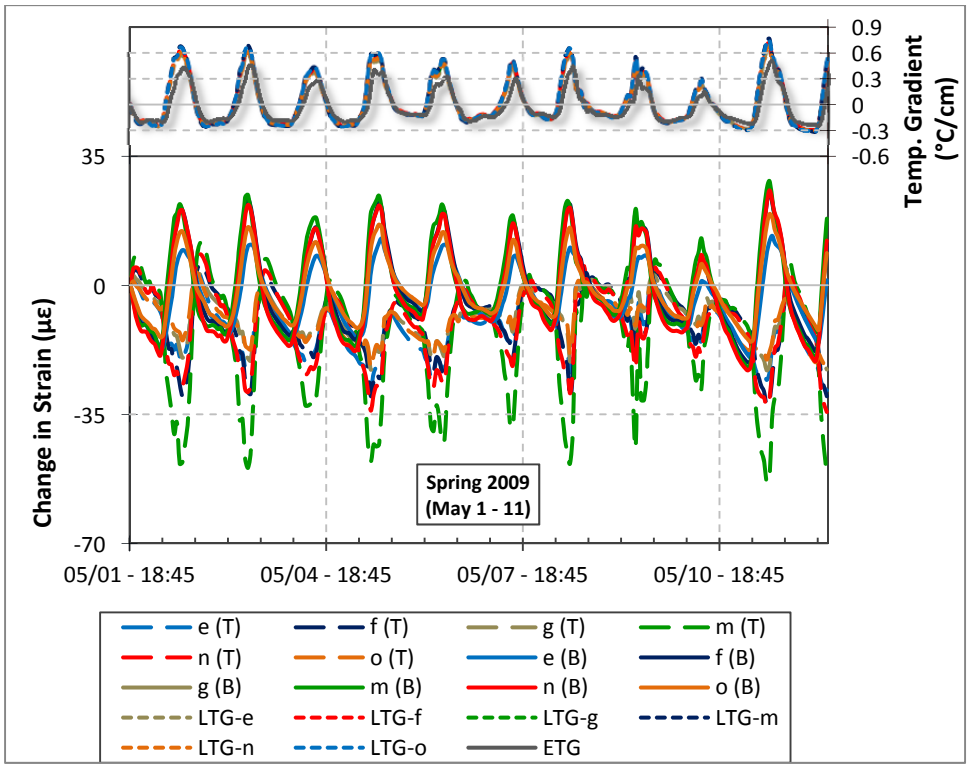
Spring 2009
(May 1 - 11)
Change in Strain (με)
Temp. Gradient (°C/cm)
0.9
0.6
0.3
0
-0.3
-0.6
35
0
-35
-70
05/01 - 18:45
05/04 - 18:45
05/07 - 18:45
05/10 - 18:45
e (T)
f (T)
g (T)
m (T)
n (T)
o (T)
e (B)
f (B)
g (B)
m (B)
n (B)
o (B)
LTG-e
LTG-f
LTG-g
LTG-m
LTG-n
LTG-o
ETG

(1°C/cm = 4.6°F/in)

Pavement Strains (Common Periods)

Untreated Section

Load-Related Strain

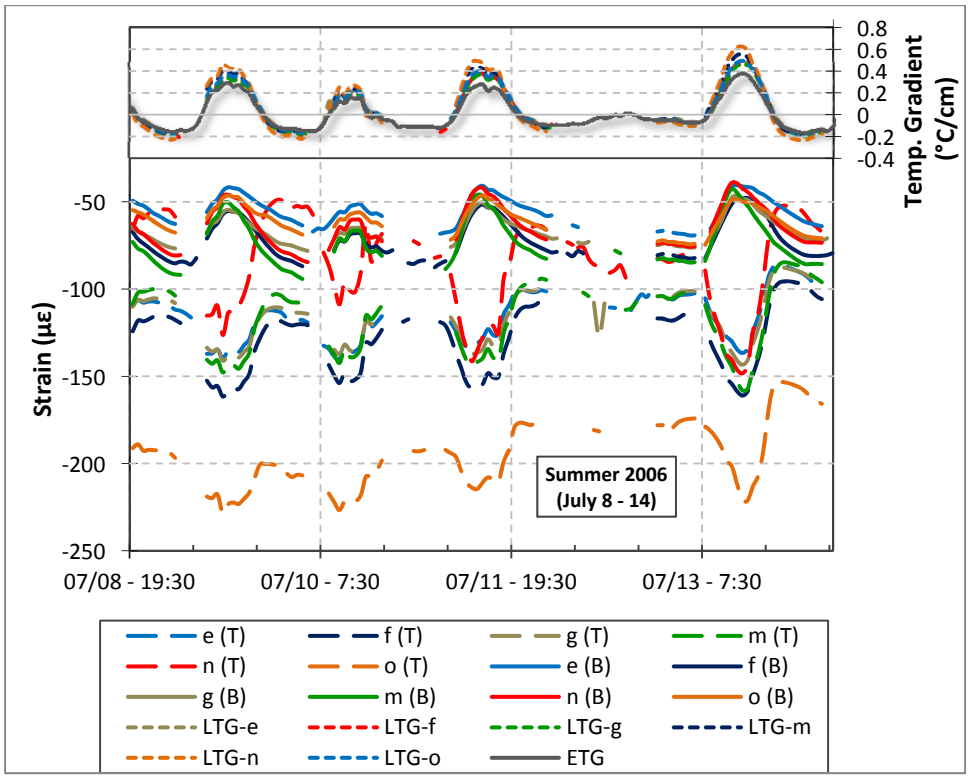

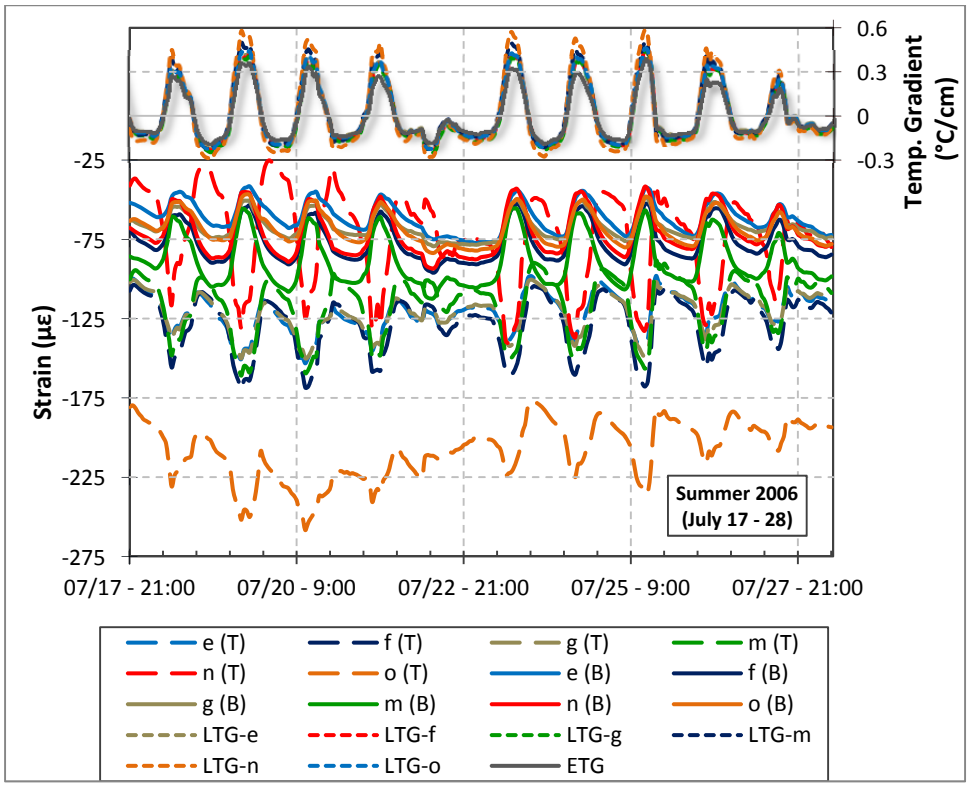

(1°C/cm = 4.6°F/in)

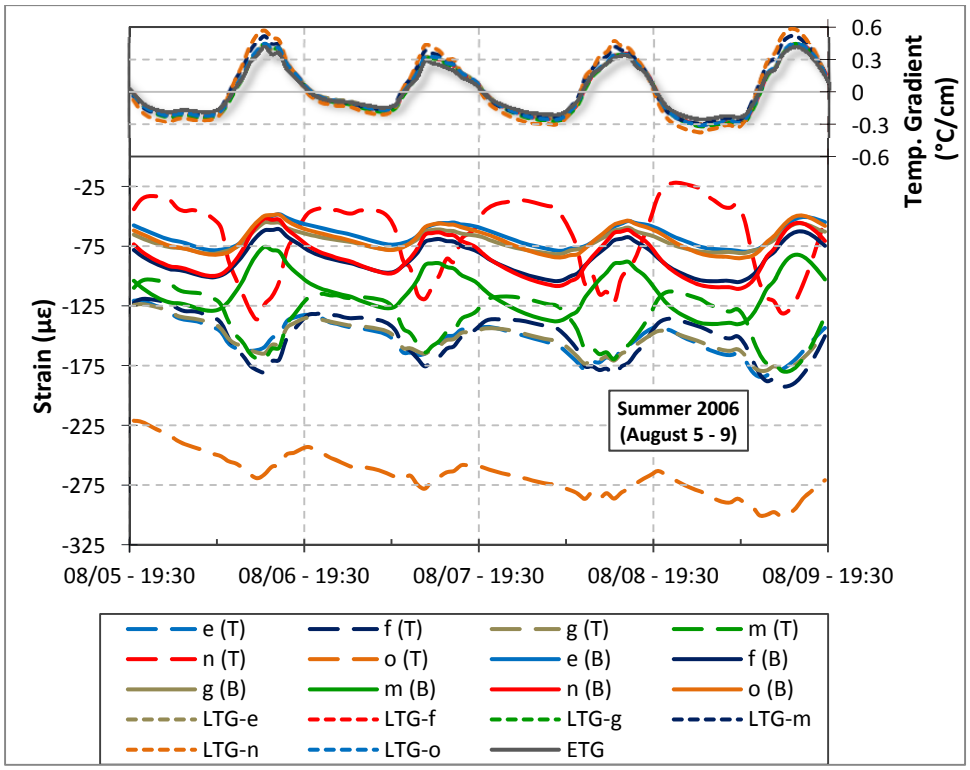
0.6
0.3
0
-0.3
-0.6
Temp. Gradient (°C/cm)
-25
-75
-125
-175
-225
-275
-325
Strain (με)
Summer 2006 (August 5 - 9)
08/05 - 19:30
08/06 - 19:30
08/07 - 19:30
08/08 - 19:30
08/09 - 19:30
e (T)
f (T)
g (T)
m (T)
n (T)
o (T)
e (B)
f (B)
g (B)
m (B)
n (B)
o (B)
LTG-e
LTG-f
LTG-g
LTG-m
LTG-n
LTG-o
ETG

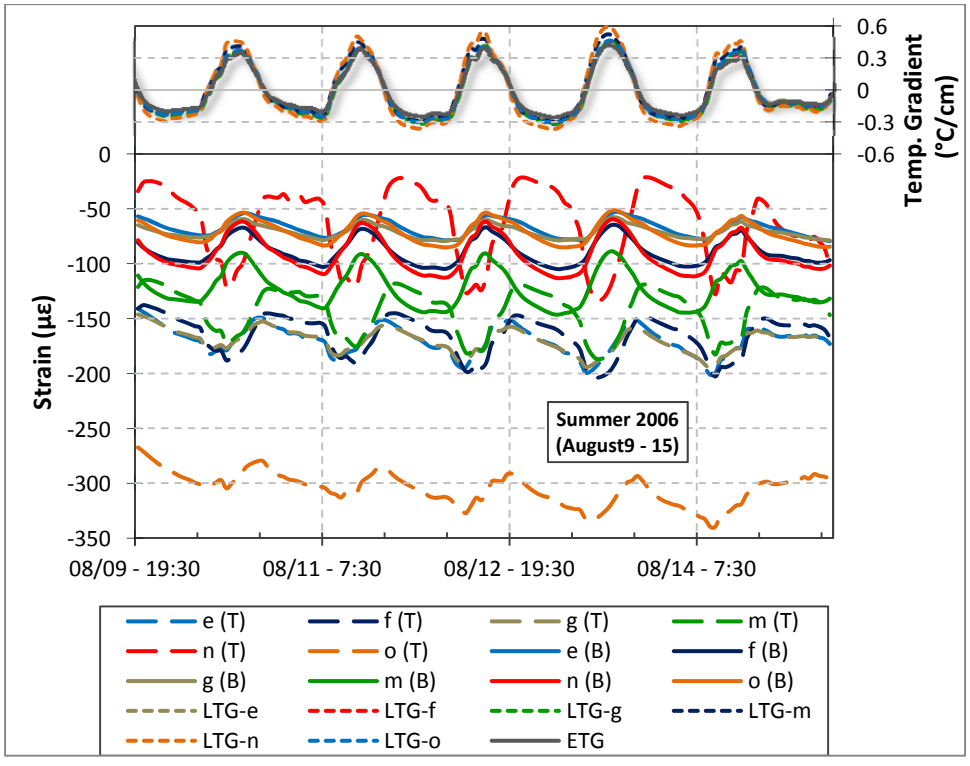
0.6
0.3
0
-0.3
-0.6
Temp. Gradient (°C/cm)
0
-50
-100
-150
-200
-250
-300
-350
Strain (με)
Summer 2006 (August9 - 15)
08/09 - 19:30
08/11 - 7:30
08/12 - 19:30
08/14 - 7:30
e (T)
f (T)
g (T)
m (T)
n (T)
o (T)
e (B)
f (B)
g (B)
m (B)
n (B)
o (B)
LTG-e
LTG-f
LTG-g
LTG-m
LTG-n
LTG-o
ETG

(1°C/cm = 4.6°F/in)

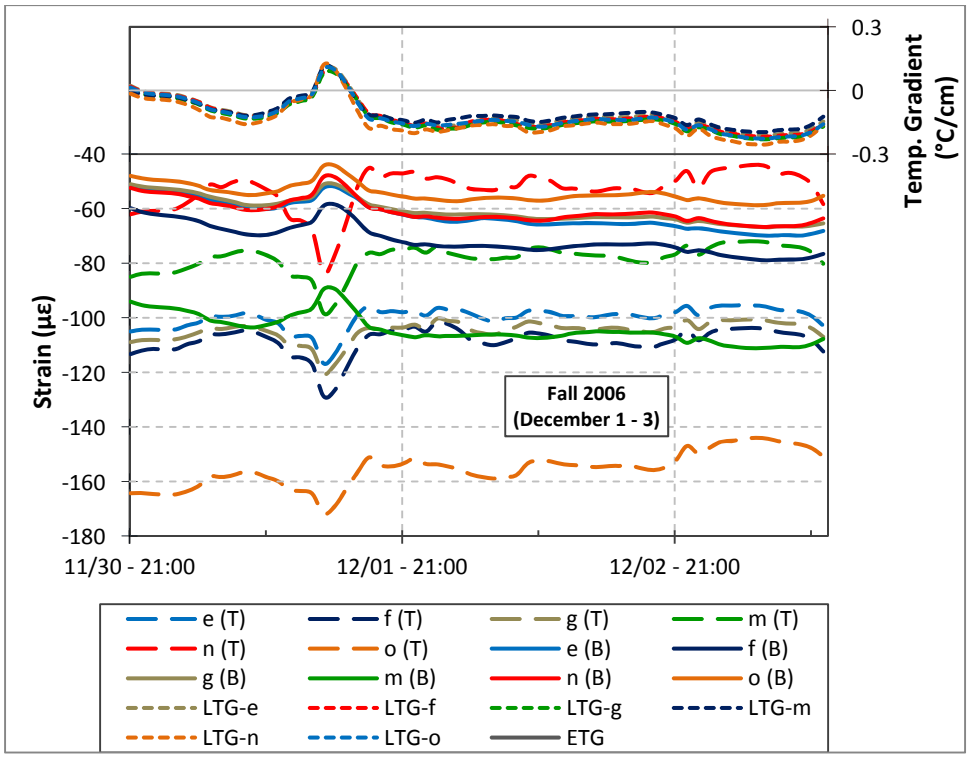
0.3
0
-0.3
Temp. Gradient (°C/cm)
-40
-60
-80
-100
-120
-140
-160
-180
Strain (με)
Fall 2006
(December 1 - 3)
11/30 - 21:00
12/01 - 21:00
12/02 - 21:00
e (T)
f (T)
g (T)
m (T)
n (T)
o (T)
e (B)
f (B)
g (B)
m (B)
n (B)
o (B)
LTG-e
LTG-f
LTG-g
LTG-m
LTG-n
LTG-o
ETG

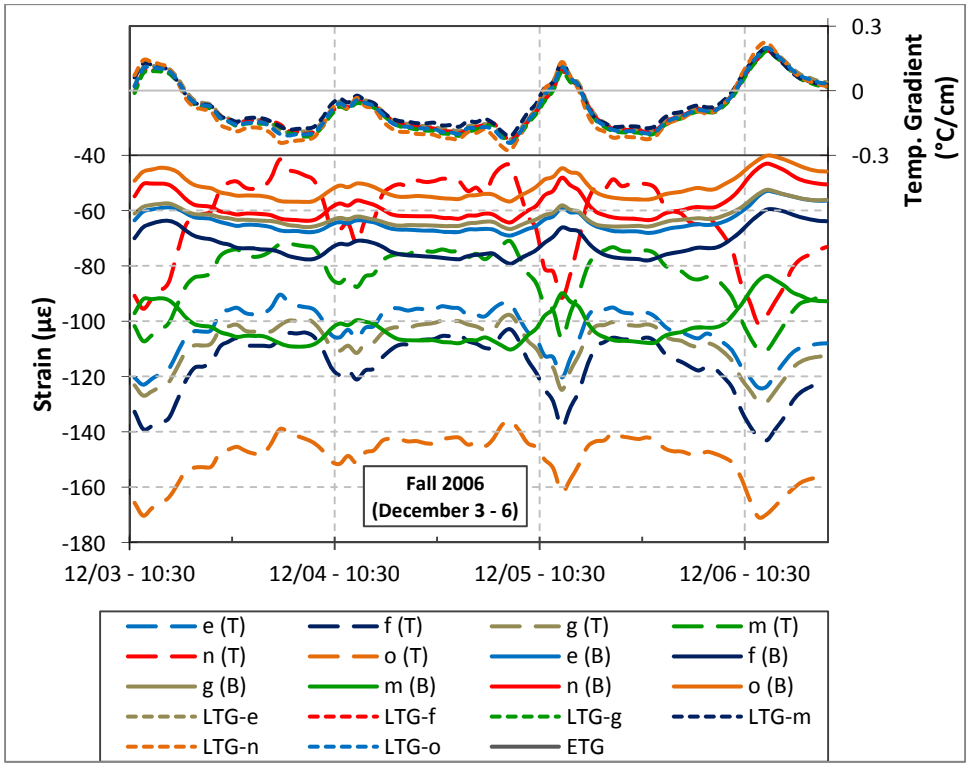
0.3
0
-0.3
Temp. Gradient (°C/cm)
-40
-60
-80
-100
-120
-140
-160
-180
Strain (με)
Fall 2006
(December 3 - 6)
12/03 - 10:30
12/04 - 10:30
12/05 - 10:30
12/06 - 10:30
e (T)
f (T)
g (T)
m (T)
n (T)
o (T)
e (B)
f (B)
g (B)
m (B)
n (B)
o (B)
LTG-e
LTG-f
LTG-g
LTG-m
LTG-n
LTG-o
ETG

(1°C/cm = 4.6°F/in)

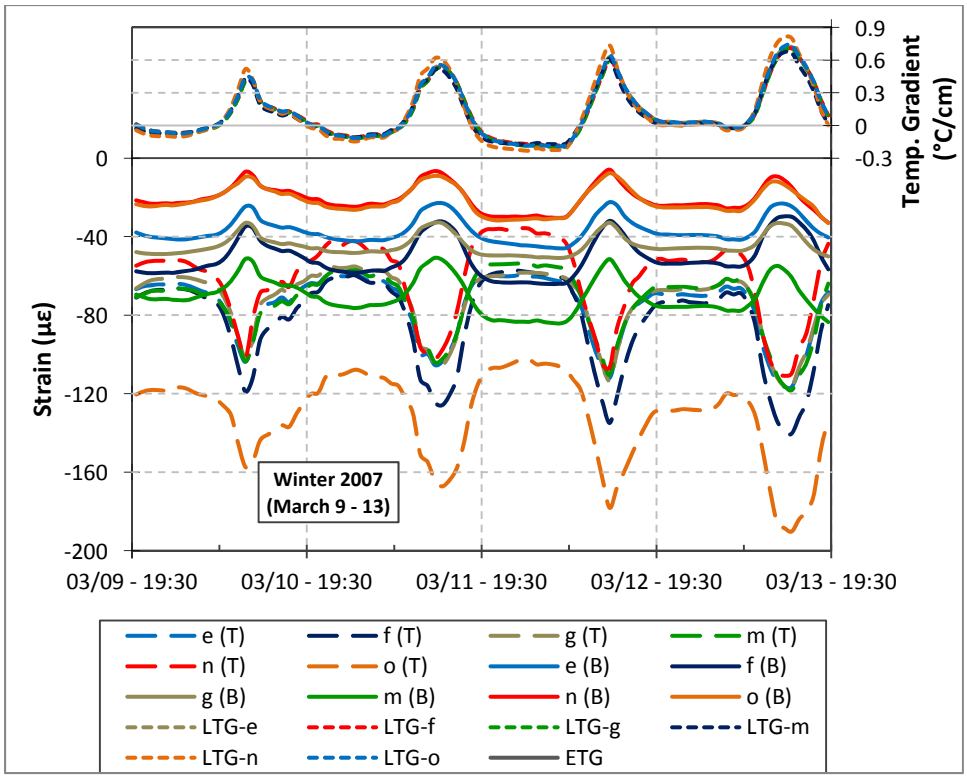
0.9
0.6
0.3
0
-0.3
Temp. Gradient (°C/cm)
0
-40
-80
-120
-160
-200
Strain (με)
Winter 2007
(March 9 - 13)
03/09 - 19:30
03/10 - 19:30
03/11 - 19:30
03/12 - 19:30
03/13 - 19:30
e (T)
f (T)
g (T)
m (T)
n (T)
o (T)
e (B)
f (B)
g (B)
m (B)
n (B)
o (B)
LTG-e
LTG-f
LTG-g
LTG-m
LTG-n
LTG-o
ETG

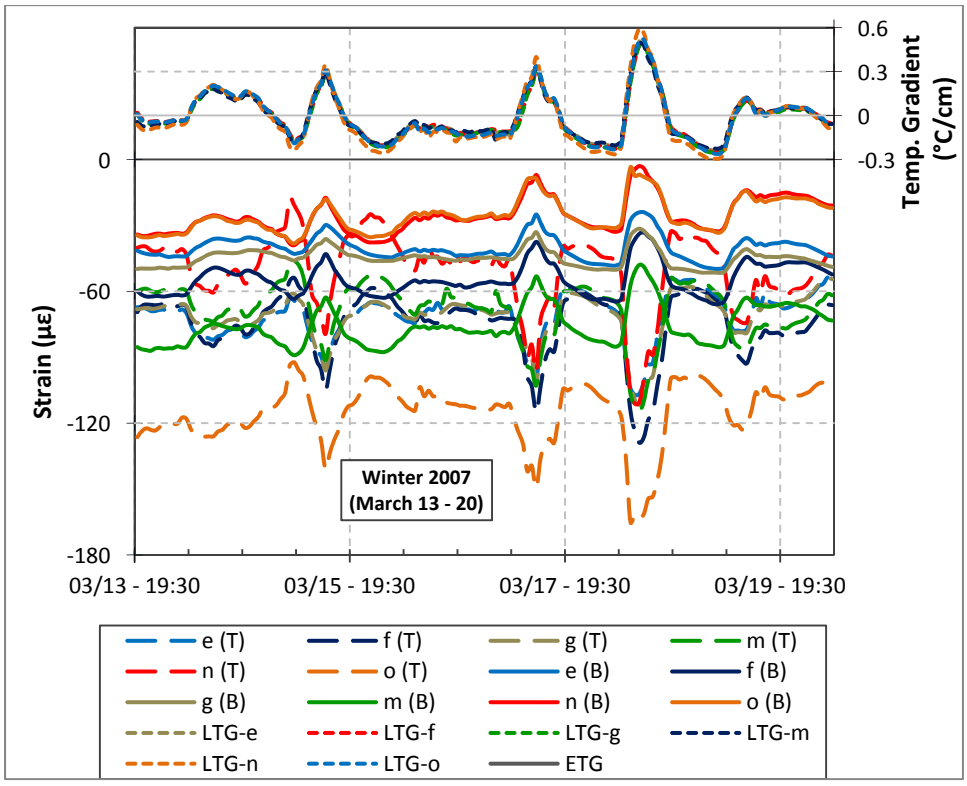
0.6
0.3
0
-0.3
Temp. Gradient (°C/cm)
0
-60
-120
-180
Strain (με)
Winter 2007
(March 13 - 20)
03/13 - 19:30
03/15 - 19:30
03/17 - 19:30
03/19 - 19:30
e (T)
f (T)
g (T)
m (T)
n (T)
o (T)
e (B)
f (B)
g (B)
m (B)
n (B)
o (B)
LTG-e
LTG-f
LTG-g
LTG-m
LTG-n
LTG-o
ETG

(1°C/cm = 4.6°F/in)

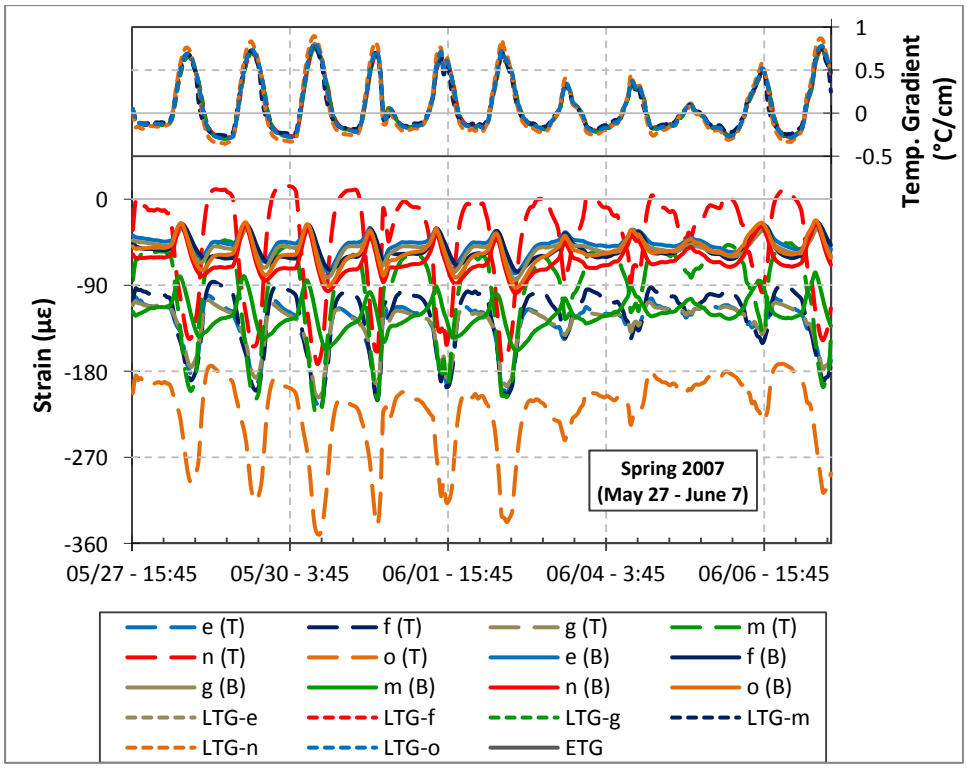
1
0.5
0
-0.5
Temp. Gradient (°C/cm)
0
-90
-180
-270
-360
Strain (με)
Spring 2007
(May 27 - June 7)
05/27 - 15:45
05/30 - 3:45
06/01 - 15:45
06/04 - 3:45
06/06 - 15:45
e (T)
f (T)
g (T)
m (T)
n (T)
o (T)
e (B)
f (B)
g (B)
m (B)
n (B)
o (B)
LTG-e
LTG-f
LTG-g
LTG-m
LTG-n
LTG-o
ETG

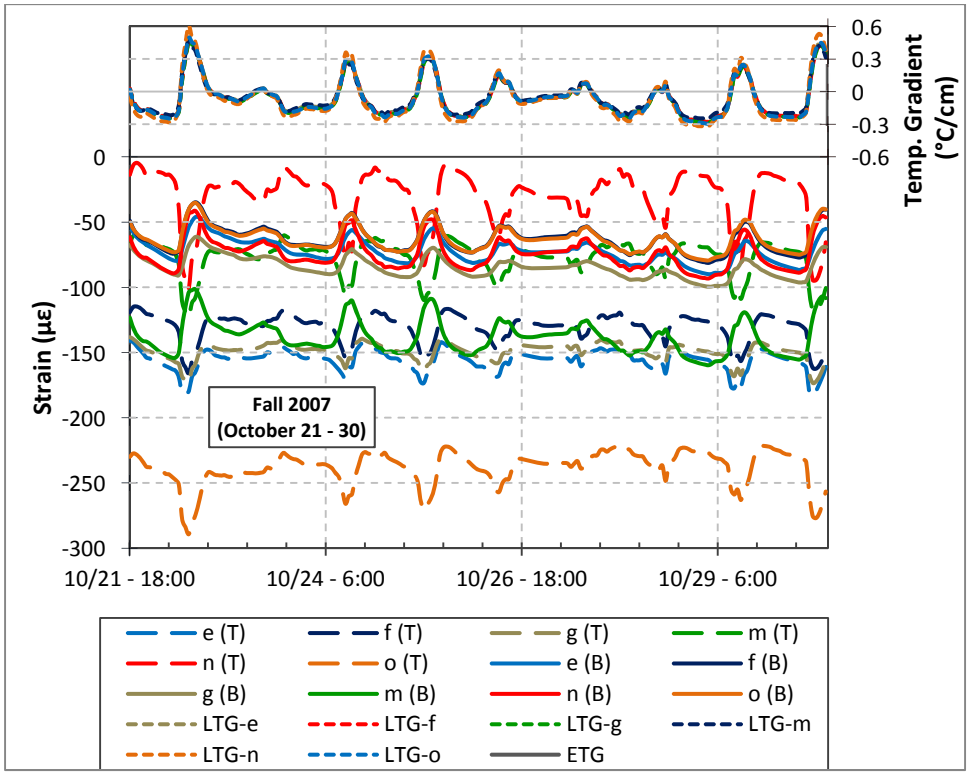
0.6
0.3
0
-0.3
-0.6
Temp. Gradient (°C/cm)
0
-50
-100
-150
-200
-250
-300
Strain (με)
Fall 2007
(October 21 - 30)
10/21 - 18:00
10/24 - 6:00
10/26 - 18:00
10/29 - 6:00
e (T)
f (T)
g (T)
m (T)
n (T)
o (T)
e (B)
f (B)
g (B)
m (B)
n (B)
o (B)
LTG-e
LTG-f
LTG-g
LTG-m
LTG-n
LTG-o
ETG

(1°C/cm = 4.6°F/in)

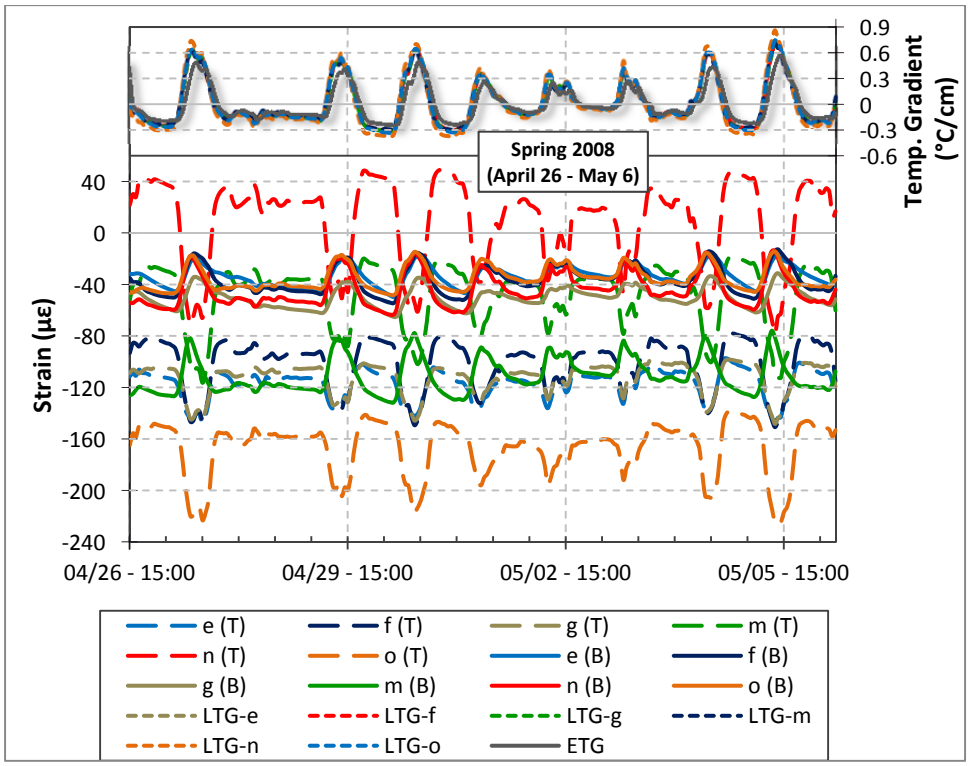
Spring 2008
(April 26 - May 6)
Strain (με)
Temp. Gradient (°C/cm)
0.9
0.6
0.3
0
-0.3
-0.6
40
0
-40
-80
-120
-160
-200
-240
04/26 - 15:00
04/29 - 15:00
05/02 - 15:00
05/05 - 15:00
e (T)
f (T)
g (T)
m (T)
n (T)
o (T)
e (B)
f (B)
g (B)
m (B)
n (B)
o (B)
LTG-e
LTG-f
LTG-g
LTG-m
LTG-n
LTG-o
ETG

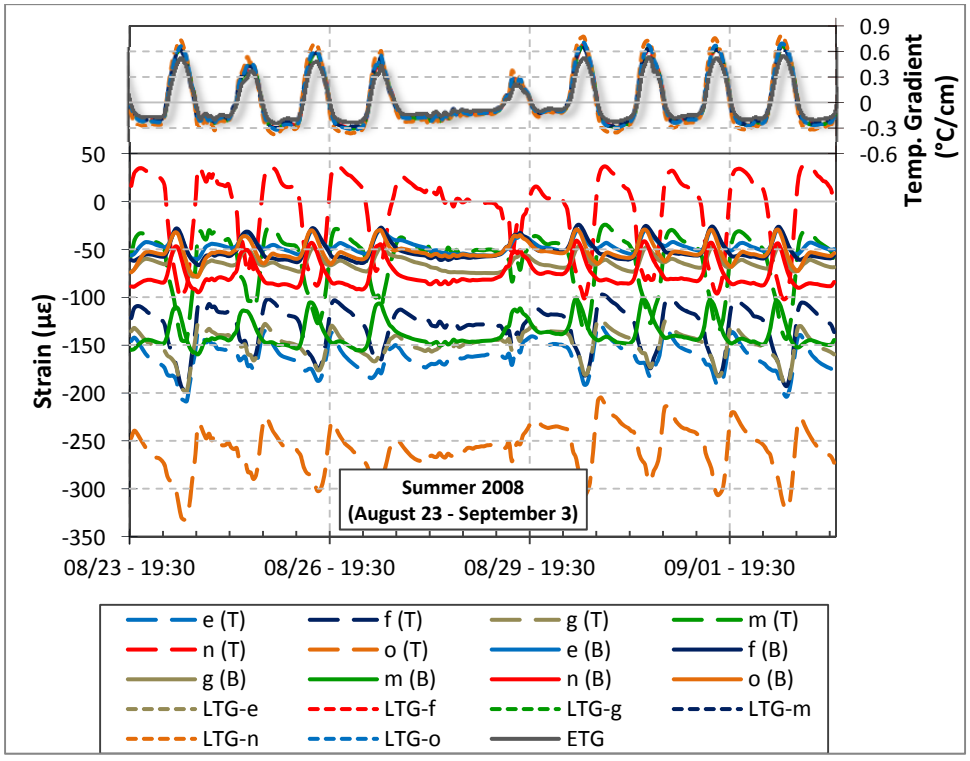
Summer 2008
(August 23 - September 3)
Strain (με)
Temp. Gradient (°C/cm)
0.9
0.6
0.3
0
-0.3
-0.6
50
0
-50
-100
-150
-200
-250
-300
-350
08/23 - 19:30
08/26 - 19:30
08/29 - 19:30
09/01 - 19:30
e (T)
f (T)
g (T)
m (T)
n (T)
o (T)
e (B)
f (B)
g (B)
m (B)
n (B)
o (B)
LTG-e
LTG-f
LTG-g
LTG-m
LTG-n
LTG-o
ETG

(1°C/cm = 4.6°F/in)

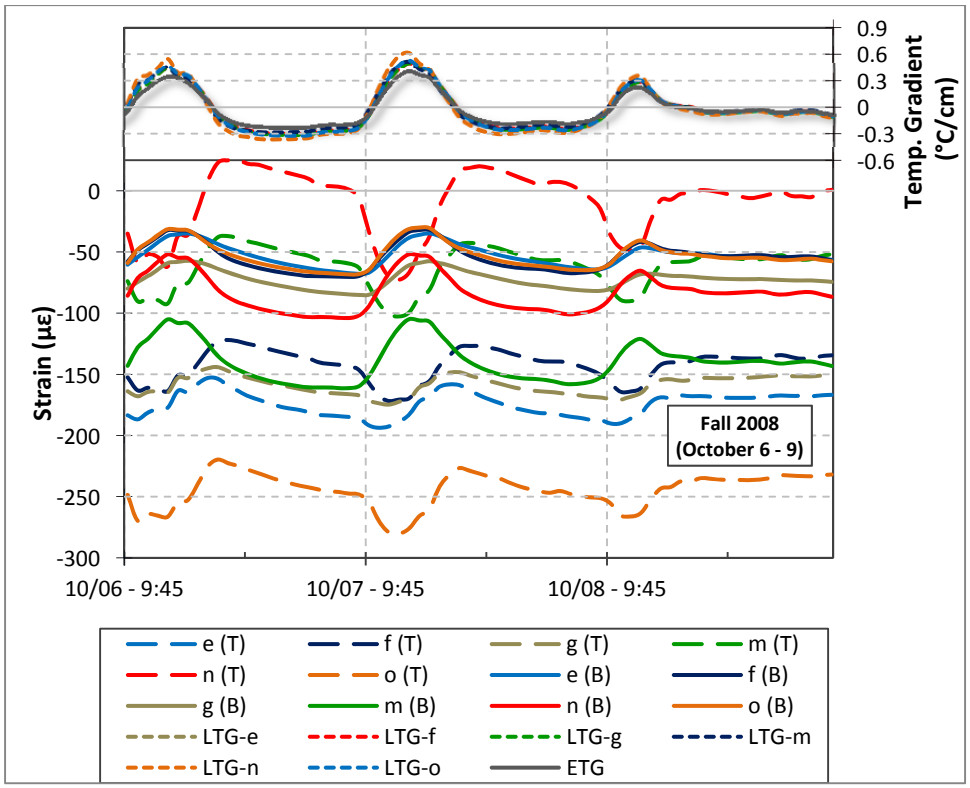
Temp. Gradient (°C/cm)
0.9
0.6
0.3
0
-0.3
-0.6
Strain (με)
0
-50
-100
-150
-200
-250
-300
Fall 2008
(October 6 - 9)
10/06 - 9:45
10/07 - 9:45
10/08 - 9:45
e (T)
f (T)
g (T)
m (T)
n (T)
o (T)
e (B)
f (B)
g (B)
m (B)
n (B)
o (B)
LTG-e
LTG-f
LTG-g
LTG-m
LTG-n
LTG-o
ETG

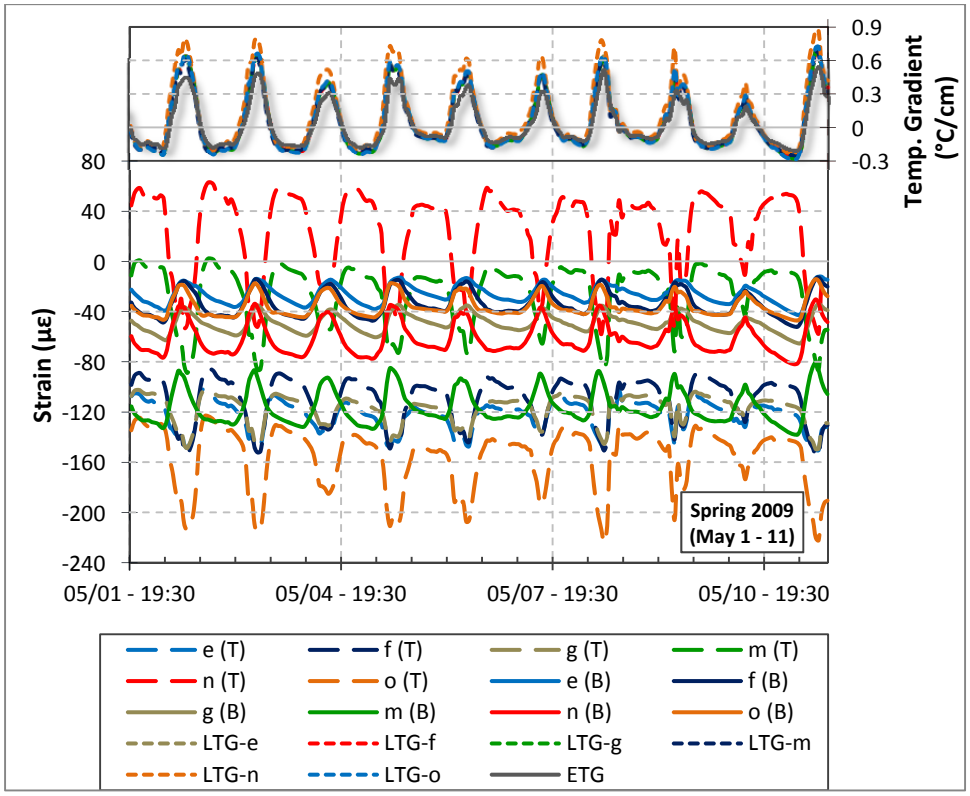
Temp. Gradient (°C/cm)
0.9
0.6
0.3
0
-0.3
Strain (με)
80
40
0
-40
-80
-120
-160
-200
-240
Spring 2009
(May 1 - 11)
05/01 - 19:30
05/04 - 19:30
05/07 - 19:30
05/10 - 19:30
e (T)
f (T)
g (T)
m (T)
n (T)
o (T)
e (B)
f (B)
g (B)
m (B)
n (B)
o (B)
LTG-e
LTG-f
LTG-g
LTG-m
LTG-n
LTG-o
ETG

(1°C/cm = 4.6°F/in)

Change in Strain

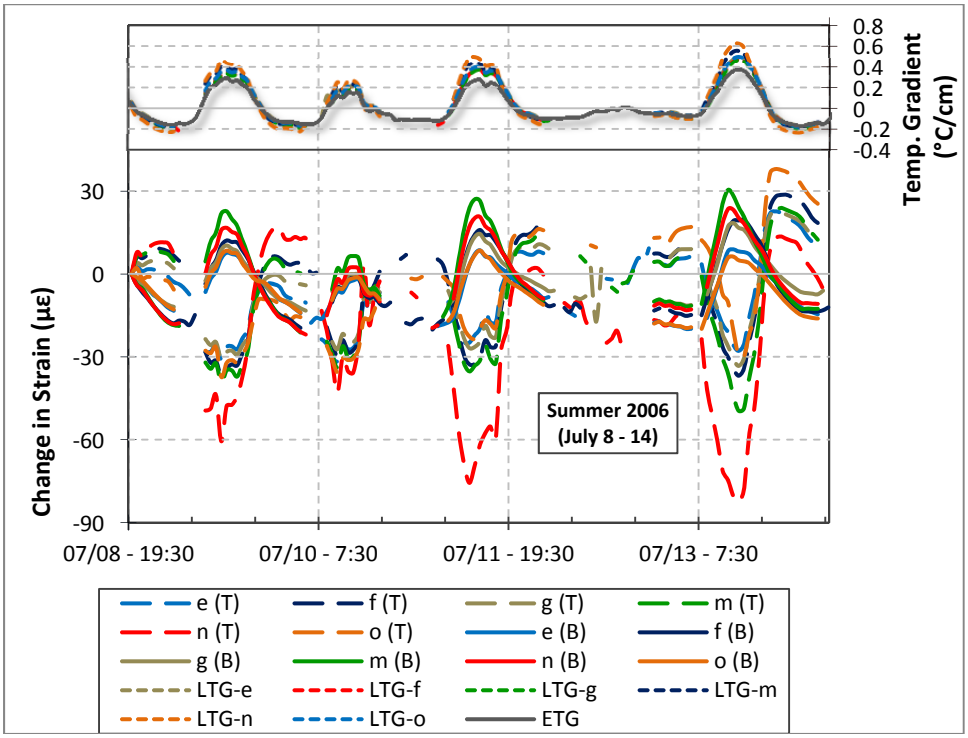

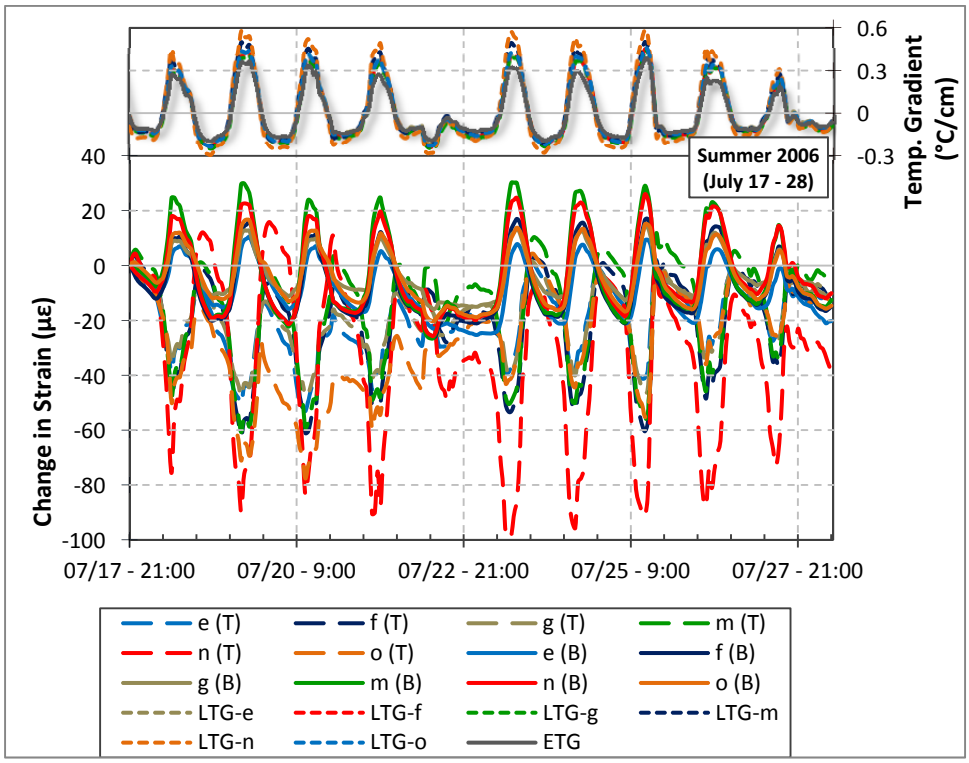

(1°C/cm = 4.6°F/in)

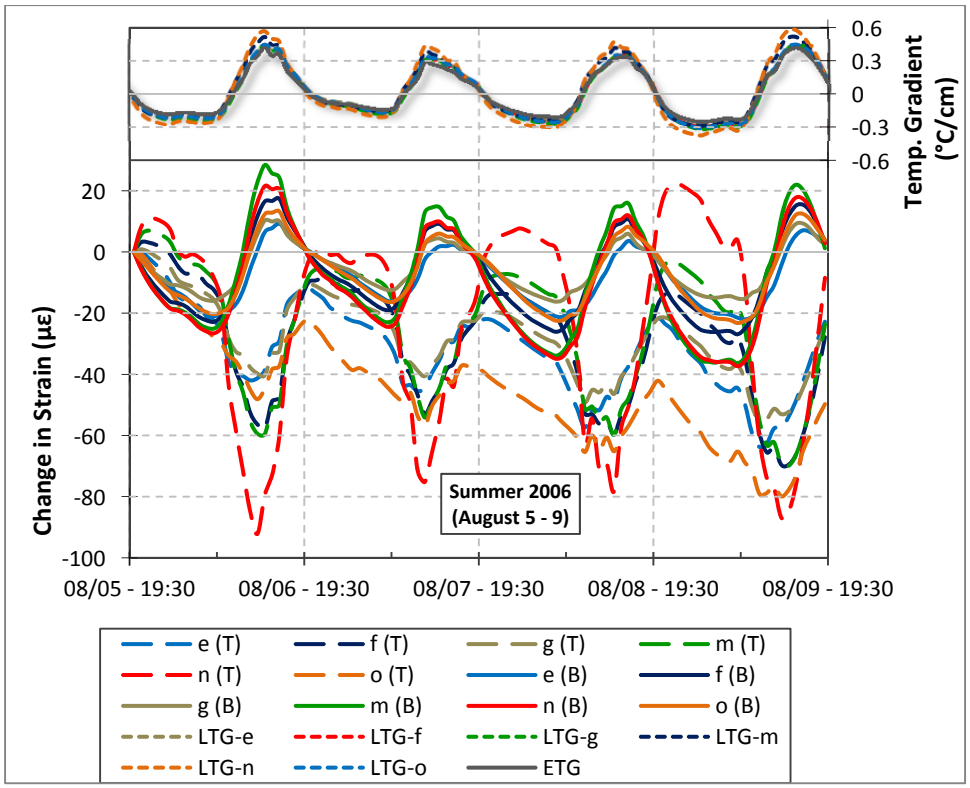
0.6
0.3
0
-0.3
-0.6
Temp. Gradient (°C/cm)
20
0
-20
-40
-60
-80
-100
Change in Strain (με)
Summer 2006 (August 5 - 9)
08/05 - 19:30
08/06 - 19:30
08/07 - 19:30
08/08 - 19:30
08/09 - 19:30
e (T)
f (T)
g (T)
m (T)
n (T)
o (T)
e (B)
f (B)
g (B)
m (B)
n (B)
o (B)
LTG-e
LTG-f
LTG-g
LTG-m
LTG-n
LTG-o
ETG

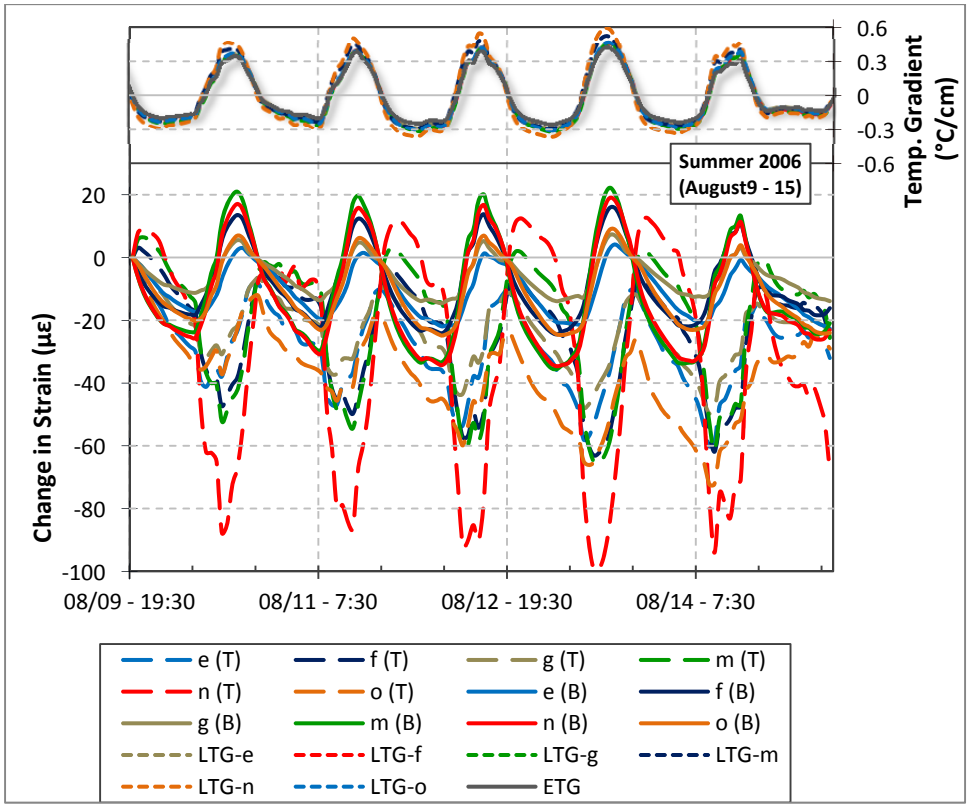
0.6
0.3
0
-0.3
-0.6
Temp. Gradient (°C/cm)
Summer 2006 (August9 - 15)
20
0
-20
-40
-60
-80
-100
Change in Strain (με)
08/09 - 19:30
08/11 - 7:30
08/12 - 19:30
08/14 - 7:30
e (T)
f (T)
g (T)
m (T)
n (T)
o (T)
e (B)
f (B)
g (B)
m (B)
n (B)
o (B)
LTG-e
LTG-f
LTG-g
LTG-m
LTG-n
LTG-o
ETG

(1°C/cm = 4.6°F/in)

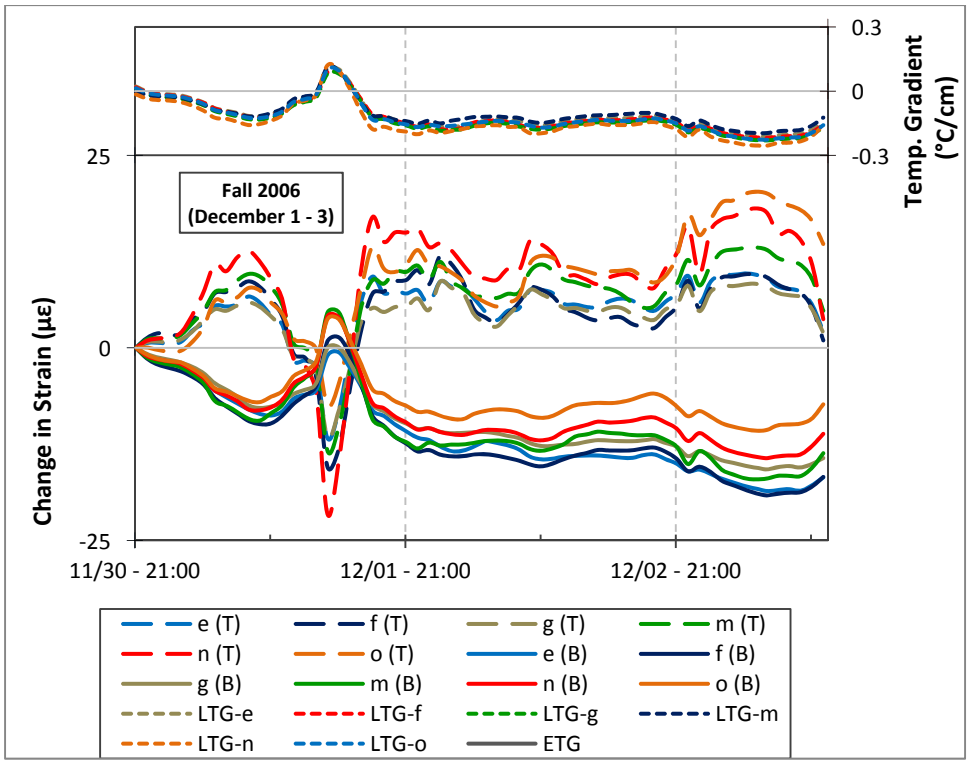
Fall 2006
(December 1 - 3)
Change in Strain (με)
Temp. Gradient (°C/cm)
25
0
-25
0.3
0
-0.3
11/30 - 21:00
12/01 - 21:00
12/02 - 21:00
e (T)
f (T)
g (T)
m (T)
n (T)
o (T)
e (B)
f (B)
g (B)
m (B)
n (B)
o (B)
LTG-e
LTG-f
LTG-g
LTG-m
LTG-n
LTG-o
ETG

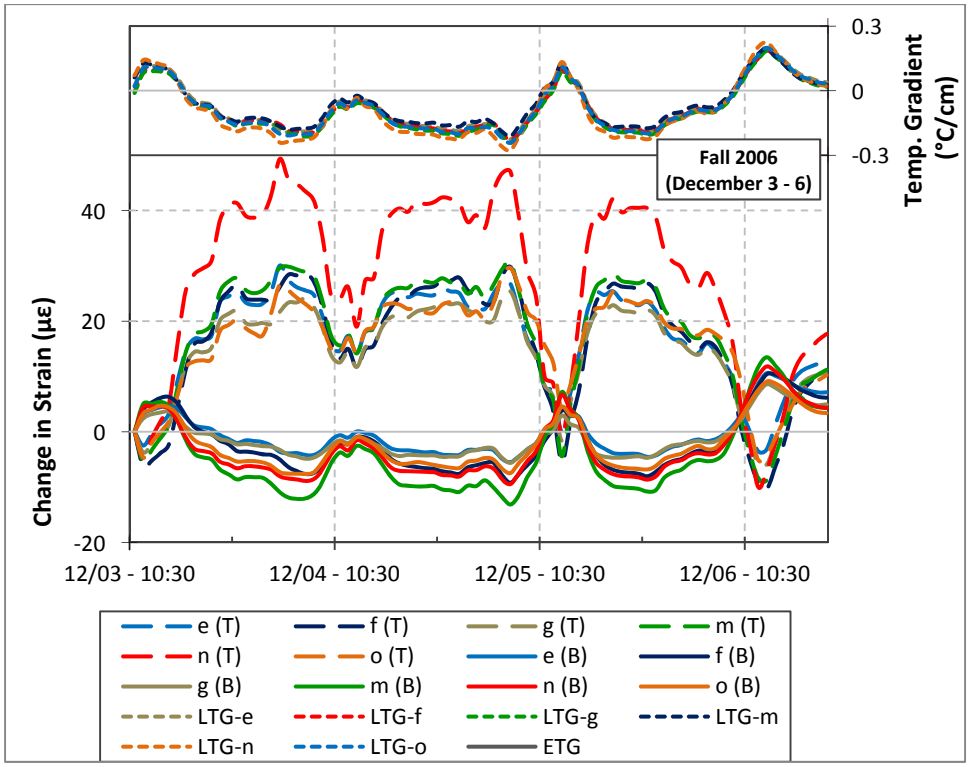
Fall 2006
(December 3 - 6)
Change in Strain (με)
Temp. Gradient (°C/cm)
40
20
0
-20
0.3
0
-0.3
12/03 - 10:30
12/04 - 10:30
12/05 - 10:30
12/06 - 10:30
e (T)
f (T)
g (T)
m (T)
n (T)
o (T)
e (B)
f (B)
g (B)
m (B)
n (B)
o (B)
LTG-e
LTG-f
LTG-g
LTG-m
LTG-n
LTG-o
ETG

(1°C/cm = 4.6°F/in)

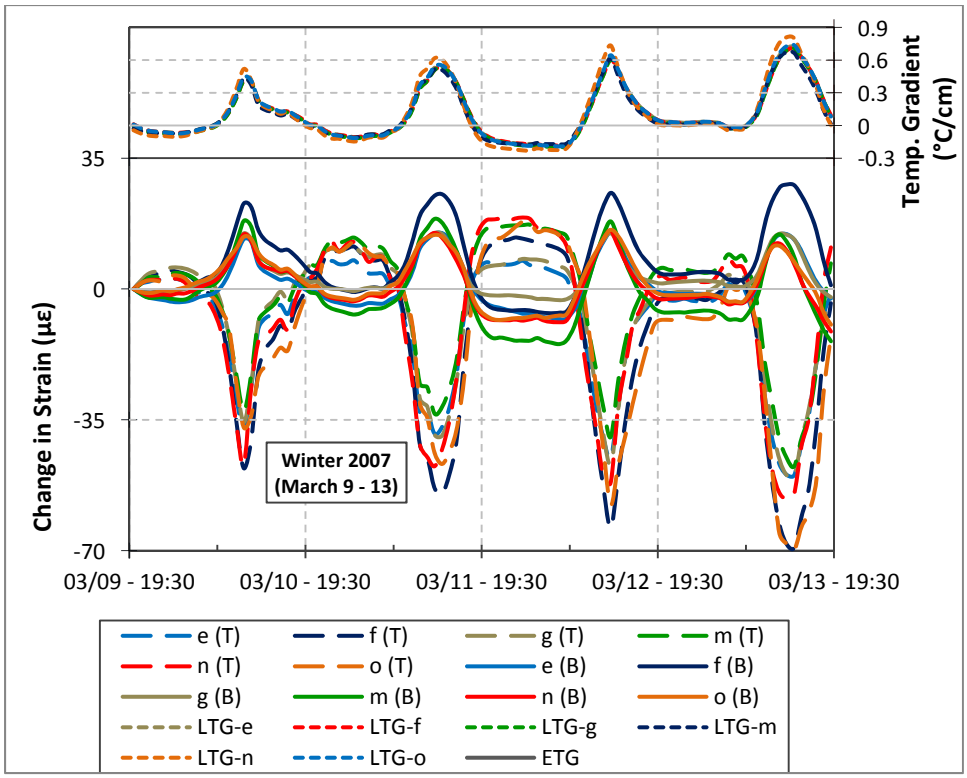
Temp. Gradient (°C/cm)
0.9
0.6
0.3
0
-0.3
Change in Strain (με)
35
0
-35
-70
Winter 2007
(March 9 - 13)
03/09 - 19:30
03/10 - 19:30
03/11 - 19:30
03/12 - 19:30
03/13 - 19:30
e (T)
f (T)
g (T)
m (T)
n (T)
o (T)
e (B)
f (B)
g (B)
m (B)
n (B)
o (B)
LTG-e
LTG-f
LTG-g
LTG-m
LTG-n
LTG-o
ETG

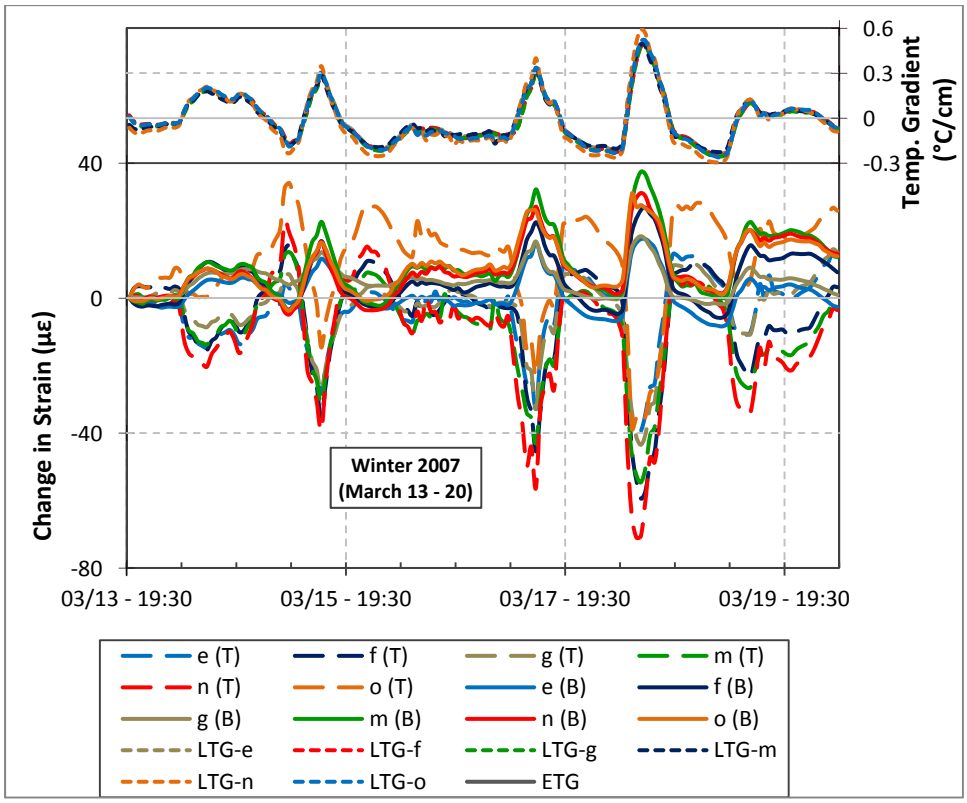
Temp. Gradient (°C/cm)
0.6
0.3
0
-0.3
Change in Strain (με)
40
0
-40
-80
Winter 2007
(March 13 - 20)
03/13 - 19:30
03/15 - 19:30
03/17 - 19:30
03/19 - 19:30
e (T)
f (T)
g (T)
m (T)
n (T)
o (T)
e (B)
f (B)
g (B)
m (B)
n (B)
o (B)
LTG-e
LTG-f
LTG-g
LTG-m
LTG-n
LTG-o
ETG

(1°C/cm = 4.6°F/in)

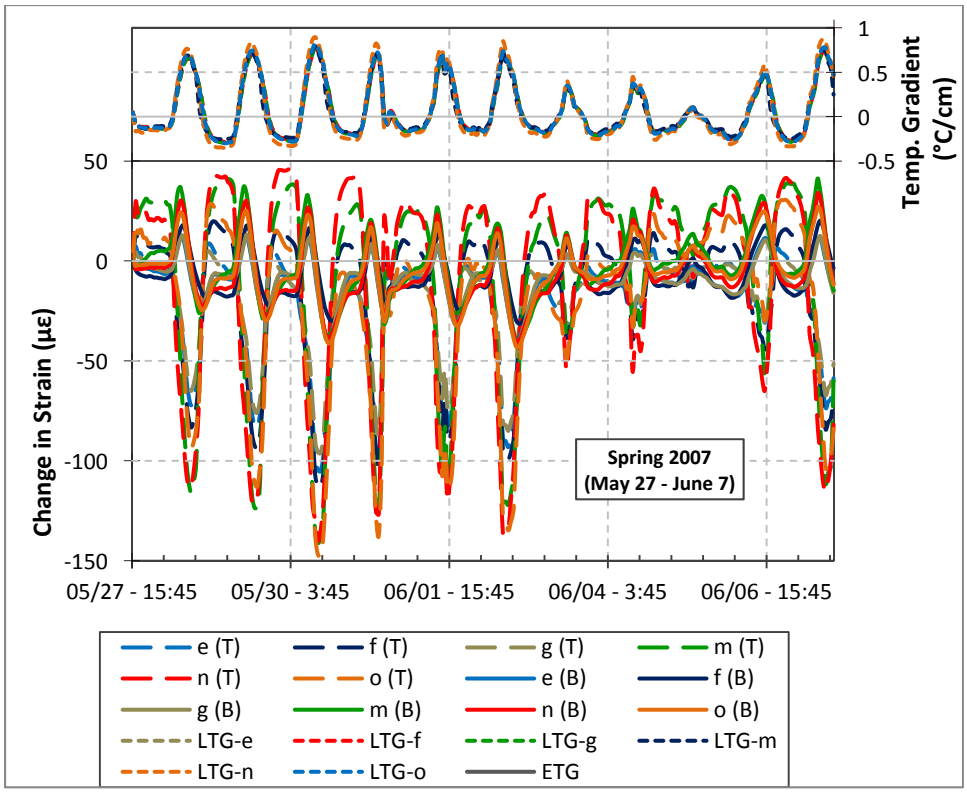
Change in Strain (με)
Temp. Gradient (°C/cm)
50
0
-50
-100
-150
1
0.5
0
-0.5
05/27 - 15:45
05/30 - 3:45
06/01 - 15:45
06/04 - 3:45
06/06 - 15:45
Spring 2007
(May 27 - June 7)
e (T)
f (T)
g (T)
m (T)
n (T)
o (T)
e (B)
f (B)
g (B)
m (B)
n (B)
o (B)
LTG-e
LTG-f
LTG-g
LTG-m
LTG-n
LTG-o
ETG

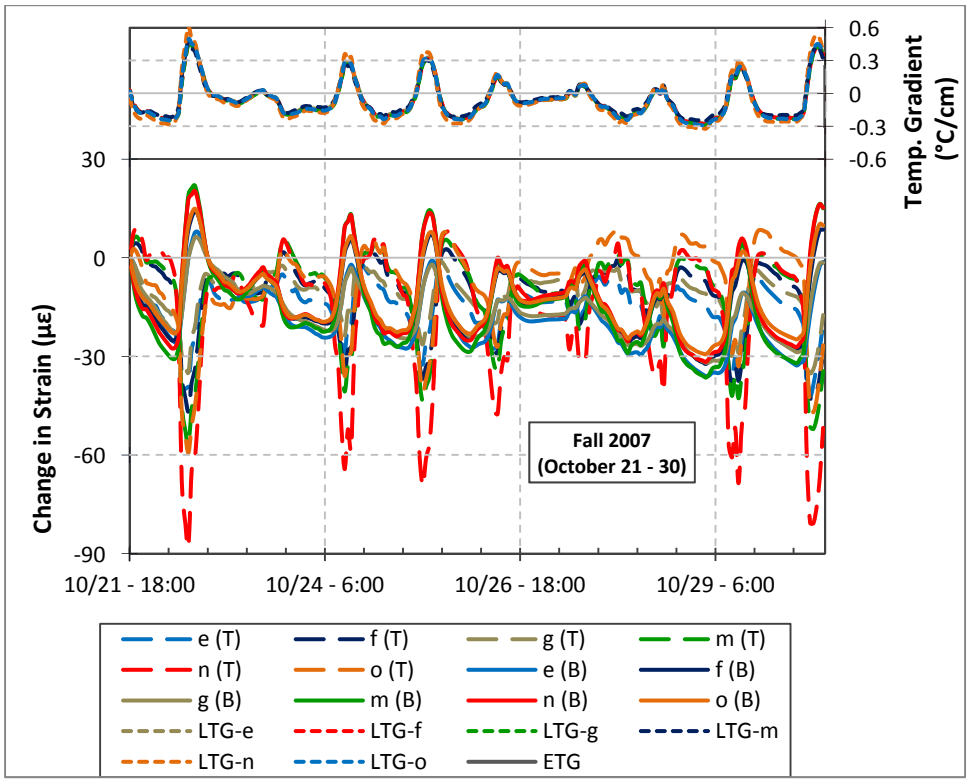
Change in Strain (με)
Temp. Gradient (°C/cm)
30
0
-30
-60
-90
0.6
0.3
0
-0.3
-0.6
10/21 - 18:00
10/24 - 6:00
10/26 - 18:00
10/29 - 6:00
Fall 2007
(October 21 - 30)
e (T)
f (T)
g (T)
m (T)
n (T)
o (T)
e (B)
f (B)
g (B)
m (B)
n (B)
o (B)
LTG-e
LTG-f
LTG-g
LTG-m
LTG-n
LTG-o
ETG

(1°C/cm = 4.6°F/in)

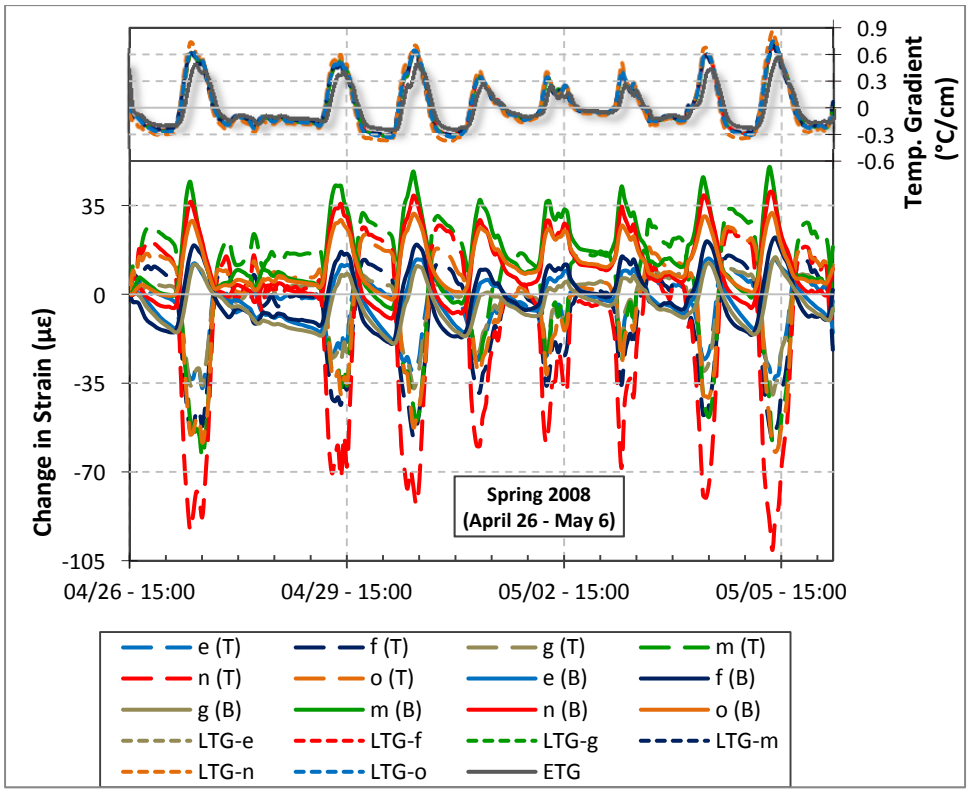
Temp. Gradient (°C/cm)
0.9
0.6
0.3
0
-0.3
-0.6
Change in Strain (με)
35
0
-35
-70
-105
Spring 2008
(April 26 - May 6)
04/26 - 15:00
04/29 - 15:00
05/02 - 15:00
05/05 - 15:00
e (T)
f (T)
g (T)
m (T)
n (T)
o (T)
e (B)
f (B)
g (B)
m (B)
n (B)
o (B)
LTG-e
LTG-f
LTG-g
LTG-m
LTG-n
LTG-o
ETG

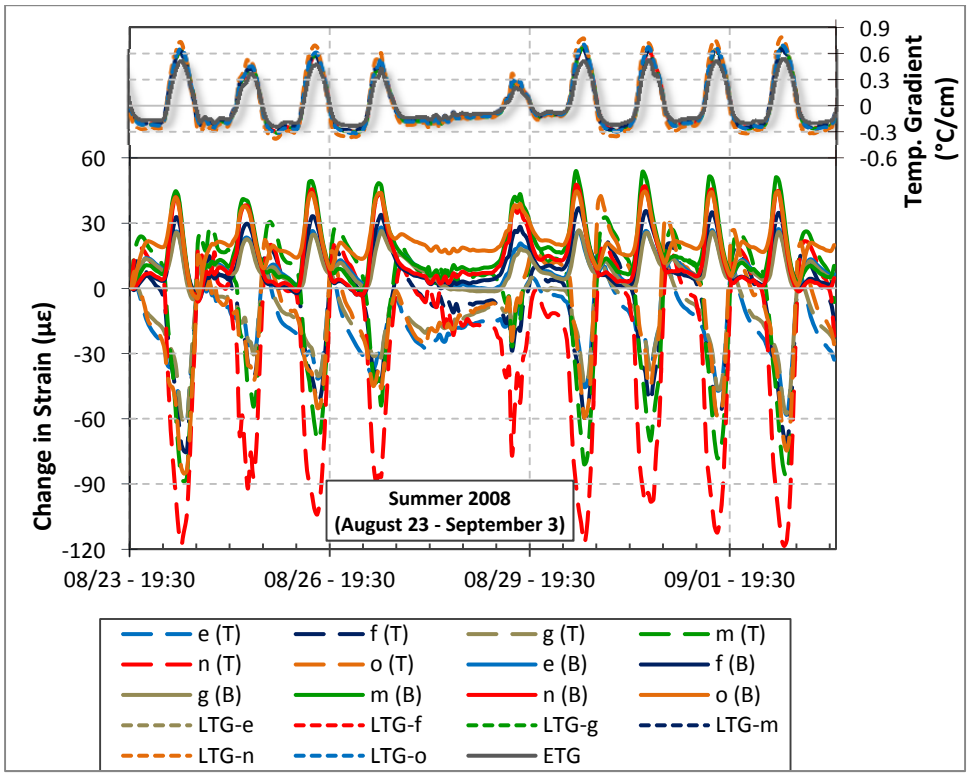
Temp. Gradient (°C/cm)
0.9
0.6
0.3
0
-0.3
-0.6
Change in Strain (με)
60
30
0
-30
-60
-90
-120
Summer 2008
(August 23 - September 3)
08/23 - 19:30
08/26 - 19:30
08/29 - 19:30
09/01 - 19:30
e (T)
f (T)
g (T)
m (T)
n (T)
o (T)
e (B)
f (B)
g (B)
m (B)
n (B)
o (B)
LTG-e
LTG-f
LTG-g
LTG-m
LTG-n
LTG-o
ETG

(1°C/cm = 4.6°F/in)

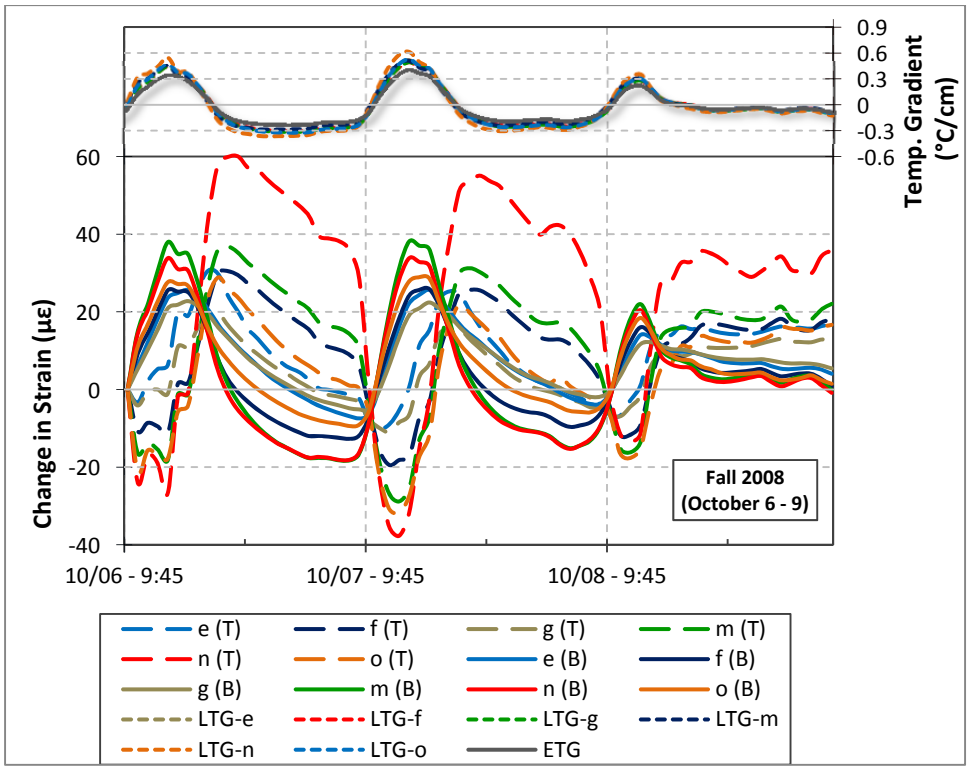
Temp. Gradient (°C/cm)
0.9
0.6
0.3
0
-0.3
-0.6
Change in Strain (με)
60
40
20
0
-20
-40
Fall 2008
(October 6 - 9)
10/06 - 9:45
10/07 - 9:45
10/08 - 9:45
e (T)
f (T)
g (T)
m (T)
n (T)
o (T)
e (B)
f (B)
g (B)
m (B)
n (B)
o (B)
LTG-e
LTG-f
LTG-g
LTG-m
LTG-n
LTG-o
ETG

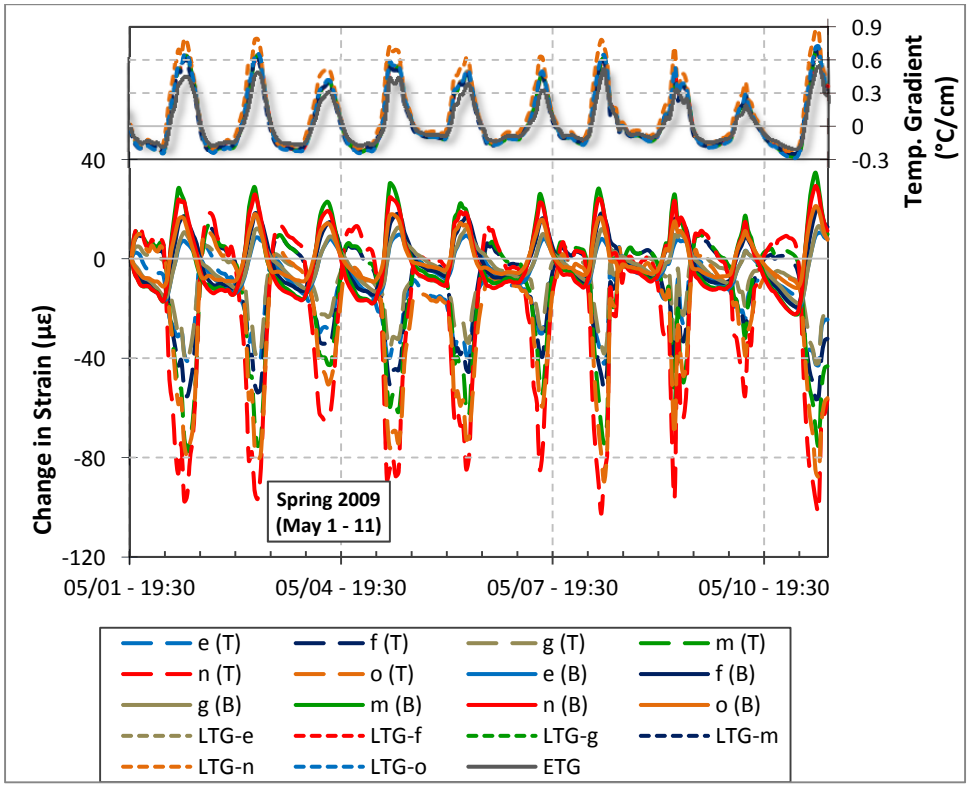
Temp. Gradient (°C/cm)
0.9
0.6
0.3
0
-0.3
Change in Strain (με)
40
0
-40
-80
-120
Spring 2009
(May 1 - 11)
05/01 - 19:30
05/04 - 19:30
05/07 - 19:30
05/10 - 19:30
e (T)
f (T)
g (T)
m (T)
n (T)
o (T)
e (B)
f (B)
g (B)
m (B)
n (B)
o (B)
LTG-e
LTG-f
LTG-g
LTG-m
LTG-n
LTG-o
ETG

(1°C/cm = 4.6°F/in)

Pavement Temperatures, Temperature Gradients, and Pavement Strains

B&S Section

Pavement Temperatures

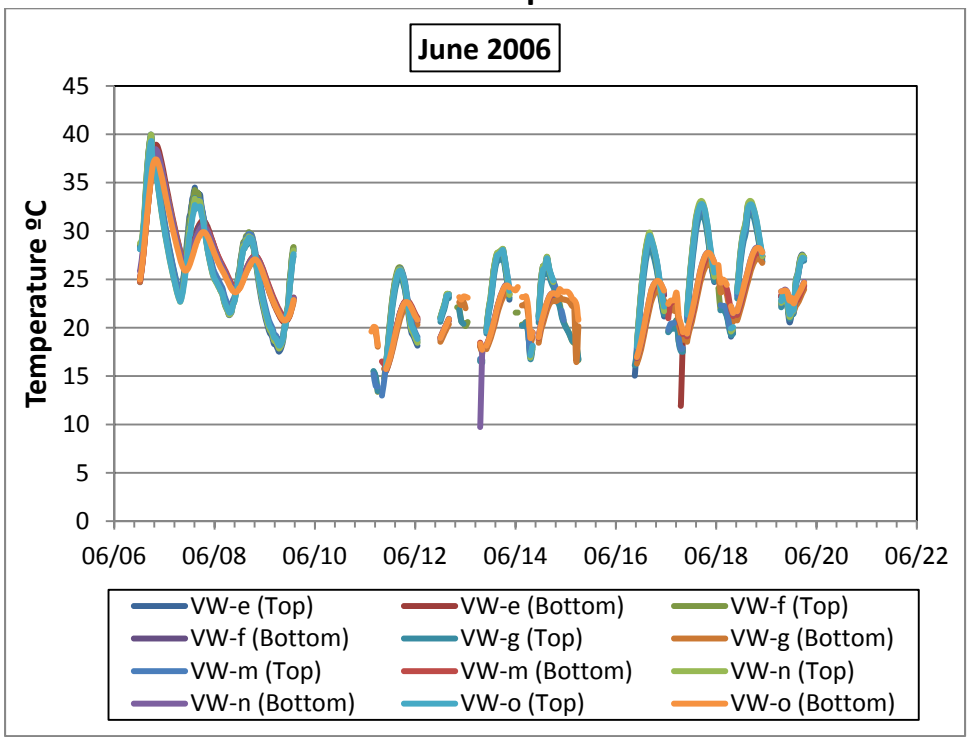

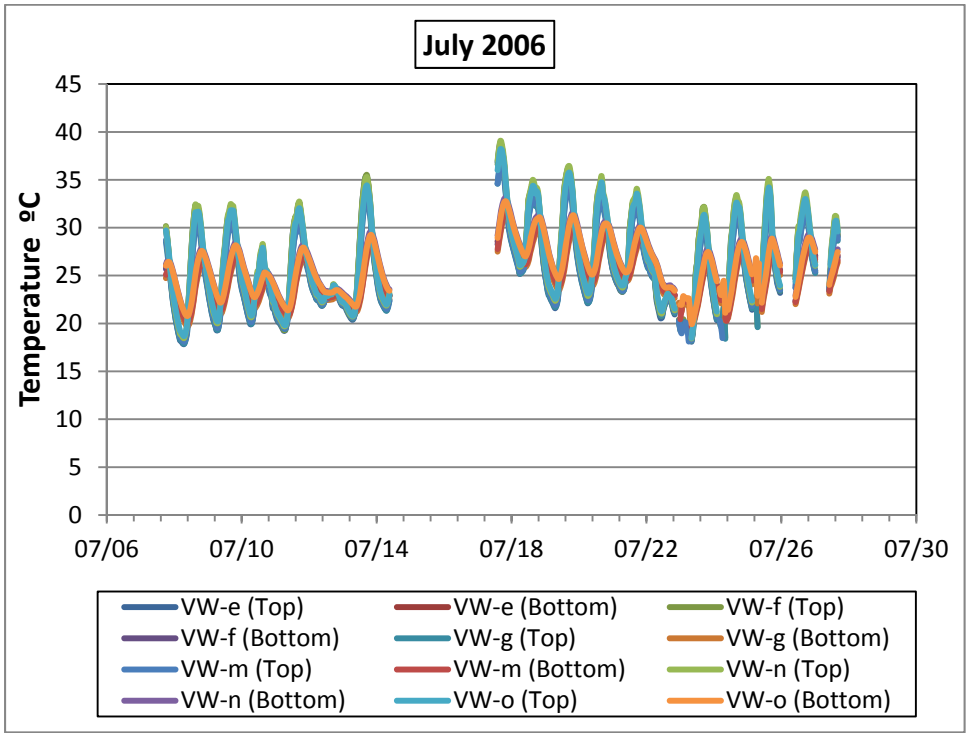

(0°C = 32°F, 45°C = 113°F)

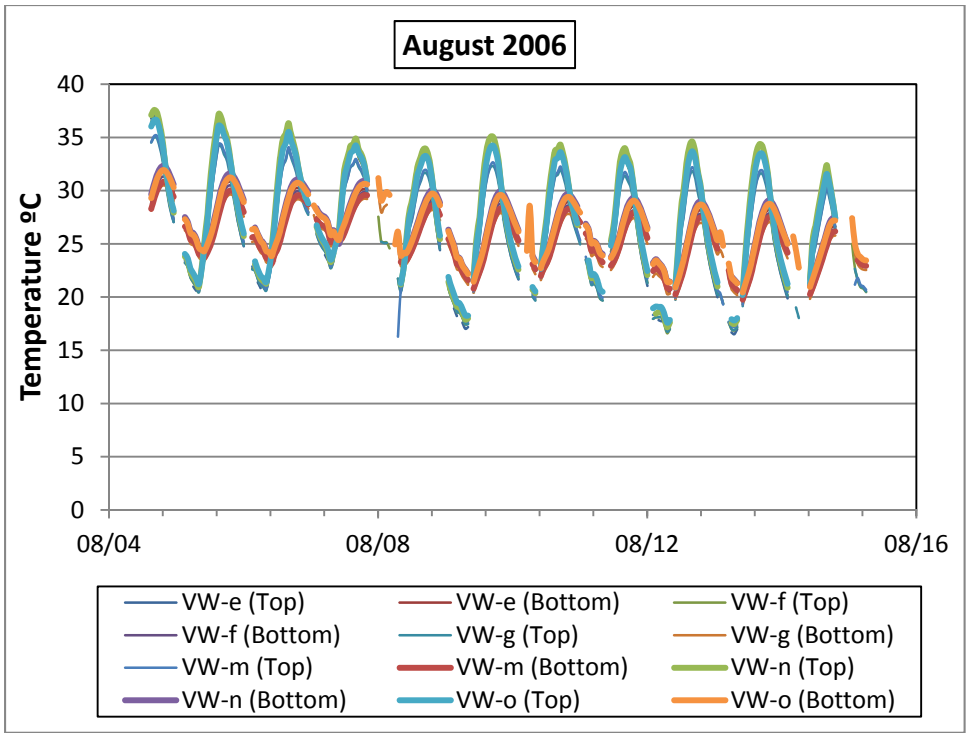

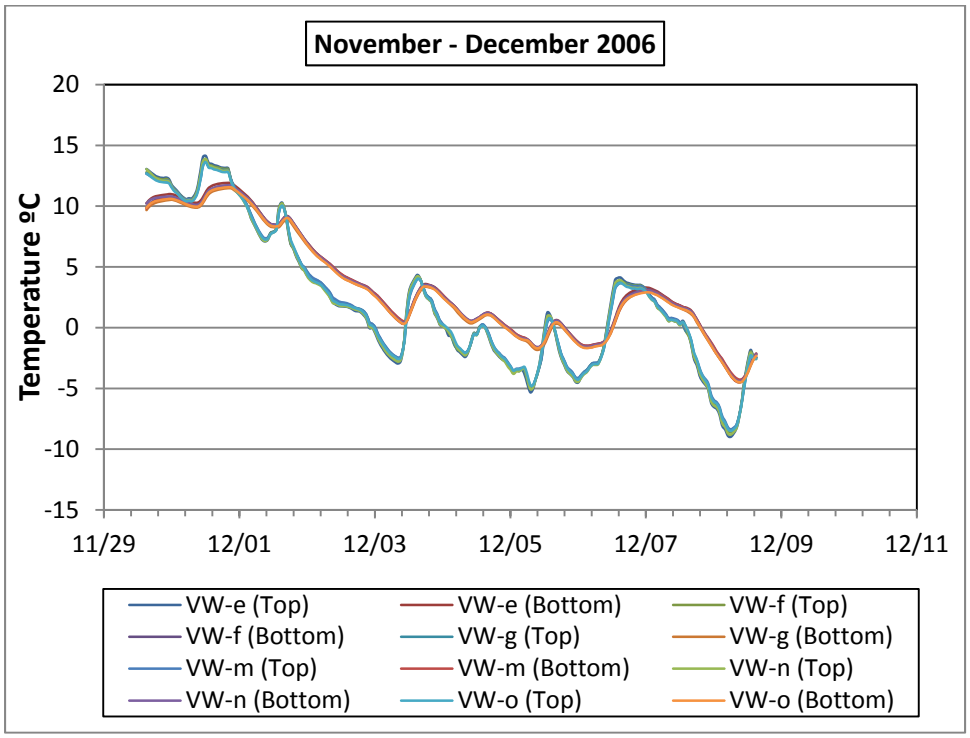

(0°C = 32°F, 40°C = 104°F)

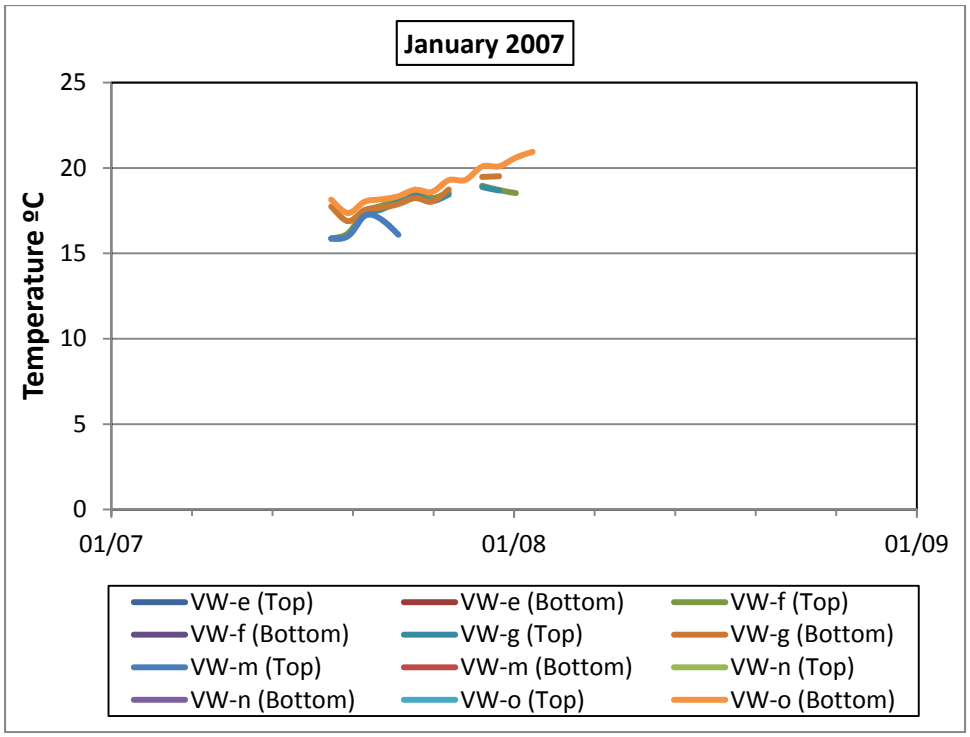

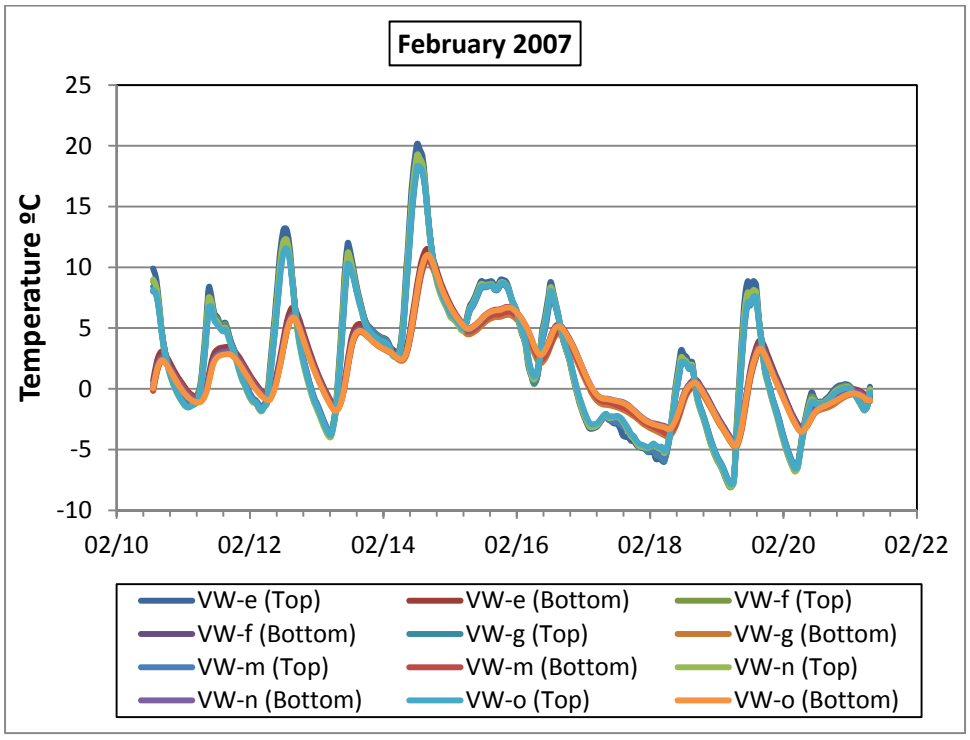

(0°C = 32°F, 25°C = 77°F)

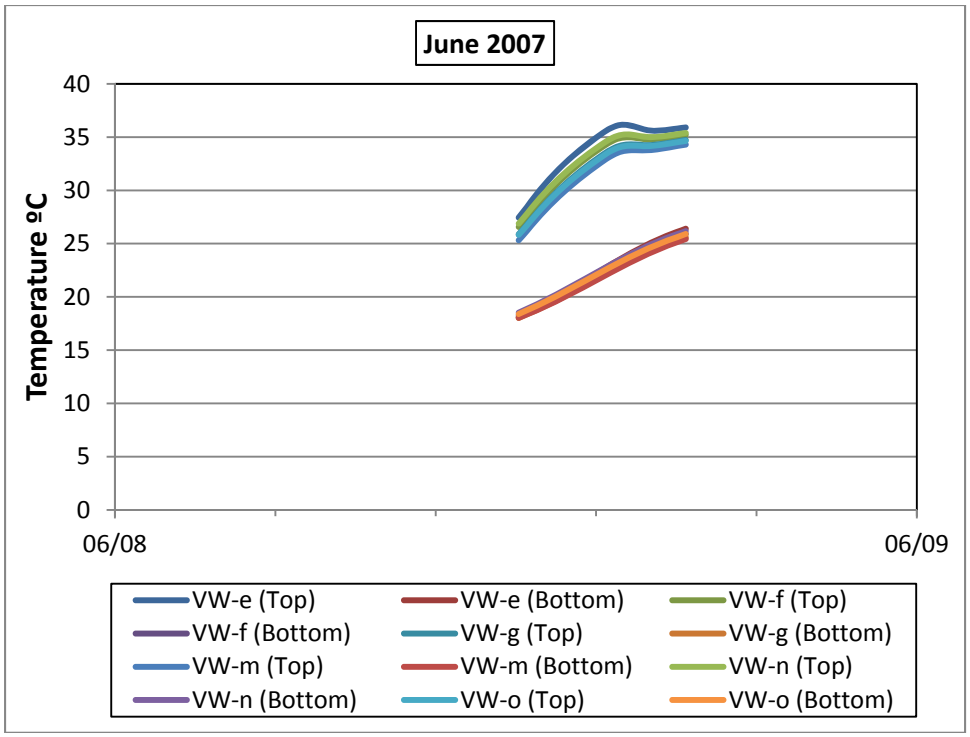

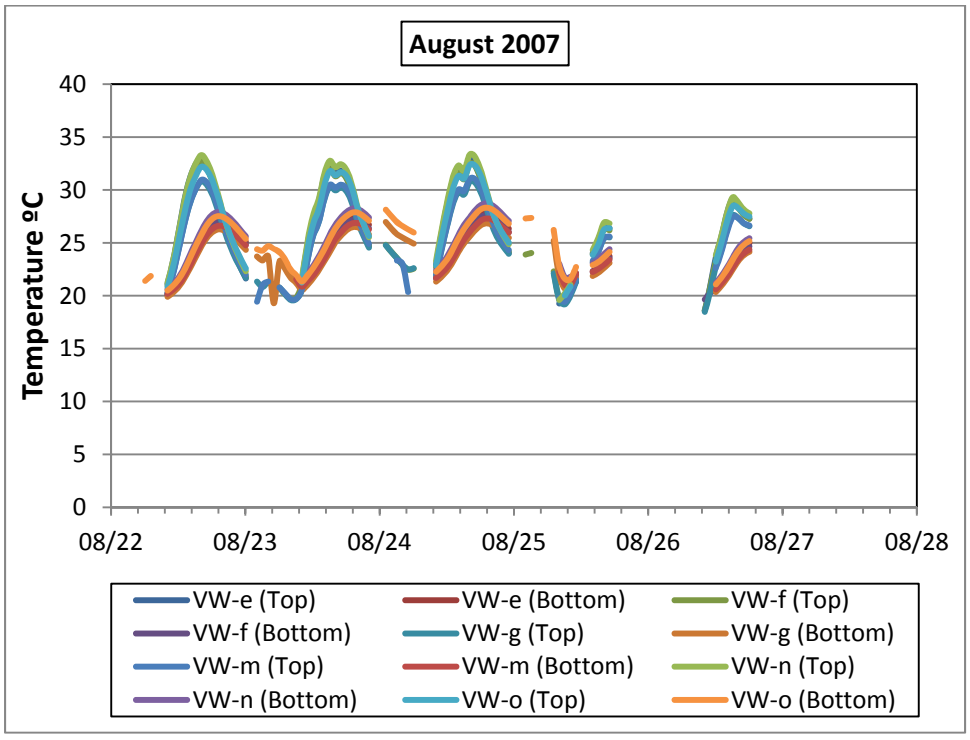

(0°C = 32°F, 40°C = 104°F)

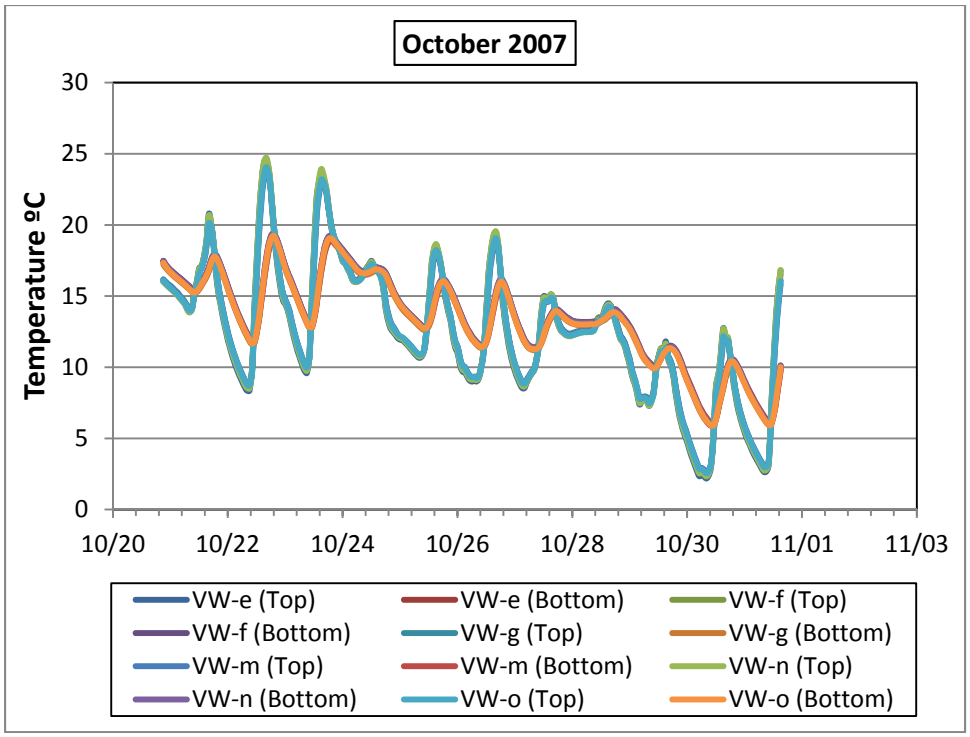

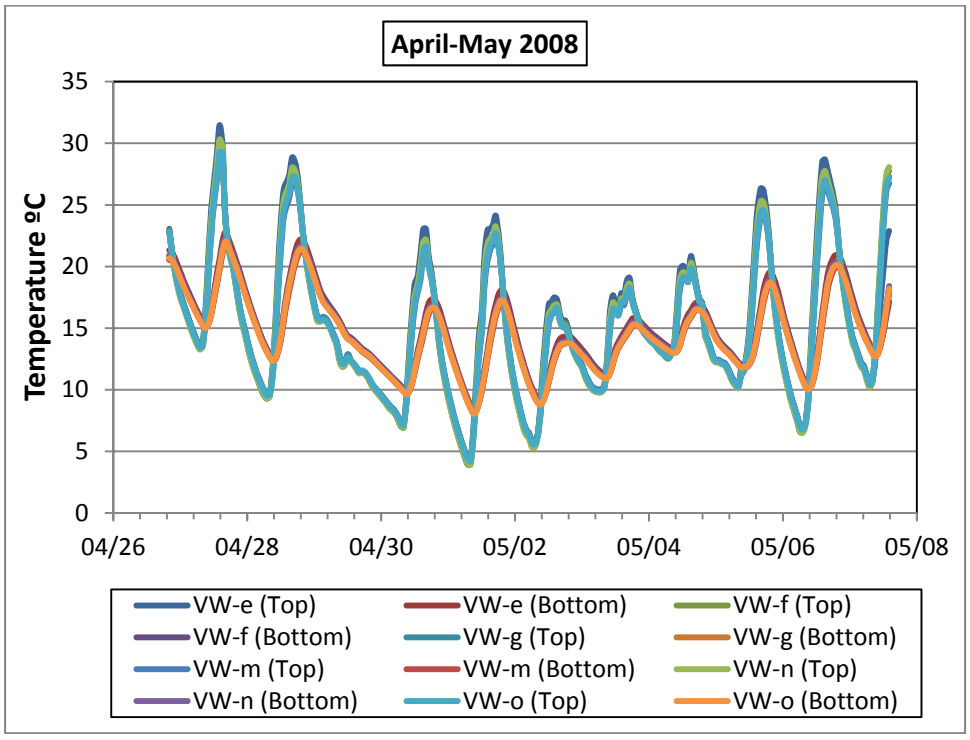

(0°C = 32°F, 35°C = 95°F)

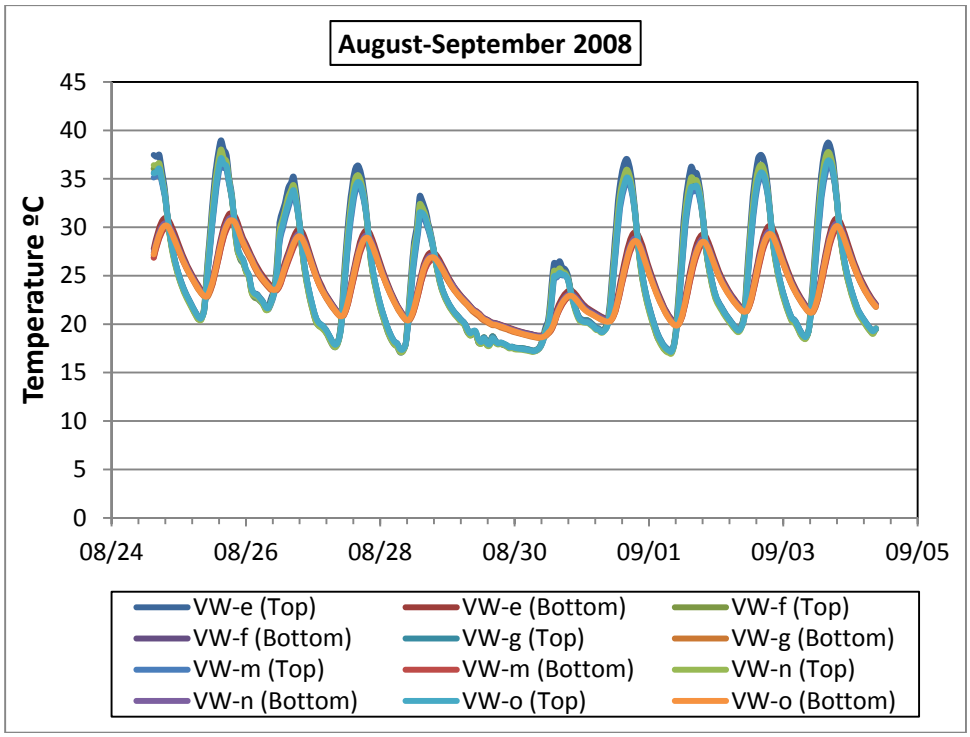

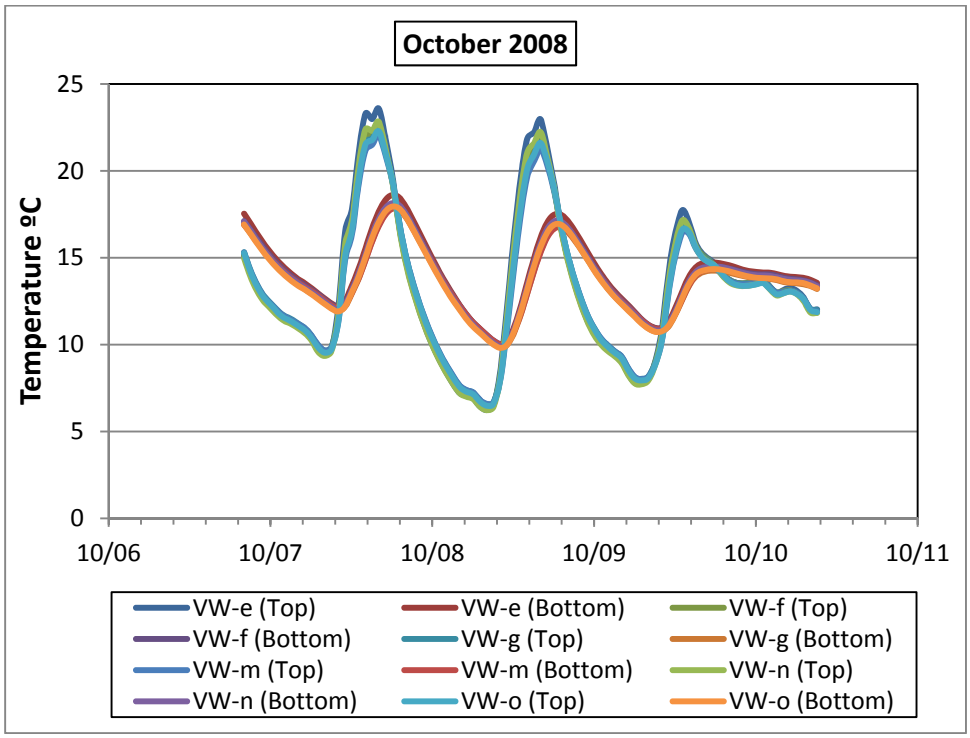

(0°C = 32°F, 45°C = 113°F)

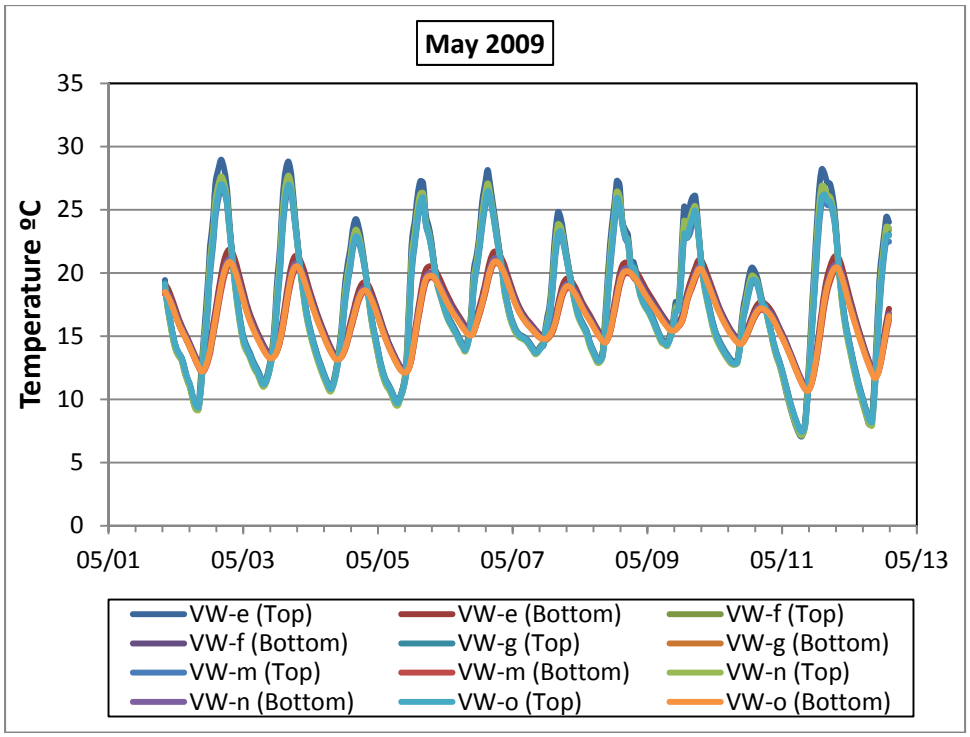

(0°C = 32°F, 35°C = 95°F)

Temperature Gradient

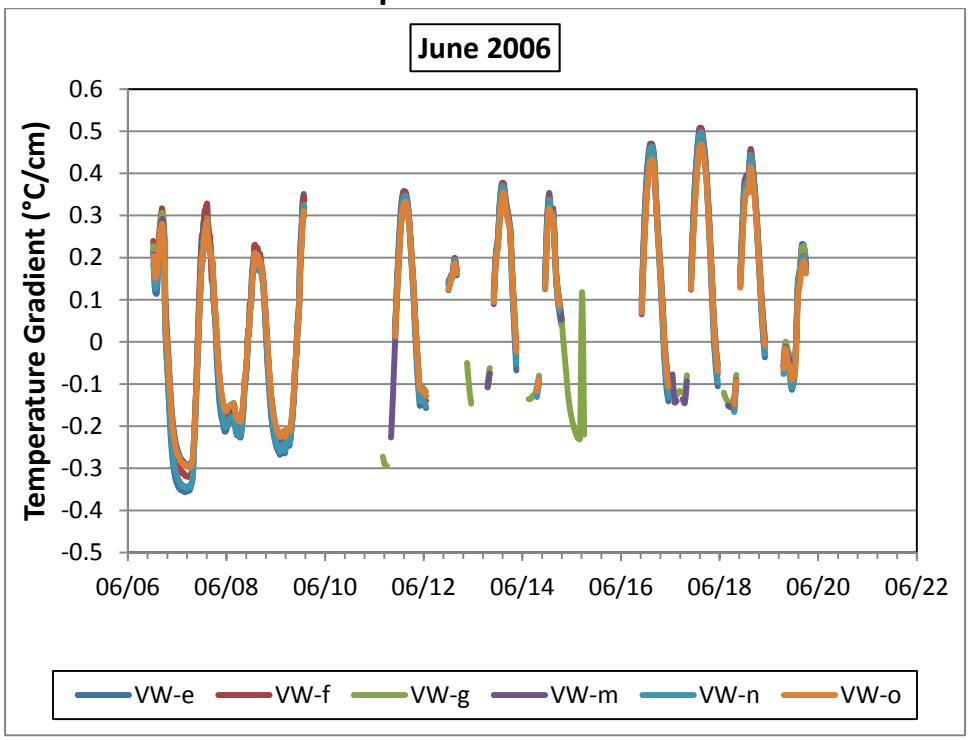

(1°C/cm = 4.6°F/in)

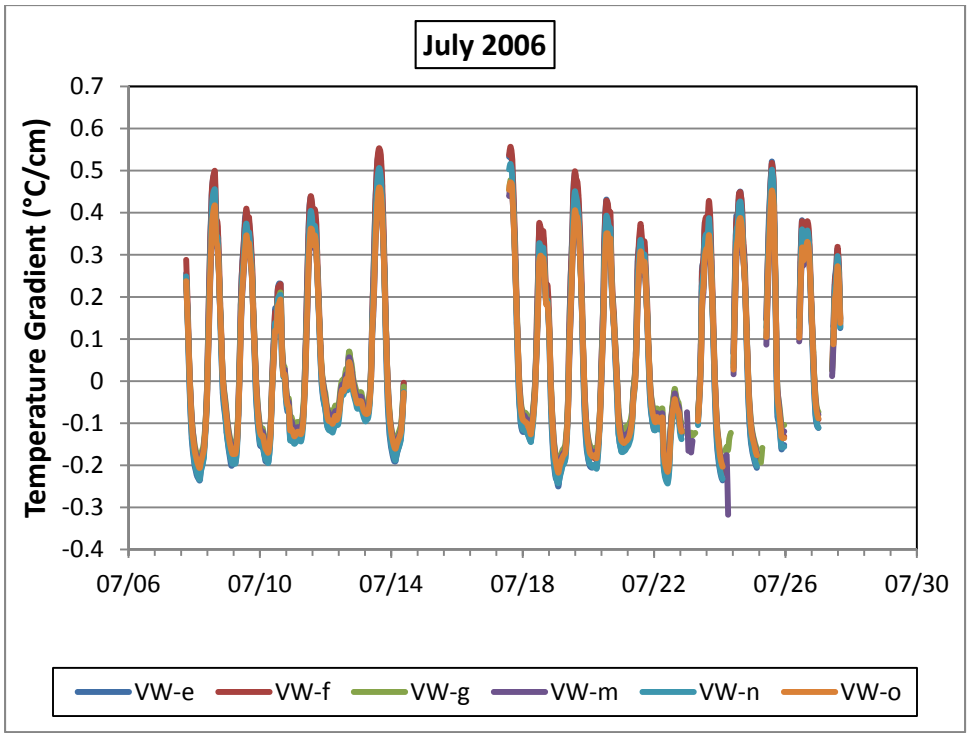
July 2006
Temperature Gradient (°C/cm)
0.7
0.6
0.5
0.4
0.3
0.2
0.1
0
-0.1
-0.2
-0.3
-0.4
07/06
07/10
07/14
07/18
07/22
07/26
07/30
VW-e
VW-f
VW-g
VW-m
VW-n
VW-o

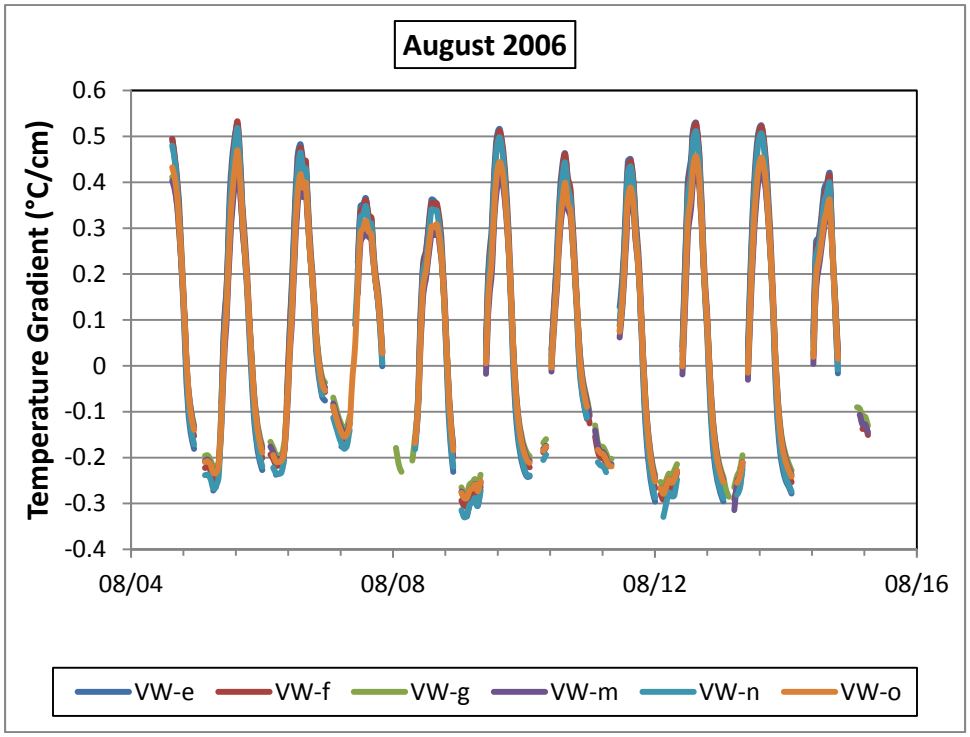
August 2006
Temperature Gradient (°C/cm)
0.6
0.5
0.4
0.3
0.2
0.1
0
-0.1
-0.2
-0.3
-0.4
08/04
08/08
08/12
08/16
VW-e
VW-f
VW-g
VW-m
VW-n
VW-o

(1°C/cm = 4.6°F/in)

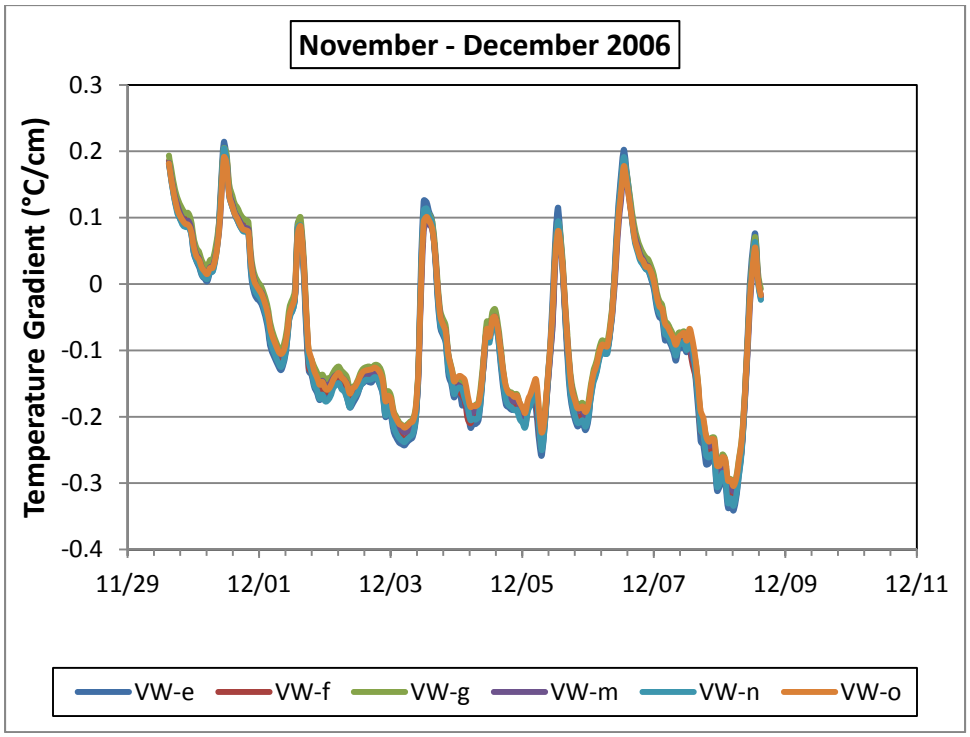
November - December 2006
Temperature Gradient (°C/cm)
0.3
0.2
0.1
0
-0.1
-0.2
-0.3
-0.4
11/29
12/01
12/03
12/05
12/07
12/09
12/11
VW-e
VW-f
VW-g
VW-m
VW-n
VW-o

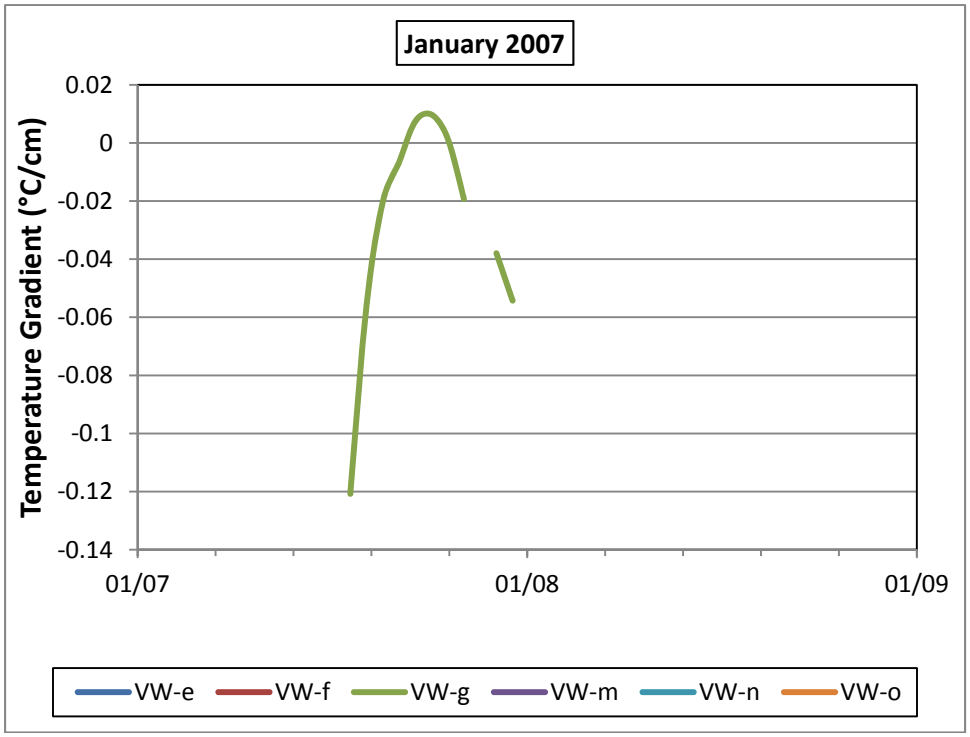
January 2007
Temperature Gradient (°C/cm)
0.02
0
-0.02
-0.04
-0.06
-0.08
-0.1
-0.12
-0.14
01/07
01/08
01/09
VW-e
VW-f
VW-g
VW-m
VW-n
VW-o

(1°C/cm = 4.6°F/in)

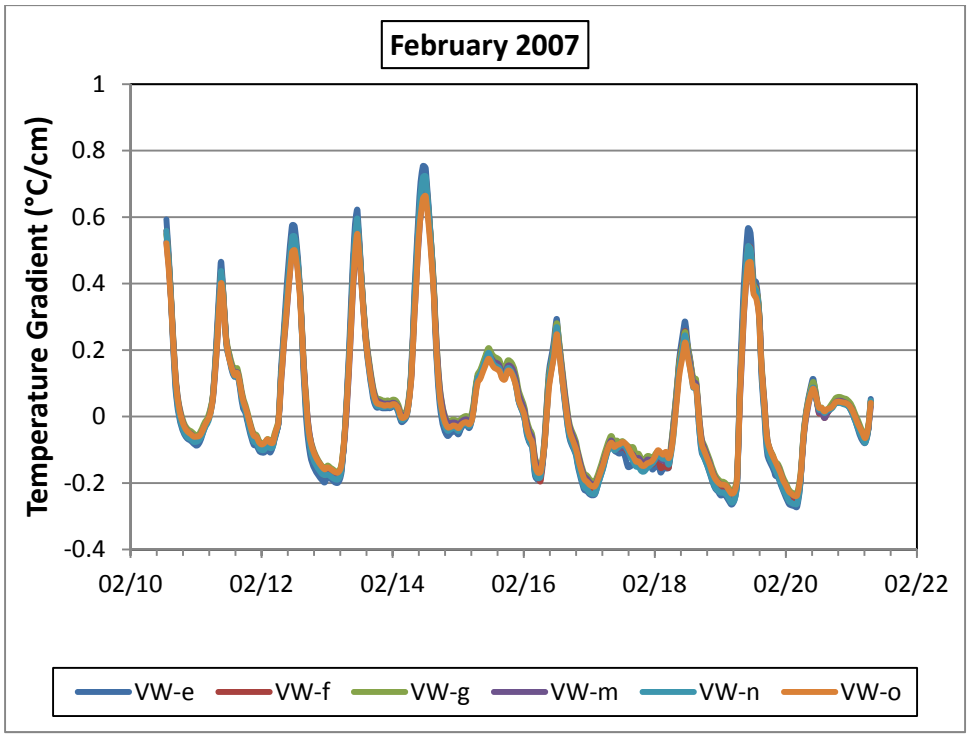
February 2007
Temperature Gradient (°C/cm)
1
0.8
0.6
0.4
0.2
0
-0.2
-0.4
02/10
02/12
02/14
02/16
02/18
02/20
02/22
VW-e
VW-f
VW-g
VW-m
VW-n
VW-o

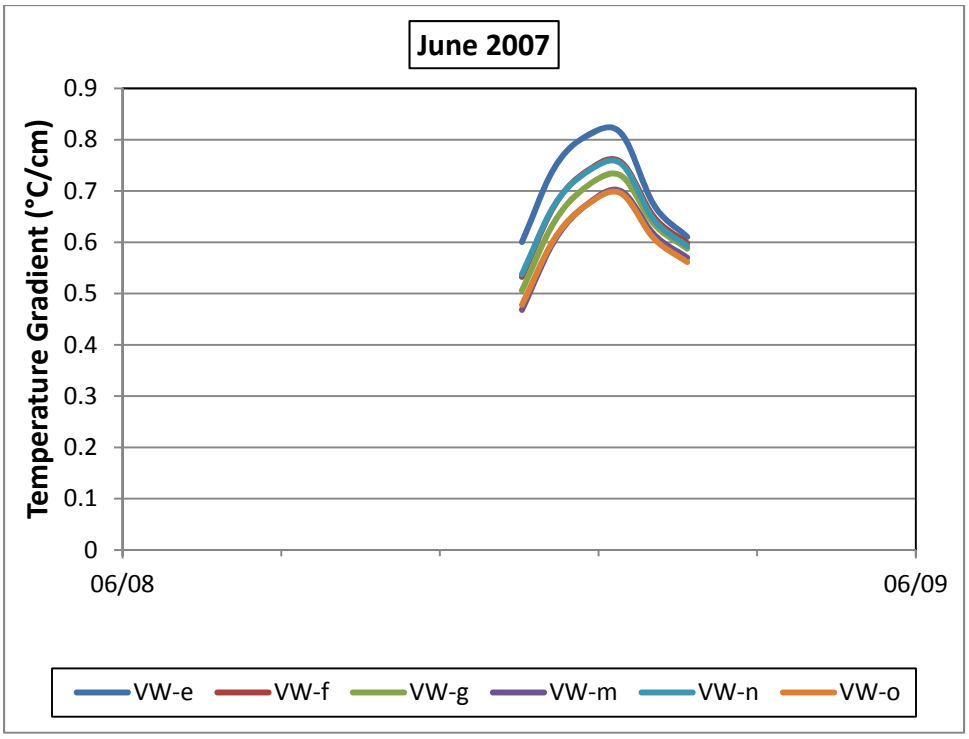
June 2007
Temperature Gradient (°C/cm)
0.9
0.8
0.7
0.6
0.5
0.4
0.3
0.2
0.1
0
06/08
06/09
VW-e
VW-f
VW-g
VW-m
VW-n
VW-o

(1°C/cm = 4.6°F/in)

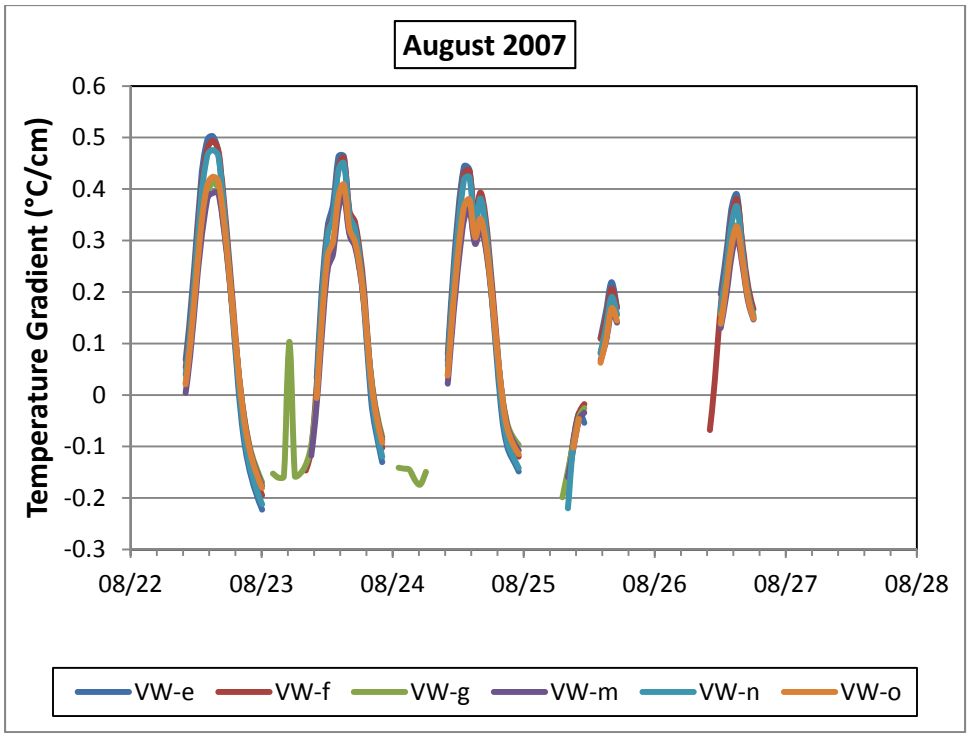
August 2007
Temperature Gradient (°C/cm)
0.6
0.5
0.4
0.3
0.2
0.1
0
-0.1
-0.2
-0.3
08/22
08/23
08/24
08/25
08/26
08/27
08/28
VW-e
VW-f
VW-g
VW-m
VW-n
VW-o

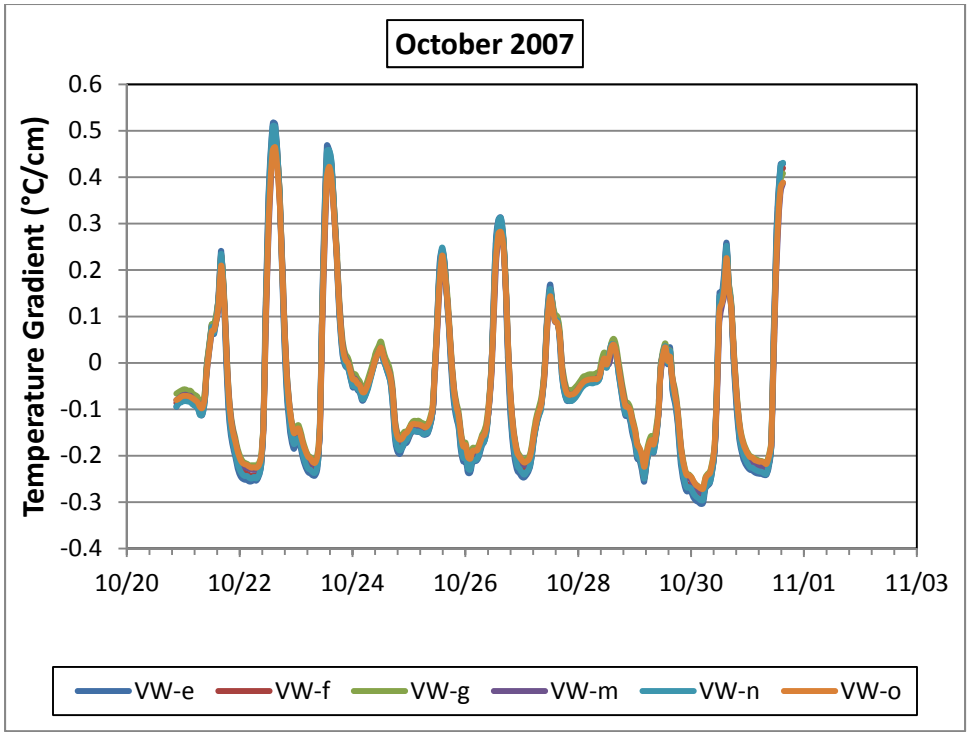
October 2007
Temperature Gradient (°C/cm)
0.6
0.5
0.4
0.3
0.2
0.1
0
-0.1
-0.2
-0.3
-0.4
10/20
10/22
10/24
10/26
10/28
10/30
11/01
11/03
VW-e
VW-f
VW-g
VW-m
VW-n
VW-o

(1°C/cm = 4.6°F/in)

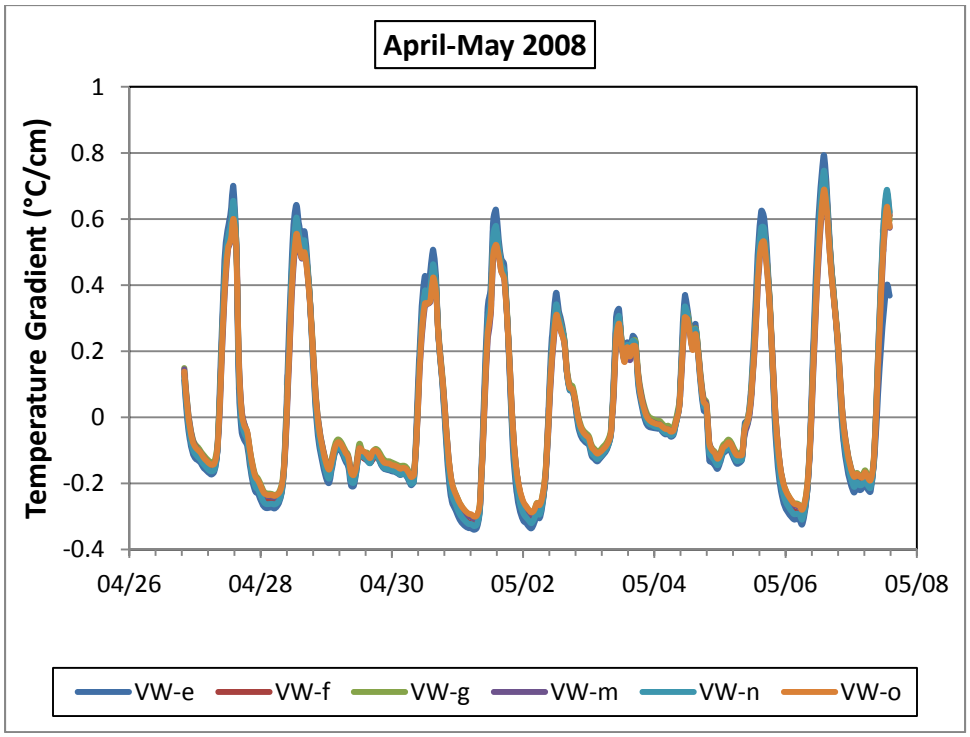
April-May 2008
Temperature Gradient (°C/cm)
1
0.8
0.6
0.4
0.2
0
-0.2
-0.4
04/26
04/28
04/30
05/02
05/04
05/06
05/08
VW-e
VW-f
VW-g
VW-m
VW-n
VW-o

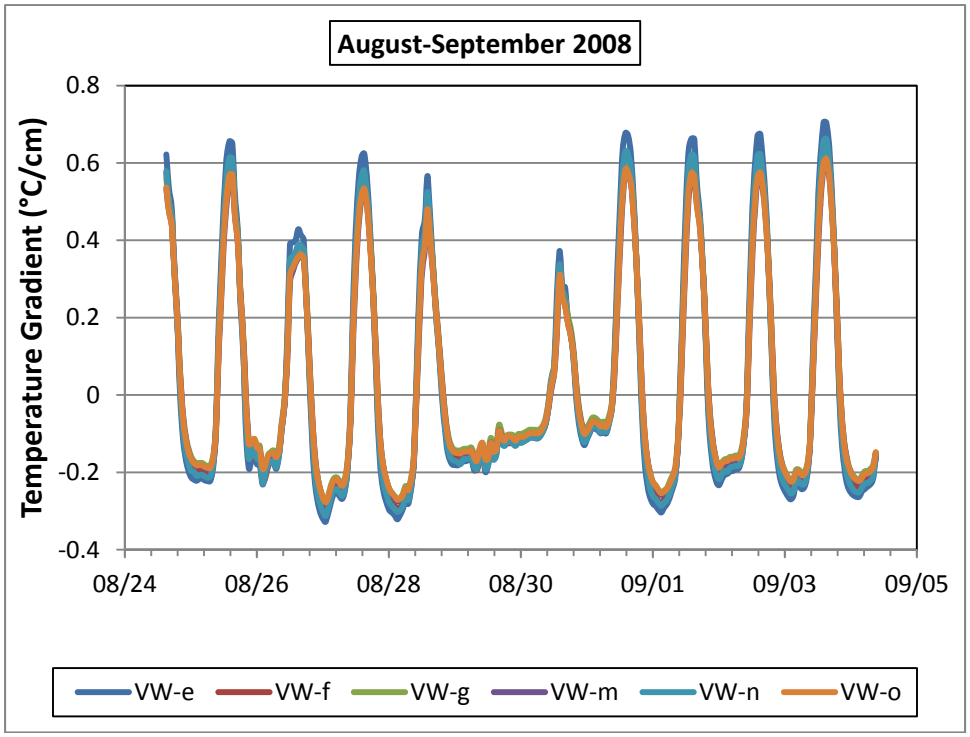
August-September 2008
Temperature Gradient (°C/cm)
0.8
0.6
0.4
0.2
0
-0.2
-0.4
08/24
08/26
08/28
08/30
09/01
09/03
09/05
VW-e
VW-f
VW-g
VW-m
VW-n
VW-o

(1°C/cm = 4.6°F/in)

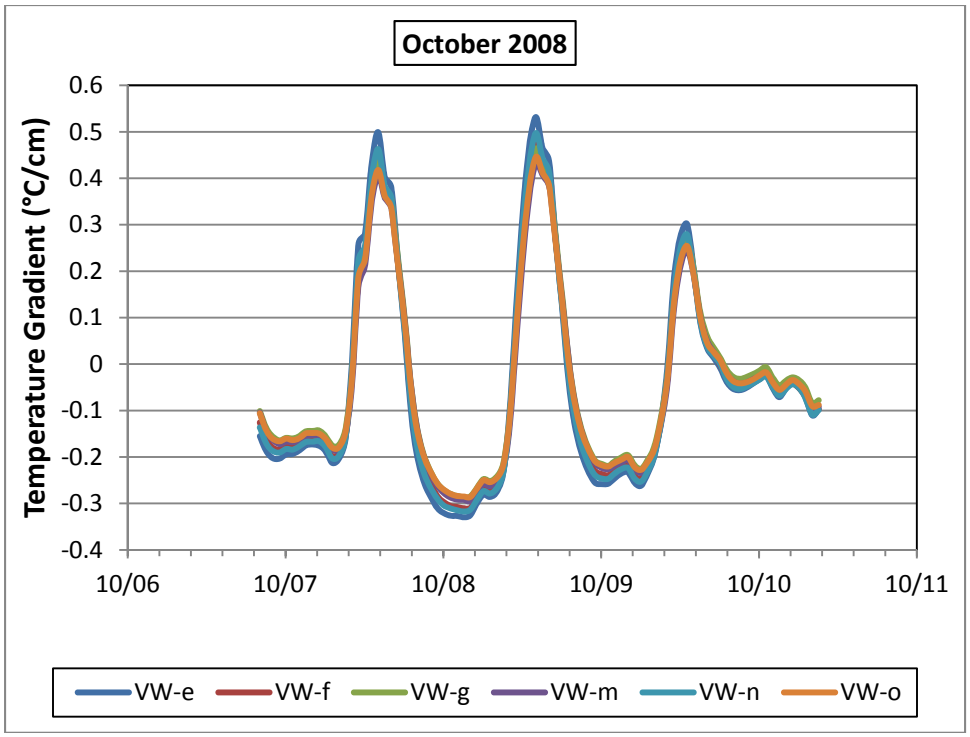
October 2008
Temperature Gradient (°C/cm)
0.6
0.5
0.4
0.3
0.2
0.1
0
-0.1
-0.2
-0.3
-0.4
10/06
10/07
10/08
10/09
10/10
10/11
VW-e
VW-f
VW-g
VW-m
VW-n
VW-o

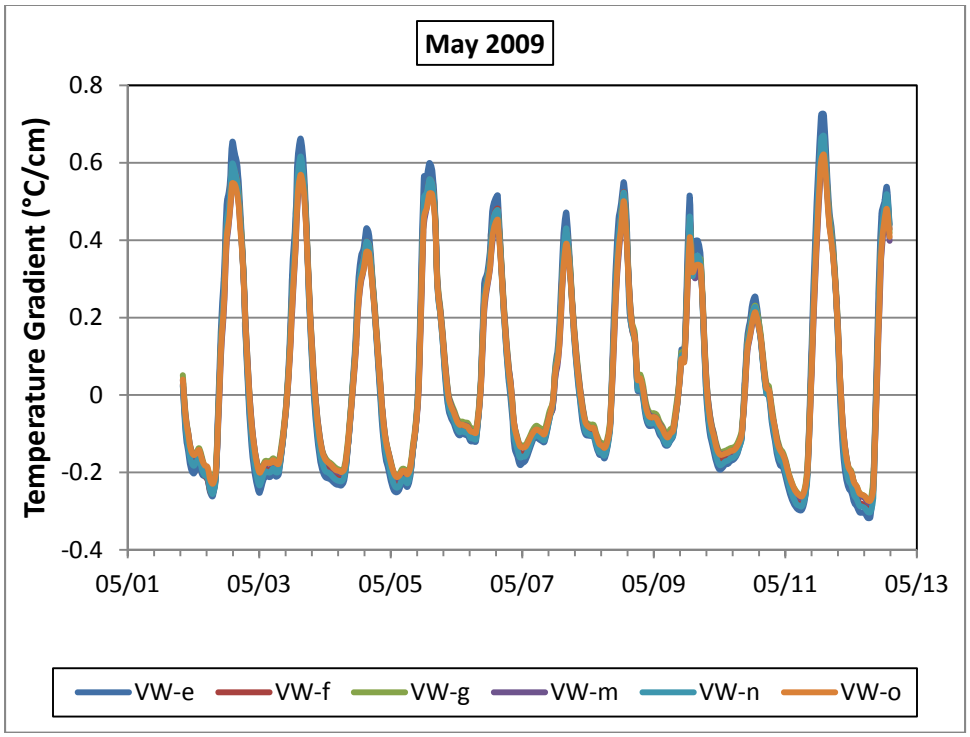
May 2009
Temperature Gradient (°C/cm)
0.8
0.6
0.4
0.2
0
-0.2
-0.4
05/01
05/03
05/05
05/07
05/09
05/11
05/13
VW-e
VW-f
VW-g
VW-m
VW-n
VW-o

(1°C/cm = 4.6°F/in)

Total Strain

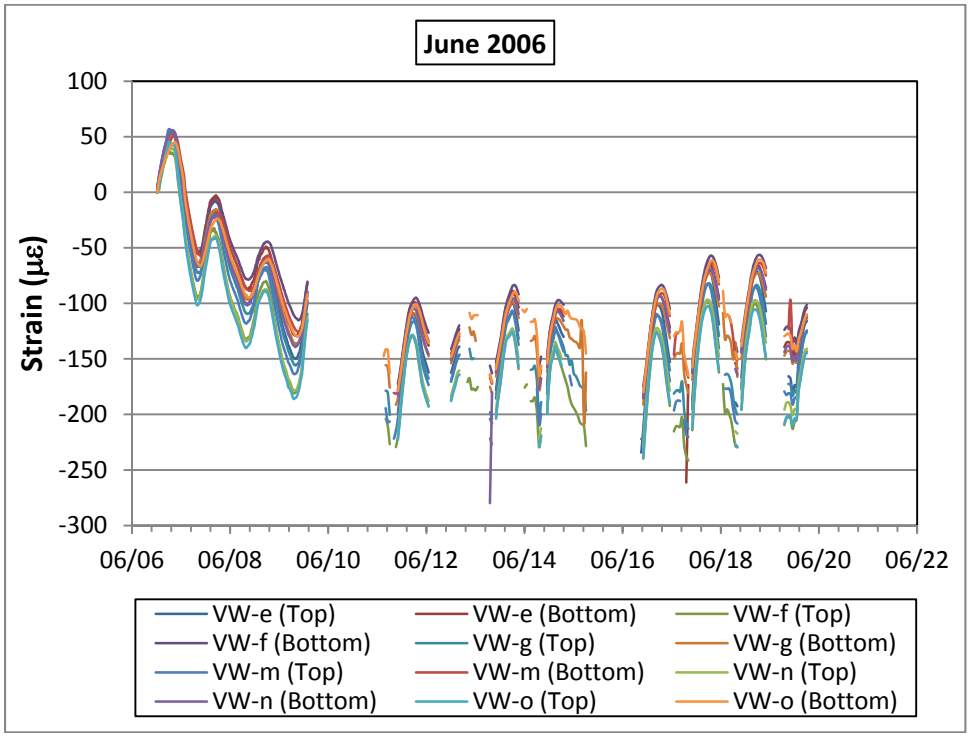

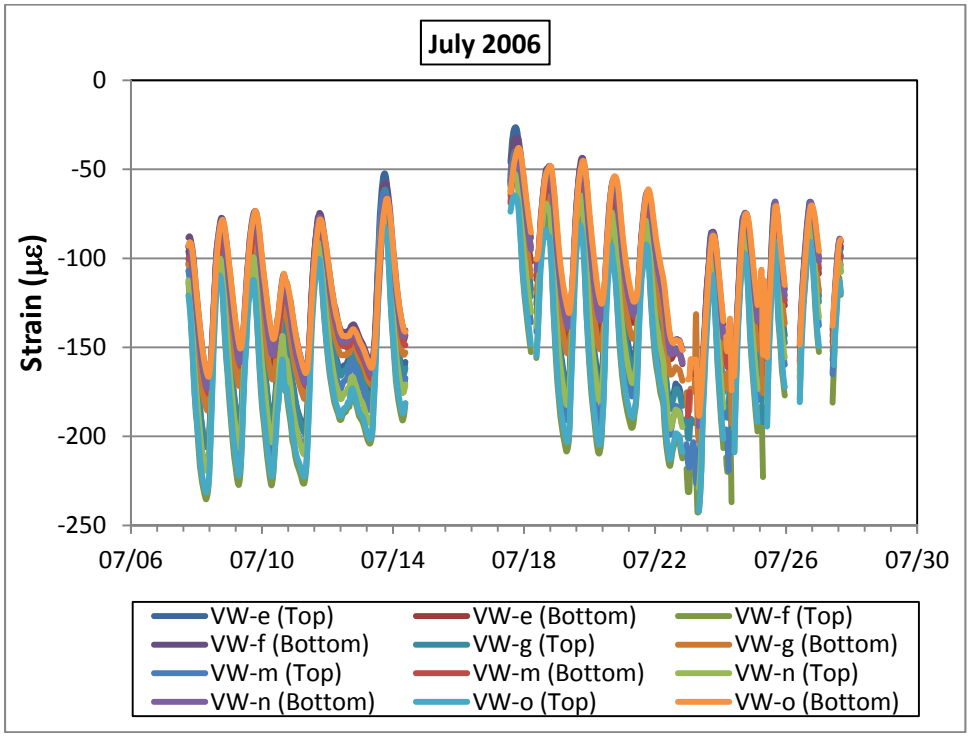

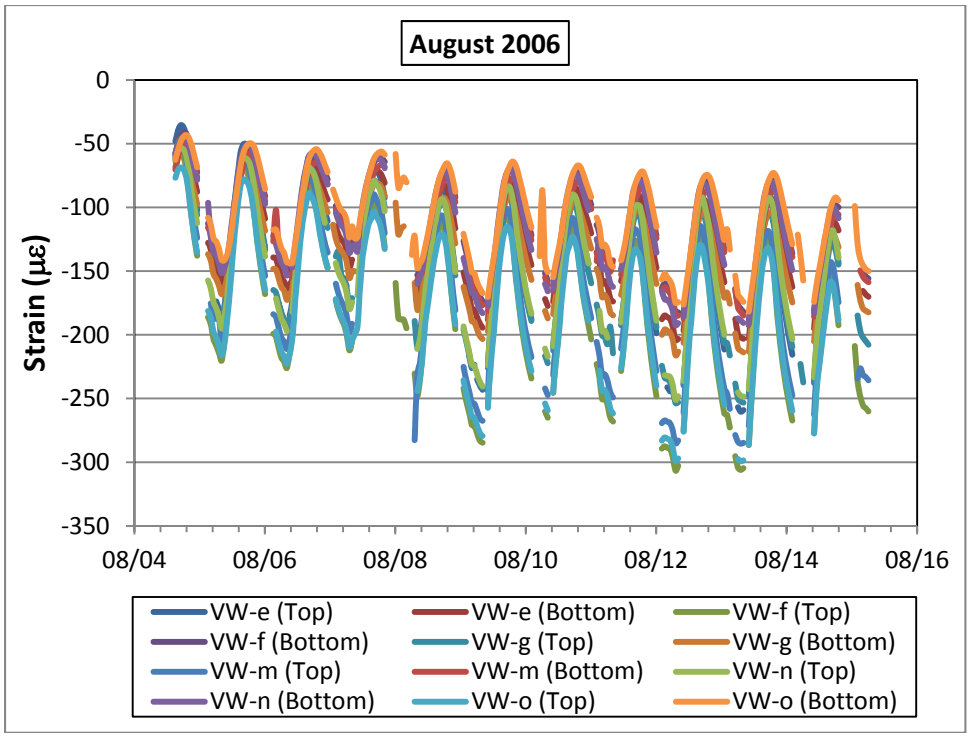
August 2006
0
-50
-100
-150
-200
-250
-300
-350
Strain (με)
08/04
08/06
08/08
08/10
08/12
08/14
08/16
VW-e (Top)
VW-e (Bottom)
VW-f (Top)
VW-f (Bottom)
VW-g (Top)
VW-g (Bottom)
VW-m (Top)
VW-m (Bottom)
VW-n (Top)
VW-n (Bottom)
VW-o (Top)
VW-o (Bottom)

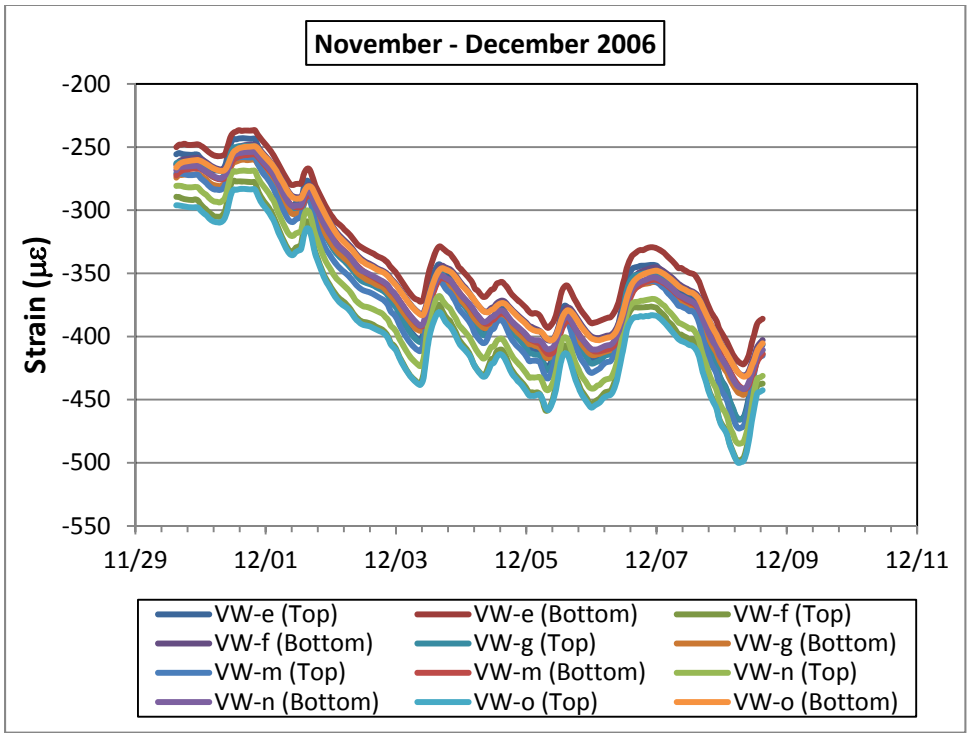
November - December 2006
-200
-250
-300
-350
-400
-450
-500
-550
Strain (με)
11/29
12/01
12/03
12/05
12/07
12/09
12/11
VW-e (Top)
VW-e (Bottom)
VW-f (Top)
VW-f (Bottom)
VW-g (Top)
VW-g (Bottom)
VW-m (Top)
VW-m (Bottom)
VW-n (Top)
VW-n (Bottom)
VW-o (Top)
VW-o (Bottom)

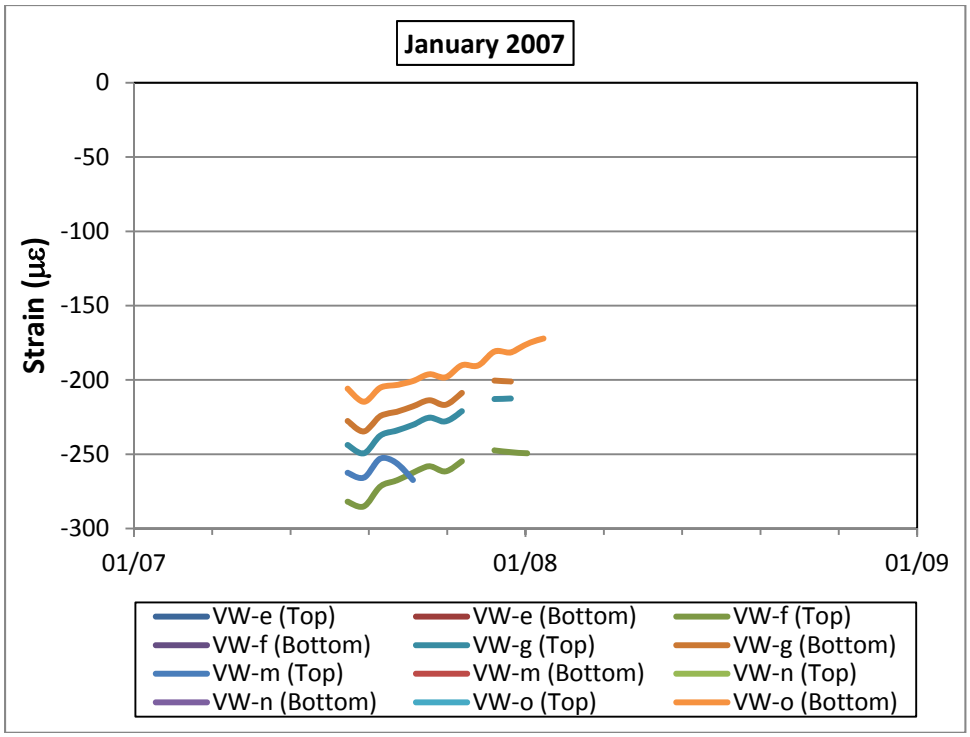
January 2007
0
-50
-100
-150
-200
-250
-300
Strain (με)
01/07
01/08
01/09
VW-e (Top)
VW-e (Bottom)
VW-f (Top)
VW-f (Bottom)
VW-g (Top)
VW-g (Bottom)
VW-m (Top)
VW-m (Bottom)
VW-n (Top)
VW-n (Bottom)
VW-o (Top)
VW-o (Bottom)

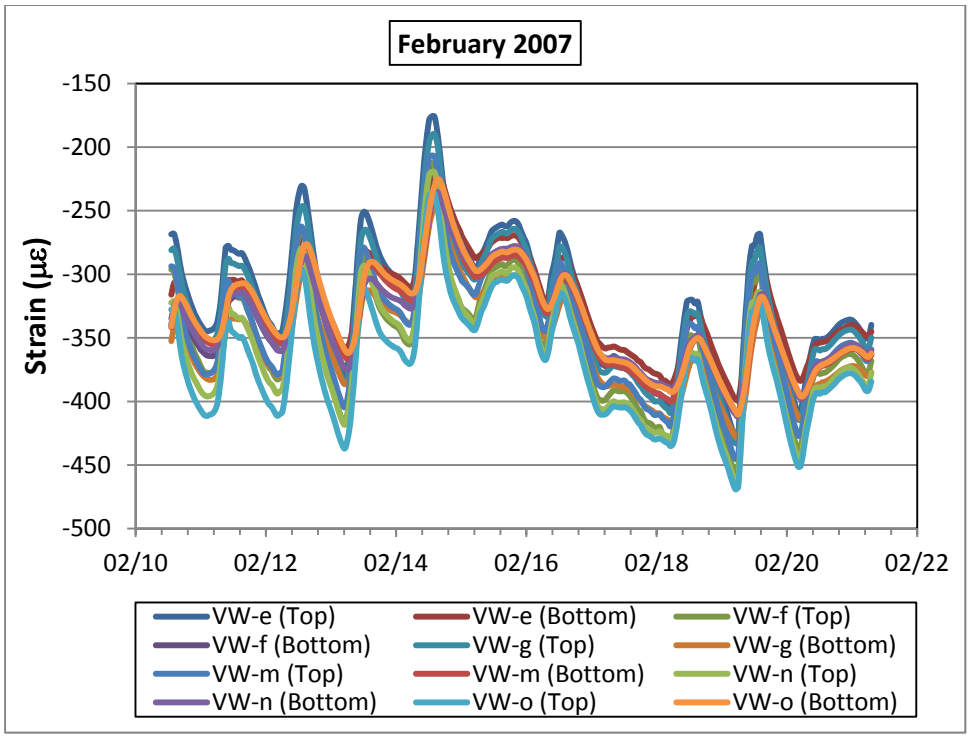
February 2007
-150
-200
-250
-300
-350
-400
-450
-500
Strain (με)
02/10
02/12
02/14
02/16
02/18
02/20
02/22
VW-e (Top)
VW-e (Bottom)
VW-f (Top)
VW-f (Bottom)
VW-g (Top)
VW-g (Bottom)
VW-m (Top)
VW-m (Bottom)
VW-n (Top)
VW-n (Bottom)
VW-o (Top)
VW-o (Bottom)

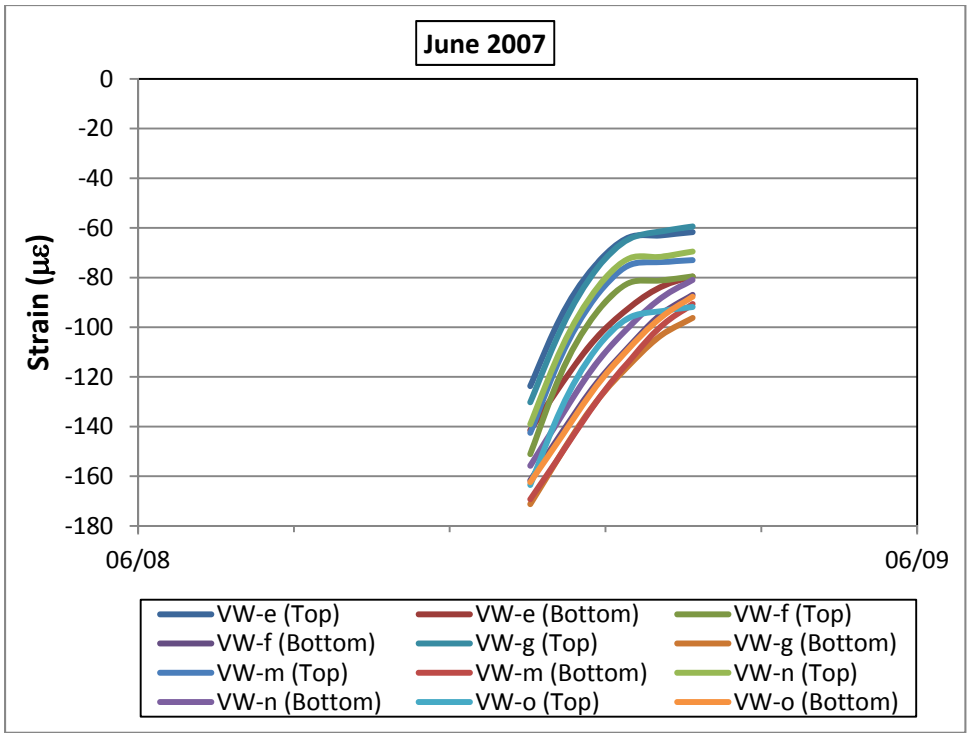
June 2007
0
-20
-40
-60
-80
-100
-120
-140
-160
-180
Strain (με)
06/08
06/09
VW-e (Top)
VW-e (Bottom)
VW-f (Top)
VW-f (Bottom)
VW-g (Top)
VW-g (Bottom)
VW-m (Top)
VW-m (Bottom)
VW-n (Top)
VW-n (Bottom)
VW-o (Top)
VW-o (Bottom)

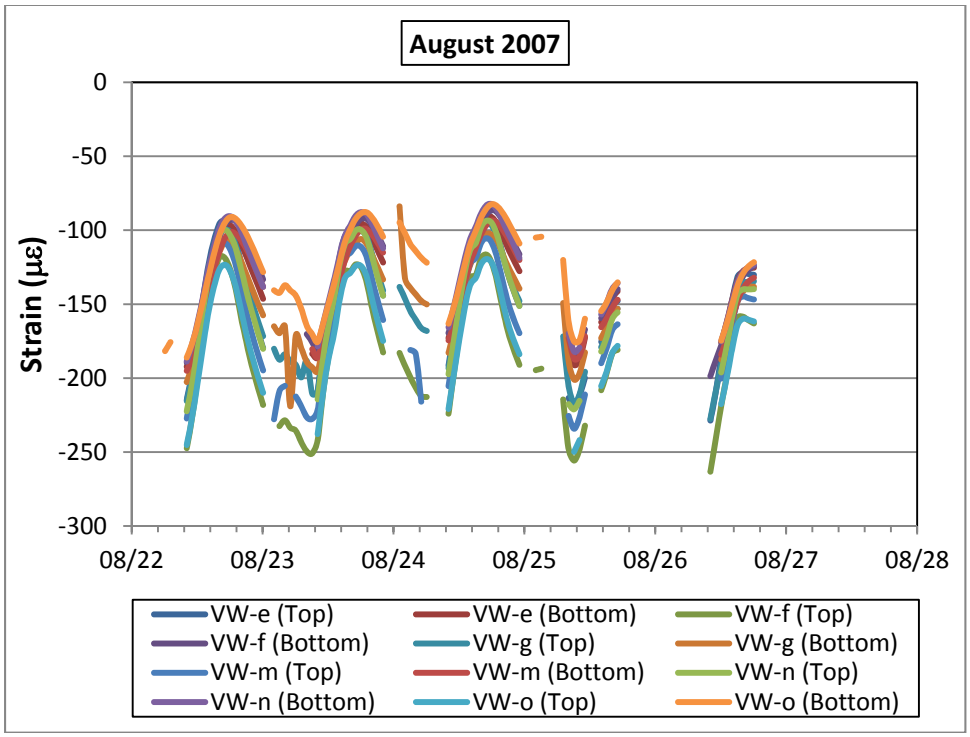
August 2007
0
-50
-100
-150
-200
-250
-300
Strain (με)
08/22
08/23
08/24
08/25
08/26
08/27
08/28
VW-e (Top)
VW-e (Bottom)
VW-f (Top)
VW-f (Bottom)
VW-g (Top)
VW-g (Bottom)
VW-m (Top)
VW-m (Bottom)
VW-n (Top)
VW-n (Bottom)
VW-o (Top)
VW-o (Bottom)

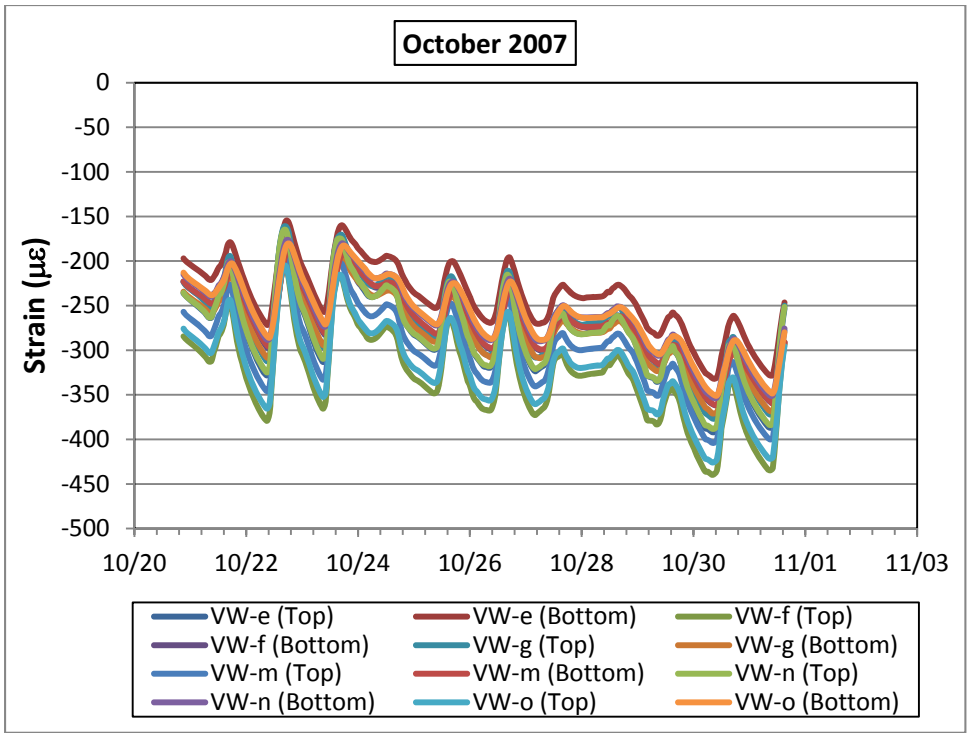
October 2007
0
-50
-100
-150
-200
-250
-300
-350
-400
-450
-500
Strain (με)
10/20
10/22
10/24
10/26
10/28
10/30
11/01
11/03
VW-e (Top)
VW-e (Bottom)
VW-f (Top)
VW-f (Bottom)
VW-g (Top)
VW-g (Bottom)
VW-m (Top)
VW-m (Bottom)
VW-n (Top)
VW-n (Bottom)
VW-o (Top)
VW-o (Bottom)

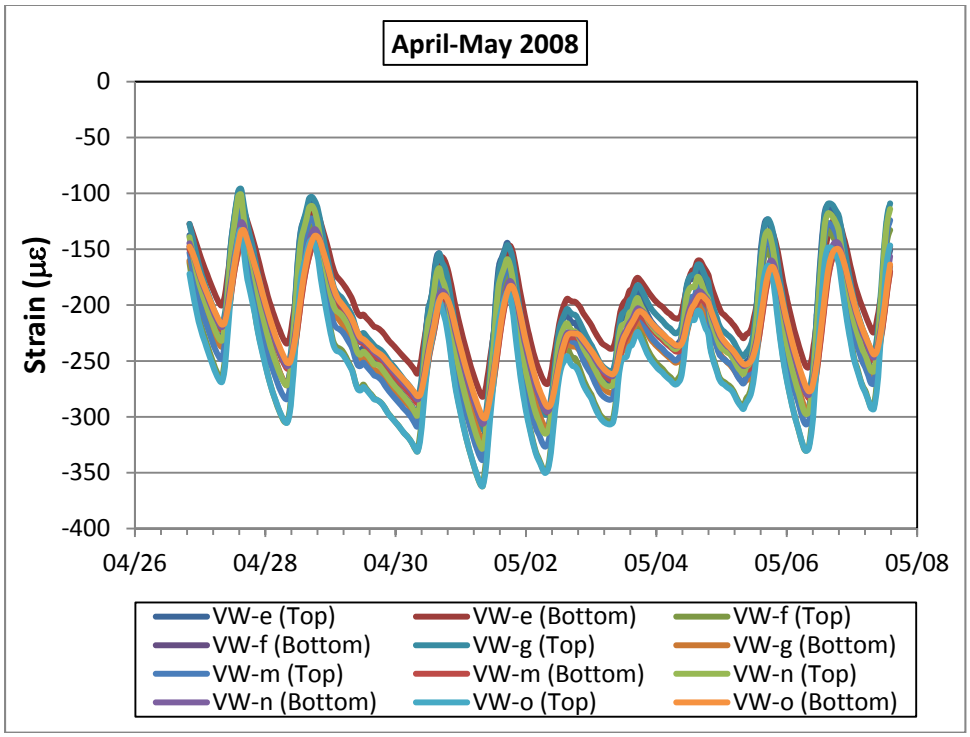
April-May 2008
0
-50
-100
-150
-200
-250
-300
-350
-400
Strain (με)
04/26
04/28
04/30
05/02
05/04
05/06
05/08
VW-e (Top)
VW-e (Bottom)
VW-f (Top)
VW-f (Bottom)
VW-g (Top)
VW-g (Bottom)
VW-m (Top)
VW-m (Bottom)
VW-n (Top)
VW-n (Bottom)
VW-o (Top)
VW-o (Bottom)

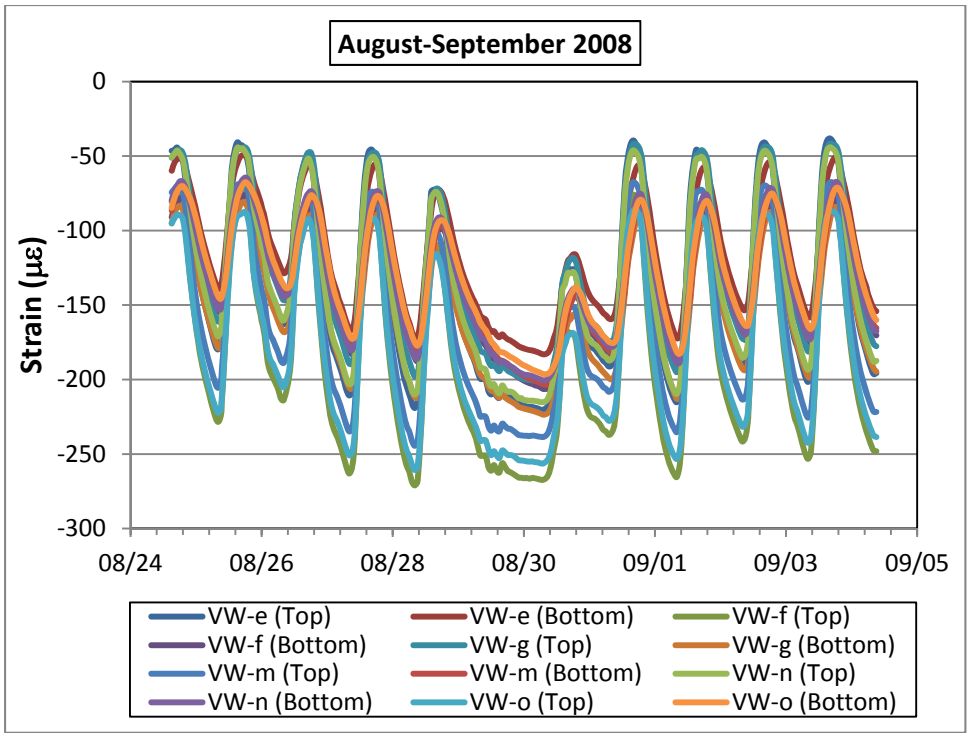
August-September 2008
0
-50
-100
-150
-200
-250
-300
Strain (με)
08/24
08/26
08/28
08/30
09/01
09/03
09/05
VW-e (Top)
VW-e (Bottom)
VW-f (Top)
VW-f (Bottom)
VW-g (Top)
VW-g (Bottom)
VW-m (Top)
VW-m (Bottom)
VW-n (Top)
VW-n (Bottom)
VW-o (Top)
VW-o (Bottom)

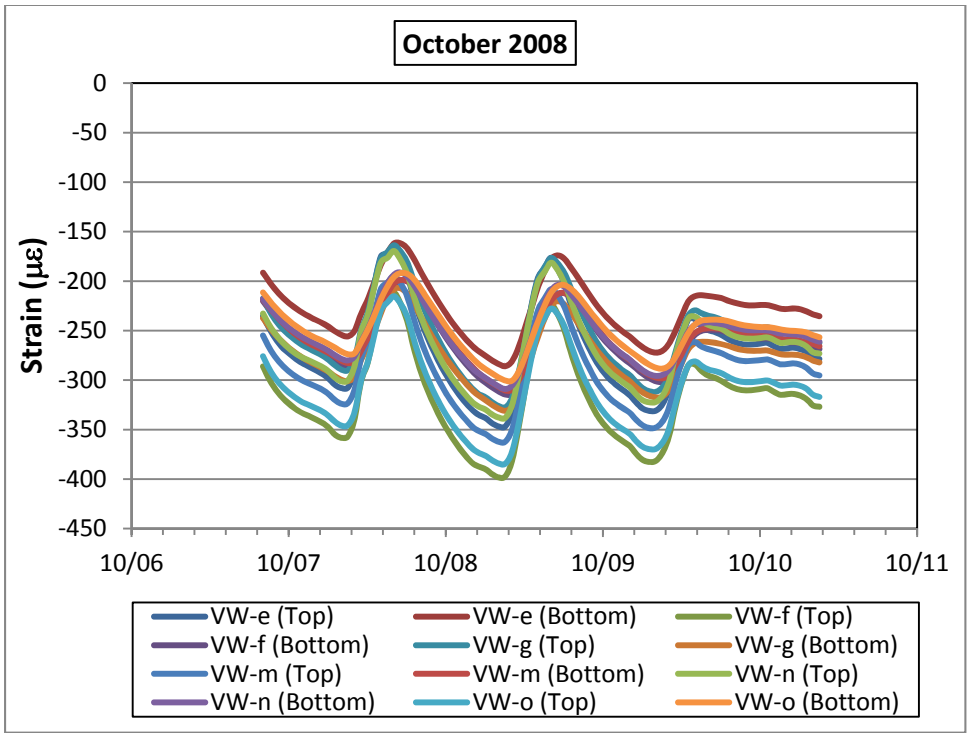
October 2008
0
-50
-100
-150
-200
-250
-300
-350
-400
-450
Strain (με)
10/06
10/07
10/08
10/09
10/10
10/11
VW-e (Top)
VW-e (Bottom)
VW-f (Top)
VW-f (Bottom)
VW-g (Top)
VW-g (Bottom)
VW-m (Top)
VW-m (Bottom)
VW-n (Top)
VW-n (Bottom)
VW-o (Top)
VW-o (Bottom)

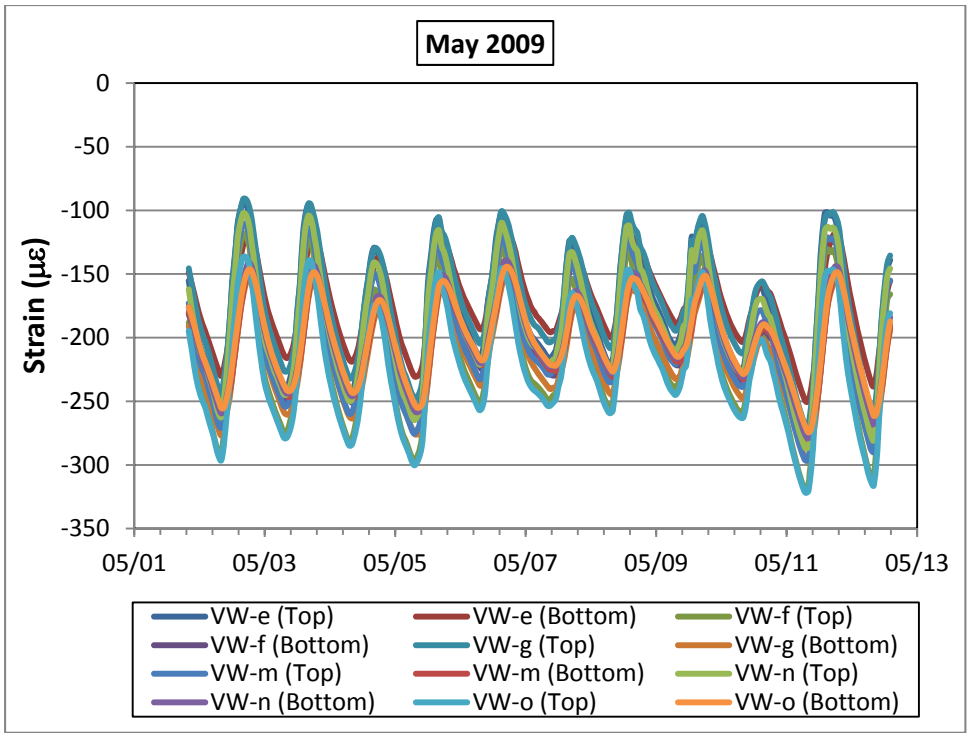

Load-Related Strain

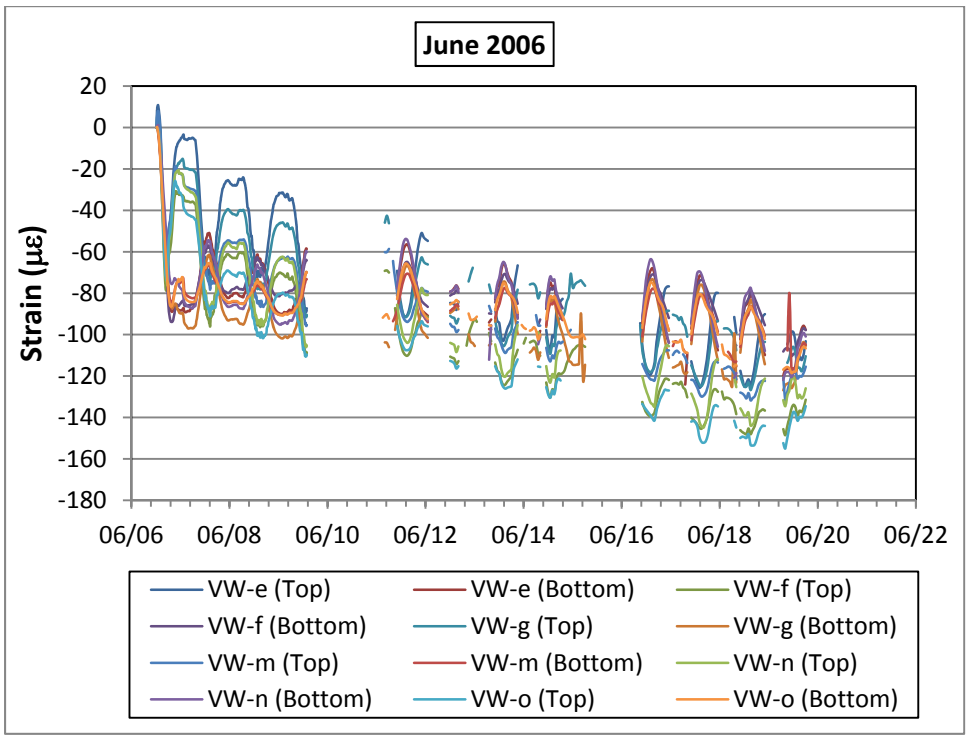

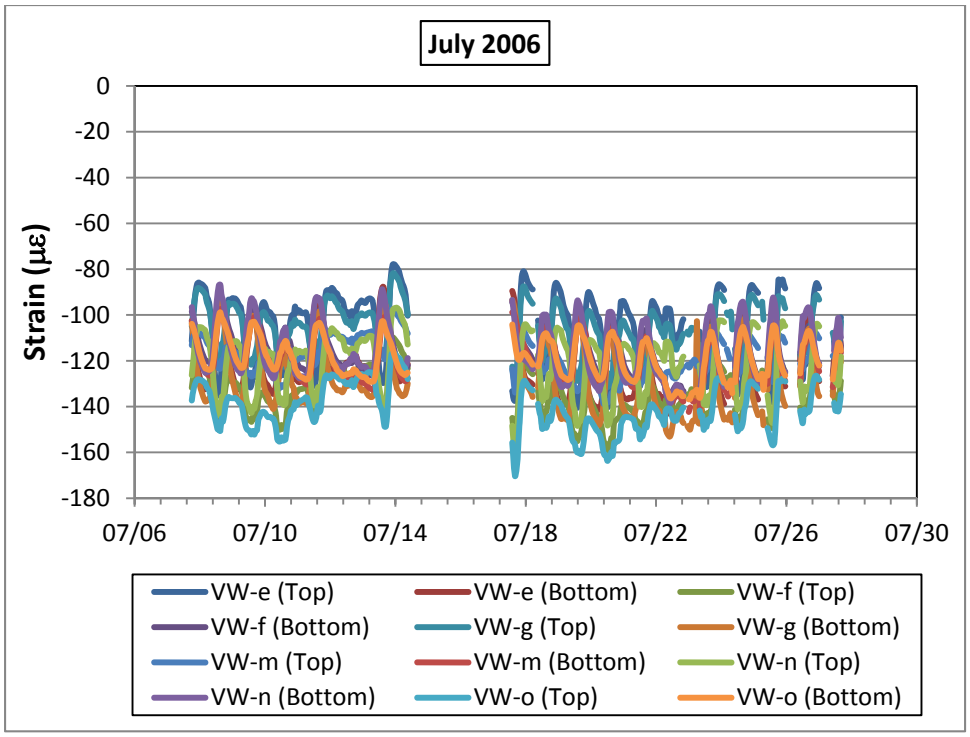
July 2006
Strain (με)
0
-20
-40
-60
-80
-100
-120
-140
-160
-180
07/06
07/10
07/14
07/18
07/22
07/26
07/30
VW-e (Top)
VW-e (Bottom)
VW-f (Top)
VW-f (Bottom)
VW-g (Top)
VW-g (Bottom)
VW-m (Top)
VW-m (Bottom)
VW-n (Top)
VW-n (Bottom)
VW-o (Top)
VW-o (Bottom)

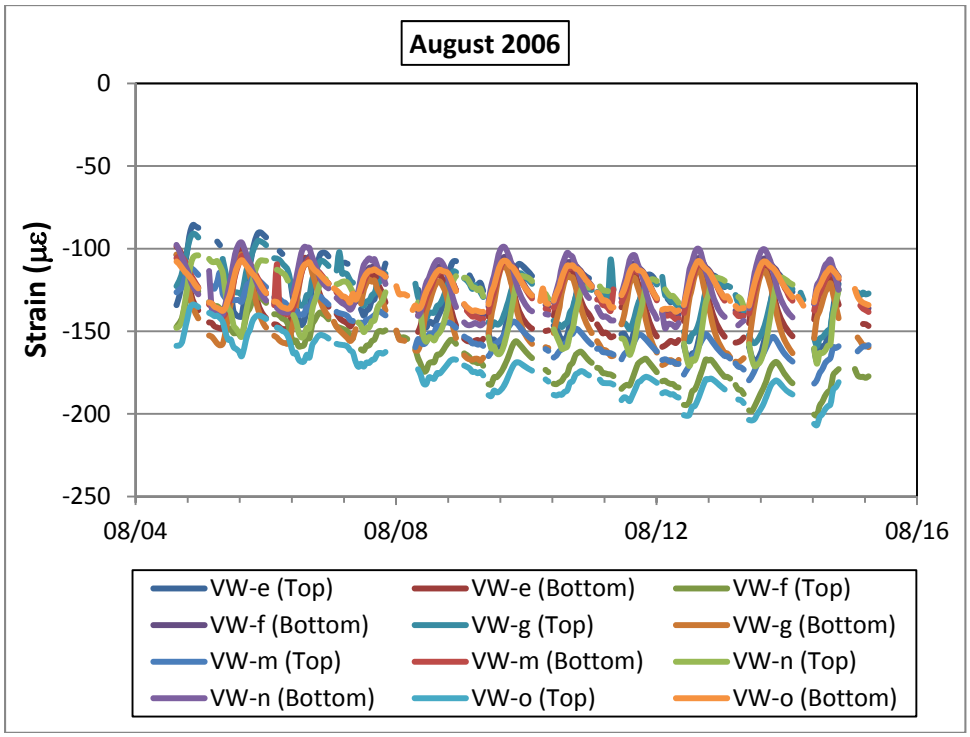
August 2006
Strain (με)
0
-50
-100
-150
-200
-250
08/04
08/08
08/12
08/16
VW-e (Top)
VW-e (Bottom)
VW-f (Top)
VW-f (Bottom)
VW-g (Top)
VW-g (Bottom)
VW-m (Top)
VW-m (Bottom)
VW-n (Top)
VW-n (Bottom)
VW-o (Top)
VW-o (Bottom)

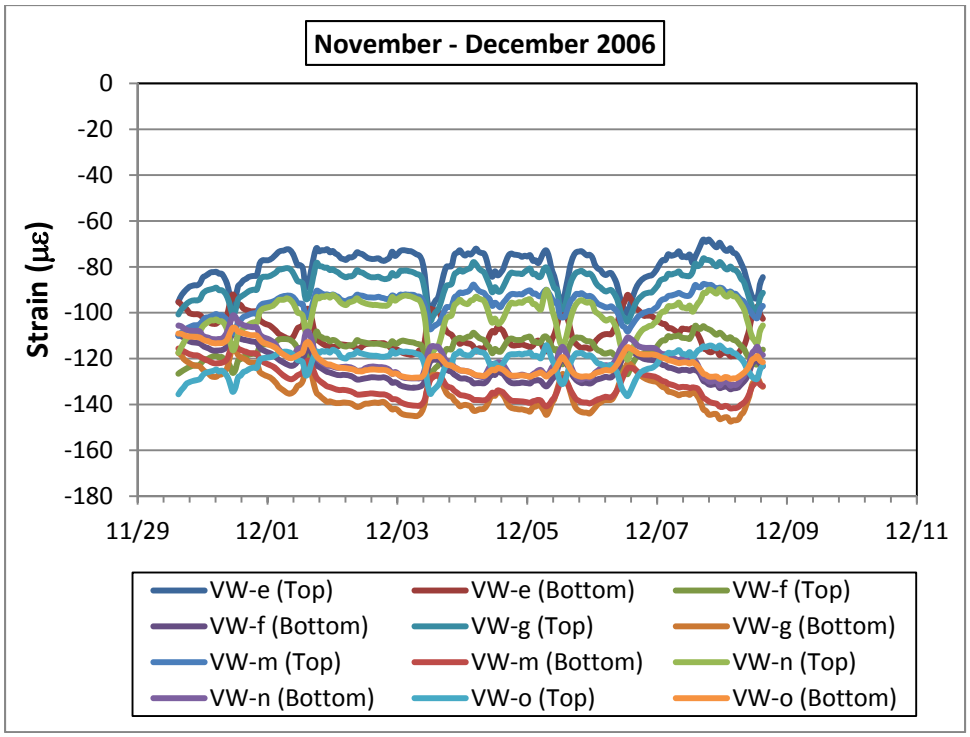
November - December 2006
Strain (με)
0
-20
-40
-60
-80
-100
-120
-140
-160
-180
11/29
12/01
12/03
12/05
12/07
12/09
12/11
VW-e (Top)
VW-e (Bottom)
VW-f (Top)
VW-f (Bottom)
VW-g (Top)
VW-g (Bottom)
VW-m (Top)
VW-m (Bottom)
VW-n (Top)
VW-n (Bottom)
VW-o (Top)
VW-o (Bottom)

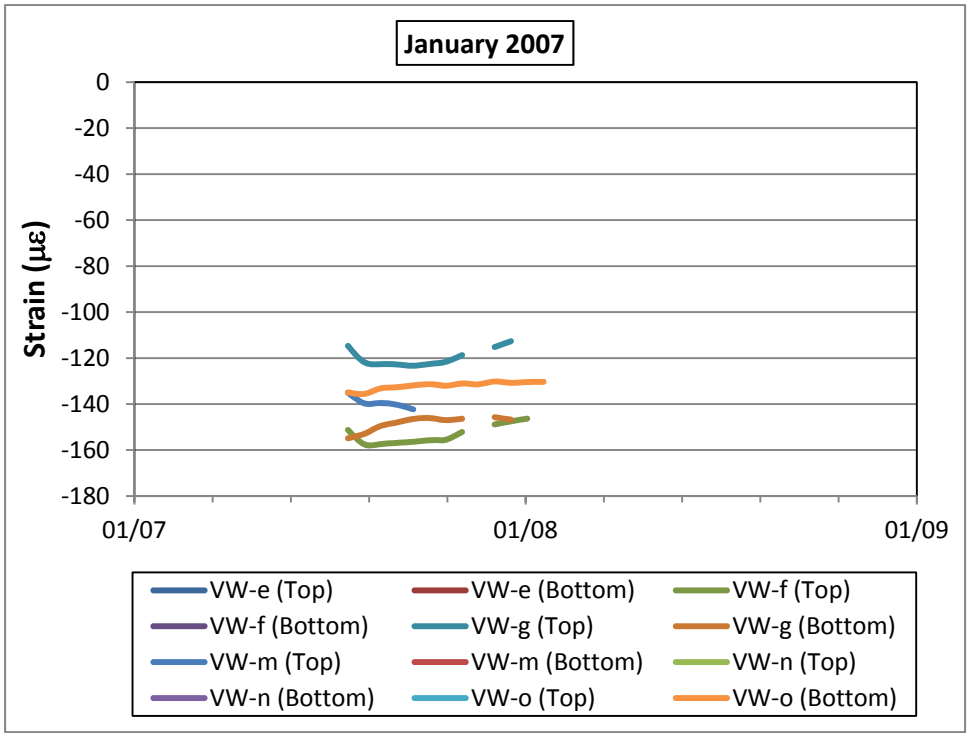
January 2007
Strain (με)
0
-20
-40
-60
-80
-100
-120
-140
-160
-180
01/07
01/08
01/09
VW-e (Top)
VW-e (Bottom)
VW-f (Top)
VW-f (Bottom)
VW-g (Top)
VW-g (Bottom)
VW-m (Top)
VW-m (Bottom)
VW-n (Top)
VW-n (Bottom)
VW-o (Top)
VW-o (Bottom)

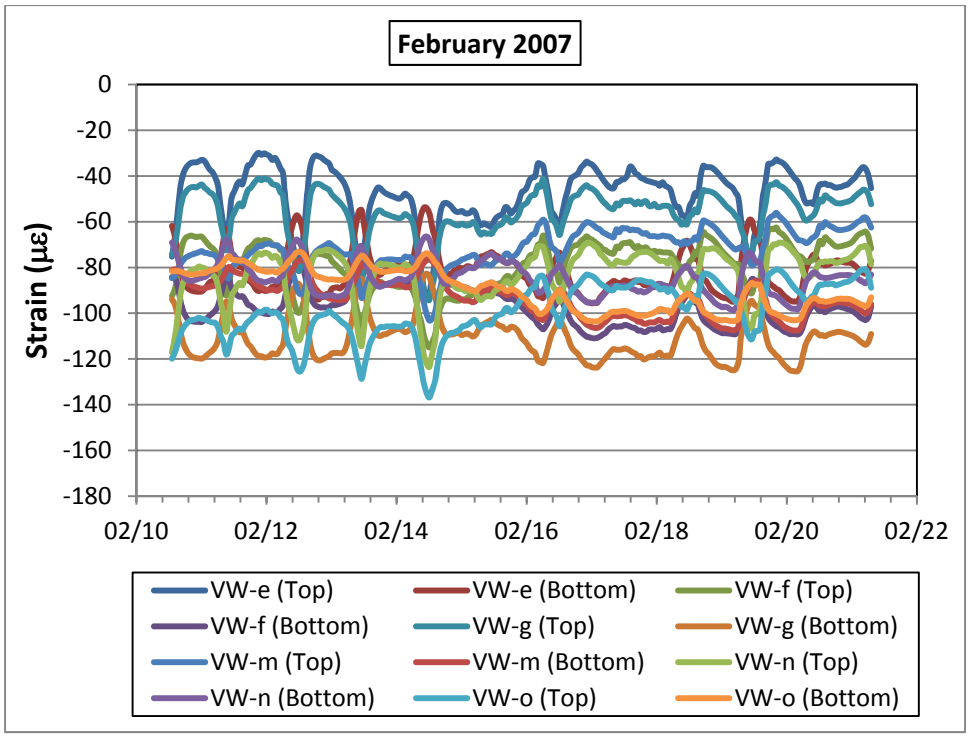
February 2007
0
-20
-40
-60
-80
-100
-120
-140
-160
-180
Strain (με)
02/10
02/12
02/14
02/16
02/18
02/20
02/22
VW-e (Top)
VW-e (Bottom)
VW-f (Top)
VW-f (Bottom)
VW-g (Top)
VW-g (Bottom)
VW-m (Top)
VW-m (Bottom)
VW-n (Top)
VW-n (Bottom)
VW-o (Top)
VW-o (Bottom)

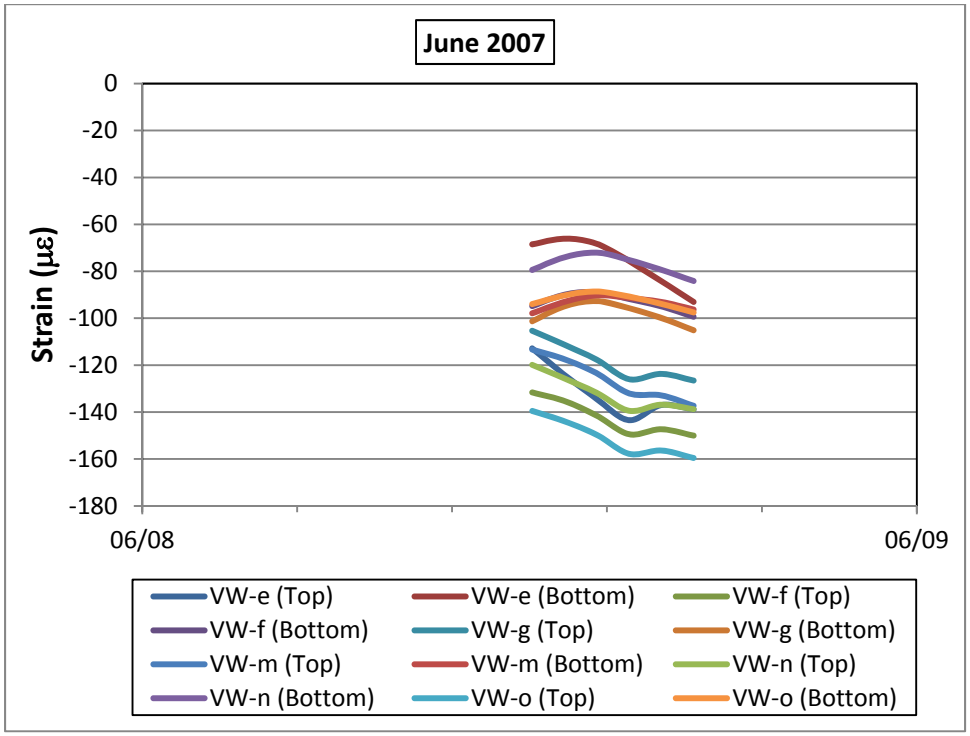
June 2007
0
-20
-40
-60
-80
-100
-120
-140
-160
-180
Strain (με)
06/08
06/09
VW-e (Top)
VW-e (Bottom)
VW-f (Top)
VW-f (Bottom)
VW-g (Top)
VW-g (Bottom)
VW-m (Top)
VW-m (Bottom)
VW-n (Top)
VW-n (Bottom)
VW-o (Top)
VW-o (Bottom)

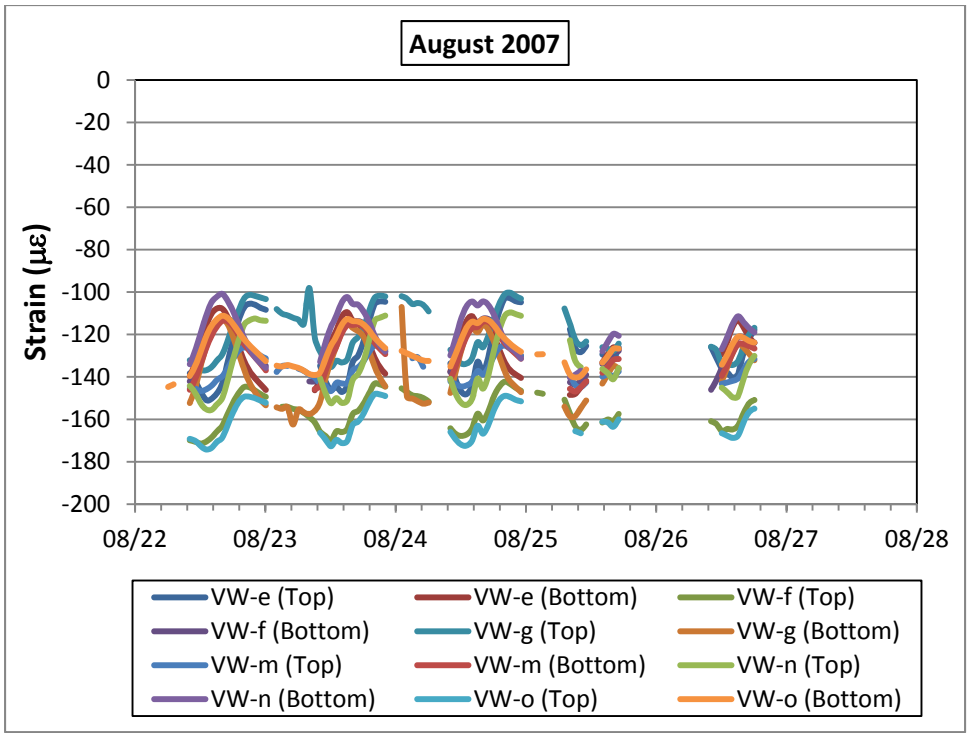
August 2007
Strain (με)
0
-20
-40
-60
-80
-100
-120
-140
-160
-180
-200
08/22
08/23
08/24
08/25
08/26
08/27
08/28
VW-e (Top)
VW-e (Bottom)
VW-f (Top)
VW-f (Bottom)
VW-g (Top)
VW-g (Bottom)
VW-m (Top)
VW-m (Bottom)
VW-n (Top)
VW-n (Bottom)
VW-o (Top)
VW-o (Bottom)

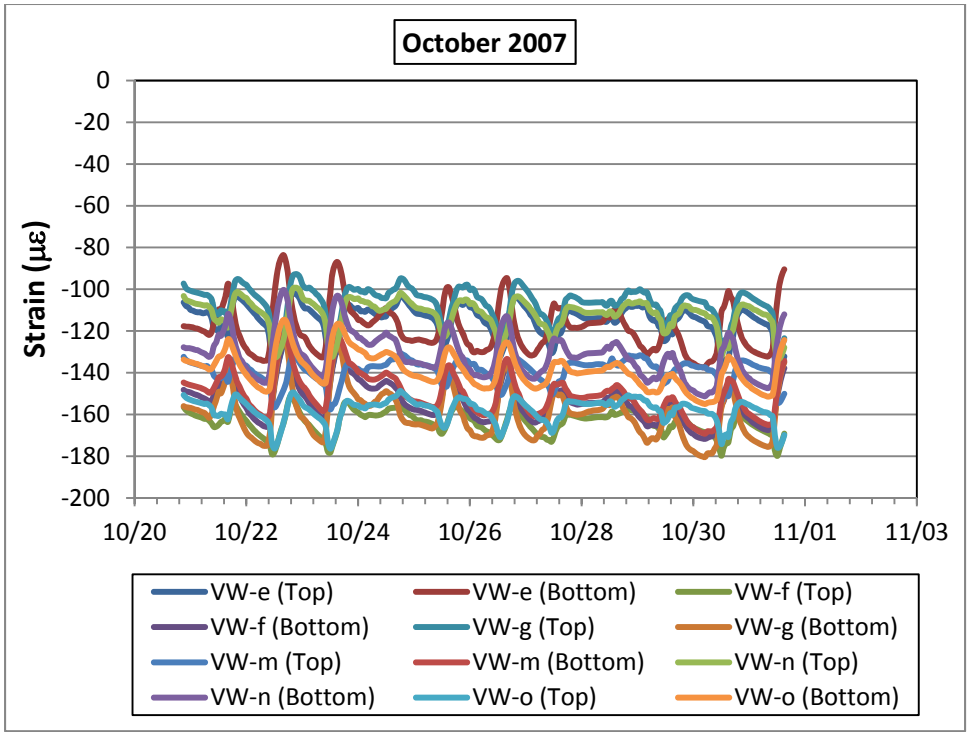
October 2007
Strain (με)
0
-20
-40
-60
-80
-100
-120
-140
-160
-180
-200
10/20
10/22
10/24
10/26
10/28
10/30
11/01
11/03
VW-e (Top)
VW-e (Bottom)
VW-f (Top)
VW-f (Bottom)
VW-g (Top)
VW-g (Bottom)
VW-m (Top)
VW-m (Bottom)
VW-n (Top)
VW-n (Bottom)
VW-o (Top)
VW-o (Bottom)

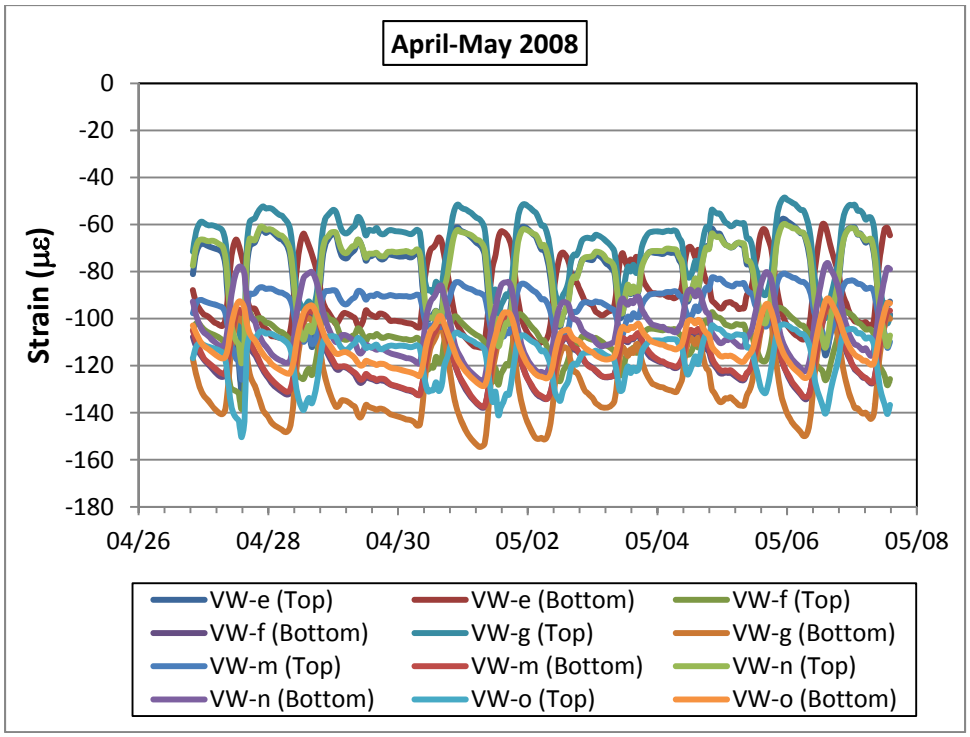
April-May 2008
0
-20
-40
-60
-80
-100
-120
-140
-160
-180
Strain (με)
04/26
04/28
04/30
05/02
05/04
05/06
05/08
VW-e (Top)
VW-e (Bottom)
VW-f (Top)
VW-f (Bottom)
VW-g (Top)
VW-g (Bottom)
VW-m (Top)
VW-m (Bottom)
VW-n (Top)
VW-n (Bottom)
VW-o (Top)
VW-o (Bottom)

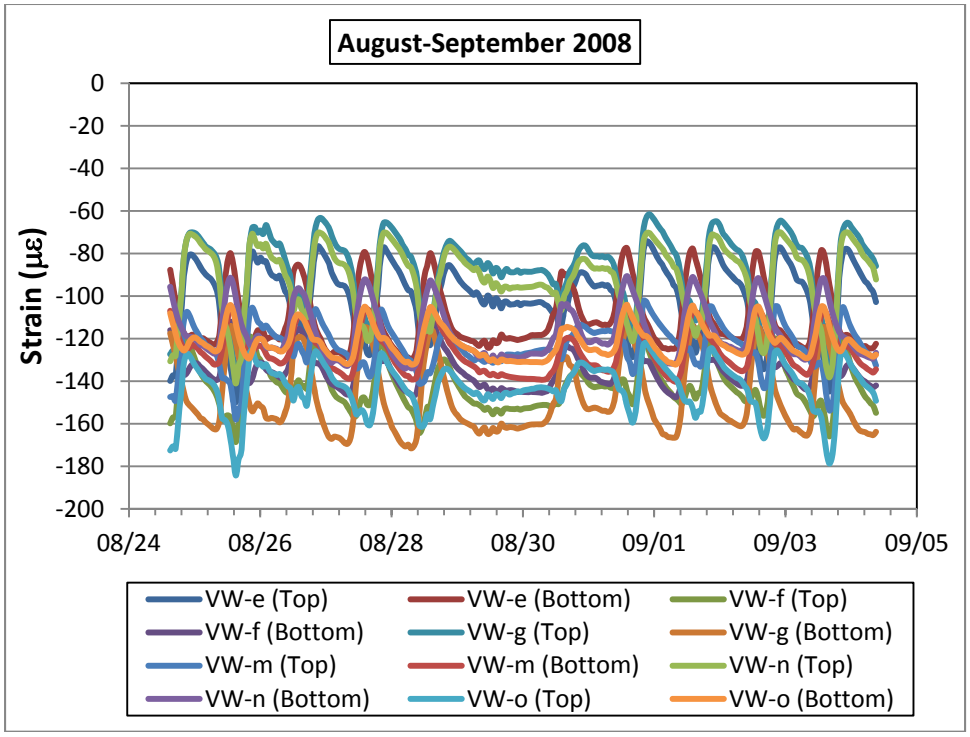
August-September 2008
0
-20
-40
-60
-80
-100
-120
-140
-160
-180
-200
Strain (με)
08/24
08/26
08/28
08/30
09/01
09/03
09/05
VW-e (Top)
VW-e (Bottom)
VW-f (Top)
VW-f (Bottom)
VW-g (Top)
VW-g (Bottom)
VW-m (Top)
VW-m (Bottom)
VW-n (Top)
VW-n (Bottom)
VW-o (Top)
VW-o (Bottom)

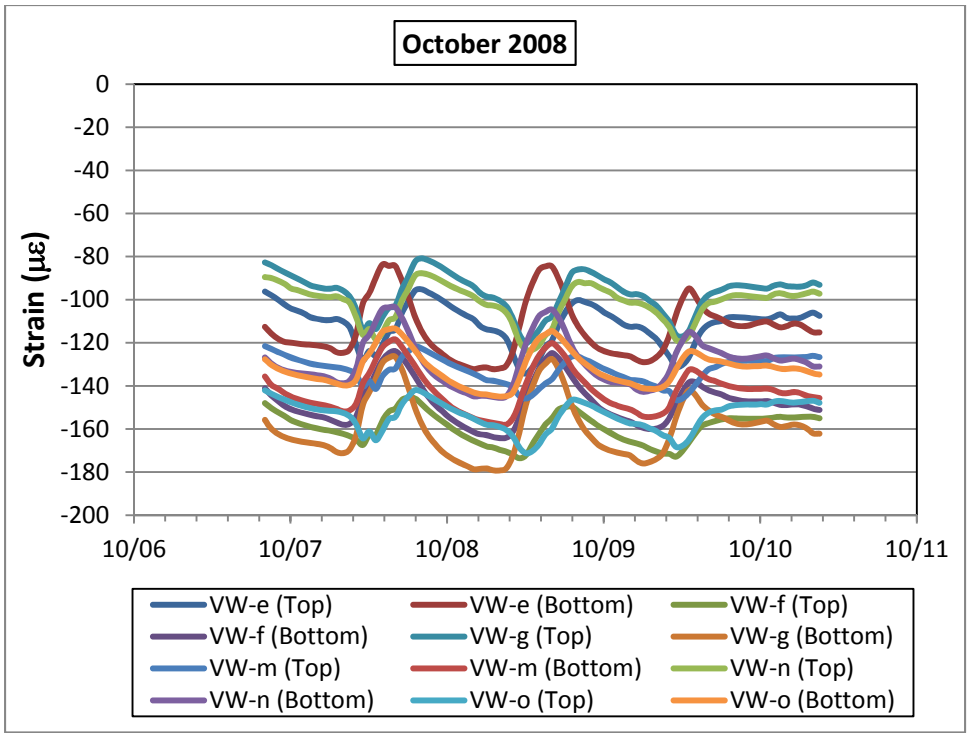
October 2008
Strain (με)
0
-20
-40
-60
-80
-100
-120
-140
-160
-180
-200
10/06
10/07
10/08
10/09
10/10
10/11
VW-e (Top)
VW-e (Bottom)
VW-f (Top)
VW-f (Bottom)
VW-g (Top)
VW-g (Bottom)
VW-m (Top)
VW-m (Bottom)
VW-n (Top)
VW-n (Bottom)
VW-o (Top)
VW-o (Bottom)

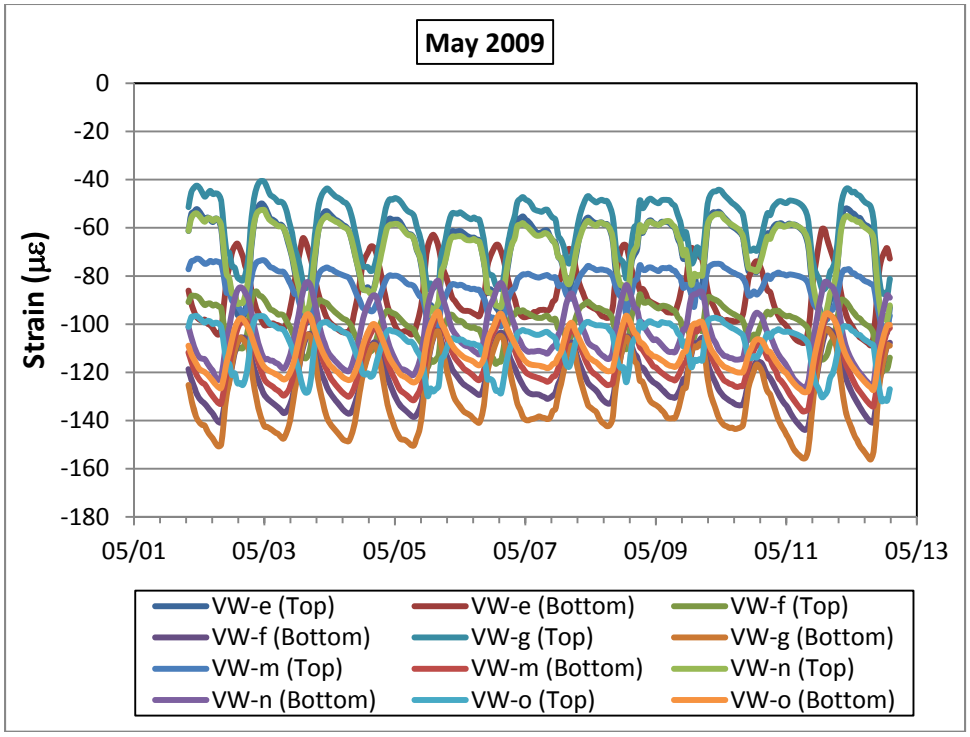
May 2009
Strain (με)
0
-20
-40
-60
-80
-100
-120
-140
-160
-180
05/01
05/03
05/05
05/07
05/09
05/11
05/13
VW-e (Top)
VW-e (Bottom)
VW-f (Top)
VW-f (Bottom)
VW-g (Top)
VW-g (Bottom)
VW-m (Top)
VW-m (Bottom)
VW-n (Top)
VW-n (Bottom)
VW-o (Top)
VW-o (Bottom)

Rubblized Section

Pavement Temperatures

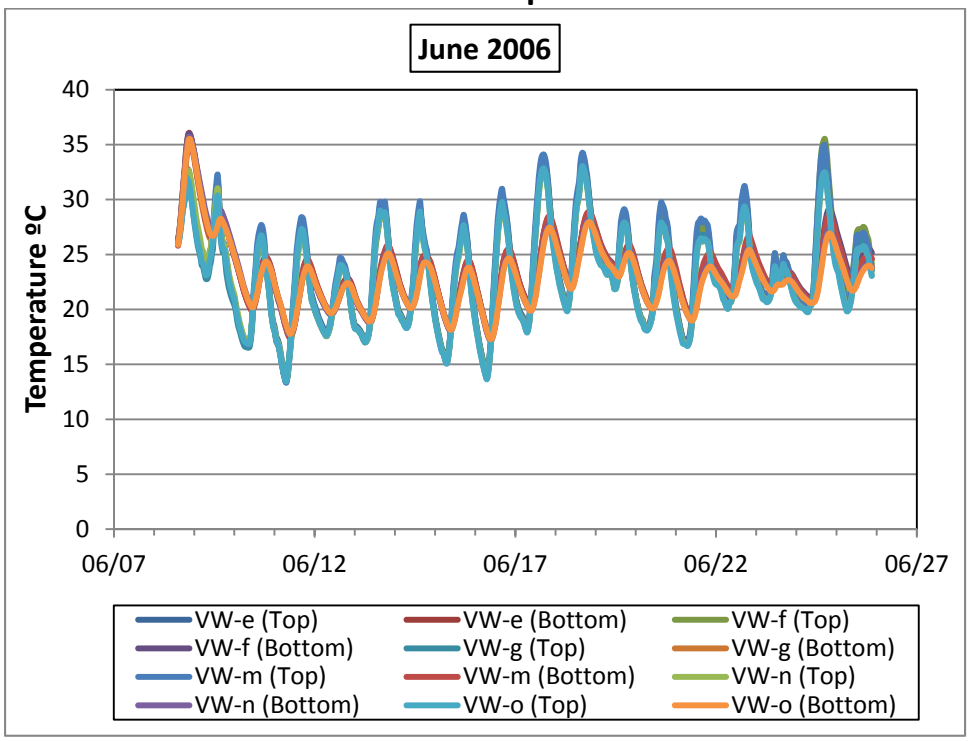

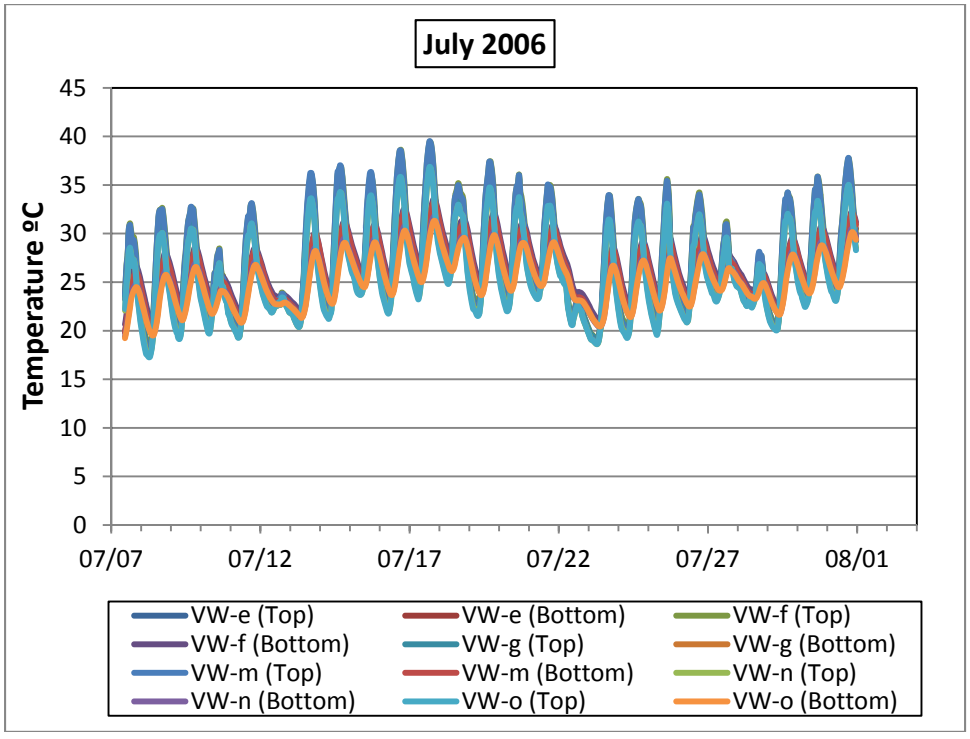

(0°C = 32°F, 40°C = 104°F)

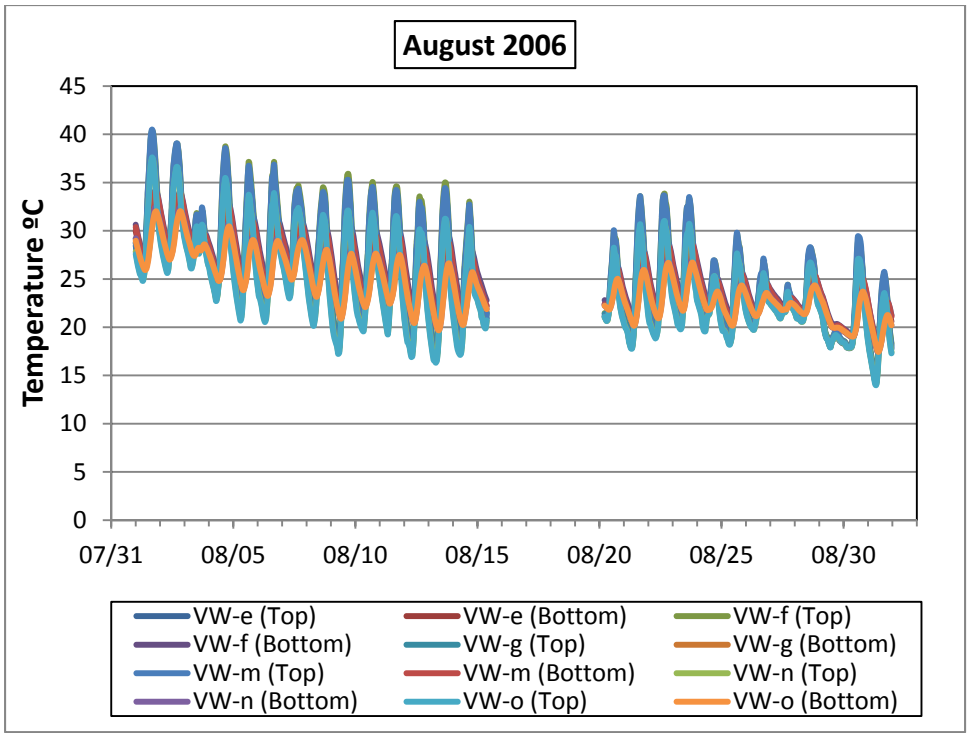

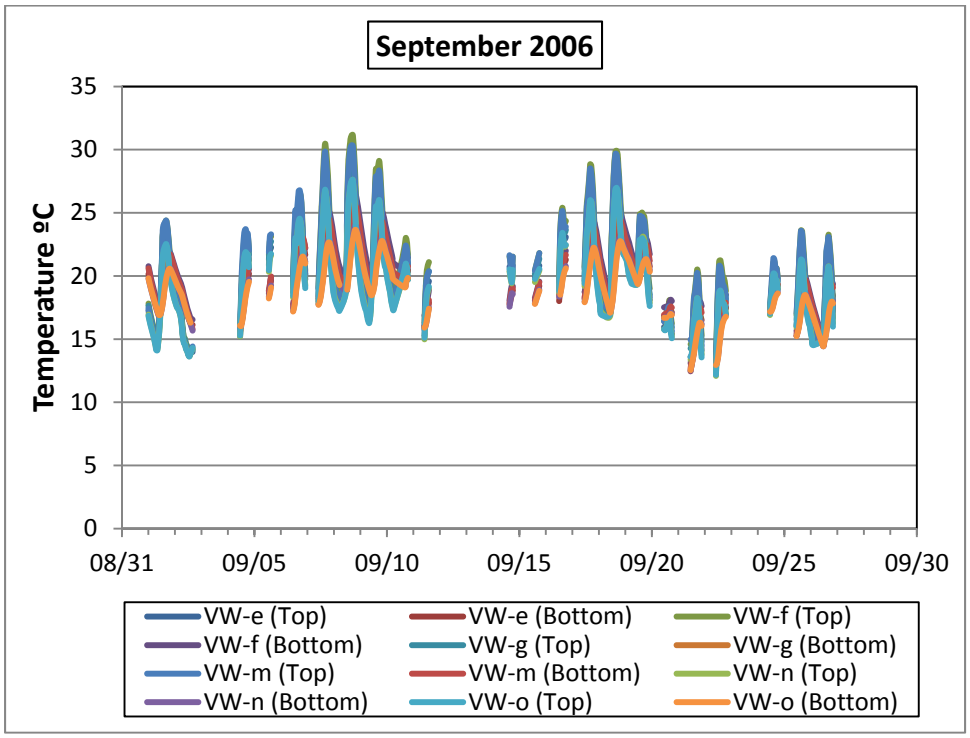

(0°C = 32°F, 45°C = 113°F)

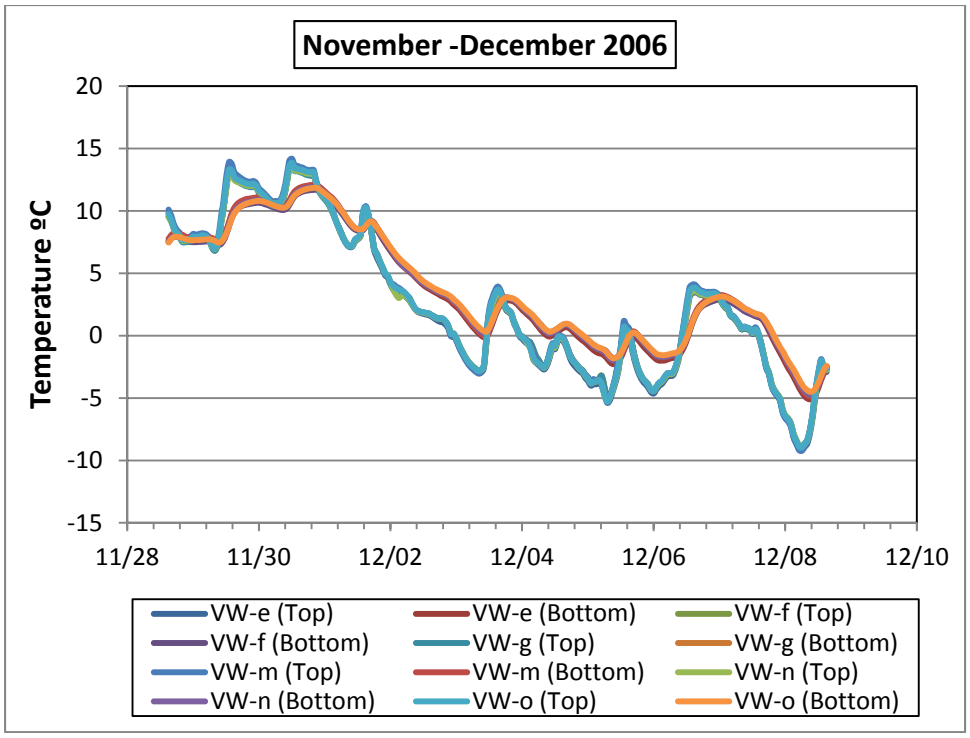

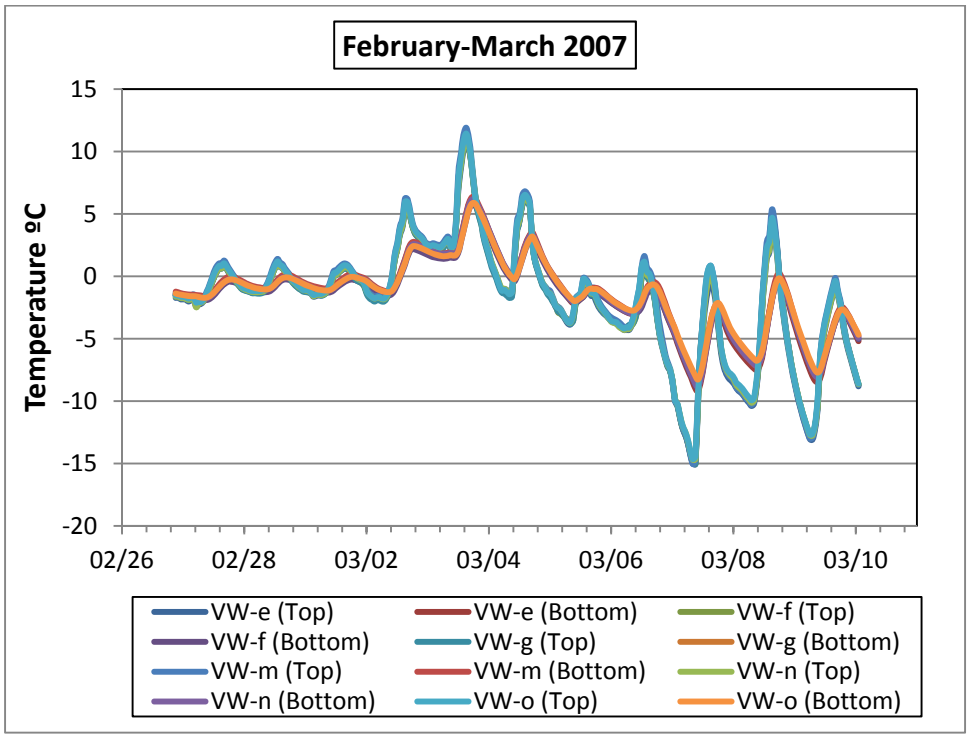

(-20°C = -4°F, 20°C = 68°F)

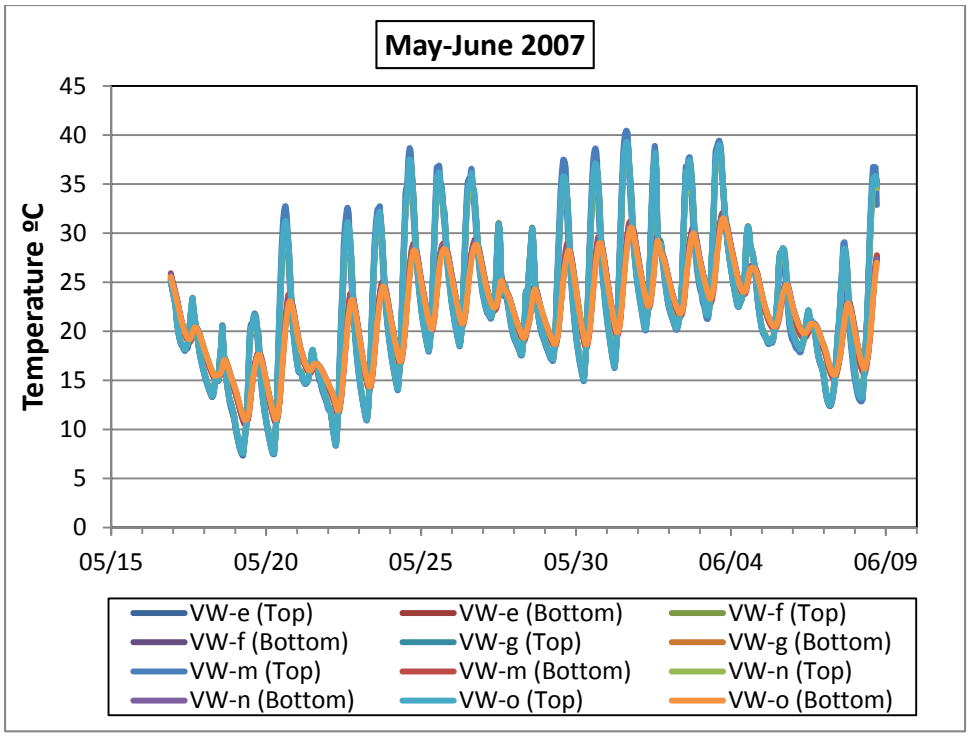

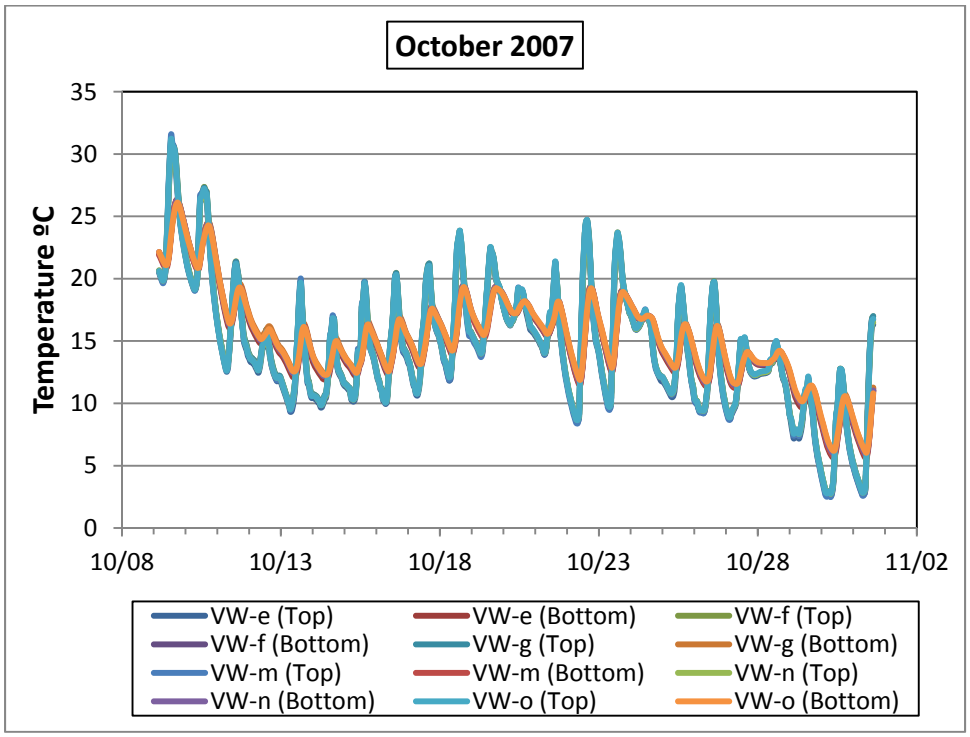

(0°C = 32°F, 45°C = 113°F)

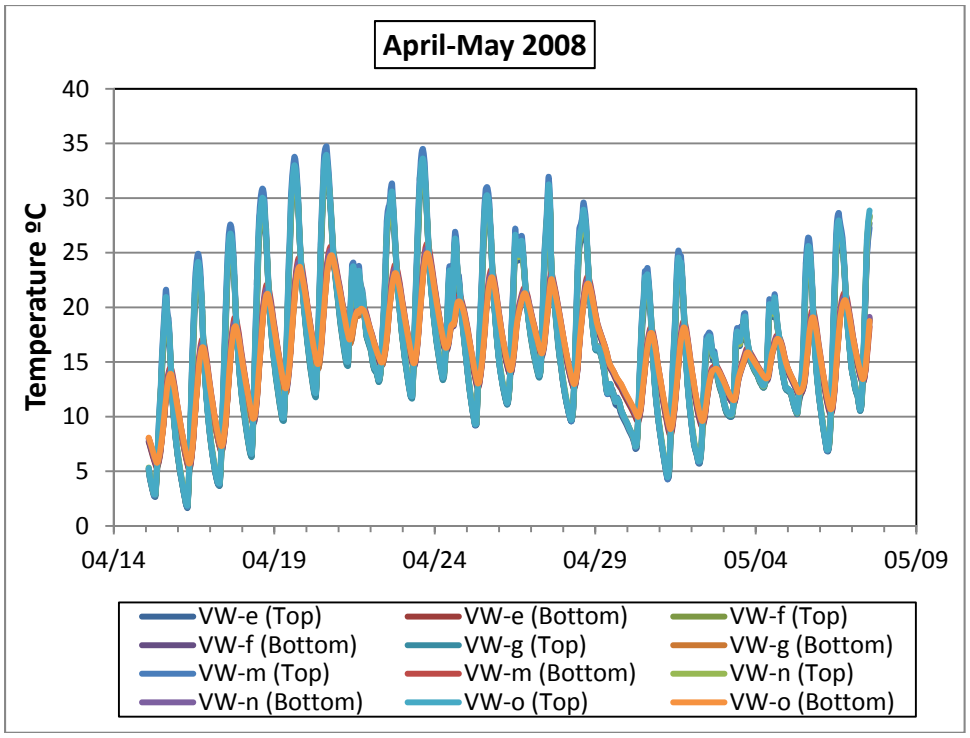

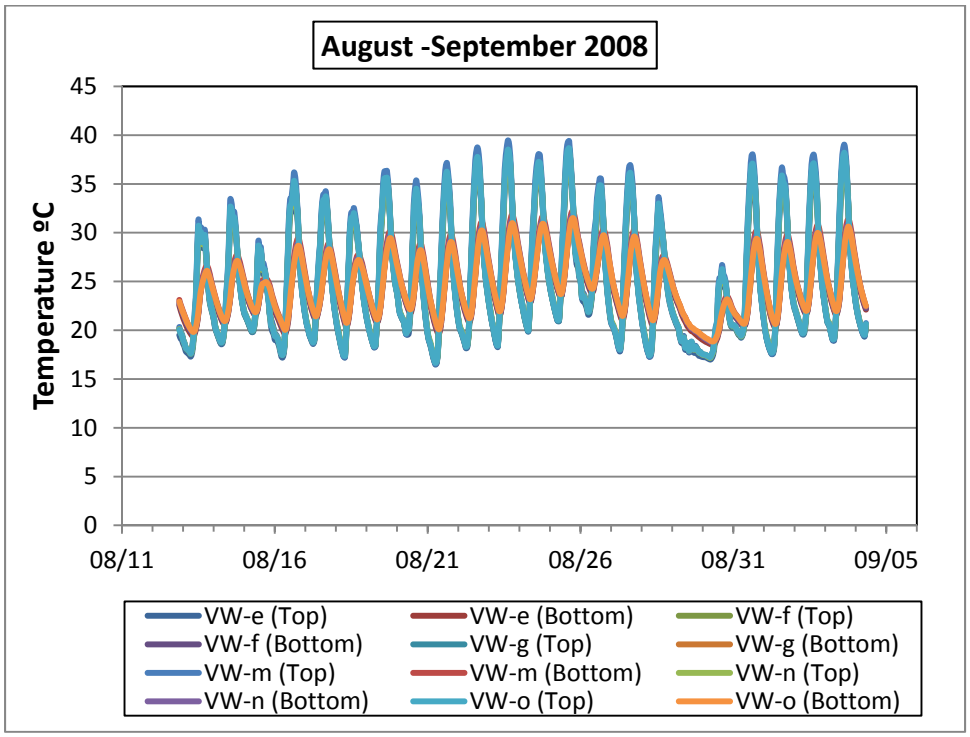

(0°C = 32°F, 40°C = 104°F)

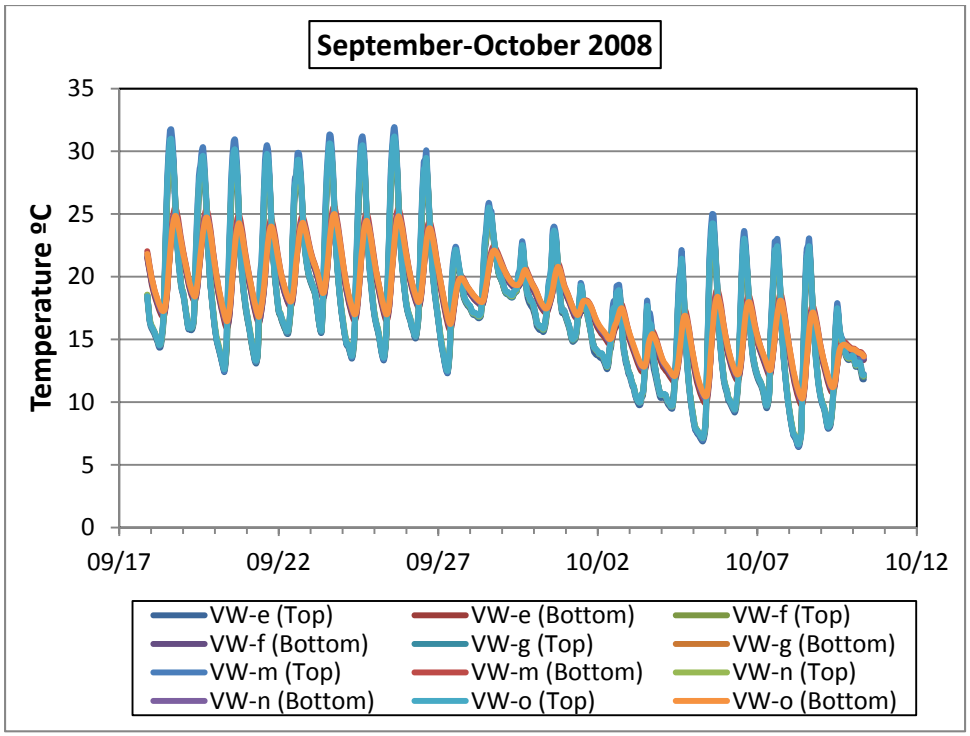

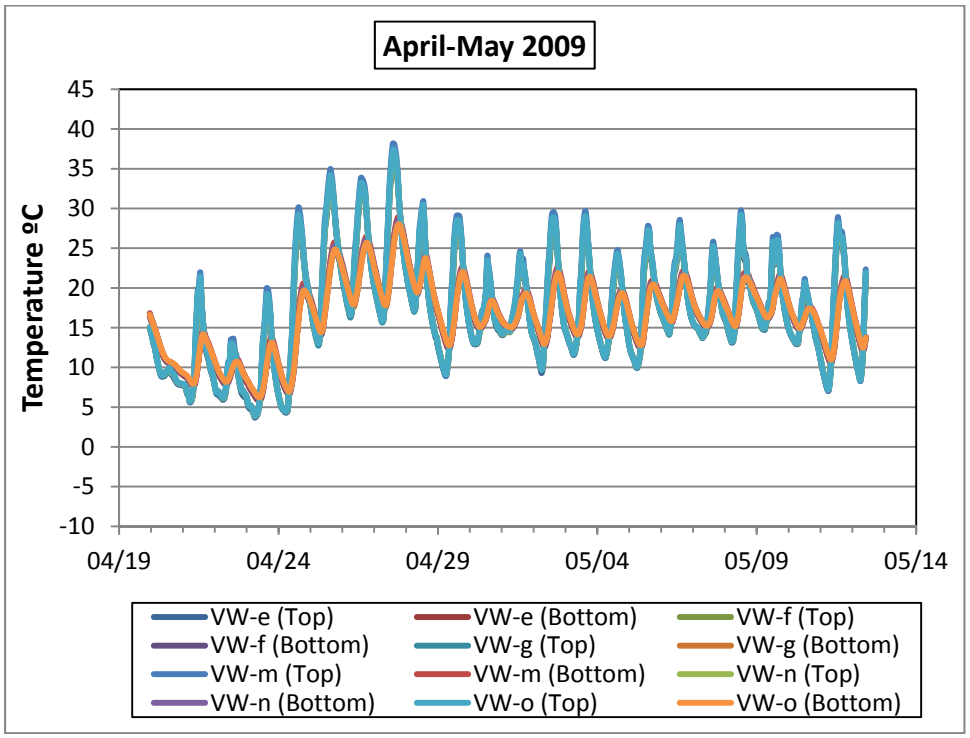

(0°C = 32°F, 45°C = 113°F)

Temperature Gradients

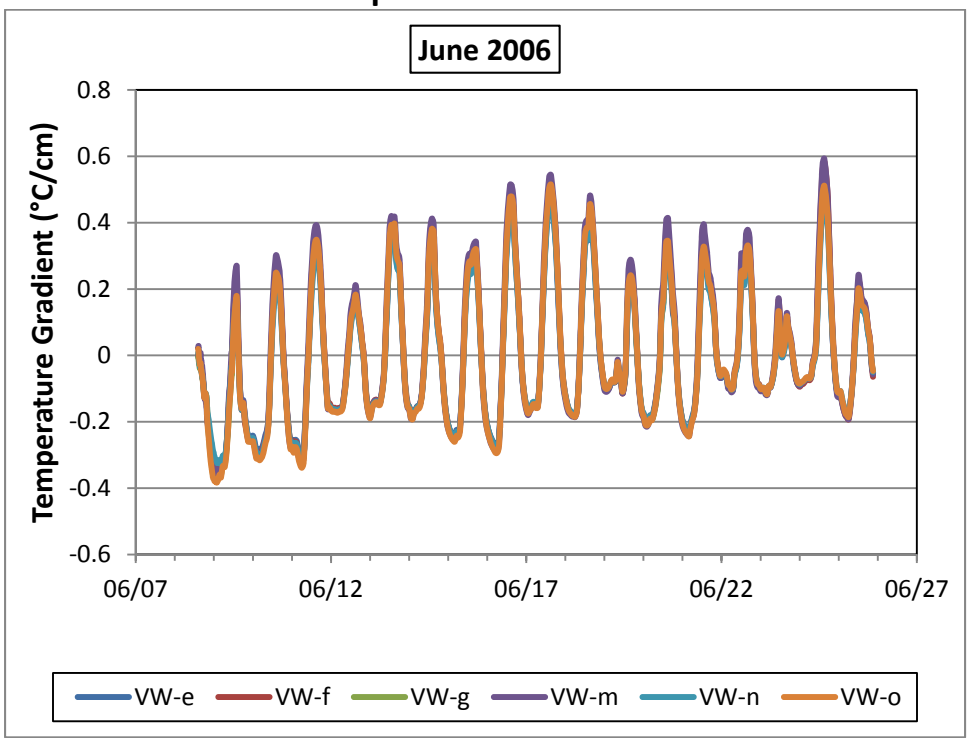

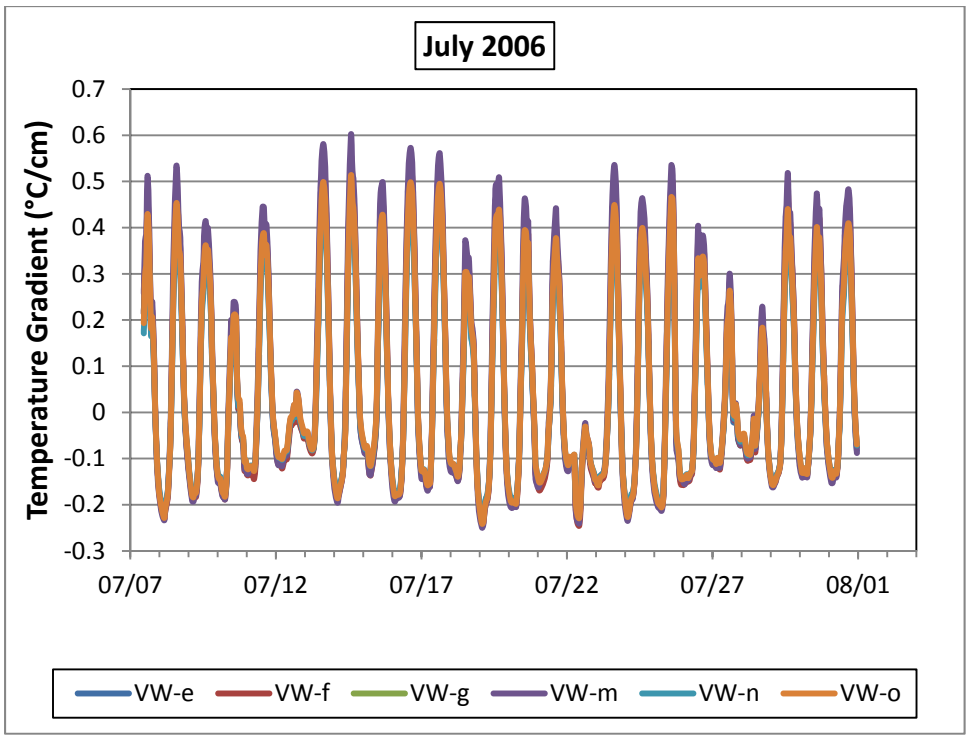

(1°C/cm = 4.6°F/in)

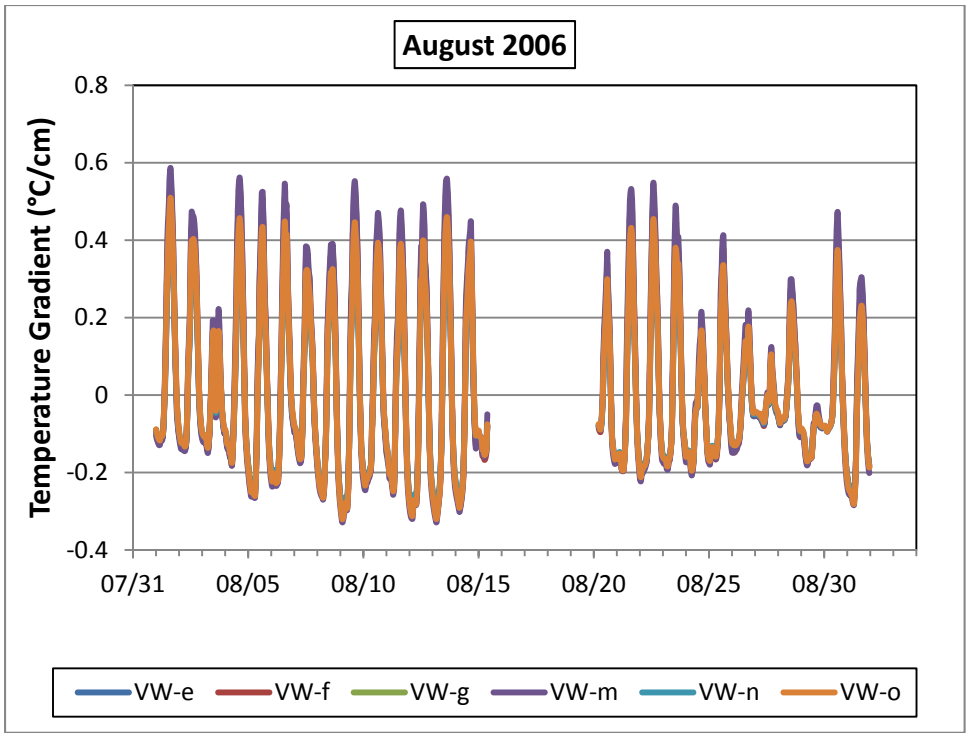
August 2006
Temperature Gradient (°C/cm)
0.8
0.6
0.4
0.2
0
-0.2
-0.4
07/31
08/05
08/10
08/15
08/20
08/25
08/30
VW-e
VW-f
VW-g
VW-m
VW-n
VW-o

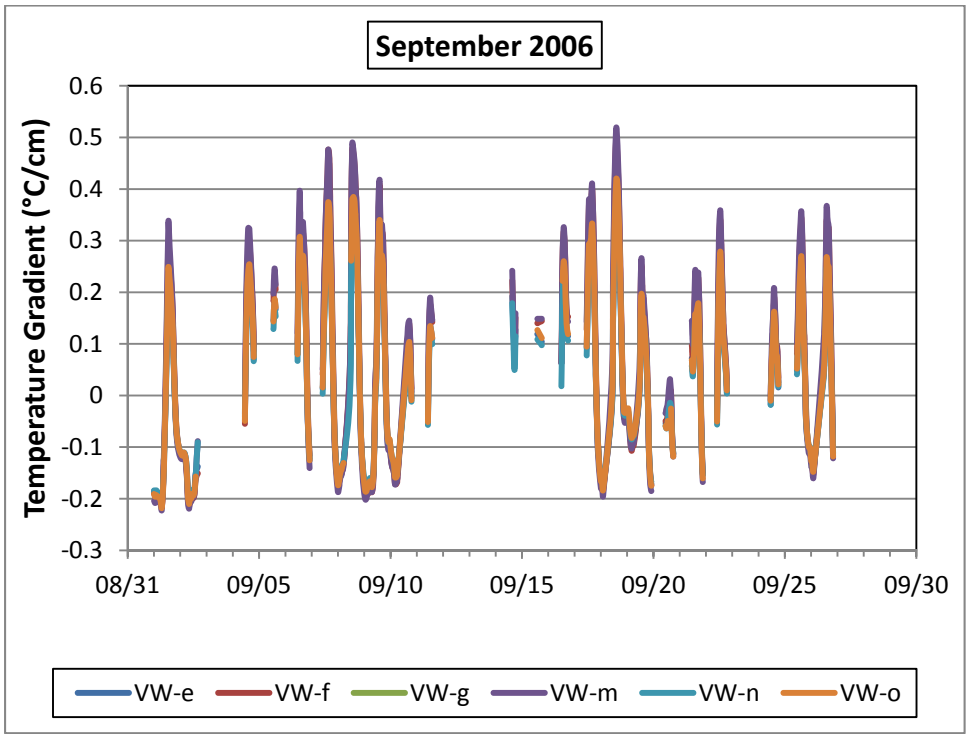
September 2006
Temperature Gradient (°C/cm)
0.6
0.5
0.4
0.3
0.2
0.1
0
-0.1
-0.2
-0.3
08/31
09/05
09/10
09/15
09/20
09/25
09/30
VW-e
VW-f
VW-g
VW-m
VW-n
VW-o

(1°C/cm = 4.6°F/in)

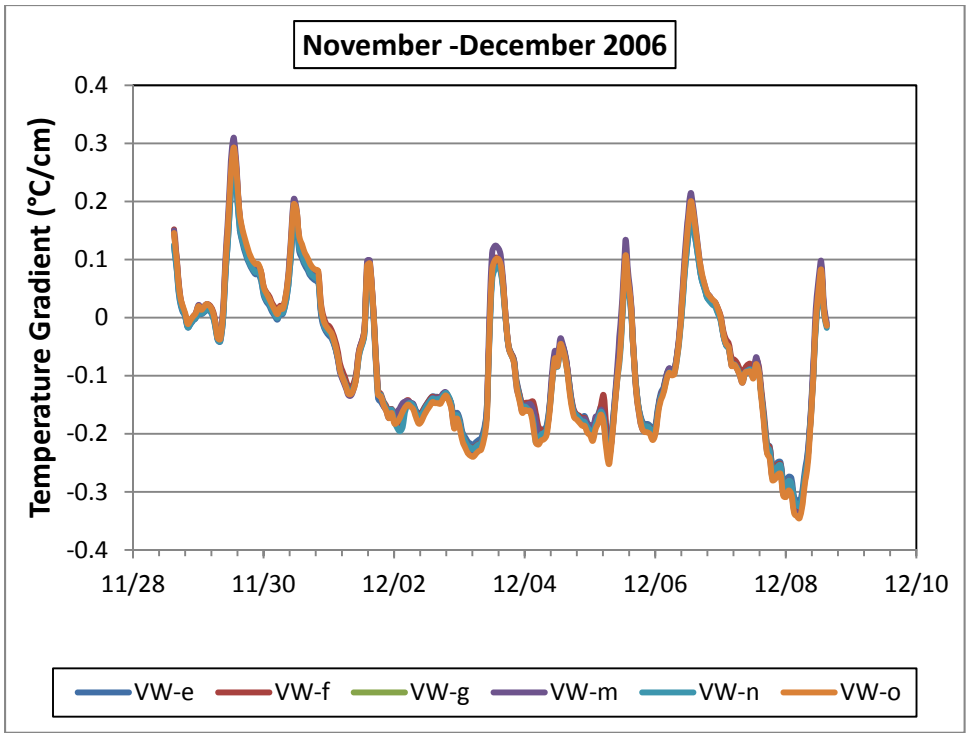
November -December 2006
Temperature Gradient (°C/cm)
0.4
0.3
0.2
0.1
0
-0.1
-0.2
-0.3
-0.4
11/28
11/30
12/02
12/04
12/06
12/08
12/10
VW-e
VW-f
VW-g
VW-m
VW-n
VW-o

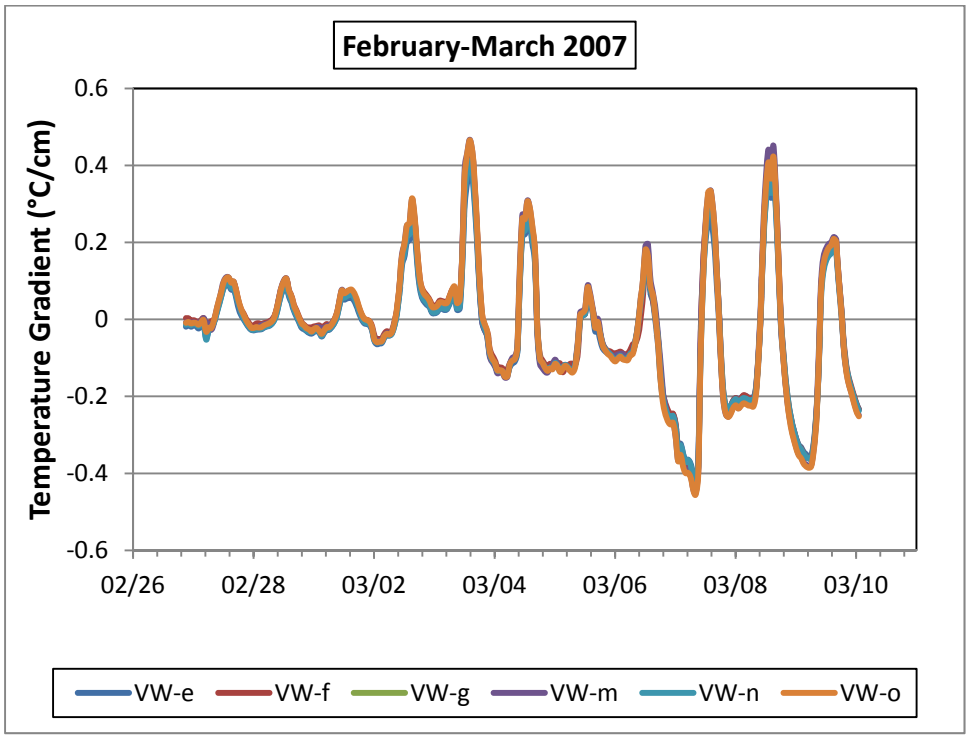
February-March 2007
Temperature Gradient (°C/cm)
0.6
0.4
0.2
0
-0.2
-0.4
-0.6
02/26
02/28
03/02
03/04
03/06
03/08
03/10
VW-e
VW-f
VW-g
VW-m
VW-n
VW-o

(1°C/cm = 4.6°F/in)

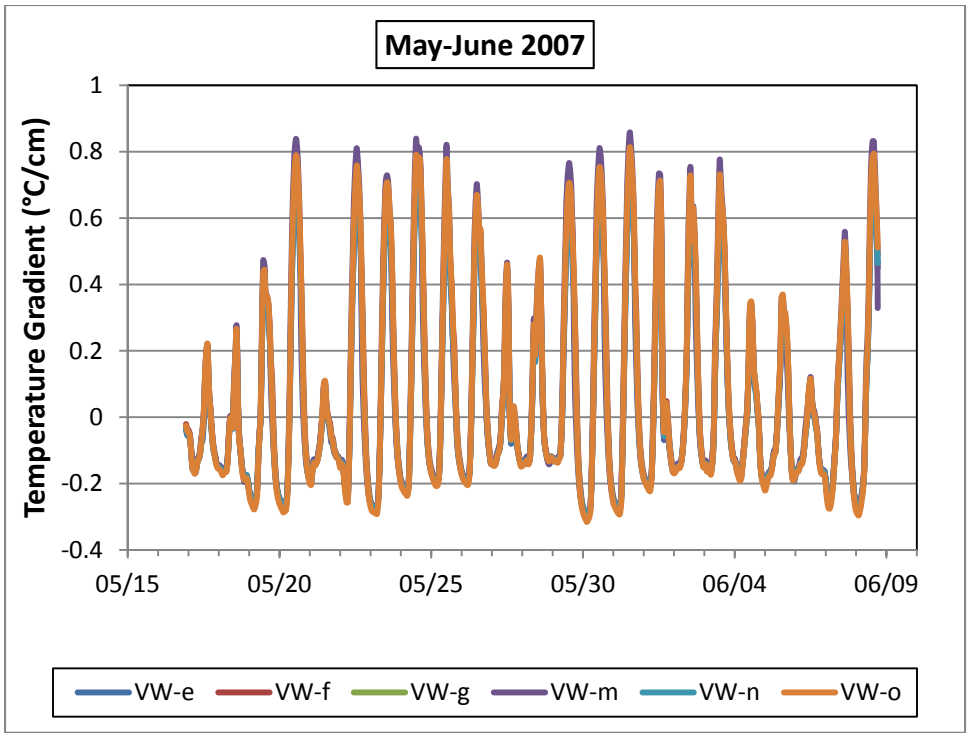
May-June 2007
Temperature Gradient (°C/cm)
1
0.8
0.6
0.4
0.2
0
-0.2
-0.4
05/15
05/20
05/25
05/30
06/04
06/09
VW-e
VW-f
VW-g
VW-m
VW-n
VW-o

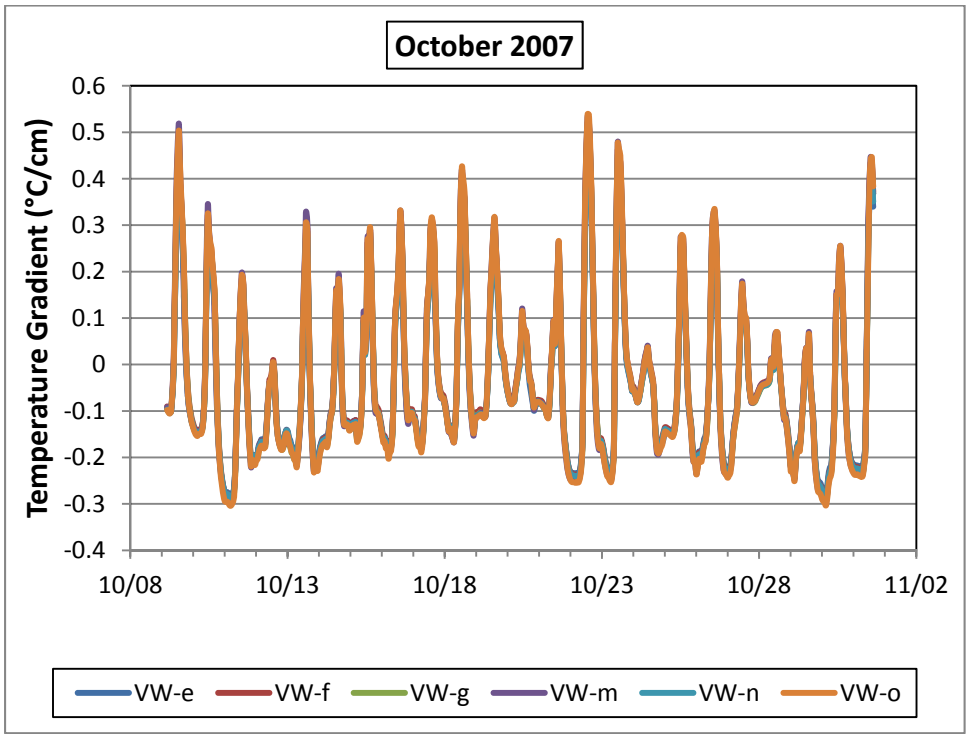
October 2007
Temperature Gradient (°C/cm)
0.6
0.5
0.4
0.3
0.2
0.1
0
-0.1
-0.2
-0.3
-0.4
10/08
10/13
10/18
10/23
10/28
11/02
VW-e
VW-f
VW-g
VW-m
VW-n
VW-o

(1°C/cm = 4.6°F/in)

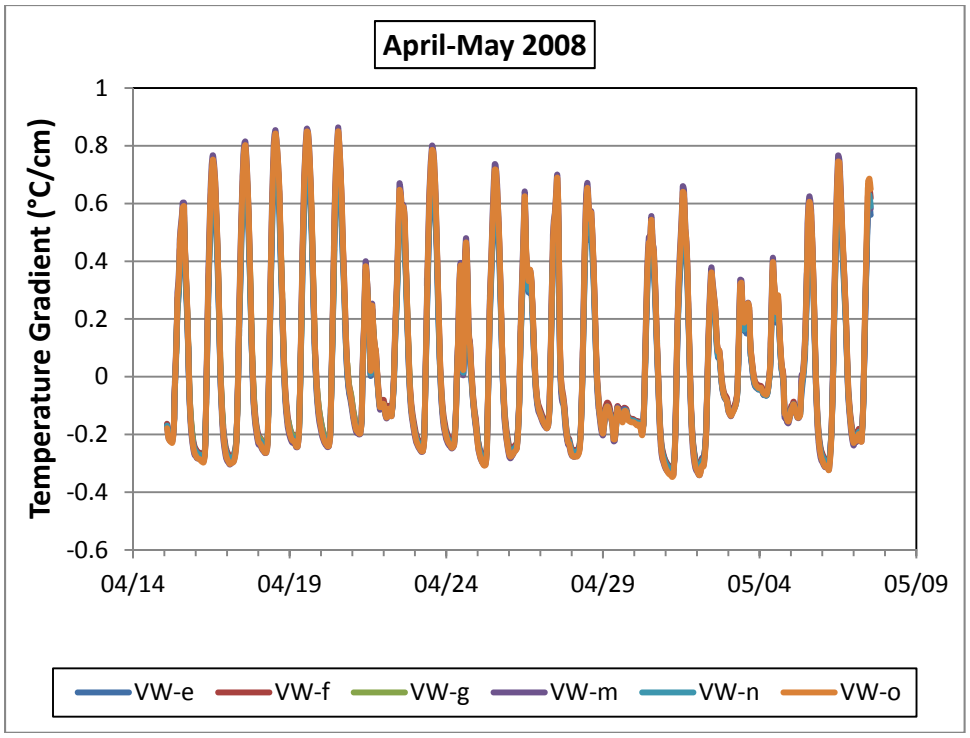
April-May 2008
Temperature Gradient (°C/cm)
1
0.8
0.6
0.4
0.2
0
-0.2
-0.4
-0.6
04/14
04/19
04/24
04/29
05/04
05/09
VW-e
VW-f
VW-g
VW-m
VW-n
VW-o

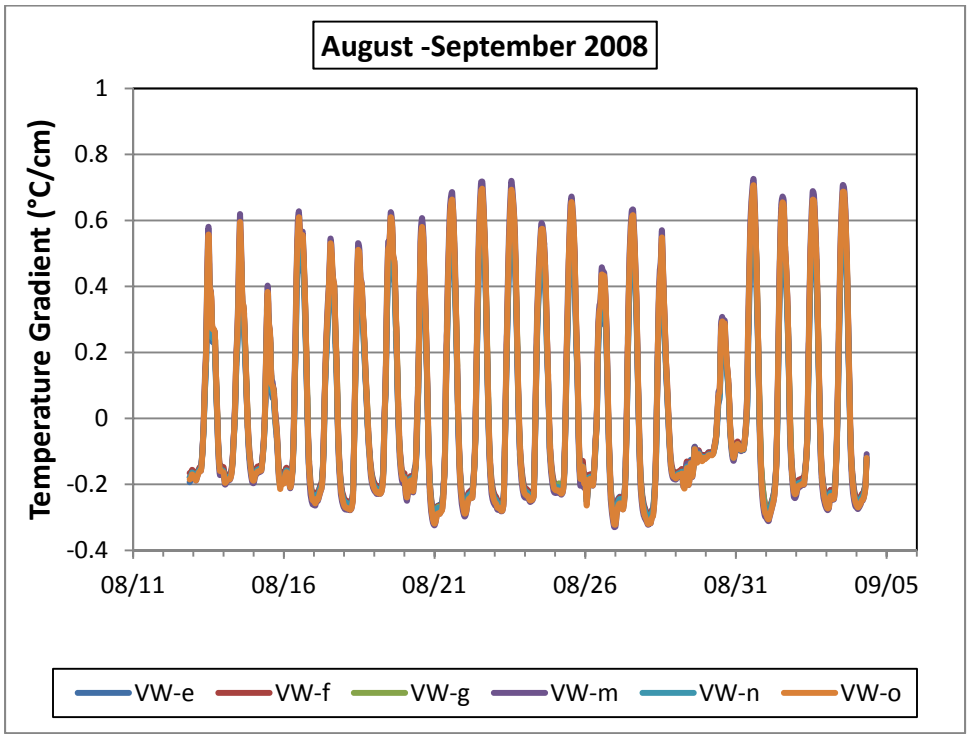
August -September 2008
Temperature Gradient (°C/cm)
1
0.8
0.6
0.4
0.2
0
-0.2
-0.4
08/11
08/16
08/21
08/26
08/31
09/05
VW-e
VW-f
VW-g
VW-m
VW-n
VW-o

(1°C/cm = 4.6°F/in)

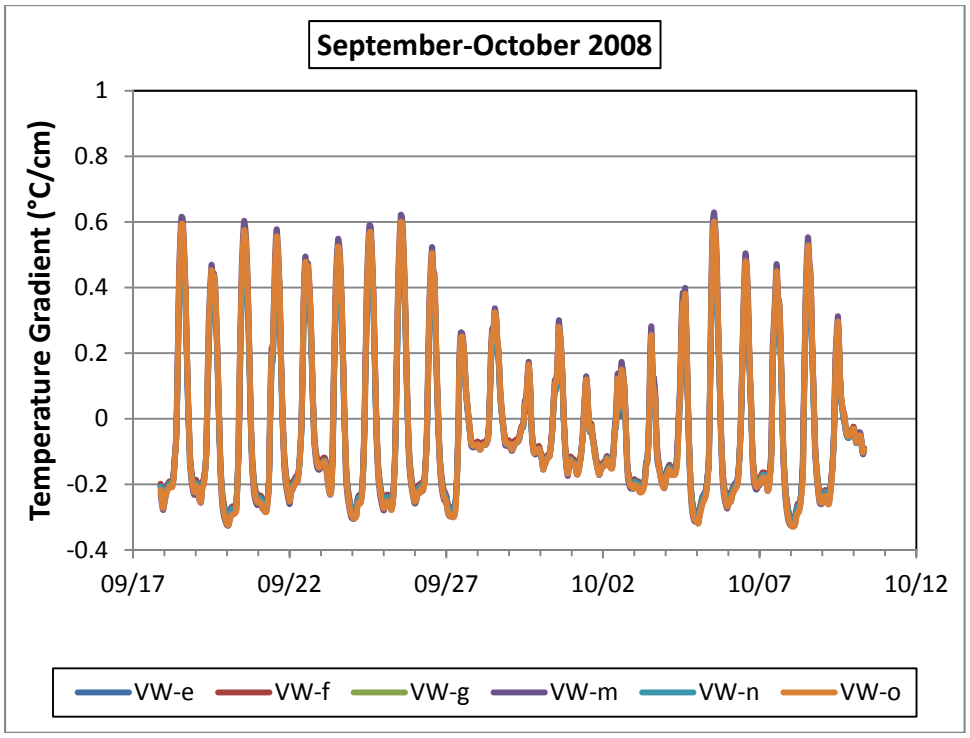
September-October 2008
Temperature Gradient (°C/cm)
1
0.8
0.6
0.4
0.2
0
-0.2
-0.4
09/17
09/22
09/27
10/02
10/07
10/12
VW-e
VW-f
VW-g
VW-m
VW-n
VW-o

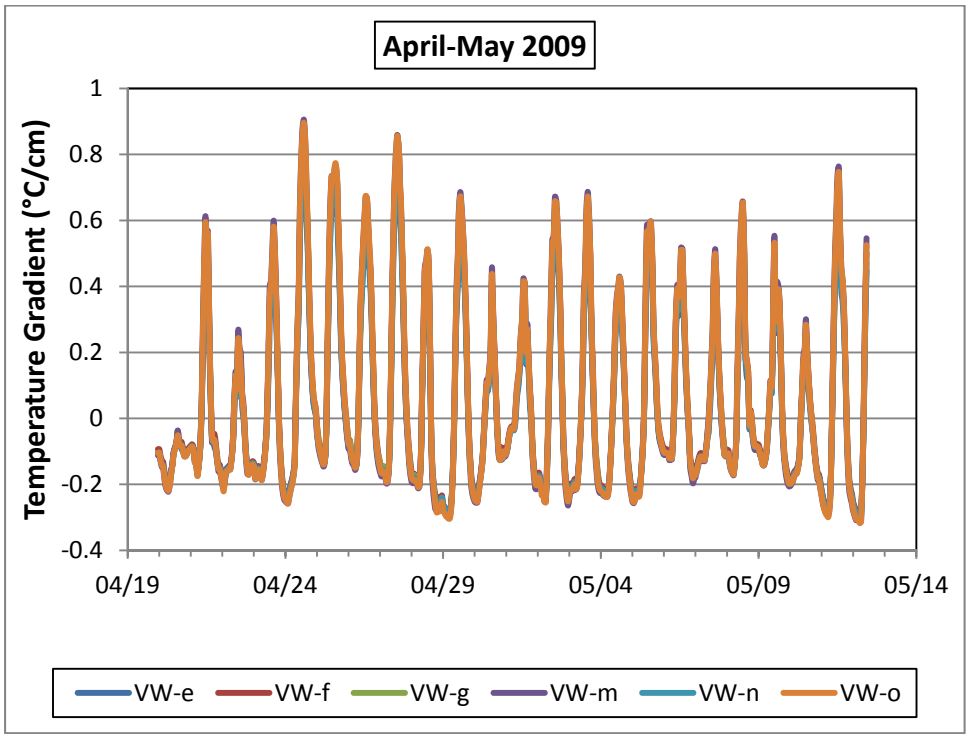
April-May 2009
Temperature Gradient (°C/cm)
1
0.8
0.6
0.4
0.2
0
-0.2
-0.4
04/19
04/24
04/29
05/04
05/09
05/14
VW-e
VW-f
VW-g
VW-m
VW-n
VW-o

(1°C/cm = 4.6°F/in)

Total Strain

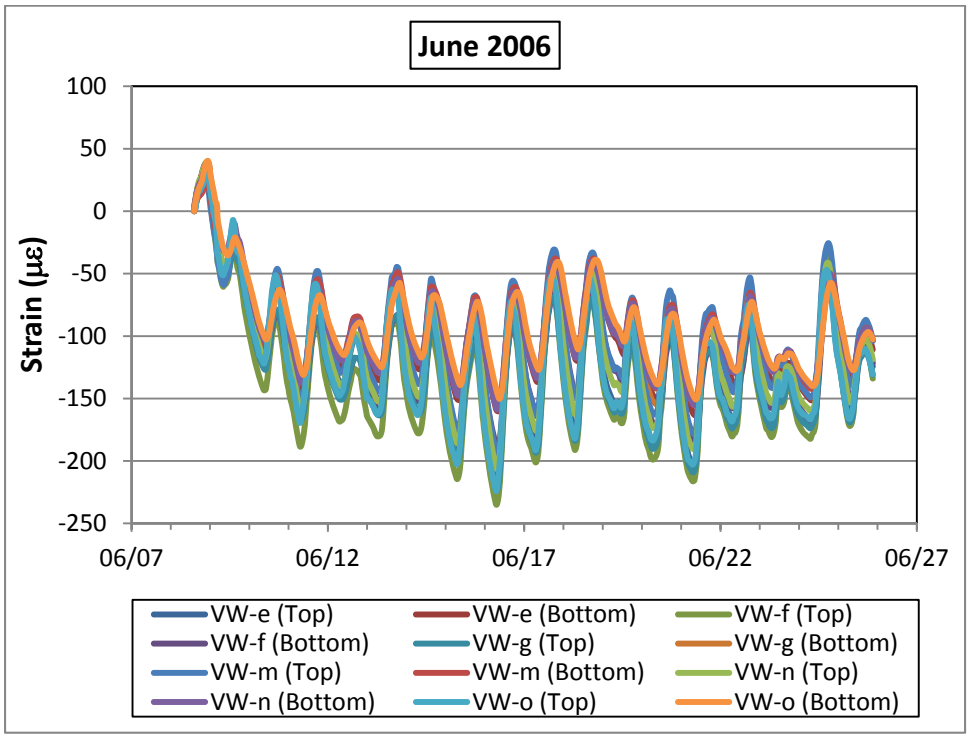

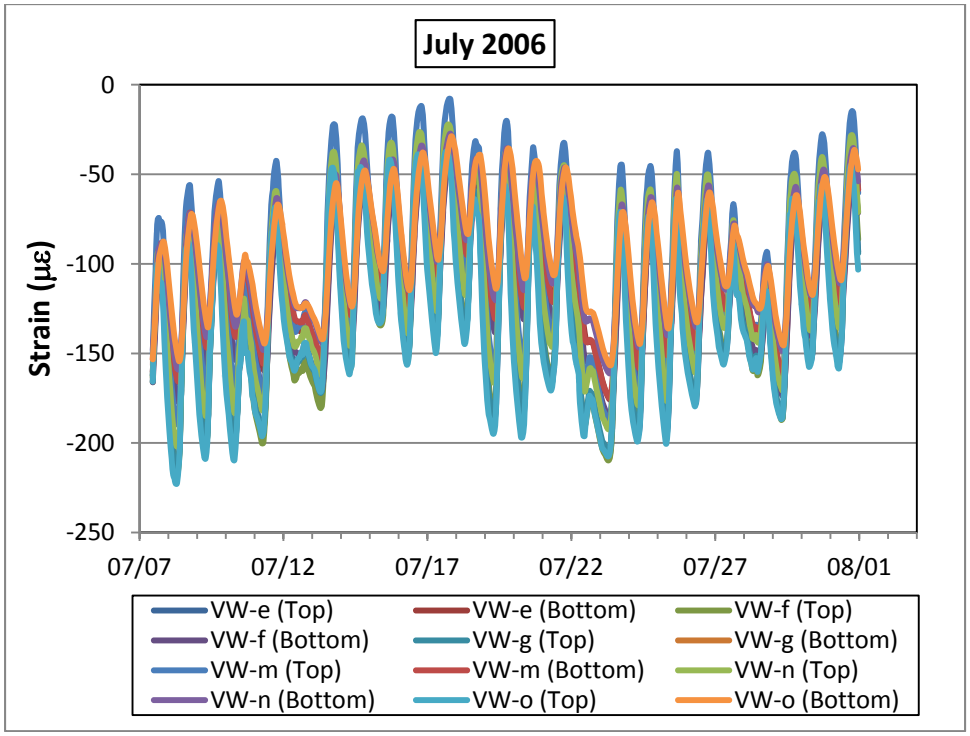

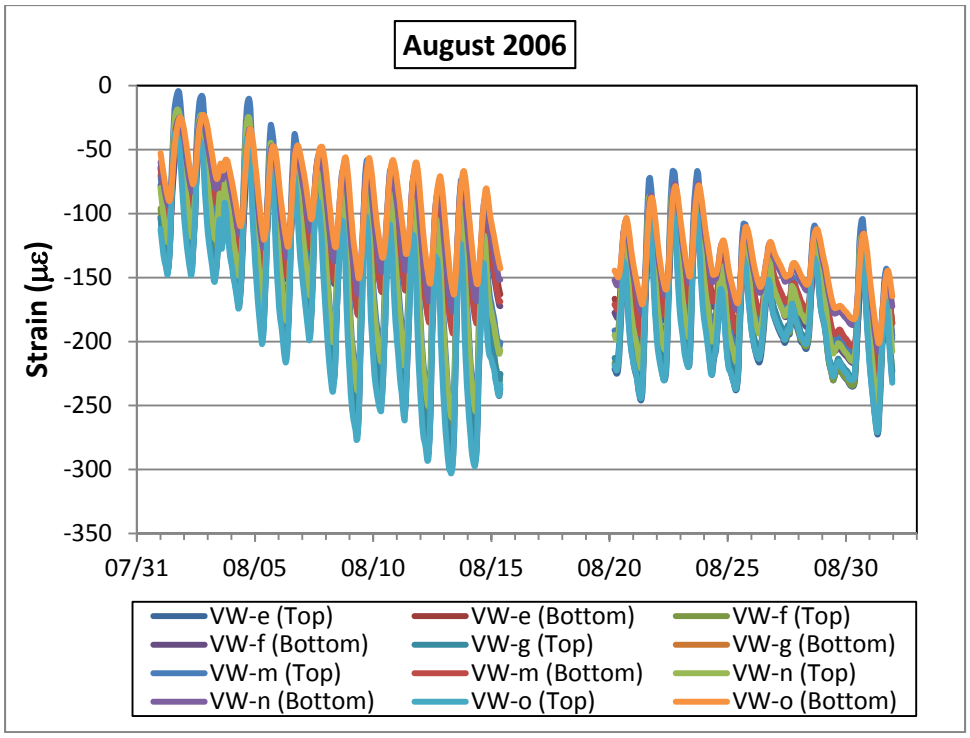
August 2006
0
-50
-100
-150
-200
-250
-300
-350
Strain (με)
07/31
08/05
08/10
08/15
08/20
08/25
08/30
VW-e (Top)
VW-e (Bottom)
VW-f (Top)
VW-f (Bottom)
VW-g (Top)
VW-g (Bottom)
VW-m (Top)
VW-m (Bottom)
VW-n (Top)
VW-n (Bottom)
VW-o (Top)
VW-o (Bottom)

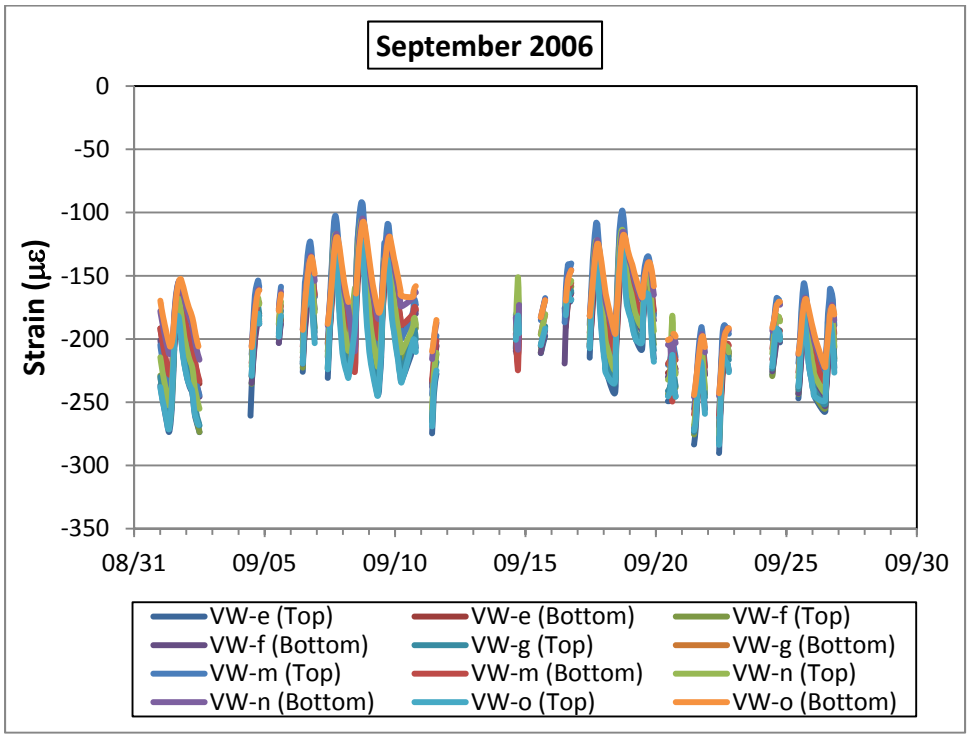
September 2006
0
-50
-100
-150
-200
-250
-300
-350
Strain (με)
08/31
09/05
09/10
09/15
09/20
09/25
09/30
VW-e (Top)
VW-e (Bottom)
VW-f (Top)
VW-f (Bottom)
VW-g (Top)
VW-g (Bottom)
VW-m (Top)
VW-m (Bottom)
VW-n (Top)
VW-n (Bottom)
VW-o (Top)
VW-o (Bottom)

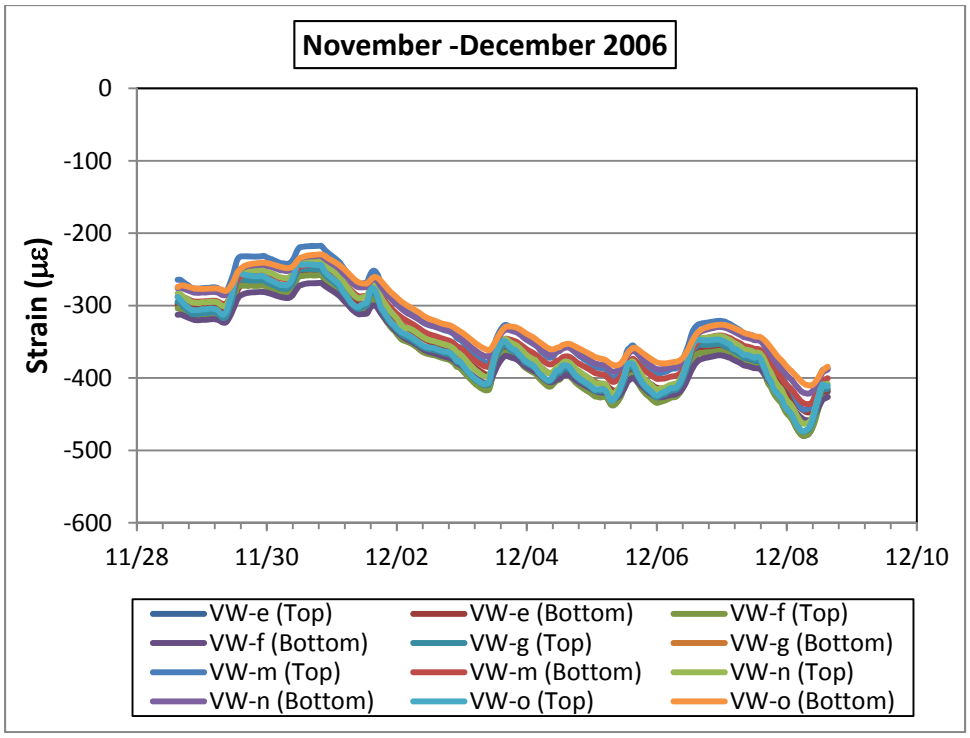
November -December 2006
0
-100
-200
-300
-400
-500
-600
Strain (με)
11/28
11/30
12/02
12/04
12/06
12/08
12/10
VW-e (Top)
VW-e (Bottom)
VW-f (Top)
VW-f (Bottom)
VW-g (Top)
VW-g (Bottom)
VW-m (Top)
VW-m (Bottom)
VW-n (Top)
VW-n (Bottom)
VW-o (Top)
VW-o (Bottom)

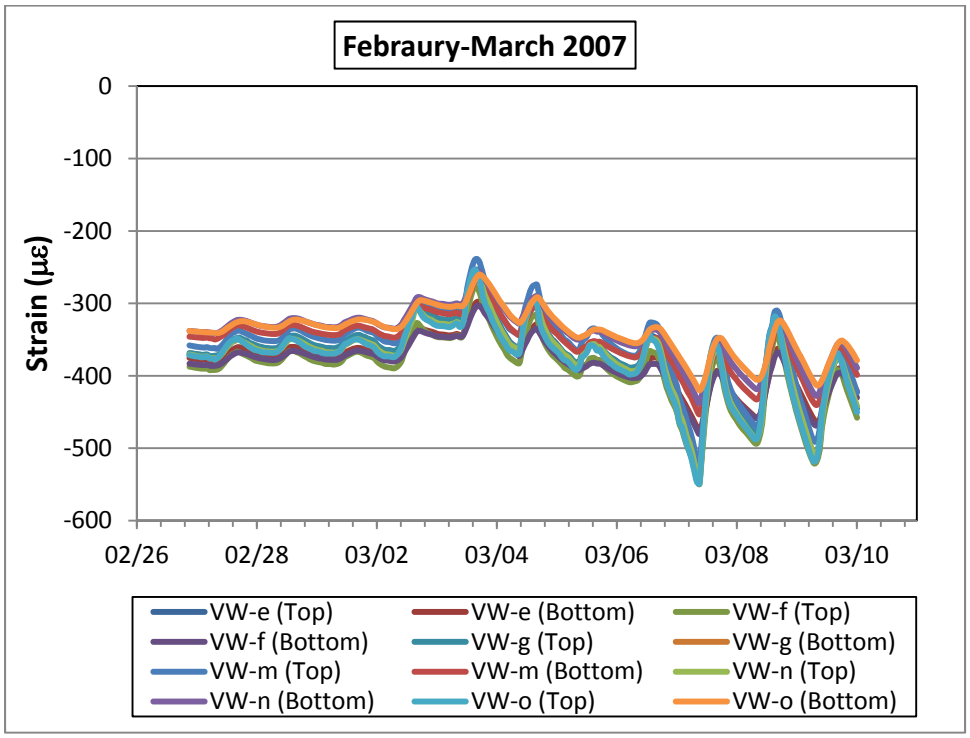
Febraury-March 2007
0
-100
-200
-300
-400
-500
-600
Strain (με)
02/26
02/28
03/02
03/04
03/06
03/08
03/10
VW-e (Top)
VW-e (Bottom)
VW-f (Top)
VW-f (Bottom)
VW-g (Top)
VW-g (Bottom)
VW-m (Top)
VW-m (Bottom)
VW-n (Top)
VW-n (Bottom)
VW-o (Top)
VW-o (Bottom)

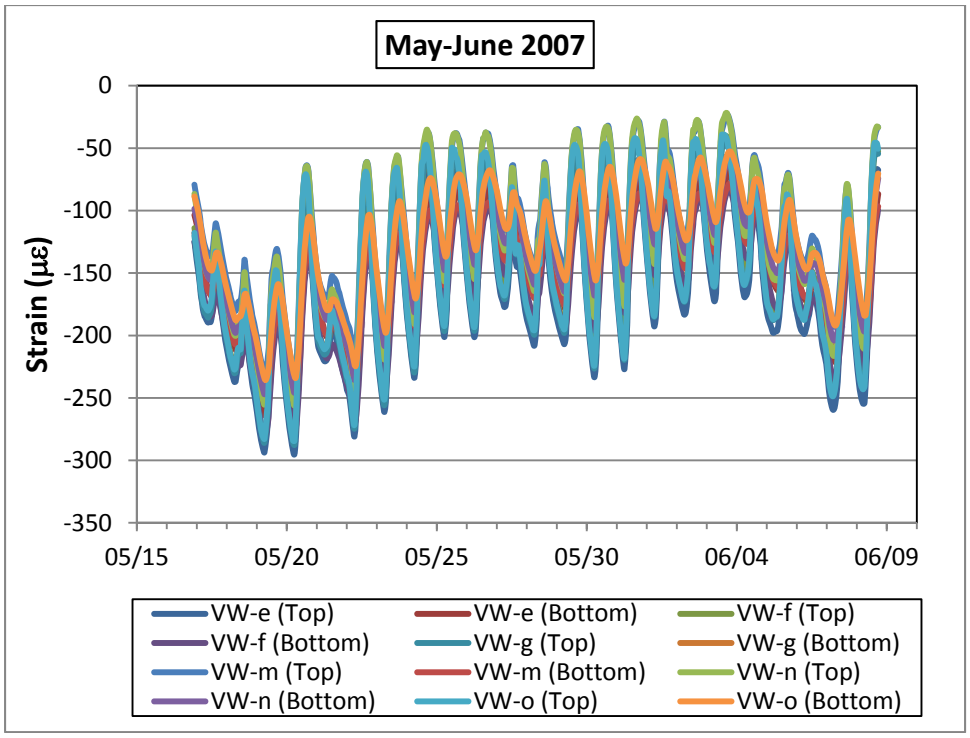
May-June 2007
0
-50
-100
-150
-200
-250
-300
-350
Strain (με)
05/15
05/20
05/25
05/30
06/04
06/09
VW-e (Top)
VW-e (Bottom)
VW-f (Top)
VW-f (Bottom)
VW-g (Top)
VW-g (Bottom)
VW-m (Top)
VW-m (Bottom)
VW-n (Top)
VW-n (Bottom)
VW-o (Top)
VW-o (Bottom)

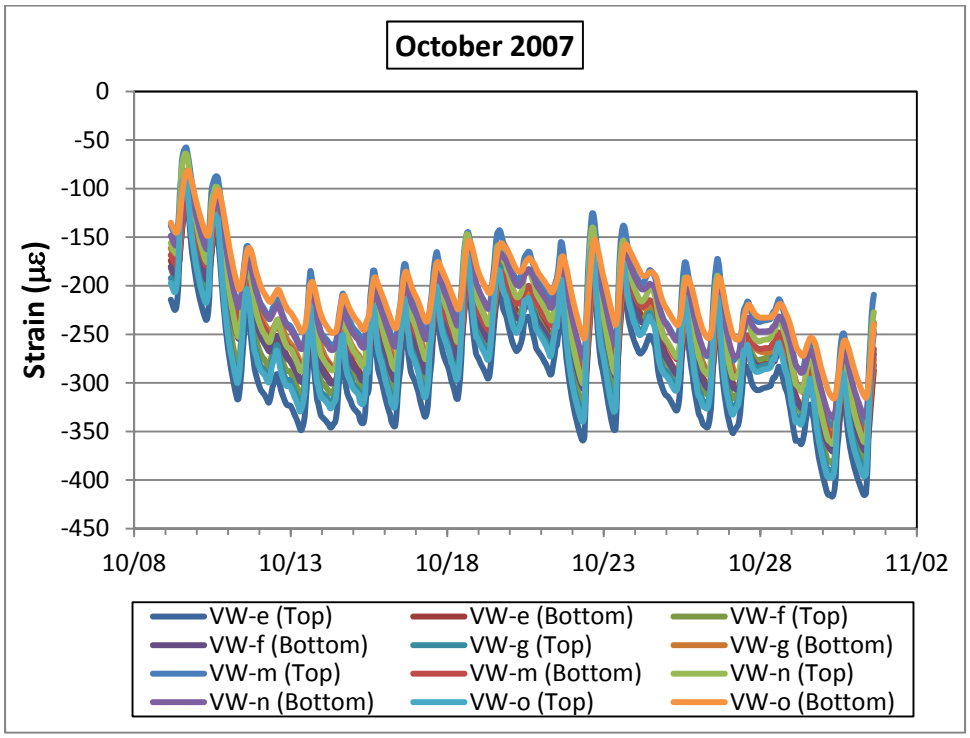
October 2007
0
-50
-100
-150
-200
-250
-300
-350
-400
-450
Strain (με)
10/08
10/13
10/18
10/23
10/28
11/02
VW-e (Top)
VW-e (Bottom)
VW-f (Top)
VW-f (Bottom)
VW-g (Top)
VW-g (Bottom)
VW-m (Top)
VW-m (Bottom)
VW-n (Top)
VW-n (Bottom)
VW-o (Top)
VW-o (Bottom)

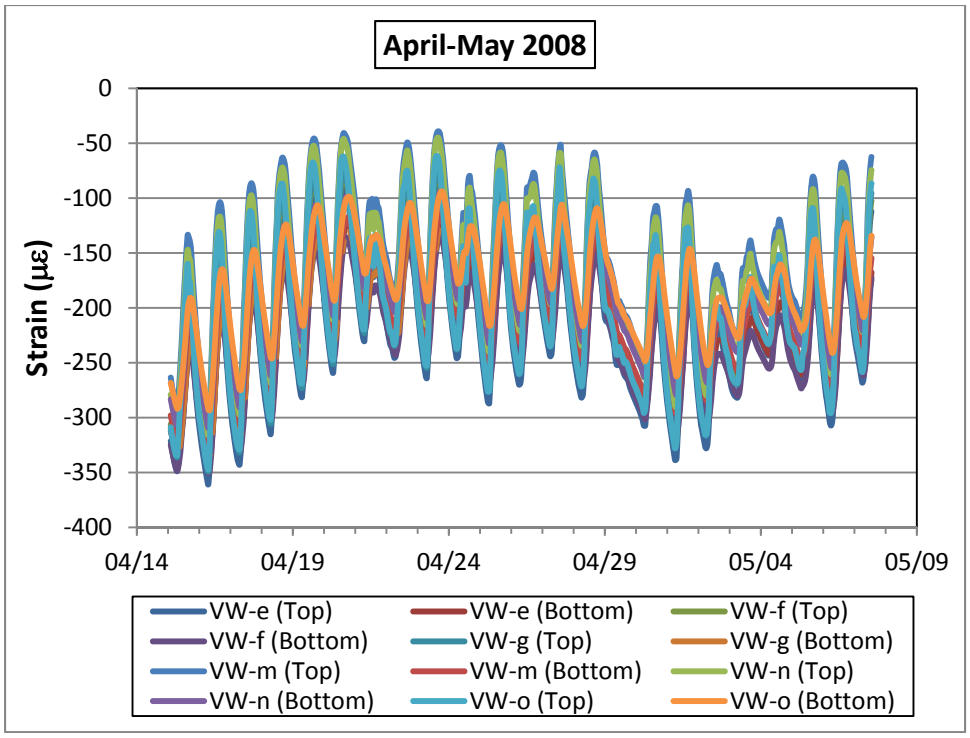
April-May 2008
0
-50
-100
-150
-200
-250
-300
-350
-400
Strain (με)
04/14
04/19
04/24
04/29
05/04
05/09
VW-e (Top)
VW-e (Bottom)
VW-f (Top)
VW-f (Bottom)
VW-g (Top)
VW-g (Bottom)
VW-m (Top)
VW-m (Bottom)
VW-n (Top)
VW-n (Bottom)
VW-o (Top)
VW-o (Bottom)

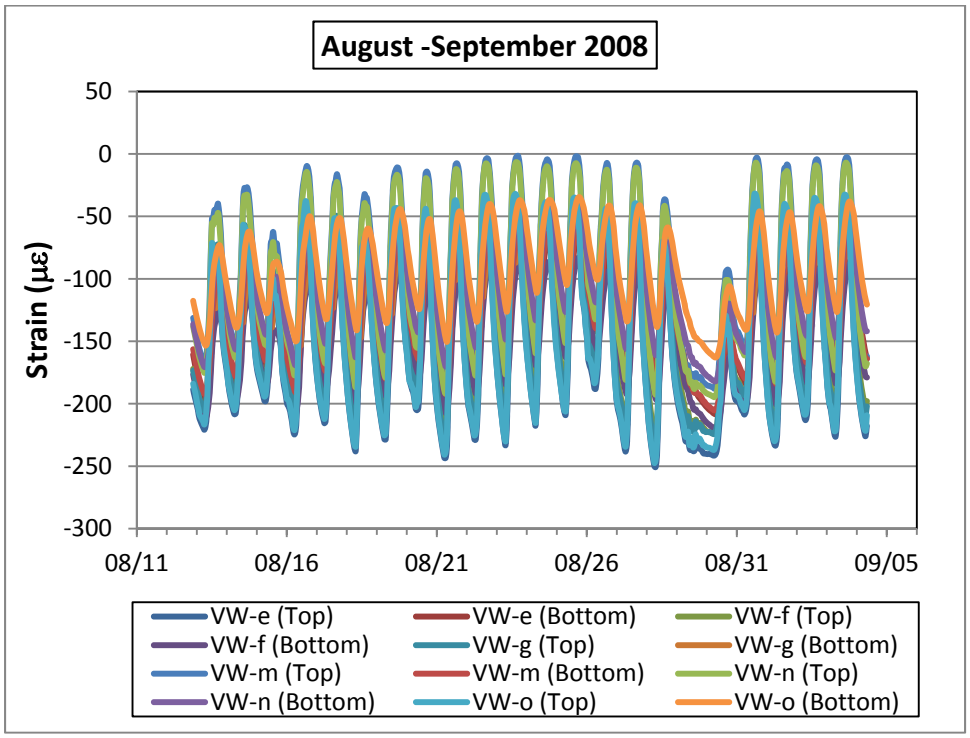
August -September 2008
50
0
-50
-100
-150
-200
-250
-300
Strain (με)
08/11
08/16
08/21
08/26
08/31
09/05
VW-e (Top)
VW-e (Bottom)
VW-f (Top)
VW-f (Bottom)
VW-g (Top)
VW-g (Bottom)
VW-m (Top)
VW-m (Bottom)
VW-n (Top)
VW-n (Bottom)
VW-o (Top)
VW-o (Bottom)

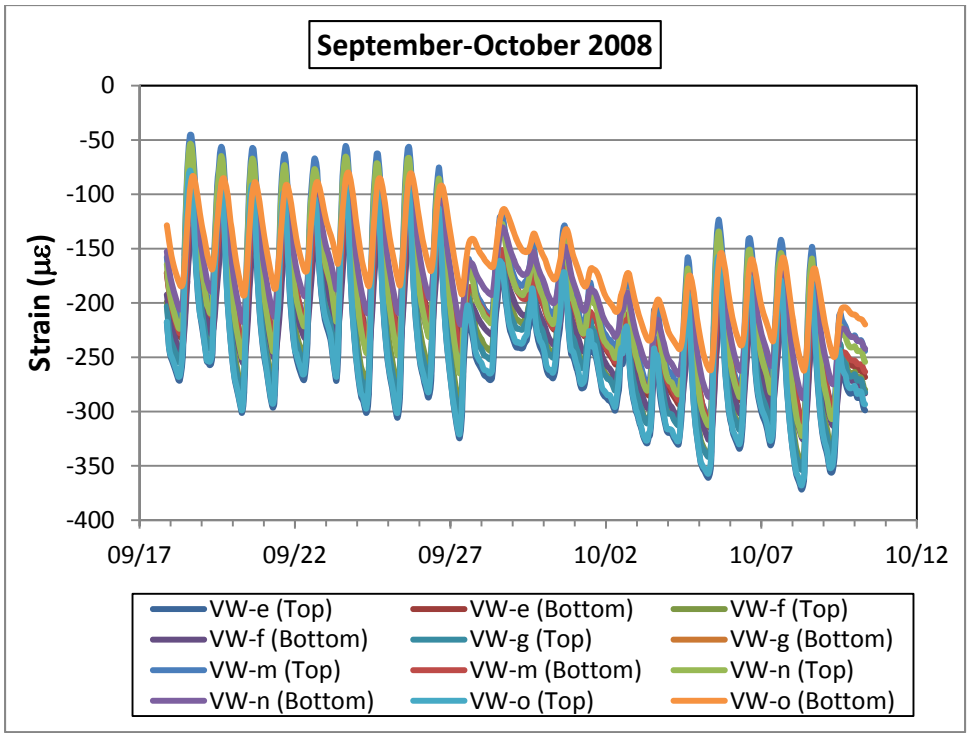
September-October 2008
0
-50
-100
-150
-200
-250
-300
-350
-400
Strain (με)
09/17
09/22
09/27
10/02
10/07
10/12
VW-e (Top)
VW-e (Bottom)
VW-f (Top)
VW-f (Bottom)
VW-g (Top)
VW-g (Bottom)
VW-m (Top)
VW-m (Bottom)
VW-n (Top)
VW-n (Bottom)
VW-o (Top)
VW-o (Bottom)

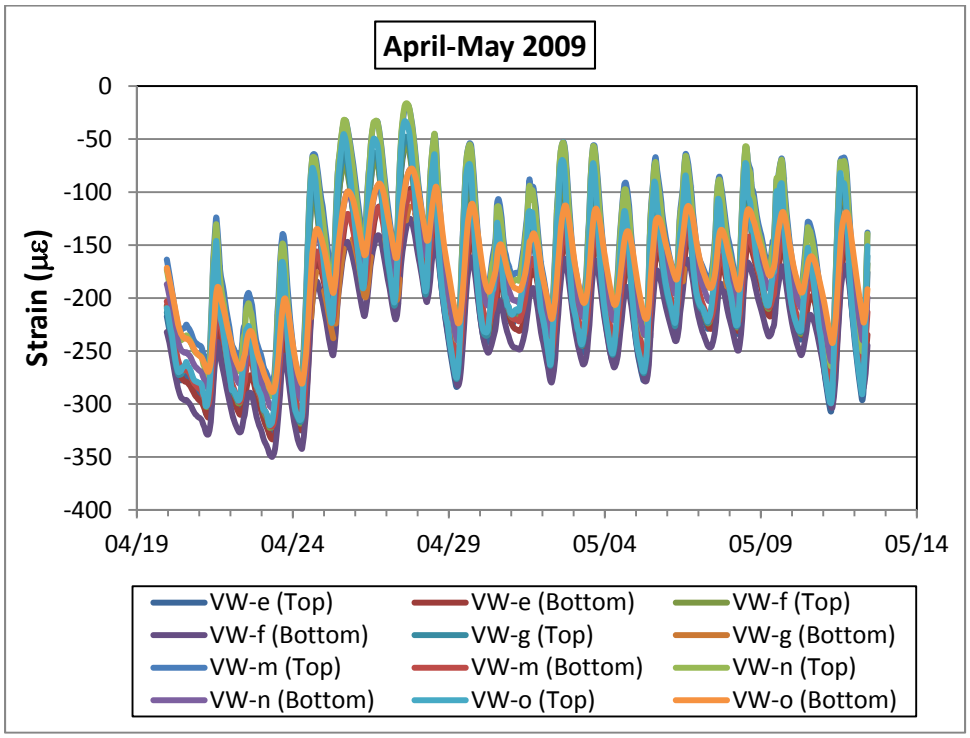
April-May 2009
0
-50
-100
-150
-200
-250
-300
-350
-400
Strain (με)
04/19
04/24
04/29
05/04
05/09
05/14
VW-e (Top)
VW-e (Bottom)
VW-f (Top)
VW-f (Bottom)
VW-g (Top)
VW-g (Bottom)
VW-m (Top)
VW-m (Bottom)
VW-n (Top)
VW-n (Bottom)
VW-o (Top)
VW-o (Bottom)

Load-Related Strain

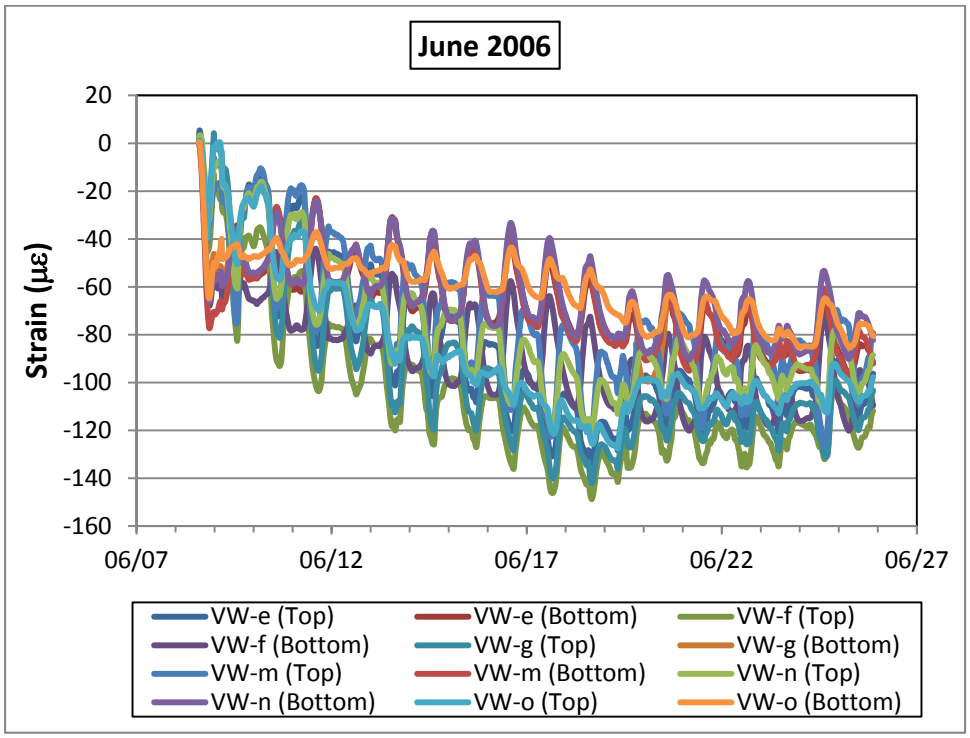

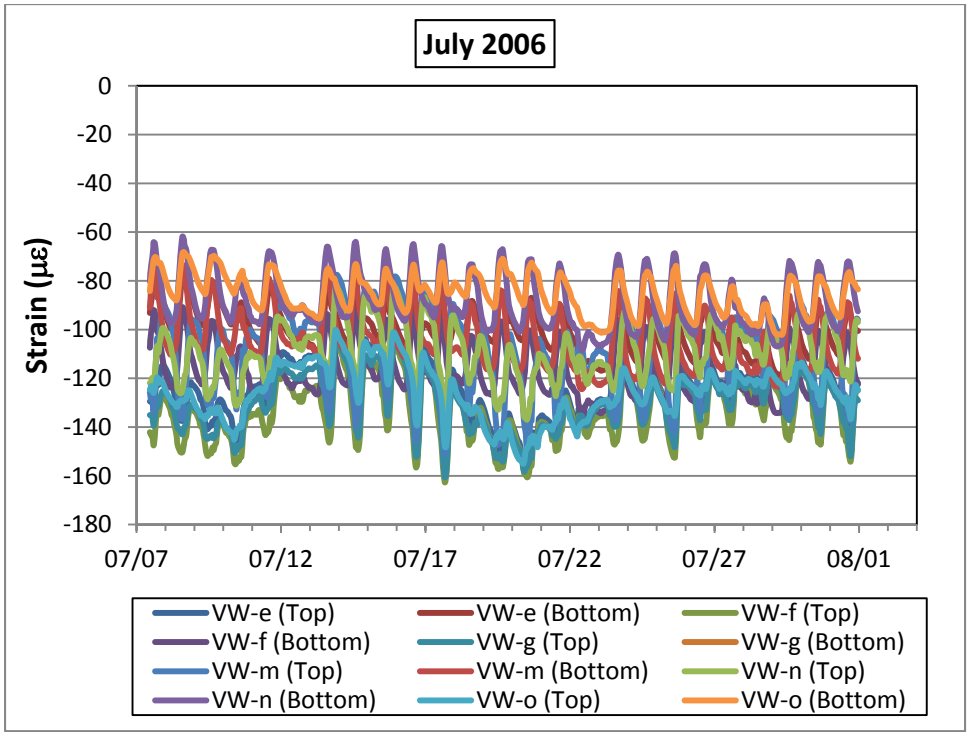

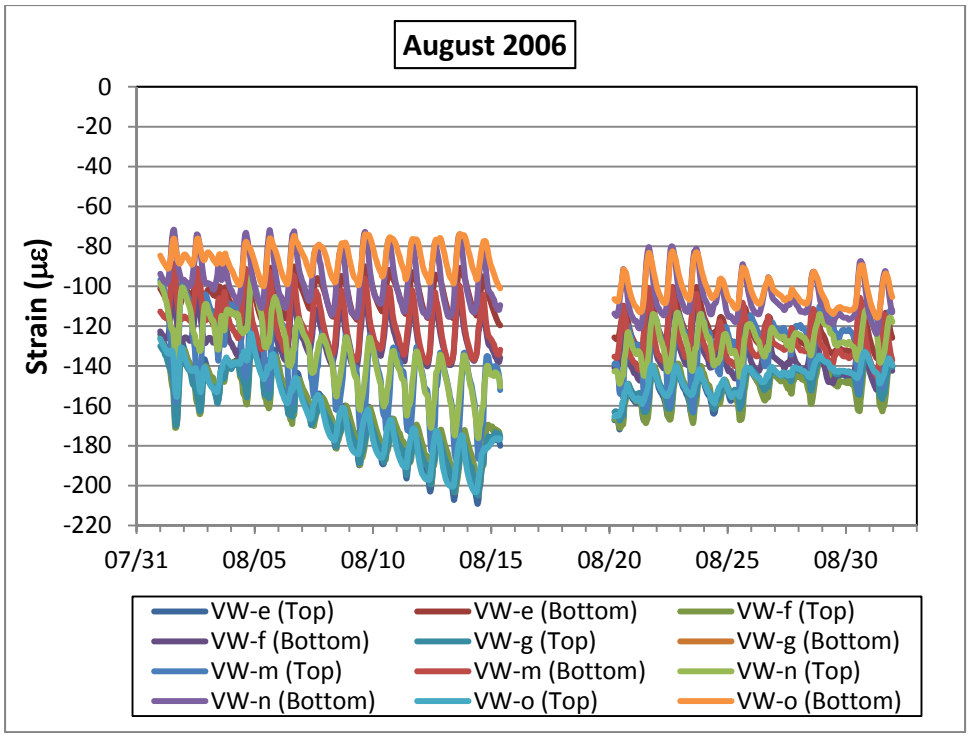
August 2006
Strain (με)
0
-20
-40
-60
-80
-100
-120
-140
-160
-180
-200
-220
07/31
08/05
08/10
08/15
08/20
08/25
08/30
VW-e (Top)
VW-e (Bottom)
VW-f (Top)
VW-f (Bottom)
VW-g (Top)
VW-g (Bottom)
VW-m (Top)
VW-m (Bottom)
VW-n (Top)
VW-n (Bottom)
VW-o (Top)
VW-o (Bottom)

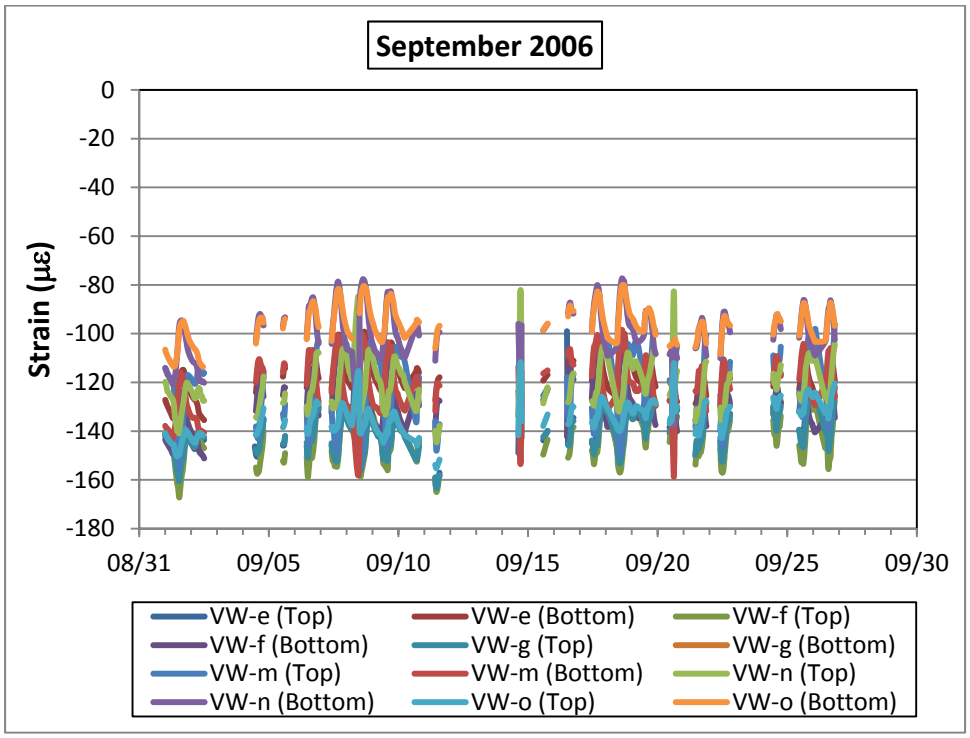
September 2006
Strain (με)
0
-20
-40
-60
-80
-100
-120
-140
-160
-180
08/31
09/05
09/10
09/15
09/20
09/25
09/30
VW-e (Top)
VW-e (Bottom)
VW-f (Top)
VW-f (Bottom)
VW-g (Top)
VW-g (Bottom)
VW-m (Top)
VW-m (Bottom)
VW-n (Top)
VW-n (Bottom)
VW-o (Top)
VW-o (Bottom)

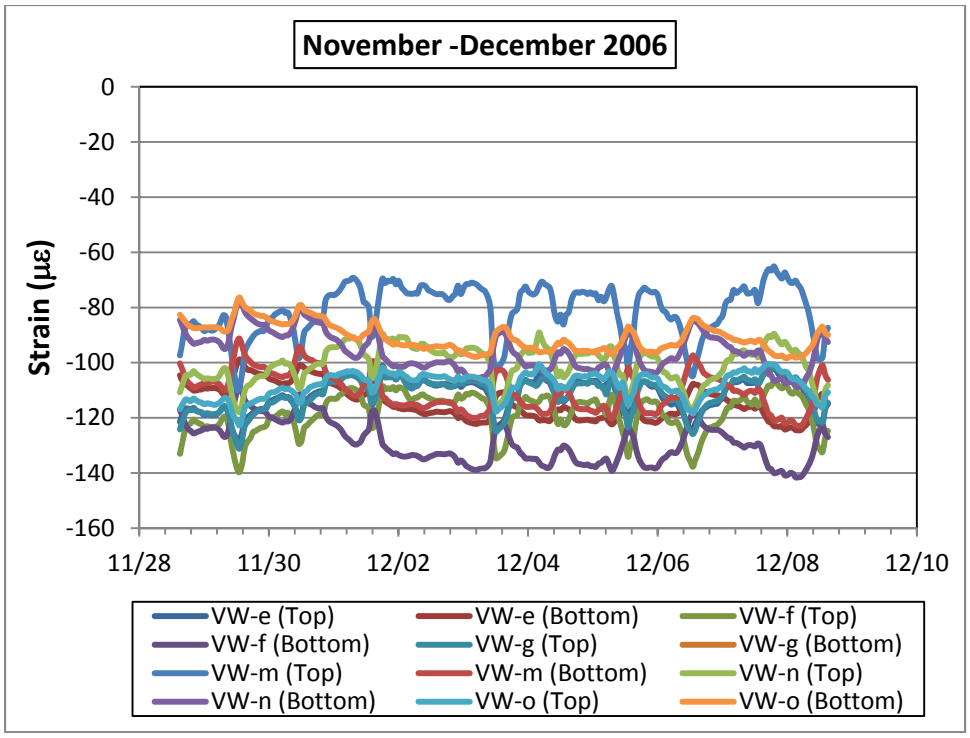
November -December 2006
Strain (με)
0
-20
-40
-60
-80
-100
-120
-140
-160
11/28
11/30
12/02
12/04
12/06
12/08
12/10
VW-e (Top)
VW-e (Bottom)
VW-f (Top)
VW-f (Bottom)
VW-g (Top)
VW-g (Bottom)
VW-m (Top)
VW-m (Bottom)
VW-n (Top)
VW-n (Bottom)
VW-o (Top)
VW-o (Bottom)

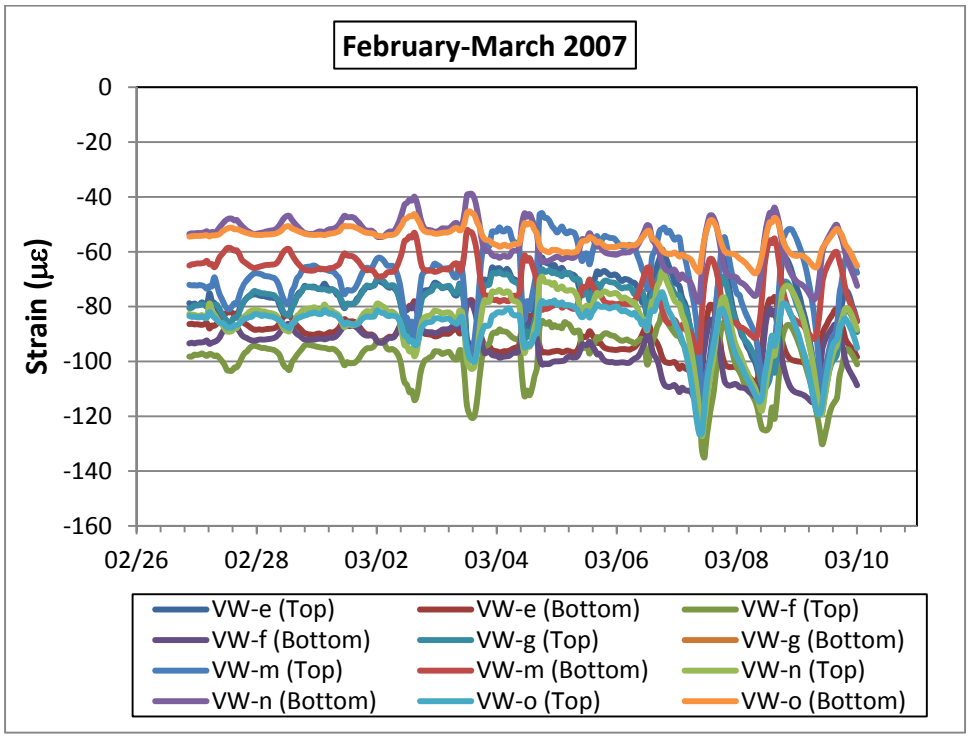
February-March 2007
Strain (με)
0
-20
-40
-60
-80
-100
-120
-140
-160
02/26
02/28
03/02
03/04
03/06
03/08
03/10
VW-e (Top)
VW-e (Bottom)
VW-f (Top)
VW-f (Bottom)
VW-g (Top)
VW-g (Bottom)
VW-m (Top)
VW-m (Bottom)
VW-n (Top)
VW-n (Bottom)
VW-o (Top)
VW-o (Bottom)

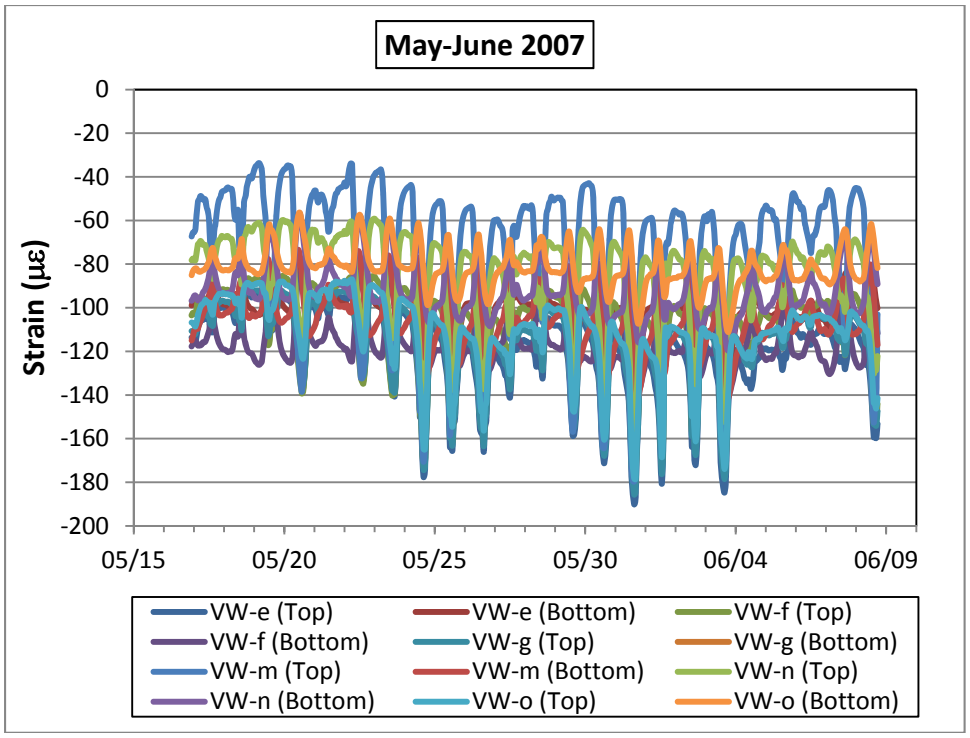
May-June 2007
Strain (με)
0
-20
-40
-60
-80
-100
-120
-140
-160
-180
-200
05/15
05/20
05/25
05/30
06/04
06/09
VW-e (Top)
VW-e (Bottom)
VW-f (Top)
VW-f (Bottom)
VW-g (Top)
VW-g (Bottom)
VW-m (Top)
VW-m (Bottom)
VW-n (Top)
VW-n (Bottom)
VW-o (Top)
VW-o (Bottom)

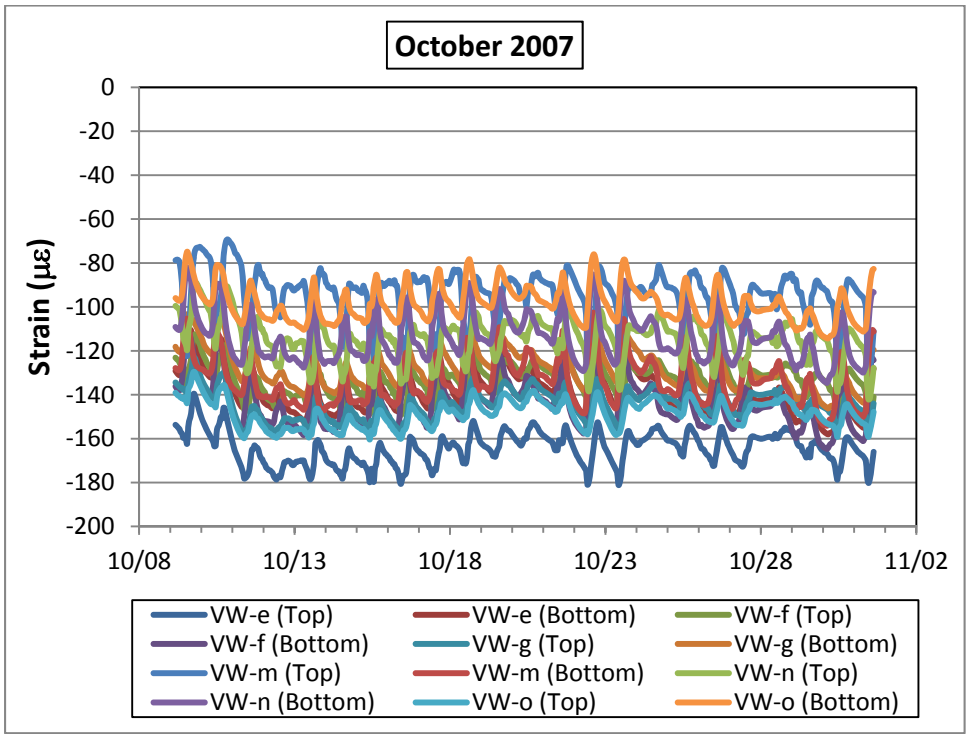
October 2007
Strain (με)
0
-20
-40
-60
-80
-100
-120
-140
-160
-180
-200
10/08
10/13
10/18
10/23
10/28
11/02
VW-e (Top)
VW-e (Bottom)
VW-f (Top)
VW-f (Bottom)
VW-g (Top)
VW-g (Bottom)
VW-m (Top)
VW-m (Bottom)
VW-n (Top)
VW-n (Bottom)
VW-o (Top)
VW-o (Bottom)

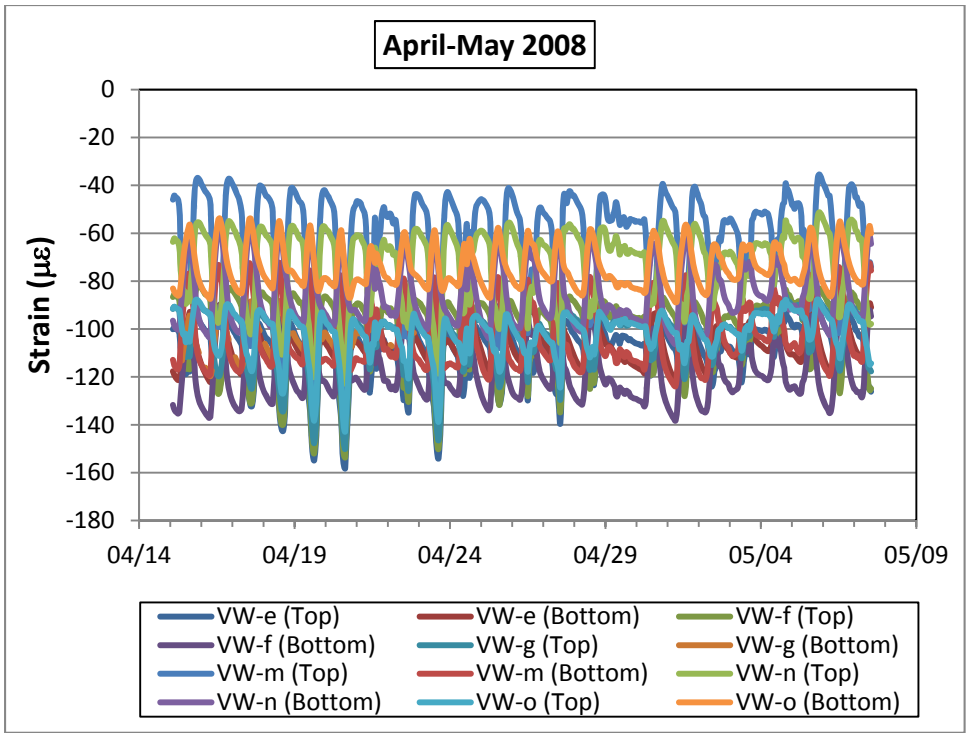
April-May 2008
Strain (με)
0
-20
-40
-60
-80
-100
-120
-140
-160
-180
04/14
04/19
04/24
04/29
05/04
05/09
VW-e (Top)
VW-e (Bottom)
VW-f (Top)
VW-f (Bottom)
VW-g (Top)
VW-g (Bottom)
VW-m (Top)
VW-m (Bottom)
VW-n (Top)
VW-n (Bottom)
VW-o (Top)
VW-o (Bottom)

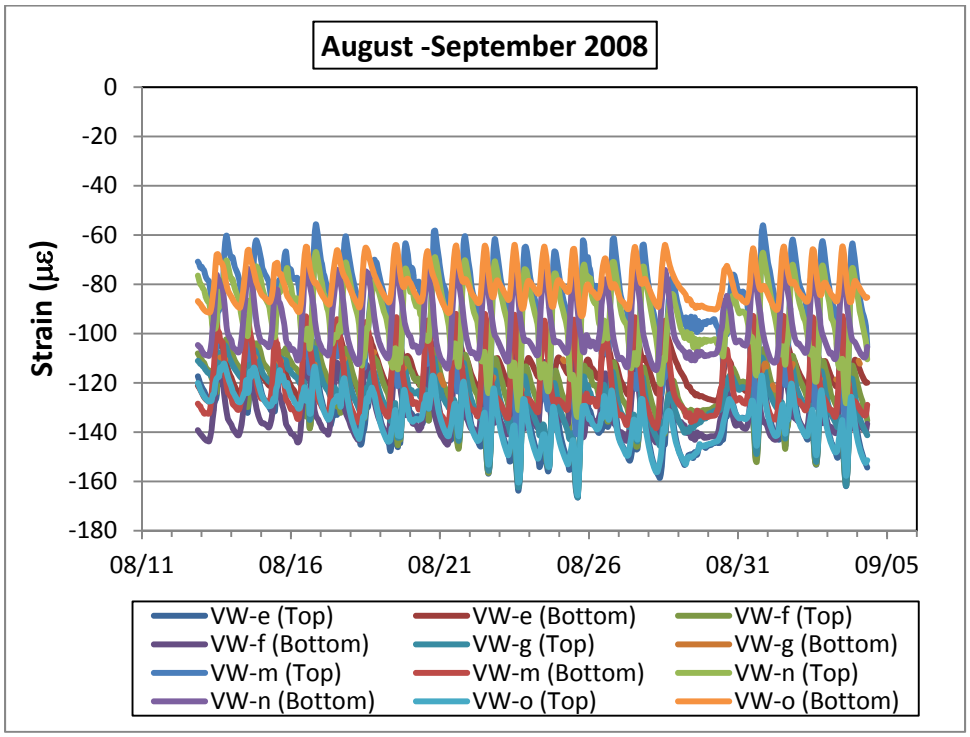
August -September 2008
Strain (με)
0
-20
-40
-60
-80
-100
-120
-140
-160
-180
08/11
08/16
08/21
08/26
08/31
09/05
VW-e (Top)
VW-e (Bottom)
VW-f (Top)
VW-f (Bottom)
VW-g (Top)
VW-g (Bottom)
VW-m (Top)
VW-m (Bottom)
VW-n (Top)
VW-n (Bottom)
VW-o (Top)
VW-o (Bottom)

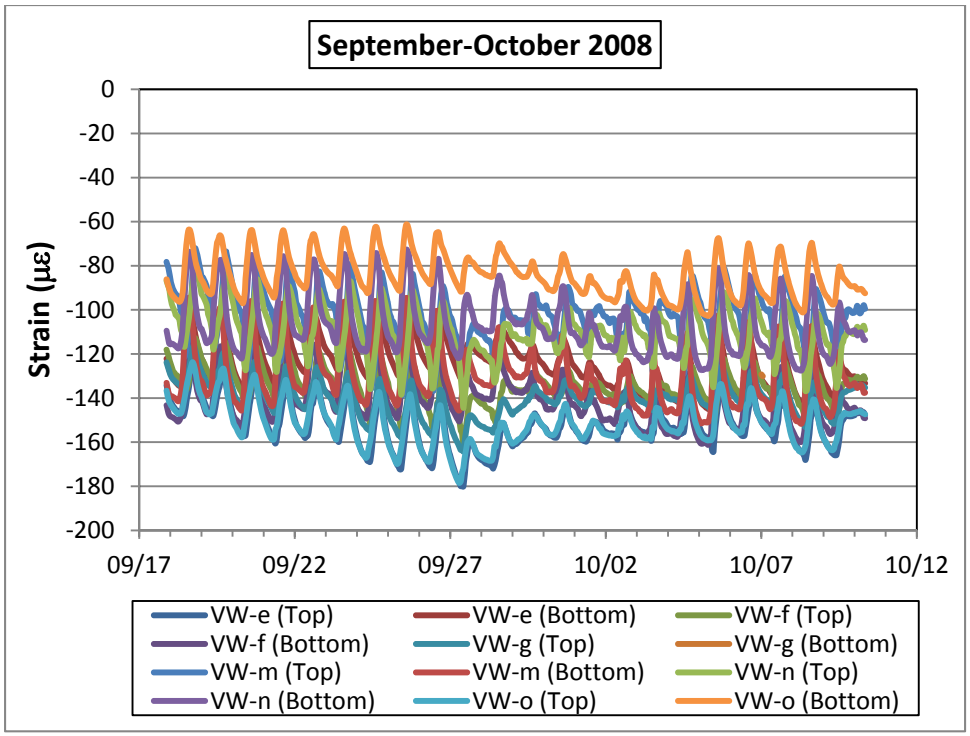
September-October 2008
0
-20
-40
-60
-80
-100
-120
-140
-160
-180
-200
Strain (με)
09/17
09/22
09/27
10/02
10/07
10/12
VW-e (Top)
VW-e (Bottom)
VW-f (Top)
VW-f (Bottom)
VW-g (Top)
VW-g (Bottom)
VW-m (Top)
VW-m (Bottom)
VW-n (Top)
VW-n (Bottom)
VW-o (Top)
VW-o (Bottom)

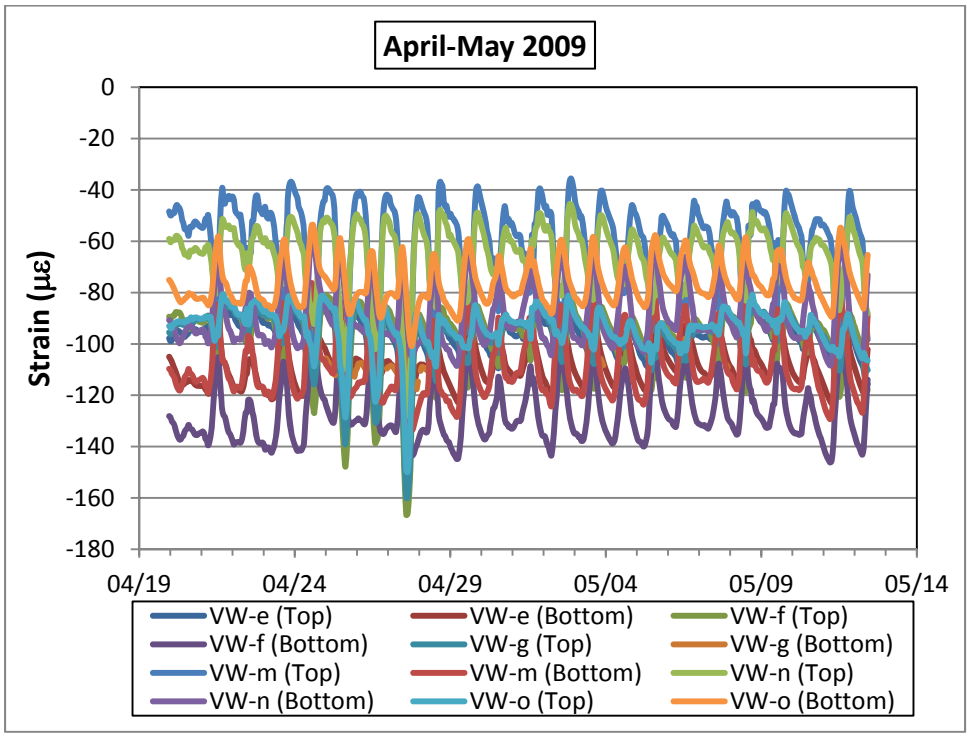
April-May 2009
0
-20
-40
-60
-80
-100
-120
-140
-160
-180
Strain (με)
04/19
04/24
04/29
05/04
05/09
05/14
VW-e (Top)
VW-e (Bottom)
VW-f (Top)
VW-f (Bottom)
VW-g (Top)
VW-g (Bottom)
VW-m (Top)
VW-m (Bottom)
VW-n (Top)
VW-n (Bottom)
VW-o (Top)
VW-o (Bottom)

Pavement Temperatures, Temperature Gradients, and Pavement Strains

Untreated Section

Pavement Temperatures

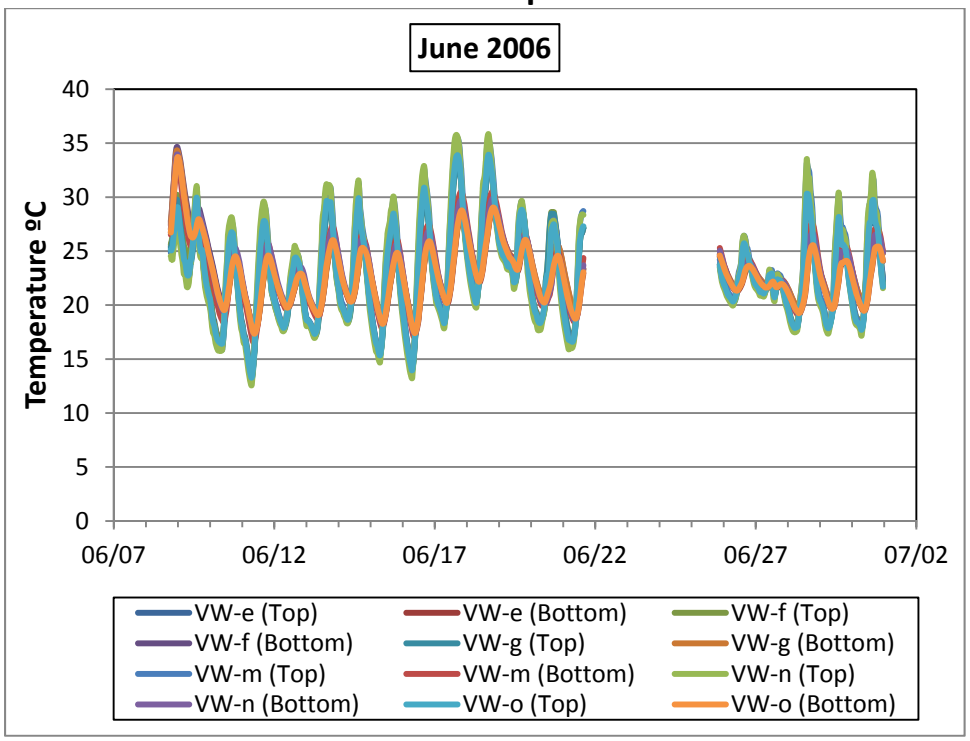

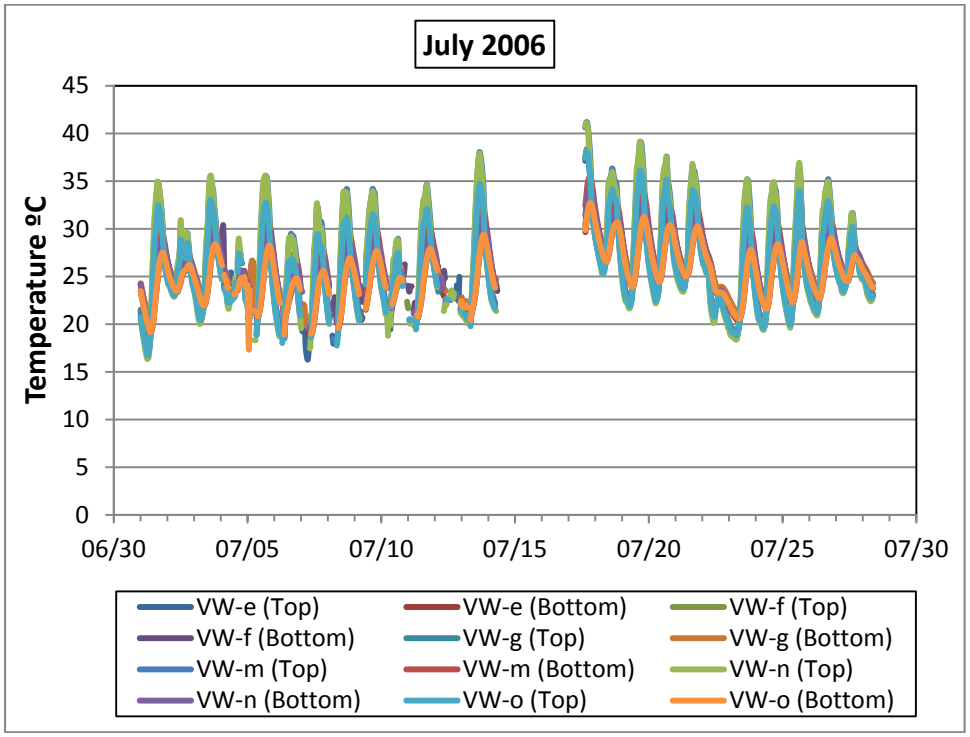

(0°C = 32°F, 45°C = 113°F)

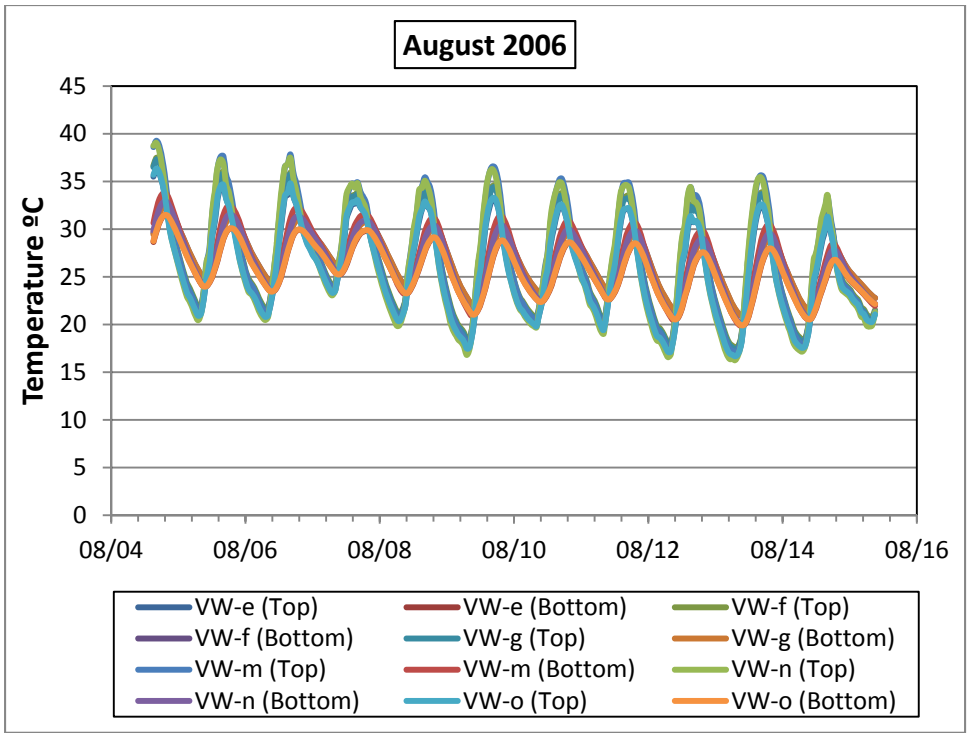

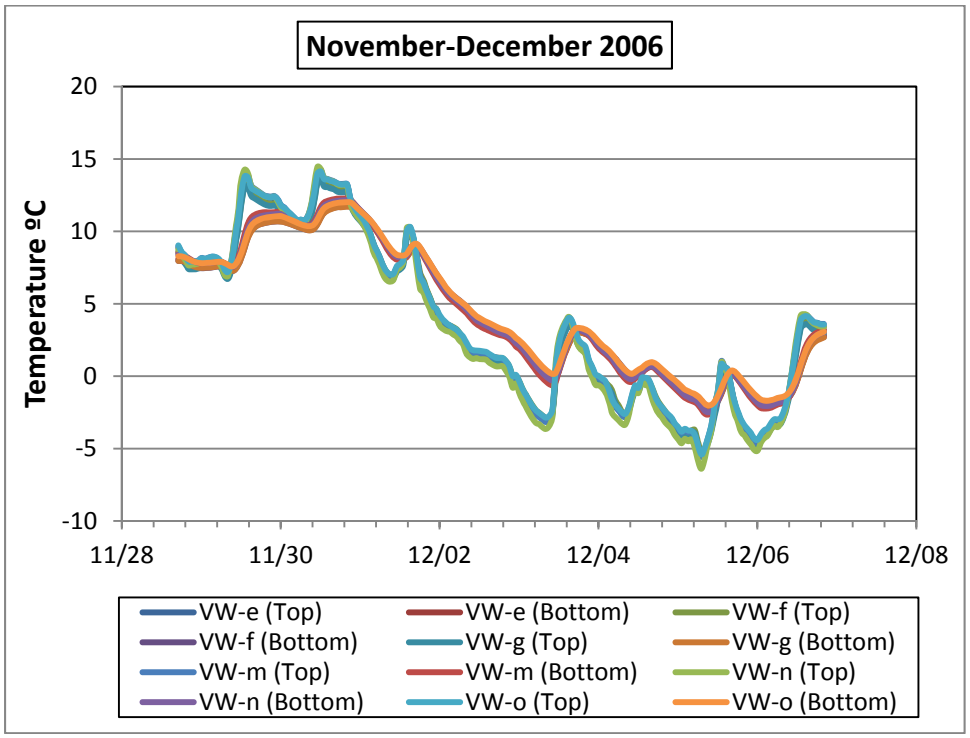

(-10°C = 14°F, 45°C = 113°F)

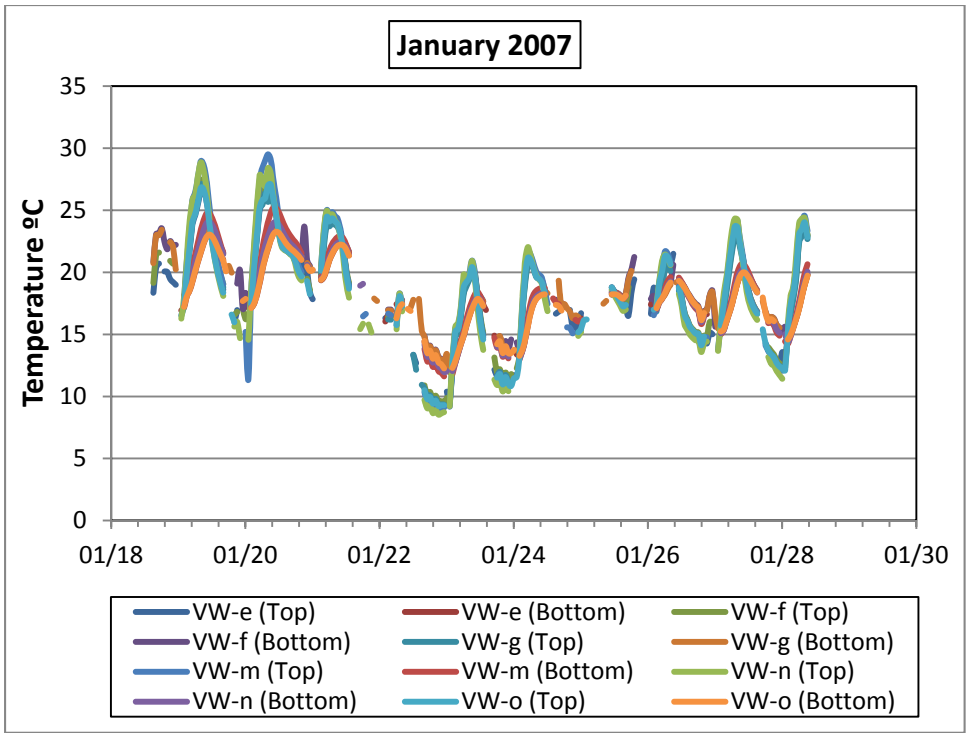

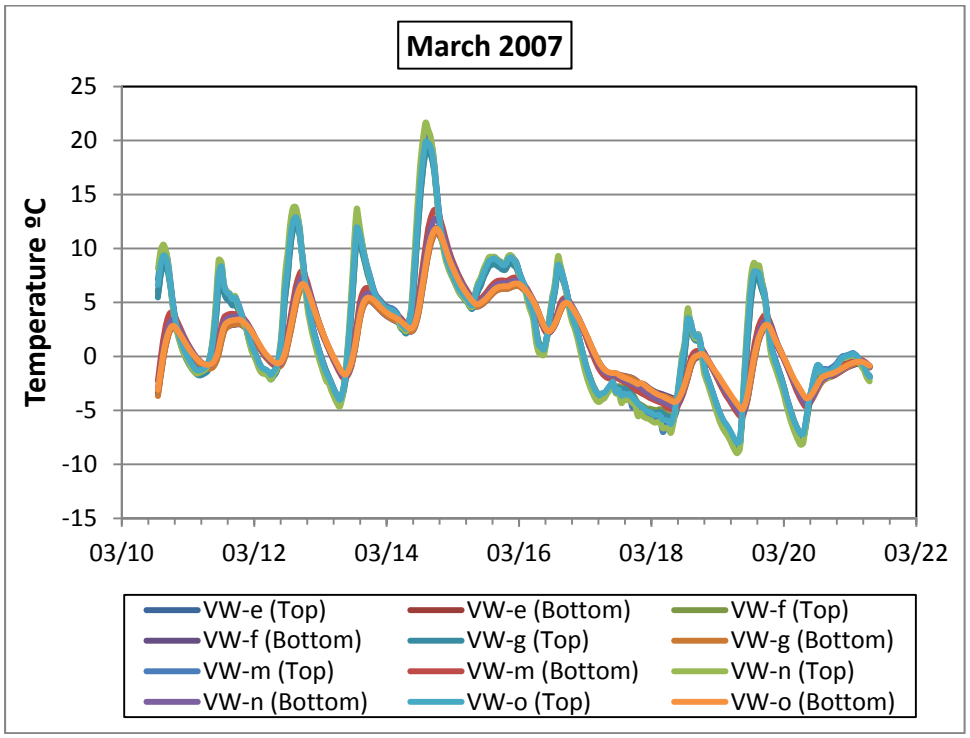

(-15°C = 5°F, 35°C = 95°F)

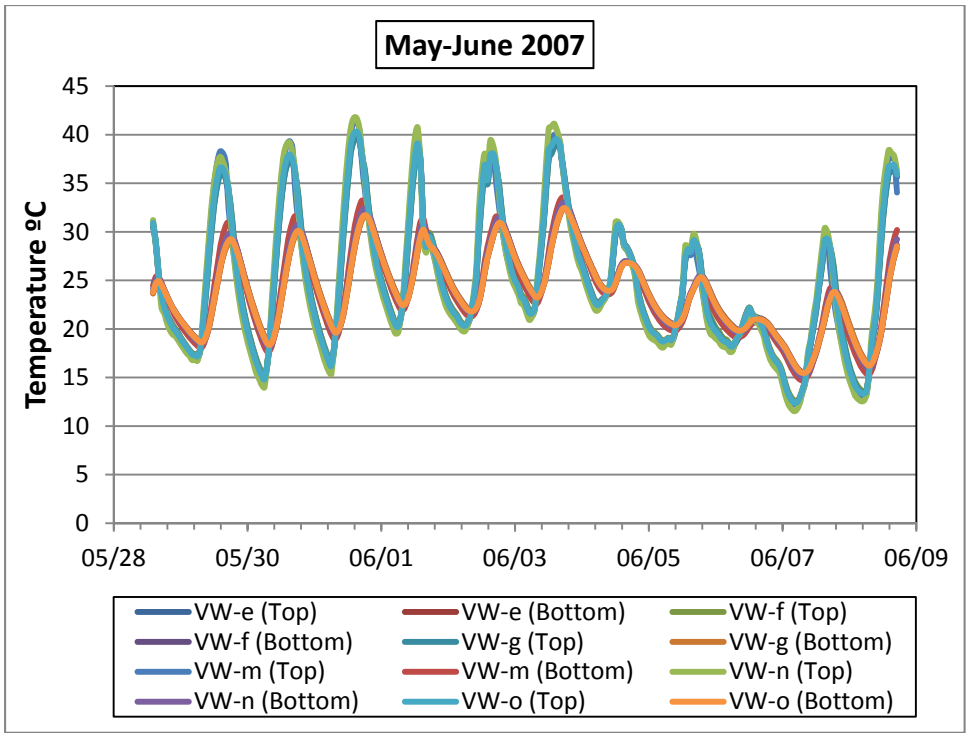

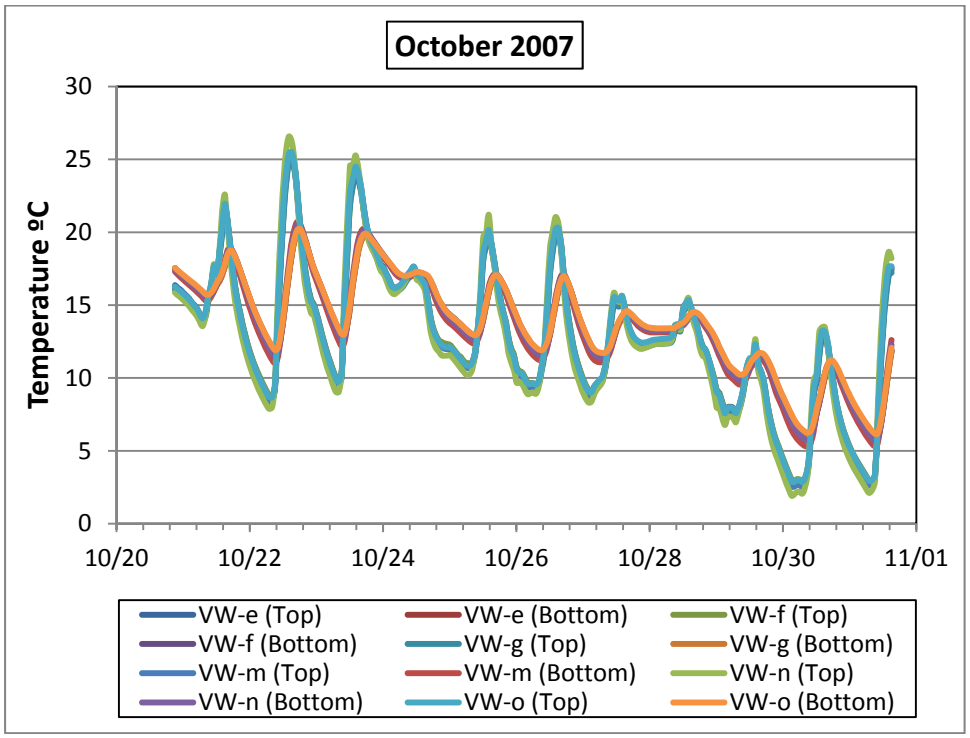

(0°C = 32°F, 45°C = 113°F)

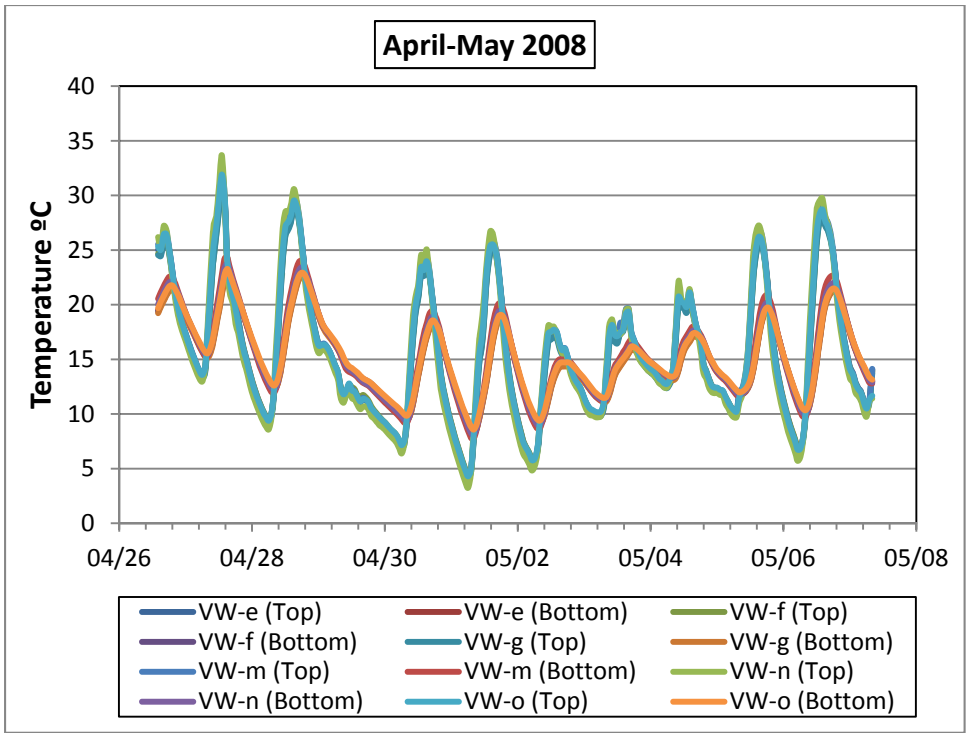

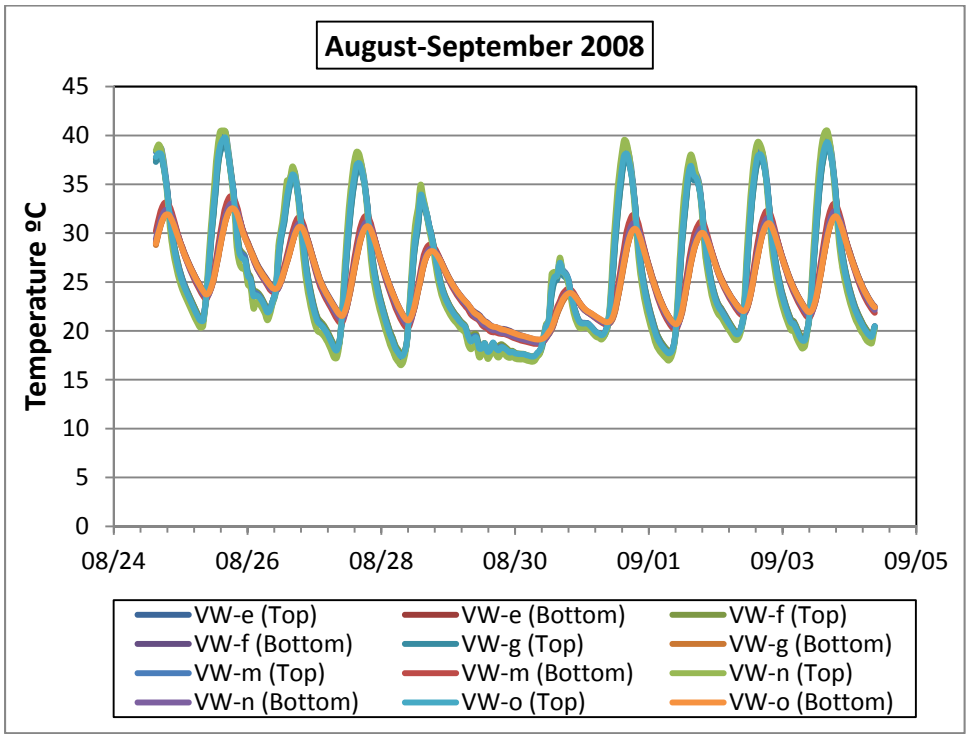

(0°C = 32°F, 40°C = 104°F)

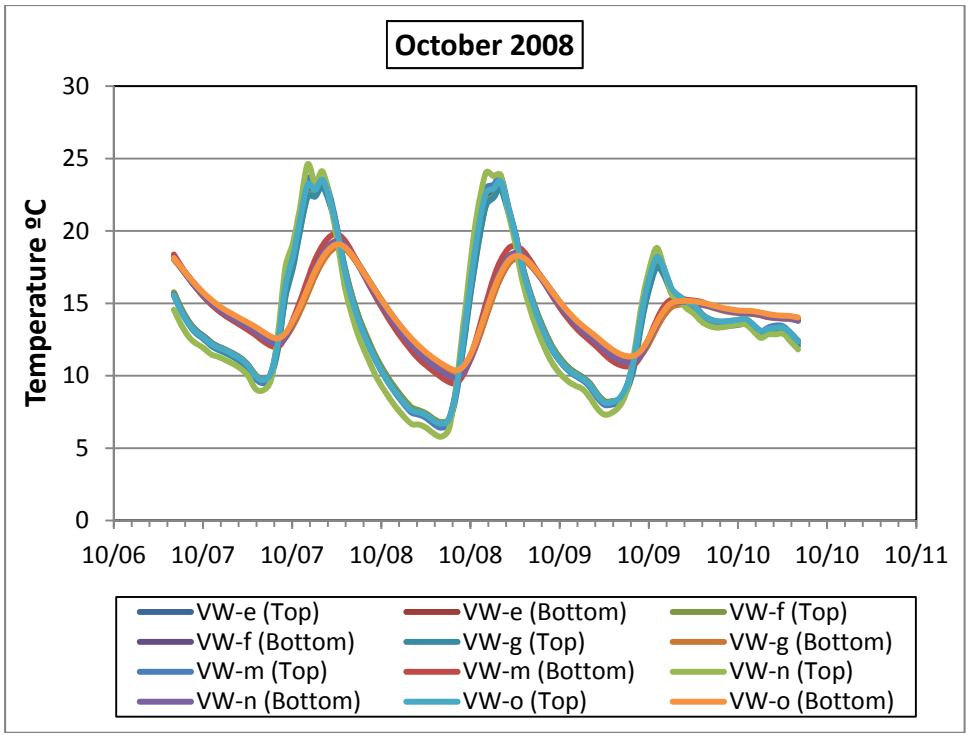

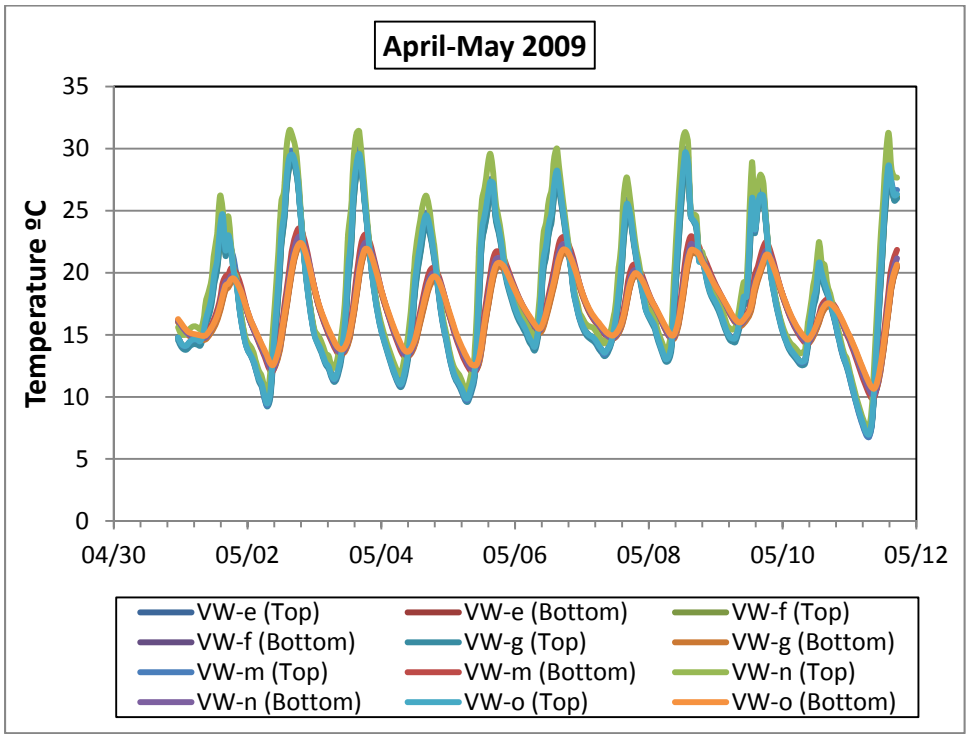

(0°C = 32°F, 35°C = 95°F)

Temperature Gradients

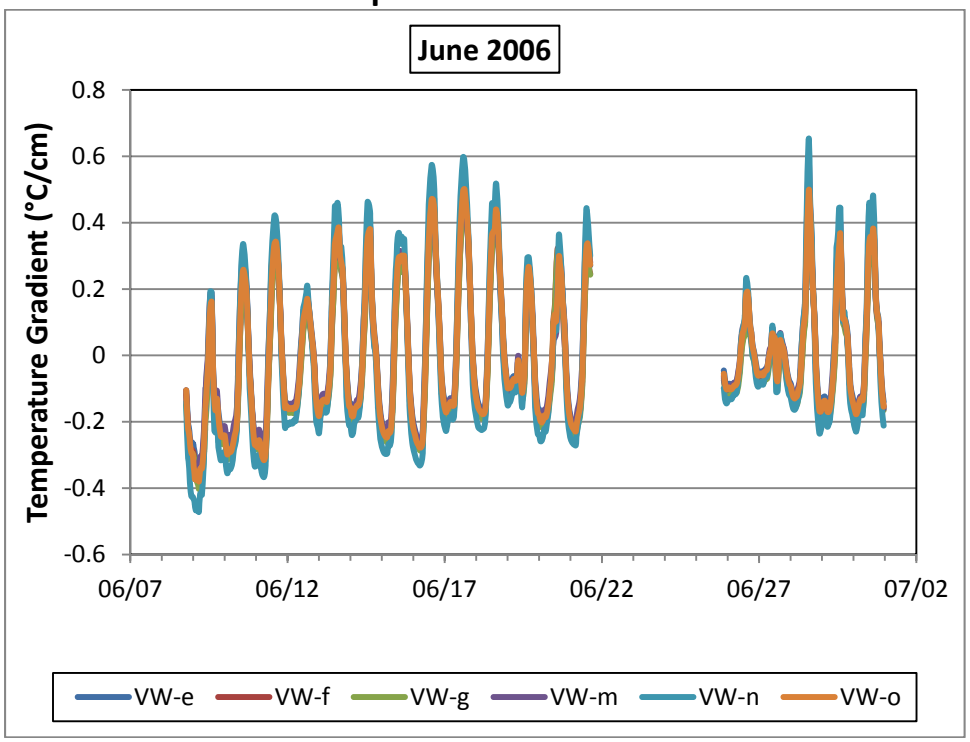

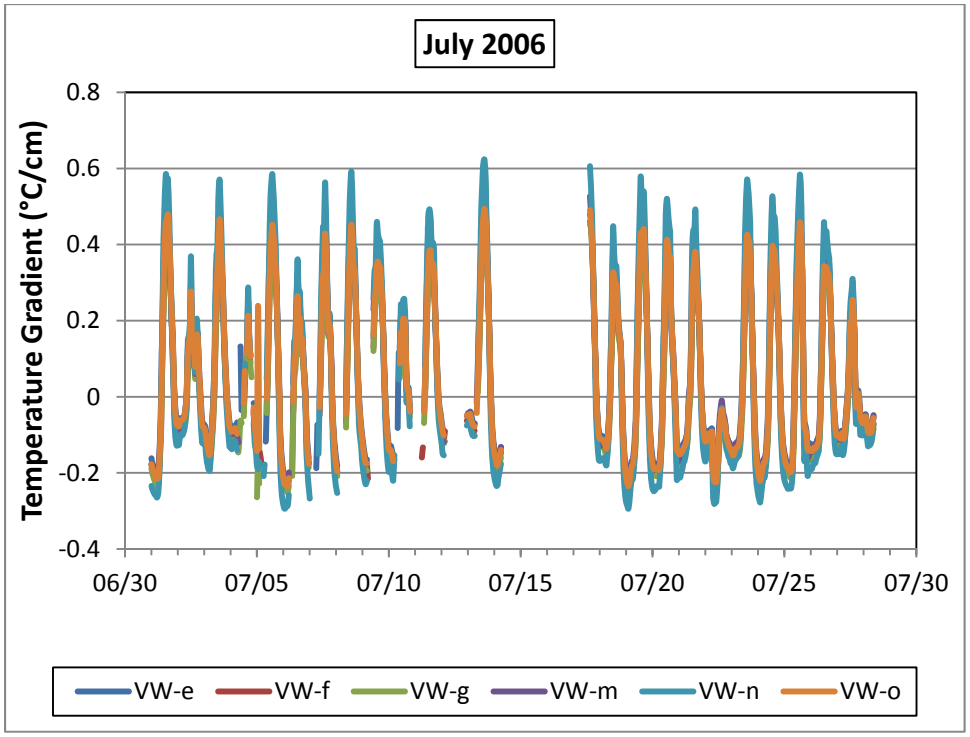

(1°C/cm = 4.6°F/in)

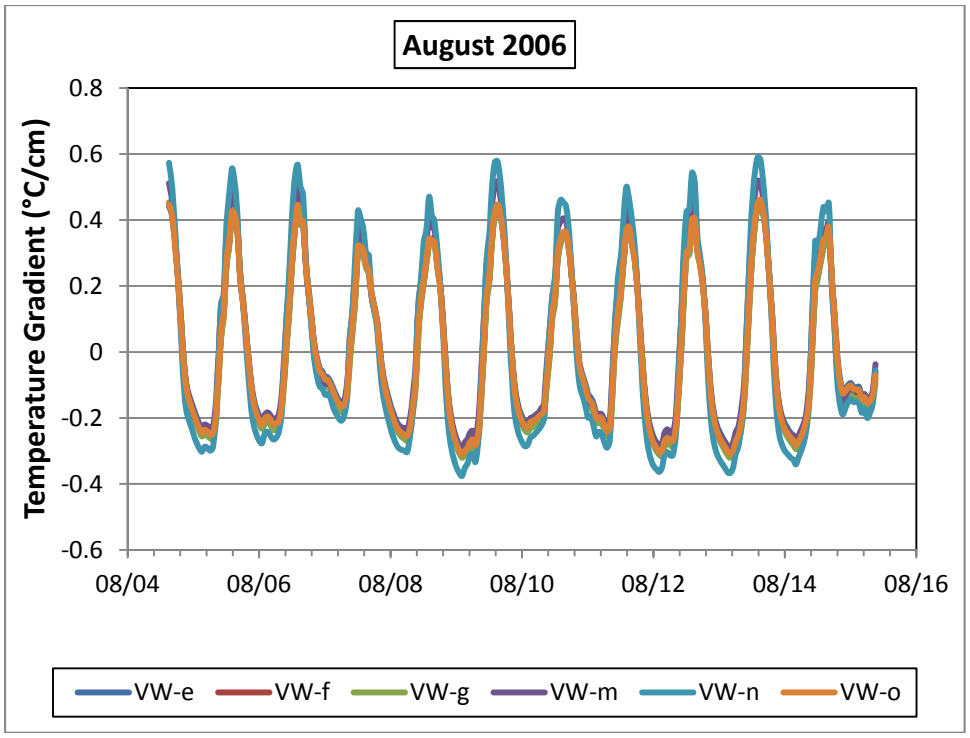
August 2006
Temperature Gradient (°C/cm)
0.8
0.6
0.4
0.2
0
-0.2
-0.4
-0.6
08/04
08/06
08/08
08/10
08/12
08/14
08/16
VW-e
VW-f
VW-g
VW-m
VW-n
VW-o

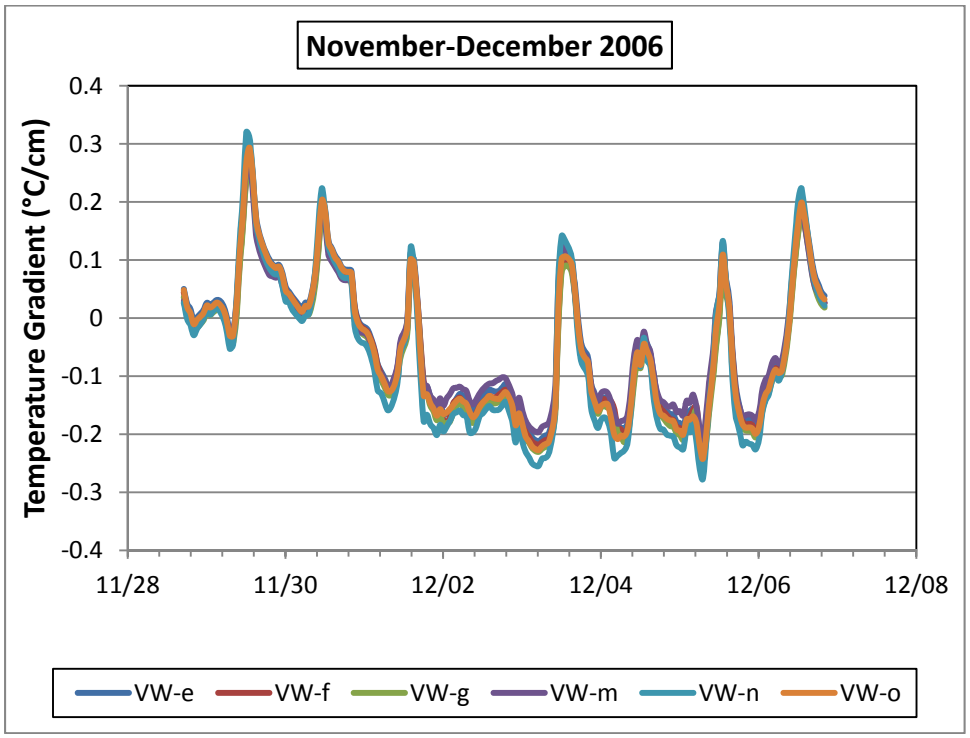
November-December 2006
Temperature Gradient (°C/cm)
0.4
0.3
0.2
0.1
0
-0.1
-0.2
-0.3
-0.4
11/28
11/30
12/02
12/04
12/06
12/08
VW-e
VW-f
VW-g
VW-m
VW-n
VW-o

(1°C/cm = 4.6°F/in)

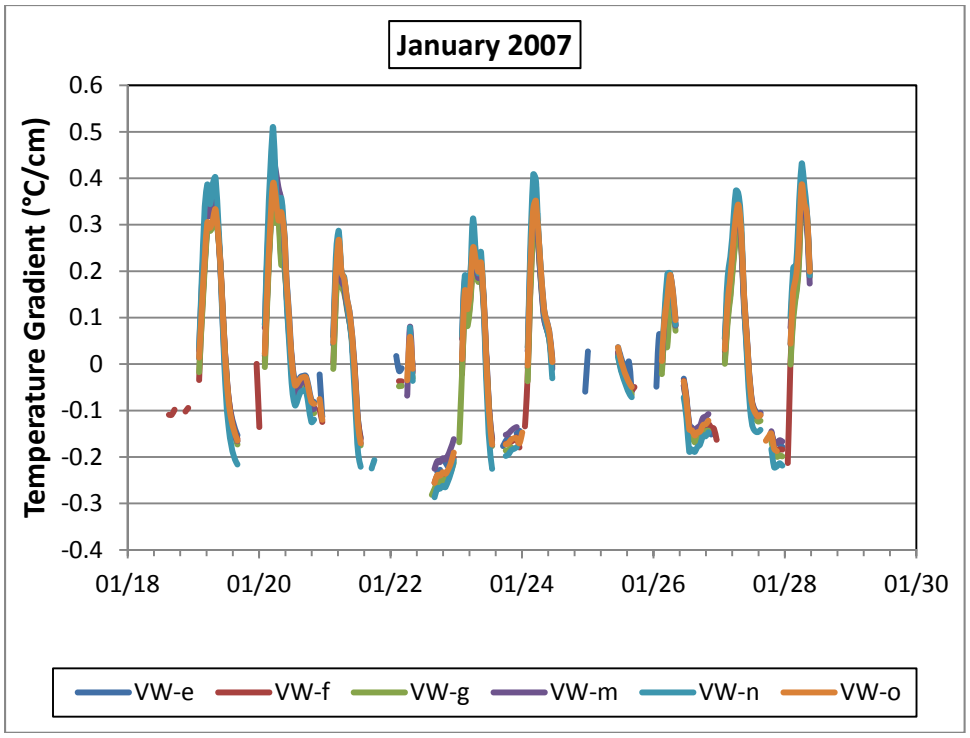
January 2007
Temperature Gradient (°C/cm)
0.6
0.5
0.4
0.3
0.2
0.1
0
-0.1
-0.2
-0.3
-0.4
01/18
01/20
01/22
01/24
01/26
01/28
01/30
VW-e
VW-f
VW-g
VW-m
VW-n
VW-o

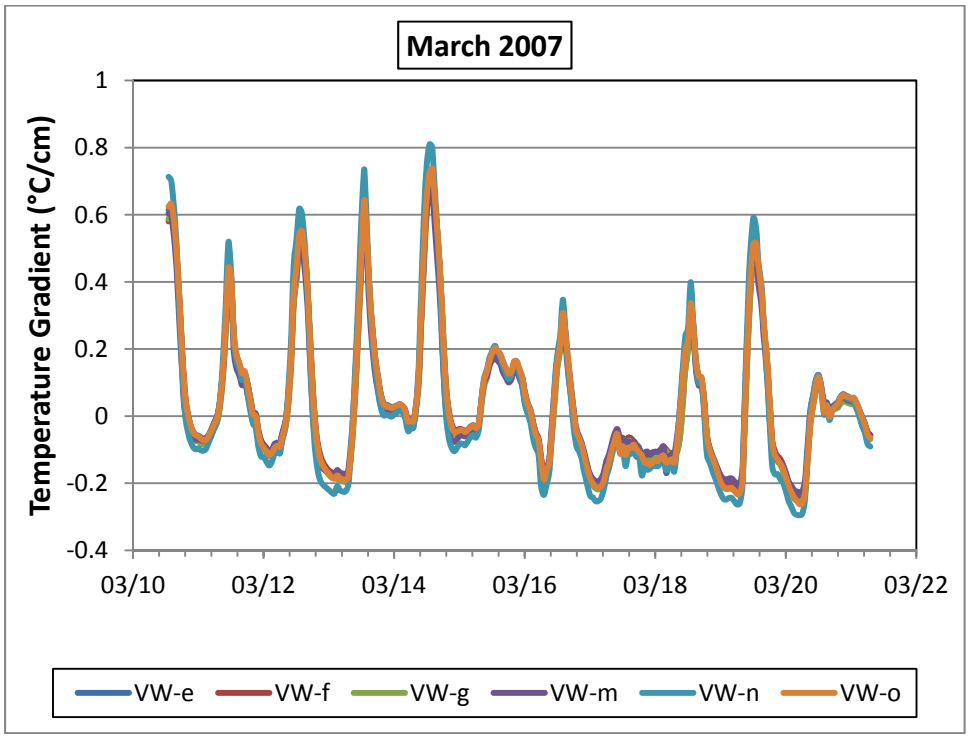
March 2007
Temperature Gradient (°C/cm)
1
0.8
0.6
0.4
0.2
0
-0.2
-0.4
03/10
03/12
03/14
03/16
03/18
03/20
03/22
VW-e
VW-f
VW-g
VW-m
VW-n
VW-o

(1°C/cm = 4.6°F/in)

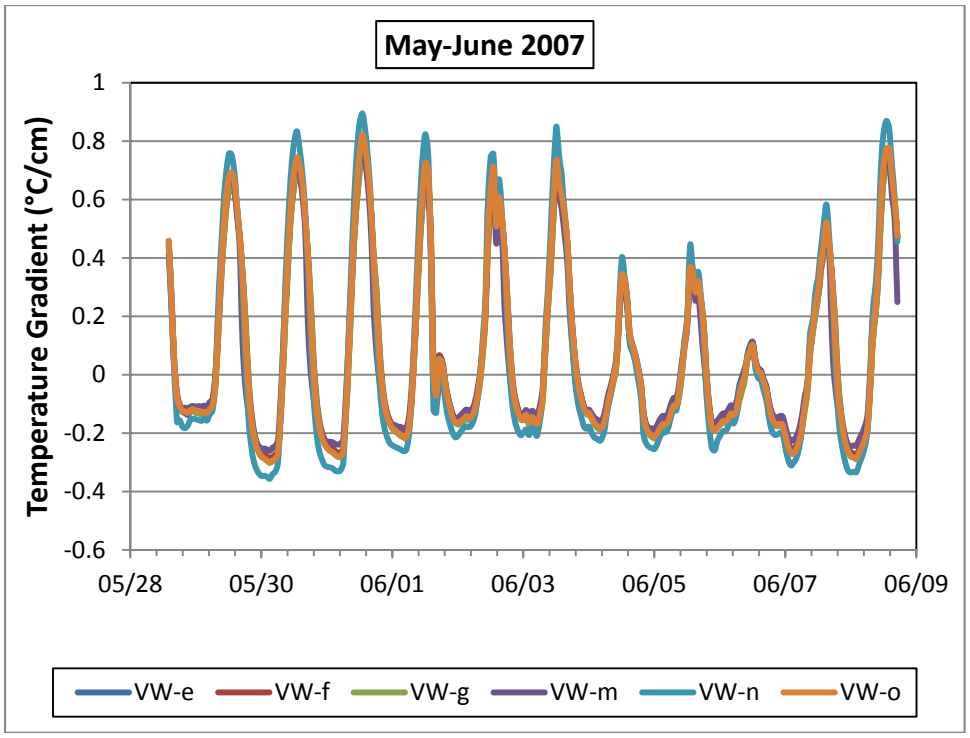
May-June 2007
Temperature Gradient (°C/cm)
1
0.8
0.6
0.4
0.2
0
-0.2
-0.4
-0.6
05/28
05/30
06/01
06/03
06/05
06/07
06/09
VW-e
VW-f
VW-g
VW-m
VW-n
VW-o

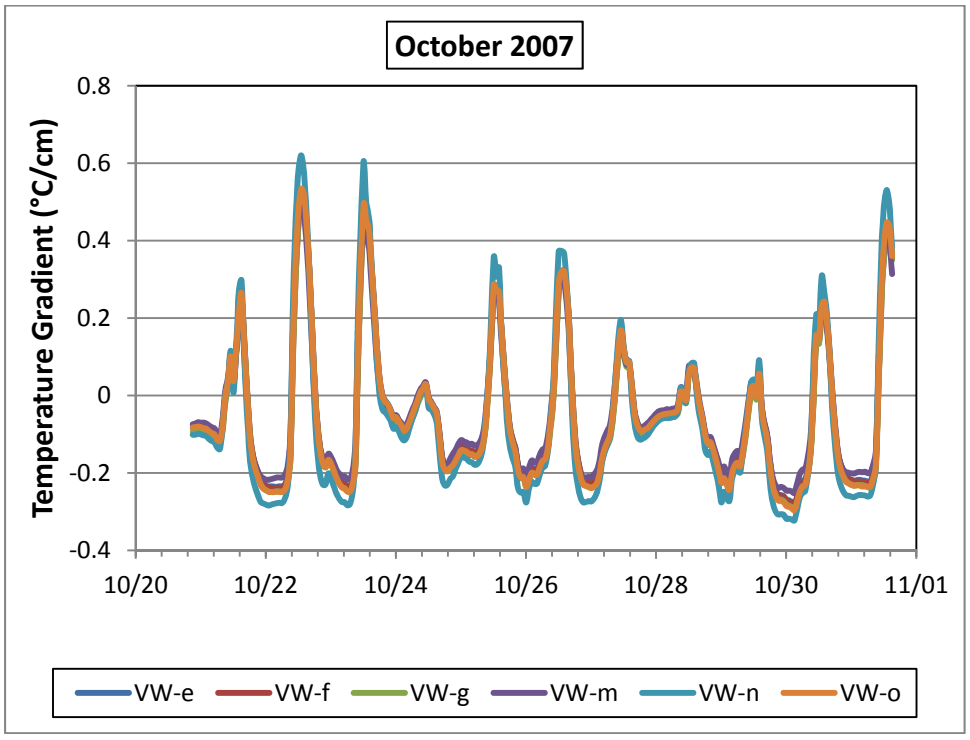
October 2007
Temperature Gradient (°C/cm)
0.8
0.6
0.4
0.2
0
-0.2
-0.4
10/20
10/22
10/24
10/26
10/28
10/30
11/01
VW-e
VW-f
VW-g
VW-m
VW-n
VW-o

(1°C/cm = 4.6°F/in)

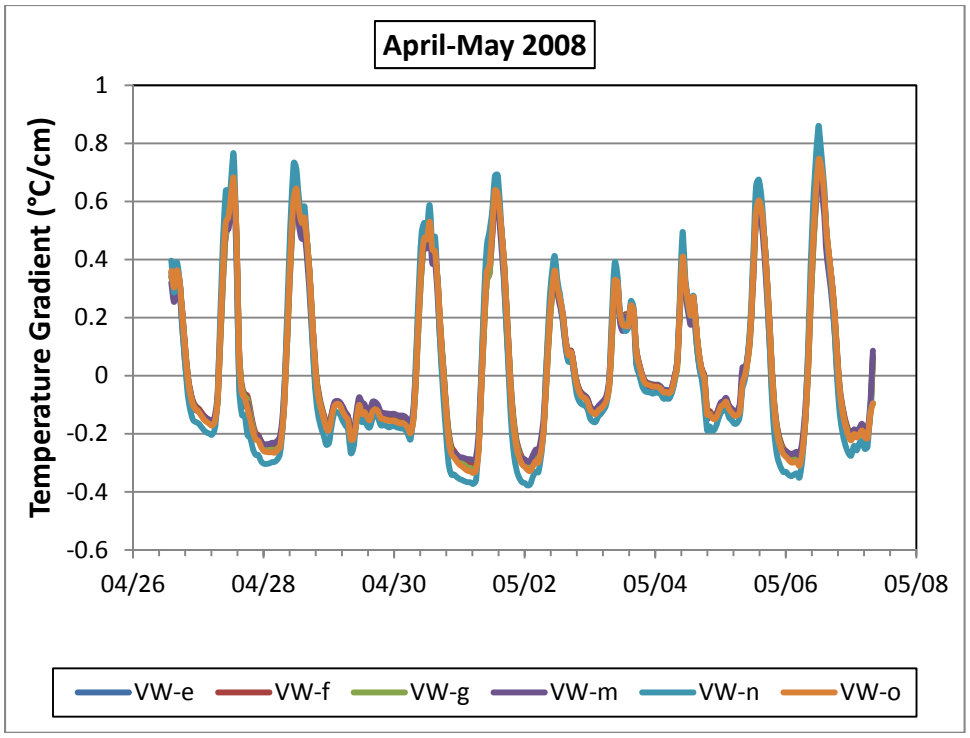
April-May 2008
Temperature Gradient (°C/cm)
1
0.8
0.6
0.4
0.2
0
-0.2
-0.4
-0.6
04/26
04/28
04/30
05/02
05/04
05/06
05/08
VW-e
VW-f
VW-g
VW-m
VW-n
VW-o

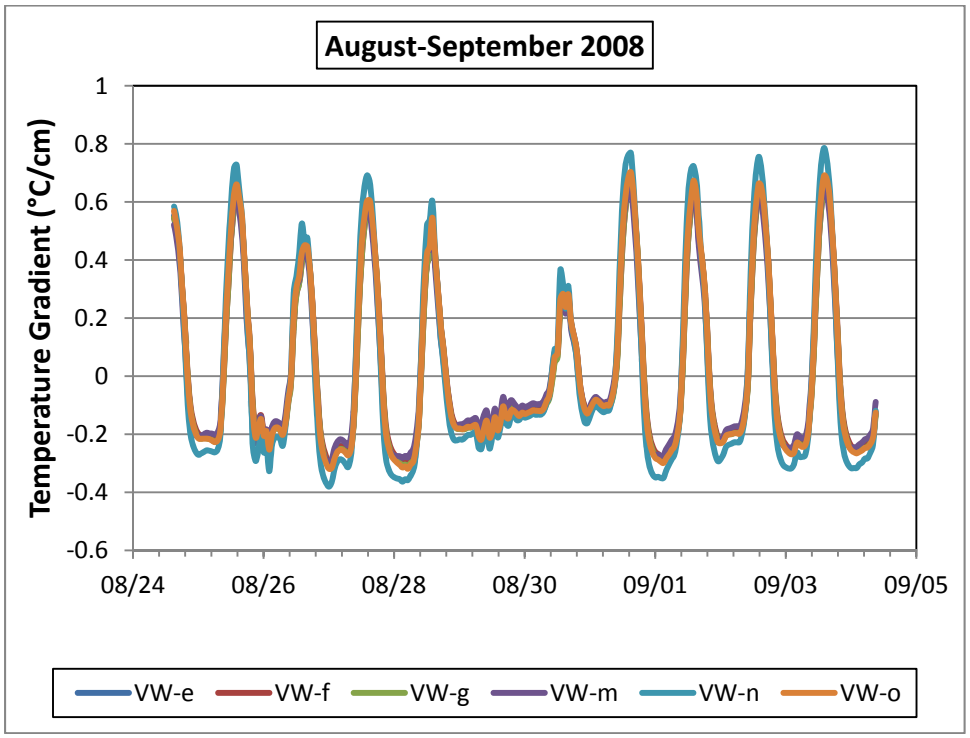
August-September 2008
Temperature Gradient (°C/cm)
1
0.8
0.6
0.4
0.2
0
-0.2
-0.4
-0.6
08/24
08/26
08/28
08/30
09/01
09/03
09/05
VW-e
VW-f
VW-g
VW-m
VW-n
VW-o

(1°C/cm = 4.6°F/in)

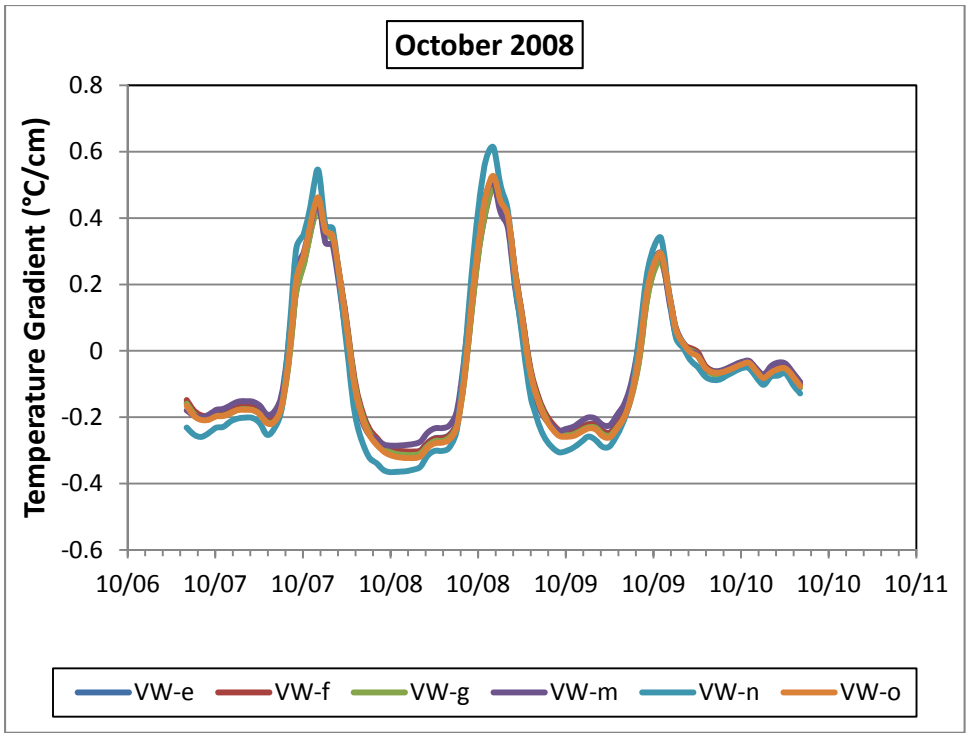
October 2008
Temperature Gradient (°C/cm)
0.8
0.6
0.4
0.2
0
-0.2
-0.4
-0.6
10/06
10/07
10/07
10/08
10/08
10/09
10/09
10/10
10/10
10/11
VW-e
VW-f
VW-g
VW-m
VW-n
VW-o

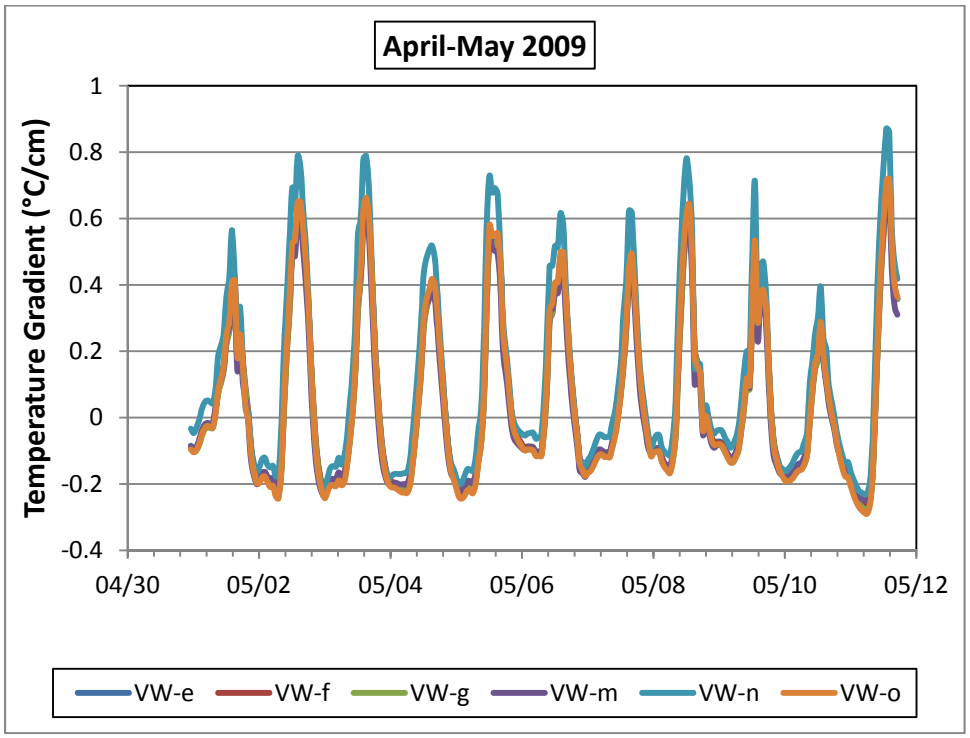
April-May 2009
Temperature Gradient (°C/cm)
1
0.8
0.6
0.4
0.2
0
-0.2
-0.4
04/30
05/02
05/04
05/06
05/08
05/10
05/12
VW-e
VW-f
VW-g
VW-m
VW-n
VW-o

(1°C/cm = 4.6°F/in)

Total Strain

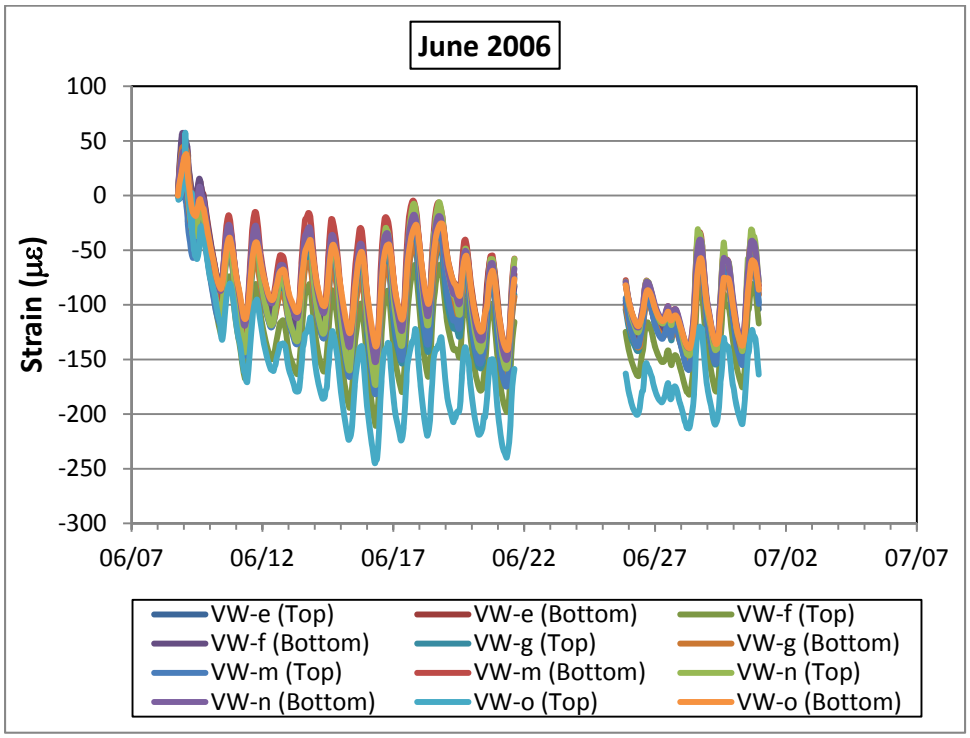

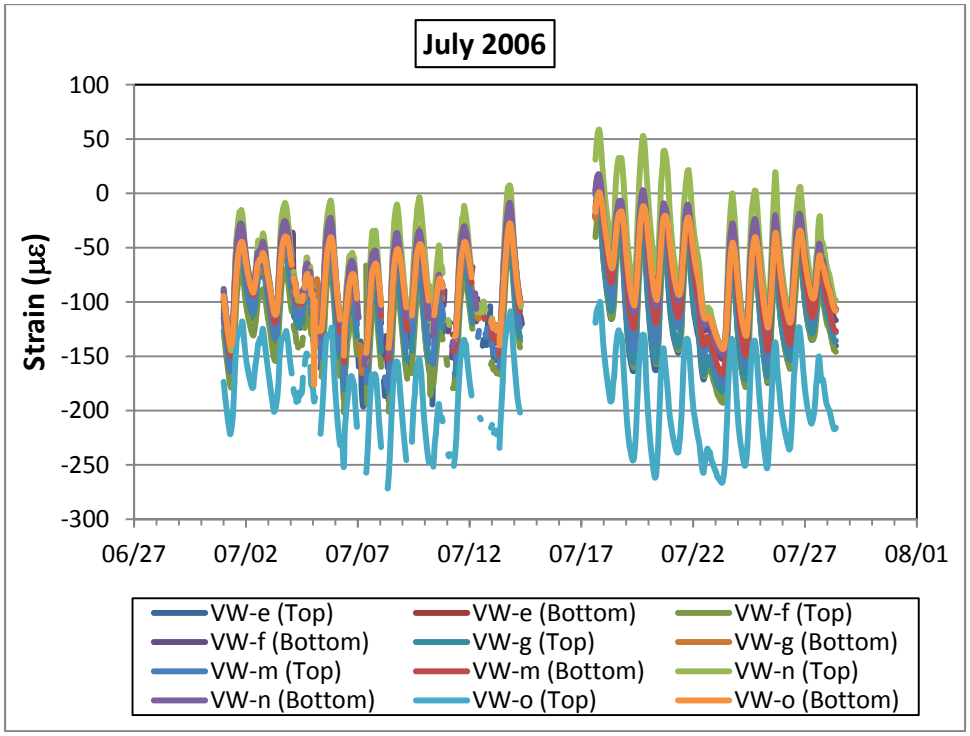

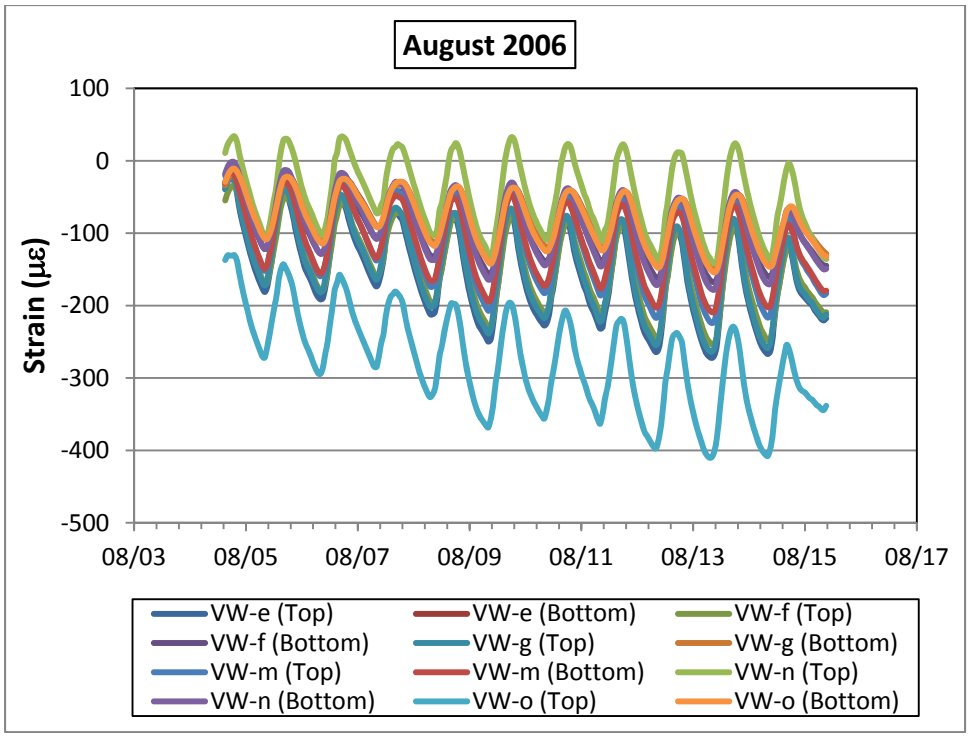
August 2006
100
0
-100
-200
-300
-400
-500
Strain (με)
08/03
08/05
08/07
08/09
08/11
08/13
08/15
08/17
VW-e (Top)
VW-e (Bottom)
VW-f (Top)
VW-f (Bottom)
VW-g (Top)
VW-g (Bottom)
VW-m (Top)
VW-m (Bottom)
VW-n (Top)
VW-n (Bottom)
VW-o (Top)
VW-o (Bottom)

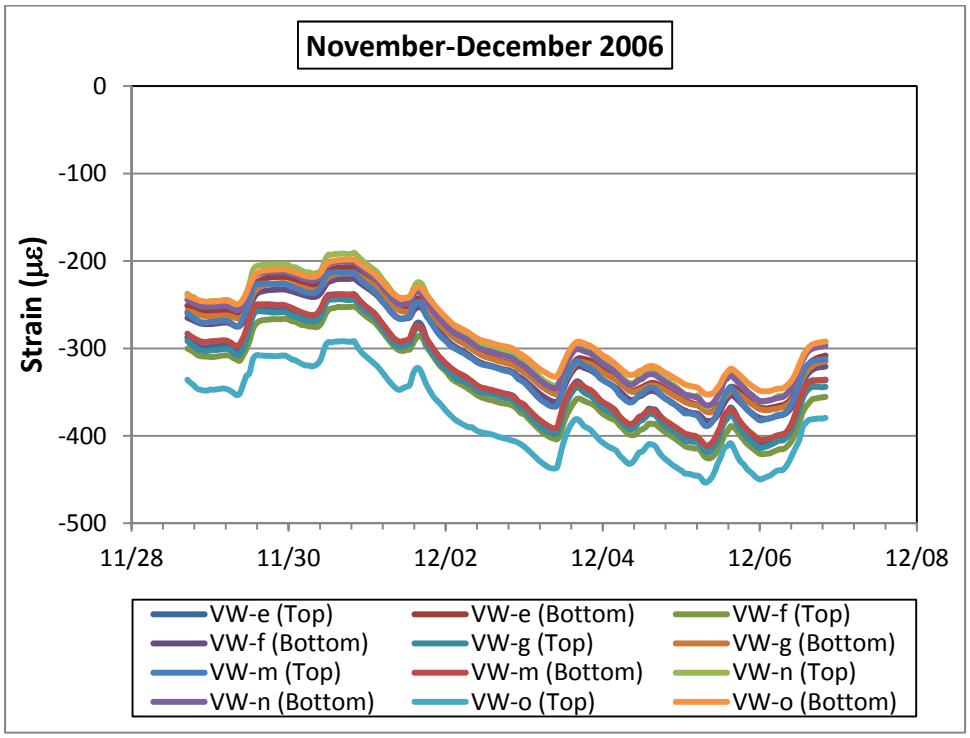
November-December 2006
0
-100
-200
-300
-400
-500
Strain (με)
11/28
11/30
12/02
12/04
12/06
12/08
VW-e (Top)
VW-e (Bottom)
VW-f (Top)
VW-f (Bottom)
VW-g (Top)
VW-g (Bottom)
VW-m (Top)
VW-m (Bottom)
VW-n (Top)
VW-n (Bottom)
VW-o (Top)
VW-o (Bottom)

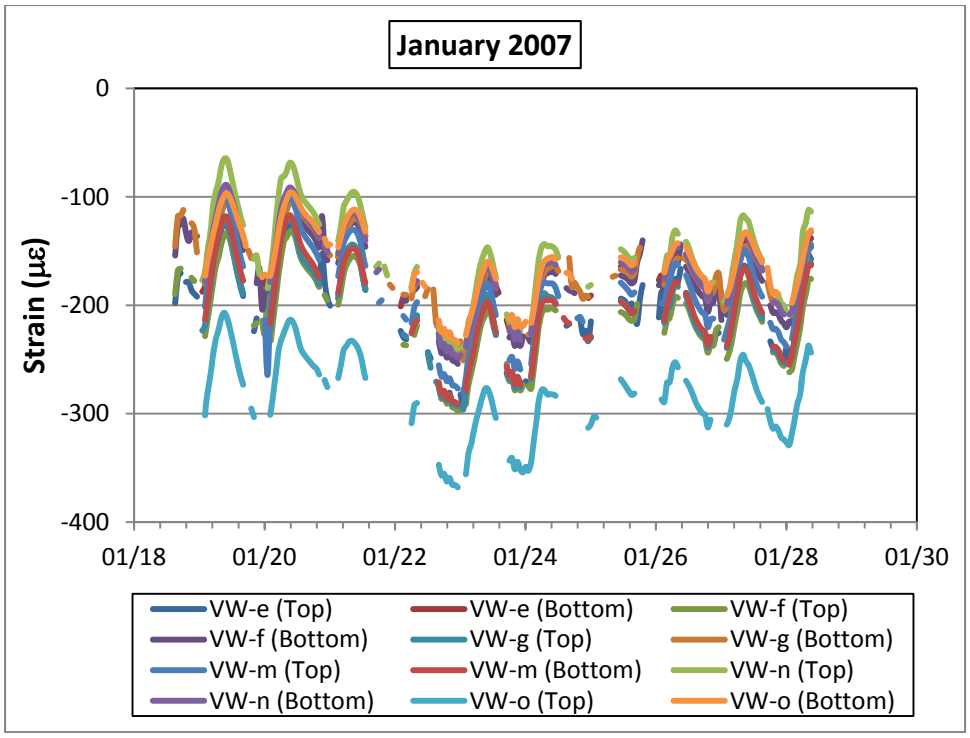
January 2007
0
-100
-200
-300
-400
Strain (με)
01/18
01/20
01/22
01/24
01/26
01/28
01/30
VW-e (Top)
VW-e (Bottom)
VW-f (Top)
VW-f (Bottom)
VW-g (Top)
VW-g (Bottom)
VW-m (Top)
VW-m (Bottom)
VW-n (Top)
VW-n (Bottom)
VW-o (Top)
VW-o (Bottom)

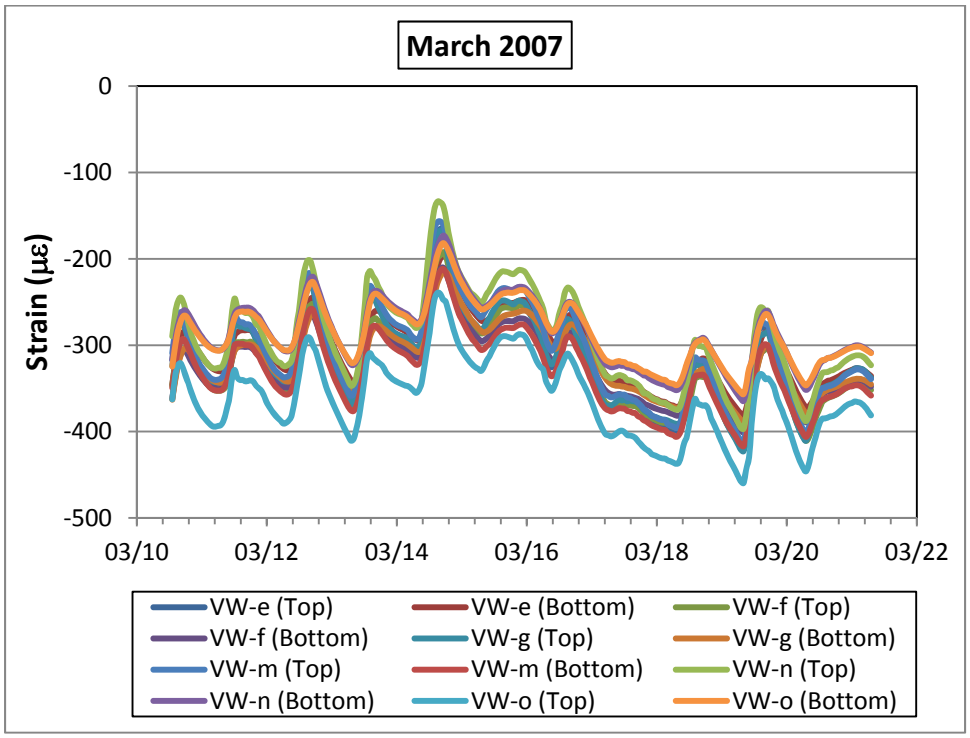
March 2007
0
-100
-200
-300
-400
-500
Strain (με)
03/10
03/12
03/14
03/16
03/18
03/20
03/22
VW-e (Top)
VW-e (Bottom)
VW-f (Top)
VW-f (Bottom)
VW-g (Top)
VW-g (Bottom)
VW-m (Top)
VW-m (Bottom)
VW-n (Top)
VW-n (Bottom)
VW-o (Top)
VW-o (Bottom)

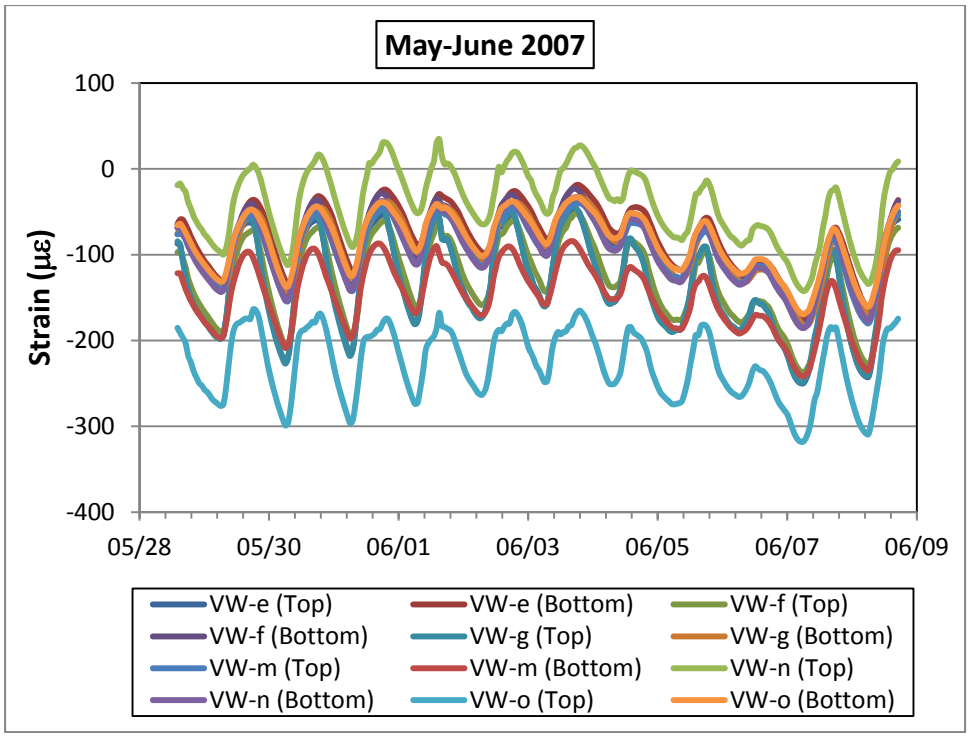
May-June 2007
100
0
-100
-200
-300
-400
Strain (με)
05/28
05/30
06/01
06/03
06/05
06/07
06/09
VW-e (Top)
VW-e (Bottom)
VW-f (Top)
VW-f (Bottom)
VW-g (Top)
VW-g (Bottom)
VW-m (Top)
VW-m (Bottom)
VW-n (Top)
VW-n (Bottom)
VW-o (Top)
VW-o (Bottom)

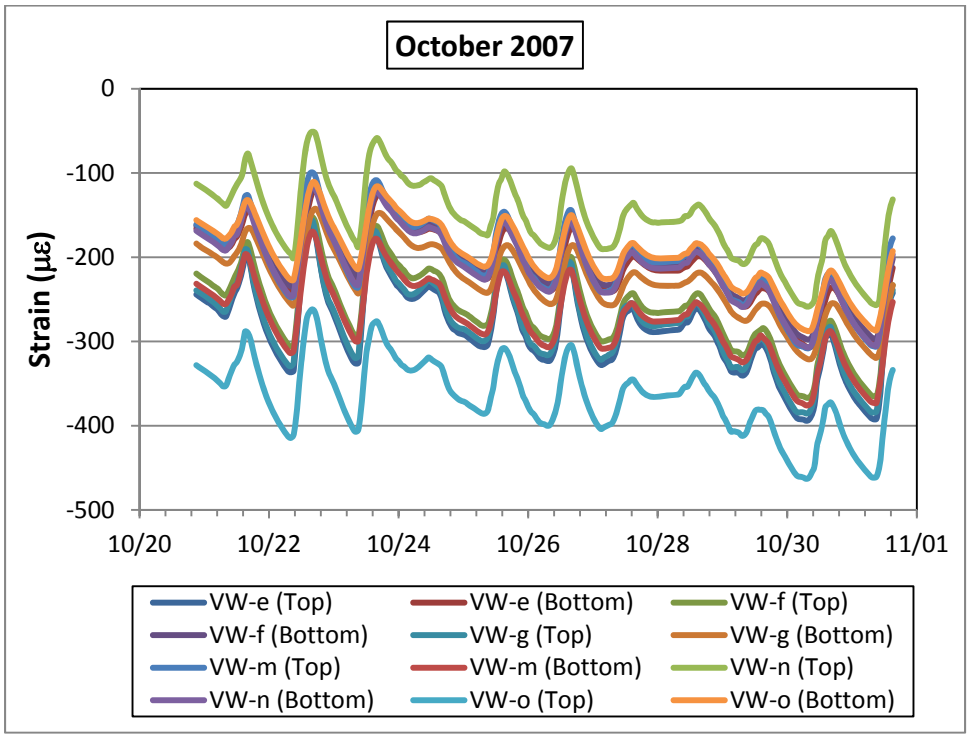
October 2007
0
-100
-200
-300
-400
-500
Strain (με)
10/20
10/22
10/24
10/26
10/28
10/30
11/01
VW-e (Top)
VW-e (Bottom)
VW-f (Top)
VW-f (Bottom)
VW-g (Top)
VW-g (Bottom)
VW-m (Top)
VW-m (Bottom)
VW-n (Top)
VW-n (Bottom)
VW-o (Top)
VW-o (Bottom)

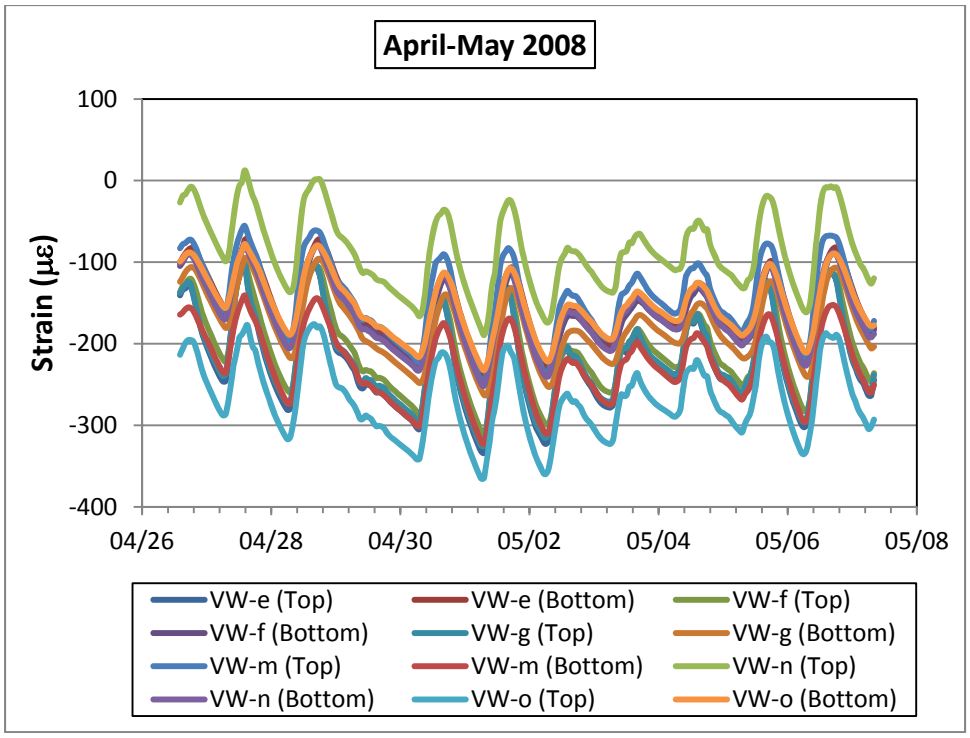
April-May 2008
100
0
-100
-200
-300
-400
Strain (με)
04/26
04/28
04/30
05/02
05/04
05/06
05/08
VW-e (Top)
VW-e (Bottom)
VW-f (Top)
VW-f (Bottom)
VW-g (Top)
VW-g (Bottom)
VW-m (Top)
VW-m (Bottom)
VW-n (Top)
VW-n (Bottom)
VW-o (Top)
VW-o (Bottom)

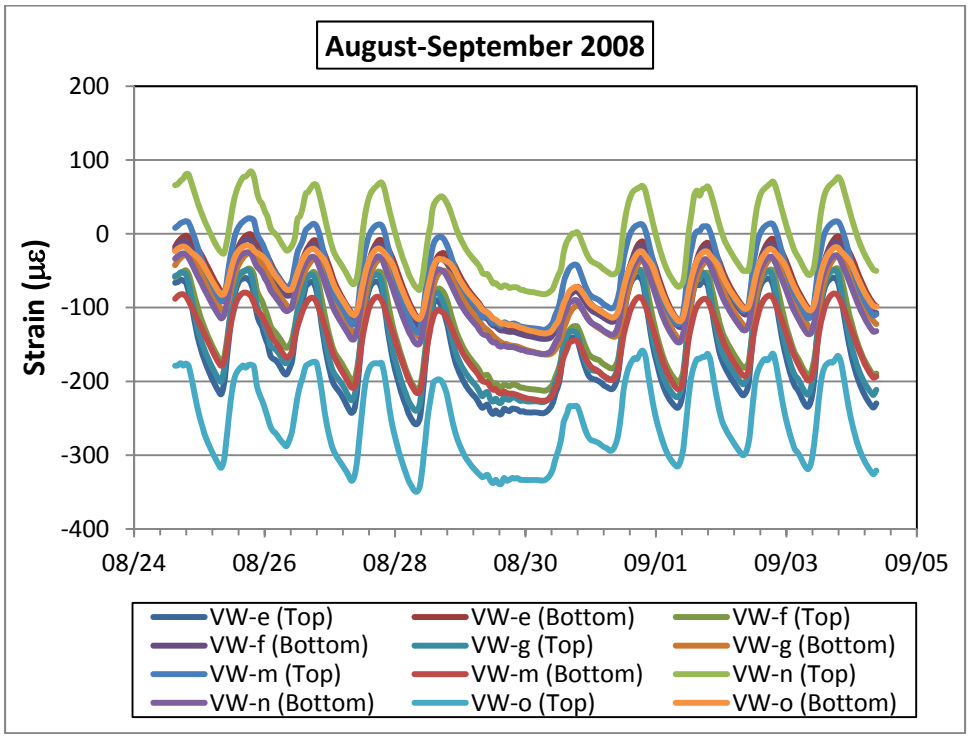
August-September 2008
200
100
0
-100
-200
-300
-400
Strain (με)
08/24
08/26
08/28
08/30
09/01
09/03
09/05
VW-e (Top)
VW-e (Bottom)
VW-f (Top)
VW-f (Bottom)
VW-g (Top)
VW-g (Bottom)
VW-m (Top)
VW-m (Bottom)
VW-n (Top)
VW-n (Bottom)
VW-o (Top)
VW-o (Bottom)

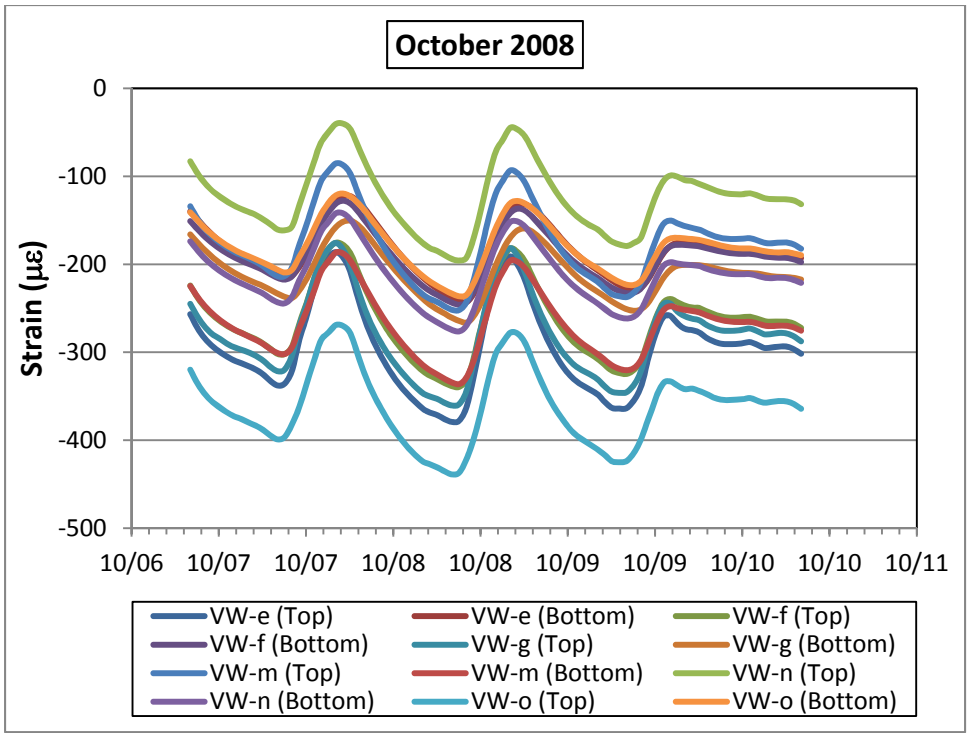
October 2008
0
-100
-200
-300
-400
-500
Strain (με)
10/06
10/07
10/07
10/08
10/08
10/09
10/09
10/10
10/10
10/11
VW-e (Top)
VW-e (Bottom)
VW-f (Top)
VW-f (Bottom)
VW-g (Top)
VW-g (Bottom)
VW-m (Top)
VW-m (Bottom)
VW-n (Top)
VW-n (Bottom)
VW-o (Top)
VW-o (Bottom)

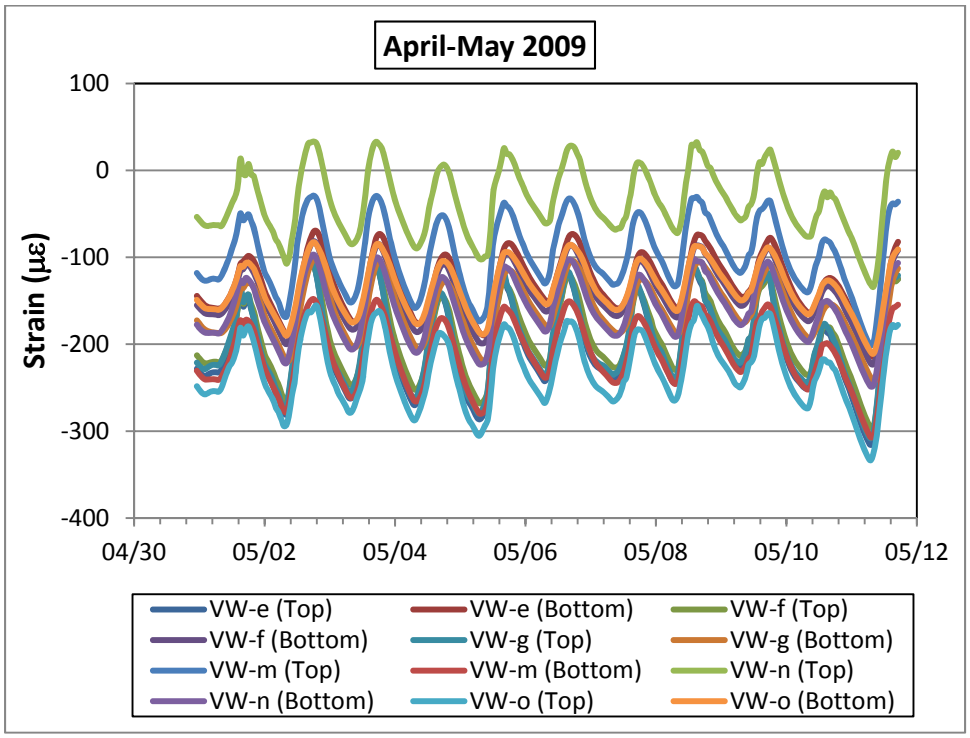
April-May 2009
100
0
-100
-200
-300
-400
Strain (με)
04/30
05/02
05/04
05/06
05/08
05/10
05/12
VW-e (Top)
VW-e (Bottom)
VW-f (Top)
VW-f (Bottom)
VW-g (Top)
VW-g (Bottom)
VW-m (Top)
VW-m (Bottom)
VW-n (Top)
VW-n (Bottom)
VW-o (Top)
VW-o (Bottom)

Load-Related Strain

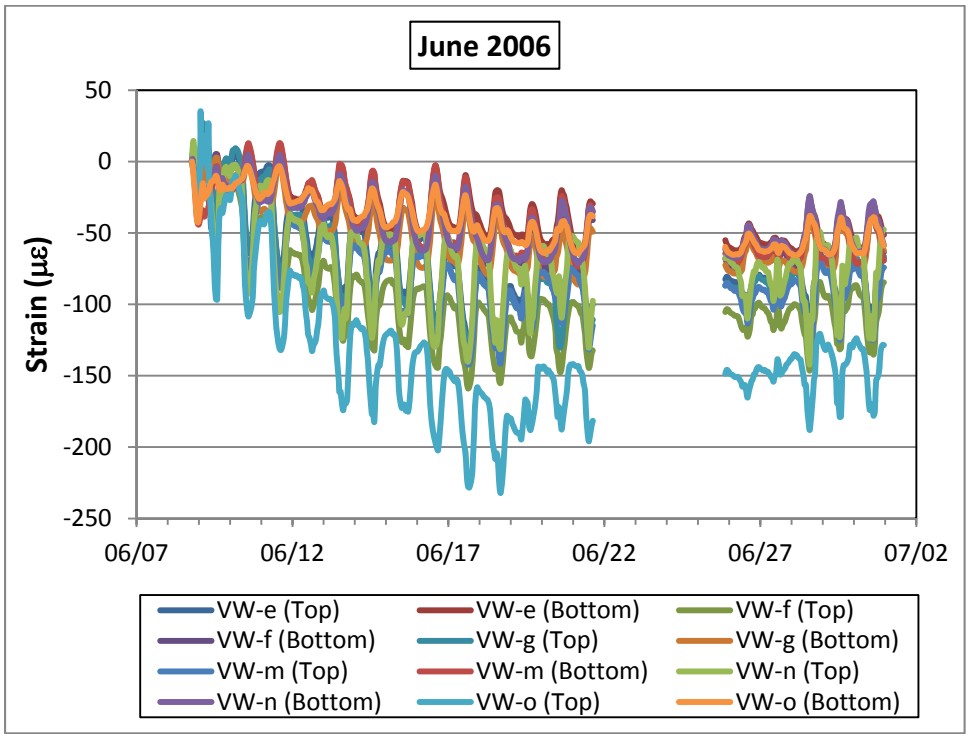

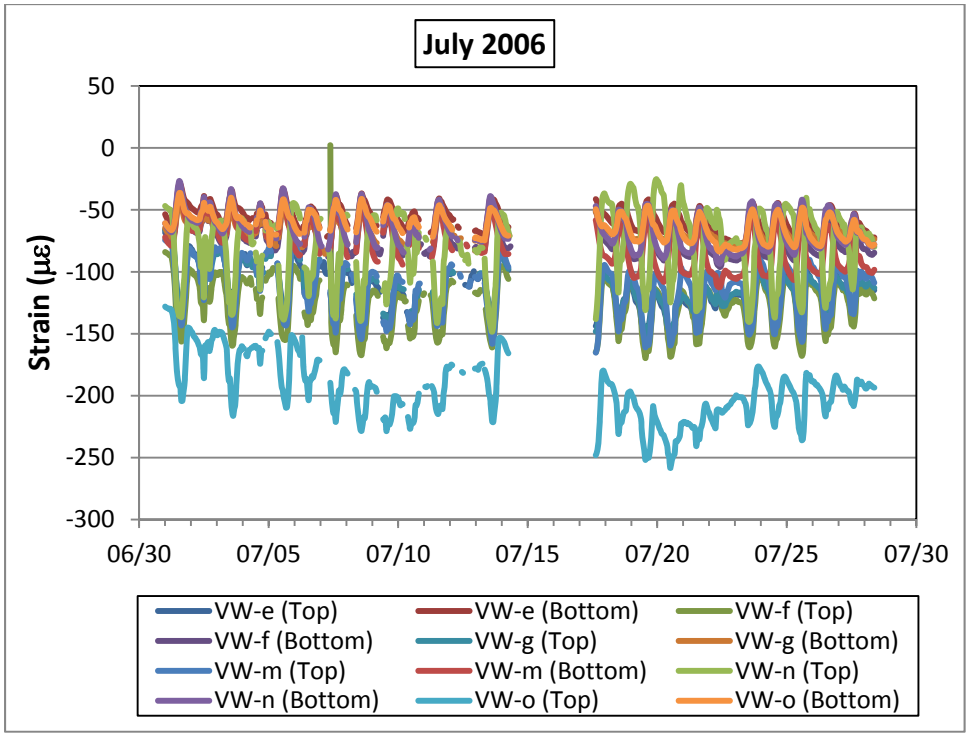

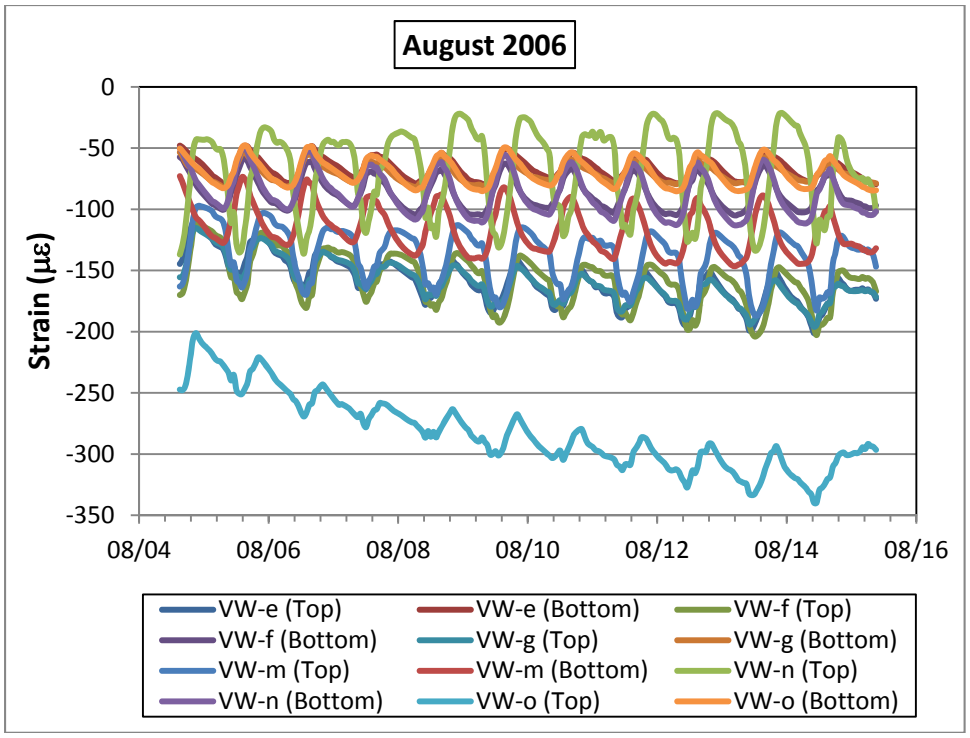
August 2006
0
-50
-100
-150
-200
-250
-300
-350
Strain (με)
08/04
08/06
08/08
08/10
08/12
08/14
08/16
VW-e (Top)
VW-e (Bottom)
VW-f (Top)
VW-f (Bottom)
VW-g (Top)
VW-g (Bottom)
VW-m (Top)
VW-m (Bottom)
VW-n (Top)
VW-n (Bottom)
VW-o (Top)
VW-o (Bottom)

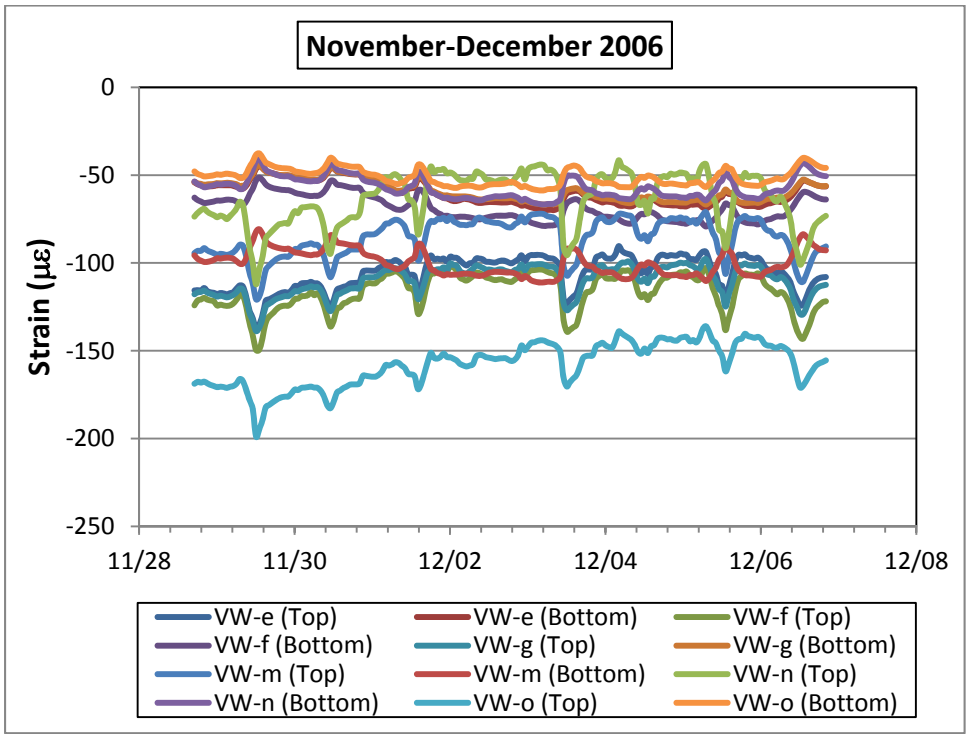
November-December 2006
0
-50
-100
-150
-200
-250
Strain (με)
11/28
11/30
12/02
12/04
12/06
12/08
VW-e (Top)
VW-e (Bottom)
VW-f (Top)
VW-f (Bottom)
VW-g (Top)
VW-g (Bottom)
VW-m (Top)
VW-m (Bottom)
VW-n (Top)
VW-n (Bottom)
VW-o (Top)
VW-o (Bottom)

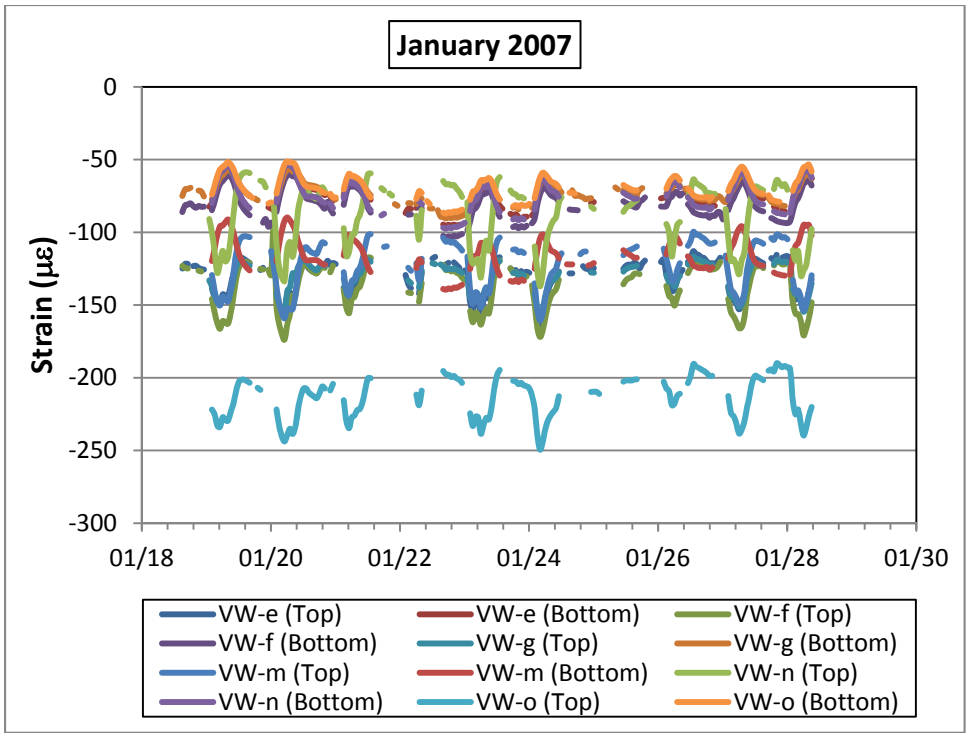
January 2007
0
-50
-100
-150
-200
-250
-300
Strain (με)
01/18
01/20
01/22
01/24
01/26
01/28
01/30
VW-e (Top)
VW-e (Bottom)
VW-f (Top)
VW-f (Bottom)
VW-g (Top)
VW-g (Bottom)
VW-m (Top)
VW-m (Bottom)
VW-n (Top)
VW-n (Bottom)
VW-o (Top)
VW-o (Bottom)

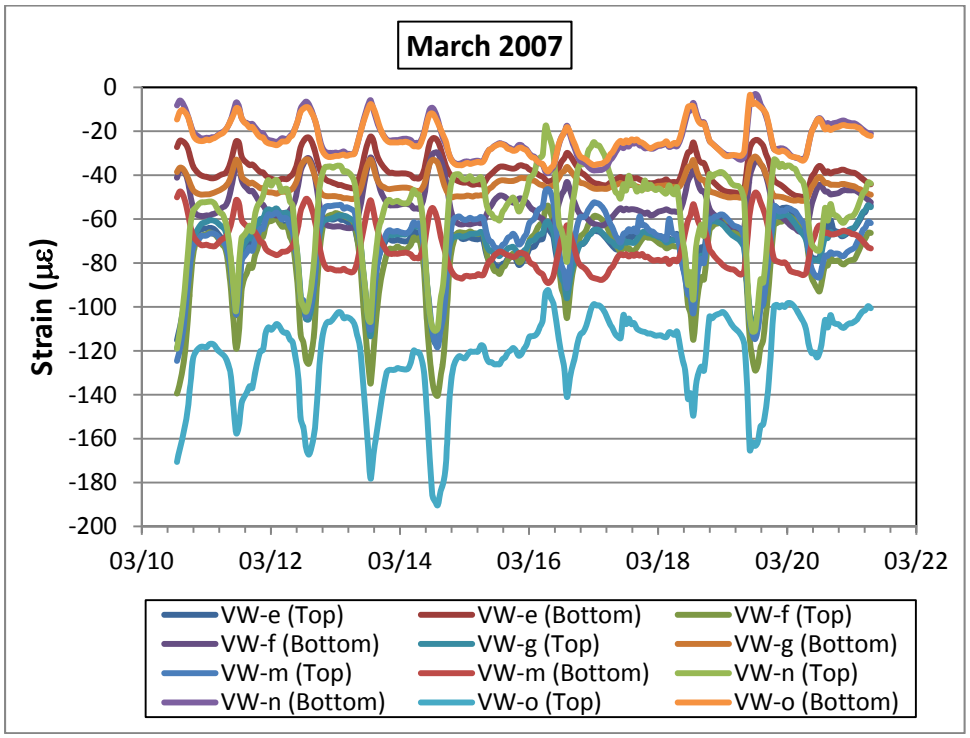
March 2007
0
-20
-40
-60
-80
-100
-120
-140
-160
-180
-200
Strain (με)
03/10
03/12
03/14
03/16
03/18
03/20
03/22
VW-e (Top)
VW-e (Bottom)
VW-f (Top)
VW-f (Bottom)
VW-g (Top)
VW-g (Bottom)
VW-m (Top)
VW-m (Bottom)
VW-n (Top)
VW-n (Bottom)
VW-o (Top)
VW-o (Bottom)

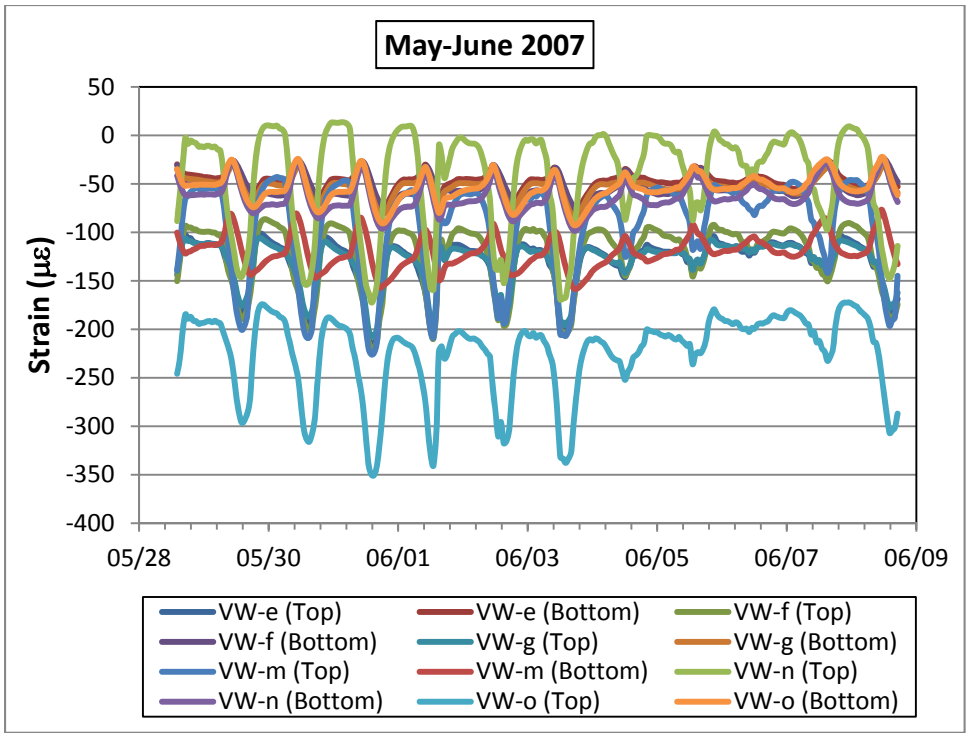
May-June 2007
Strain (με)
50
0
-50
-100
-150
-200
-250
-300
-350
-400
05/28
05/30
06/01
06/03
06/05
06/07
06/09
VW-e (Top)
VW-e (Bottom)
VW-f (Top)
VW-f (Bottom)
VW-g (Top)
VW-g (Bottom)
VW-m (Top)
VW-m (Bottom)
VW-n (Top)
VW-n (Bottom)
VW-o (Top)
VW-o (Bottom)

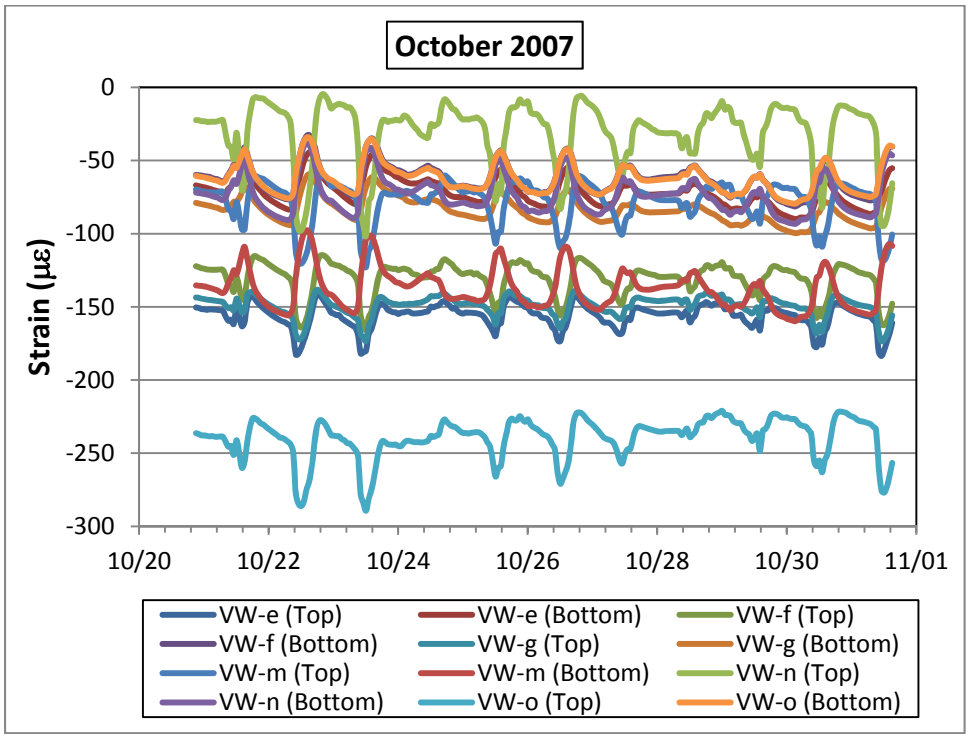
October 2007
Strain (με)
0
-50
-100
-150
-200
-250
-300
10/20
10/22
10/24
10/26
10/28
10/30
11/01
VW-e (Top)
VW-e (Bottom)
VW-f (Top)
VW-f (Bottom)
VW-g (Top)
VW-g (Bottom)
VW-m (Top)
VW-m (Bottom)
VW-n (Top)
VW-n (Bottom)
VW-o (Top)
VW-o (Bottom)

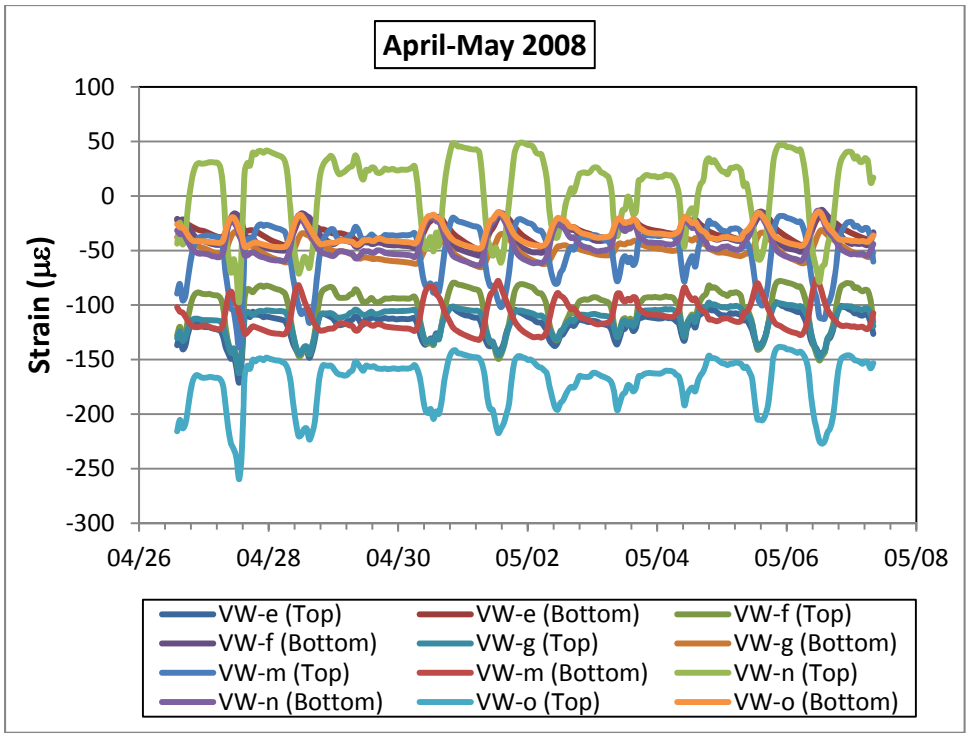
April-May 2008
Strain (με)
100
50
0
-50
-100
-150
-200
-250
-300
04/26
04/28
04/30
05/02
05/04
05/06
05/08
VW-e (Top)
VW-e (Bottom)
VW-f (Top)
VW-f (Bottom)
VW-g (Top)
VW-g (Bottom)
VW-m (Top)
VW-m (Bottom)
VW-n (Top)
VW-n (Bottom)
VW-o (Top)
VW-o (Bottom)

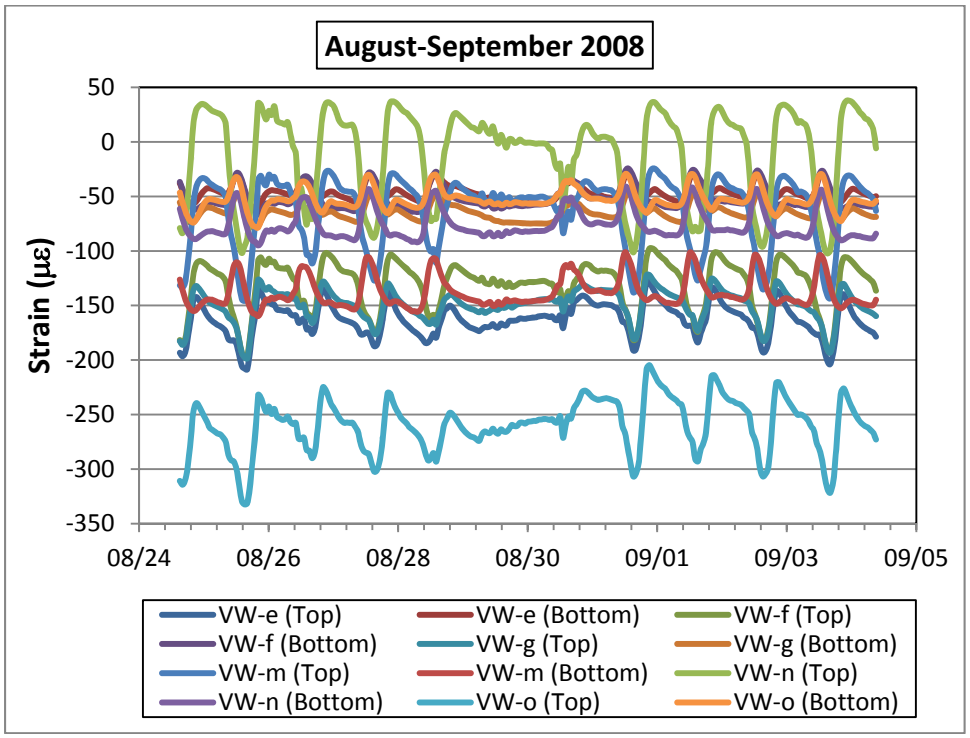
August-September 2008
Strain (με)
50
0
-50
-100
-150
-200
-250
-300
-350
08/24
08/26
08/28
08/30
09/01
09/03
09/05
VW-e (Top)
VW-e (Bottom)
VW-f (Top)
VW-f (Bottom)
VW-g (Top)
VW-g (Bottom)
VW-m (Top)
VW-m (Bottom)
VW-n (Top)
VW-n (Bottom)
VW-o (Top)
VW-o (Bottom)

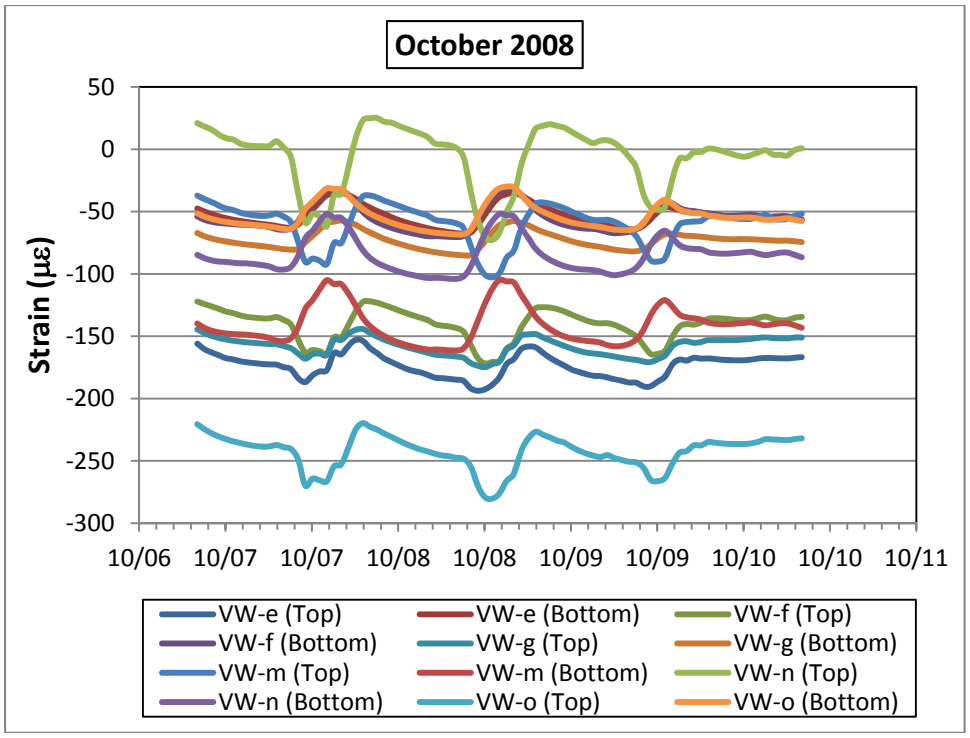
October 2008
Strain (με)
50
0
-50
-100
-150
-200
-250
-300
10/06
10/07
10/07
10/08
10/08
10/09
10/09
10/10
10/10
10/11
VW-e (Top)
VW-e (Bottom)
VW-f (Top)
VW-f (Bottom)
VW-g (Top)
VW-g (Bottom)
VW-m (Top)
VW-m (Bottom)
VW-n (Top)
VW-n (Bottom)
VW-o (Top)
VW-o (Bottom)

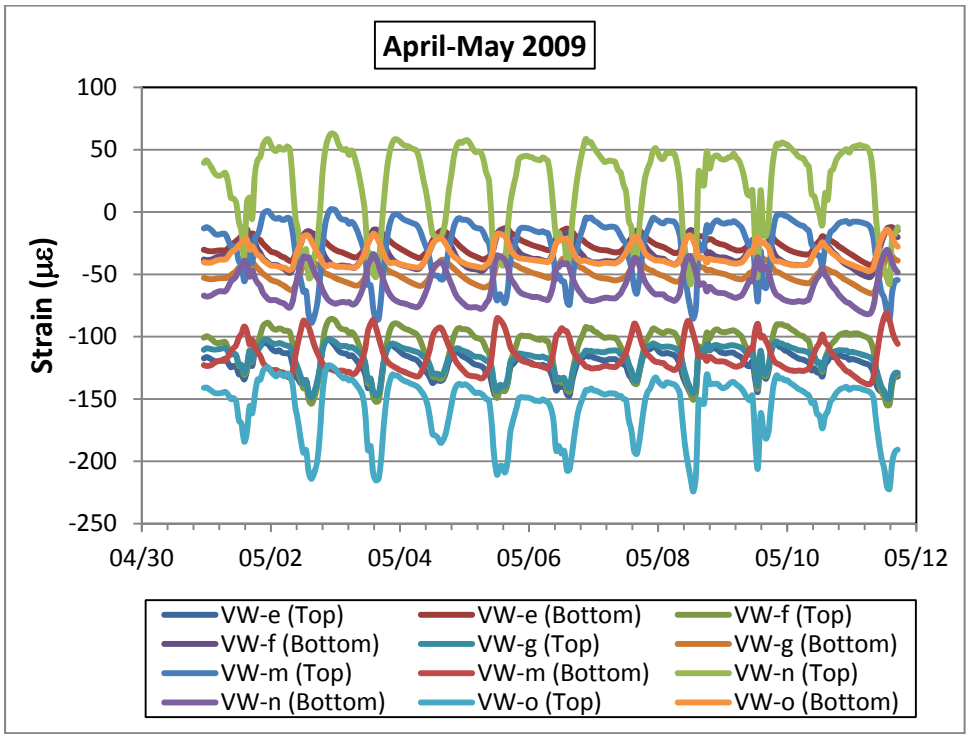
April-May 2009
Strain (με)
100
50
0
-50
-100
-150
-200
-250
04/30
05/02
05/04
05/06
05/08
05/10
05/12
VW-e (Top)
VW-e (Bottom)
VW-f (Top)
VW-f (Bottom)
VW-g (Top)
VW-g (Bottom)
VW-m (Top)
VW-m (Bottom)
VW-n (Top)
VW-n (Bottom)
VW-o (Top)
VW-o (Bottom)

ORITE • 141 Stocker Center • Athens, Ohio 45701-2979 • 740-593-2476
Fax: 740-593-0625 • orite@ohio.edu • http://www.ohio.edu/orite/